

092083

CONTRACT NAS 7-436 - INTERIM REPORT 06641-6014-R000 - NOVEMBER 1967

(NASA-CR-96636) ADVANCED VALVE TECHNOLOGY.
VOLUME 1: SPACECRAFT VALVE TECHNOLOGY
Interim Report, Jan. - Nov. 1967 R.J.
Salvinski, et al (TRW Systems Group) Nov.
1967 467 p

N72-74686

Unclas

CO/99 39293

ADVANCED VALVE TECHNOLOGY

FACILITY FORM 602

780 10 13 71

(ACCESSION NUMBER) 467

(PAGES) 20

(THRU) 20

(CODE) 78

(NASA CR OR TASK OR AD NUMBER) CR-96636

(CATEGORY) 3

"Available to U.S. Government Agencies and
U.S. Government Contractors Only"

VOLUME 1: SPACECRAFT VALVE TECHNOLOGY

Reproduced by
NATIONAL TECHNICAL
INFORMATION SERVICE
US Department of Commerce
Springfield, VA. 22151

PREPARED FOR
CHIEF FIELD OFFICE FOR TECHNOLOGY CODE APL
NATIONAL AERONAUTICS AND SPACE ADMINISTRATION
WASHINGTON, D.C.

N72-74686

ADVANCED VALVE TECHNOLOGY

VOLUME I

SPACECRAFT VALVE TECHNOLOGY

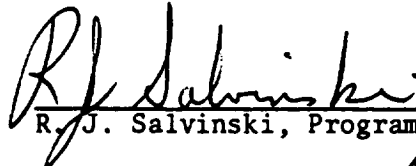
CONTRACT NAS 7-436

INTERIM REPORT

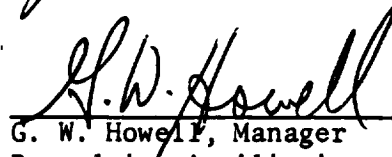
06641-6014-R000

NOVEMBER 1967

PREPARED FOR
CHIEF, LIQUID PROPULSION TECHNOLOGY, CODE RPL
NATIONAL AERONAUTICS AND SPACE ADMINISTRATION
WASHINGTON, D. C.



R. J. Salvinski, Program Manager



G. W. Howell, Manager
Propulsion Auxiliaries and
Component Technology Department



D. H. Lee, Assistant Manager
Technology Laboratory

TRW SYSTEMS GROUP
ONE SPACE PARK • REDONDO BEACH, CALIFORNIA

REPRODUCED BY
NATIONAL TECHNICAL
INFORMATION SERVICE
U.S. DEPARTMENT OF COMMERCE
SPRINGFIELD, VA. 22161

467

FOREWORD

This report was prepared by TRW Systems Group, Redondo Beach, California, and contains the results of work undertaken for the purpose of advancing valve technology for liquid propulsion spacecraft engines. The report is published in two volumes. The work was accomplished from January 1967 to November 1967 for the Chief, Liquid Propulsion Technology, Code RPL, Headquarters, National Aeronautics and Space Administration, Washington, D. C. The Headquarters Project Manager is Mr. Frank E. Compitello. The program was administrated under the technical direction of Mr. Louis R. Toth of the Jet Propulsion Laboratory, Pasadena, California.

The work performed on the program was accomplished by TRW Systems Group, Power Systems Division. Mr. R. J. Salvinski of the Propulsion Auxiliaries and Component Technology Department, Technology Laboratory, is the Program Manager. Technical efforts provided for the work reported in Volume I of this report, by several TRW Systems Group personnel, are acknowledged:

Dr. P. Bhuta	Advanced Technology Department, Systems Laboratories
Mr. O. Fiet	Propulsion Auxiliaries and Component Technology Department
Mr. R. Hammel	Materials Science Department, Systems Laboratories
Mr. S. Lieberman	System Analysis Department
Mr. R. Lovejoy	Reliability Engineering Department, Product Assurance
Mr. M. Makowski	Propulsion Auxiliaries and Component Technology Department
Mr. C. Mangion	Propulsion Auxiliaries and Component Technology Department
Dr. H. Mann	Thin Film Department, Systems Laboratories
Mr. J. Reger	Materials Science Department, Systems Laboratories
Mr. M. Weiner	Advanced Technology Department, Systems Laboratories

The results of efforts made on two subcontracts in support of this program are also acknowledged:

Professor R. W. Christy	Dartmouth College, Hanover, New Hampshire
Professor M. W. Roberts	University of Bradford, Bradford, England
Dr. J. R. H. Ross	University of Bradford, Bradford, England

ABSTRACT

This report describes the work performed by TRW Systems Group during a 12-month period with the objective of advancing the state of the art of valves used on spacecraft liquid propulsion systems. Current problems and future requirements relating to valve design, operation and test were determined. Interviews were held with personnel of NASA, Air Force, and prime manufacturers of propulsion systems to identify valve problems. New technology was utilized where necessary, to solve problems. Areas of study included propellant valves, valve actuators, and fluidic controls, instrumentation and measurements, liquid propellants and thin polymeric films. The results of the effort are reported in two volumes.

Volume I - Spacecraft Valve Technology

The valve technology study included problem analysis and problem identification; a review of reliability techniques in the specific area of valve redundant systems; seal leakage; and conceptual studies. A bipropellant valve concept requiring no-moving parts is described. Surface tension of liquids to provide valve sealing was studied and test data presented. A no-moving parts valve based on the principle of electroplating to effect a zero leak shutoff and throttling function was fabricated and tested. Conceptual tests were performed in a simple shutoff valve utilizing the interaction of magnetic fields on liquids to shift the liquid from off or on flow positions.

The applications and limitations of valve actuators were determined and new technology reported included a high speed actuator study. Reported are a monopropellant and bipropellant actuator, and a thermal actuator concept. The monopropellant actuator was fabricated and tested to determine feasibility. An investigation of thin film beryllium for use as an electrical conductor at low temperatures showed constant electrical resistance within 1 percent over a temperature range from ambient to liquid N_2 . Actuation techniques studied include electromechanical, hydraulic, pneumatic, chemical and thermal.

The advantages of applying fluidics to liquid propulsion systems are reduced size, and weight, with increased reliability. The most common fluidic devices were studied relative to configuration, performance, fabrication and materials, specific functional parameters, propellant compatibility, and the space environment. The technical problems and standard application criteria were reviewed, and the analytical techniques used to synthesize and design fluidic systems from the components level were outlined. Conceptual studies were initiated in the areas of pressure references and fluid flow regulation. An extensive bibliography is included.

In-flight leakage and valve positioning measurements criteria were established. The application of thin polymeric films as compatible coatings and valve seals were considered. In support of the work, an investigation was made of the formation kinetics of the films applied by electron bombardment techniques.

Volume II - Materials Compatibility and Liquid Propellant Study

This volume includes the results of surveys pertaining to the materials compatibility, shock sensitivity, lubricity, viscosity, radiation tolerances, and effects of leakage for 21 liquid propellants in present use or anticipated use within the next ten years. The information contained herein results from review of the literature listed in the Bibliography at the conclusion of this section. A new test method was studied pertaining to the evaluation of materials compatibility with propellants for long term storage.

Also included in this volume is a report on clogging of filters and orifices during flow with N_2O_4 .

CONTENTS

VOLUME I

<u>Section</u>		<u>Page</u>
I	INTRODUCTION	1-1
	PROGRAM PLAN	1-3
	SUMMARY OF SPECIFIC TASKS	1-4
II	VALVE STUDY	2-1
	VALVE COMPONENT RATING ANALYSIS CHART	2-4
	REDUNDANCY STUDY	2-8
	DIAPHRAGM VALVE	2-25
	ELECTROFLUID CONTROLS	2-27
	ELECTROSEAL CONCEPT	2-36
	SURFACE TENSION CONCEPTUAL STUDY	2-42
	SEAL LEAKAGE STUDY	2-59
III	ALL FLUID CONTROLS	3-1
	INTRODUCTION	3-6
	SURVEYS	3-8
	FLUIDIC COMPONENT STUDY	3-14
	COMPONENT APPLICATION CRITERIA	3-93
	CONCEPTUAL STUDIES	3-108
	ANALYSIS	3-141
	REFERENCES	3-148
IV	VALVE ACTUATOR STUDY	4-1
	VALVE ACTUATOR RATING ANALYSIS CHART	4-3
	ACTUATOR STUDY	4-4
	HIGH SPEED SOLENOID VALVE ACTUATION STUDY	4-16
	CONCEPTUAL STUDIES	4-36
V	INSTRUMENTATION AND MEASUREMENTS	5-1
	IN-FLIGHT LEAKAGE MEASUREMENTS	5-2
	VALVE POSITIONING INDICATORS	5-7
	CONCEPTUAL STUDIES	5-18

CONTENTS (con't)

VOLUME I

<u>Section</u>	<u>Page</u>
VI THIN FILM STUDY	6-1
THE FORMATION OF SURFACE FILMS BY ELECTRON BOMBARDMENT	6-2
PHYSICAL AND CHEMICAL PROPERTIES OF THIN POLYMER FILMS	6-24

VOLUME II

<u>Section</u>		
I MATERIALS COMPATIBILITY		1-1
INTRODUCTION		1-1
DISCUSSION		1-2
MATERIALS COMPATIBILITY TEST METHODS		1-6
RECOMMENDATIONS		1-9
PROPELLANT RATING CHART		1-11
EARTH STORABLE PROPELLANTS		1-12
SPACE STORABLE PROPELLANTS		1-61
HARD CRYOGENICS		1-84
GELLED PROPELLANTS		1-99
REFERENCES		1-106
II CLOGGING OF FILTERS AND ORIFICES		2-1

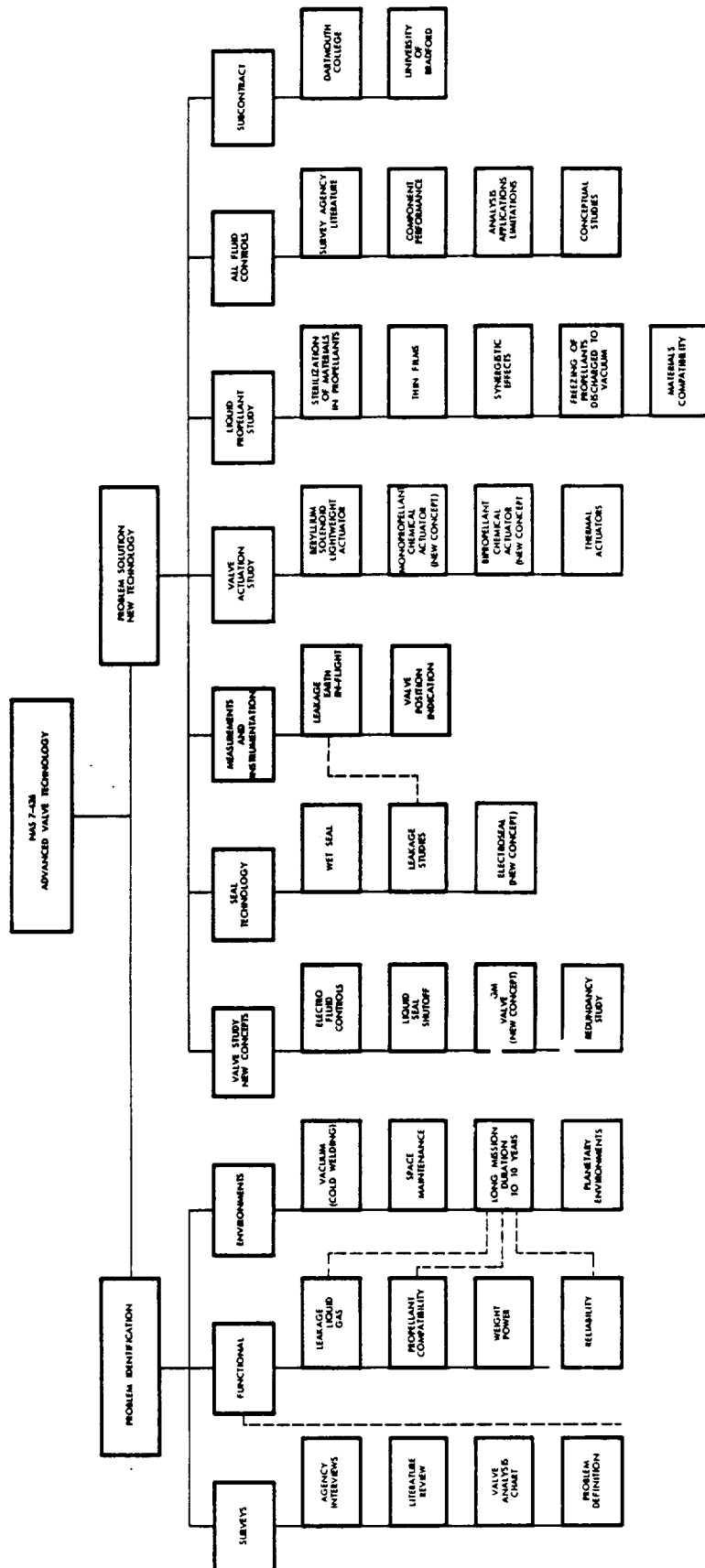
I INTRODUCTION

This Interim Report represents the work accomplished under the Advanced Valve Technology Program between 1 November 1966 and 1 November 1967. The objective of the work is to advance the state of the art of valves used on spacecraft liquid chemical rocket engines. The approach taken to meet the objectives during the program period involved two major steps: 1) problem definition, and 2) problem solutions. Problem definition resulted from efforts expended on interviews with personnel working in the propulsion control areas and a literature search. Problem solution was approached through conceptual design and analytical methods. Technological disciplines not normally utilized in valve design were employed where their application to solutions to problems appeared promising. "Brain storming" techniques were applied freely as well as the systematic approach to concepts evolution.

The types of valves studied included those necessary for the regulation and flow control of liquid propellants and gas pressurants. The propellants considered were the earth and space storables and the hard cryogenics. Gas pressurants at pressures up to 1000 psia for both hot and cold service were considered. Electrical, pneumatic, and hydraulic actuators and actuating concepts were included in the valve study. The functional parametric requirements for valves and actuators studied included zero leakage, minimum pressure drop, minimum power consumption, service life to 10,000 cycles, and maximum response. Environmental parameters included the space and planetary environments, shock and vibration, sterilization, materials compatibility, thermal cycling and thermal shock, low weight, low cost, and minimum size.

The above requirements and other effects anticipated were considered for valves operating for periods of two, five and ten years in the space and planetary environments. The ten year requirements were considered for longer missions beyond Jupiter to the outer planets, Saturn, Uranus, Neptune and Pluto.

An outline of the program plan showing specific areas of study is given on the next page. A summary chart of specific tasks undertaken during this reporting period is given on Page 1-4. Task I through V depicted in the summary chart are reported in Volume I. Task VI is reported on in Volume II.



NAS 7-436 ADVANCED VALVE TECHNOLOGY

SUMMARY OF SPECIFIC TASKS - Period November 1966 to November 1967

Objective: To advance the state of the art of valves used in liquid propulsion spacecraft engines.

I. VALVE STUDY

A. Valve Analysis Chart

Program management aid in defining and evaluating problems related to propulsion valves operating in the space environment. Includes functional parameters and valve performance with propellants.



- B. Redundancy Study
- C. Diaphragm Valve (concept)
- D. Electrofluid Control Study
Electric Interaction Control (concept) (Fabrication and Test)
- E. Electroseat (concept) Fabrication and Test
- F. Surface Tension Conceptual Study
Electromagnetic Capillary Valve (new concept)
Relief Valve (new concept)
Check Valve (new concept)
- G. Seal Leakage Study

II. ALL FLUID CONTROLS - DETERMINE THE APPLICATION OF FLUIDICS TO LIQUID CHEMICAL PROPULSION CONTROLS

- A. Agency Surveys
- B. Fluidic Component Study
State of the Art Review
Operation and Performance
Fabrication and Materials
Functional Parameters
Space Environments
- C. Application Criteria
- D. Conceptual Studies
Fluidic Pressure Regulation
Fluidic Control Systems
Vortex Regulation (concept)
Vented Jet Performance Tests
- E. Analysis
Analytical techniques
Analytical tools

III. ACTUATOR STUDY

- A. Investigate beryllium for low temperature (to -420°F)
Electrical Resistivity
Thin Films
- B. HI-Speed Solenoid Actuator Study
- C. Conceptual Studies
Thermal Actuators
Chemical Actuators - Fabrication and Test

IV. INSTRUMENTATION AND MEASUREMENTS

- A. In-flight leakage
- B. Valve Position Indicators
- C. Conceptual Studies
Electromagnetic Meter
Acoustic Meters

V. THIN FILM STUDY

Investigate the application of thin polymeric films applied by electron bombardment techniques.

Materials	Physical Properties	Functional Parameters	Environments	Subcontracts
Cyclic Siloxane Linear Siloxane Cyclic Hydrocarbons	Thermal Stability Solvent Attack Flexibility Substrate Adhesion Physical Continuity	Cold Welding Propellant Compatibility Lubrication Sealing	High Temperature >1200°F High Vacuum to 10 ⁻¹³ mm Hg Acids Solvents	Dartmouth College University of Bradford

VI. LIQUID PROPELLANT STUDY (VOLUME II)

A. Effects of propellants on valve design

Earth Storables	Space Storables	Hard Cryogenics	Parameters
Hydrazine Monomethylhydrazine Unsymmetrical Dimethylhydrazine Aerozine-50 Pentaborane	Diborane Hydrazine A5 Liquidified Petroleum Gases Chlorine Trifluoride Oxygen Difluoride Perchloryl Fluoride Nitrogen Trifluoride Nitryl Fluoride Tetrafluorohydrazine	Liquid Fluorine Liquid Hydrogen Liquid Oxygen FLOX Gels Metalized Nonmetalized	Materials Compatibility Control of Flow Leakage Lubricity Radiation Tolerance Shock Sensitivity Viscosity Sterilization

- B. Clogging of Filters and Orifices
Gel Formation During N₂O₄ Flow

R. J. Salvinski
R. J. Salvinski, Program Manager

II. VALVE STUDY

This section presents the results of work performed with the objective of advancing the state of the art of valves used on liquid propulsion engines operating in space. A rating analysis chart is used as an aid in defining areas where advancements in valve technology is required. A redundancy study is included in this section and includes a discussion on the application and limitations imposed on series and redundant valve configurations using present analytical techniques. Also reported are the results of several conceptual studies, and a permeation leakage study, undertaken to investigate analytical techniques for predicting leakage through seal glands.

	<u>Page</u>
Valve Component Rating Analysis Chart	2-4
Redundancy Study	2-8
Diaphragm Valve	2-25
Electrofluid Controls	2-27
Electroseal Concept	2-36
Surface Tension Conceptual Study	2-42
Seal Leakage Study	2-59

VALVE COMPONENT RATING ANALYSIS CHART (TABLE 2-1)

The valve analysis chart is used as a management aid in defining the areas where advancement in valve technology is required. A reliability rating technique is used for defining and evaluating problems relating to the state of the art of valves used on liquid chemical propulsion systems. The reliability rating is assigned to each valve and valve element which make up a valve assembly and qualitatively relates to a functional parameter; the performance of the valve or valve elements operating in a propellant; and the space environment.

Reliability ratings assigned to various combinations and components and parameters have the following definitions:

Rating

1	A serious problem exists for which there is no satisfactory solution.
2	A problem exists, but a remedy may be available.
3	Satisfactory; i.e., within the state of the art.
U	Necessary information upon which to base a judgment was unavailable.
NA	Parameter is not applicable.

The planetary characteristics and mission parameters presented in the chart were considered for mission durations of five to ten years. Missions of five to ten years may be categorized as those in earth orbit such as communications satellites and those intended for planetary exploration such as missions to Jupiter and beyond to the outer planets. Probably the most significant parameter to consider for long term missions are problems relating to the effects of space environment on materials, materials' aging and materials' compatibility with propellants and pressurants.

The ratings depicted on the analysis chart, Table 2-1, were based on the results of survey studies and work performed under this program. The surveys conducted include:

- Agency Interview
- Literature Search
- Propellant Study

A propellant study was performed under this program and is reported in Volume II. Personnel knowledgeable in the valve development and associated technical fields were interviewed for the purpose of establishing the state of the art of valves used in liquid rocket engines and to determine valve problems relating to present valve technology and to establish valve requirements which are applicable in five to ten years.

The agencies contacted during the reporting period were:

Bell Aerosystems, Buffalo, New York
Bendix Research Laboratories, Detroit, Michigan
General Electric Company, Advanced Technology Laboratories,
Schenectady, New York
Hughes Aircraft Company, Los Angeles, California
Hydraulic Research Corporation, Burbank, California
Jet Propulsion Laboratory, Pasadena, California
Marquardt Corporation, Los Angeles, California
McDonnell Douglas Aircraft, St. Louis, Missouri
NASA Goddard Spaceflight Center, Greenbelt, Maryland
NASA Lewis Research Center, Cleveland, Ohio
NASA Manned Spacecraft Center, Houston, Texas
NASA Marshall Spaceflight Center, Huntsville, Alabama
Parker Valve Company, Los Angeles, California
Stanford Research Institute, Palo Alto, California
Sterer Valve Company, Los Angeles, California

FUNCTIONAL PARAMETERS										SPACE ENVIRONMENTAL PARAMETERS									

[illegible]

REFERENCES

1. Harry E. Bailey, Planetary Atmospheres (Mars), NASA SP-3021 (1965).
2. Peter J. Brancagio, Planetary Atmospheres (Gen.), NASA Conference held 1963, Libr. Congress QB 505.B7.
3. Dallas E. Evans, Planetary Atmospheres (Venus and Mars), NASA SP-3016, (1965).
4. Conference on the Science and Technology of Space Exploration, 1962 NASA SP-14, (1963).
5. Joseph H. Jackson, Pictorial Guide to the Planets, T. Y. Crowell Co., New York, 1965.
6. William W. Kellogg and Carl Sagan, The Atmospheres of Mars and Venus, Publication No. 944, 1961, National Academy of Sciences - National Research Council, Washington, D. C.
7. L. R. Koenig, F. W. Murray, C. M. Michaux and H. A. Hyatt, Handbook of the Physical Properties of the Planet Venus, NASA SP-3029, 1967, Washington, D. C.
8. Gerald P. Kuiper, The Atmospheres of Earth and Planets, Chicago, University of Chicago Press 1952, (Presented 1947).
9. C. M. Michaux, Handbook of Physical Properties of the Planet Mars, NASA Washington, D. C., 1967.
10. Patrick Moore, The Planet Venus, The McMillan Company, New York, 3rd Edition, 1960.
11. James Muirden, Stars and Planets, Crowell, New York, 1965.
12. NATO Advanced Study Institute on Planetary and Stellar Magnetism, Edit: W. R. Hindmarsh, New York, American Elsevier Publishing Co., 1967.
13. Planetary Atmospheres (Bibliography and Indexes), NASA SP-7017 (1965).
14. Dr. Werner Sander, The Planet Mercury, Faber and Faber 24 Russel Square, London, England, 1963.
15. Significant Achievements in Planetary Atmospheres, NASA SP-98 (Pub. 1966).
16. Significant Achievements in Planetology, 1958-1964, NASA SP-99 (1966).

17. Significant Achievements in Space Science, NASA SP-136, (1965 pub. 1967).
18. The Earth, The Planets and The Stars: Their Birth and Evolution, New York, MacMillian, 1961.
19. Nicholas A. Weil, Lunar and Planetary Surface Conditions, New York, Academic Press 1965.
20. D. Christensen, Engine Operating Problems in Space - The Space Environment, NASA CR-294, September 1965.

REDUNDANCY STUDY

Introduction

In order to achieve the maximum system reliability, space systems are normally analyzed by combining the success (or failure) probabilities of their components in their appropriate series or parallel operating modes. The required elements are then rearranged and redundancies introduced until the required reliability values are obtained. The analytic method normally used to determine reliability of series, redundant and series-redundant valve arrays is described below. The analysis takes into account the difference which occurs between the fail-open and fail-closed probabilities normally encountered in real valving elements. This gives a better indication of actual system reliability and the most probable overall failure mode.

The objectives of this study are to examine the analytical procedure for determining the application of redundant valving arrangements and to assess their merits in relation to functional parameters and effects on system performance not normally considered in the analysis. A review of the analytical procedures used in determining redundancy requirements is reported. Several functional parameters were considered which are not normally included in the redundancy analysis and which may affect engine performance and valve design.

Redundancy In Valving Arrangements

The reliability of a system may be defined as the probability of its performing properly over the required period of time. Basic system reliabilities may be computed approximately from the individual availabilities of the component parts. However, establishing these individual reliabilities required extensive test data on the components. Even so, the numbers may not apply due to differences in applications. This is particularly true in mechanical systems where in many cases it is difficult or impossible to obtain data on test conditions exactly matching those in the real system. Most system reliability data, therefore, must be obtained by actual system

testing in the use environment in order for it to be reliable itself. Presented below is a discussion of the reliability of various valving arrangements. The approach presented may be used to obtain the reliability of shutoff valve arrangements for which individual valve reliabilities are available. It considers both open and closed failure modes.

The overall reliability of a multi-unit system is normally calculated by applying the well-known additive and multiplicative probability relations to the units with no consideration given to specific modes of failure. The reliability estimated in this manner for a system comprised of a number of interconnected "on-off" devices, such as valves and switches, can be in considerable error since the probability of an "open" failure is not normally the same as for a "closed" failure.

The effects of a different fail "open" as opposed to a fail "closed" probability are relatively simple to account for and this has been done in the discussion below. This gives a more accurate assessment of actual system behavior. The actual system reliability calculated in this manner may be higher or lower than that obtained by assuming equal failure probabilities for closing and opening.

Flow diagrams and the derivations of overall system reliability equations for a number of valve configurations and equations describing series, parallel, series-parallel and quad systems are presented below.

Unit Failure Modes

The probability of success or failure are related by:

$$R = 1 - Q \quad (1)$$

where

R = probability of success

Q = probability of failure

For convenience, the total failure probability Q is divided into two parts so that Equation (1) may be rewritten as:

$$R = 1 - q_a - q_b \quad (2)$$

where

q_a = probability of failure for a valve to open on command

and q_b = probability of failure for a valve to close on command

NOTE: All relationships derived may be applied directly to electric switch systems if the equivalent q_a and q_b definitions are selected.

A General Case

In general, a valve system may be considered as comprised of parallel connections of a number of identical multi-unit series strings as shown in Figure 2-1 below.

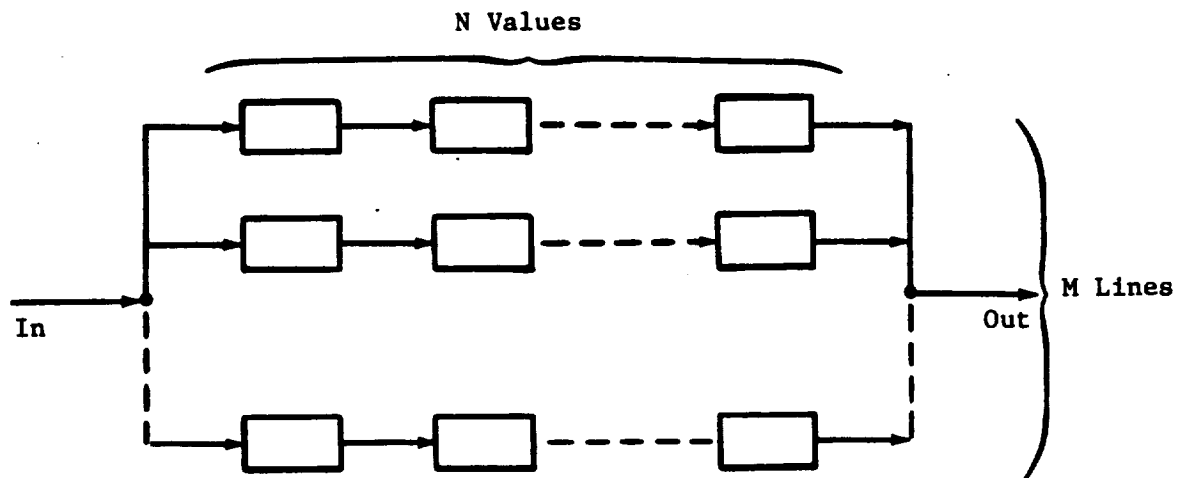


Figure 2-1.

For opening commands, the system is considered to have failed if one or more of the m lines do not allow a flow through. The probabilities are:

$$\begin{aligned} (1 - q_a)^n &= \text{probability all valves in one line open} \\ 1 - (1 - q_a)^n &= \text{probability at least one valve in one line fails to open} \\ [1 - (1 - q_a)^n]^m &= \text{probability at least one valve in each of } m \text{ lines fails to open} \end{aligned} \quad (3)$$

For closing commands, the system is considered to have failed if any one or more of the m lines allows flow to continue. This is represented by:

$$\begin{aligned}
 q_b^n &= \text{probability all valves in one line fail to close} \\
 1 - q_b^n &= \text{probability at least one valve in one line closes} \\
 (1 - q_b^n)^m &= \text{probability at least one valve in all } m \text{ lines closes} \\
 1 - (1 - q_b^n)^m &= \text{probability all valves in at least one line fail to close}
 \end{aligned}
 \tag{4}$$

The overall System Failure Probability Q_s is given by the sum of Equations (3) and (4):

$$Q_s = [1 - (1 - q_a)^n]^m + 1 - (1 - q_b^n)^m \tag{5}$$

and the System Reliability R_s is:

$$R_s = 1 - Q_s = 1 - \{[1 - (1 - q_a)^n]^m + 1 - (1 - q_b^n)^m\} \tag{6}$$

Series Systems

For a dual unit series system such as shown in Figure 2-2, $n = 2$ and $m = 1$.

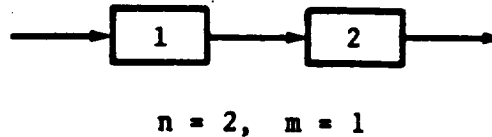


Figure 2-2.

Substituting these values in Equation (6) gives:

$$R_s = 1 - 2q_a + q_a^2 - q_b^2 \tag{7}$$

$$\text{or } R_s = (1 - q_a)^2 - q_b^2 \tag{8}$$

Similarly, for a 3-unit series system, substitution of $n = 3$ and $m = 1$ reduces Equation (6) to:

$$R_s = 1 - 3q_a + 3q_a^2 - q_a^3 - q_b^3 \quad (9)$$

$$\text{or } R_s = (1 - q_a)^3 - q_b^3 \quad (10)$$

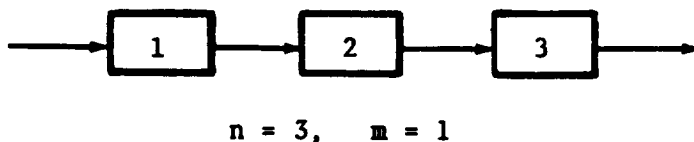


Figure 2-3.

The reliability for a series arrangement of any number of units can now be written as:

$$R_s = (1 - q_a)^n - q_b^n \quad (11)$$

where: n = number of individual units in a single series string ($m = 1$).

Parallel Systems

For a 2-unit system of Figure 2-4, $n = 1$ and $m = 2$. Upon inserting these values, Equation (6) becomes:

$$R_s = 1 - q_a^2 - 2q_b + q_b^2 \quad (12)$$

$$\text{or } R_s = (1 - q_b)^2 - q_a^2 \quad (13)$$

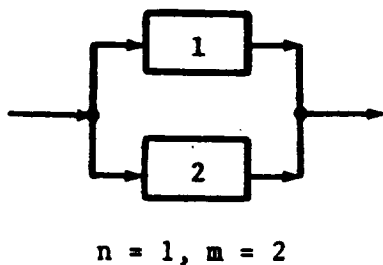
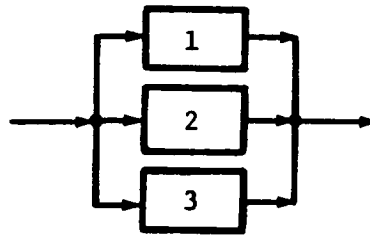


Figure 2-4.

In like manner, $n = 1$ and $m = 3$ for the 3-unit parallel system of Figure 2-5. Substitution of these values in Equation (6) results in:

$$R_s = 1 - q_a^3 - 3q_b + 3q_b^2 - q_b^3 \quad (14)$$

$$\text{or } R_s = (1 - q_b)^3 - q_a^3 \quad (15)$$



$n = 1, m = 3$

Figure 2-5.

A general equation may be written for any number of single units arranged in parallel:

$$R_s = (1 - q_b)^m - q_a^m \quad (16)$$

where: m = number of single units ($n = 1$) in a parallel configuration.

Note that Equations (11) and (16) are of identical form with the failure probabilities q_a and q_b and the constants n and m interchanged.

Series-Parallel System

The reliability of the 3-unit series-parallel system in Figure 2-6 cannot be determined by means of Equation (6). Nor is it permissible to consider the system as one unit in series with two parallel units with the reliability of the latter determined by Equation (6) because the conditions of system success or failure assumed in deriving Equation (6) are not valid here. The reliability equation for the system in Figure 2-6, however, may be determined by inspection. To accomplish this, the probabilities of all the number of various ways the system can fail are first summed. Thus:

$$\begin{aligned} \text{System Failure Probability } Q_s = & q_a^3 + 3q_a^2 (1 - q_a) + q_a (1 - q_a)^2 \\ & + q_b^3 + 2q_b^2 (1 - q_b) \end{aligned} \quad (17)$$

which may be expanded and reduced to:

$$Q_s = q_a + q_a^2 - q_a^3 + 2q_b^2 - q_b^3 \quad (18)$$

and the system reliability then is:

$$R_s = 1 - Q_s = 1 + q_a^3 - q_a^2 - q_a + q_b^3 - 2q_b^2 \quad (19)$$

or rearranged:

$$R_s = (1 - q_a)^2 (1 + q_a) - q_b^2 (2 - q_b) \quad (20)$$

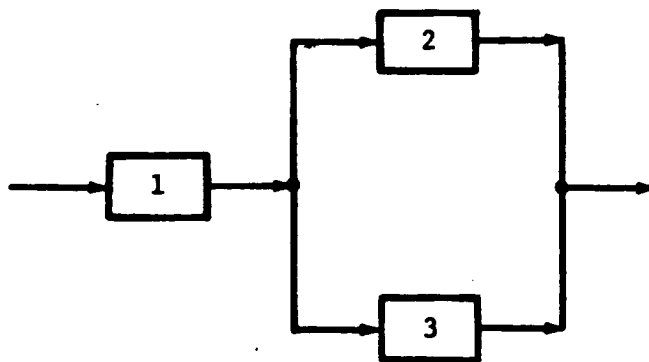


Figure 2-6.

The 4-element system shown in Figure 2-7 may be treated in an identical manner. Thus:

$$\begin{aligned} Q_s = & q_a^4 + 4q_a^3 (1 - q_a) + 6q_a^2 (1 - q_a)^2 + 2q_a (1 - q_a)^3 \\ & + q_b^4 + 2q_b^3 (1 - q_b) \end{aligned} \quad (21)$$

$$Q_s = q_a^4 - 2q_a^3 + 2q_a^2 + 2q_b^3 - q_b^4 \quad (22)$$

$$R_s = 1 - Q_s = 1 - q_a^4 + 2q_a^3 - 2q_a^2 - 2q_b^3 + q_b^4 \quad (23)$$

or rearranged: $R_s = (1 - q_a)^3 (1 + q_a) - q_b^3 (2 - q_b)$ (24)

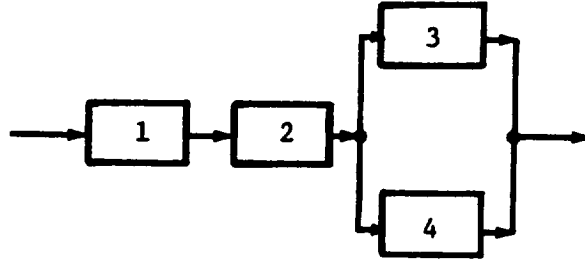


Figure 2-7.

The reliability equation for the system in Figure 2-8 also may be written by inspection:

$$Q_s = q_a^4 + 4q_a^3 (1 - q_a) + 3q_a^2 (1 - q_a)^2 + q_a (1 - q_a)^3 + q_b^4 + 3q_b^3 (1 - q_b) + 3q_b^2 (1 - q_b)^2$$
 (25)

$$Q_s = q_a + q_a^3 - q_a^4 + 3q_b^2 - 3q_b^3 + q_b^4$$
 (26)

$$R_s = 1 - Q_s = 1 - q_a - q_a^3 + q_a^4 - 3q_b^2 + 3q_b^3 - q_b^4$$
 (27)

or by rearranging:

$$R_s = (1 - q_a) (1 - q_a^3) - q_b [1 - (1 - q_b)^3]$$
 (28)

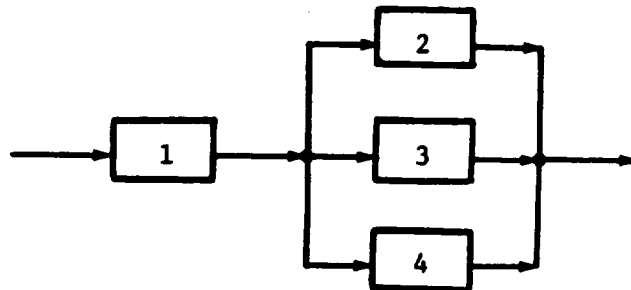


Figure 2-8.

Quad Systems

Quad configuration systems are of two types — the "open" quad shown in Figure 2-9 and the "Bridged" quad of Figure 2-10. While the "open" quad reliability may be ascertained by means of Equation (6) that for the "Bridged" quad cannot. For convenience, therefore, both systems will be analyzed by the previously described inspection method.

By inspection, the system failure probability for Figure 2-9 is:

$$Q_s = q_a^4 + 4q_a^3 (1 - q_a) + 4q_a^2 (1 - q_a)^2 + q_b^4 + 4q_b^3 (1 - q_b) + 2q_b^2 (1 - q_b)^2 \quad (29)$$

$$\text{This reduces to: } Q_s = q_a^4 - 4q_a^3 + 4q_a^2 - q_b^4 + 2q_b^2 \quad (30)$$

and the system reliability is:

$$R_s = 1 - Q_s = 1 - q_a^4 + 4q_a^3 - 4q_a^2 + q_b^4 - 2q_b^2 \quad (31)$$

$$\text{which can be reduced to: } R_s = (1 - q_b^2)^2 - q_a^2 (2 - q_a)^2 \quad (32)$$

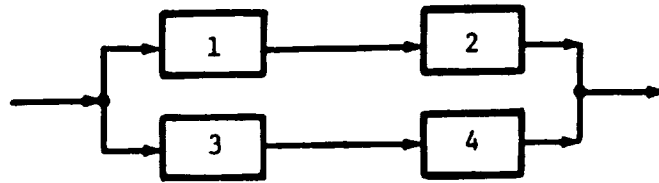


Figure 2-9. "Open" Quad

For the "Bridged" quad of Figure 2-10, the system failure probability is:

$$Q_s = q_a^4 + 4q_a^3 (1 - q_a) + 2q_a^2 (1 - q_a)^2 + q_b^4 + 4q_b^3 (1 - q_b) + 4q_b^2 (1 - q_b)^2 \quad (33)$$

which reduces to:

$$Q_s = 2q_a^2 - q_a^4 + 4q_b^2 - 4q_b^3 + q_b^4 \quad (34)$$

and this corresponds to a system reliability of:

$$R_s = 1 - Q_s = 1 + q_a^4 - 2q_a^2 - q_b^4 + 4q_b^3 - 4q_b^2 \quad (35)$$

which can be rearranged:

$$R_s = (1 - q_a^2)^2 - q_b^2 (2 - q_b)^2 \quad (36)$$

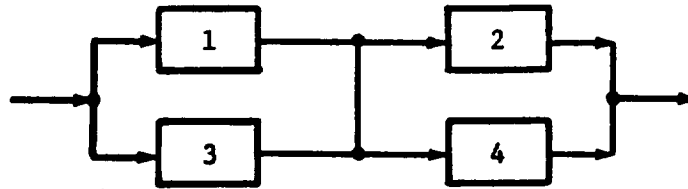


Figure 2-10. "Bridged" Quad

Inspection of Equations (32) and (36) reveals they are of identical form with the failure probabilities q_a and q_b interchanged. This indicates the "open" and "bridged" quads are dual configurations.

It is difficult to get a "feel" for the manner in which valve fail-to-open or fail-to-close probabilities affect the reliability of an over-all system configuration. To illustrate the complex relationships, reliability variations for the valve arrangements shown in Figures 2-2, 2-6, 2-8, 2-9, and 2-10, are plotted in Figures 2-11, 2-12, 2-13, 2-14, and 2-15 respectively. Calculations were made using hypothetical values for the individual valve failure probabilities (q_a and q_b in the appropriate reliability models, namely Equations (8), (20), (28), (32) and (36).

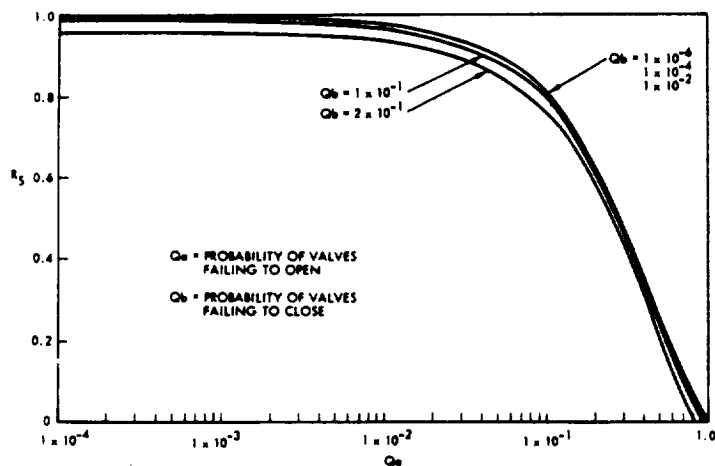


Figure 2-11.

System Reliability vs.
Valve Failure Probabilities

[Figure 2-2 Configuration-Equation (8)]

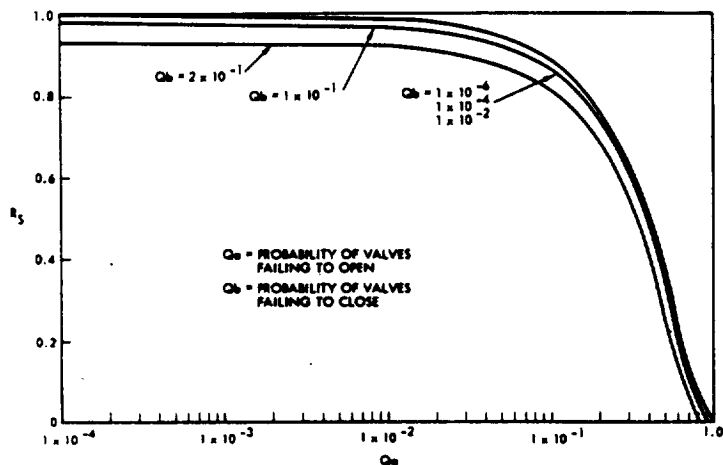


Figure 2-12.

System Reliability vs.
Valve Failure Probabilities

[Figure 2-6 Configuration-Equation (20)]

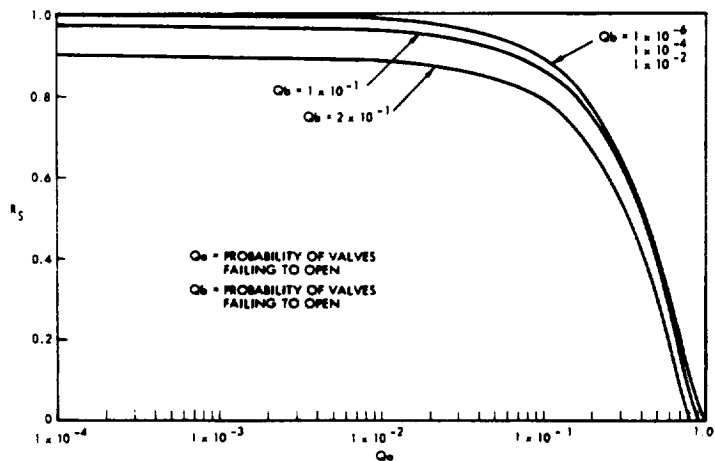


Figure 2-13.

System Reliability vs.
Valve Failure Probabilities

[Figure 2-8 Configuration-Equation (28)]

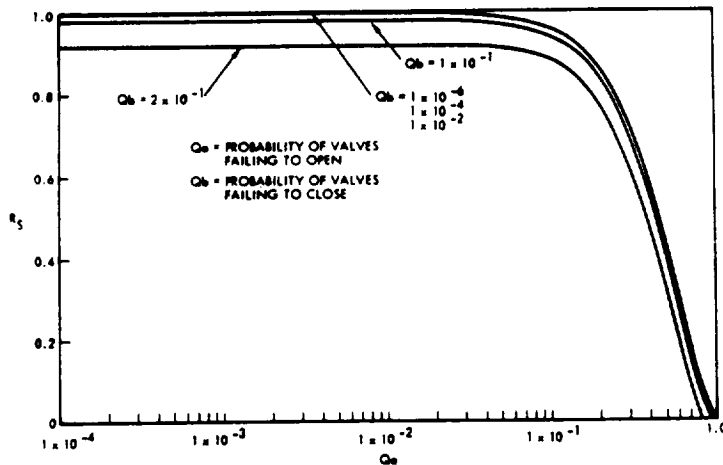


Figure 2-14.

System Reliability vs.
Valve Failure Probabilities

[Figure 2-9 Configuration-Equation (32)]

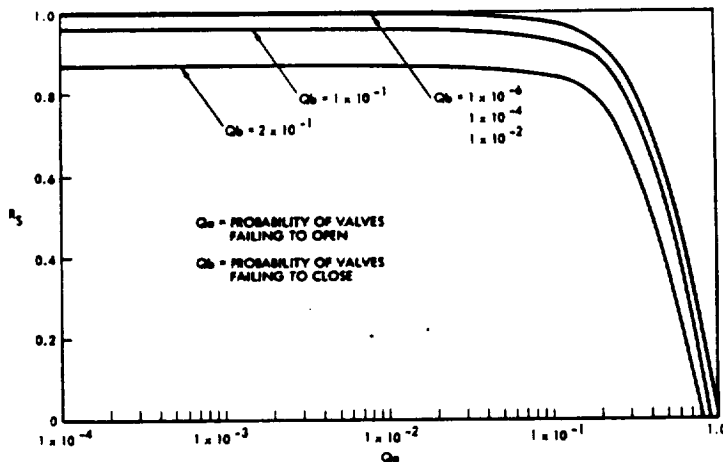


Figure 2-15.

System Reliability vs.
Valve Failure Probabilities

[Figure 2-10 Configuration-Equation (36)]

In all cases it is seen that if valve failure probabilities are low, there is relatively little effect upon system reliability. However, as failure probabilities increase, the reliability falls, giving a pronounced "knee" to each curve. Although these graphs were drawn with valve fail-to-open probabilities (q_a) as abscissae, similarly shaped curves (but not the same absolute values) would be obtained with values of the fail-to-close probabilities (q_b) as one coordinate.

It should be noted that the system choice for the two quad arrangements of Figures 2-9 and 2-10 would depend upon whether a closed or open failure is more critical in terms of mission effect, and which of these is more probable. From Equations (32) and (36) it is seen that the reliability for

each is the same if failure probabilities q_a and q_b are equal. This is not normally the case. Of special interest then are the curves of Figures 2-14 and 2-15. At the knees of the curves it can be seen that the "open" quad of Figure 2-9 has higher reliability if the fail-to-close failure probability q_b is predominant; whereas the "bridged" quad of Figure 2-10 exhibits better reliability if the fail-to-open failure probability q_a is of larger magnitude.

Unit Failure Probabilities

It should be noted the unit failure mode probabilities q_a and q_b used in the preceding paragraphs are not considered as functions of operating time. Involvement of time would have necessitated use of joint probability distributions at the expense of a very considerable increase in complexity.

The reliability equations given, however, may be viewed as the expressions for system reliability for exactly one open-close operating cycle. Failure probability per cycle for on-off devices, such as switches, relays and valves may be calculated from test and field data.

For any system operating time profile, if the number of required operation cycles is known or can be estimated, the system reliability for a complete mission is simply:

$$R_S (\text{mission}) = \left[R_s (\text{one cycle}) \right]^N \quad (37)$$

where: N = required number of complete on-off operating cycles in the mission.

Limitations in Redundancy Analysis

The preceding reliability analysis represents the standard approach to defining redundant systems based on probability of success or failure. However, several factors have been ignored which can affect the designer's approach to redundant systems. These factors, for example, include system effects such as pressure drop variations, depending on which valves in the arrangement are operating, and effects of qualification testing such as leakage measurement of the upstream valve seat in a series arrangement. These factors are problems which may be solved by adding additional complexity to the valve, impairing its reliability. A quad redundant shut-off

valve arrangement for example, requires consideration of a complex actuator which may reduce the overall reliability of the system. The counteracting effects of added valve elements are the added weight and complexity which are not represented in redundant analysis.

The changes in major parameters affected by introducing redundant valving arrangements into the system are presented in Table 2-2 below.

TABLE 2-2.

	INCREASED	DECREASED
Effects of Redundancy on:		
Size	✓	
Weight	✓	
Pressure Drop	✓	
Service Required	✓	
Test Time	✓	
Power Consumption	✓	
Cost	✓	
Complexity	✓	
Performance		✓
Space Maintenance		✓

The effects of redundancy on the parameters shown in the above table indicate that reliability should be obtained through basic simplicity of design and function rather than through use of redundant systems, as a matter of course.

If an unmanned mission is involved, the cost effectiveness of the overall program might be better served through the use of redundancy of the overall spacecraft in some cases. The costs involved in added valve weight must be evaluated on the basis of cost of payload and in many cases abbreviated mission capabilities.

In addition to the factors noted above, the relative effectiveness of different redundant systems must be compared. Since reliability criteria is black or white, "failed" or "not failed", the effects of partial failures may not be handled by standard reliability techniques. In redundant systems, or in systems consisting of a number of interconnected elements, there may be significant differences in system performance due to partial system failure, such as the effects of system performance due to a change in pressure drop. The effects may be taken into account by relating to a failure mode or indicate the need for a reliability figure of merit. If a value is assigned to each failed state, then a reliability figure of merit might be used as proposed in Reference 1. That is:

$$V(t) = \sum_{\substack{\text{all} \\ \text{states}}} P(S_i, t) V(S_i, t) P \quad (1)$$

or the expected value (V) at any time (or after any number or cycles) t is the value (V) of the i^{th} state (S) at time t , multiplied by the probability (P) of being in the i^{th} state at time t , and summed over all noneligible states. Equation (1) holds for a time period $t + \Delta t$ where Δt is small. The accrued value is normally of more interest, say over a mission time of 0 to t (or over same number of cycles from 0 to N). The averaged value over the interval may then be stated as

$$\bar{V}(\tau) = \frac{1}{\tau} \int_0^t V(t) dt \quad (2)$$

Equation (2) is a figure of merit expression for accrued value obtained by integrating equation (1) over a time period from 0 to t (or 0- N in the cyclic case).

Equations (1) and (2) may then be used in conjunction with basic reliability data to choose the more reliable system. However, the relative values of the failed states must still be assigned. All critical system

performance parameters must be considered, and an itemization of the effects on system performance are required. The assessment will in some cases be somewhat arbitrary.

The examination of the reliability/redundancy area indicates a definite need for new systemized techniques for evaluating the optimum system in terms of over-all system objectives. In order to attain this, a methodology placing values on items such as size, weight, power, etc., must be developed. At present this seems to fit best in the area of the systems engineer and analyst where studies including all pertinent factors may be included and traded off against one another to optimize over-all system performance. The studies would give results for use in component specifications or requirements to guide the component designer.

REFERENCES

1. Captain E. L. Battle, Basic Reliability Concepts, Air University Quarterly Review.
2. P. A. Hiltz and R. T. Burks, Fundamentals of Reliability Mathematics, North American Space and Information Systems Division, Publ 542-D, new 11/62.
3. Donald E. Johnson and Duane T. McRuer, A Summary of Component Failure Rate and Weighing Function Data and Their Use in System Preliminary Design, WADC Technical Report 57-668, ASMA Document No. AD-142120.
4. Morris I. Kaufmann and Roger A. Kaufman, Predicting Reliability, Machine Design, August 1960.
5. R. E. Lovejoy, TRW Systems Interoffice Correspondence, 67-4002.1-031, Reliability Estimation for Systems Involving Open-Closed Failure Modes.
6. Manned Space Reliability Symposium, Proceedings of a Symposium Sponsored by the American Astronautical Society at Anaheim, California, 9 June 1964.
7. R. M. McClung, First Aid for Pet Projects Injured in the Lab or on The Range or What to do Until the Statistician Comes, NOTS Tech Memo No. 113, Naval Ordnance Test Station, China Lake, California.
8. G. E. Neuner, TRW Systems Interoffice Correspondence 63-9701.3-75, LEMDE Reliability Reports for September.
9. Reliability Training Test, Second Edition, Institute of Radio Engineers, 1960.
10. Clifford M. Ryerson, Simplified Reliability Mathematics and Statistics, Space/Aeronautics, December 1961.
11. E. J. Tangerman, A Manual of Reliability, Product Engineering, May 16, 1960, (McGraw-Hill Publishing Co., Inc.).
12. Jerome Toffler, System Reliability, Electronic Industries, July 1959.

DIAPHRAGM VALVE

Conceptual studies are an important part of the objectives of this program. Bipropellant valves capable of flow control and shutoff, high response, having no sliding surfaces, and requiring cavitation for the throttling function are established requirements. A semitoroidal diaphragm cavitating valve designed to meet these requirements was reported in the Advanced Valve Technology Interim Report 06641-6004-R000, November 1966.

Conceptual development of throttling and pulsing propellant valves has continued. The preliminary design of a throttling valve incorporating a diaphragm closure is presented in Figure 2-16 below. The valve has no sliding parts. One metal diaphragm is used as the control element and to effect a seal in the shutoff condition. This feature is utilized to design a very compact single or dual propellant valve.

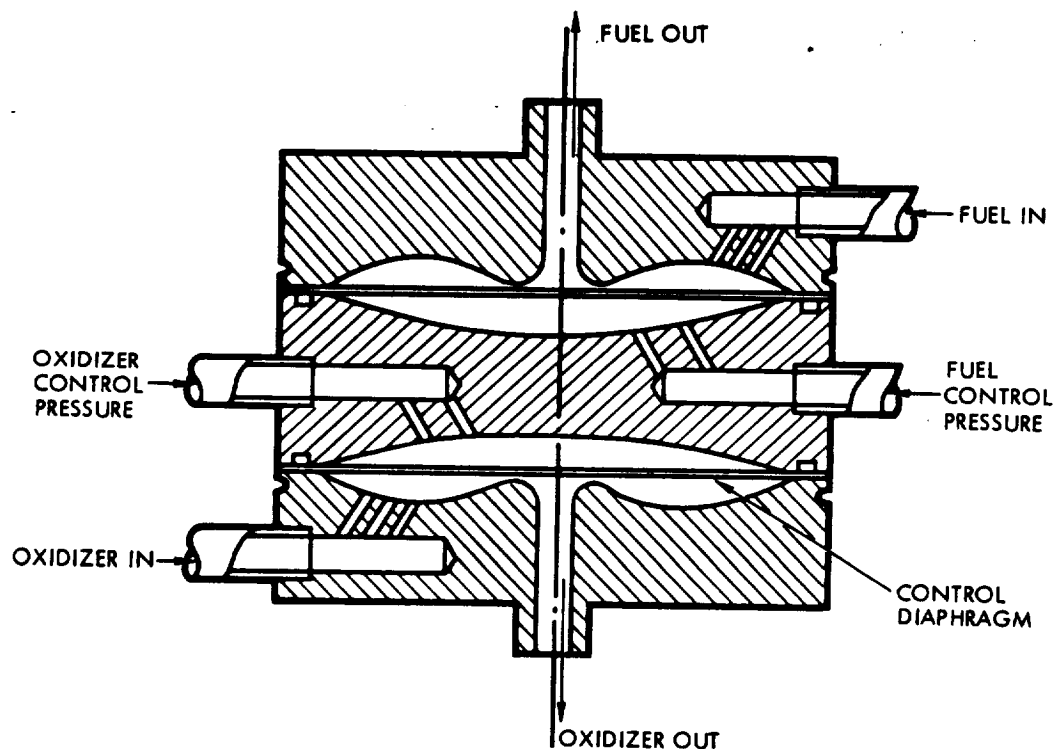


Figure 2-16. Diaphragm Valve

The valve can be used for throttling and flow shutoff in conjunction with fluidic or conventional piloting methods. Diaphragm mass is extremely low, allowing high response in pulsing applications. The control diaphragms can be welded to the seal plates resulting in a hermetically sealed valve design. Only the metal diaphragm and seal plate are exposed to the flow, minimizing materials compatibility problems. With proper material choice the valve may be used from cryogenic to elevated temperature services. Leakage should be comparable to lapped metal-to-metal seal valves. Improved leakage characteristics may be obtained through polymeric coatings on the diaphragm and/or the seal plate.

The valve operation is described for the oxidizer side; the fuel side operation is identical. The oxidizer flows in through the inlet port and, with control pressure off, deflects the diaphragm upward allowing free flow through the outlet port. When reduced flow is required, pressure is applied to the control port, deflecting the diaphragm toward the seal plate reducing flow. The seal plate may be shaped to allow cavitation. When complete shutoff is required the pressure at the control port is raised so that the diaphragm is firmly pressed against the seal plate, thus sealing the outlet port.

Analysis has shown that a valve with a 2-inch diameter diaphragm could operate with a full stroke of .012 inch without overstressing the diaphragm based on a fatigue life of over a million cycles. If the seat diameter is 0.125 inch the flow area is $4.72 \times 10^{-3} \text{ in}^2$ or equivalent to a .078 diameter hole. The seat diameter may be increased further without hindering valve action. It is felt that equivalent orifice in excess of 0.093 diameter using a 2-inch diaphragm is entirely possible.

The valving arrangement described has advantages in single as well as bipropellant applications. Its shape makes it attractive for use as a "built in" propellant valve, where it could form part of the propellant tank or engine structure. This would reduce weight and minimize injector dribble volume. A model to demonstrate feasibility of this concept should be considered.

ELECTROFLUID CONTROLS

The use of direct electrofluid interaction was investigated to determine its potential in applications to a valve with no moving parts. Various mechanisms of electrofluid interaction have been examined and some testing performed.

Interactions between liquids and electrical fields usually are considered to be electrostatic phenomena. This terminology, with respect to liquids, loosely connects phenomena concerned with the deformation or physical change of the fluid by an electric field. The deformation primarily occurs because one or more of the following phenomena takes place: direct ionization or conduction charging of the fluid or one of its components, interaction due to the differential dielectric constants of the fluid constituents, or interaction due to the induced polarization of one or more of the molecular species of the material. In addition, there are also conditions wherein an electric field is produced by the movement of the fluid. Presence of ionizing radiation and impurities in the liquids complicates the understanding of the phenomena occurring, and it is sometimes difficult to determine the exact interaction process.

It must be emphasized that the categorization of the various phenomena as presented here has been somewhat arbitrary. Since the usage of the terms in the past has been applied to a number of quite different liquids, and in view of the disagreements among investigators, it was felt that the following characterization would prove useful.

The general types of fluids have been utilized in studying these interactions: "pure" liquids (in that the impurity content is minimized as much as possible), regular solutions where the solute is evenly distributed in the solvent, and liquid systems containing dispersed particles, such as colloids, charged particles, or "cybotatic regions" (Reference 1). A more detailed discussion concerning these systems follows.

Pure Liquids

There are three main effects that are observed when a pure liquid interacts with an electrical field:

- Electroendosmosis, which is the movement of the liquid through a membrane or capillary when a charged surface is fixed (Reference 2)
- Streaming potentials, produced by a movement of a liquid relative to a solid surface (Reference 2)
- Electrostriction, which is the compression of a dielectric liquid due to the anisotropy of the interacting electric field (Reference 3)

Some investigators also include electrophoretic and dielectrophoretic effects in the behavior of pure liquids with electric fields. However, these two effects depend on the injection or presence of charged particles such as electrons in the liquid, or else the presence of a differential dielectric, such as liquid and vapor forms of the same molecule, and as such more properly belong in the third liquid category.

Of the three effects, electrostriction gives the strongest interaction between the liquid and an electric field. Schatt and Kaghan (Reference 3) tested various pure liquids (some were molten polymers) to determine the influence of viscosity and dielectric constant on electrostriction.

It was found that by introducing a liquid between two steel disc electrodes of different size, a column of the liquid would rise above the bulk liquid level when a high dc voltage was applied. The conclusions were as follows: (a) viscosity was unimportant, with the maximum rise being highest (2.3 cm) for the liquids having the highest dielectric constants and polarizabilities and lowest (1.0 cm) for those having the smallest values, (b) the electrostriction was producing the effect rather than electrophoresis or dielectrophoresis since uncharged or charged particles were immobilized in the viscous

polymers, and reversing the dc field gave the same result, (c) by raising the voltage above a critical point, the liquids could be made to pulsate, form a disruptive spray, or in the case of the polymers, to be repulsed by the electrode, (d) high frequency ac fields produced no effect. Thus, the ability of the molecules to be polarized is of major importance. The necessity of having a non-uniform field was demonstrated by the failure of the normal approximations to the classical equations to predict such large rises, since these approximations assume infinite electrodes with no fringe effects. This point is brought out by Felici (Reference 4) on the use of formulae in electrostatic generators. Laplace's equation is replaced by a quadratic of the third or fourth order (depending on diffusion effects) which necessitates the use of modern analysis and computers in order to be solved. Since there has been little incentive to solve these types of equations, in terms of a practical application, little work has been done in this field. It should be pointed out that this deficiency is evident in the analysis of almost all of the areas of liquid-electric field effects, and is further complicated in that many of the more interesting fluids possess non-Newtonian flow characteristics with attendant non-linear behavior.

Regular Solutions

The effects produced on regular solutions are complicated to an extent by the limitations imposed due to their electrical conductivity. If one of the electrodes can be electrically separated by a dielectric such as a glass partition, then the solutions should behave as pure liquids. In addition, two other effects may take place:

- Electrocapillarity, in which the surface tension of a metal in contact with a conducting solution is changed by polarization of the metal (Reference 2)
- Electrophoresis, where migration of the solute occurs due to the presence of an electric field (Reference 3)

The surface tension of a metal can be appreciably varied by use of suitable electrolytic solutions. For example, the surface tension of a mercury

electrode has been shown to increase as much as 20 percent in some electrolytes (Reference 2).

As mentioned previously, electrophoretic phenomena is more properly associated with the third class of liquids; however, by the use of a suitable support media such as chromatographic paper, migration of the solute can be made to occur.

Liquids Containing Dispersed Particles

This class of liquids has probably been the subject of the majority of the investigations of liquid-electric field phenomena. Most of the practical applications of electrostatic engineering have arisen from the use of these types of fluids, and the bulk of future applications will probably arise from these types of materials, and the pure liquids.

With the exception of electrocapillarity effects, all of the above phenomena also occur with these fluids, and the following additional effects are applicable:

- Cataphoresis in which an applied electric field causes movement of charged particles (Reference 2)
- Potential differences arising from the movement of charged particles in liquid (Reference 2)
- Dielectrophoresis, in which an anisotropic electric field causes a material in the liquid, possessing a higher dielectric constant than the liquid, to move to the region of greatest flux (Reference 5)
- Electroviscosity, in which a fluid becomes rigid upon application of an electric field (References 1 and 2)

Cataphoresis, dielectrophoresis, and electroviscosity effects give the strongest interaction between liquids and electric fields.

Cataphoresis effects have been applied to a number of engineering applications, such as electrostatic coating, and have been proposed for use as dielectric pumps (Reference 6).

Dielectrophoresis has also been utilized in a number of applications of which separation and heat transfer enhancement are probably the most important examples (Reference 7).

Electroviscosity, although theoretically proposed in 1916 (Reference 2), and demonstrated in 1939 (Reference 1), has only recently had practical application (References 8 and 9). The effect is now used to make clutches which are electrical analogs of the magnetic fluid clutch. In this case, application of an electric field across two metal discs separated by a fluid "freezes" the fluid and allows mechanical power to be transferred from one disc to the other.

There is one other phenomena which appears to be associated with the effects discussed above, but not enough information is available for assessment. This is the effect produced on suspended particles, both living and non-living, when they are subjected to a radiofrequency field (Reference 10). In this case, small particles such as polystyrene, carbon black, and one-celled organisms, suspended in a liquid medium, aligned themselves along the electrical lines of force when a uniform, pulsed RF field was turned on, yet gave random arrangements when the field was off. The field was pulsed in order to avoid thermal effects. Moreover, the alignment appears to be frequency dependent. Electrophoretic migration of polystyrene latex was also found to be frequency dependent, with a reduction in mobility occurring at specific frequencies, depending on a number of parameters.

Applications

Examination of the various types of interactions of electric fields with liquids, as presented above, shows that there are a number of potentially useful effects for use in fluid control devices. Since the fluids of

interest range from pure liquids to those containing particulate matter, however, one single type of interaction probably would not suffice for all of them. In particular, electroendosmosis, electrostriction, electrocapillarity and electroviscosity effects would appear to have the greatest potential for fluid control. Investigation of the physical limitations (e.g., voltage, electrode configurations and spacings, etc.) of proposed control devices would be necessary since most of the effects have been examined from the standpoint of the phenomenon itself and not from the viewpoint of practical application. An outline of such an investigation is given in the following:

1) Determination of the Electrical Properties of the Fluids of Interest

This portion of the investigation is concerned with characterizing the liquids now being utilized in spacecraft engines. In most cases, the electrical conductivity, voltage breakdown conditions, and behavior in intense electrical fields are not known for the liquids. These characteristics, then, should be obtained so that the proper interaction can be utilized.

2) Parametric Investigation of the Physical Limitations of Prototype Control Devices

Most of the interactions have not been investigated under varying conditions. Evaluation of the parameters which produce the interaction should be performed. As an example, if electroendosmosis is to be considered, the capillary size, voltage and fluid conductivity limits, and system pressurization requirements would have to be determined. These tests would be run with fluids simulating actual liquids of interest.

3) Simulated Usage Tests Under Operational Conditions

This portion of the investigation would be concerned with the design and fabrication of a fluid control device which would simulate control devices now in operational use. Information derived from the first two parts of the program will enable a choice to be made of the type of fluid to be

controlled, and in what manner. By using the design specifications of devices now in use, a control unit based on electrical field interaction would be fabricated and tested under simulated operational conditions. In this manner a comparison of operational characteristics and an evaluation of the potential usefulness of such a device could be made.

Electric Field Interaction Tests

A test apparatus was constructed to investigate experimentally the effect of electrical fields on simulated propellants. This apparatus is schematically illustrated in Figures 2-17 and 2-18. Although simulated propellants were the guidelines utilized in the construction of the apparatus, it was felt that an initial experiment with a real propellant would give meaningful preliminary information on the technical approach to utilize in this investigation. Accordingly, N_2O_4 (MSC-PPD-2) was selected as the propellant to test initially.

N_2O_4 , flowing under gravity feed, was passed through the test section at varying voltage settings. Interaction of the N_2O_4 with the relatively intense, asymmetric ac electric field was noted. Agitation and disruption of the normal flow pattern was noted at all voltages from approximately five KV upward. Flow was either stopped, or considerably reduced, at 12 KV for two runs made at this voltage setting, and normal flow was resumed when the voltage was turned off. The uncertainty of the extent of flow reduction is due to the low pressures involved in the runs, which allowed some N_2O_4 to back up from the receiver, and to leakage of N_2O_4 past the outer electrode. The results are sufficiently encouraging, however, that the fabrication of an apparatus capable of handling N_2O_4 under more typical operating conditions is being considered.

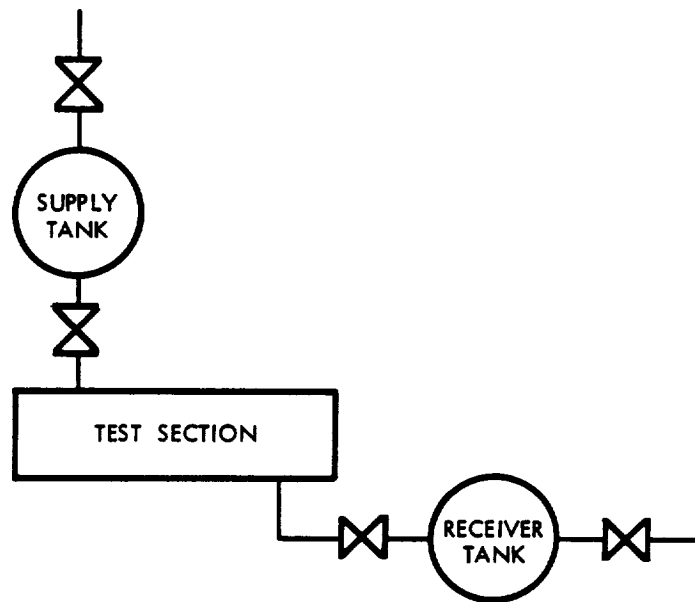


Figure 2-17. Schematic: Apparatus Utilized in Examination of Electro-Fluid Interactions

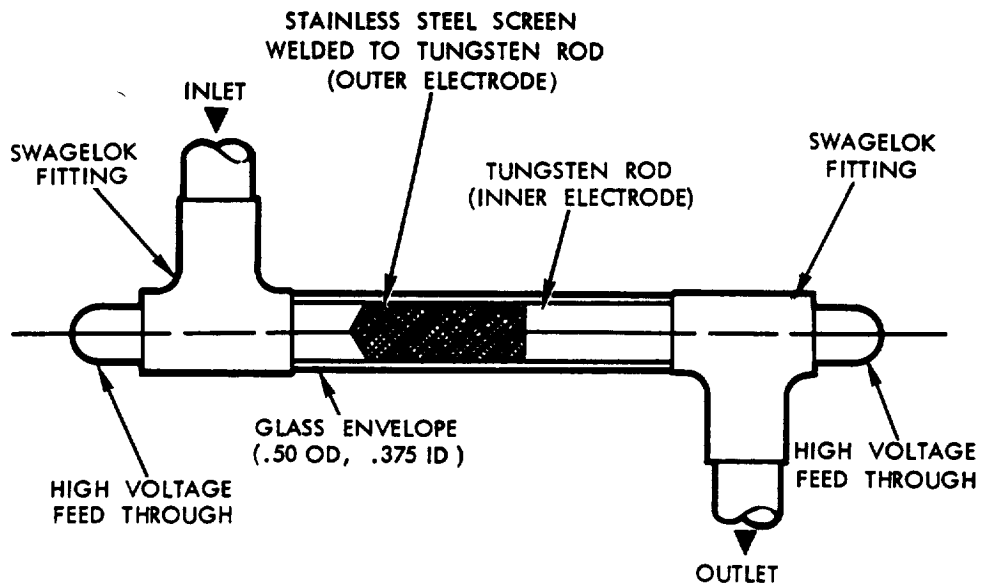


Figure 2-18. Schematic: Illustration of Test Section

REFERENCES

1. Anonymous, Electro-Technology, September 1966.
2. P. Auer and A. Sharbaugh, General Electric Review, Page 37, July 1958.
3. J. Butler, Electrocapillarity, Chemical Publishing Company, Inc., New York, N. Y., 1940.
4. N. Felici, Contemporary Physics, Volume 5, 377 (Part I) and 419 (Part II), 1954.
5. J. Freeborn, IEEE Student Journal, Page 3, July 1964.
6. J. Frenkel, Kinetic Theory of Liquids, Dover Publications, New York, N. Y., 1955.
7. H. Pohl, Journal of Applied Physics, 29, 1182, 1958.
8. H. Schatt, and W. Kaghan, Journal of Applied Physics, 36, 3399, 1965.
9. W. Tucker, Machine Design, Page E-2, January 5, 1967.
10. R. Williams, International Science and Technology, Page 38, January 1967.

ELECTROSEAL CONCEPT

In order to obtain a zero leakage valve, the poppet and seat must be in intimate contact so that all the surface asperities forming passages between them are filled. A method of eliminating these leak paths is to coat the interface of the seal and poppet with some material impervious to the fluid to be sealed. A schematic representation of a valve utilizing this technique is shown in Figure 2-19. To effect a zero leakage seal the valve is closed and a coating of some material, such as copper, gold, etc., is electroplated across the interface between the seat and poppet. To open the valve the material may be plated back onto the source electrode or the joint may be broken open by the valve actuation.

The electroseal concept can be utilized in the design of a no moving parts valve, (see Figure 2-20). In this valve, a porous plug, screen, or any system of fine passages is placed in the flow stream. When valve closure is required, material is electroplated over the plug, shutting off the flow. Valve opening is obtained by plating the material back onto the source electrode. This technique may also be used to throttle flow.

An electrolyte is required in the plating process. Preliminary investigations indicate that some currently used propellants contain enough water to act as effective electrolytes. Experimental verification of the use of propellants as electrolytes in the plating process is required. In certain systems where the propellant is not a suitable electrolyte, an additional electrolyte might be required.

The introduction of an electrical potential into the fluid lines could possibly cause long term corrosion problems. These must also be investigated and control measures instituted if required.

The use of chemical deposition might also be possible as an alternate sealing technique. This would be particularly applicable to one shot systems.

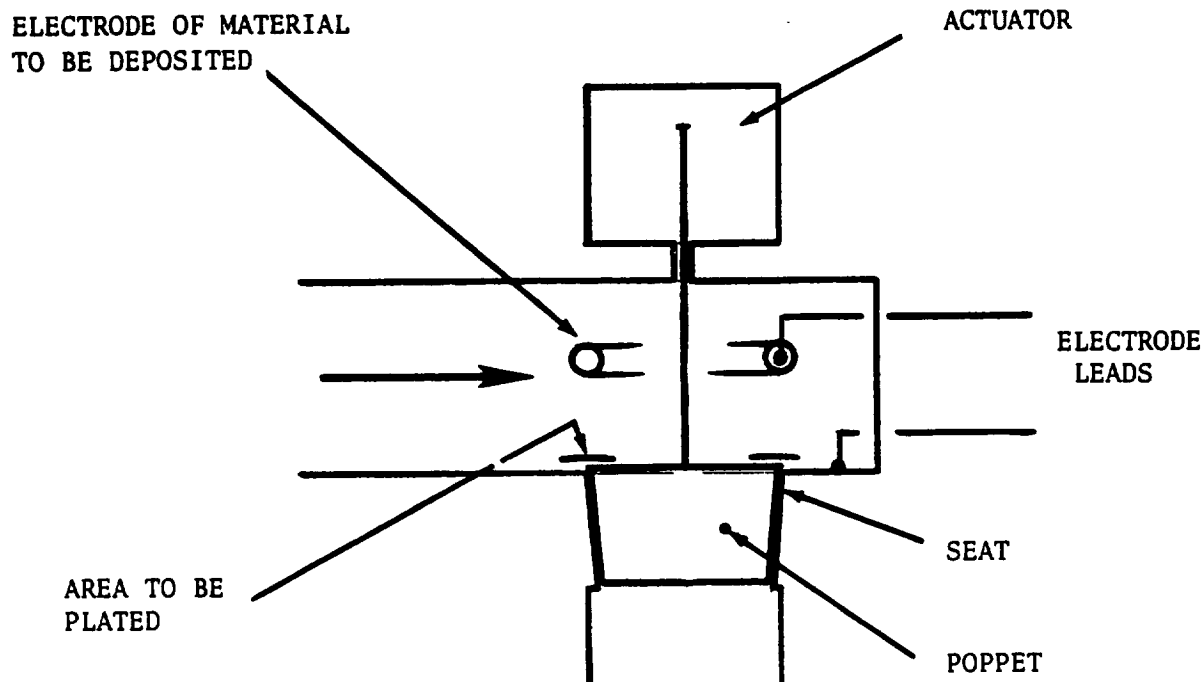


Figure 2-19. Schematic: Electroseat Moving Parts Type Valve Concept

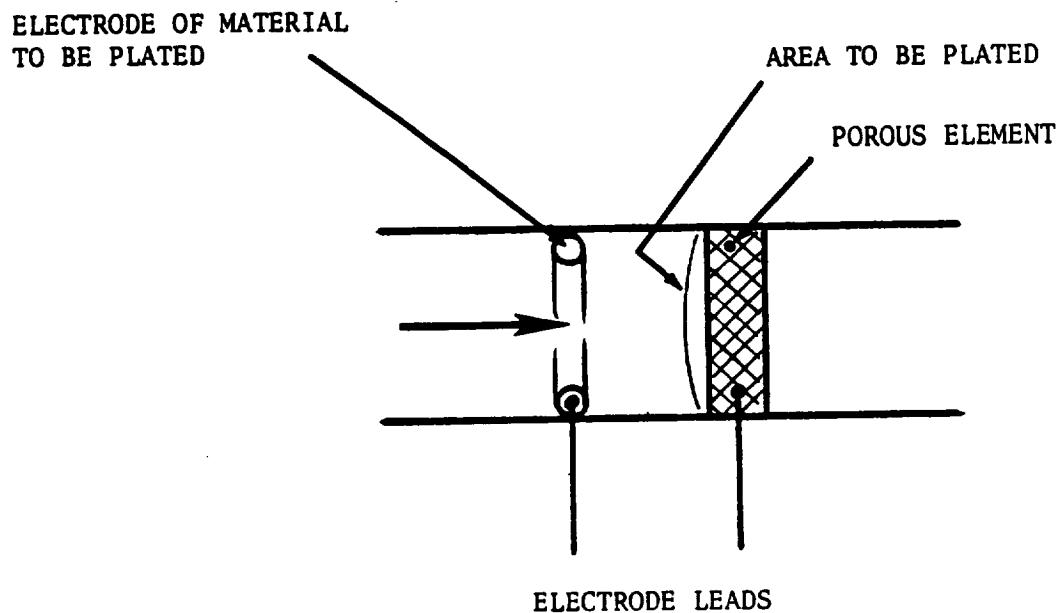
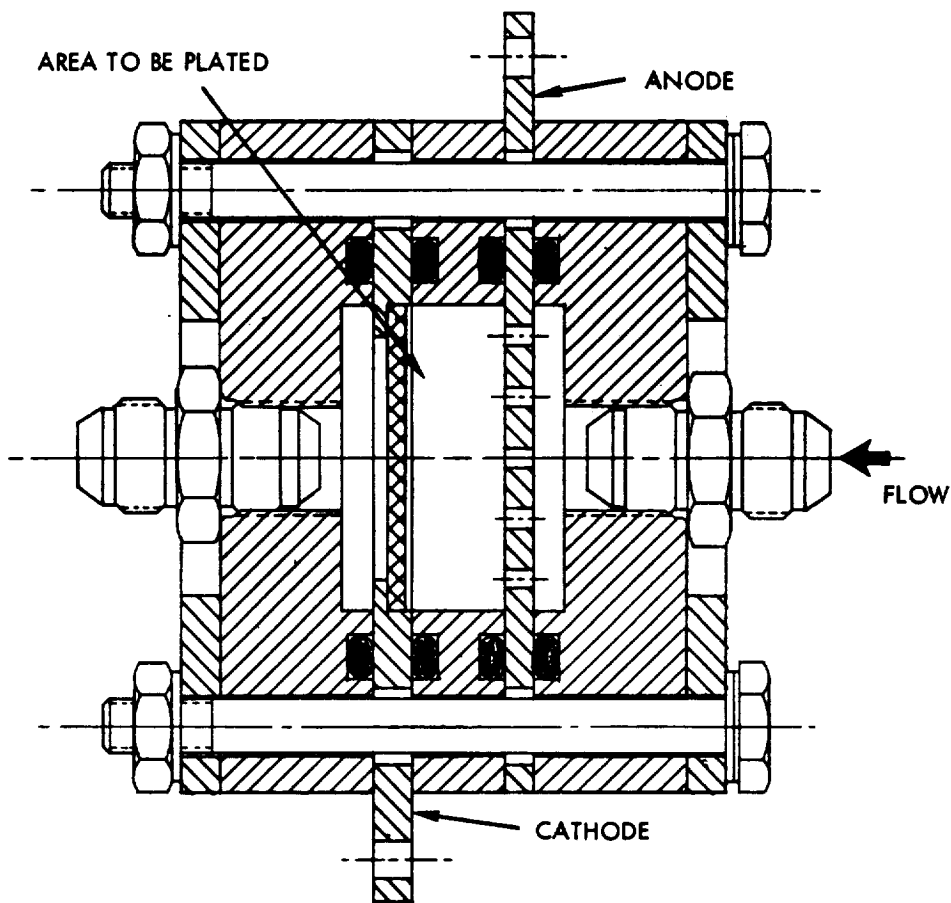


Figure 2-20. Schematic: Electroseat Non-Moving Parts Type Valve Concept

Test Program

A no moving parts electroseal valve as described above was fabricated and tested. It consisted of a copper cathode and stainless steel anode. The anode was a porous stainless steel plug, the cathode had several drilled holes to allow flow of the solution. A cross-sectional view of the no moving parts electroseal valve built and tested is shown in Figure 2-21. The cathode and anode were insulated from one another by a Lucite plate. Lucite plates were also used for the end pieces in order to eliminate short circuits through the bolts holding the unit together. A photograph, Figure 2-22, shows an external view of the actual electroseal unit.



CROSS SECTION - ELECTROLYTIC NO MOVING PARTS VALVE

Figure 2-21. Cross Section - Electrolytic No Moving Parts Valve

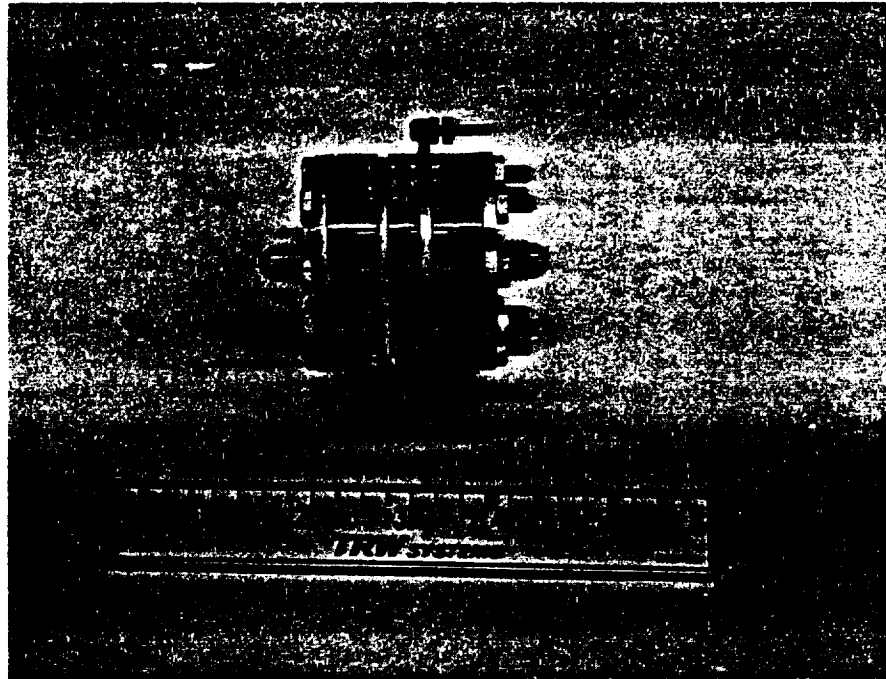


Figure 2-22.

Feasibility Model - Electrolytic
No Moving Parts Flow Control and Shutoff Valve

Electrolytic
No Moving Parts Type

- Reliable
- Flow Control
- Complete Shutoff
- All Metal Seal

Electroreel
Moving Parts Type

- Quick Response
- Zero Leakage
- All Metal Seal

In order to test the feasibility of the concept it was decided to attempt operating the unit in a copper sulphate solution with approximately 5 percent sulphuric acid added. In actual practice propellants such as hydrazine could probably provide an effective electrolyte for the plating operation. The test setup consisted of a pump, flow meter, throttling valve, and electroseal valve and a fluid catch tank for the solution. It is shown schematically in Figure 2-23.

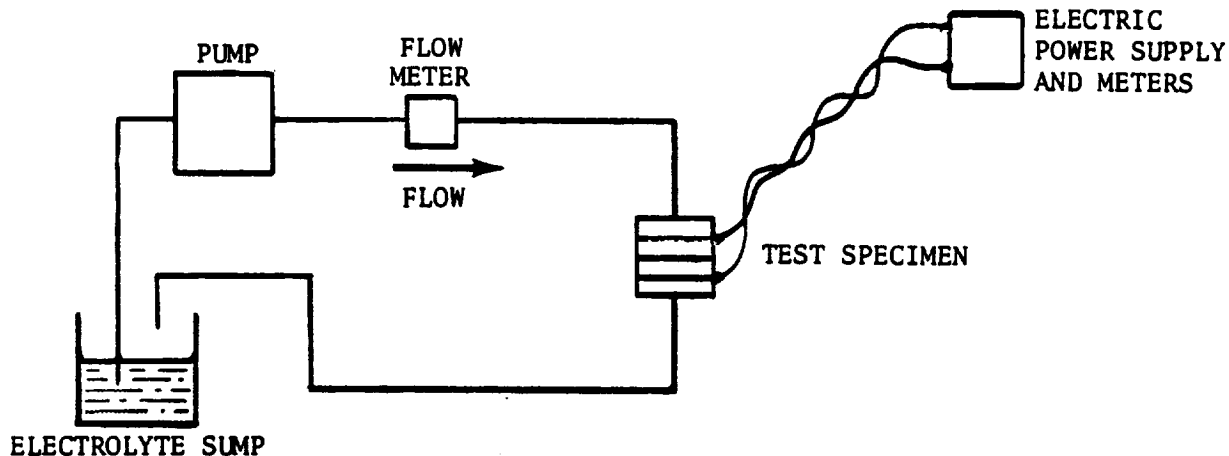


Figure 2-23. Schematic: Electrodeal Test Setup

It was originally planned to observe the flow decay utilizing the flow meter. However, the flow meter malfunctioned shortly after the beginning of the test and all flow observations were made visually at the exit tube from the electroseal valve for a period of approximately 2 hours utilizing the copper plate as the cathode and the stainless steel screen as the anode as stated above. The initial flow through the electroseal valve was greater than 1000 cc's per minute and at the end of the 2-hour test had been reduced to approximately 1-1/2 cc's per minute. The valve at this point was left to sit overnight in the solution. In the morning some added power was applied; however, the growth of copper crystals was observed within the unit. The unit was therefore disassembled and examined. Photographs of the disassembled unit are presented in Figure 2-24. Some copper crystals were deposited on the stainless steel anode to a height that could contact the copper cathode. This was probably a result of the use of an essentially saturated solution of copper sulphate and the acid balance which renders an extremely effective plating solution.

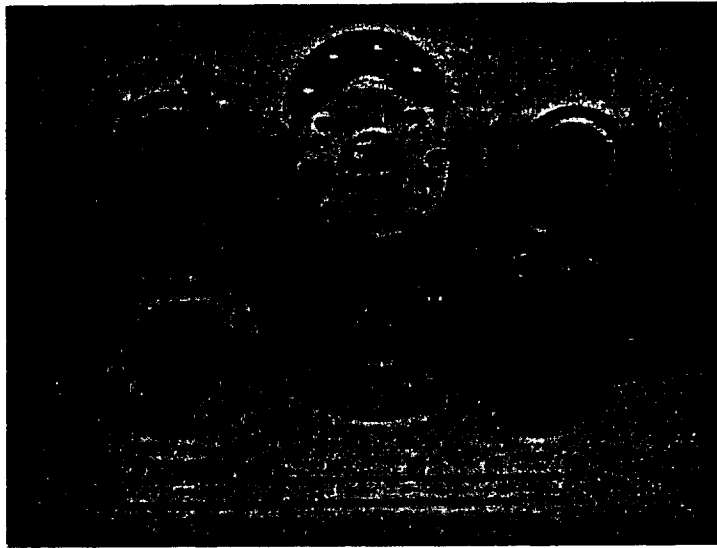


Figure 2-24: Electrovalve Disassembled After Closure

After examination, the loose crystals were removed, the unit reassembled and flow started once again. The flow was unchanged from before unit disassembly which indicated that actually an excess of power had been used. The polarity on the plates was reversed, making the stainless steel, porous member the anode and the copper plate the cathode. The unit was operated in this mode for a period of approximately 3 hours with a steadily increasing flow as the copper was plated back on to the copper plate from the stainless steel anode.

While this test did not shut off the flow completely and has indicated several potential development problems, it is felt that it has demonstrated the feasibility of the electroseal concept and certainly further development work is warranted. The quantity of copper which must be deposited to reinforce the sealing of a moving parts electroseal valve with a conventional poppet is considerably less than that required for a no moving parts design. Such a unit might be extremely useful where tight shutoff for long periods of time is required. Capability of bridging the gap between the poppet and seat by plating remains to be demonstrated.

SURFACE TENSION CONCEPTUAL STUDIES

The objectives of this program are to gain a better understanding of surface tension and the part it plays in fluid component function and leakage. The application of known surface tension effects to valve design results in several new concepts which are applicable to spacecraft valving. Results of a literature search analysis and test program on the effects of surface tension on seal technology are presented.

LITERATURE SEARCH

A literature search was conducted to obtain data on contact angle of various liquids on materials such as fluorinated polymers, paraffin, polyethylene, and others. These polymers were considered to be typical of the materials that might be employed in surface tension seals. Data relating the cosine of the contact angle, θ , and θ to the liquid surface tension is given in Figure 2-25 for several materials.

The indications are that surfaces exhibiting close packed CF_3 surface structures, such as might be expected with a perfluorolauric acid monolayer, have the lowest critical surface tensions. The critical surface tension is defined as the value of surface tension of a liquid, placed on the subject surface, below which the liquid will wet and spread over the surface. The lowest surface energy polymers presently available appear to be the Teflons with a CF_2 surface structure. Materials such as polyethylene and nylon have critical surface tensions approximately 1.7 to 2.5 times greater than Teflon surfaces. Table 2-3 presents critical surface tension data for several selected materials.

The fluorinated polymers have the lowest surface energies of commonly available materials and therefore when used for both sides of a valve seat should maximize the surface tension sealing effects of the liquid being used.

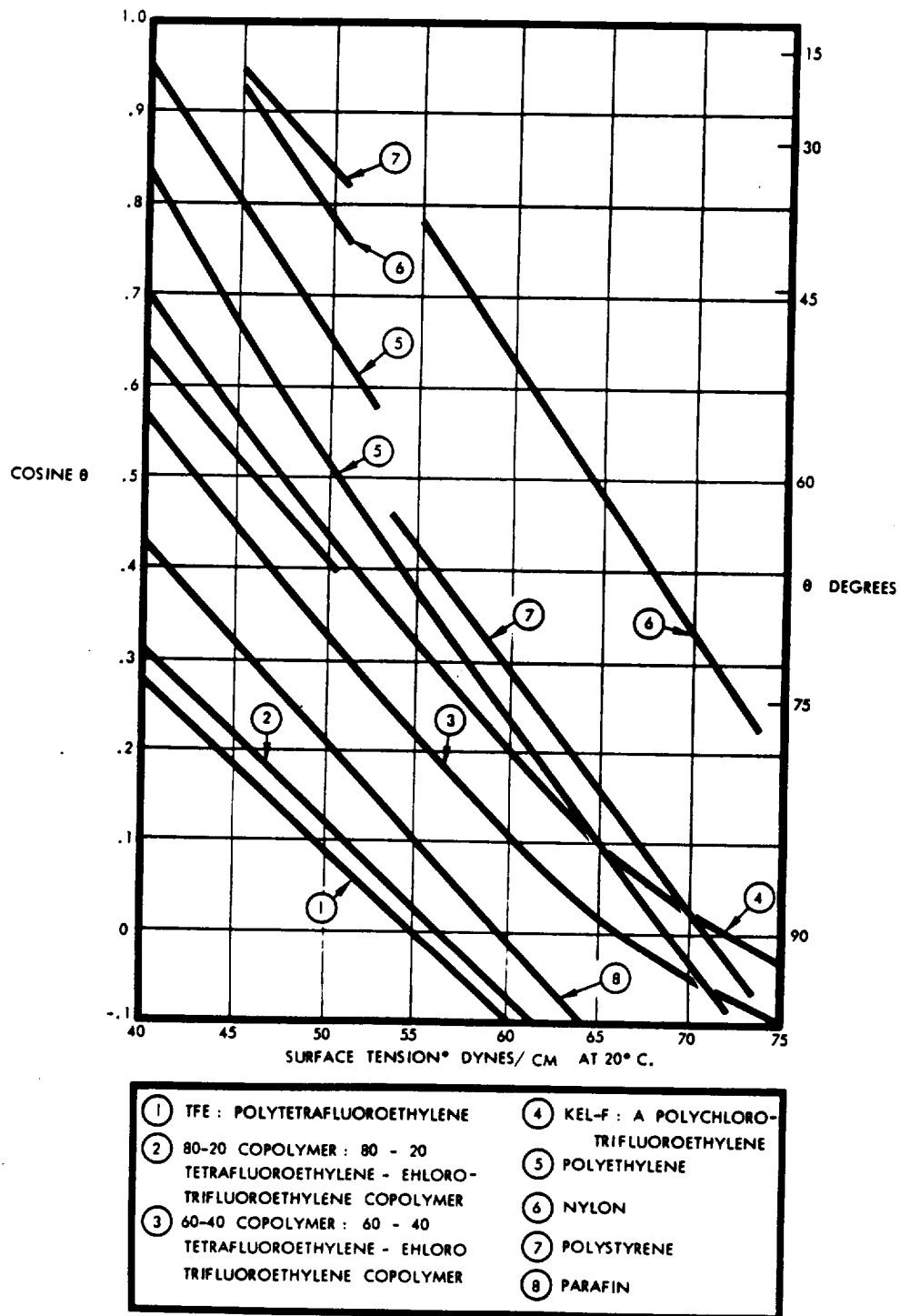







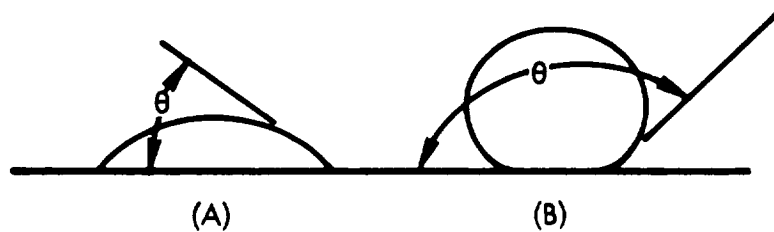
Figure 2-25: Contact Angle vs. Surface Tension for Several Polymers

TABLE 2-3. The Critical Surface Tension of Low Energy Solid Surfaces

Surface	Chemical Structure of Surface	Critical Surface Tension γ_c (dyne/cm)
Perfluorolauric acid, monolayer	CF_3 , close packed	5.6
Perfluorobutyric acid, monolayer	CF_3 , less closely packed	9.2
Perfluorokerosene, thin liquid film	CF_2 , some CF_3	17.0
Polytetrafluoroethylene, solid	CF_2	18.2
Octadecylamine, monolayer	CH_3 , close packed	22.
α -amyl myristic acid, monolayer	CH_3 and CH_2	26.
2-ethyl hexyl amine, monolayer	CH_3 and CH_2	29.
n-hexadecane, crystal	CH_2 , some CH_3	29.
Polyethylene, solid	CH_2	31.
Naphthalene, crystal	 , edge only	25.
Benzoic acid, monolayer	 , edges and faces	53.
2-naphthoic acid, monolayer	 , edges and faces	58.
Polystyrene, solid	CH_2 , some 	32.8-43.3
Polyethylene terephthalate, solid	 , CH_2 , ester	43.0
Nylon, solid	CH_2 , amide	42.5-46.0

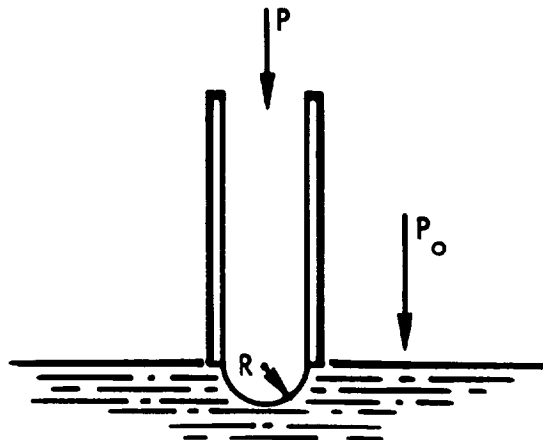
ANALYSIS

The contact angle may be determined from a drop placed on a surface by measurement of the angle of the liquid drop at contact with the solid, as shown.



When the contact angle, θ , is less than 90 degrees, as in A above, the fluid will rise in a capillary tube of the material in question. If the contact angle, θ , is greater than 90 degrees, the fluid will be depressed in the capillary.

The pressure that may be supported across a curved liquid gas interface may be derived from a consideration of the work required to form the surface. The surface formed is assumed to be spherical, as shown in the sketch below, such as might occur at the entrance or exit to a fine capillary tube or surface scratch.



Then the surface area of a hemisphere is:

$$A = 2\pi R^2 \quad (1)$$

and if the radius of the sphere is increased to $R + dR$, the surface area is increased by:

$$dA = 4\pi R dR \quad (2)$$

This results in an expenditure of work. From the definition of surface tension the work to form a new surface

$$dW = \gamma dA \quad (3)$$

where γ is the coefficient of surface tension.

Therefore $dW = 4\pi\gamma R dR \quad (4)$

The work required to form the new surface is also represented in terms of the pressure on the concave and convex surfaces. Since the bubble size is small, we neglect hydrostatic head. The forces on an element of the spherical surface of area ds are:

$$(P - P_o) ds$$

and as the bubble increases in size by dR , the work done is the product of force times distance or:

$$(P - P_o) ds dR$$

Considering the total surface of the hemisphere, the work done by the pressure is:

$$dW = (P - P_o) 2\pi R^2 dR \quad (5)$$

and combining (4) and (5)

$$(P - P_o) 2\pi R^2 dR = 4\pi\gamma R dR$$

therefore

$$(P - P_o) = \frac{2\gamma}{R} \quad (6)$$

where P_o is the pressure on the convex side and P on the concave side of a spherical surface.

Through a similar derivation it can be shown that for a long thin gap such as defined by two parallel plates, the pressure difference is

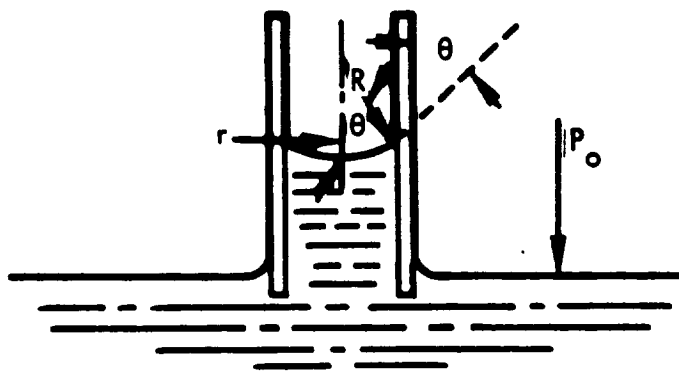
$$(P - P_o) = \frac{\gamma}{R} \quad (7)$$

or half that for a spherical surface. In general, the pressure difference may be defined for an arbitrary surface by

$$(P - P_o) = \gamma \left(\frac{1}{R_1} + \frac{1}{R_2} \right) \quad (8)$$

where R_1 and R_2 are taken in mutually perpendicular directions.

Normally, the radius of curvature of a fluid being forced into or coming out of a restriction is not the radius of the capillary or gap, due to forces of adhesion and cohesion between the liquid and the solid surface. There is a contact angle, as noted above, which describes these interactions and affects the pressure which may be supported across a physical gap. The effect of contact angle may be determined from examination of the rise, or drop of a fluid in a capillary as shown below.



The surface can be considered spherical with radius R. The radius of the capillary is taken as r and θ is the contact angle. Then:

$$R = \frac{r}{\cos \theta} \quad (9)$$

and substituting in (6), (7) and (8) for:

a round capillary;

$$(P - P_o) = \frac{2 \gamma \cos \theta}{r} \quad (10)$$

for a long narrow gap;

$$(P - P_o) = \frac{\gamma \cos \theta}{r} \quad (11)$$

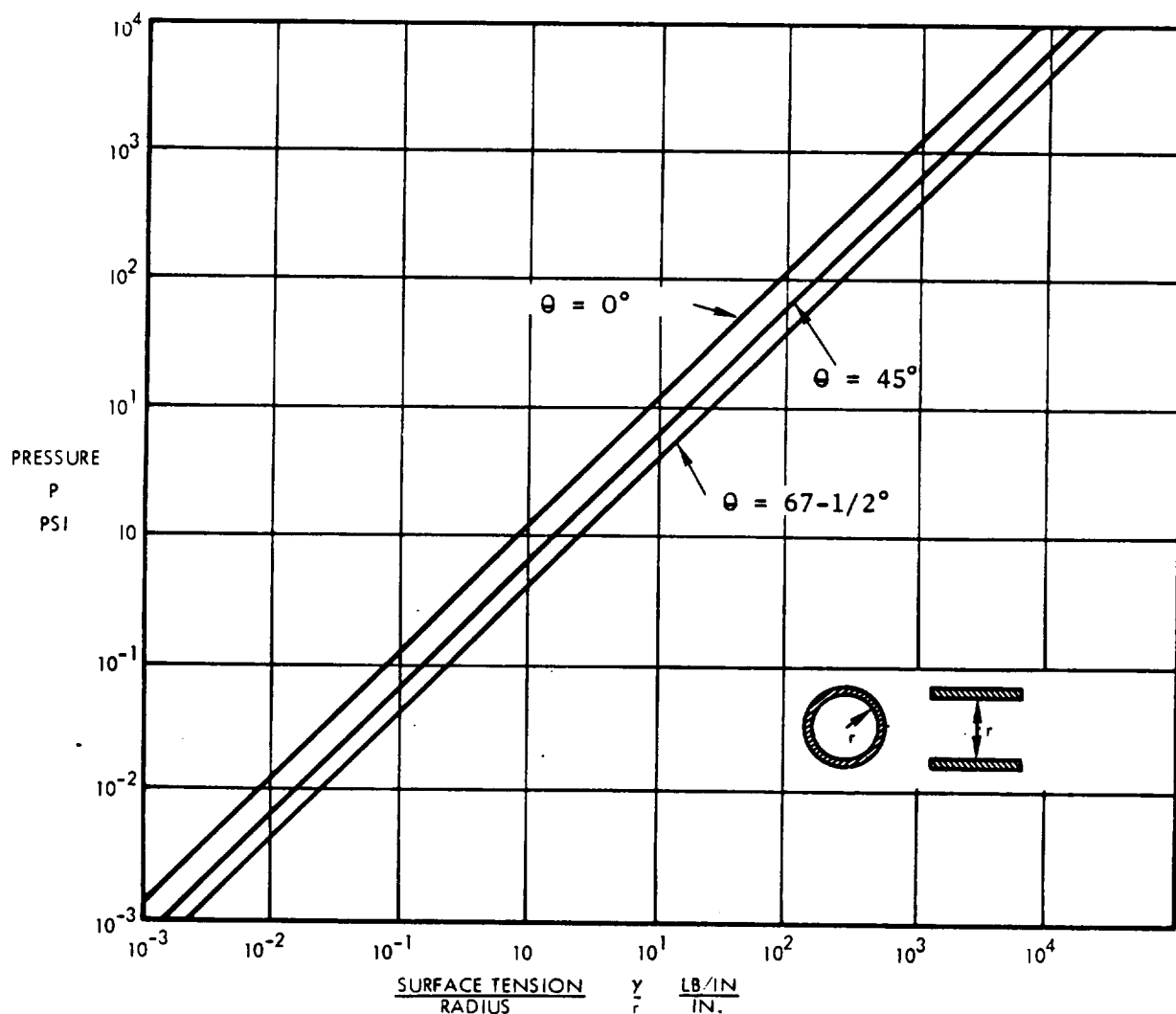
and for any gap;

$$(P - P_o) = \gamma \cos \theta \left(\frac{1}{r_1} + \frac{1}{r_2} \right)$$

A summary of pressure holding capabilities for round capillaries, as a function of size and contact angle, is shown in Figure 2-26. The pressure holding capability is reduced by a factor of two for long narrow gaps. The surface tensions of some typical propellants are shown in Table 2-4.

TEST FIXTURE FABRICATION

A test fixture was fabricated for use in testing of pressure sealing capabilities of various fluid-material combinations. The fixture is shown in cross-section in Figure 2-27. It consists of upper and lower test samples, which are held in intimate contact by the upper and lower housing. The samples are pressure-balanced to eliminate the effects of undesired pressure load. A port is, however, provided in the upper housing to allow gauging or loading of the specimens if desired. Pressure is applied through a port in the side of the lower housing and leakage is monitored through the port in its bottom. The lower test sample is machined to provide a controlled "leakage" gap and is pierced to allow leakage to flow to the exhaust port.



1. AT $\theta=90^\circ$ $\cos \theta = 0$ AND NO PRESSURE CAN BE SUPPORTED-
2. PRESSURE VALUES FOR $\theta = 180^\circ$, 135° , AND $112\frac{1}{2}^\circ$ RESPECTIVELY ARE EQUAL TO MINUS THE VALUES FOR $\theta = 0^\circ$, 45° , AND $67\frac{1}{2}^\circ$ RESPECTIVELY-
3. MINUS PRESSURES INDICATE THE PRESSURE AT WHICH A LIQUID WOULD BE FORCED INTO A CAPILLARY WHICH IT WOULD NOT NORMALLY ENTER-
4. POSITIVE PRESSURES INDICATE THE PRESSURE TO FORCE LIQUID OUT OF A CAPILLARY WHICH IT NORMALLY ENTERS.
5. PRESSURE VALUES FOR A SLIT GAP ARE ONE HALF THOSE SHOWN FOR ROUND CAPILLARIES ABOVE.
6. TO OBTAIN THE SURFACE TENSION, γ , IN LB/IN MULTIPLY THE VALUE IN DYNES/CM BY 5.72×10^{-6}

Figure 2-26. Flow-through Pressure vs. Surface Tension to Radius Ratio

TABLE 2-4. Surface Tensions of Several Propellants

No.	Propellant	Temperature °F	Surface Tension lb/in
1	NH ₃ Ammonia	-68.8	2.23×10^{-4}
2	ClF ₃ Chlorine Trifluoride	53.	1.417×10^{-4}
3	H ₂ O ₂ Hydrogen Peroxide	64.8	5.446×10^{-4}
4	CH ₃ NHNH ₂ Monomethyl Hydrazine (MMH)	68.	1.96×10^{-4}
5	White Fuming Nitric Acid	68.	2.34×10^{-4}
6	N ₂ O ₄ Nitrogen Tetroxide MIL-P-26539	67.6	1.58×10^{-4}
7	B ₅ H ₉ Pentaborane MIL-P-27403	70.2	1.21×10^{-4}
8	ClO ₃ F Perchloryl Fluoride	-68.	1.218×10^{-4}
9	UDMH (CH ₃) ₂ N ₂ H ₂	68.	1.58×10^{-4}
10	LF ₂ Liquid Fluorine	-313.	$.593 \times 10^{-4}$
11	LHe Liquid Helium	-453.	$.00639 \times 10^{-4}$
12	LH ₂ Liquid Hydrogen	-424.	$.1285 \times 10^{-4}$
13	LN ₂ Liquid Nitrogen	-307.	$.411 \times 10^{-4}$
14	LO ₂ (LOX) Liquid Oxygen	-298.	$.755 \times 10^{-4}$
15	N ₂ H ₄ Hydrazine	68.	3.83×10^{-4}

SOURCE: Reference 2 - Page 2-67.

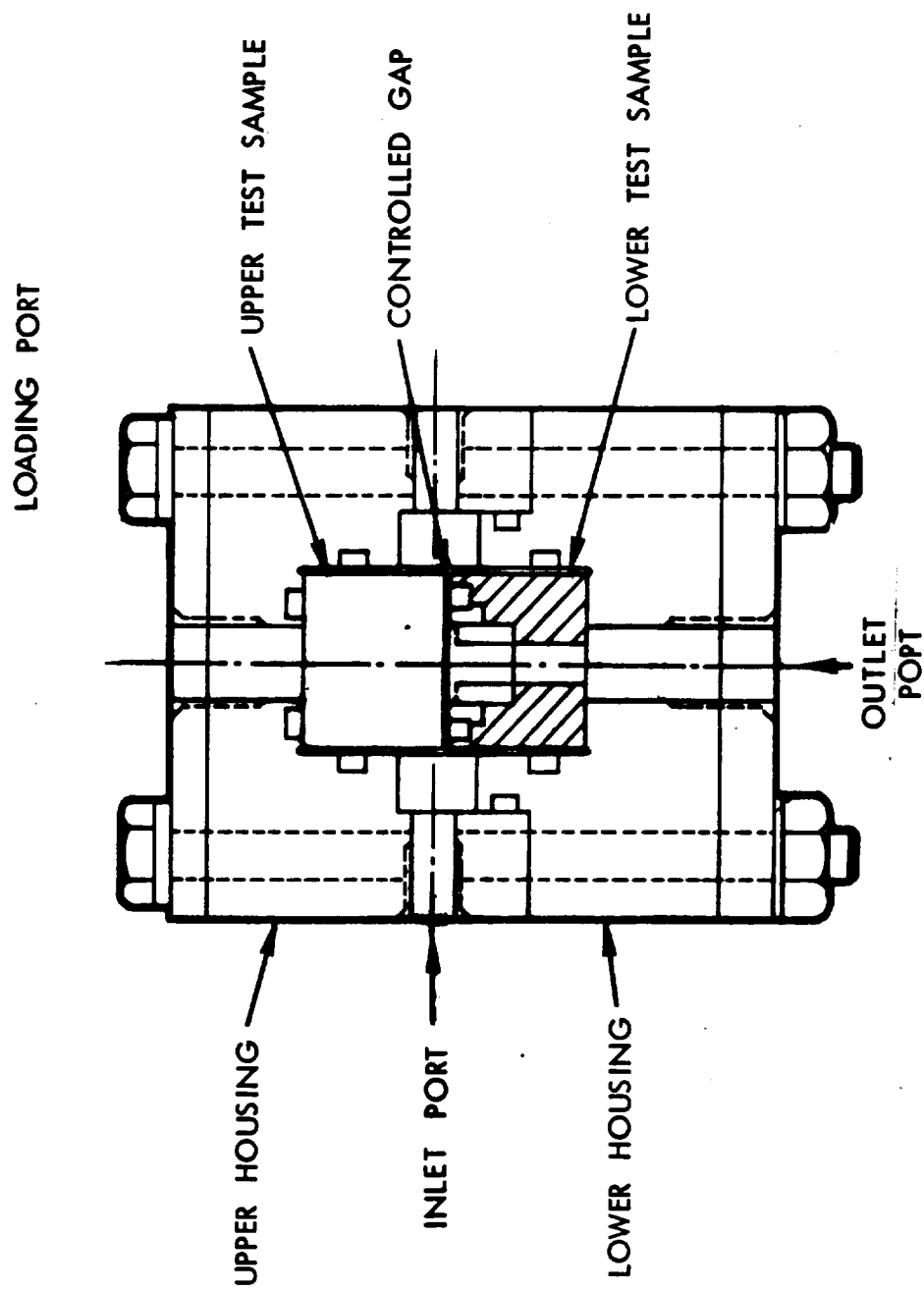


Figure 2-27. Surface Tension Test Fixture

TESTING

Some limited testing was performed utilizing the above fixture to determine the flow-through pressures for water and Mercury with varying gaps and materials. The basic sample materials used were Teflon and CRES 347. The CRES samples were also tested with coatings of Nyebar C* and Nyebar H*. In addition, capillary, rise or drop, experiments were performed utilizing a .023 inch inside diameter glass capillary. Fluids tested were water, Mercury, Dow-Corning 704 oil, and a petroleum-based detergent motor oil, Penzoil with Z-7.

The results of these experiments are shown in Table 2-5. The samples were typically cleaned ultrasonically in Freon TF, then rinsed and wiped with acetone.

It should be noted that, even though the low surface energy "Nyebar" films showed positive effects with Hg in the capillary tests, this was not the case in the pressure tests, particularly with Nyebar "C". During the pressure tests the films were applied on a CRES substrate rather than glass. It is postulated that a Hg, CRES, film reaction occurred, improving the surfaces wetability.

It was observed that the flow-through pressure for both the wettable and non-wettable surfaces was reduced to a very low value after initial flow through occurred.

*A low-surface energy fluorocarbon polymer in a solvent carrier, produced by William F. Nye, Inc., New Bedford, Massachusetts.

TABLE 2-5. Flow-Through Pressure Test Results

MATERIAL (2)	COATING	FLUID	CAPILLARY RISE (1)	FLOW-THROUGH PRESSURE	REMARKS
Glass	--	Hg	-.625"	--	
Teflon	--	H ₂ O	--	14" Hg	No sharp break-through.
Teflon	--	Hg	--	30" Hg	No sharp break-through.
CRES (3)	--	Hg	--	7.13" Hg	Break-through much sharper than with Teflon sample.
Glass	--	H ₂ O	+.250	--	Tube cleaned with Freon Tf.
Glass	Nybar H (4)	H ₂ O	-1.00"	--	After stabilization.
Glass	Nybar H (4)	Hg	-.687	--	
CRES	--	H ₂ O	--	Very low <.25"	Run through after wetting.
CRES	Nybar H (4)	Hg	--	6.25" Hg	
CRES	Nybar C (5)	Hg	--	3.75" Hg	
CRES	Nybar C (5)	H ₂ O	--	.63" Hg	Cannot support press after first flow-through.
Glass	Nybar C (5)	704 Oil (6)	-.06	--	
Glass	Nybar H (4)	704 Oil (6)	-.04	--	
Glass	WD-40 (7)	H ₂ O	+.75	--	
Glass	--	Penzoil (8)	+1.0	--	
Glass	Parafin (9)	Penzoil (8)	+.37	--	
Glass	Nybar C	Penzoil (8)	+.18	--	
Glass	Nybar H	Penzoil (8)	-.20	--	
CRES (10)	--	H ₂ O	--	45 psi	Could support less than 4 psi after flow-through.

(1) Using a .023 ID capillary tube, negative numbers indicate a depression.

(2) For test samples in the fixture shown in Figure 2-27, gap for all CRES samples was .001; gap for all Teflon samples was .0005; however, this could have been reduced somewhat due to cold flow.

(3) All CRES samples are AISI Type 347.

(4) A low surface energy fluorocarbon resin solution in a chlorinated solvent. Manufactured by William F. Nye, Inc., New Bedford, Mass.

(5) A low surface energy fluorocarbon resin solution in a fluorinated solvent. Manufactured by William F. Nye, Inc., New Bedford, Mass.

(6) A silicone oil manufactured by Dow Corning Corp., Midland, Michigan.

(7) WD-40, a protective oil manufactured by Rocket Chemical Company, San Diego, California.

(8) Penzoil with Z-7, a petroleum base detergent motor oil, manufactured by the Penzoil Company, Oil City, Pa.

(9) A solution of Gulfwax; Gulf Oil Corporation, Houston, Texas; in trichloroethylene.

(10) Two touching lapped surfaces



APPLICATION OF CONCEPTS

Electromagnetic Capillary Valve

An electromagnetic capillary valve concept utilizing mercury or another high surface tension conductive liquid actuated by an electrical signal has been originated. This valve approach is applicable for use as a fluidic system shutoff and may be adaptable to other low pressure gas systems. A cross-sectional illustration of the valve is shown in Figure 2-28.

The valve functions as follows: A conductive, high surface tension liquid, such as mercury, is trapped in a channel between two fine screens, slits or porous plugs. The channel is constructed so that the Hg may be placed blocking the main valve flow channel or withdrawn into a storage chamber. When the Hg is in the flow channel, it prevents any flow through the slit, or porosities in the exit side of the valve. It is held in place, since its surface tension will not allow it to penetrate the pores, until some critical pressure is reached. When the Hg is withdrawn, the working fluid is free to flow through the slit, screen or porous plug with no more than the normal pressure drop for a filter of equivalent size. The motion is imparted to the mercury by placing it in a magnetic field, and then flowing a current through it, perpendicular to the direction of the field. A permanent or electromagnet may be used to provide the field. The current through the mercury need only be applied long enough to accomplish the shutoff function.

Two preliminary test models of the valve described were built and some feasibility testing has been performed. A photograph of the first valve is shown in Figure 2-29.

Planar construction, similar to construction of some fluidic logic elements, was used in producing the test models. The valves were fabricated from two sheets of Lucite between which are sandwiched two pieces of stainless steel shim stock, which were shaped to the desired flow channels. Due to the geometry selected, these pieces of shim stock are also used as the electrodes for applying a current through the mercury.

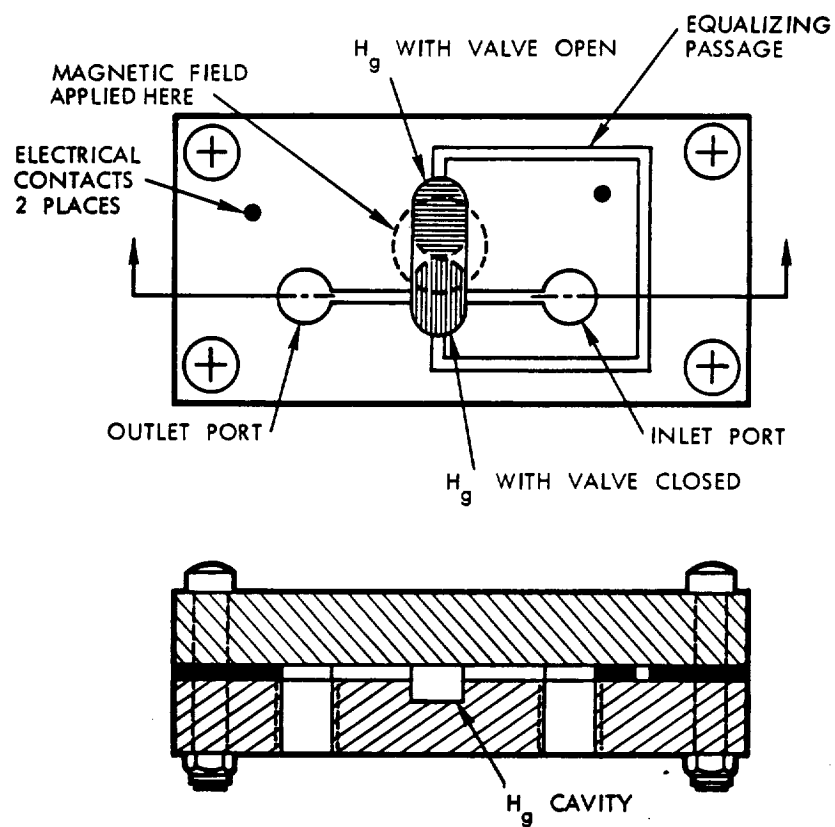


Figure 2-28. Drawing - Electromagnetic Capillary Valve

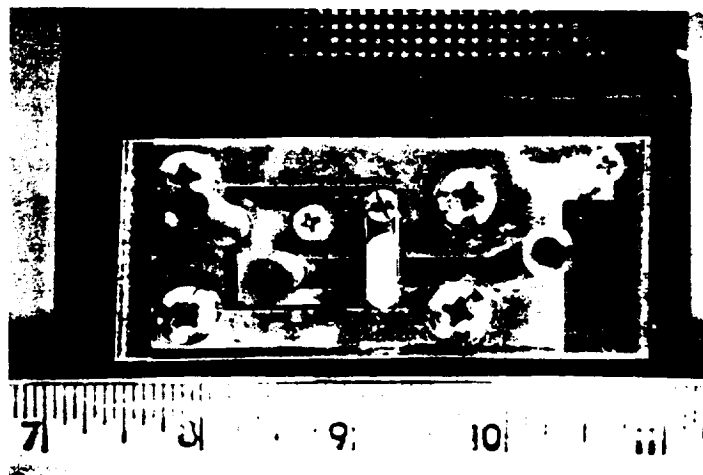


Figure 2-29. Photograph - Electromagnetic Capillary Valve

In the first valve the mercury channel was produced by milling a groove approximately .03 inch deep into one of the Lucite plates. The shim used to separate the Lucite plates was .001 inch thick and no porous plug was used in the gas flow channel. A large permanent magnet was used for applying the required field; a piece of magnetic material being employed to reduce the gas as much as possible.

Testing performed, demonstrated an ability to move the mercury from the open to the closed position by applying a current to the electrodes. Current pulses of approximately eight amperes were used. It is probable that in actual practice a capacitor can be used, thus reducing the average power used to a negligible value. Nitrogen was used as the test fluid.

Flow changes of a factor of three, from closed to open, were accomplished at a pressure of 4.5 psi. This pressure sealing capability is adequate for some low pressure fluidic and gas thruster applications. Since the slit holding the mercury in place was .001 inch thick, this is close to the maximum pressure capability of this particular unit.

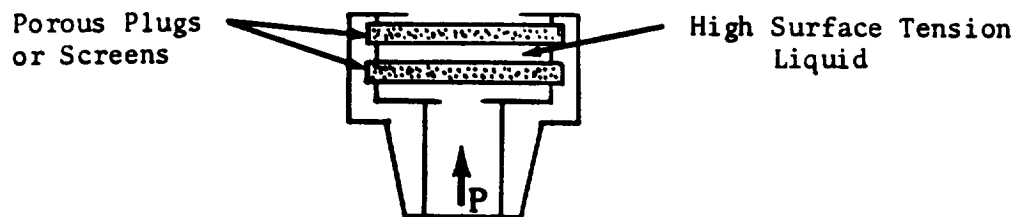
The second valve utilized a mercury channel formed between .04 inch thick pieces of stainless steel sheet spaced approximately .080 inch apart. The mercury was kept from entering the gas passages by a pair of 12μ absolute retention porous stainless steel filter plugs which were bonded into slots in the stainless sheet material. The spacer plates were cut to allow four electrodes rather than two as formerly used. This allows the proper current to be applied to the segment of mercury to be moved without short circuits due to the mercury that has already been transferred.

Testing performed demonstrated the ability to move the mercury from the open to the closed position by applying current to the proper pair of electrodes. The mercury was retained in place after opening or closing by a restriction between the two chambers.

The mercury was contained in the closed position with pressures of 15 psi applied to the gas inlet ports. The valve exhibited leakage characteristics considerably superior to the first unit, including leak-free shutoff at low pressures. It is felt that the initial testing done has demonstrated the electromagnetic capillary valve concept to be a feasible and promising one.

Relief Valve

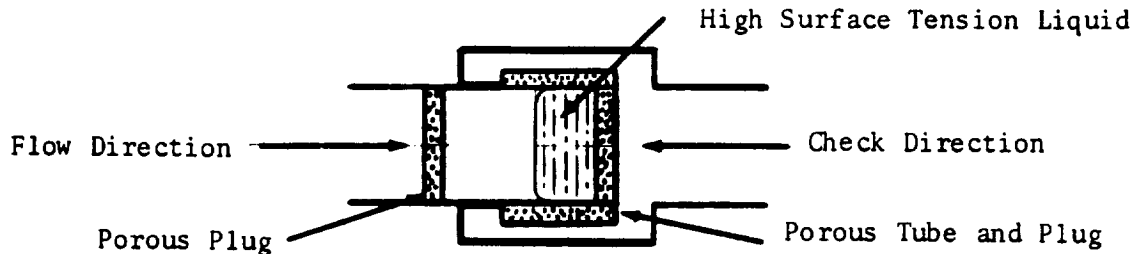
A relief valve may be made by trapping a high surface tension liquid between two restrictions, such as fine screens or porous plugs as shown below.



The liquid will form a seal preventing any fluid applied to the inlet port from leaking through until a critical pressure is reached. This critical pressure is a function of the pore size of the plug or screen, the surface tension of the sealing liquid, and the contact angle between the sealing liquid and the plug or screen material. This relationship is described in the Analysis section. A device such as this would have application as a replacement for burst discs and similar devices. If required, a combined temperature-pressure relief function may be supplied by using a sealing material that is solid below a certain pressure or exhibits particularly large changes in surface tension with temperature. A test model was fabricated and feasibility tests performed. Relief pressures of approximately 10 psi were obtained using porous stainless steel plugs with mercury as the sealing liquid and up to 30 psi using porous Teflon plugs with mercury.

Check Valve

A possible check valve configuration is shown below.



If pressure is applied in the flow direction, the high surface tension liquid is blown into the cup-shaped cavity, formed by a porous tube and plug. There is not sufficient liquid to completely fill the porous tube, and the working fluid flows freely through the unfilled portion. When pressure is applied in the check direction, the high surface tension liquid is blown against the porous plug and forms a seal preventing further flow.

REFERENCES

1. F. W. Sears, Mechanics, Heat and Sound, Addison-Wesley Press, Inc., Cambridge, Massachusetts, 1950.
2. Norbert A. Lauge and Gordon M. Forker, Handbook of Chemistry, Handbook Publishers, Inc., Sandusky, Ohio, 1956.
3. B. Kitt and D. S. Everet, Rocket Propellant Handbook, MacMillan, 1960.
4. Lloyd I. Osipow, Surface Chemistry, Theory and Industrial Application, Reinhold Publishing Corp., New York, 1962.
5. W. C. Reynolds, N. A. Laad and H. M. Satterley, Capillary Hydrostatics and Hydrodynamics at Low G, NSS-G 20090, Stanford University, September 1964.
6. L. S. Marks, Mechanical Engineers Handbook, McGraw-Hill Book Company, Inc., New York, Fifth Edition.

SEAL LEAKAGE STUDY

The objective of this study is to provide a greater understanding of permeation-type leakage phenomena and determine a correlation between liquid and gaseous medium permeation leakage characteristics.

The leakage study has been primarily concerned with the development of the mathematical model to aid in the predicting of leakage through seal glands containing polymeric seals. The analytical model used in the analysis takes geometry into account directly and seal properties by the introduction of the permeability coefficient. A non-dimensional geometry factor to correct for the effects of seal geometry is developed. The analysis presented here is a simplified treatment, and it is felt that a more complete analytic study including the effects of items such as seal stress vacuum conditioning and other material pre-treatments should be undertaken.

ANALYSIS

Two basic models which closely approximate leakage past O-ring seals are the radial leakage model shown in Figure 2-30 and the axial leakage model shown in Figure 2-31 (Reference 4).

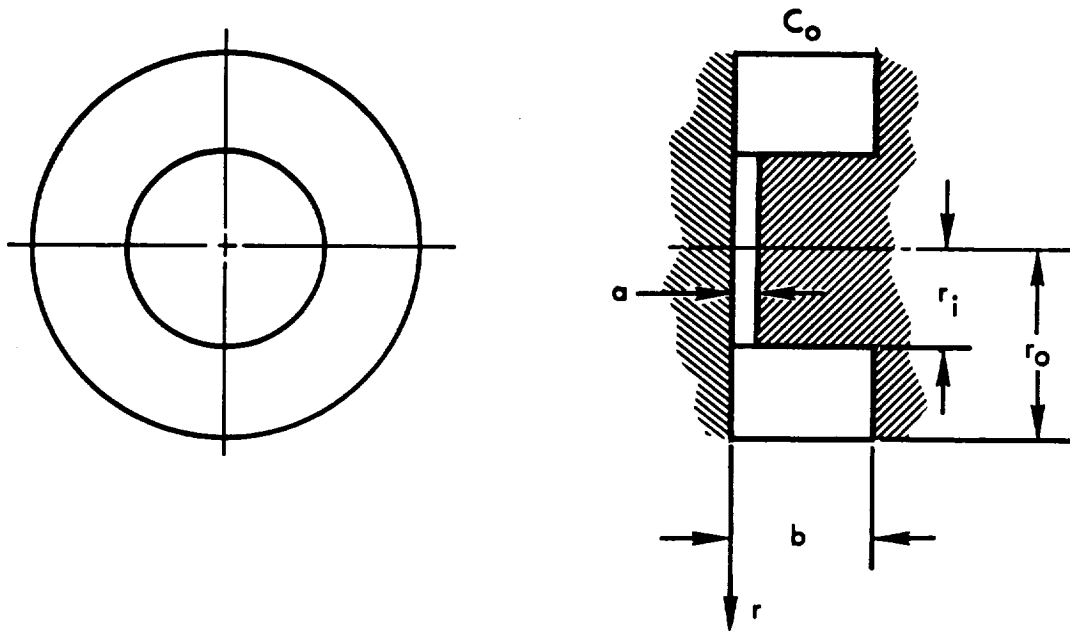


Figure 2-30. Radial Leakage Model

The boundary conditions for the radial flow model are:

$$C(r_o, z) = C_o$$

$$\frac{\partial C}{\partial z}(r, b) = 0$$

$$\frac{\partial C}{\partial z}(r, 0) = 0$$

$$\frac{\partial C}{\partial r}(r_i, z) = 0 \quad a \leq z \leq b$$

$$D \frac{\partial C}{\partial r}(r_i, z) = \omega \quad 0 \leq z \leq a$$

where C is the concentration of species which are leaking, ω the leakage rate per unit length of seal material, and D the diffusivity of the seal.

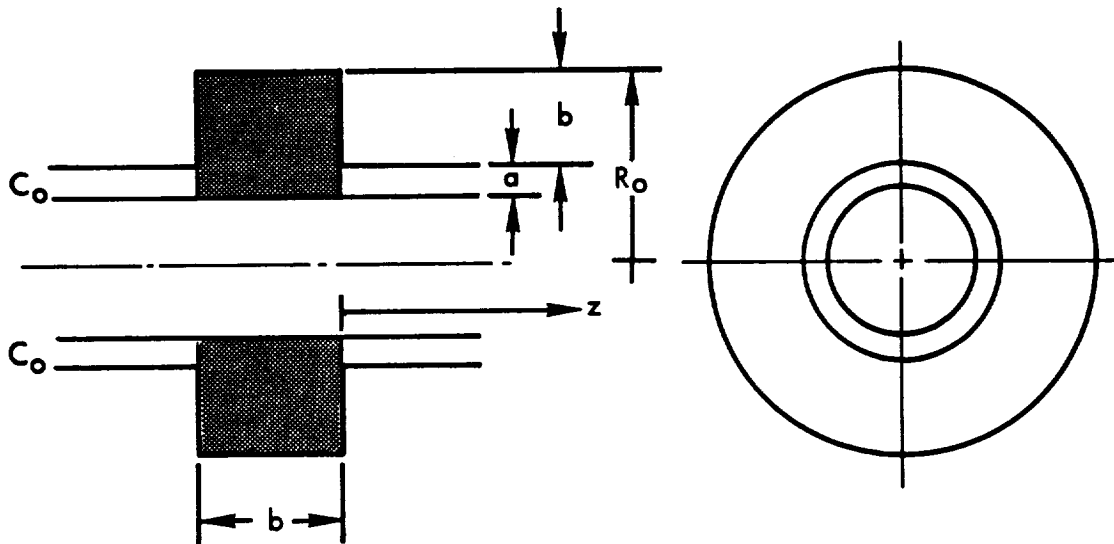


Figure 2-31. Axial Leakage

The boundary conditions for the axial leakage model are:

$$C(a \leq r \leq b, 0) = C_0$$

$$\frac{\partial C}{\partial z}(b \leq r \leq R_0, 0) = 0$$

$$\frac{\partial C}{\partial z}(b \leq r \leq R_0, h) = 0$$

$$\frac{\partial C}{\partial r}(R_0, z) = 0$$

$$D \frac{\partial C}{\partial z}(a \leq r \leq b, h) = \omega$$

In the above model, it was assumed that the O-ring completely fills the groove. In reality, this is not necessarily the case.

Therefore the case to be examined is shown in Figure 2-32.

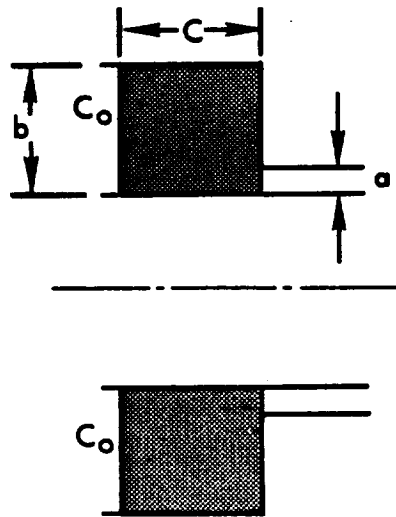


Figure 2-32. Final Permeation Leakage Model

Here the boundary conditions were modified on the left-hand side leaving this edge open to the permeating gas. It can be seen that there is a great deal of similarity between the radial and axial leakage problems. That is, the boundary conditions are similar; namely, a constant concentration on one surface, impermeable boundaries normal to this surface, and diffusion through the remaining surface governed by convection from this surface.

If the dimensions b and c are very large compared with a and the diameter R_0 is also large compared with a , each of the models can be approximated by a model which is semi-infinite in one direction. Such a model is shown in Figure 2-33.

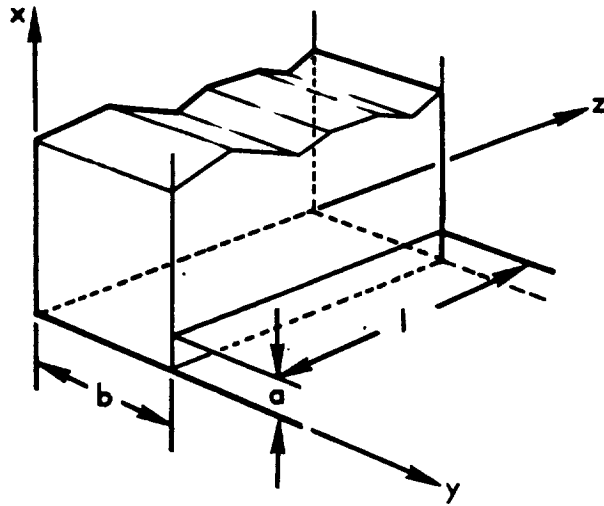


Figure 2-33. Simplified Final Permeation Leakage Model

The solution to this problem was obtained as part of a study to analyze the permeation of high density gases and propellant vapors through single layer Teflon or Teflon structure materials and laminations performed by TRW Systems for NASA (Reference 1). The leakage rate for the above geometry is given by:

$$\frac{W}{L} = \omega = \frac{2aD C_d}{h \left[1 - \frac{2}{\pi^2} G \frac{a}{h} \right]} \quad (1)$$

Where ω is given in mass per unit time per unit length. For the particular problem described, ω is multiplied by $2\pi R_0$ ($L \approx 2\pi R_0$) to obtain mass per unit time. The function G is given by:

$$G\left(\frac{a}{h}\right) = \sum_{h=0}^{\infty} \frac{\left[I_0 \left((h + 1/2) \pi \frac{a}{h} \right) \right]}{(h + 1/2)^2} e^{-(h + 1/2) \pi \frac{a}{h}} \quad (2)$$

where I_0 denotes the zero order modified Bessel function. The details of the solution are given in Reference 1.

In the above case, both the radial and axial problems become the same, and the geometry of the problem becomes cartesian. Only the steady-state solution is presented due to the complexity involved in obtaining the transient solution in the original mathematical models.

The above discussion has not included mention of the physical properties of the seal and the leakage fluid. These properties are considered in obtaining the constants D and C_0 for Equation (1).

The mass transfer of a gas from one surface of a permeable material to the other involves

- Absorption on the barrier surface
- Solution in the material
- Diffusion
- Dissolution
- Evaporation at the other side

It is assumed that diffusion is the rate-controlling factor and Fick's Law is used as the starting point of the analysis. The concentration gradient in the seal will be dependent on the solubility of the leakage gas or liquid in the seal material and the pressure difference across the seal. In addition, the diffusivity D will be dependent upon such factors as the

stress on the seal, and chemical reaction between the seal and the leakage fluid which may change seal surface characteristics, and on the temperature of the system.

$$\frac{\omega}{DC_0} = \frac{2\alpha}{\left[1 - \frac{2}{\pi^2} G(\alpha)\right]} \quad (3)$$

where $\alpha = a/h$, the ratio of the leakage path to the width of the seal. These dimensions are usually known for a gland design, and therefore leakage rate for a given seal configuration may be calculated if one knows the concentration of the fluid to which the seal will be exposed, and the diffusivity of the seal material.

Since most data on seal material is given in terms of permeability rather than diffusivities, we can transform Equation (3) by noting that Henry's Law

$$C_0 = kp \quad (4)$$

states that the concentration is equal to the product of the solubility constant k and the absolute pressure p . In addition, the product of the solubility constant and the diffusivity is defined as the permeability. Therefore, Equation (3) becomes:

$$\frac{\omega}{S p p} = \frac{2\alpha}{\left[1 - \frac{2}{\pi^2} G(\alpha)\right]} \quad (5)$$

Figure 2-34 shows a plot of $\frac{\omega}{p p}$ versus $\frac{2\alpha}{\left[1 - \frac{2}{\pi^2} G(\alpha)\right]}$

indicating the effects of seal geometry on leakage rate.

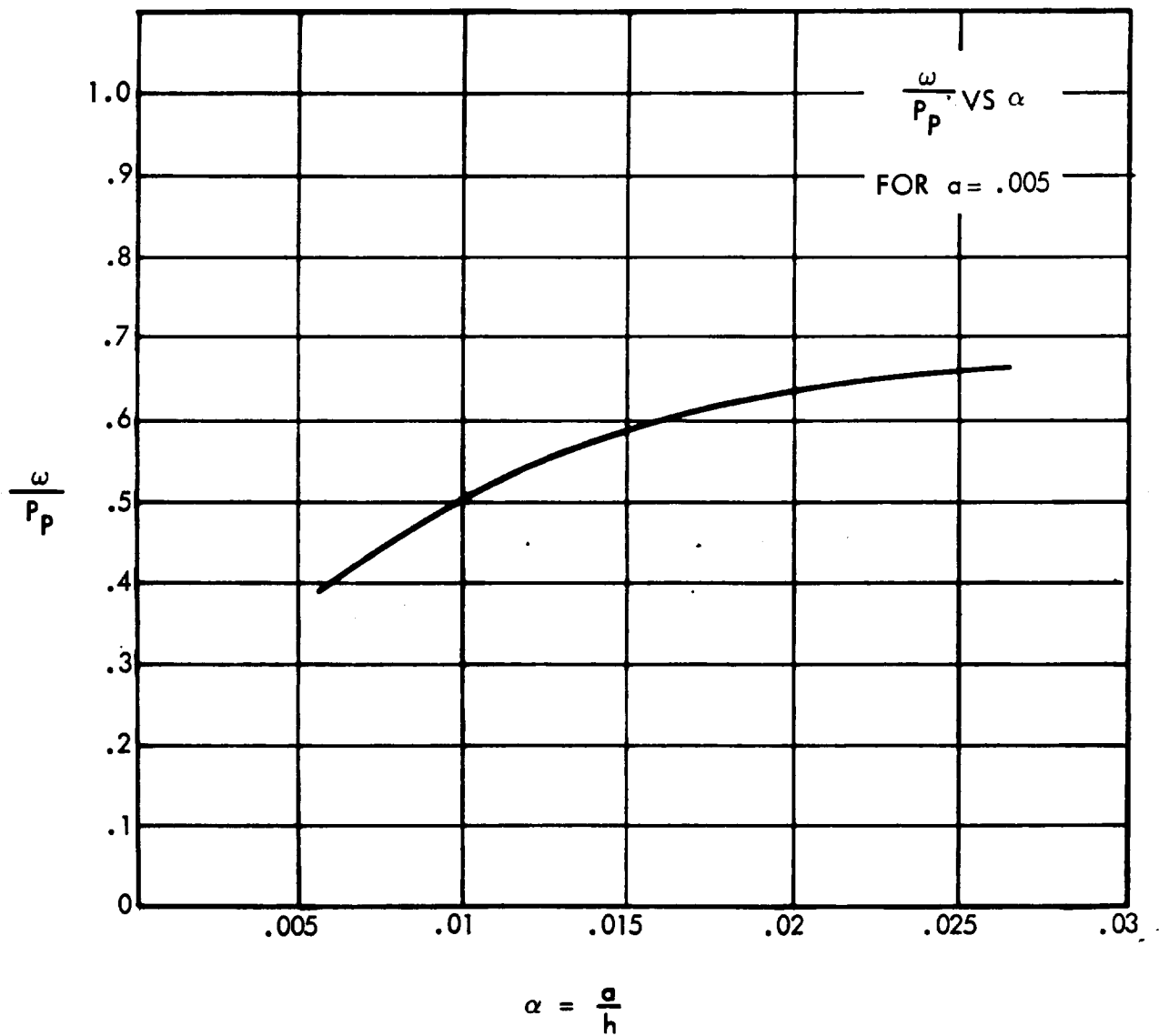


Figure 2-34. Plot of Flow Per Unit Length and Pressure vs. α , the Ratio of Gland Thickness to Leakage Gap

Sample Calculation

Consider a typical O-ring configuration which can be approximated by the situation pictured in Figure 2-35.

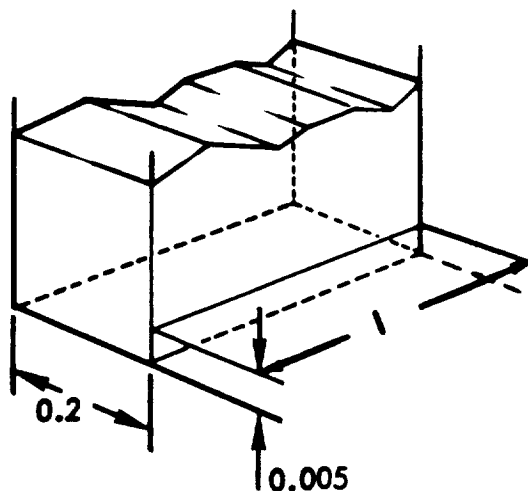


Figure 2-35.

It is seen that $\alpha = a/h$ is .025. From Figure 2-35 for this value of α :

$$\frac{\omega}{P_p} = 0.65$$

Assuming that the O-ring is made of natural rubber and that the pressurant is He at one atmosphere, Reference (3) shows:

$$P_p = 23 \times 10^{-8} \frac{\text{cc(STP)}}{\text{cm/sec}}$$

Therefore

$$W = \omega (2\pi R_o)$$

i.e., the rate of flow in cc (STP)/sec is obtained by multiplying through by the circumference of the flange which is sealed. For $R_o = 1.5$ cm the flow rate, $w = 2.1 \times 10^{-6}$ cc/sec.

REFERENCES

1. Advanced Valve Technology for Spacecraft Engines, TRW Systems Final Report, NASA Report 8651-6016-RU-000, Contract NAS 7-107, March 1963.
2. Aerospace Fluid Component Designers' Handbook, RPL-TDR-64-25, Volume I and II, Revision B, Contract AF04(611)-8385 and AF04(611)-11316, March 1967.
3. A Study to Analyze the Permeation of High Density Gases and Propellant Vapors through Single Layer Teflon or Teflon Structure Materials and Laminations, TRW Systems Interim Final Progress Report, Contract NAS 7-505, October 25, 1967.
4. Cryenco Data Sheet, Cryogenic Engineering Company, Denver, Colorado.
5. Design Data for Pressurized Gas Systems, Stanford Research Institute, Menlo Park, California, Contract NAS 7-105, November 1963.
6. P. J. Lare, et. al., Investigation of the Effects of Mechanical Stress on the Permeability of Engineering Materials to Certain Cryogenic and Storable Propellants used in Launch Vehicles, Annual Summary Report, Melpar, Inc., Falls Church, Virginia, June 30, 1964 to June 30, 1965, NASA-CR-68411, Contract NAS 8-11322, Abstract No. N66-13088, September 1965.
7. R. F. Muraca, Investigation of the Storability of Pressurizing Gases, Stanford Research Institute, Menlo Park, California, Monthly Status Report No. 2, March 1962 to April 1962, Contract NAS 7-105, Abstract No. N62-13141, April 27, 1962.
8. J. William Marr, Leakage Testing Handbook, General Electric Company, Schenectady, New York, NASA-CR-952, NAS 7-396, Abstract No. N68-20389, April 1968.
9. Seal Compound Manual, Parker Seal Company, Culver City, California, July 1964.
10. Telecon between M. J. Makowski and Dr. Muraca (TRW Systems and Stanford Research Labs.), March 28, 1967.

III ALL FLUID CONTROLS

This section presents the results of work performed with the objective of determining the applicability of fluidics to liquid propulsion systems. Included are the results of surveys, component and system analysis, and conceptual studies. Fluidic literature and patent bibliographies, a subject index, and standards which were prepared from the survey material are listed in the appendices.

	<u>Page</u>
Introduction.....	3-6
Surveys.....	3-8
Literature and Patent Search.....	3-8
Agency Interviews.....	3-10
Fundamentals and Definitions.....	3-12
Fluidic Component Study.....	3-14
Component Rating Chart.....	3-15
Fluidic Components.....	3-17
Component Fabrication and Materials.....	3-80
Component Performance With Propellants.....	3-84
Component Functional Parameters.....	3-87
Space Environments.....	3-92
Component Application Criteria.....	3-93
Technical Problem Areas.....	3-93
Propulsion Applications.....	3-98
Standard Criteria.....	3-100
Typical Subsystem.....	3-102
Conceptual Studies.....	3-108
Fluidic Pressure References.....	3-108
Fluidic Pressure Regulation.....	3-117
Vortex Regulation Concepts.....	3-126

	<u>Page</u>
Proportional Pressure Control System.....	3-133
New Regulator Concepts.....	3-133
Vented Jet Performance.....	3-137
Analysis.....	3-141
Analytical Techniques.....	3-141
Analytical Tools.....	3-142
References.....	3-148
Appendix III-A Fluidic Literature Bibliography.....	3-A1
Appendix III-B Fluidic Patent Bibliography.....	3-B1
Appendix III-C Fluidic Subject Index.....	3-C1
Appendix III-D Fluidic Standards.....	3-D1

ILLUSTRATIONS

		<u>Page</u>
3-1	Illustration of the Coanda Effect.....	3-17
3-2	Basic Wall Attachment Device.....	3-18
3-3	Switching Mechanism in Bistable Wall Attachment Device.	3-20
3-4	Methods of Reducing Load Sensitivity.....	3-21
3-5	Wall Attachment Logic Elements.....	3-22
3-6	Load Insensitive Flip-Flop Performance.....	3-26
3-7	Flip-Flop Performance.....	3-27
3-8	Or/Not Performance.....	3-28
3-9	Turbulence Amplifier Configuration and Operation.....	3-29
3-10	Induction Amplifier Configuration.....	3-31
3-11	Edgetone Amplifier Configuration.....	3-32
3-12	Focused Jet Amplifier - Configuration and Operation....	3-33
3-13	Proportional Amplifier - Interaction Region Shapes.....	3-35
3-14	Proportional Amplifier Configuration.....	3-36
3-15	Stream Interaction Proportional Amplifier Performance..	3-39
3-16	Stream Interaction Rectifier Performance.....	3-40
3-17	Center Dump Proportional Amplifier Performance.....	3-41
3-18	Illustration of Vortex Amplifier Operation.....	3-42
3-19	Vortex Valve Configuration.....	3-44
3-20	Optimized Vortex Valve Configuration.....	3-44
3-21	Vortex Valve Static Performance Characteristic.....	3-46
3-22	Single Exit Vortex Valve Performance.....	3-47
3-23	TRW Systems Vortex Valve Performance - Unloaded.....	3-48
3-24	TRW Systems Vortex Valve Performance - Loaded.....	3-49
3-25	Vented Vortex Amplifier Operation.....	3-52
3-26	Vented Vortex Amplifier - Nomenclature and Symbology...	3-53
3-27	Typical Pressure Gain Characteristics Vented Vortex Amplifier.....	3-54
3-28	Vented Jet Amplifier Configuration.....	3-58
3-29	Vented Jet Amplifier - Typical Performance Map.....	3-59
3-30	Typical Performance - Vented Jet.....	3-63

	<u>Page</u>
3-31	Flow Diverter Configuration..... 3-65
3-32	Boundary Layer Amplifier Operation..... 3-66
3-33	Boundary Layer Amplifier Configuration..... 3-67
3-34	Double-Leg Elbow Amplifier Configuration..... 3-68
3-35	Transverse Impact Modulator..... 3-69
3-36	Direct Impact Modulator..... 3-70
3-37	Transverse Impact Modulator Performance..... 3-71
3-38	Vortex Diode Performance..... 3-74
3-39	Electrical to Fluid Transducer-Torque Motor Driven..... 3-76
3-40	Electrical to Fluid Transducer-Diaphragm Oscillator Type..... 3-76
3-41	Fluid to Electrical Transducer-Hot Film Type..... 3-77
3-42	Fluid to Electrical Transducer-Strain Element Type..... 3-77
3-43	Mechanical to Fluid Transducer-Flapper Type..... 3-79
3-44	Mechanical to Fluid Transducer-Interruptable Jet..... 3-79
3-45	Fluidic Element Time Response as a Function of Size and Fluid..... 3-88
3-46	Fluidic vs Conventional Attitude Control System..... 3-103
3-47	System Weight Ratio Versus Mission Time..... 3-106
3-48	Optimum System Weight Regions..... 3-107
3-49	Illustration of Operating Point Pressure Ratio..... 3-109
3-50	Laminar vs Orifice Restrictor Circuit Configuration.... 3-109
3-51	Graph of Laminar vs Orifice Restrictor ΔP 3-111
3-52	Laminar vs Orifice Restrictor Pressure Reference..... 3-112
3-53	Characteristics of Linear-Nonlinear Resistors as a Pressure Reference..... 3-113
3-54	Fluidic Tuning Fork Oscillator..... 3-118
3-55	Series Connected Vortex Valves..... 3-122
3-56	Vortex Amplifier-Vortex Valve Cascade..... 3-122
3-57	Single vs Multiple Orifice Bridge..... 3-125
3-58	Vented Jet-Single Stage Feedback Amplifier..... 3-127
3-59	Dual Volume Regulation System..... 3-129
3-60	Lag Circuit Regulator..... 3-130
3-61	Hybrid Regulator Scheme..... 3-132

		<u>Page</u>
3-62	Proportional Pressure Control System.....	3-134
3-63	Vented Jet-Vortex Valve Regulator Concept.....	3-135
3-64	Vented Jet-Vortex Valve Regulator Performance.....	3-138
3-65	Monopropellant Gas Generator System.....	3-139
3-66	Variable Geometry Vented Jet Configuration.....	3-140

TABLES

3-I	Fluidic Component Rating Analysis Chart.....	3-16
3-II	Performance of Bistable Wall Attachment Devices.....	3-25
3-III	Performance of Stream Interaction Proportional Amplifiers.....	3-38
3-IV	Nonhysteretic Vortex Valve Performance.....	3-51
3-V	Fluidic Attitude Control System Parameters.....	3-104

INTRODUCTION

The field of fluid power, which is an outgrowth of fluid mechanics, has to do with the use of fluids at high pressures for the transmission of power and with the control and utilization of the power thus transmitted. Conventional control of sophisticated fluid power circuits has been based primarily on electronics. However, the recent development of fluid control devices that use no moving parts and in which the fluid itself is the working medium has led to completely new concepts in fluid control. From this unique concept, a distinct technology known as fluidics* has emerged.

Fluidics offers unique capabilities which should lead to a new generation of valves and controls for liquid propulsion systems. Practically any fluid can be used and often a particular fluidic element will operate equally well on both gases and liquids. The operation of these elements is based on various fluid mechanic principles, including momentum exchange, wall attachment (Coanda effect), and vortex generation. While fluidics promises potential weight savings, the primary advantage is that fluids are used for operation and components can be conveniently coupled with other fluid control components, eliminating the need for a transducer. This characteristic as well as a wide range of fabrication materials, including high temperature alloys and ceramics, make fluidic systems relatively insensitive to extreme temperature, radiation, vibration, and shock environments.

The overall objectives of this study are to advance the state-of-the-art of fluid controls used on spacecraft liquid propulsion power systems through evaluating fluidic technology, defining problem areas and evolving new concepts. The specific tasks which were undertaken to meet these objectives include:

*As defined by the National Fluid Power Association, a fluidic system is one in which "sensing, control, information processing, and/or actuation functions are performed primarily through utilizing fluid dynamic phenomena."

- o Comprehensive literature and patent searches and a survey of the leading government agencies and companies in the fluidics business.
- o Review of the properties and parameters of fluid mechanics pertaining to fluidics and the definition of accepted terminology and symbology.
- o A study of the operating principles, configurations, and applications of the basic fluidic components and consideration of performance relative to propellants, specific functional parameters, and space environments.
- o Application studies and investigations of new concepts.

SURVEYS

The initial efforts to ascertain the present state-of-the-art of fluidic technology consisted of searches and agency interviews to determine the extent of existing data and to evaluate the major applications and the problem areas. These efforts included a comprehensive literature and patent search, and interviews with cognizant personnel in industry and government agencies. In addition, generally accepted fluidic fundamentals and definitions were identified. A discussion of this work follows.

Literature and Patent Search

Much material covering almost all aspects of fluidics has been published. However, the literature search was limited to material covering fluidic devices and systems and the supporting technology. This technical literature is almost entirely in the form of symposia notes, technical papers, and reports which have been written within the last six years with the greater proportion over the last two years.

Over 600 literature references were recorded, primarily from TRW Systems Group, Technical Information Center; and Monthly Bibliography Service for Fluidic Technology, General Fluidics Corporation, Chatsworth, California. The fluidic literature was arranged in alphabetical order by author and a listing is presented in Appendix III-A, Fluidic Literature Bibliography.

A search was also made of the U.S. patent files to determine the scope of the patents issued in the field of fluidics. Of primary interest were those patents which are directly or indirectly related to propulsion system applications. Copies of about 350 patents were reviewed, and each patent was examined only to the extent necessary to determine its applicability. The fluidic patents were arranged in alphabetical order by the discloser's name, and are listed in Appendix III-B, Fluidic Patent Bibliography.

In summarizing the fluidic literature and patent searches, it may be stated

that a significant amount of basic information was obtained on fluidic components, systems, and applications. This information was useful in defining fluidic fundamentals and definitions, and in the selection of accepted nomenclature, drawing techniques, and symbology. Fundamental theory, configurations, and performance also were obtained to support the fluidic component study effort.

A subject index was organized so that the literature and patent bibliographies could be used effectively in obtaining information in a specific area of interest. The following categories were selected and presented in Appendix III-C, with cross reference identifications to the literature and patent listings in Appendices III-A and III-B.

Fluidic Subject Index

- I Capabilities
- II Commercial Applications
- III Aerospace Applications
- IV Propulsion Applications
- V Basic Fluid Flow
- VI Digital Elements
- VII Analog Elements
- VIII Valves and Power Elements
- IX Passive Elements and Interconnects
- X Sensors and Interface Devices
- XI Pneumatic Logic - Moving Parts
- XII Digital Systems
- XIII Analog Systems
- XIV Hybrid Systems
- XV Component Performance
- XVI System Analysis and Design
- XVII Instrumentation Techniques
- XVIII Fabrication
- XIX Symposia and Abstracts

Agency Interviews

Visits were made to the major aerospace and commercial companies and government agencies engaged in fluidics. Knowledgeable personnel were interviewed with the purpose of establishing the state of the art of fluidics relative to spacecraft liquid propulsion power systems. Information concerning problem areas, future component and system requirements, and expected performance gains in the next five years were also sought.

The agencies contacted during the reporting period were:

NASA Lewis Research Center, Cleveland Ohio
NASA Goddard Space Flight Center, Greenbelt, Maryland
NASA Manned Space Flight Center, Houston, Texas
NASA Marshall Space Flight Center, Huntsville, Alabama
Wright-Patterson Air Force Base, Dayton, Ohio
MIT, Cambridge, Massachusetts
Corning Glass Works, Corning, New York
Genge Fluorics, North Hollywood, California
ASME and Harry Diamond Laboratories Fluidics Symposium,
Chicago, Illinois
Honeywell Incorporated-Aerospace Division, Minneapolis,
Minnesota
The Marquardt Corporation, Van Nuys, California
Harry Diamond Laboratories, Department of the Army,
Washington, D. C.
Bowles Engineering, Silver Springs, Maryland
The Bendix Corporation-Research Laboratories Division,
Southfield, Michigan
Martin-Marietta Corporation, Orlando, Florida
General Electric Company-Advanced Technology Laboratories,
Schenectady, N. Y.

Propulsion applications of fluidics were identified; the more important ones are itemized below:

1. Secondary injection thrust vector control
2. Rocket engine throttling

3. Liquid rocket engine start-run-shutdown logic systems
4. Pressure and flow regulation
5. Controllers, compensation, sensors, and actuators for radiation hardened applications
6. Proportional and bistable attitude control
7. Pressurization system controls - cold gas, monopropellant, and solid propellant
8. Propellant management - oxidizer/fuel ratio control
9. Temperature sensing in severe environments
10. Servo systems for gimbal actuation

The significant problem areas and future development requirements determined during the agency interviews are summarized below:

1. Temperature effects on fluidic elements presently are determined for the most part on an analytical basis, with little or no supporting test data. These effects need to be identified for design purposes.
2. Although exploratory testing has been performed with many fluids, very little development effort has been expended on elements specifically designed for operation with liquid.
3. The scaling of elements is a major problem, particularly when going from laboratory models to miniature sizes.
4. More compatible electrical to fluid and fluid to electrical transducers are required. Many of the presently available transducers utilize a mechanical interface, which detracts from the reliability of the devices.
5. Several passive circuit elements are required, in particular, a wide range laminar flow restrictor, a series capacitance, an efficient nonvented fluid diode, and a sharp cutoff low pass filter.
6. Performance information is needed on fluidic elements exhausting to space vacuum or a controlled back pressure.
7. Consideration needs to be given to shutoff functions and power supplies with no moving parts.
8. Materials, fabrication, and interconnection techniques need to be established which are particularly suited to spacecraft propulsion components. An optimum size and arrangement for fluidic circuit modules should be considered.

9. Analytical design procedures are noticeably lacking. Work needs to be done to establish the analytical techniques and tools that could be used to help synthesize and design fluidic systems from the component level and to reduce the long time, cost, and uncertainty involved with present repetitive "cut and try" methods.
10. Production runs are necessary to provide insight into the reproducibility of elements and ultimate cost - present estimates are misleading.
11. Service data are required on elements and systems before realistic reliability estimates can be made.

Fundamentals and Definitions

Fluidic fundamentals and definitions as determined during the literature search and agency interviews are presented in this section. The intent is to provide common generally accepted ground rules which will enhance the understanding of subsequent tasks undertaken during this study.

The important properties and parameters of fluid mechanics pertaining to fluidics should be understood. This includes a firm understanding of fluid pressure, fluid current, and fluid resistance. A complete discussion of these parameters is incongruous with the objectives of this study program and is adequately covered elsewhere. The reader is therefore directed to Reference 3-1 for a general treatment of fluidic parameters and Reference 3-2 for a more detailed treatment.

The first set of symbols for fluidic circuitry was presented by General Electric personnel at the October 1962, Fluid Amplification Symposium, held at the Harry Diamond Laboratories, Washington, D.C. Since then, the National Fluid Power Association and the Fluidics Panel, SAE Committee A-6, Aerospace Fluid Power Technologies, have both done a great deal of work in the definition of fluidic terminology, symbology, and performance rating. The primary differences between the NFPA Proposed Standard (Reference 3-3) and SAE ARP 993 (Reference 3-4) are in symbology:

1. The SAE uses a circle as the basic symbol, whereas the

NFPA uses a square.

2. The SAE makes maximum use of existing logic standards, whereas the NFPA has redefined all of the basic logic functions.

Symbology is still suffering growing pains, but since this study is aerospace oriented, the SAE standards which are generally accepted in the aerospace field would appear more appropriate. The SAE standards have been adopted by the Navy and are soon to be published in MIL-STD-1306, which is very similar to the SAE document.

For reference purposes, the SAE accepted fluidic terminology, nomenclature, drawing techniques, symbology, and definitions of circuit and performance parameters are included in Appendix III-D, Fluidic Standards.

FLUIDIC COMPONENT STUDY

Devices utilizing fluid flow phenomena are fundamental to fluidics technology. Most fluidic elements can be classified in one of the following categories: digital devices, proportional devices, passive elements, and interface devices. These basic building blocks of the technology can perform a variety of circuit functions. Consequently, an understanding of the operating principles, performance, and limitations of these elements is essential to their successful application, and to the analysis, design, and test of circuits.

In this section, a Fluidic Component Rating Analysis Chart is presented as a summary of the state-of-the-art performance of the most common fluidic devices relative to various propellants, specific functional parameters, and the space environment. The theory of operation, configuration, and applications of each of the devices are covered, also state-of-the-art performance and expected performance gains in the next five years. Subsequently, component fabrication and materials and component performance relative to propellants, specific functional parameters, and the space environment are discussed. The literature and patent searches, the agency surveys, component evaluations, and analysis were all used to support the discussion.

Component Rating Chart

The Fluidic Component Rating Analysis Chart is presented as a management aid in defining the state-of-the-art of basic fluidic devices and interface elements relative to propellant compatibility, functional parameters, and space environments. This chart, Table 3-I, presents ratings which are the best estimates based on the results of the literature and patent search, agency interviews, in-house evaluation, and performance analysis. The space environment data used for this rating chart were based on the Aerojet-General report, NASA CR-294, "Engine Operating Problems in Space - The Space Environment."

Reliability ratings assigned to the various combinations of fluidic components, propellants, and parameters have the following definitions:

<u>RATING</u>	<u>DEFINITION</u>
1	Poor - a serious problem exists for which there is no satisfactory solution.
2	Fair - a problem exists, but a remedy may be available.
3	Satisfactory - i.e., within the state of the art.
U	Information upon which to make a judgement is unavailable.
NA	Combination is not applicable.

TABLE 3-1. FLUIDIC COMPONENT RATING ANALYSIS CHART

[illegible]

Fluidic Components

Wall-Attachment Devices - Wall-attachment devices occupy a very important position in fluidics. These devices provide a fairly high speed of response, average efficiency, and relatively high fan-out. Versatility and relatively good performance in a number of applications are strong recommendations for their continued widespread use. Several basic logic elements utilizing this principle have been developed including a flip-flop, monostable switch, or/nor element, half adder, and a pulse converter.

The Coanda effect is the primary fluid dynamic phenomenon influencing the performance of a wall attachment device. In 1932, Henri Coanda observed that a free jet emerging from a nozzle will tend to follow a nearby curved or flat plate and also attach to and flow along the surface of the plate even though the flow path is divergent to the initial jet direction. Consider a jet emerging into the area bounded by one right angle wall near the direction of jet flow (Figure 3-1).

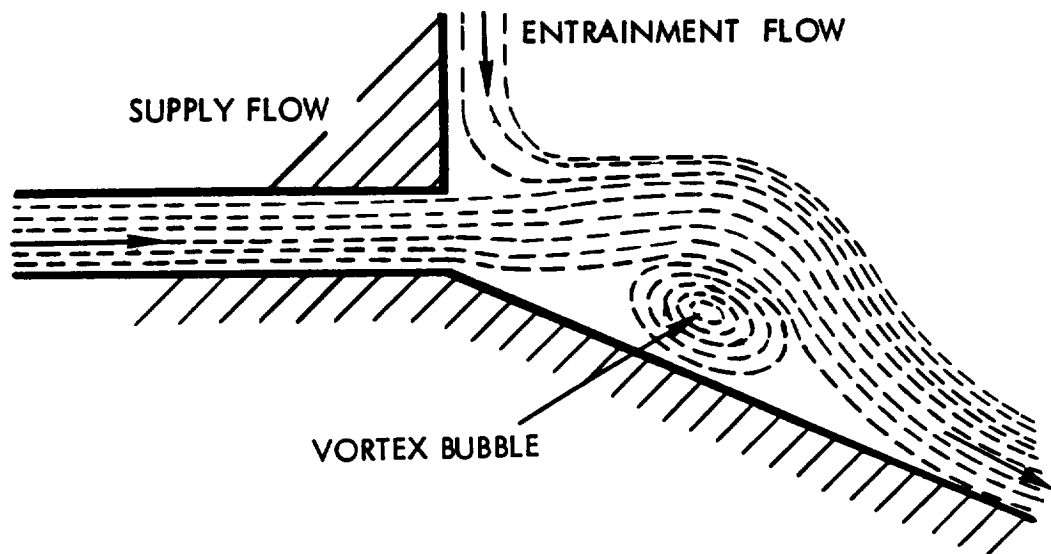


Figure 3-1 Illustration of the Coanda Effect

The emerging jet normally entrains ambient fluid because of high shear at the edges of the jet. This entrained fluid is not easily replaced on the side near the adjacent wall, whereas fluid is easily replaced by ambient fluid on the opposite side of the jet. The result is a transverse pressure gradient across the jet which bends the jet and forces it to attach to the adjacent wall as the entrainment on the adjacent wall side is further reduced. A low pressure vortex region, or bubble, is formed between the jet and the point of attachment, and within the bubble fluid is entrained near the jet nozzle and replenished by separated flow near the point of attachment.

The configuration of the basic wall attachment device is shown in Figure 3-2.

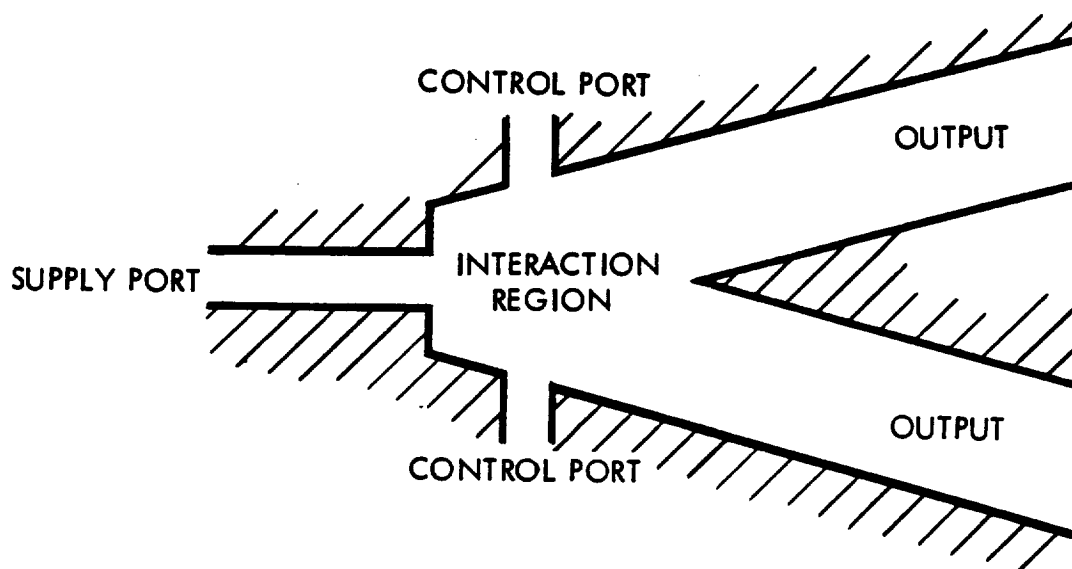


Figure 3-2 Basic Wall Attachment Device

The device utilizes two walls set back from the nozzle, control ports, and channels to define two downstream outputs. The device is bistable, i.e. because of the Coanda effect, a turbulent free jet emerging from the supply nozzle can stably attach to either wall. The operating characteristics of the unit can be varied by the relative position of the splitter with respect

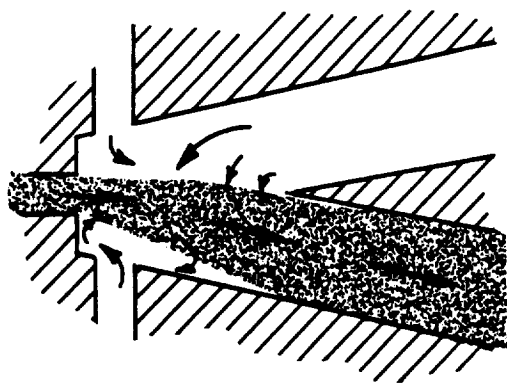
to the power jet nozzle, the control port size, the attachment wall angle, and by asymmetry in the supply port and splitter locations.

The switching mechanism in a bistable wall attachment device is illustrated in Figure 3-3. Presuming the jet is initially attached to the lower wall, fluid is injected through the lower control port into the vortex bubble. When the rate of injected fluid exceeds the rate at which fluid is removed by entrainment, the pressure on the lower edge of the jet will increase. As this pressure becomes greater than the pressure on the upper edge of the jet, the pressure differential is reversed and the jet will detach and cross over to and attach to the upper wall, and will remain attached even after the lower control flow is removed.

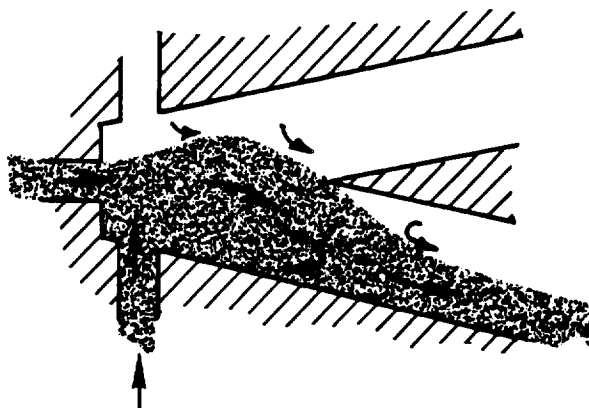
The elimination of load sensitivity has been a major problem in the design of wall attachment devices, since it is impractical to design interconnecting impedances for each separate case. Consequently, most wall attachment elements are vented or bled off to a suitable sink, so that over an appreciable operating range, each element is automatically matched to its applied load. This approach, although inefficient in terms of input fluid power considerations, is quite adequate in many circuit applications where total fluid power is not critical.

The configurations shown in Figure 3-4 are representative of the many methods utilized to decrease load sensitivity in a wall-attachment device. A few examples of the many logic elements which utilize wall attachment principles are shown in Figure 3-5.

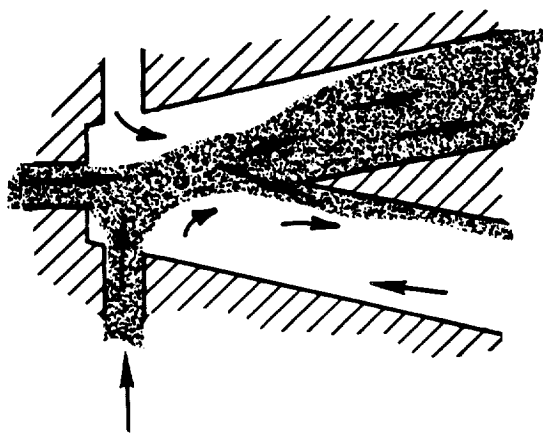
The size of a wall attachment device is established by the width of the power nozzle, i.e., a 10 mil element refers to one which has a power nozzle width of 0.010 inch. Logically all of the internal amplifier dimensions are then defined as ratios of the power nozzle width. Consequently, since most wall attachment elements are two dimensional devices, the depth of the element profile is expressed as the aspect ratio, which is the ratio of the profile depth to the power nozzle width. Normally, these devices are designed with aspect ratios from 1 to 4.



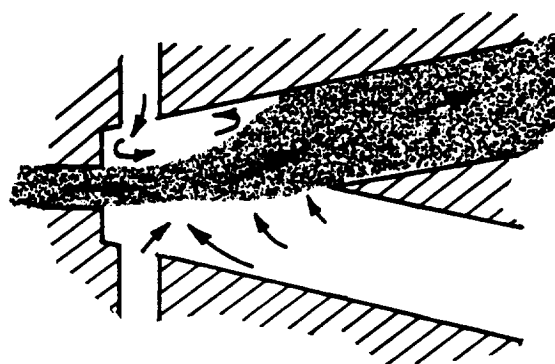
(A)



(B)

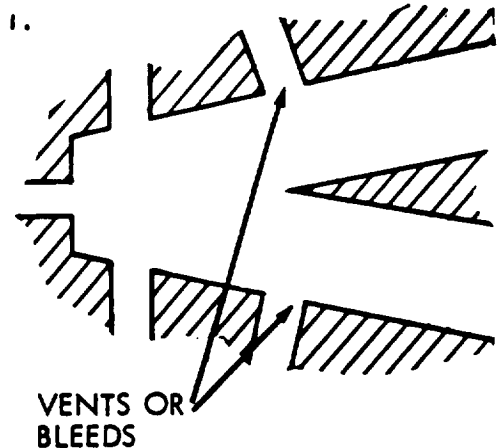


(C)



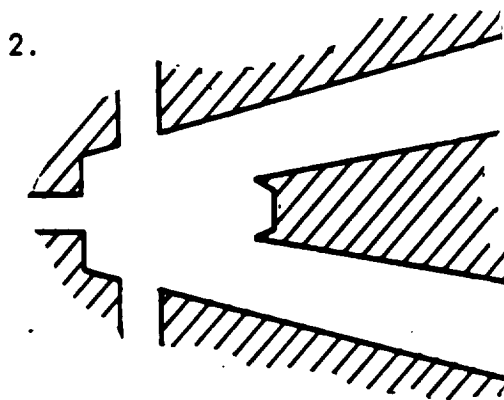
(D)

Figure 3-3 Switching Mechanism in Bistable Wall Attachment Device



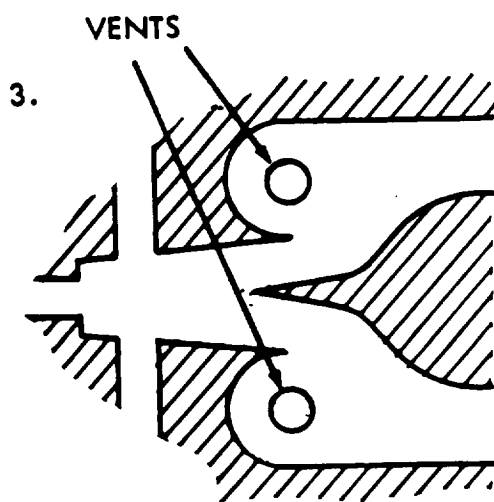
VENTED OUTPUTS

Vents or bleeds in the output channels isolate the interaction region fairly well from downstream conditions.



CUSPED SPLITTER

The cusp in the splitter generates a latching vortex on the passive output side of the power jet, consequently, the pressure, flow, and power recovery of the device are considerably increased. In addition, the active and passive output ports are effectively decoupled.

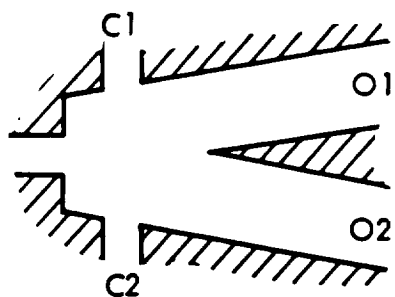


LATCHED VORTEX VENT

This vent configuration allows impedance matching over a wide range of load conditions, from zero load up to and including reverse flow into the amplifier. Compression pulses propagated back into the amplifier interaction region are also attenuated.

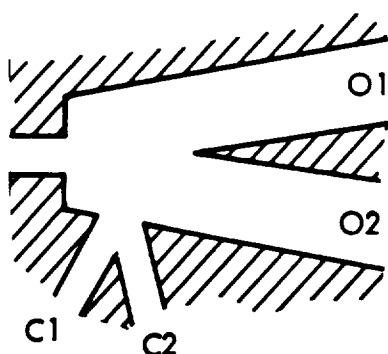
Figure 3-4 Methods of reducing Load Sensitivity

1. FLIP FLOP



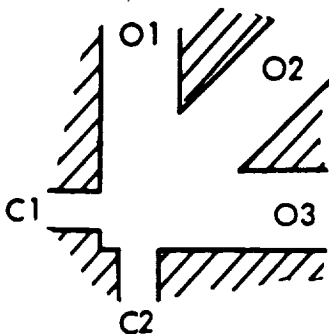
C1	C2	O1	O2
X	O	O	X
O	O	O	X
O	X	X	O
O	O	X	O

2. OR-NOR GATE



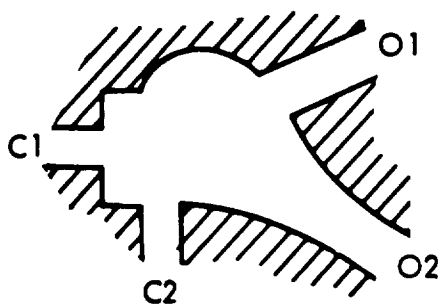
C1	C2	O1	O2
O	O	O	X
X	O	X	O
O	O	O	X
O	X	X	O
O	O	O	X
X	X	X	O

3. AND GATE



C1	C2	O1	O2	O3
X	O	O	O	X
O	X	X	O	O
O	O	O	O	O
X	X	O	X	O

4. HALF ADDER



C1	C2	O1	O2
O	O	O	O
X	O	O	X
O	X	O	X
X	X	X	O

Figure 3-5 Wall Attachment Logic Elements

Performance considered herein is general, and slight performance variations due to aspect ratio (in the range of 1 to 4) were not considered. Quoted performance is for sizes ranging from 10 to 25 mil. The 10 mil size appears to be the smallest practical size. Air was the primary test fluid considered, however, present data indicates that performance with water or other low viscosity fluid should be similar except that time response may be considerably slower.

Time response of a digital element is defined as the time between a measurable change of input signal to a measurable change of output signal when the device is switched with a step input. The load is specified if the element is load sensitive. Changes in design and operating conditions will affect the switching speed of elements, but typical time response for wall attachment elements range from 0.1 to 2 milliseconds. Faster switching speeds have been achieved with high supply pressures (50 psig) and with unstable geometries; however, this obviously is done at the expense of power consumption and reliability.

Time responses of 0.5 to 1 millisecond are state-of-the-art for elements with 10 mil wide power nozzles. Within the next five years switching times should be reduced about 50 percent. However, it must be kept in mind that response time is equal to the sum of the transport time and switching time, where the transport time is the interval between the issuance of a particle of fluid from the power jet nozzle and the arrival of the particle at the output of an element, and is fixed by the geometry of an element. Presuming more efficient element geometries will be designed, the response time of a 10 mil element should decrease to about 0.2 millisecond in the next five years.

Power recovery in nonvented wall attachment devices presently is a maximum of about 50 percent at a pressure recovery of 60 percent. Maximum pressure recovery is about 85 percent at low flow recovery and maximum flow recovery is about 90 percent at low pressure recoveries. Typically, for state-of-the art vented wall-attachment devices, pressure recovery is about 50 percent at near zero output flow and flow recovery is about 85 percent at near zero output pressure.

Fan-in capability of wall attachment devices is limited by the configuration, i.e., there is a practical limit to the number of control input ports which can be present in the interaction region. A fan-in of four is considered state-of-the-art, and potentially this should increase to about eight. Fan-out is defined as the number of digital elements which can be controlled from the output of a single identical element operating at a common power nozzle pressure. Fan-out of up to 32 has been reported, however, present practical fan-out capability is 4 to 6.

Typical pressure and flow gains range from 1 to 15 depending on fan-out. Control pressures of 2 to 15 percent of supply pressure are normally required to switch a device. However, switching pressure can increase up to about 50 percent with increase in fan-out from 1 to 4. Present state-of-the-art for a 10 mil element is a switching pressure 5 to 10 percent of supply for a fan-out of 1.

State-of-the-art performance of bistable wall attachment devices is summarized in Table 3-II along with the expected performance gains in the next five years. Typical performance curves of three commercially available wall attachment elements are shown in Figures 3-6, 3-7 and 3-8.

Table 3-II
Performance of Bistable Wall Attachment Devices

Parameter	State-of-the-Art		In 5 years
	Typical	Best	
Power Nozzle Size (mil)	5 - 40	10	2 - 10
Aspect Ratio	0.8 - 4	1 - 2	1 - 2
Supply Pressure (psig)	0.1 - 40	1 - 10	0.05 - 5
Switching Pressure* (% of supply)	5 - 15	2	1 - 5
Fan-in	2 - 6	4	8
Fan-out	1 - 16	2 - 4	6 - 8
Nonvented Devices:			
Pressure Recovery @ $Q_o = 0$ (%)	60	85	90 +
Flow Recovery @ $P_o \rightarrow 0$ (%)	70	90	80
Power Recovery (%)	40	50	70
Vented Devices:			
Pressure Recovery @ $Q_o = 0$ (%)	25 - 40	50	75
Flow Recovery @ $P_o \rightarrow 0$ (%)	40 - 70	85	90
Power Recovery (%)	20 - 30	30	40 - 50
Pressure Gain	1 - 15	15	25
Flow Gain	5 - 20	20	30
Response Time (millisecond)	0.1 - 2	0.5 (10 mil nozzle)	0.2 (10 mil nozzle)

* For fan-out of 1, i.e., with the control port of an identical device as a load.

Power & Control Nozzles:

.020" wide x .080" deep

Power Nozzle Pressure:

1.5 psig minimum

3.0 psig normal

20 psig maximum

Switch Pressure:

5% to 15% of supply

Pressure Recovery:

33% maximum

Frequency Response over 1000 cps

Fan-out of 4 similar devices

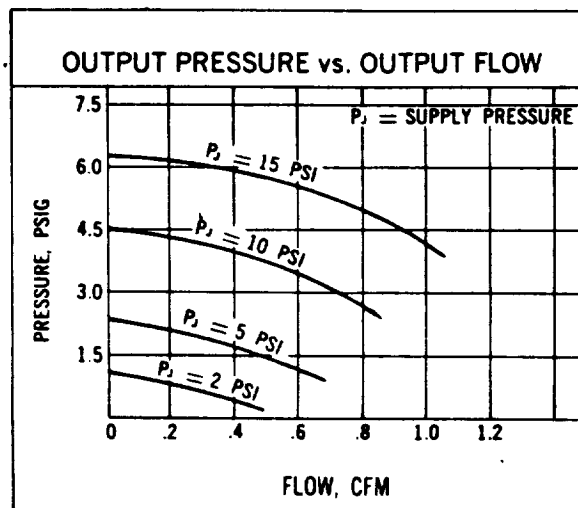
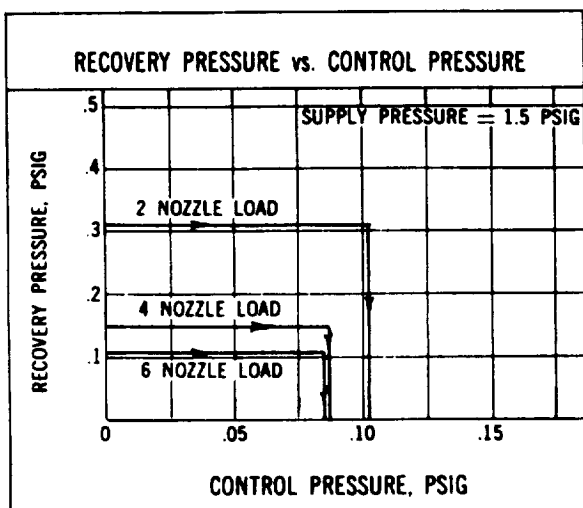
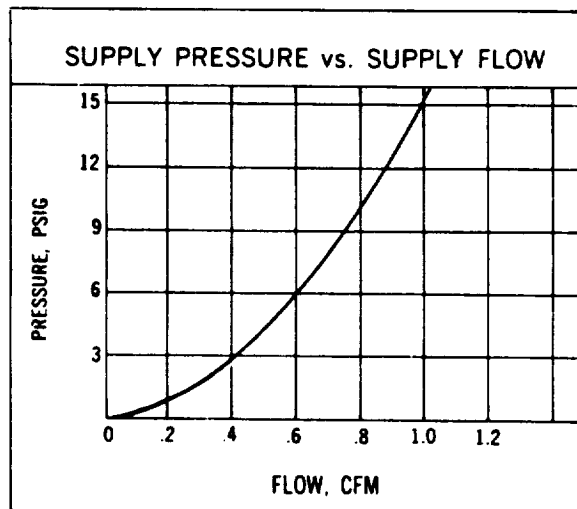


Figure 3-6 Load Insensitive Flip-Flop Performance

(Courtesy of Corning Glass Works)

Power Nozzle:

Flow $W_s = 55 \mu\text{lb/sec}$

Pressure $P_s = 1.0 \text{ psig}$

Notation:

P = Pressure

W = Flow

R = Flow Resistance

Subscripts:

s - Supply

c - Control

o - Output

NOTE: R_L is a load approximating the flow resistance of a control port of an OR/NOT element operating at the same supply pressure.

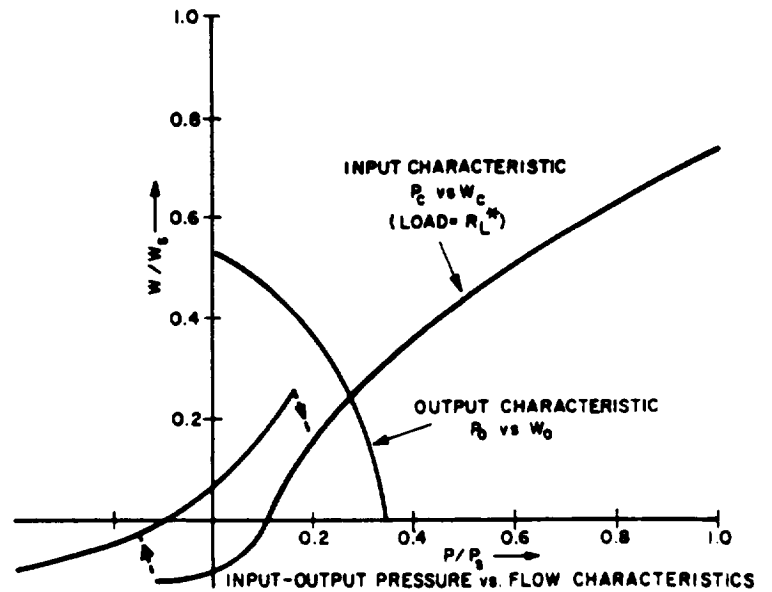
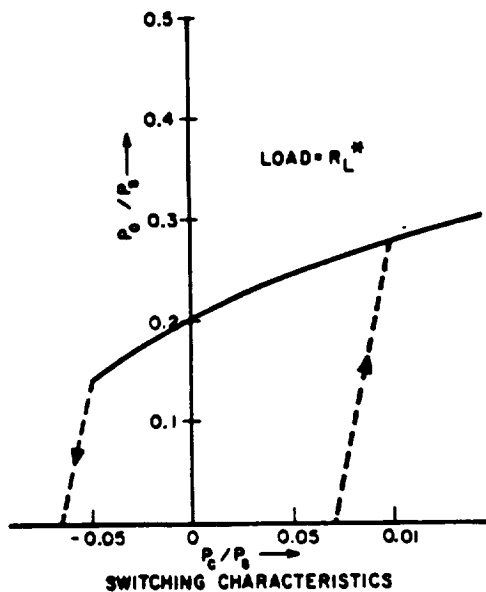
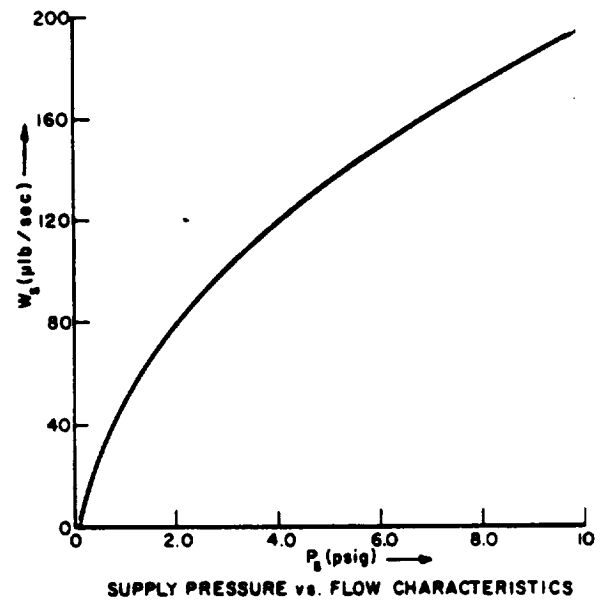


Figure 3-7 Flip-Flop Performance
(Courtesy of General Electric)

Power Nozzle:

Flow $W_s = 135 \mu\text{lb/sec}$

Pressure $P_s = 3.0 \text{ psig}$

Notation:

P = Pressure

W = Flow

R = Flow Resistance

Subscripts:

s - Supply

c - Control

o - Output

Note: R_L is a load approximating the flow resistance of a control port of an identical element operating at the same supply pressure.

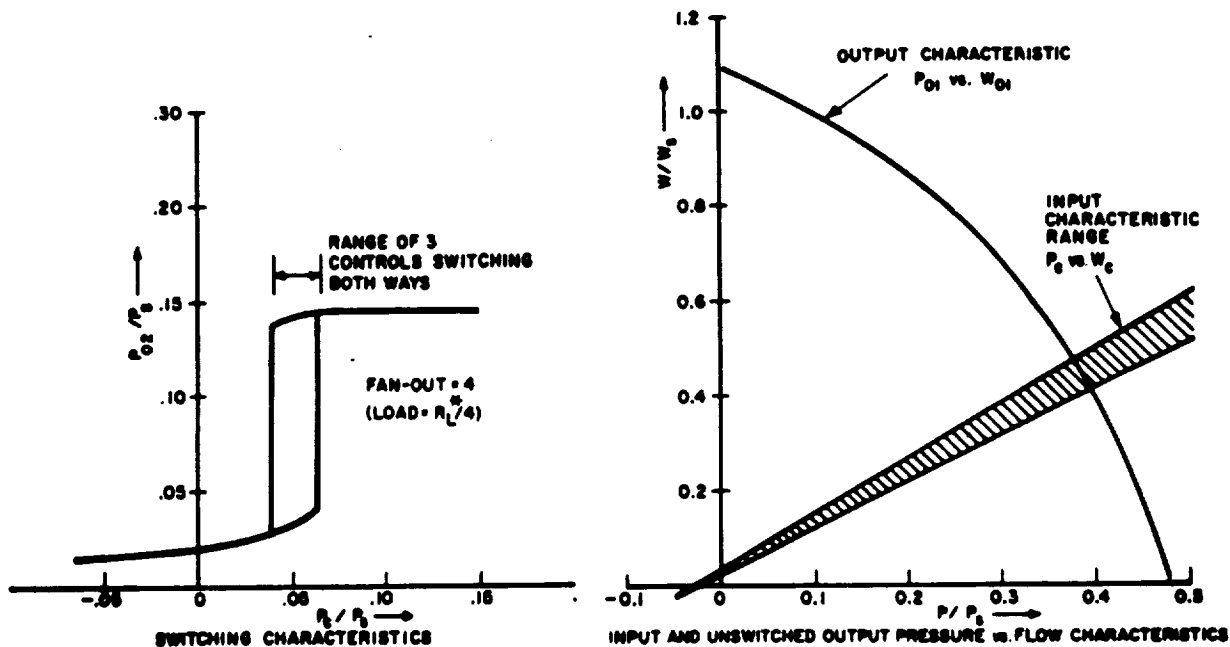
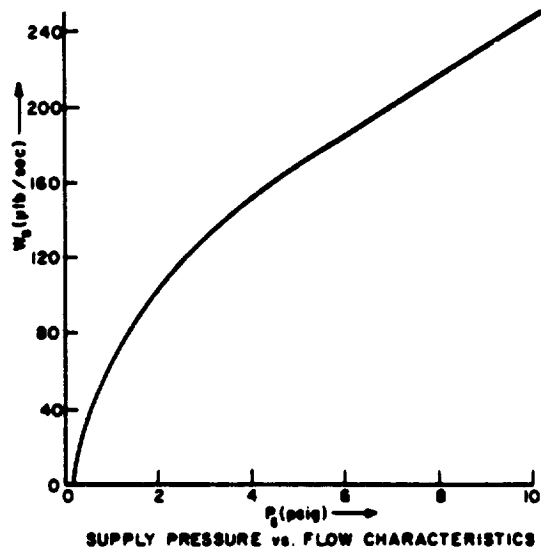


Figure 3-8 Or/Not Performance
(Courtesy of General Electric)

Turbulence Amplifier - The turbulence amplifier consists of a supply tube and an output tube precisely aligned in a vented cavity, and one or more control input tubes perpendicular to the power tube axis. The power jet is introduced into the cavity as a laminar stream, so that in the absence of control flow, much of the original jet power can be recovered at the output. When one or more of the control flows are introduced perpendicular to the power stream, as shown below (Figure 3-9), the jet becomes turbulent before reaching the receiver and the output pressure drops sharply.

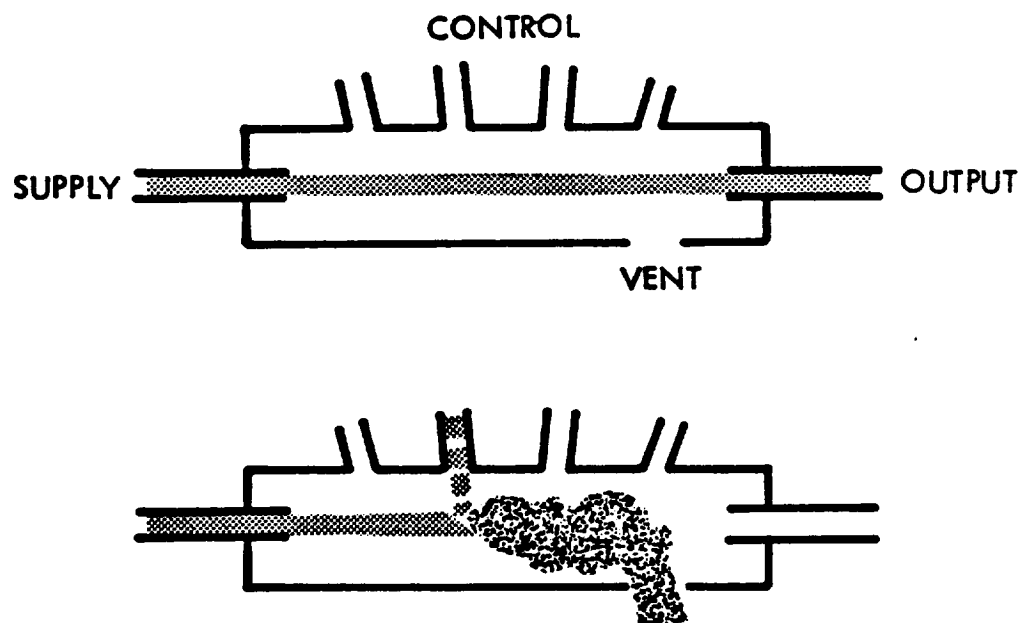


Figure 3-9 Turbulence Amplifier Configuration and Operation

The power supply pressure is normally adjusted so that the laminar jet starts to become turbulent as it enters the output tube. Consequently, only a small disturbance by the control flow will cause the power stream to become totally turbulent.

Time response of the turbulence amplifier is considerably slower than wall attachment devices. Normal switching times are 5 to 10 milliseconds,

and the shortest practical cyclical switching period is about 3 milliseconds, i.e., the relatively long interval (2 to 6 milliseconds) required to re-establish laminar flow after transition to turbulent conditions. It has the advantage of excellent input-output isolation, and typical fan-in and fan-out are 8 to 10.

The major applications for the turbulence amplifier appear to be in the areas of logic, sensing, and counting particularly in industrial areas where its comparatively low speed is adequate. Application of this device in propulsion systems does not appear practical at present, because of the acoustic sensitivity of the power stream which makes it relatively unreliable in severe vibrational and shock environments.

Induction Amplifier - This device is essentially a back-to-back arrangement of two airfoils as shown in Figure 3-10.

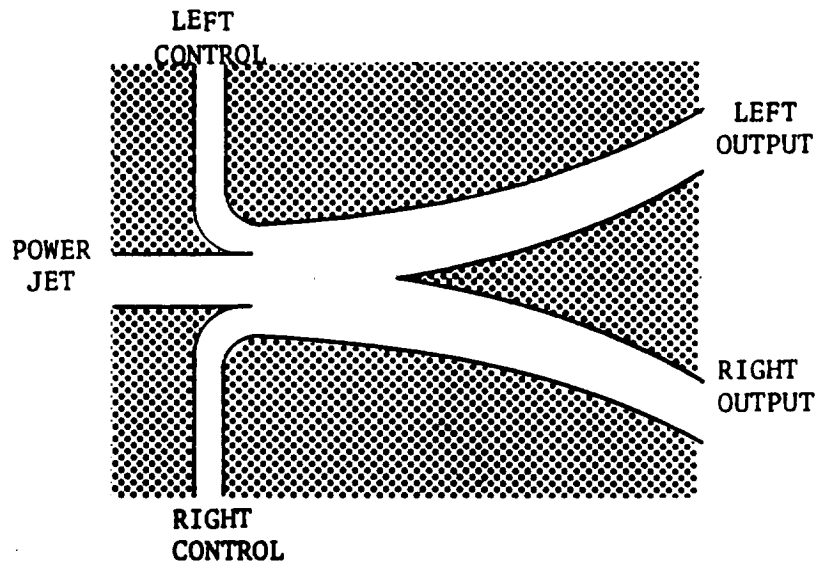


Figure 3-10 Induction Amplifier Configuration

When flow is applied to the power jet, the flow will adhere to one of the airfoil shaped boundaries downstream of the power jet. With flow originally flowing out of the left output duct, to switch the flow a control signal must be applied to the right control duct. The stream from the right control duct adheres to the outside wall of the right output duct. Since the control flow is tangential to the power flow in the interaction region, the transverse pressure gradient is reversed which causes the power jet to switch and flow through the right output duct.

Except for the switching principle, the characteristics of this device are similar to those of the bistable wall attachment amplifier. No performance information is specifically available on this device, although it is expected it would perform somewhat like a boundary layer amplifier. Typical pressure gains are 2 to 3, flow gains 20 to 30, and power gains 60 to 80.

Edgetone Amplifier - The edgetone amplifier is a high-speed planar flip-flop which uses a fluid dynamic phenomenon called the edgetone effect. To understand the effect, consider a fluid jet impinging on a wedge. Under the proper conditions, the jet will continuously oscillate back and forth across the wedge tip, shedding a vortex on each side. In the edgetone amplifier, as shown in Figure 3-11, the power jet stably oscillates between the wedge shaped splitter and the cusp of the output duct in use, until a signal is applied to the control duct to switch the flow.

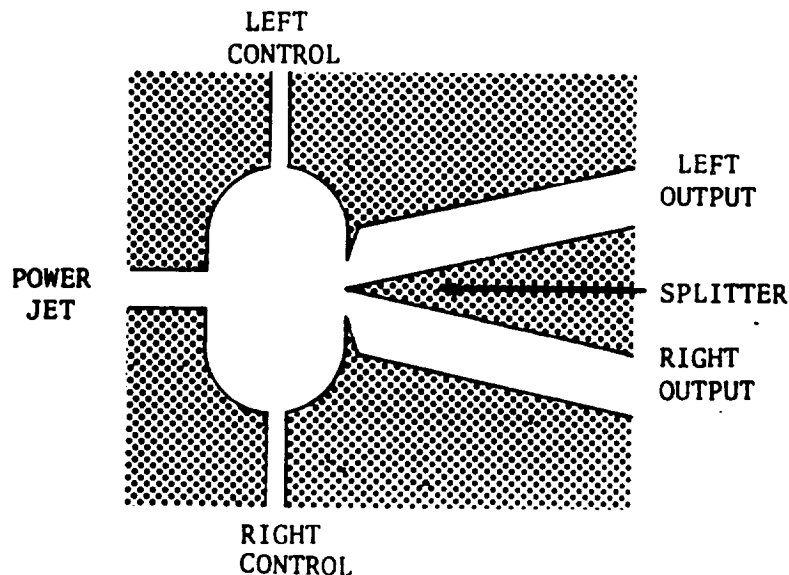


Figure 3-11 Edgetone Amplifier Configuration

A relatively small signal is required to switch the output, because the power jet is oscillating. The primary functional difference in the edgetone amplifier from a typical wall attachment bistable element, is the 0.1 millisecond or less switching time for a typical device. Little information about this device is presently available, and apparently it is not in widespread use. The possible reasons are low signal to noise ratio and reduced reliability in shock and vibrational environments.

Focused Jet Amplifier - Operation of the focused jet amplifier is based on the tendency of an inwardly directed annular jet to adhere to the upper surface of a flow separator by wall attachment and to form a focused jet (Figure 3-12), which is collected at the output tube. When an annular control signal is present it prevents collapsing of the power jet and the flow is directed away from the output tube so that the output is greatly reduced.

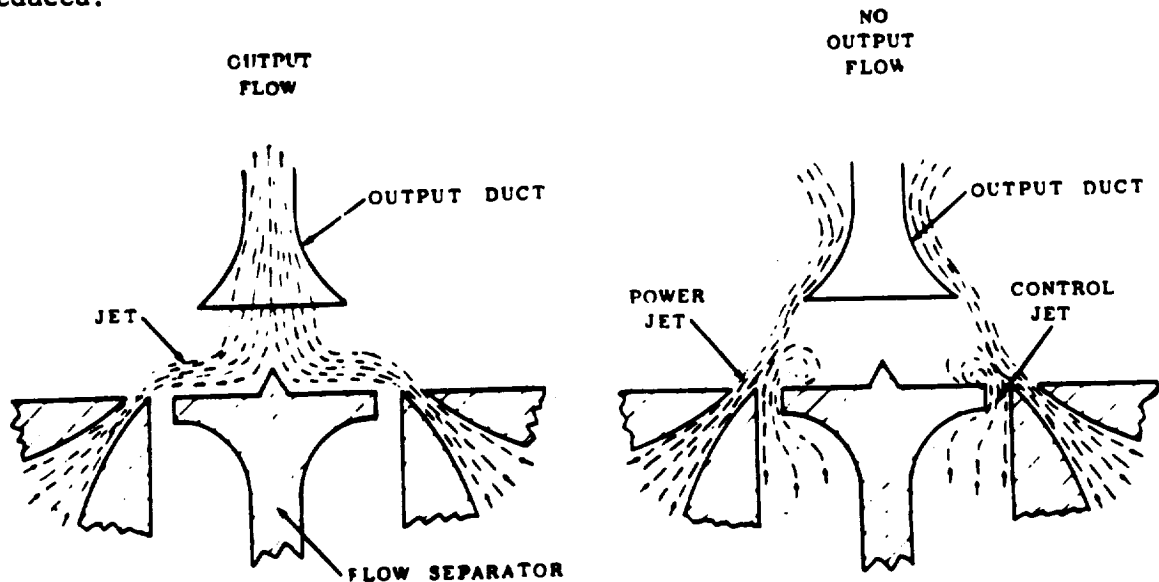


Figure 3-12 Focused Jet Amplifier Configuration and Operation

Operating pressure range of this device is 3 to 14 psig. However, a large volume flow is required because of the large aspect ratio. Switching speeds range from 0.3 to 0.6 millisecond. Fan-in and fan-out capabilities are only average. The switching of the jet is not completely snap action, but the device is not suited for proportional operation.

The high flow requirements with no significant performance gains will limit the application of this device. In addition, the axisymmetric configuration is considerably more expensive to manufacture than a two-dimensional bistable element.

Stream Interaction Amplifier - The stream interaction amplifier fulfills many critical system functions. The amplifier is particularly suited to applications in which the input control signals are continuously compared and continuous proportional output changes are required. Applications include sensors, stabilization systems, speed control, temperature control, pressure control, and analog computation. Proportional deflection of the power jet is achieved in the stream interaction amplifier because of changes in the control stream energy level. This has given rise to a variety of terms to describe the main operating principle. These include beam deflection, stream interaction, momentum exchange, and jet-on-jet.

For proportional operation, a device is specifically designed to avoid the Coanda effect. This is done by shaping the interaction region so as to prevent wall attachment (Figure 3-13). The entrainment requirements of the power jet are then easily satisfied, since under normal operating conditions there is no effective limitation on the rate at which ambient fluid can be replaced in the side regions.

The shape and dimensions of the cutout areas have considerable influence on the performance of the amplifier. Any fluid that is not picked up in the outputs must be removed efficiently and with minimum disturbance. Any disturbance can be reflected from the walls of the interaction region back toward the power jet to produce a feedback effect, which could result in unstable operation, oscillation, or reduced gain. The two side regions of the interaction region are either connected together or vented to atmosphere so as to equalize the pressure against the power jet. The stream interaction amplifier is also extremely sensitive to high impedance loads which present a problem even when the bleeds are adequate. A center dump or bleed port is often used between the output ports to help alleviate this effect.

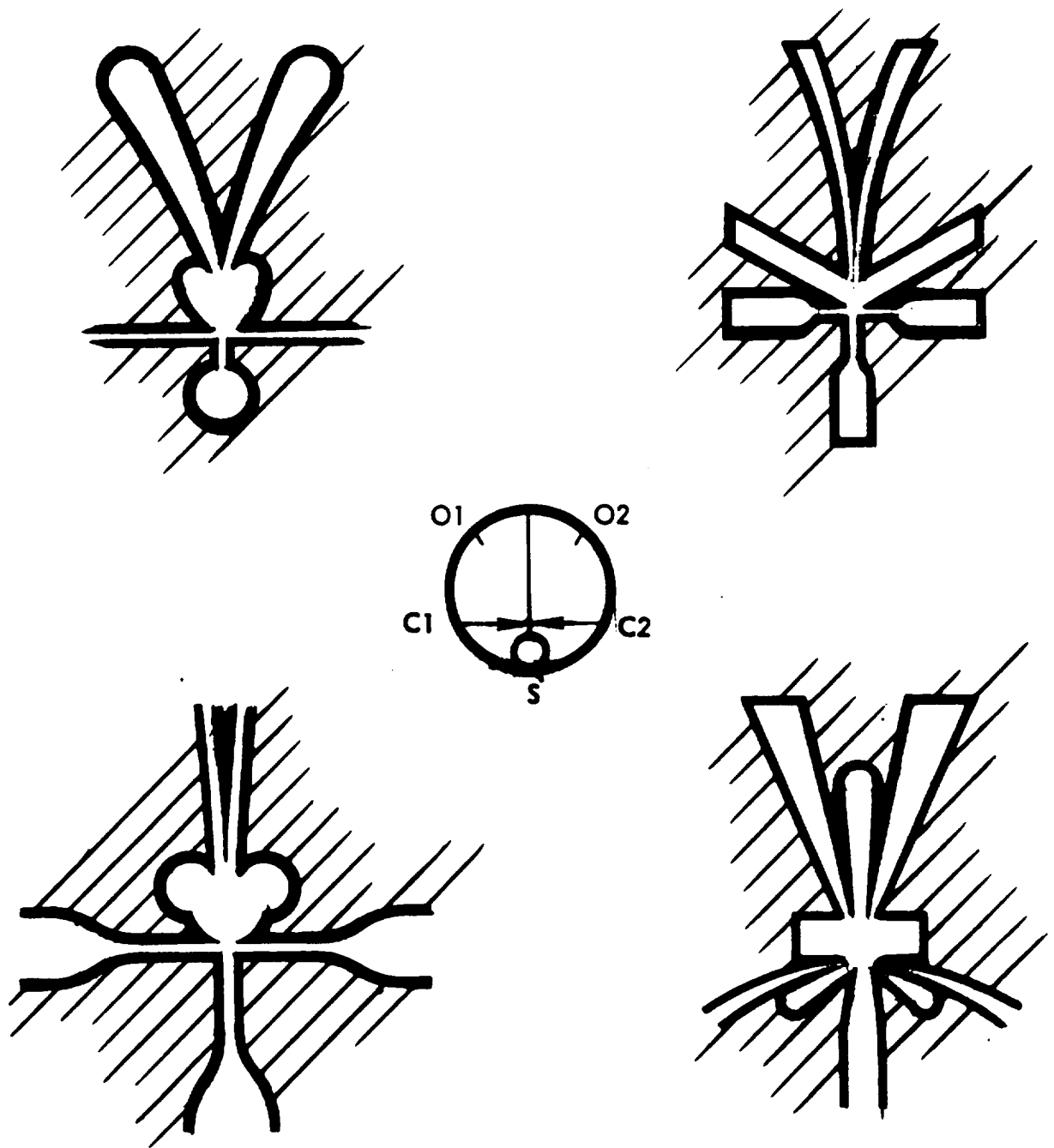


Figure 3-13 Proportional Amplifier - Interaction
Region Shapes

Control ports are located on either side of the power input nozzle as shown in Figure 3-14.

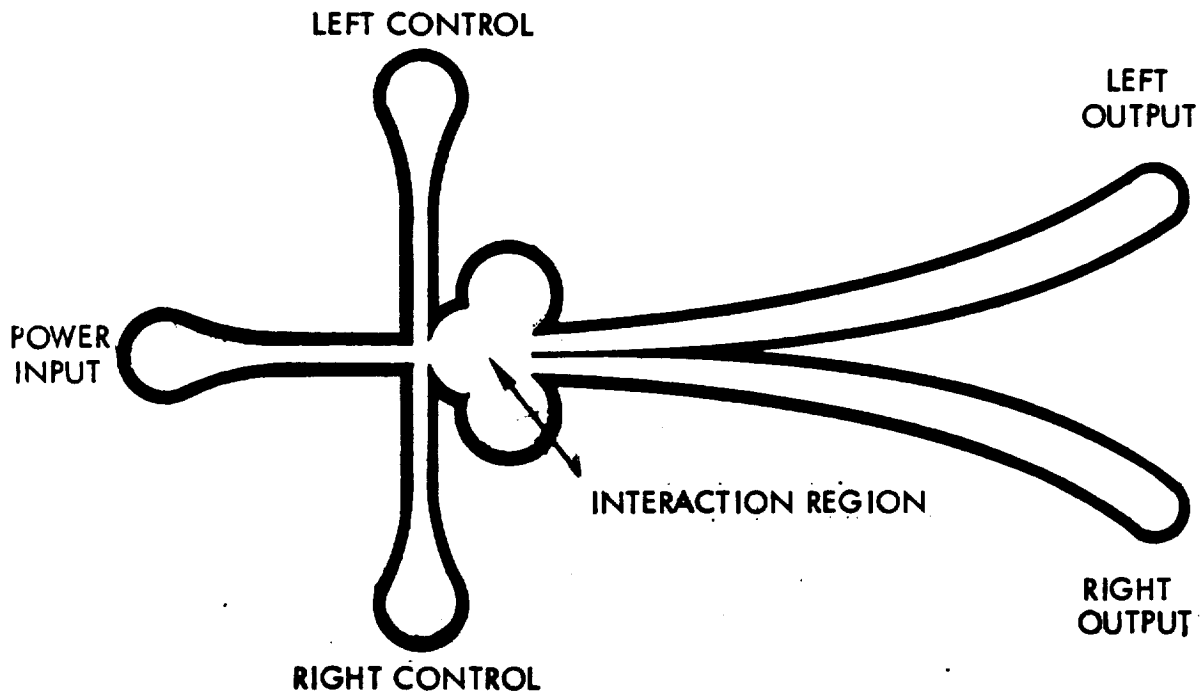


Figure 3-14 Proportional Amplifier Configuration

With equal or no control flow present, the jet input flow crosses the interaction region, strikes the splitter, and flows equally out through the two outputs. When a center dump is used, a large percentage of the flow vents through the center dump and the remainder is equally divided between the two outputs. If one control force is made greater than the other, the power jet is deflected away from the center line in the direction of the weaker force and a greater portion of the jet enters the output receiver on that side. The deflecting force of the control streams may be either a pressure force or a momentum flux force; both types are present in all stream interaction amplifiers. In general, momentum forces predominate when the controls are set back several nozzle widths from the power jet, and the pressure force is increased as the controls are brought closer to the edge of the power jet.

Stream interaction amplifiers are generally proportional and two dimensional

and are sized the same as a wall attachment device, i.e., by the power nozzle width and the aspect ratio. Performance is affected by the aspect ratio, the control location and direction, output and vent locations, and the configuration of the interaction region.

Pressure gain is usually the parameter of general interest, but there are several other important criteria which should be considered before a fair judgement can be made, i.e., flow gain, power gain, pressure recovery, linearity, etc. Of course, optimum pressure gain is achieved at the expense of flow and power gain, so that a useful amplifier must be a compromise between the three. The theoretical maximum pressure gain for momentum deflection devices is about 20, but when the pressure forces are included no theoretical limit presently exists.

Signal-to-noise ratio usually becomes the most important criterion, and it is felt this ratio should be greater than 100, and in some cases 150 to 200 has been achieved. Noise is defined as the peak-to-peak pressure fluctuations measured at null and full output, from zero to about 100 cps when working into a load equivalent to one-third the power nozzle area.

The present state-of-the-art performance of stream interaction proportional amplifiers is summarized in Table 3-III, along with the expected performance gains in the next five years. Typical performance of three commercially available amplifiers is shown in Figures 3-15, 3-16 and 3-17.

Table 3-III
Performance of Stream Interaction Proportional Amplifiers

Parameter	State-of-the-Art		In 5 Years
	Typical	Best	
Power Nozzle Size (mil)	5 - 40	10	5
Aspect Ratio	1 - 3	2	1 - 2
Supply Pressure (psig)	1 - 100	1 - 10	1 - 5
Pressure Gain:			
No Load	2 - 15	20	20 - 25
With Equivalent Load	1 - 10	8	12
With Signal to Noise Ratio > 100	1 - 8	6	10
Flow Gain	10	15 - 20	25
Power Gain	50 - 100	150	200
Pressure Recovery @ $Q_o = 0$ (%)	35	50	70
Flow Recovery @ $P_o \rightarrow 0$ (%)	40	50	60
Power Recovery (%)	20 - 30	30	50
Linearity (%) Of Best Straight Line	2 - 5	1	1 - 2
Linear Range (%) Of Supply Pressure	± 25	± 30	± 50
Maximum Range (%) Of Supply Pressure	± 30	± 40	± 60
Operating Frequency-Gas (kc)	0.1 - 5	1 - 2	2 - 6

Power Nozzle:

Flow $W_s = 58 \text{ mlb/sec}$

Pressure $P_s = 1.0 \text{ psig}$

Notation:

P = Pressure

W = Flow

R = Flow Resistance

ΔP = Pressure Differential
between Opposite Sides

Subscripts:

s - Supply

c - Control

o - Output

NOTE: R_L is a load approximating
the flow resistance of a control port
of an identical element operating
push-pull at the same supply pressure.

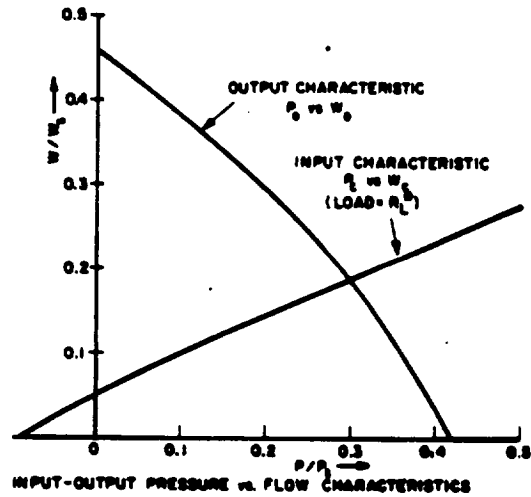
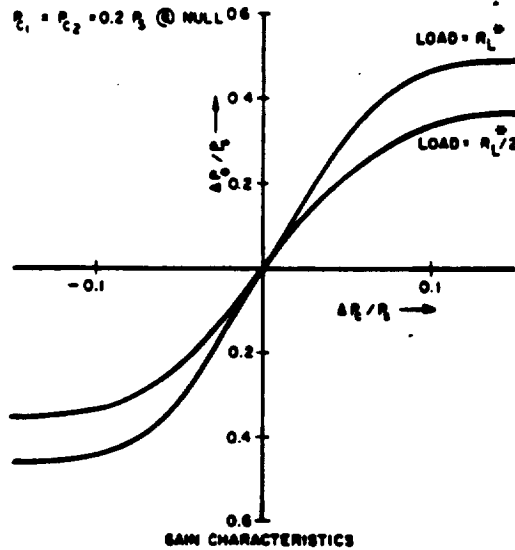
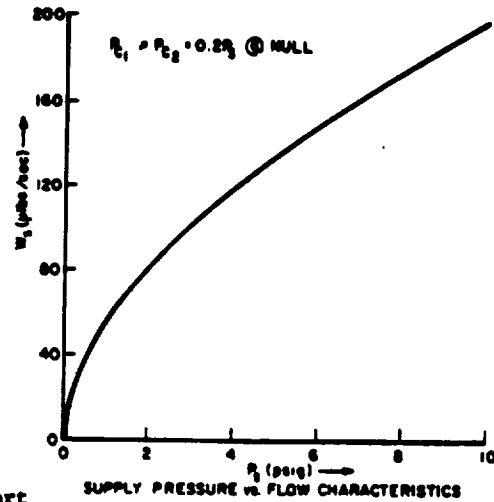


Figure 3-15 Stream Interaction Proportional Amplifier Performance
(Courtesy of General Electric)

Power Nozzle:

Flow $W_s = 58 \mu\text{lb/sec}$

Pressure $P_s = 1.0 \text{ psig}$

Notation:

P = Pressure

W = Flow

R = Flow Resistance

ΔP = Pressure Differential
between Opposite Sides

Subscripts:

s - Supply

c - Control

o - Output

NOTE: R_L is a load approximating
the flow resistance of a control
port of an identical element operating
at the same supply pressure.

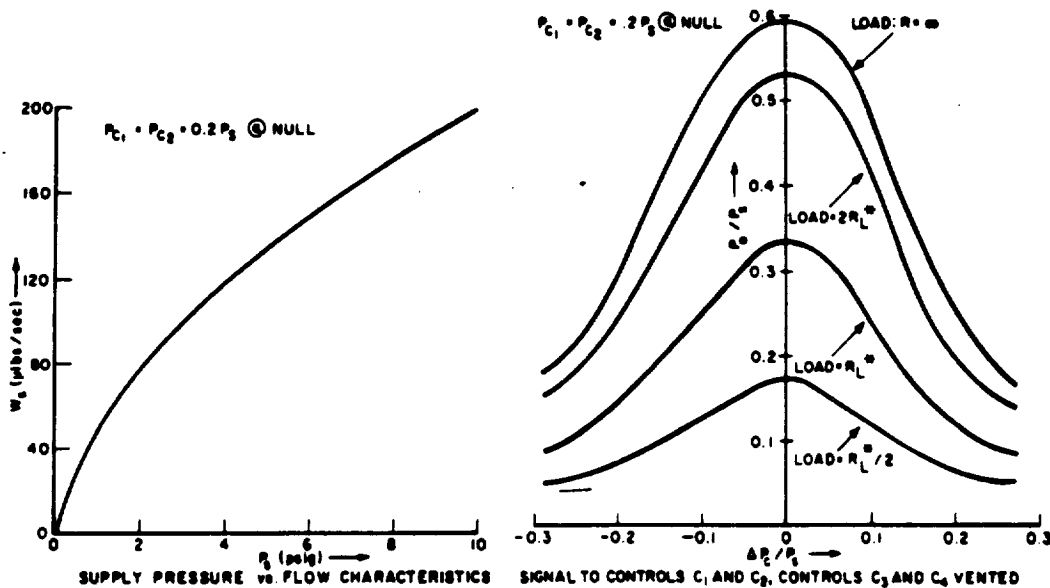
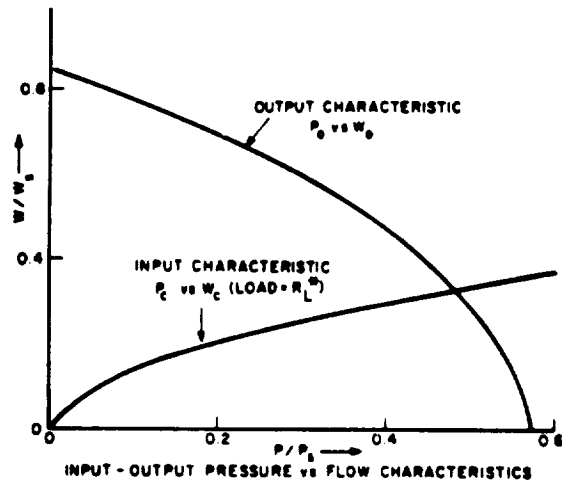


Figure 3-16 Stream Interaction Rectifier Performance
(Courtesy of General Electric)

Dimensions:

Power Nozzle -

.010" wide x .025" deep

Control Nozzle -

.015" wide x .025" deep

Performance:

Power Nozzle Pressure -

5 psi nominal

.1 psi minimum

Pressure Recovery -

25% of supply pressure
maximum (See curve)

Pressure Gain -

6 (max. when $P_c = .1 P_j$)

Frequency Response -

Over 1000 cps

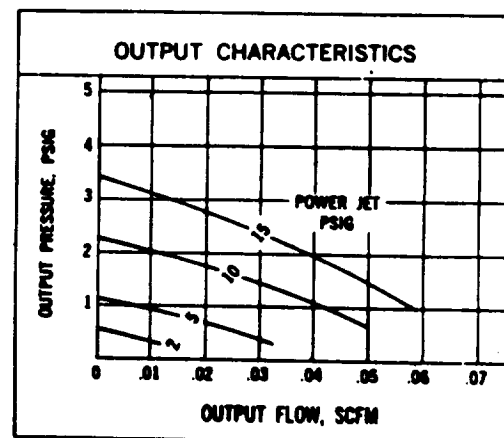
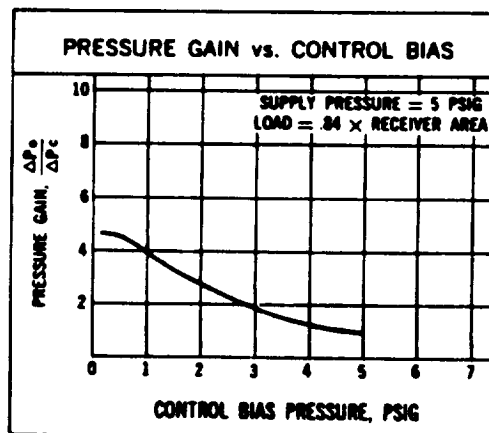
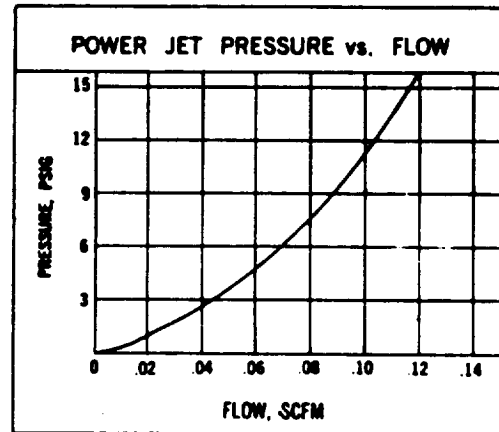


Figure 3-17 Center Dump Proportional Amplifier Performance
(Courtesy of Corning Glass Works)

Vortex Amplifiers - A vortex amplifier utilizes the properties of a vortex to regulate flow. It is a pure fluid device in which a radial primary flow is controlled by a tangential control flow. In operation, the control flow generates a vortex and thereby restricts and reduces the larger primary flow. The modulated primary flow exhibits negative flow gain, since an increase in the vortex generating control flow results in a reduction in the net outlet flow.

Vortex amplifiers will modulate flow from full output down to about 5 to 10 percent of full output. At the lowest output flow the primary flow to the amplifier is essentially zero and the total output flow is supplied almost entirely by the control flow. Vortex amplifiers can control the flow of gases and liquids and consequently have potential application in propulsion system controls. They can be used in hydraulic and pneumatic systems as power stages for driving cylinders and motors and for piloting conventional control valves.

The basic vortex amplifier consists of a cylindrical chamber with supply and control flow inlets and an outlet orifice as illustrated in Figure 3-18.

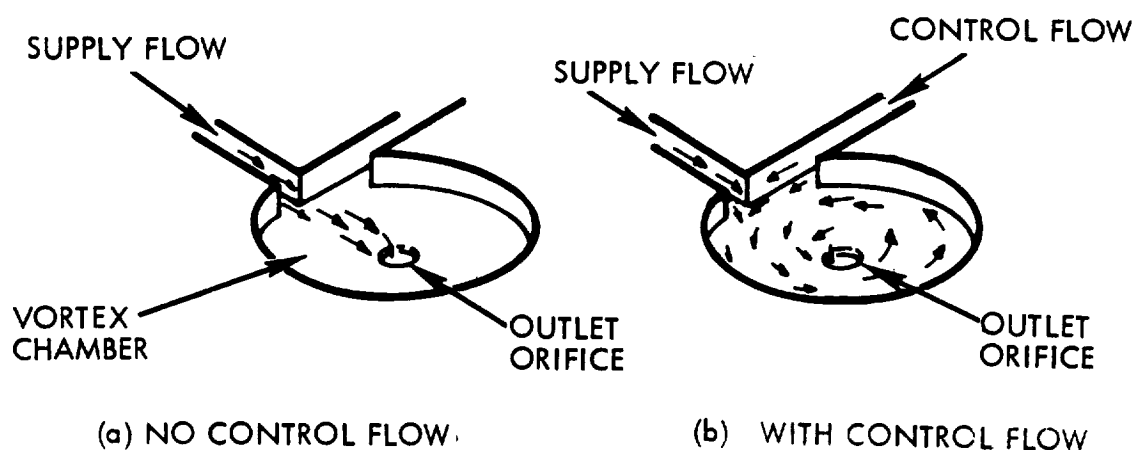


Figure 3-18 Vortex Amplifier Operation

With no control flow present, the supply flow enters the vortex chamber and proceeds radially inward with minimal resistance and flows through the outlet orifice. The supply port is generally much larger than the outlet orifice, so that with no control flow the outlet flow rate is determined by the area of the exit orifice and system pressures. When control flow is injected tangentially into the chamber, a rotational component is imparted to the supply flow. The combined flow has both a tangential and a radial velocity component which must increase as the flow moves inward to conserve angular momentum. Centrifugal force due to the fluid rotation results in a radial pressure gradient, which reduces the pressure differential across the outlet orifice, and thus reduces the outlet flow.

Vortex Valve - The vortex amplifier in its simplest form is shown in Figure 3-19.

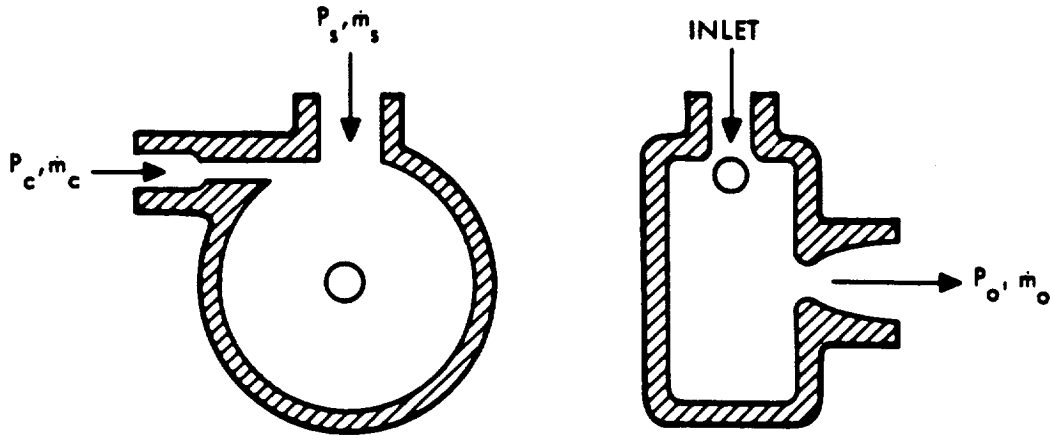


Figure 3-19 Vortex Valve Configuration

This device is known as a nonvented vortex amplifier or vortex valve. In this form, the vortex valve can be easily constructed in a two dimensional configuration, and although performance is not optimized, it is adequate for many applications. In a typical optimized configuration the supply flow is introduced through an annular slot at the periphery of the chamber (Figure 3-20).

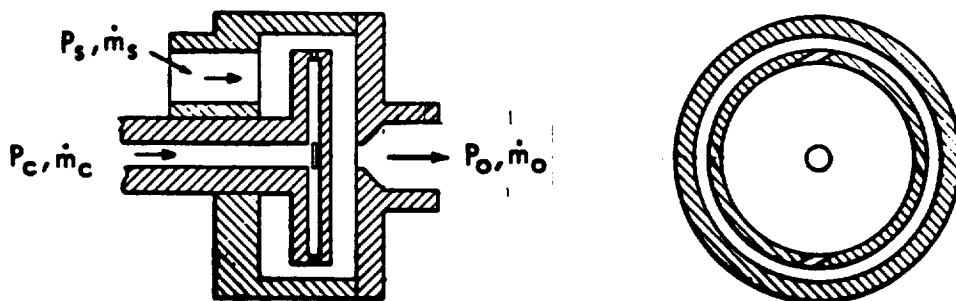


Figure 3-20 Optimized Vortex Valve Configuration

This configuration allows a uniform sheet of supply fluid to enter the vortex chamber and control flow can be introduced at several points. The more uniform the mixing of the control and supply flows, the better the valve performance. This three-dimensional configuration is more complex and consequently harder to build.

A second outlet port can be added to either of the above vortex valve configurations, which will provide a 50 to 75 percent increase in performance. However, this adds further to the complexity of the valve. In particular, it becomes a major design problem to connect the two outlets, which discharge 180 degrees apart, without affecting valve performance.

The static performance characteristics of a vortex valve is conveniently represented by a family of curves of outlet flow, \dot{m}_o , versus supply pressure, P_s , for a constant control pressure, P_c (Figure 3-21). The upper envelope of the curves is the flow characteristic of the outlet orifice when $P_c < P_s$ and presuming that the pressure drop from the inlet of the vortex chamber to the edge of the outlet orifice is negligible. The lower bound of the constant control pressure curves indicates the point at which supply flow is completely shut off and the outlet flow is equal to the control flow. Typical performance curves are shown in Figures 3-22, 3-23, and 3-24.

The most widely used performance criterion of vortex valves is the turndown ratio. This is defined as the ratio of output flow with $P_c \leq P_s$ to the output flow when the supply flow, \dot{m}_s , is zero at a constant supply pressure.

$$\text{Turndown Ratio} = \frac{\dot{m}_o (P_c \leq P_s)}{\dot{m}_o (\dot{m}_s = 0)} \bigg|_{P_s = \text{constant}}$$

A vortex valve can be optimized for maximum turndown by utilizing relatively small control port areas and chamber to outlet hole diameter ratios of less than 8, however, a bistable hysteretic device will result. Normal useful designs are non-hysteretic with minimum noise in the high gain region. To accomplish this:

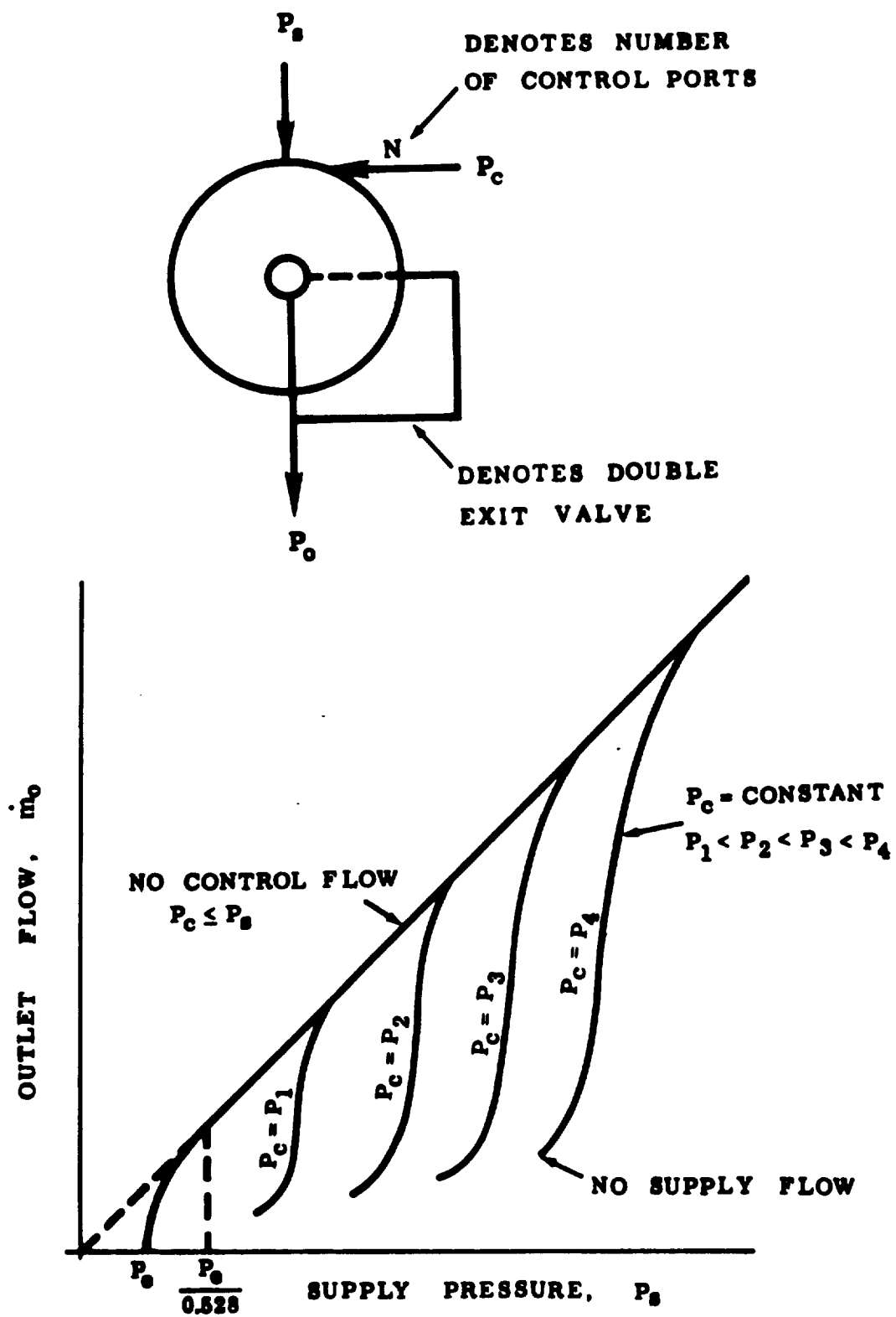


Figure 3-21 Vortex Valve Static Performance Characteristic

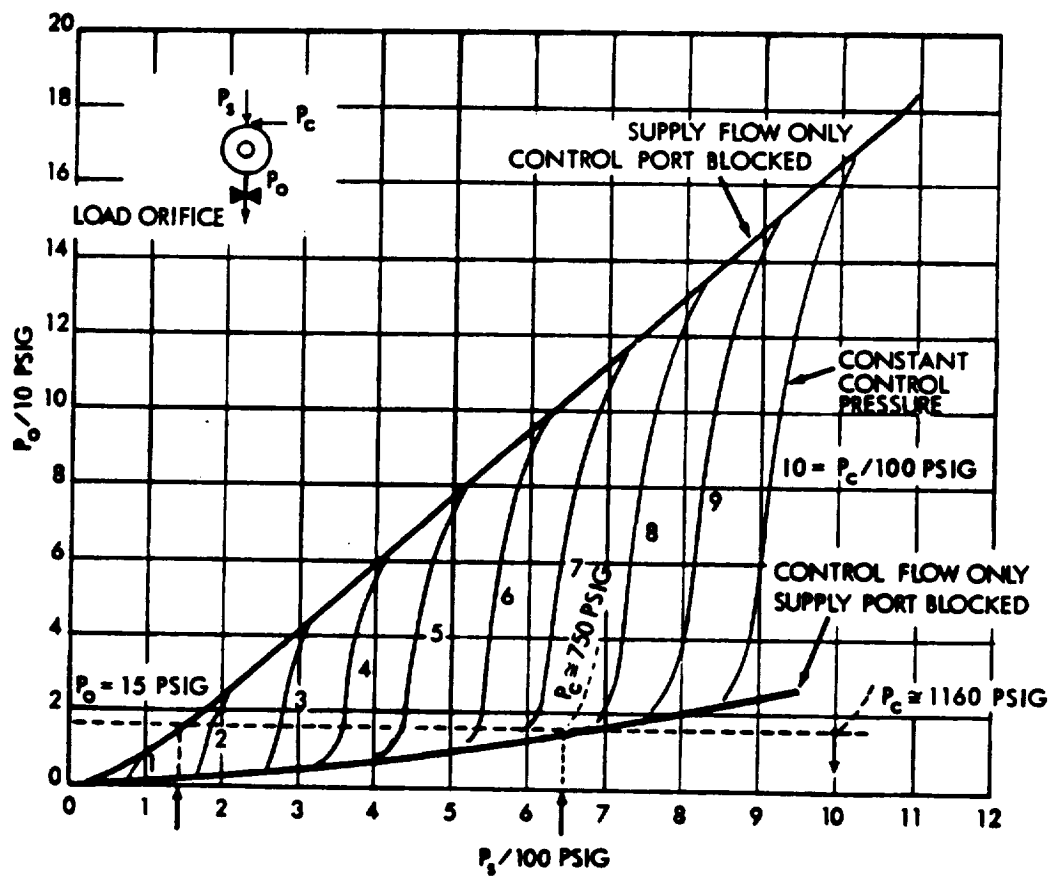


Figure 3-22 Single Exit Vortex Valve Performance
(Courtesy of Bendix)

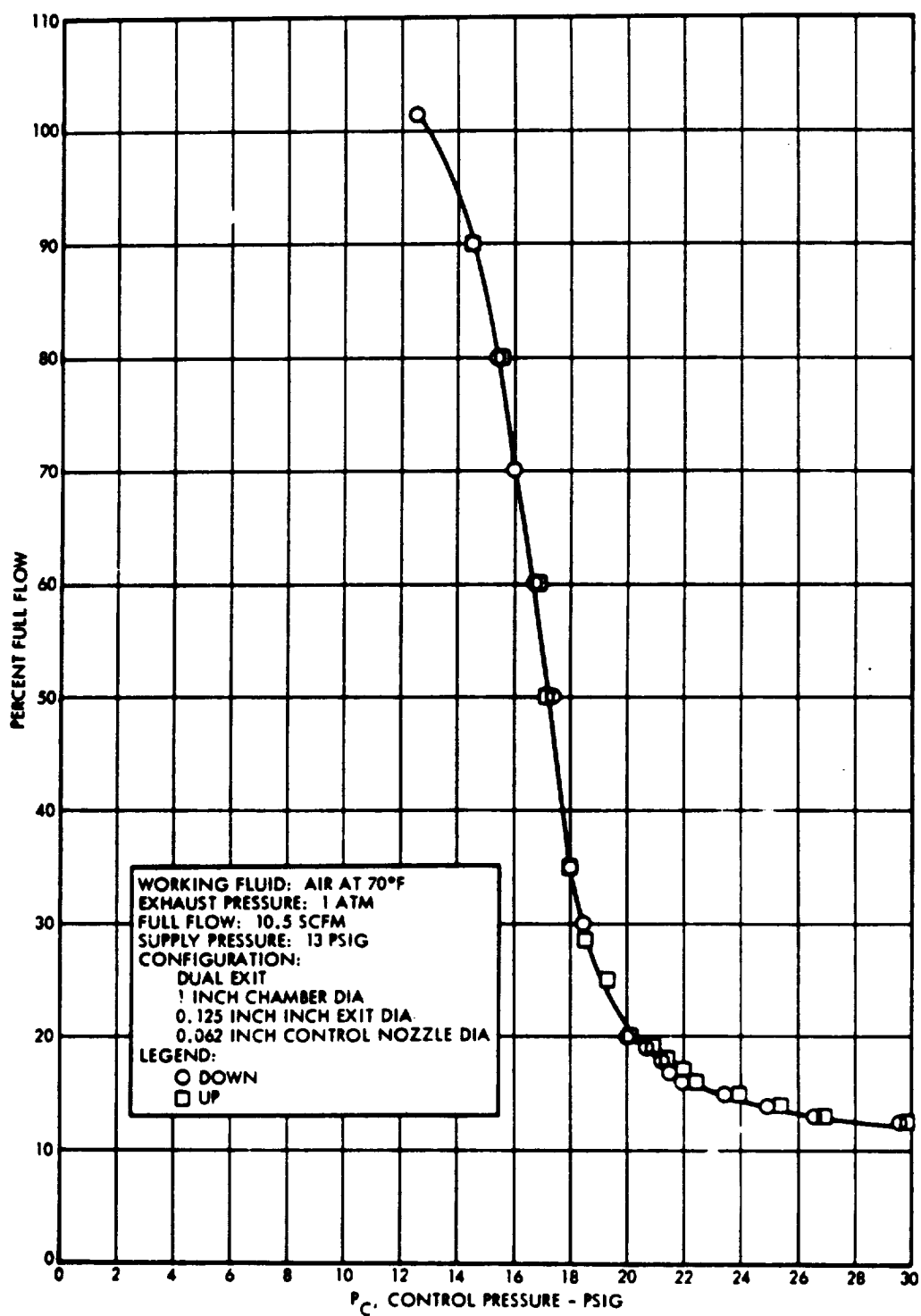


Figure 3-23 TRW Systems Vortex Valve Performance - Unloaded

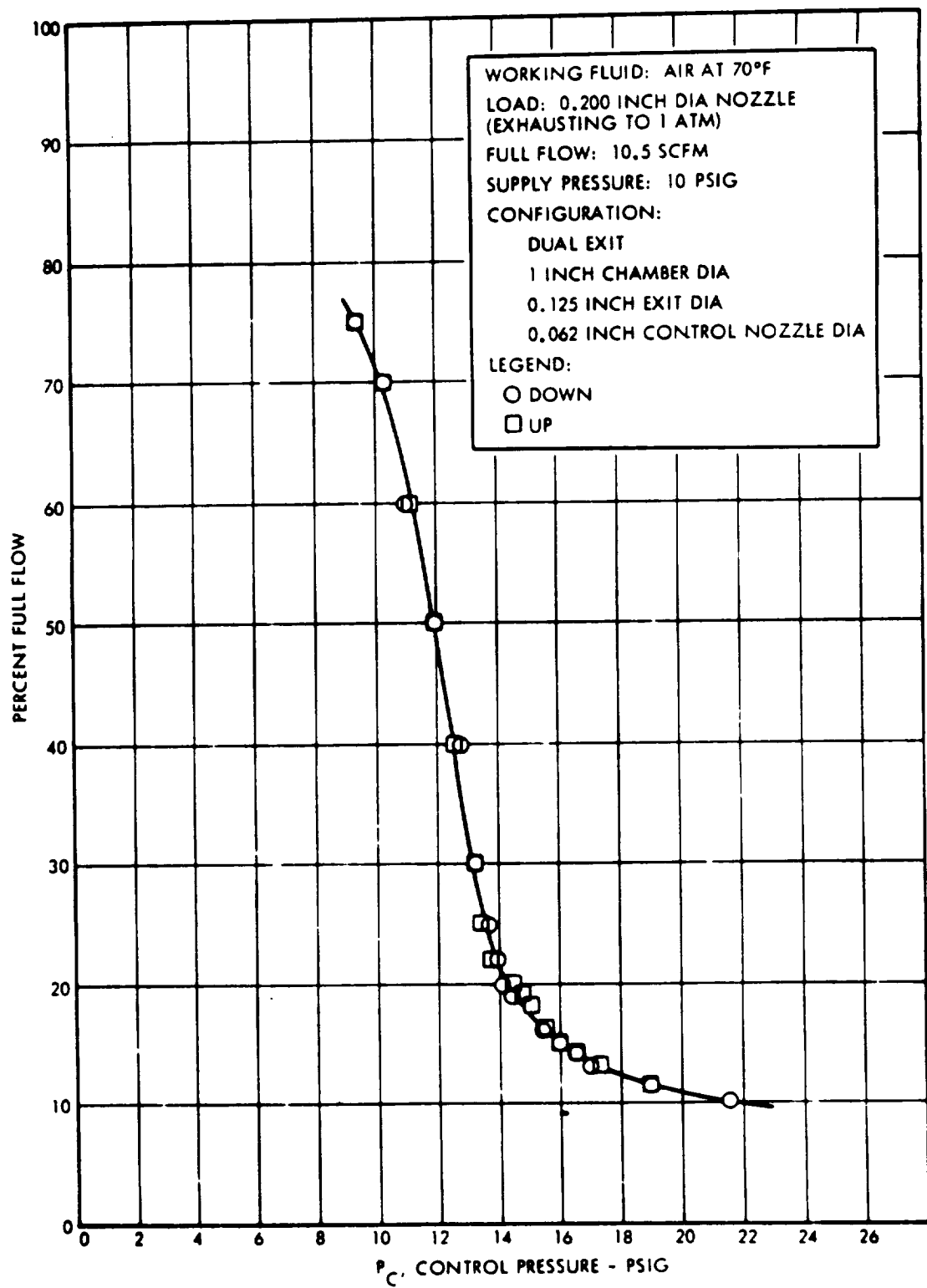


Figure 3-24 TRW Systems Vortex Valve Performance - Loaded

1. Chamber to outlet hole diameter ratio is usually between 8 and 12,
2. Outlet hole to control port area should be about 8, and
3. Chamber length is usually greater than $1/2$ the exit hole diameter.

Since the control pressure must be higher than the supply pressure, a vortex valve cannot operate with full line pressure on its load. Consequently, another important criterion, often overlooked when specifying vortex valve performance, is the control to supply pressure ratio at turndown. This ratio varies from about 1.05 to 2 depending on how the valve was optimized.

Present vortex valve performance is summarized in Table 3-IV along with estimates of expected performance gains in the next five years. Vortex valve sizes are assumed to be about 1 inch. Wall effects become a factor below a chamber diameter of 1 inch and performance will be lower than estimated in Table 3-IV. The outlet orifice is also presumed to be sonic, although performance will improve somewhat with a subsonic orifice. A sufficient number of control nozzles are also required to insure minimum pressure drop and uniform mixing in the vortex chamber.

A vortex valve can operate with any type of fluid. It has been used with gases, water, hydraulic fluids, liquid propellants, and liquid metals. The most efficient operation is obtained with low viscosity fluids such as air and water; modulation range is reduced with the higher viscosity fluids. Units have been built in sizes ranging from 0.072 inch to 9 inch chamber diameter.

One type of vortex valve, the vortex throttle, utilizes a gas to control fluids such as water or liquid propellants. Turndown ratios of up to 50 have been reported for the vortex throttle. This device should find wide application in liquid throttling applications where the mixing of small percentages of gas with the controlled liquid is either not detrimental or beneficial. For instance, low molecular weight gases have been used to stabilize combustion in several small deep-throttling bipropellant rocket engines.

Table 3-IV
Nonhysteretic Vortex Valve Performance

FLUID	P_c/P_s	TURNDOWN RATIO			
		Single Exit		Double Exit	
		S.O.A.	In 5 Years	S.O.A.	In 5 Years
AIR	1.05	2.5	3.5	U	U
AIR	1.2	5.5	7	8	10
AIR	1.5	8	12	11	16
AIR	2	9	14	U	18
WATER	1.05	U	U	U	U
WATER	1.2	7	9	U	12
WATER	1.5	10	15	U	17
WATER	2	12	18	U	20
HYDRAULIC OIL	1.05	2	4	U	6
HYDRAULIC OIL	1.2	7	9	U	14
HYDRAULIC OIL	1.5	11	15	U	19
HYDRAULIC OIL	2.0	U	20	U	22

S.O.A. - State-of-the-art

U - Information presently unavailable

Vented Vortex Amplifier - The vortex valve has a limited range of flow modulation. To overcome this limitation, a vented vortex amplifier utilizes a receiver tube which is located and displaced axially away from the outlet orifice (Figure 3-25).

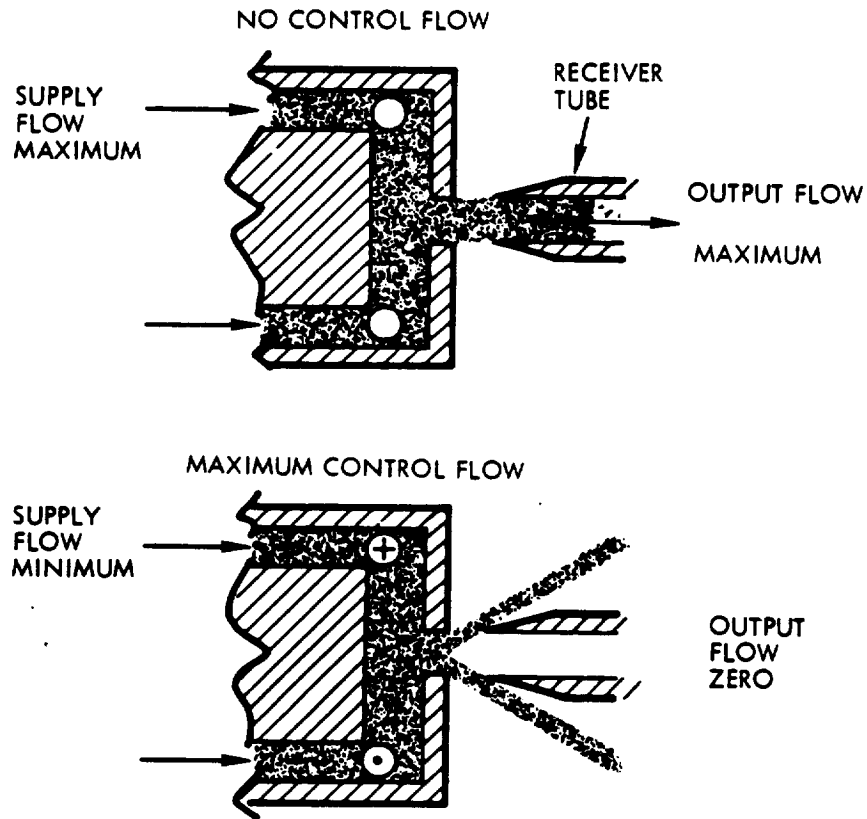


Figure 3-25 Vented Vortex Amplifier Operation

With no control flow to the vortex amplifier, the flow exiting from the vortex chamber is a well-defined jet. This flow is recovered in the receiver tube, and the recovery characteristic is similar to that achieved in a jet pipe. As control flow is applied, a vortex is generated and the flow out of the exit orifice forms into a hollow conical shape, such that some of the flow is diverted to the exhaust. When a sufficiently strong vortex is generated, all of the exiting flow fans out to miss the receiver tube. This then produces a valving action with full modulation of flow to zero.

Conventional vented vortex amplifier nomenclature and symbology are shown in Figure 3-26. The most widely used symbol for a vented vortex amplifier consists of three concentric circles. The largest represents the outer diameter of the vortex chamber; the intermediate circle represents the vent port; and the inner circle represents the load flow receiver. Supply flow is shown by a radial arrow pointing at the outer circle and control flow is shown by an arrow tangent to the outer circle. Load flow and vent flow are shown by radial arrows originating from the inner and intermediate circles respectively.

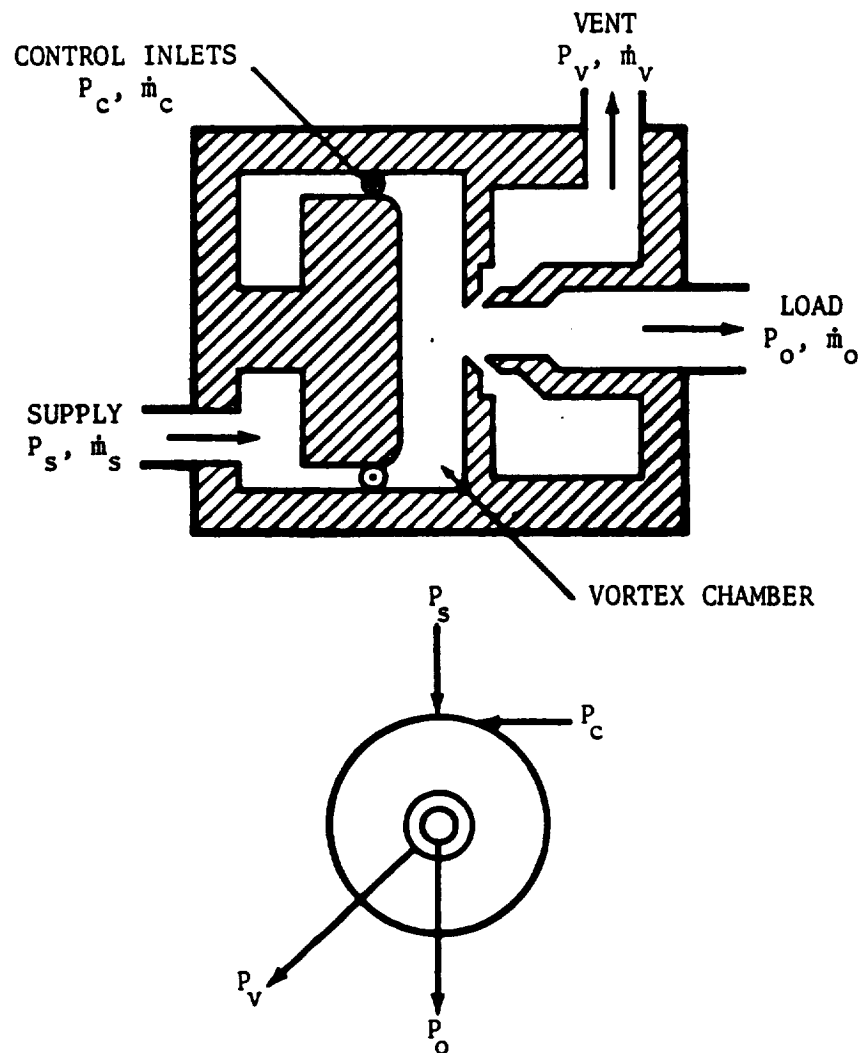


Figure 3-26 Vented Vortex Amplifier-Nomenclature and Symbology

Typical pressure gain characteristics for the vented vortex amplifier at several supply pressures and under blocked load conditions are shown in Figure 3-27.

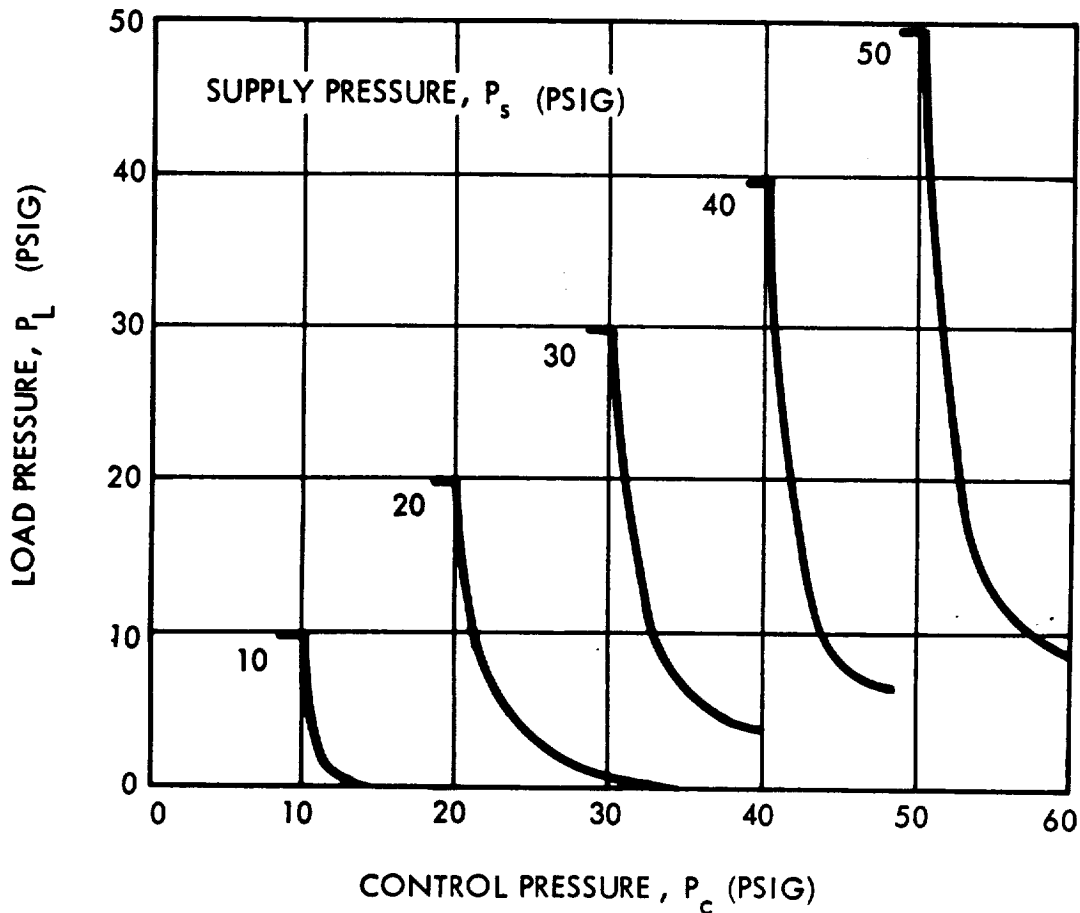


Figure 3-27 Typical Pressure Gain Characteristics
Vented Vortex Amplifier

It should be noted that the control pressure must exceed the supply pressure level before the characteristic turndown pressure recovery curves are achieved; i.e., no incremental gain is exhibited until the control pressure exceeds supply pressure. Consequently, this type of amplifier requires a

bias pressure at the control input higher than the supply pressure. The gain shown by the characteristic curves, i.e., the change in load pressure for an incremental change in control pressure, is about 10.

Other important aspects of properly designed vented vortex amplifiers are as follows:

1. Incremental gain is virtually independent of load over a wide range. Consequently, this type amplifier has a very low incremental output impedance and can be cascaded effectively with virtually no gain loss.
2. Increased vent pressure does not degrade performance.
3. Load output pressure is virtually independent of vent pressure over a considerable range.

The performance of vented vortex amplifiers is hard to define, and is best described by the incremental pressure gain and the power efficiency at the load. The incremental pressure gain is the change in load pressure for an incremental change in control pressure in the linear range of the amplifier. Power is defined as the product of pressure and flow. Load power efficiency is the percentage ratio of delivered load power to output power. Although pressure recovery can be extremely high (95 percent) under blocked load conditions with no turndown, the flow recovery is zero. However, large size ($W_L = 0.5$ lb/sec) vented vortex amplifiers have been operated at a point with flow recovery of about 95 percent and pressure recovery of about 30 percent.

Performance of vented vortex amplifiers is summarized below in terms of useful pressure gain (i.e., capable of driving another stage) and power efficiency at a point.

VENTED VORTEX AMPLIFIER PERFORMANCE

Pressure Gain:

0.25" diameter	500
2" to 3" diameter	5000

Power Efficiency with Gases:

State of the Art	50%
Within 5 years	60-65%

Power Efficiency with Liquids:

State of the Art	65%
Within 5 years	75%

Error detection circuitry is readily implemented with vented vortex amplifiers, since there is sufficient room around the outer periphery of the vortex chamber to accommodate a multiplicity of control ports, which can be arranged to either aid or oppose each other. For instance, the Bendix Research Laboratories have demonstrated the use of up to 16 separate summing control ports on a 1-inch amplifier. This is compared to a typical jet-on-jet amplifier where it is very difficult to sum more than two pairs of control ports without significant loss in gain and pressure recovery.

Vented Jet - The vented jet amplifier, or confined-jet, utilizes the properties of a freely expanding jet impinging on a receiver (Figure 3-28). By confining the jet, and controlling the vent rate of gas from the chamber, useful amplification is achieved. Vented jets have been used to control vortex valves and have exhibited high flow and pressure recoveries in this application. The vented jet is also beginning to find application in fluidic pressure regulation circuitry and servovalves.

To understand the operation of the vented jet, presume that the supply flow is essentially fixed (Figure 3-28) and the output pressure (P_o) and the exit flow are controlled by the vent pressure (P_v), which regulates the spread of the supply jet. With the receiver outlet blocked, i.e. $\dot{m}_o = 0$, a vented jet exhibits three different characteristic regions (Figure 3-29):

1. At low vent pressures there is a region of moderate pressure gain ($\Delta P_o / \Delta P_v$ between 1 and 3), but due to the low vent pressure, the logarithmic gain is poor $\left(\frac{\Delta P_o / P_o}{\Delta P_v / P_v} \right) \sim 1$.
2. At intermediate vent pressures, there is a high gain region which is unstable (at least when using conventional receiver configurations), which for certain geometries can be stabilized by pulling sufficient flow from the receiver.
3. At high vent pressures, there is a stable low gain region ($\Delta P_o / \Delta P_v < 1$).

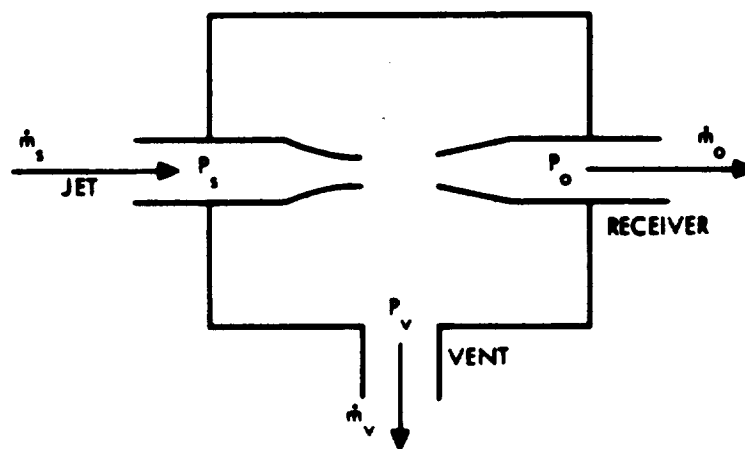
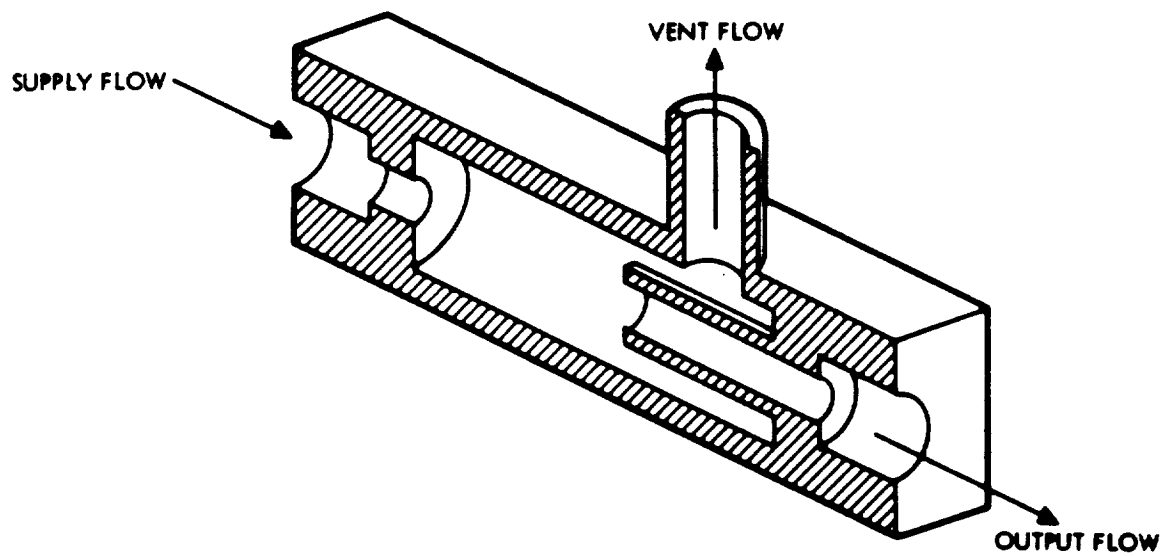


Figure 3-28 Vented Jet Amplifier Configuration

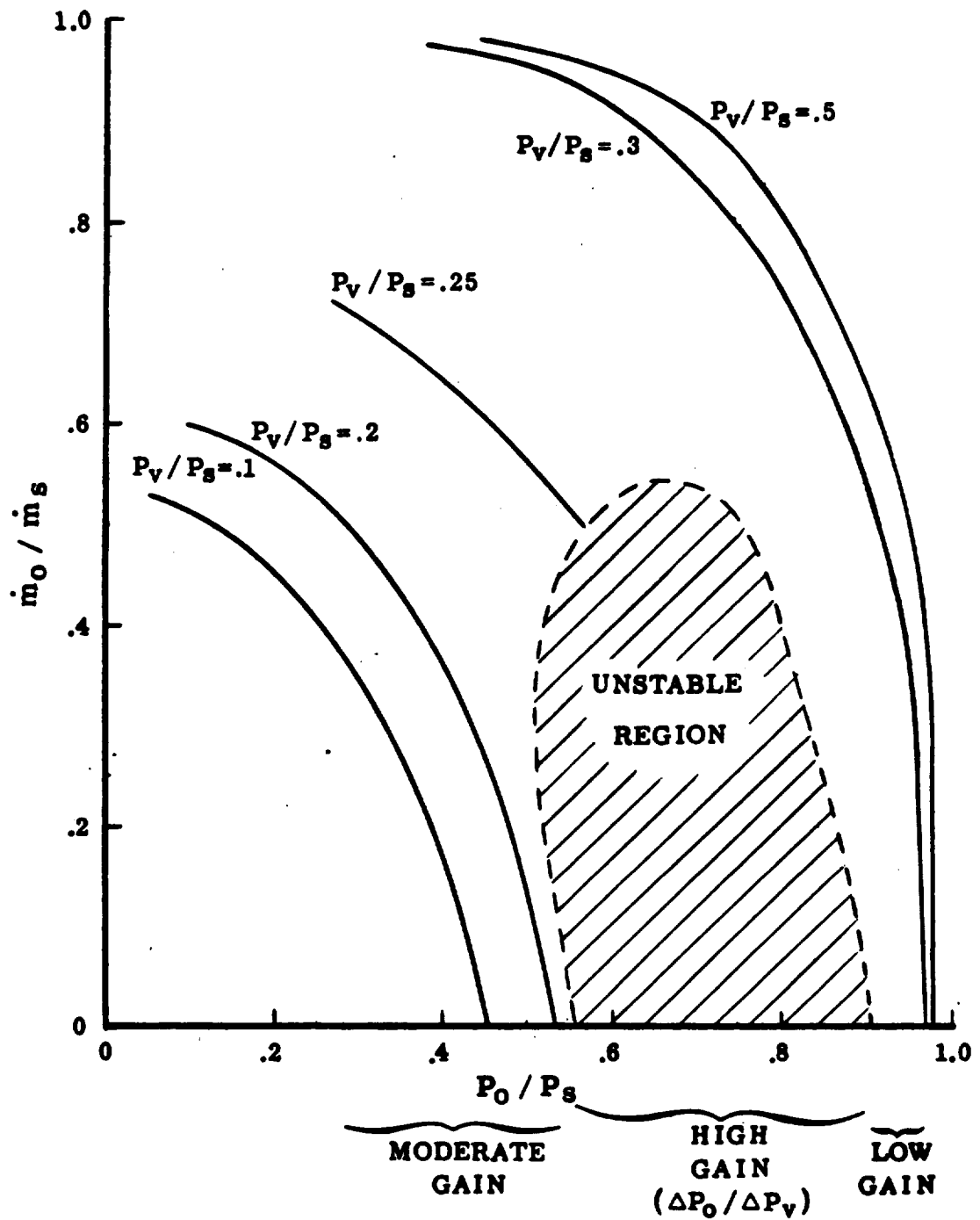
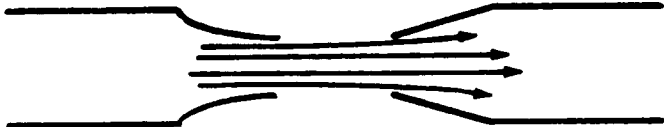
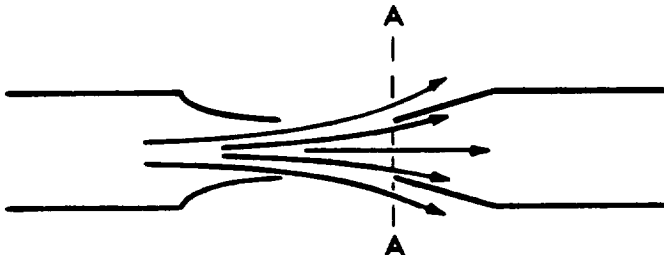
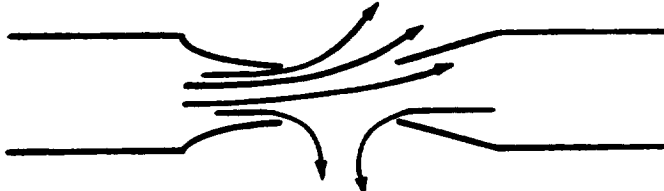


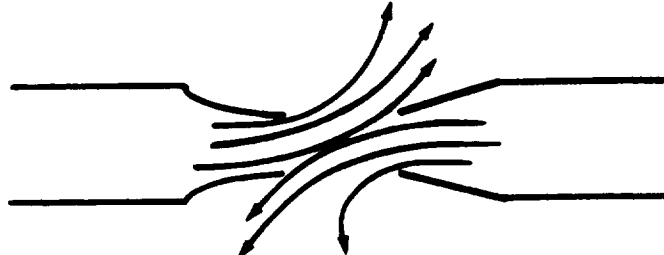
Figure 3-29 Vented Jet Amplifier - Typical Performance Map

The instability in the high gain region may be explained as follows
(considering the blocked output case):

1. 

The downstream volume charges up and total pressure increases.
2. 

As flow decelerates in the receiver, the total pressure at plane A approaches the jet total pressure.
3. 

Due to high total pressure in the receiver, flow tends to backflow out of the receiver to the vent.
4. 

The jet is deflected and the volume downstream of the receiver vents down to the vent pressure.
5. The jet returns to its normal position and the cycle restarts at (1).

The plausibility of the above explanation is supported by qualitative observations made during vented jet testing. One is that flow from the receiver will stabilize things at times. Another is that the frequency of oscillation goes up when the volume downstream of the receiver is reduced.

Many possible remedies have been suggested to improve vented jet stability. Improvement has been noted when the receiver is just a chamfered hole in a flat plate. Normal receivers are conical on the O.D. and chamfering produces little or no improvement. When size permits, devices to provide stabilizing negative feedback from the receiver to the vent cavity might help, or the receiver may be slotted to facilitate stable venting or contoured to improve pressure recovery.

Aside from such items as receiver shape, location of vents, etc., the two most important vented jet parameters are (1) the ratio of jet diameter to the receiver diameter, and (2) the spacing between the jet and receiver. For a fixed ratio between the jet and receiver diameters, increasing the spacing does the following:

1. The blocked output pressure recovery at high vent pressures is not significantly affected.
2. With significant output flow and high vent pressures, output pressure recovery drops slightly.
3. The unstable high gain region extends across a wide range of output and vent pressures, and the average gain across the region increases.
4. Gain increases at the lower vent pressures, although flow recovery becomes poorer.

Vented jet amplifiers are primarily fabricated in three dimensional configurations (Figure 3-28) and are sized by the internal diameter of the supply nozzle. Two dimensional vented-jet configurations are currently being investigated, since they are easier to integrate with other fluidic circuit elements.

The supply jet is controlled by vent pressures of 15 to 30 percent of the supply pressure, with maximum output flow and pressure recoveries on the order of 70 to 90 percent. Preliminary testing has shown that vented jets are relatively insensitive to gas temperature and supply pressure variations. To date very little information is available on the performance of the vented jet, although several investigators are experimenting with it. Wider application of this device is expected, once the instability in the high gain region is solved. Typical performance is shown in Figure 3-30 for a unit with a supply nozzle diameter of .040 inch and a fixed area load.

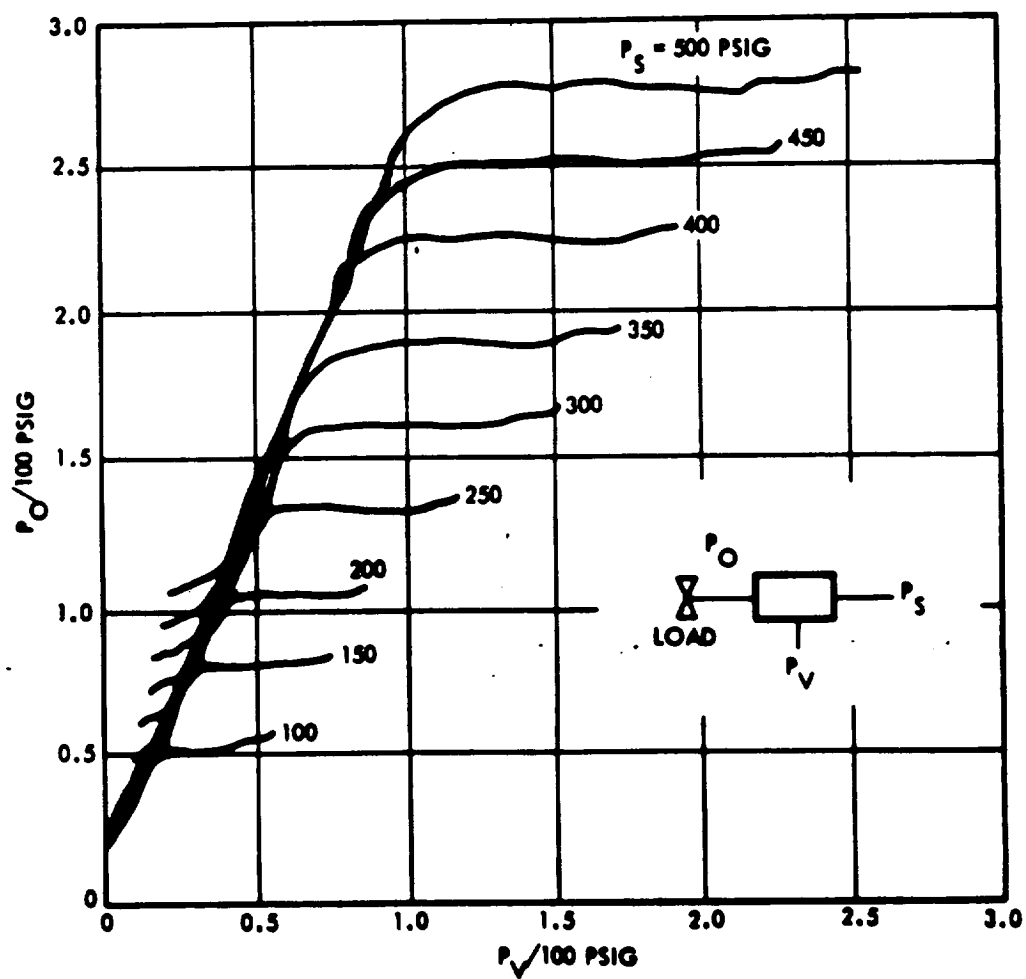


Figure 3-30 Typical Performance - Vented Jet
(Courtesy of Bendix)

Flow Diverter - Fluid flow diverters, or switches, are nonvented wall attachment amplifiers which are designed to achieve maximum pressure recovery in the output ducts. Whenever a fluid jet passes through a region of similar fluid, entrainment, momentum exchange, and frictional losses occur, which cause degradation of the stream. The loss of energy and pressure of the stream increases directly with the length of the interaction region. Therefore, to obtain maximum output pressure and power, it is necessary to locate the output ducts as close as possible to the input ducts.

The splitter in the flow diverter (Figure 3-31) is normally located 0 to 2 supply nozzle widths downstream from the exit of the supply port. Without control flow, the side wall influence is insufficient to deflect the supply jet, because of the small differential pressure developed by entrainment over an effective sidewall distance of only 2 supply port widths, and the power stream flow divides about equally between the output ducts. However, the pressure differential developed over this short length, results in a larger deflection by a given control signal than possible in an open system without bounding walls. The flow diverter essentially uses stream interaction for switching and is not bistable, because a continuous control signal is required to keep the supply flow switched to the opposite output port.

Pressure recovery of this device ranges from 60 to 90 percent, which is accomplished at the expense of pressure and flow gain. Time response is equivalent to or better than normal wall attachment devices, because of the unstable load sensitive geometry. Air has been used in a flow diverter to switch water flow with pressure recovery as high as 80 percent.

Application of this device has been limited to date, consequently very little performance information is available.

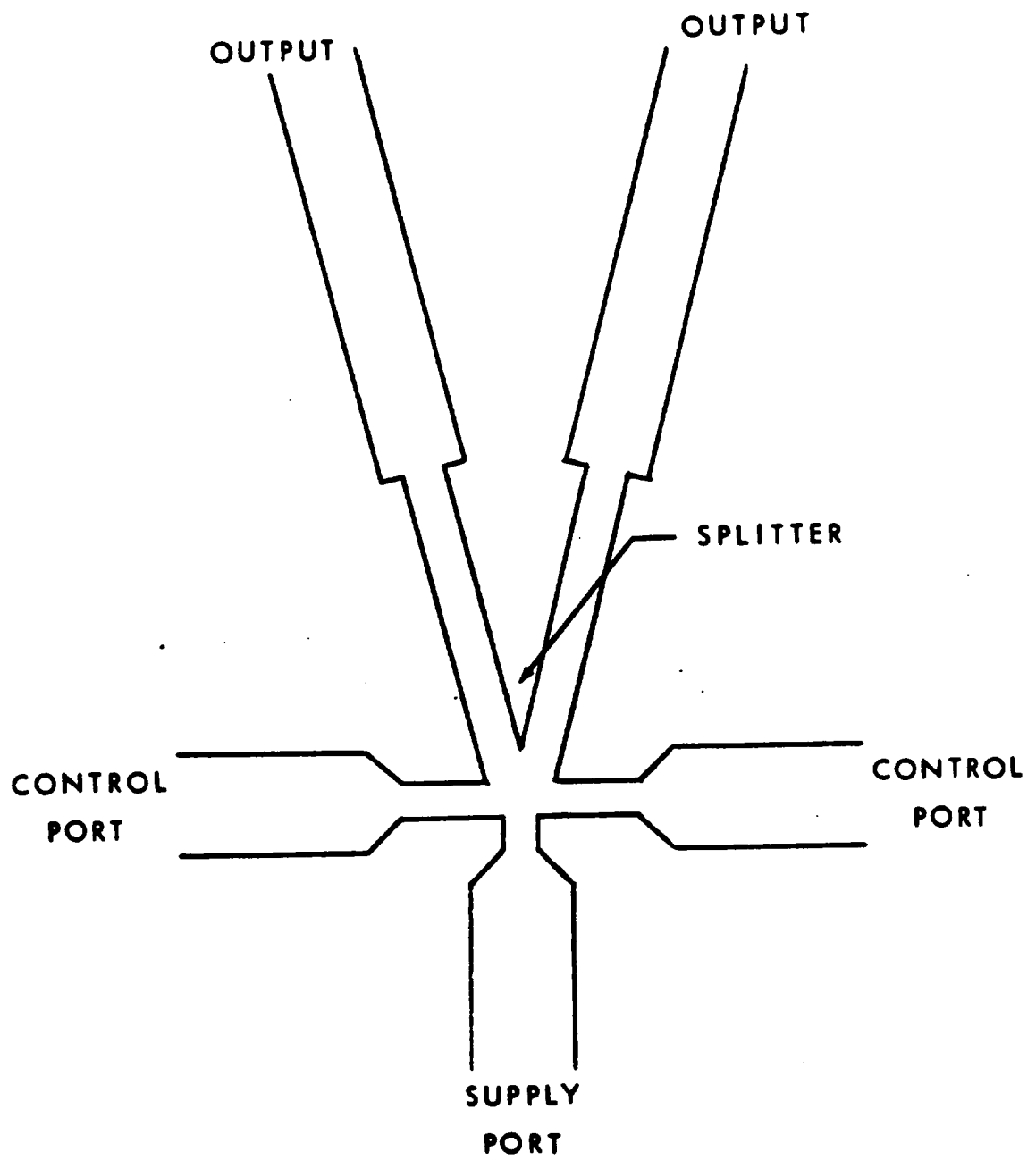


Figure 3-31 Flow Diverter Configuration

Boundary Layer Amplifier - This two dimensional device uses the principle of forced separation of a stream flowing over a curved surface. With no control flow (Figure 3-32), the supply flow adheres to the adjacent curved surface until well downstream of the control duct so that the flow is vented. When control flow is injected into the boundary layer of the curved surface, the point of separation moves upstream so that the supply flow is directed into the output duct.

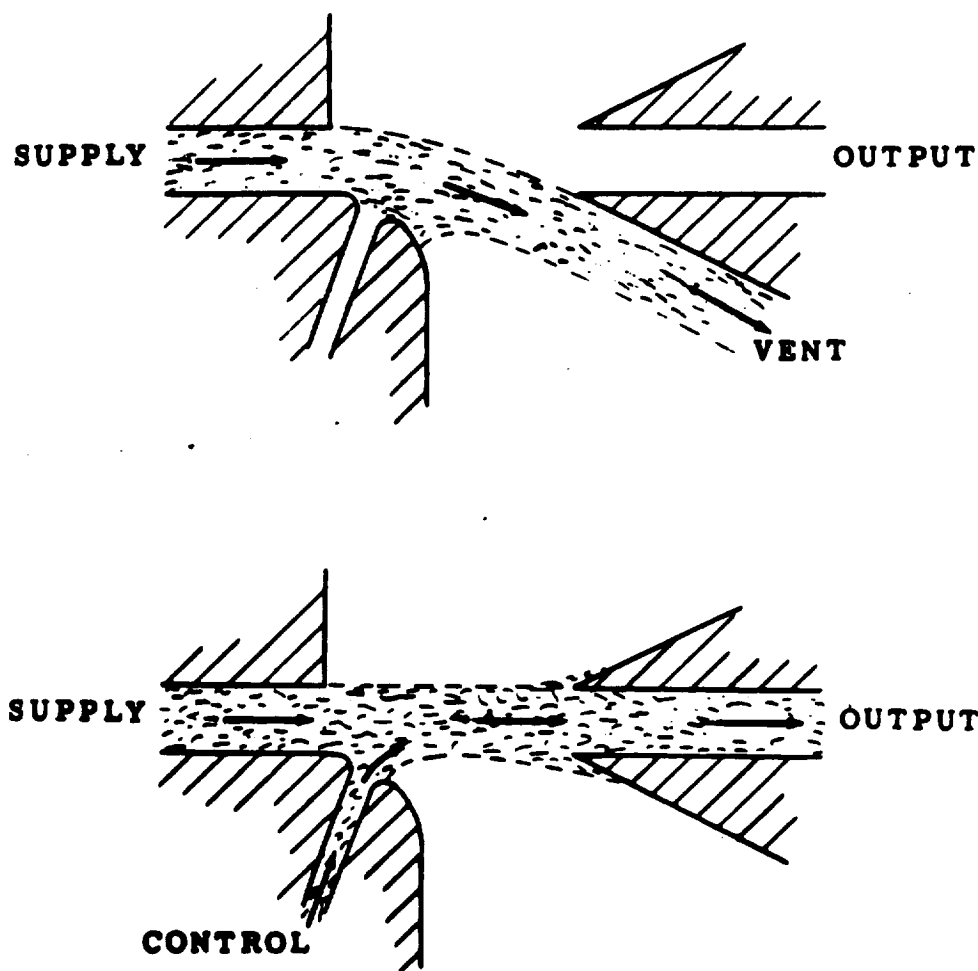


Figure 3-32 Boundary-Layer Amplifier Operation

A prototype model of a boundary layer amplifier is shown in Figure 3-33. A low, but constant bias flow is required to force the power jet to unlock and return to the off position when control flow is removed. The location of the control slots have significant effect on the characteristics of the amplifier. An island is necessary in this device to eliminate output hysteresis effects.

The boundary layer amplifier is used primarily when a high input impedance power amplifier is required. Typical pressure gains are 2 to 3, flow gains 20 to 30, and power gains 60 to 80, at relatively low pressures (about 5 psig).

This device is limited by its low pressure gain, complexity of construction, and relatively slow response time.

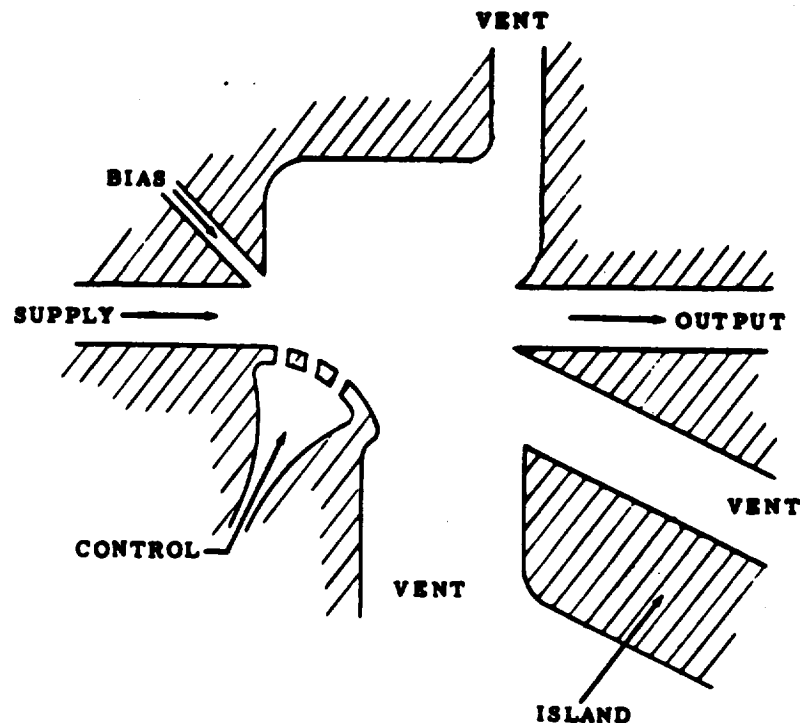


Figure 3-33 Boundary Layer Amplifier Configuration

Double Leg Elbow Amplifier - This device is essentially a more complex version of the boundary layer amplifier. The double leg elbow amplifier (Figure 3-34) has two output ducts. With no control flow, the momentum flux in the active leg is low near the outlet of the passive leg, hence the combined flow is directed into the left output duct. When a control flow is applied, the point at which the flow in the active leg separates from the channel wall moves upstream, so that the momentum distribution across the flow changes and the combined flow is directed toward the right output duct. The action is proportional, since the proportion of the power stream which flows into either of the output ports depends upon the momentum distribution of the combined active and passive flows.

The double leg elbow amplifier provides very high flow amplification at low pressures and low operating frequencies. Maximum gains under static conditions are flow gain 300, pressure gain 3, and power gain 500. Typical flow gain is 200 and power gain 40. However, the performance of the device drops drastically as the operating frequency is increased, i.e., down 3 db at 10 cps and down 10 db at 40 cps. Application of this device will be limited by the low pressure gain, complex construction, and slow response time.

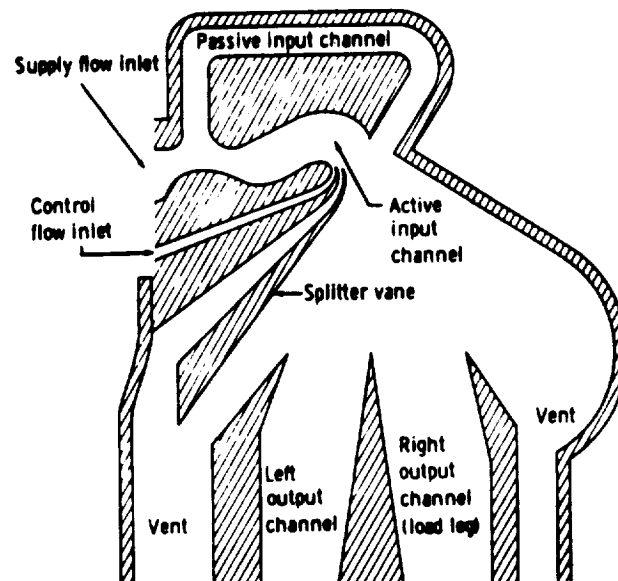


Figure 3-34 Double Leg Elbow Amplifier Configuration

Impact Modulator - The impact modulator is a proportional amplifier concept that uses two axially opposed power jets to provide a planar impact region. Its operation depends on varying the axial momentum of one of the supply jets, so as to vary the position of the planar impact region. There are two versions of this device, the transverse and the direct impact modulator.

In the transverse impact modulator, Figure 3-35, when a control signal is applied, the momentum of the left supply jet is decreased and the impact region moves to the left. Consequently, the output flow and pressure decrease and, since the output pressure decreases with increase in control pressure, the device has negative gain.

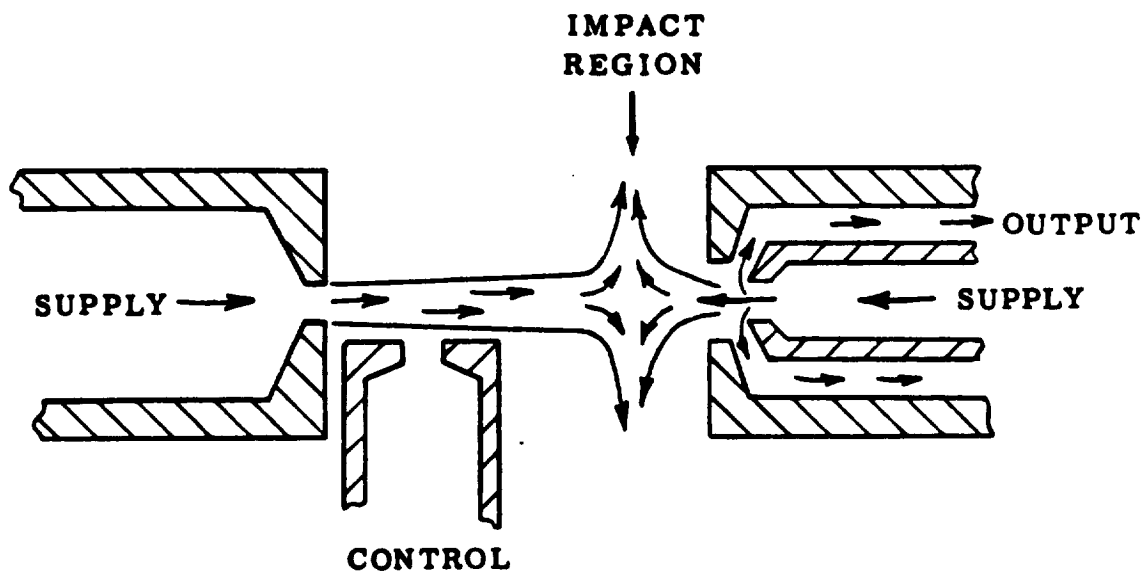


Figure 3-35 Transverse Impact Modulator

In the direct impact modulator, Figure 3-36, when a concentric control signal is applied, the momentum of the left supply jet is increased and the impact region moves to the right. This results in increased output flow and pressure and, since the output pressure increases with increased control pressure, the device has positive gain.

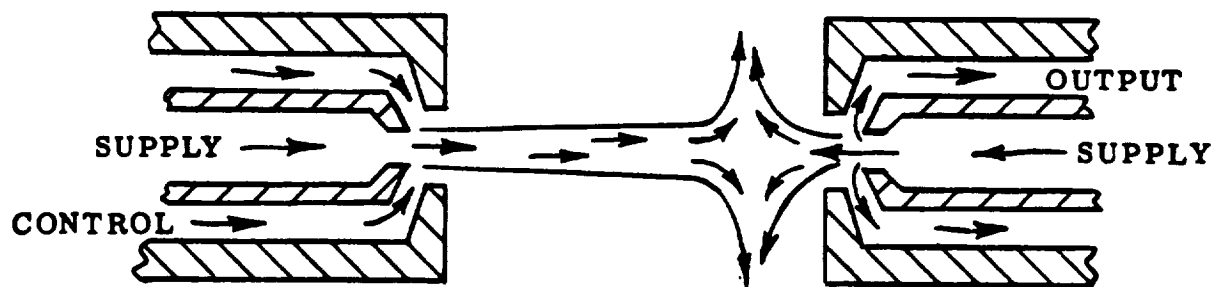


Figure 3-36 Direct Impact Modulator

Typical performance of the transverse impact modulator is full output flow gain of 5 to 30, and no load pressure gain of 20 to 40. A characteristic curve is shown in Figure 3-37. Optimized four-stage cascades have given pressure gains of about 12,000, which reduces the average pressure gain per stage to about 10.5. This is necessary to insure output linearity and proper interstage impedance matching.

The direct impact modulator is a significant improvement over the transverse impact modulator. Pressure gains up to 200 have been reported for this device, and the input impedance is variable and can be adjusted so as to approach infinity. Unloaded frequency response is reportedly quite high, 300 to 400 cps; however, this has not been related to a particular element size and response will decrease markedly when the element is loaded. Signal to noise ratio information is not generally available for either device, however, this ranges from 60 to 300.

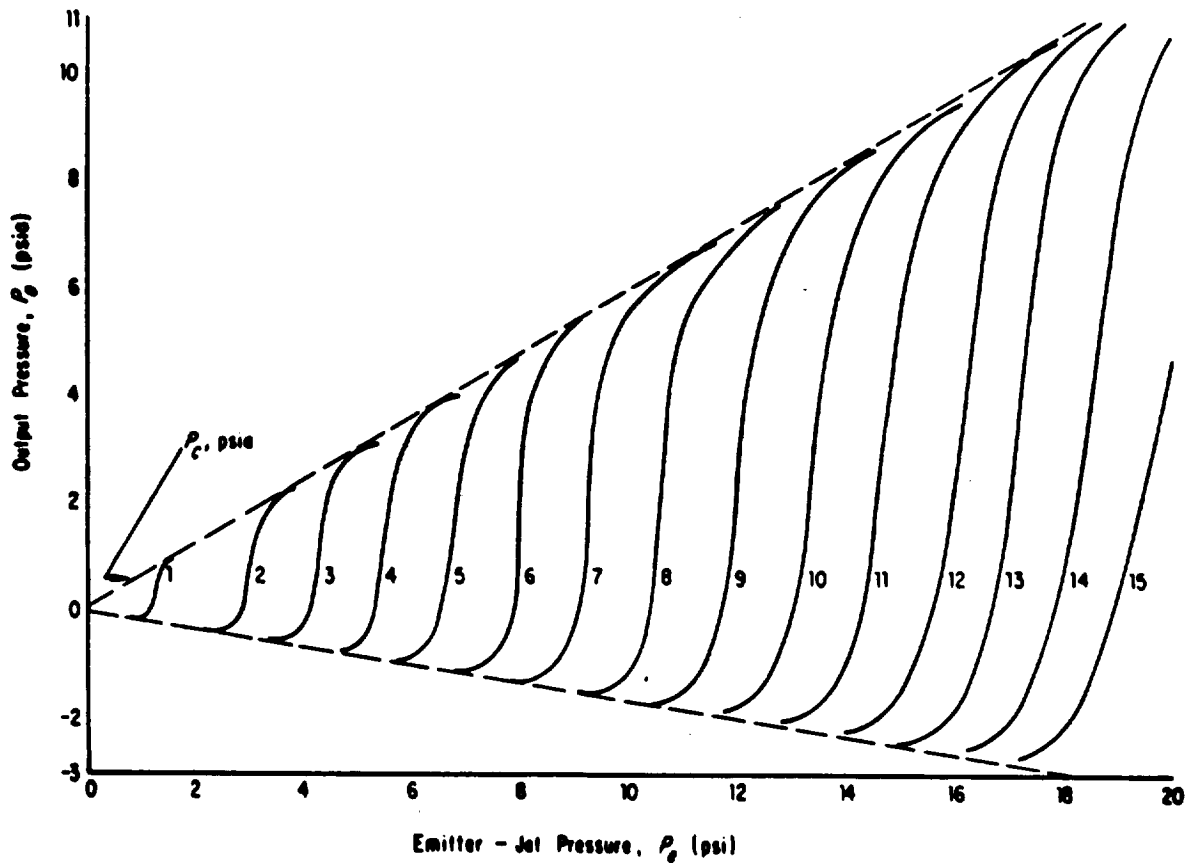
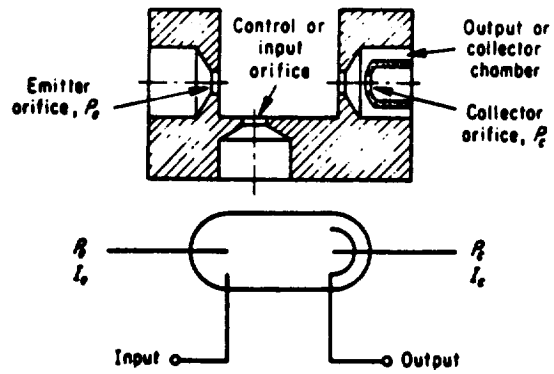


Figure 3-37 Transverse Impact Modulator Performance

The difficulty of obtaining reproducible characteristics from one device to another is one of the major obstacles to the development of the impact modulators. This is primarily due to the three dimensional concentric nozzle configurations, which are expensive to manufacture. Some effort is being expended in developing a two dimensional version of the direct impact modulator, however, even if this is successful, lower pressure gains are expected. Although very attractive for proportional control application, additional development is necessary before the true value of these devices can be assessed.

Passive Elements - Passive circuit elements are generally needed when assembling fluidic elements in digital or analog circuits. Since passive elements have been used in hydraulic and pneumatic circuitry for a long time, their performance is well documented. The reader is referred to the TRW Systems Group - AFRPL "Aerospace Fluid Component Designers' Handbook," Reference 3-5, for a good outline of fluid mechanics and for the static and dynamic performance of passive elements.

Passive elements produce no gain, and consequently require no separate power supply. Mass flow is considered analogous to current and pressure analogous to voltage. A fluid impedance produces a pressure drop as a function of the flow through it. Algebraic representation of the impedance may be composed of either real or pure imaginary parts or both.

Simple orifices are generally used to provide a fluid resistance. When orifices are used with low pressure gases or incompressible fluids, their pressure-flow characteristics follow the square law relationship and hence are nonlinear. Tube resistors fabricated from metal or glass capillaries and porous plugs, can provide essentially linear characteristics, but may also have significant inductance. The primary problem with present laminar fluid resistors is a narrow linear range, which must be carefully selected. A wide range laminar resistor is definitely needed.

In a capacitor, the pressure drop lags the flow by a phase angle of 90 degrees. Ideally, only compressible fluids show capacitive effects, and in low pressure designs capacitive effects on most liquids are neglected. In circuits employing compressible fluids, the analog of the electrical capacitor is simply a volume. Shunt capacitance is the only type that can be obtained without moving parts. The series capacitance (i.e., coupling capacitor) requires a diaphragm, or the same effect can be accomplished fluidically by the use of differentiating circuits employing operational amplifiers.

In an inductor, the pressure drop leads the flow by a phase angle of 90 degrees. An acceptable fluid inductor can be made from long tubes, however, in most cases fluid inductance can be neglected with respect to resistance.

Fluid diodes are used when a large impedance to flow in one direction and little or no impedance to flow in the opposite direction is desired. Telsa's valvular conduit was the first fluid diode, and the vortex diode is one of the most widely used at present. In the vortex diode (Figure 3-38), when flow is introduced into the center duct it follows a radial path to the tangential duct, encountering small impedance. When an input flow is applied to the tangential duct, the flow establishes a vortex and follows a long circular path before exiting through the center duct, thus encountering high impedance. Optimized nonventing vortex diodes have been reported to have front to back ratios (i.e., ratio of forward flow to reverse flow at constant pressure) as high as 5. Vented vortex diodes are available with front to back ratios as high as 20.

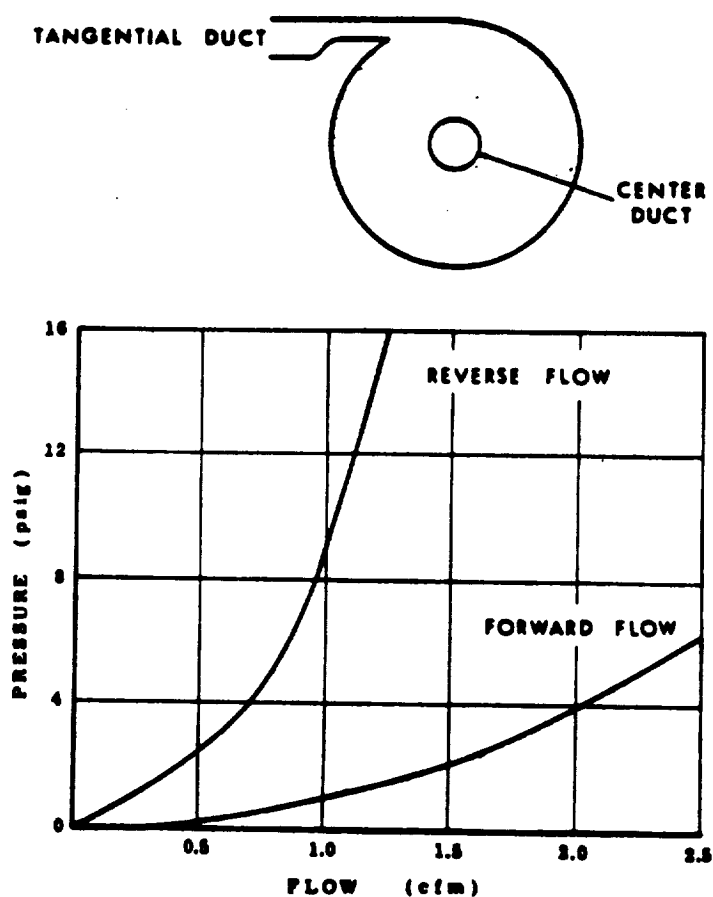


Figure 3-38 Vortex Diode Performance

Interface Elements - The ideal fluidic application is one where a single fluid medium can be used for all control functions and the need to translate information from one medium to another is eliminated. However, the bulk of the present applications are of the hybrid variety in which interface elements are required. Interface elements include the broad range of sensors and transducers required in the applications where the input and/or the output must be either electrical or mechanical. To date, very little original work has been done in this area, and most interface elements are adaptations of commercially available hardware.

Electrical to fluid (E-F) transducers in general use are solenoid valves, torque motor driven flapper valves (Figure 3-39), and a wide variety of devices in which an electrical or mechanical signal produces a mechanical movement of an element into the active area of a fluidic device. The present trend is toward more compatible E-F transducers, i.e., those in which an electrical signal is converted directly into a fluidic signal with a minimum number or essentially no moving parts. An E-F transducer which utilizes the basic principle of a speaker cone, in that a diaphragm is oscillated in a closed chamber by a controller to induce pressure variations, is shown in Figure 3-40. Experimental investigation of many other types are in progress, including the switching of digital elements by electrophoresis, deflection of an ionized fluid, and spark discharge.

Many fluid to electrical (F-E) transducers are possible, and the most widely used are a simple pressure switch, thermistor probes, and hot-film anemometers. A proportional type cooled filament F-E transducer (Figure 3-41) consists of two heater filaments or hot-films in the output ducts of a proportional amplifier, connected in a bridge circuit. The bridge output voltage is then proportional to the differential cooling of the two sensors. Another proportional type F-E transducer utilizes a small differential semiconductor or wire strain element mounted between the output legs of a proportional amplifier (Figure 3-42). A transducer of this type, with a close coupled strain element, will provide a sensitive and accurate output signal directly proportional to the amplifier differential output pressure.

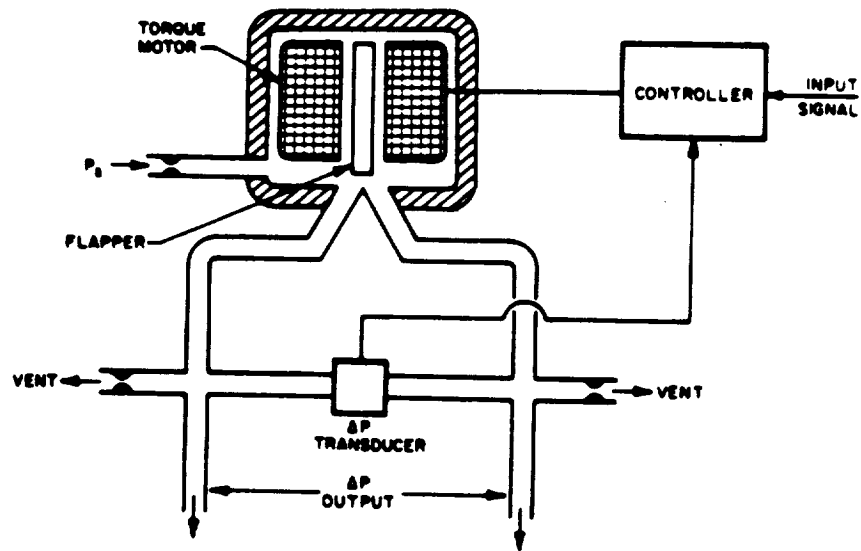


Figure 3-39 Electrical to Fluid Transducer - Torque Motor Driven

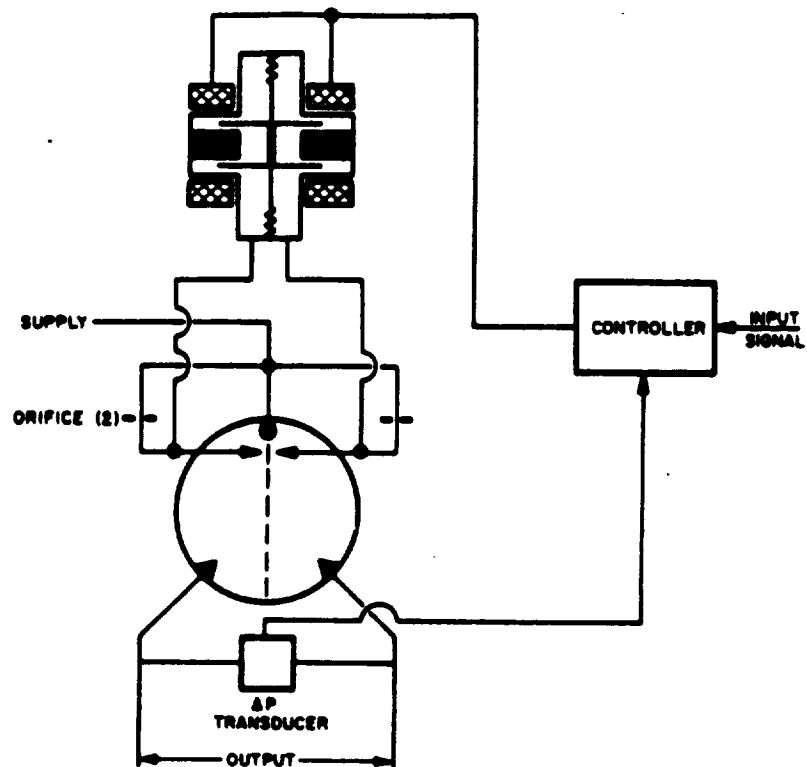


Figure 3-40 Electrical to Fluid Transducer - Diaphragm Oscillator Type

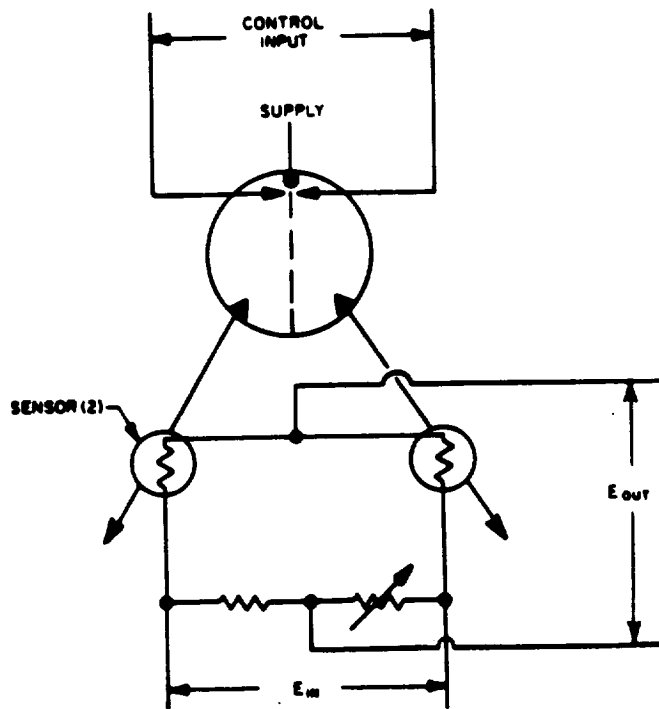


Figure 3-41 Fluid to Electrical Transducer - Hot Film Type

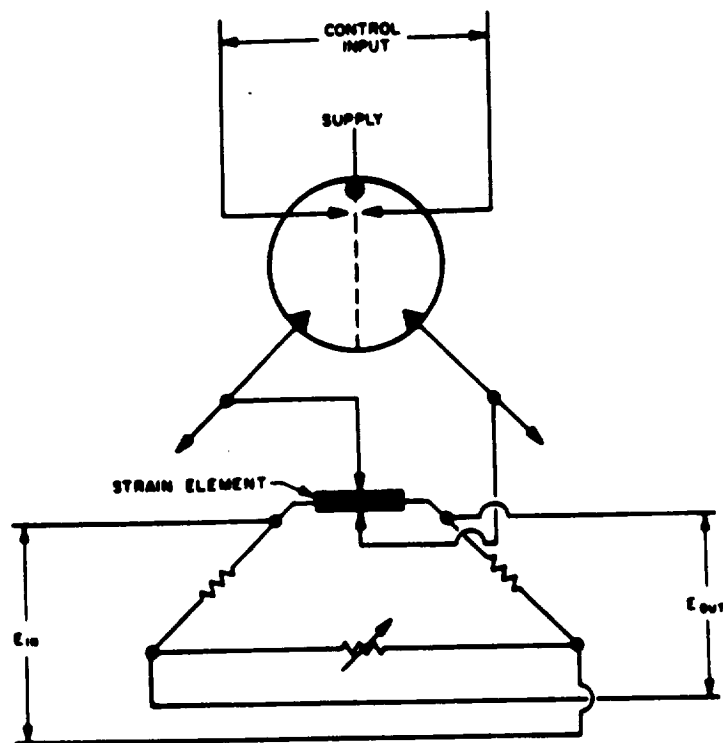


Figure 3-42 Fluid to Electrical Transducer - Strain Element Type

Mechanical to fluidic (M-F) sensors are normally used to detect linear and angular displacement. The flapper valve (Figure 3-43) is one of the most widely used M-F transducers. Another M-F device is the interruptable jet (Figure 3-44), which can detect the presence of a thread or wire, or the edge of almost any material. For digital circuitry, standard punched cards or tapes can be used to interrupt jets and provide complex programmed inputs.

Fluidic to mechanical transducers simply utilize the output of a fluidic device to drive a bellows or diaphragm, which can be used to drive a variety of devices. The output of fluidic devices are also used to directly position the pilot valve of a power element.

Efficient and compatible interface elements are necessary to bridge the gap between fluidic systems and other kinds of systems, primarily electrical and mechanical. At present, required accuracies are achieved through the utilization of less reliable mechanical components. Environmentally insensitive interface elements, preferably with no moving parts and specifically designed for space application, are required.

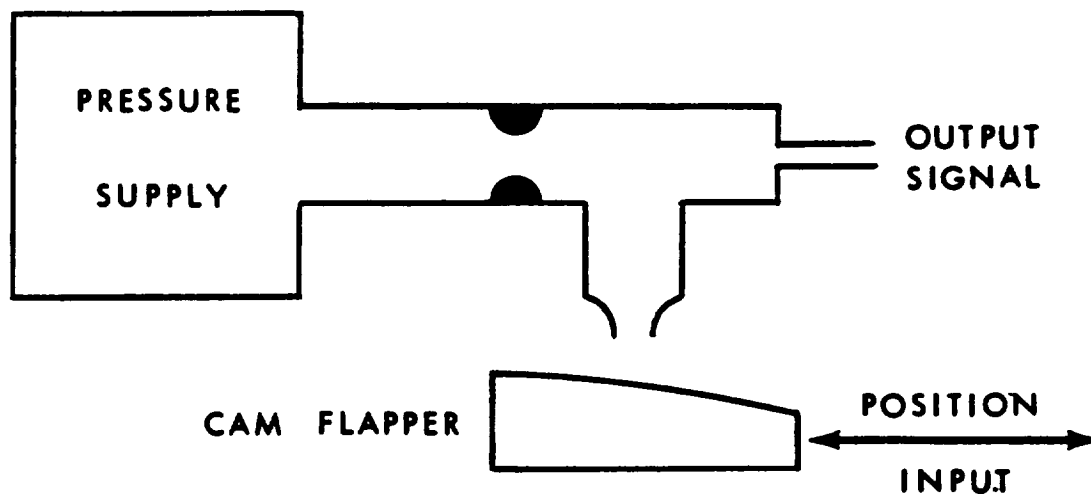


Figure 3-43 Mechanical to Fluid Transducer - Flapper Type

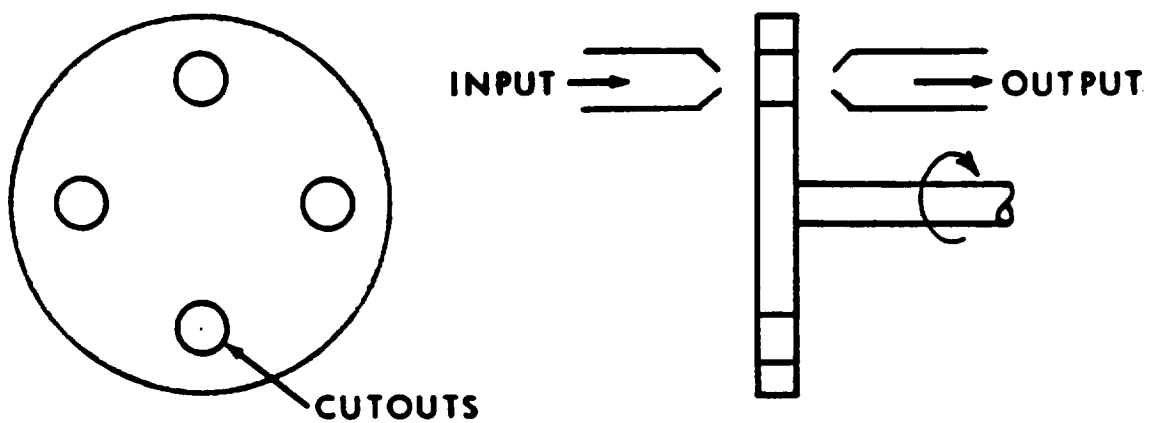


Figure 3-44 Mechanical to Fluid Transducer - Interruptable Jet

Component Fabrication and Materials

Fluidic devices can be made by a wide variety of manufacturing processes, and in almost any type of rigid material. Techniques for the fabrication of these devices are well known and not difficult. The most important consideration is that the performance and characteristics of a fluidic device are closely related to its geometric shape, so that in fabricating fluidic devices intricate shapes must be held to precise dimensions.

The size of fluidic devices varies widely because of the many different types and also because of the different uses for the same device. For example, fluidic elements used as logic elements in aerospace applications are miniaturized to minimize power consumption. Whereas, a similar device used as a switch to divert flow in a pipeline is much larger. Because of this wide diversity in the size, quantities involved, tolerances required, and materials used, there is no singularly best fabrication technique for fluidic devices. Manufacturing processes in common use include the casting, thermoforming, photoetching, and molding of plastics; chemical milling, photoetching, electrical discharge machining, electroforming, die casting, and powder metallurgy of metals; and photoetching, ultrasonic machining and electron beam machining of ceramics. This is by no means the end, but only representative of the wide range of choices available.

Environmental tolerance required of a fluidic element is a consideration in selecting a fabrication process, but more important is the choice of material. Fluidic devices are subjected to both structural and hydraulic forces, so that materials must have sufficient strength to withstand these forces without undue distortion. Surface hardness of the material must also be considered, particularly if the working fluid carries abrasive particles. Wear in stream interaction devices is critical in the nozzles, and on the splitter. Other factors, such as operating temperature and compatibility with the working fluid, also enter into the selection.

Injection molding of thermoplastic material appears to offer the cheapest method of fabricating large quantities of fluidic elements. However, these elements are limited to operation at near room temperature conditions and

with noncorrosive media. In industrial application, injection molded devices should provide long term reliable operation, particularly in digital systems.

There are several fabrication methods which are suitable for use in making two dimensional elements for aerospace application, these include:

1. Compression Molding - This is perhaps the most economical production method for manufacturing parts from thermosetting materials. Tolerances can be held as close as required for most fluidic elements. Fillers are used to add stiffness, control shrinkage, and reduce the coefficient of thermal expansion. Maximum operating temperature is about 400°F for the best filled thermosetting plastic elements, and filled epoxy elements are limited to about 300°F.
2. Photoetching Ceramics - This process was originally developed by the Corning Glass Works to prepare substrates for electronic circuits and has been adapted to the manufacture of fluidic elements. A high contrast negative is placed upon a thin sheet of Fotoform glass, which is a silicate glass containing a photosensitizing ingredient such as the cesium radical, Ce^{+3} . In the presence of ultraviolet light, the exposed glass absorbs the ultraviolet radiation, creating a contact print in depth. The glass is then heated to about 1200°F, so that colloidal particles of crystallized lithium metasilicate are formed in the exposed areas of the glass, which appear as a white opal image. When the glass sheet is immersed in a hydrofluoric acid bath, the exposed areas dissolve 20 to 30 times faster than the clear unexposed glass. Further processing converts the Fotoform glass to a higher strength partially crystalline material called Fotoceram.

The finished Fotoceram elements offer several important advantages which are normally associated with ceramic

material, i.e., high dimensional stability, low moisture absorption, good shock resistance, and operating temperatures approaching 1000°F. This process can produce intricate two dimensional elements down to a nozzle width of .005 inch. An important consideration in circuit fabrication, is that both the Fotoform and Fotoceram plates can be thermally laminated to form a monolithic structure.

3. Photoetching Metals - This process has recently become very important in the manufacture of fluidic elements for aerospace application. Essentially the process removes metal by the chemical etching of preferentially exposed surfaces. The process is presently limited to metal sheets of about .020 inch thick, since the dimensional tolerances that can be achieved increase with increasing metal thicknesses. For a .001 inch thickness of stainless steel channels can be cut .005 inch wide with a tolerance of $\pm .0005$ inch or about ± 10 percent. Whereas tolerances jump to about ± 40 percent for a .005 inch thickness of the same material with the same channel width.

In the fabrication of two dimensional fluidic elements, several laminations of etched sheets are required to provide the required aspect ratio. Photoetching can be used with the following metals, in order of increasing difficulty: copper, nickel, carbon steel, stainless steel, aluminum, titanium, and molybdenum. Operating temperature depends primarily on the metal used and/or the method used to seal the laminated devices.

Many new methods are being considered for the fabrication of fluidic elements. Techniques such as electron and laser beam machining may eventually make it possible to pack 1000 fluidic elements in one cubic inch. Coining techniques may soon make it possible to manufacture interconnected fluidic elements by indexing a die and stamping in the right location. However, much work still needs to be done in the sealing of fluidic elements, particularly those for

use with high temperature working fluids. To date diffusion bonding and furnace brazing have been used with moderate success in the sealing of photoetched metal elements, but more efficient sealing methods are required if the inherent reliability of fluidic elements is to be maintained.

One way of overcoming the sealing problem is a ceramic molding process, where a polystyrene mold is made from a metal master. Ceramic is then molded around the polystyrene and fired at about 2000°F. The polystyrene is vaporized, leaving a one piece ceramic device. Although the process is complex, it does eliminate the basic problem of sealing a two dimensional element with a cover plate.

Component Performance with Propellants

Gases - The gases commonly available in spacecraft include pressurants, propellant boiloff, and combustion products. Any of these gases may be used as a working fluid for fluidic devices. Particulate contamination such as fine rust particles can cause detrimental erosion in elements, particularly when in hydrogen and helium because of the high sonic velocities. Ice crystals formed from impurities such as water vapor and carbon dioxide in the gases can clog orifices and filters. Normal care to ensure that systems are clean and dry and the use of adequate filters will obviate most problems.

Hydrogen, helium, and high temperature combustion products are extremely difficult to seal and will leak through exceedingly small openings such as are found in connectors and body seals. Under these conditions the erosive effects of these gases can be quite significant. Boiloff gases from the various propellants such as N_2O_4 and fluorine and combustion product gases, may be corrosive and adequate provisions must be made to ensure materials compatibility. Monopropellant hydrazine gas generator systems generate a relatively clean gas and should find wide application in providing working fluid for fluidic systems.

Liquid Propellants - The liquid propellants used for spacecraft propulsion are classified as either earth storables, space storables, or hard cryogenics. In most cases more serious problems exist with liquid flow than with gas, primarily because of the more stringent materials compatibility and sealing problems. As with gases, the purity of the liquid flow media must be maintained to avoid problems. Of particular significance is the case of cryogenic fluids that may become contaminated with gases whose freezing points are higher than the storage temperature of the cryogenic fluid.

Fluidic elements can be successfully operated with any of the liquid propellants, however, the development of gaseous fluidic systems has progressed much more rapidly than those which use liquids. There are several reasons for this. Liquid operated fluidic elements tend to be an order of magnitude slower than pneumatic elements because of fluid density, however, liquid

elements are still fast enough for most applications. Many elements rely on a laminar to turbulent transition which will occur when the Reynolds number is high enough. Since the Reynolds number decreases as fluid viscosity is increased, a more viscous fluid will require a much higher fluid velocity to operate with the same degree of turbulence as it would with a less viscous fluid.

Another problem is that whenever a viscous fluid passes around a sharp bend, the fluid separates from the bend and a region of low pressure is formed between the bend and the separated jet. In this low pressure region, a vapor or gas pocket can form which affects the efficiency of the jet. When the jet is directed into a receiver, the pressure recovery will be strongly affected by the upstream bubble. The removal of entrapped gases from liquids and the prevention of vapor formation are substantial problems which must be considered in the design of liquid operated fluidic systems.

Gelled Propellants - A liquid propellant which has been conditioned so that it exhibits non-Newtonian properties is normally called a gel. For spacecraft propulsion the gels are classified into two types: nonmetalized and metalized. In a nonmetalized gel the additives used to cause gelling (carbon black, silica, etc.) do not normally modify the chemical characteristics of the propellant, whereas a metalized gel is generally prepared with propellant mixed with metal having an average particle size range of 5 to 50 microns and it has been necessary to gel the mixture in order to suspend the metal in the propellant. The gels are characterized by thixotropic properties, i.e. the viscosity decreases with increasing shear rate and stress decreases with time at constant shear. As the gel flows through lines and components, the shear becomes greater, the viscosity becomes less and the gel behaves more like a low viscosity liquid.

The properties of gelled propellants can present several problems in fluidic devices. Pressure drops through lines and elements are larger than those of comparable liquids and are unpredictable, i.e., the viscosity keeps varying. Nozzles can cause evaporation of the liquid phase of the gel, which leaves a solid matrix as a residue that can hinder and/or restrict the flow. The abrasive action of metal particles can cause erosion of nozzles and passages. The compatibility of gelled propellants with the materials of construction is generally comparable to the base liquid propellant.

Component Functional Parameters

Temperature - The temperature range of interest is from -420°F to 2500°F . Fluidic devices can be operated at any discrete temperature in this range, limited only by the materials of construction. Digital elements can be operated over broad temperature ranges, however, analog devices are quite sensitive to temperature variation. This sensitivity is due to such things as viscosity variations, sonic velocity changes, and orifice and nozzle size variations due to thermal expansion or contraction. Differential circuits are used to compensate for small temperature ranges, and temperature sensitive gain changing networks are required for compensation over broad temperature ranges.

Pressure - Operating pressure up to 5000 psi may be considered for fluidic elements. The primary problems seen at high pressure levels are structural strength and seals. The external or ambient pressures also must be considered since it can vary from 10^{-16} mm Hg in interplanetary space to about 225 psia in the Venus atmosphere and several thousand psi in the Jupiter atmosphere. Consequently the structural strength and seals of elements must be made effective in both directions. Back pressure regulation or a constant pressure dump source may be necessary if elements are required to operate over a wide range of ambient or vent conditions.

Time Response - The response time of fluidic elements refers to the propagation delay which occurs in digital elements when stimulated by a step control signal of predetermined amplitude and the frequency at which the output signal lags the control signal by 45 degrees for specified conditions in an analogue element. Practical time responses with gases are presently limited to about 1000 cps and should be extended to about 10,000 cps in a few years.

Fluidic elements operated on liquid propellants tend to be an order of magnitude slower than elements operated on gases because of fluid density. Consequently, the time response of many fluidic elements decreases as density increases as shown in Figure 3-45. The response times shown in the figure are only approximate and should be used only as a rough idea of the

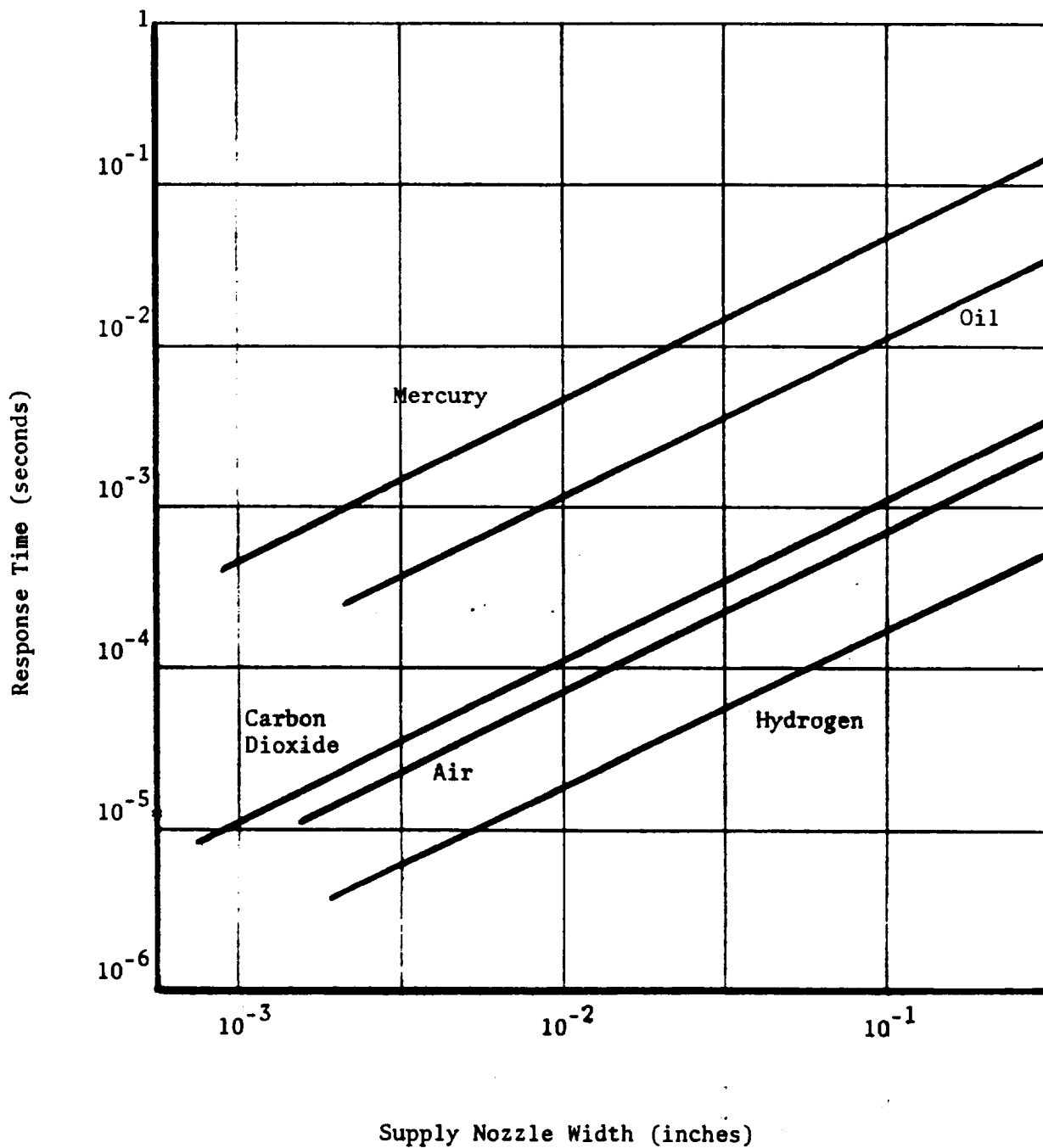


Figure 3-45 Fluidic Element Time Response
As a Function of Size and Fluid

comparative speed capability of fluidic elements. In addition, the figure indicates that elements will operate faster as they are made smaller.

Power Requirements - Fluidic component operation requires a continuous flowing supply of working fluid. In analogue control and digital circuitry the individual component supplies can add up to a sizable power drain. This power drain can be minimized by the use of efficient element geometries and by miniaturization. Some elements can be made to operate with power jet pressures of just a few inches of water, but then the increased susceptibility to vibration and shock can become a problem. In general, fluidic elements operated on low pressure high temperature gas is the right direction to take when power needs to be conserved.

Operating Life - The actual required operating life of a fluidic element can vary from a few cycles to several hundred thousand cycles depending on mission requirements. Since there are no moving parts that can wear out, the operating life of an element is not usually a problem. The most significant effects on operating life are materials compatibility, seals, erosive action of the working fluid, and space environment.

Leakage - The primary concern here is the leakage in fluidic elements that is not normally vented during operation. For a basic two dimensional fluidic element sealed with a cover plate, consider the leakage paths across the seal layer. In a cold gas or liquid system some leakage can be tolerated across the seal without adversely affecting component performance. However, in a hot gas system even minute leaks can cause severe erosion in the seal layer which will soon develop into a severe leak and ultimate component malfunction. Non-vented leakage of this type is generally hard to detect unless it is external to the component vent ports. Manufacturing techniques and the careful inspection of seals during component assembly are perhaps the best methods of maintaining the integrity of the seals.

As in conventional fluid systems leakage can result in severe loss of propellants, may interfere with spacecraft experiments, can cause fire and/or explosions, and in some cases toxicity hazards to personnel.

Signal to Noise Ratio - Noise is defined as the peak-to-peak pressure fluctuations on the signals of a fluidic device, so that in high gain circuits the signal to noise ratio becomes a comparative measure of element performance. Of primary concern are element geometry, method of fabrication, and operating conditions.

There are several fluidic elements potentially capable of operating with relatively high signal to noise ratio (>200). Some element geometries are much noisier than others, however, these devices are generally of the digital variety. In particular, the turbulence amplifier is susceptible to external vibration and shock, and the edgetone amplifier generates considerable internal noise since the device is purposely designed unstable so as to enhance switching speed.

Sterilization - Complete sterilization of all components on a spacecraft may be necessary for planetary missions or fly by missions to the planets. One method of sterilization involves a soak at temperatures up to 300°F for 60 hours, which is repeated for 6 cycles. A mixture of 12 percent ethylene oxide and 88 percent Freon is also used in a spray for surface sterilization. In a fluidic system, the materials of construction, the methods of fabrication and assembly, and the subsequent handling required must all be considered.

Contamination - Fluidic elements can be designed to be contamination insensitive by utilizing large nozzle widths ($>.025$ inch). For aerospace application this is inconsistent with the normal requirements for low power systems. Therefore, .005 inch to .010 inch nozzle widths are considered more practical for gas systems with normal filtration and contamination control during assembly. Estimates as to the smallest practical power nozzle width for liquid operated systems range from .007 inch to .025 inch. The decision as to width must be tempered by the required operational life and the liquid or propellant properties.

Space Maintenance - The maintenance of manned and unmanned spacecraft is a requirement that will involve new designs, techniques, and procedures.

Periodic service of unmanned satellites is envisioned in which rendezvous and docking techniques are employed to permit personnel to effect the necessary maintenance or repair. In-flight maintenance will be necessary during space travel or in orbiting space stations, and major repairs may be required on vehicles which have landed on the moon or other celestial bodies.

Fluidic elements will not be interchangeable, because integrated circuitry will be employed in spacecraft applications. Maintenance or replacement then must be considered on a subsystem basis. The problem then becomes one of the usual difficulties which would be imposed on an astronaut who must connect and disconnect conventional normal fittings or even specially designed quick disconnect fittings.

Space Environments

The space environment is characterized by radiation, vacuum, zero gravity, and meteoroids. Radiation in space includes the earth Van Allen belts, solar flares, and interplanetary radiation. Considering that fluidic elements can be fabricated from stainless steel and assembled by diffusion bonding or molded in ceramics, radiation exposure is not a serious problem even for spacecraft orbiting within the Van Allen belts.

Interplanetary space vacuum is characterized as a low density gas mixture consisting primarily of hydrogen and helium at an estimated pressure of 10^{-16} mm of mercury. In this environment the primary problem would be the sublimation and/or evaporation of the materials in fluidic elements. Sublimation is negligible for most structural metals and generally the lower the vapor pressure of the material the lower the rate of sublimation. Cadmium and zinc have relatively high vapor pressures and should be avoided. High molecular weight polymers such as Teflon are also very stable in space vacuum, although a weight loss is commonly experienced due to outgassing of contaminants such as absorbed gases, moisture, and solvents.

Zero gravity should not affect the performance of fluidic elements. However, careful consideration should be given to low pressure liquid systems where the wettability of the liquids on the element walls may affect performance. It is generally believed that no significant effects on materials will be encountered due to zero gravity conditions in space.

Meteoroidal hazards to fluidic elements and/or systems in space must be considered and could possibly exert some influence on the system design. Protective measures can be taken without imposing a high weight penalty. Fluidic elements should be less susceptible to meteoroid damage than components with moving mechanical parts, which could malfunction due to deformation on the inner surfaces resulting from external meteoroidal impingement.

COMPONENT APPLICATION CRITERIA

Rocket propulsion engines must operate reliably in a combination of environments including temperature, space vacuum, zero gravity, shock, vibration and radiation (natural and/or produced by nuclear weapons). For many materials and components, the combined effect of these environments is hard to predict, and it is difficult to test components in a simulated combined environment to obtain design data. However, because of the inherent simplicity and ruggedness of fluidic elements, fluidic components appear to be more reliable than conventional counterparts.

The purpose of this section is to identify the technical problem areas and the major propulsion application areas, and to classify the uses of fluidic components. Standard criteria for evaluating engineering systems are reviewed relative to the selection of fluidic components for propulsion system use.

Technical Problem Areas

Prototype applications of fluidic rocket propulsion systems are increasing rapidly, particularly when the operational environments and the reliability requirements are severe. Progress to operational status has been delayed by the normal technical problems involved in assembling a working system; i.e., dynamic interaction, circuit noise, power consumption, power sources, sensors, and instrumentation. In addition, there have been a number of fabrication problems such as difficulty in sealing elements, physical connections and interconnections, allowable tolerances on physical dimensions, and manifolding. A major operational problem in propulsion systems is that shutoff is required to prevent venting during long standby periods.

Response Time - Comparison of various published fluidic element switching speeds is difficult because analytical techniques vary and a wide variety of test conditions are involved which are not directly comparable. In addition, the element size, the effect of connections and interconnecting lines, loading, etc., must be taken into account. In general, response time depends upon at least the following:

- 1) The compressibility or compliance of the fluid
- 2) The displacement of fluid mass required to switch the power jet
- 3) The flow which is entrained
- 4) The inertia of the jet to lateral deflections
- 5) The action of the vortex in the control region

Practical speed of response is currently limited to between 500 to 1000 cps. Time response is improved by miniaturization, but must be degraded (elements made larger) to maintain reliability.

Noise - The peak-to-peak amplitude of the pressure fluctuations in a fluidic element is defined as noise. These pressure fluctuations can make the discrimination of signals difficult and can result in erroneous outputs. The magnitude of the noise problem depends upon the specific elements and the system application.

Analog systems are generally more sensitive; consequently, signal-to-noise ratios in these applications must be high. This is especially important in staged amplifiers, where the noise in the output of the previous stage is amplified along with the signal in each successive amplifier. High signal-to-noise ratio is not quite as important for digital amplifiers where the output is at one of two discrete levels, and as long as noise does not exceed tolerable limits, the amplifier will still function properly.

Noise can be attributed to either external or internal factors as follows:

External Noise:

- o Turbulence in the input power or control streams because of environmental factors (i.e., vibration, shock, localized radiation heating, etc.)
- o Power supply fluctuations resulting from poor pressure regulation or fluid impurities

Internal Noise:

- o Primarily dependent on geometry, method of fabrication and operating condition
- o Influenced by surface roughness, abrupt transitions, sharp edges in a flow channel, edge-tone, impedance mismatches, jet velocity, and operating frequency
- o Also affected by downstream instabilities which are propagated back through the element interaction region.

Power Consumption - Fluidic control or logic circuits can consume relatively large amounts of power, depending on the application. For example, an aircraft gas turbine ingests hundreds of pounds of air per second and compresses it to 150 to 200 psi. With such a plentiful supply, the few cubic feet per minute required by a sensor and control system becomes less important. On the other hand, if high pressure stored gas is the only supply available for a low duty cycle application, a miniaturized fluidic element would be a significant power drain even with the gas throttled to a few psi, since continuous power jet flows are required. Consequently, if long standby periods occur, useful energy becomes a small part of the power supplied. Power consumption can be reduced by:

- o Efficient element geometries
- o Miniaturization
- o Use of moving part components in the power stages of high output systems
- o Development of efficient fluidic shutoffs.

Operational Problems - Fluid filtration, power source performance, element interchangeability, and system maintenance are the most frequently encountered operational problems to date. Conventional filters have been found adequate for most applications; however, in atmospherically vented circuits, care must be taken to avoid the aspiration of contaminants from the environment. The use of liquid propellants in the fluid circuits will offer other considerations, such as propellant compatibility, rheopectic or thixotropic behavior, and contamination of the environment. Many available power

sources do not deliver a constant power supply, and component selections and the circuit design must be made on this basis. Conventional pressure regulators are the only answer for the present, but good fluidic pressure regulators are expected in the future. Monopropellant gas generation systems and closed-loop power supplies hold the answers for aerospace application.

Unless absolutely necessary, miniature devices with small nozzle dimensions must be avoided to ensure low sensitivity to variations in operating conditions, fabrication, and contamination. Many new fluidic element designs are less sensitive to geometry variations, and manufacturing techniques are also being improved constantly. Instrumentation is presently inadequate; consequently, it is difficult to verify system performance and, more important, to pinpoint malfunctions. Concentration on satisfying the need for special purpose instrumentation should help; however, in the long run, the most promising solution is self-contained miniaturized instrumentation.

Analytical Techniques - Earlier development and a large percentage of the current development of fluidic elements and systems were done on an empirical basis, although current macroscopic mathematical models (the statistical averaging of fluid properties over relatively large regions) have provided useful results. This reflects the difficulty of mathematically analyzing steady-state device operation and the formidable problems encountered in representing transient phenomena. Major efforts are underway in industry, government agencies, and universities (notably MIT) to formulate and to commit to practice the tools and techniques required to facilitate the analytical design of fluidic components and systems.

The formulation of an analytical model is complicated by the fact that fluid flow phenomena are very sensitive to several interrelated variables. For example, wall attachment amplifier performance is influenced by many factors which include Reynolds number, the ratio of control jet to power jet pressure, several features of the element's geometry, size, surface roughness, and upstream and downstream loading. Then the complete solution of the model will require the use of numerical analysis techniques and probably could be done only by making some simplifying assumptions. Marked improvements in fluidic

technology will result when there is a successful extension of the numerical solutions of the fluid flow equations to a treatment of the jet-edge problems, the optimization of device parameters, the solution of pressure and flow transients, and the stability of a free jet in the presence of acoustic disturbances.

System Design - All fluidic elements must overcome similar conditions for their successful interconnection into circuits and systems. These include the effects of nonlinearities and dynamics in active and passive circuit elements and in connecting passageways, plus similar effects due to temporary and permanent instrumentation. Noise in supply lines and active element power jets is also an important factor. Transient circuit instability can result from any of these sources, and amplified noise can saturate analog stages or switch digital elements, just as it will in electronic circuits. Consequently, small changes in element and line geometries and/or surface finish can also cause significant changes in performance.

Optimum system performance requires a compromise among gain, stability, and speed of response. Each fluidic element must be carefully matched to its load characteristic for good power transfer and to provide sufficient signal power to drive successive stages. Besides providing maximum power transfer, the matching of line and port impedance minimizes the reflection of waves at the junctions of lines and ports. In general, it has been found practical to work with fluidic element static pressure-flow curves, which are usually nonlinear over wide ranges, but can be assumed linear for small swings about a chosen operating point. These curves can also be used to represent element dynamic characteristics up to about 400 cps.

Power supply regulation and reliability are necessary prerequisites to proper system performance. Fluid supply lines should be smooth and sized for sufficient capacity. If the flow area of supply lines and connectors is too small, unobserved pressure drops can occur so that supply pressures at individual element power nozzles will be less than specified. An even more serious consequence of small flow areas is the increased possibility of noise being generated from the resulting abrupt velocity changes.

In the design of analog systems:

- 1) Problems exist in matching component characteristics because of the inherent sensitivity of analog devices.
- 2) Noise is a major problem, particularly in high gain circuits where staging is required.
- 3) Most systems are directly proportional; i.e., the fluidic elements operate at a frequency and output level dependent on the input signal.
- 4) Carrier techniques are currently being applied to minimize signal to noise problems in critical applications.

Regarding digital system design:

- 1) More theoretical and experimental work has been done.
- 2) Vented digital elements are normally less sensitive to noise and load conditions.
- 3) Vented digital circuits are in the most widespread use; however a vented circuit is not the best choice where maximum power is desired (such as in most aerospace applications).

Propulsion Applications

For the purposes of classifying the uses of fluidic components, six major propulsion subsystem categories have been defined with various sublevels dependent upon the type of propellant used. Each of these areas involves different accuracy, power, and reliability requirements and thus will provide a basis for determining the best applications of fluidics technology. These categories are as follows:

- A. Ground Support Equipment
 - o Propellant handling
 - o Pressurant handling
- B. Propellant Pressure Control
 - o Pressure regulation
 - o Turbopump control

Stored gas

- o Pressure relief
- o Gas generator control

Liquid
Solid

C. Primary Flow Control

- o Thrust modulation
 - Cavitating venturi
 - Gas ingestion
 - Injector control
- o Chamber pressure control
- o Mixture ratio control
- o Reactor control

D. Thrust Vector Control

E. Attitude Control/Stabilization

F. Flight Instrumentation

- o Flow
 - Propellant
 - Pressurant
- o Transducers
 - Electro/Fluidic
 - Mechanical/Fluidic

The above areas represent extensive requirements for fluid control and parameter monitoring. While other areas can undoubtedly be added, these represent the primary interest for current fluidic applications.

The following types of propulsion engines are being considered in this study.

- o Chemical
 - Liquid bipropellant
 - Liquid monopropellant

Cold/Warm gas
Hybrids
Gels/slurries

- o Nuclear (Interface with chemical)
- o Electrical (Interface with chemical)

Due to the operating principles of fluidics which are based almost exclusively on continuously flowing systems, the above areas should be evaluated within the framework of potential mission phases. For the purposes of this study, the following are considered to be the major phases:

- o Prelaunch
- o Launch
- o Midcourse
- o Orbital
- o Reentry
- o Planetary Landing

The above phases can be further subdivided, however, as discussed in a subsequent section, the primary concern is the relationship between mission time, subsystem duty cycle, and the operating environments. These factors to a large degree, determine the limits of the use of fluidic components.

Standard Criteria

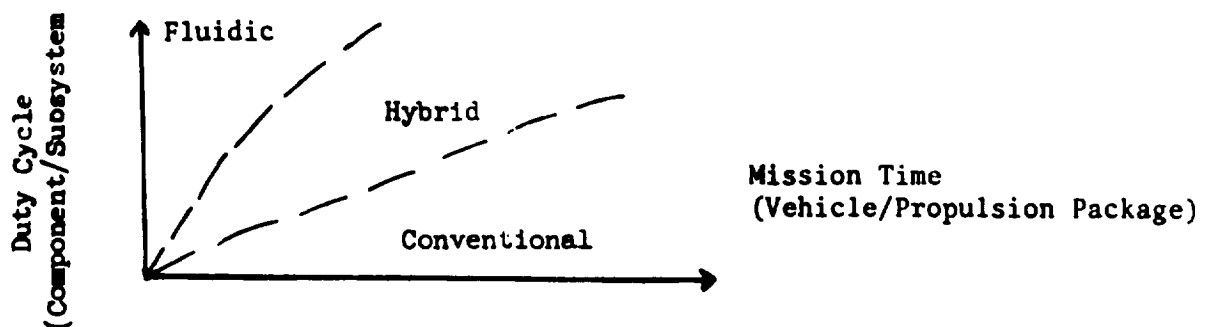
The most prominent potential improvements fluidic components offer are in the size, weight, and reliability of systems where it is advantageous to use a single fluid medium for all control functions and the need to translate information from one medium to another is eliminated. In evaluating systems, the ease or difficulty with which a mechanization concept meets a particular requirement is reflected in these parameters (size, weight, and reliability) which can be effectively compared. For example, a fluidic vortex valve can be designed to operate in a 2000°F environment without cooling. An electrically operated valve can also be made to operate in the same 2000°F environment, but only with additional cooling devices which add

to the size and weight and reduce the reliability of the valve. This means that stability, response, and ambient temperature capability are not direct items of comparison but are basic requirements for all components.

Standard criteria should be used in comparing fluidic elements and systems with their currently used counterparts. While a number of factors are involved in the evaluation, it is ultimately the cost or cost effectiveness of the proposed item which determines its acceptance or rejection. Thus, reliability, weight, performance, etc., are ultimately expressed in the cost necessary to employ the system and obtain the desired return. The cost of a program may be divided into conceptual development (acquisition) and maintenance (operational) phases with the primary contributing factors being the following:

- o System Weight
- o System Performance
 - Accuracy
 - Repeatability
 - Power Consumption
- o System Packaging

These criteria are thus being used to evaluate fluidic components and subsystems for propulsion system use. In the case of fluidics, a decision on its applicability to a particular use cannot be limited to a "yes" or "no," but must also consider the particular hybrid use of a few elements in conjunction with electromechanical, pneumomechanical, electrohydraulic, and other currently available components. The decision on the extent to which fluidics can be used is heavily dependent upon the mission length and duty cycle (on time/total mission time) as shown in the following sketch.



The dividing lines between the regions shown above will be flexible from system-to-system and dependent upon the cost factors previously described. System weight is the major factor in defining these regions while reliability is the deciding factor where a final selection is not clearcut. An attempt therefore will be made to establish wherever possible the operational regions for each subsystem previously described.

Typical Subsystem

One fluidic application will be in the area of hot gas or monopropellant attitude control systems which work from solid or liquid gas generator systems. This would, for example, be the case where a high chamber pressure, high thrust main engine is used plus low thrust attitude control engines. The attitude control engines might be of the hydrazine monopropellant or hot gas type while the main engine is a liquid bipropellant.

Consider the attitude control system as an example in determining a means of comparing a fluidic to a conventional system. Regulated gas is supplied at 1400 psia to each system (Figure 3-46) and the following requirements are presumed:

Chamber Pressure (P_c)	= 75 psia
Thrust (F)	= 10 lbs
Specific Impulse (I_{sp})	= 150 seconds
Engine Flowrate (\dot{w}_4)	= 0.067 lbs/sec

It is further assumed that the secondary pressure regulator, shown in Figure 3-46, can be either mechanical or fluidic and thus dictates whether this subsystem is pure fluidic or hybrid. When no signal (engine off) is received from the guidance system, the vortex valve control pressure (P_4) minimizes power flow which is dumped as \dot{w}_3 or used to augment main thrust. When an "on" signal ($P_7 = 140$ psia) is received, the power amplifier control pressure (P_5) switches power flow (\dot{w}_4) to the thruster at a maximum flow rate. For purposes of sizing a fluidic system, conservative pressure recovery factors were assumed and the guidance signal input (P_7)

was assumed to be of the same gas composition. This "on-off" characteristic can be provided using an electrofluidic transducer or even through the use of a fluidic guidance system. The electrofluidic transducers can be based on the electrostatic phenomena also being evaluated under this program.

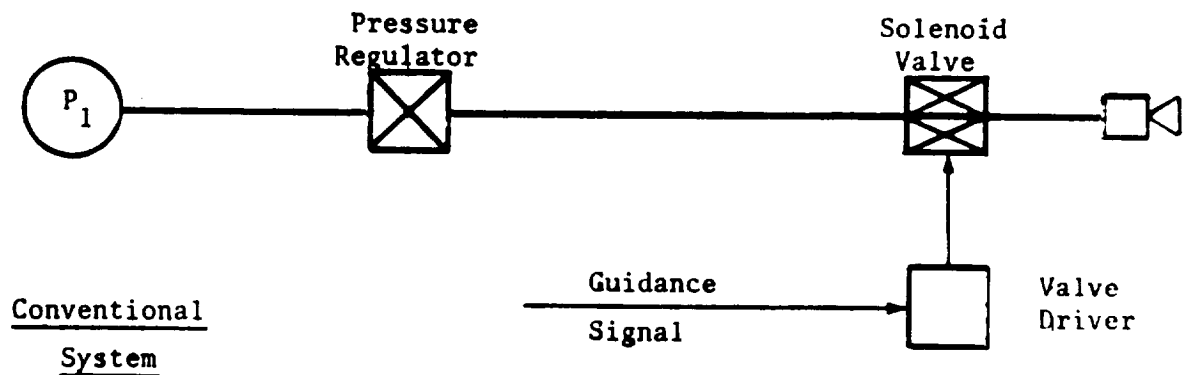
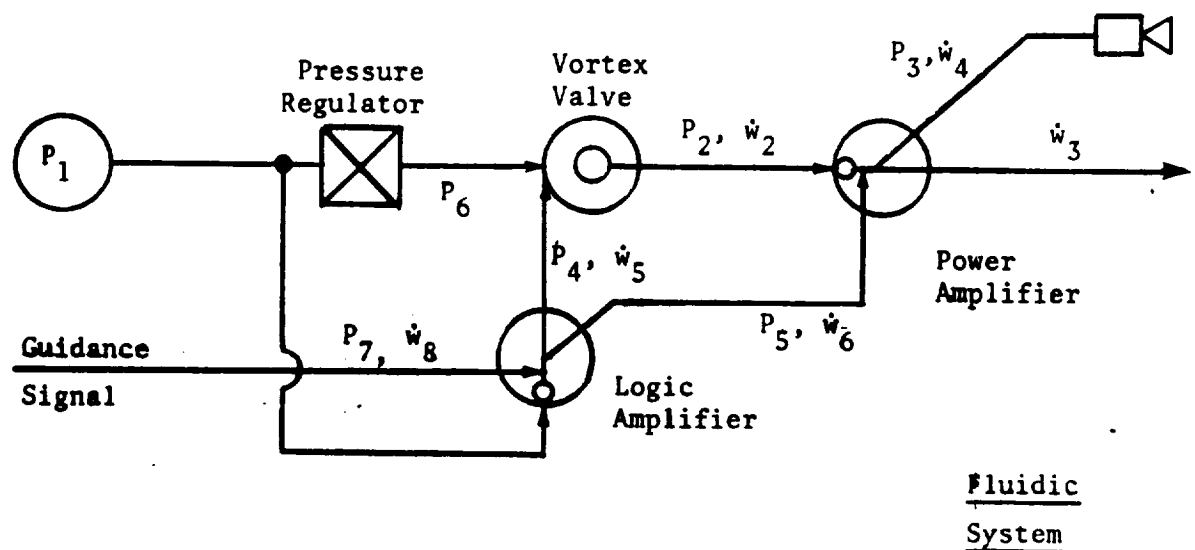


Figure 3-46 Fluidic Vs. Conventional Attitude Control System

The pressure recovery of the vortex valve is approximately 50 percent:

$$P_2/P_6 = 0.5 \quad (1)$$

The pressure recovery of the power amplifier is approximately 70 percent:

$$P_3/P_2 = 0.7 \quad (2)$$

The pressure recovery of the logic amplifier is also 70 percent:

$$P_4/P_1 = P_5/P_1 = 0.7 \quad (3)$$

The ratio of total flow to control flow through the bistable amplifier when the engine is firing is about 20:1.

$$\dot{w}_8/\dot{w}_6 = 0.05 \quad (4)$$

When the engine is turned off, the ratio of total flow to control flow through the vortex valve is about 1.1:1.

$$\dot{w}_5/\dot{w}_2 = 0.9 \quad (5)$$

Using these basic relationships, the operating characteristics (pressure and flow) of the fluid system controller can be determined as presented in Table 3-V.

Table 3-V
Fluidic Attitude Control System Parameters

P_1 (psia)	ON	OFF	\dot{w}_1 (lbs/sec)	ON	OFF
P_1	1400	1450	\dot{w}_1	.0638	.000638
P_2	250	25	\dot{w}_2	.0638	.00638
P_3	175	0	\dot{w}_3	0	.00638
P_4	0	980	\dot{w}_4	.067	0
P_5	17.5	0	\dot{w}_5	0	.00574
P_6	490	490	\dot{w}_6	.0032	0
P_7	140	0	\dot{w}_7	.00304	.00574
P_c	75	0	\dot{w}_8	.00016	0

The propellant consumption for the fluidic and electromechanical systems can be compared on the basis of duty cycle (ϕ) and mission time (T) with the former having the higher level as expected. The fluidic propellant consumption is given by Equation (6) and the solenoid valve system by Equation (7).

$$W_{p_T} = \left[\dot{w}_4 \phi + \dot{w}_3 (1 - \phi) \right] T \quad (6)$$

$$W_{p_T}' = \phi \dot{w}_4 T \quad (7)$$

The total system weight must also include the pressure regulator and the vortex and monostable amplifiers for the fluidic system and the pressure regulator, relief valve, valve driver and solenoid valve for the standard system. Assuming a fluidic system weight of 0.25 lb and a conventional system weight of 1.35 lb, eliminating the weight of the pressure regulator which is equal in both cases (a fluidic regulator could, however, be lighter) the total weights of the two systems can be compared for various duty cycles (Figure 3-47). The equivalent duty cycle (ϕ) versus mission time (T) curve based on a weight comparison only is presented in Figure 3-48. The two areas represent minimum system weights respectively. Again, the actual selection would also have to involve the other cost factors.

This type of analysis can be useful in evaluating the applicability of fluidic systems. However, the analysis is only as good as the assumptions made. Before continuing the analysis, the current state-of-the-art performance capabilities of fluidic components must be determined. In addition, fluidic systems should be designed so as to minimize system dry weight as well as power consumption. New concepts and/or components will be considered in an effort to optimize the fluidic system.

In examining Figure 3-48, it becomes apparent that in many cases a supply shutoff capability should extend the application of fluidic systems to longer mission times at the smaller duty cycles. Reliable shutoff concepts directly applicable to fluidic systems are also being studied under this task.

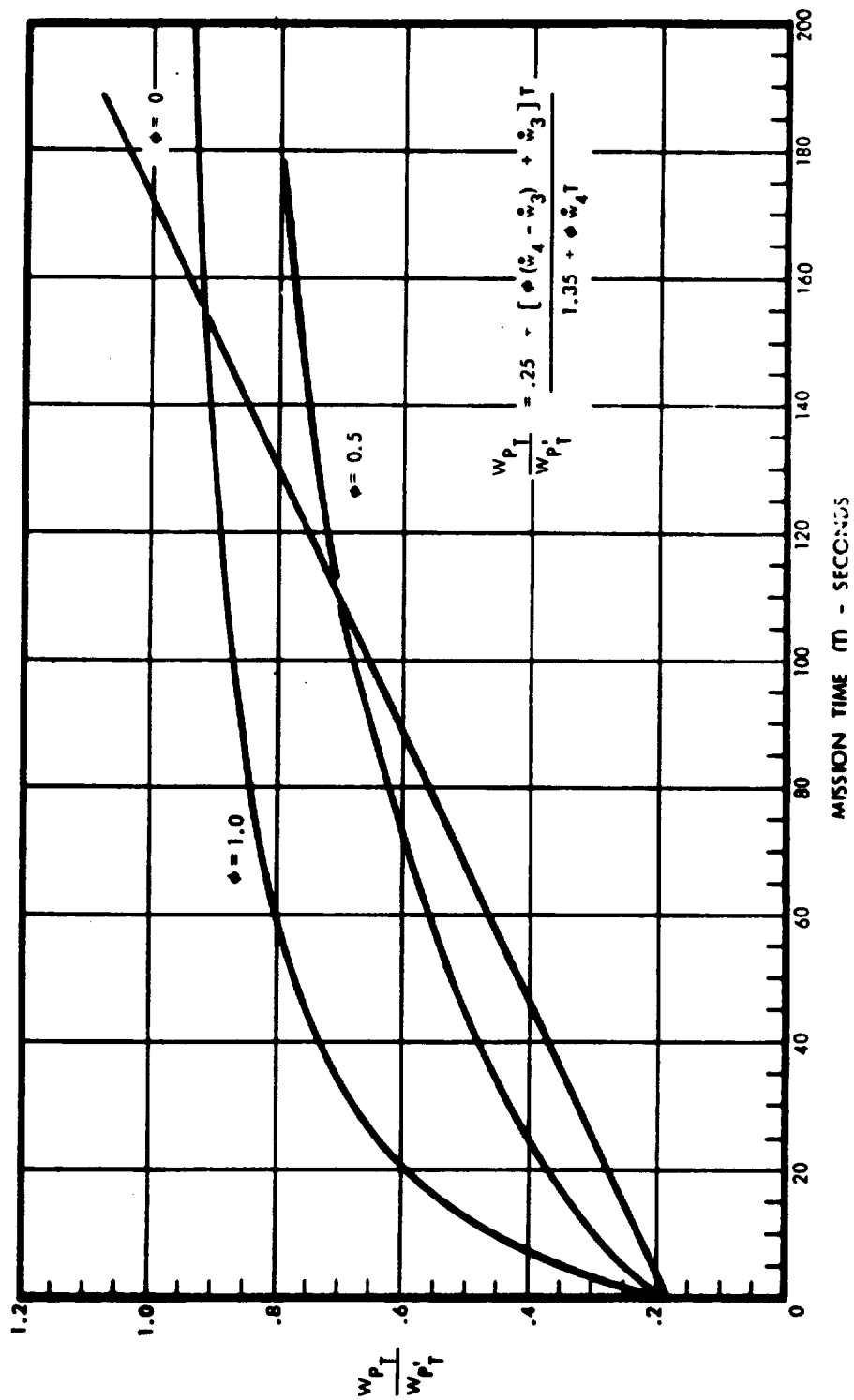


Figure 3-47 System Weight Ratio Versus Mission Time

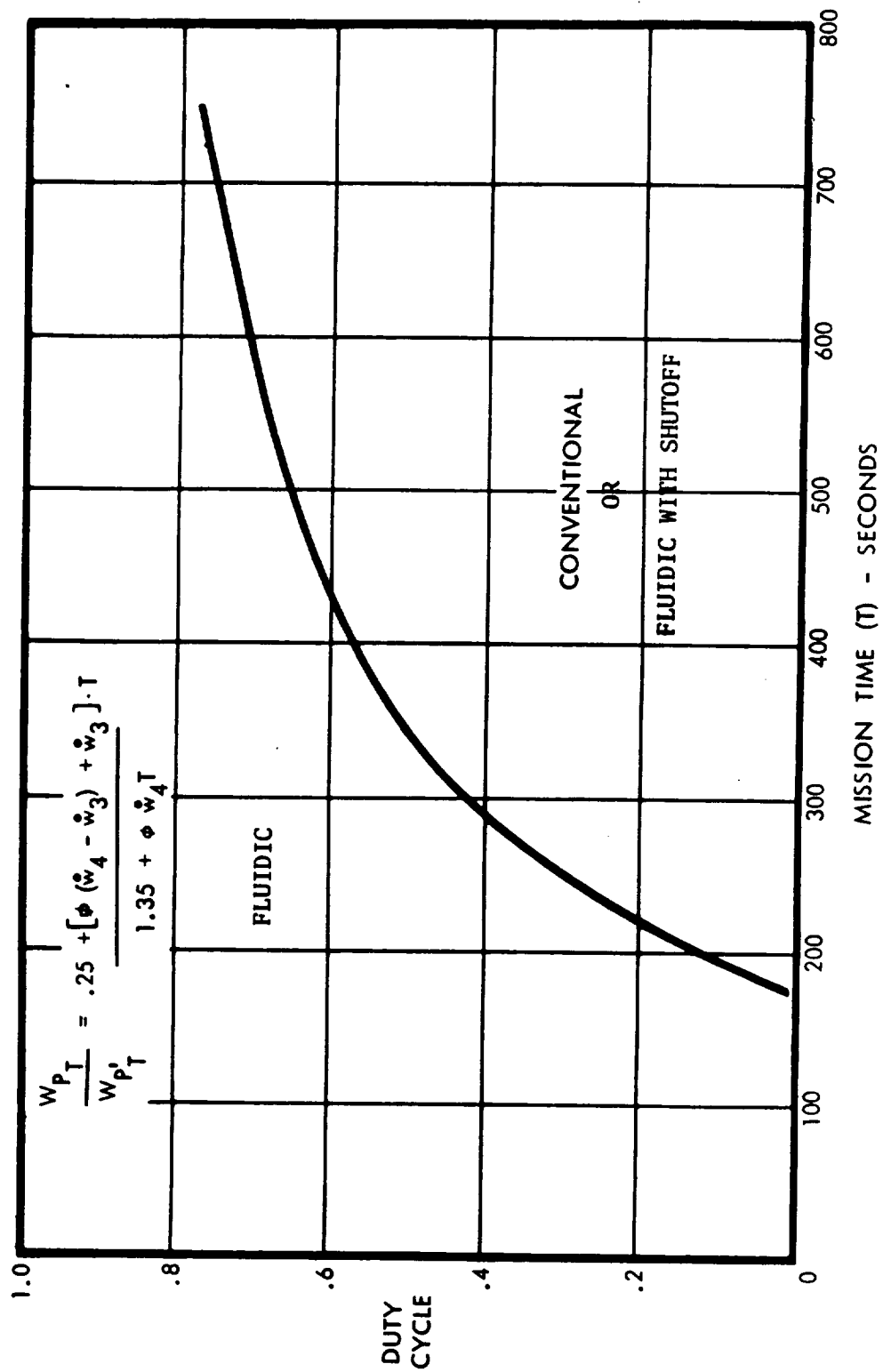


Figure 3-48 Optimum System Weight Regions

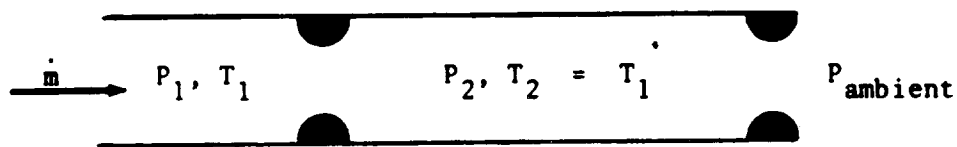
CONCEPTUAL STUDIES

The objectives of these studies are to describe fluidic concepts which have potential application to propulsion control systems and to evaluate these concepts both analytically and experimentally. A further objective is the evaluation of new concepts, particularly those related to propellant pressure and flow regulation, pressure regulation, and shutoff functions.

Fluidic Pressure References

Precise reference pressure signals should have a variety of uses in spacecraft power systems. The primary uses are seen as set points for fluidic pressure regulators, reference signals for fluidic controllers, and a necessary prerequisite to accurate time delays in sequential fluidic circuits.

Nonlinear versus Linear Resistors - Given two orifices in series,



if the second orifice is choked, the pressure ratio across the first orifice is independent of supply pressure and temperature for adiabatic flow, i.e.,

$$\dot{m} = \frac{K_1 P_1}{\sqrt{T_1}} f\left(\frac{P_2}{P_1}\right) = \frac{K_2 P_2}{\sqrt{T_2}} \quad (8)$$

$$\frac{P_2}{P_1} = K f\left(\frac{P_2}{P_1}\right), \quad (9)$$

where K , K_1 and K_2 are constants and $f\left(\frac{P_2}{P_1}\right)$ indicates a function of.

Therefore the operating point pressure ratio is given by the point of intersection of two curves, and is independent of supply pressure and temperature as shown in Figure 3-49:

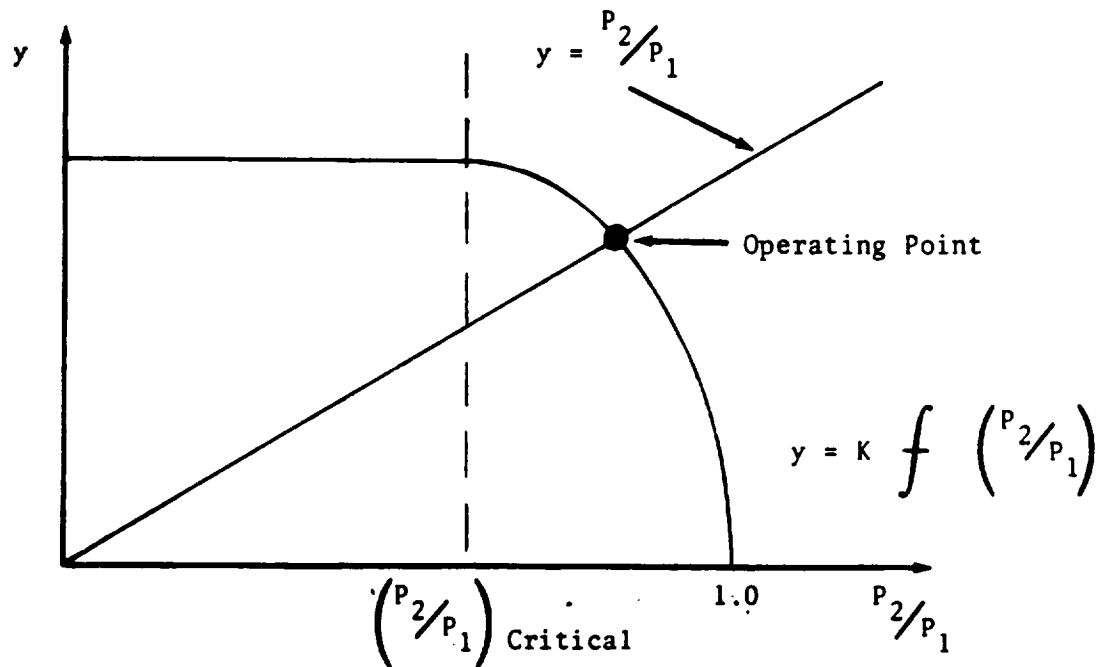


Figure 3-49 Illustration of Operating Point Pressure Ratio

Consider the following laminar resistor (linear) and fixed orifice (non-linear) circuit configuration.

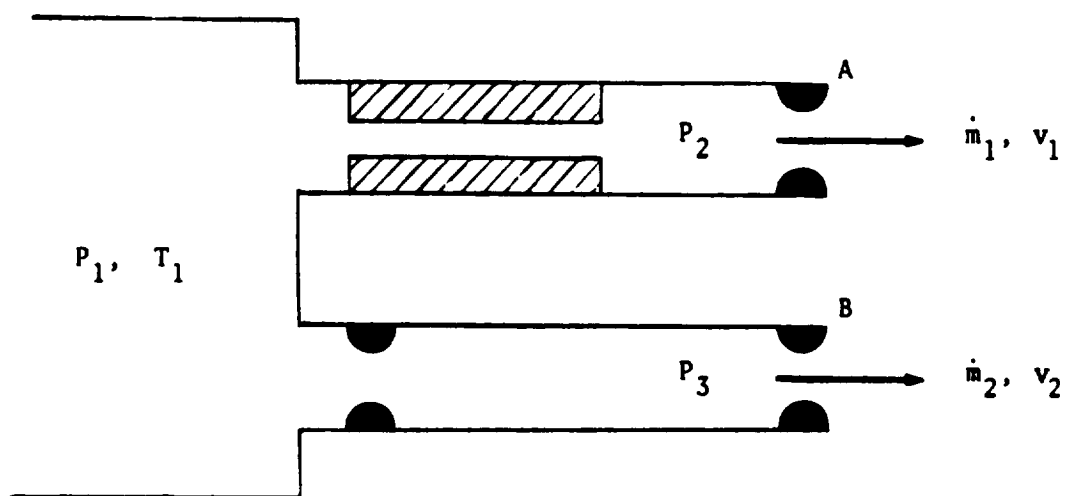


Figure 3-50 Laminar vs Orifice Restrictor Circuit Configuration

Assuming orifices A and B are of equal area and choked, $P_3 = C_1 P_1$ by the above, however, for laminar flow and small values of $(P_1 - P_2)/P_1$

$$P_1 - P_2 = \frac{64 \rho v^2 l}{2 g d R_n} = \frac{C_2 \mu \dot{m}_1 T_1}{P_1}, \quad (10)$$

and

$$\dot{m}_1 = \frac{P_1 (P_1 - P_2)}{C_2 \mu T_1} \quad (11)$$

NOTE: C_1, C_2, C_3 , etc., are constants.

For gases, the viscosity μ may be approximated by

$$\mu(T) = \mu_0 \left(\frac{T}{T_0} \right)^\alpha = C_3 T^\alpha \quad (12)$$

where α is a constant and in the range $0 < \alpha < 1$. Therefore,

$$\dot{m}_1 = \frac{P_1 (P_1 - P_2)}{C_4 T_1^{(\alpha+1)}} = \frac{C_5 P_2}{\sqrt{T_1}} \quad (13)$$

which can be rearranged to

$$P_2 = \frac{P_1^2}{P_1 + C_4 C_5 T_1^{(\alpha+1/2)}} \quad (14)$$

Now, since $P_3 = C_1 P_1$

$$P_2 - P_3 = \left[\frac{1}{1 + \frac{C_4 C_5 T_1^{(\alpha+1/2)}}{P_1}} - C_1 \right] P_1 \quad (15)$$

For a fixed T_1 , a graph of Equation (15) would be represented by (Figure 3-51):

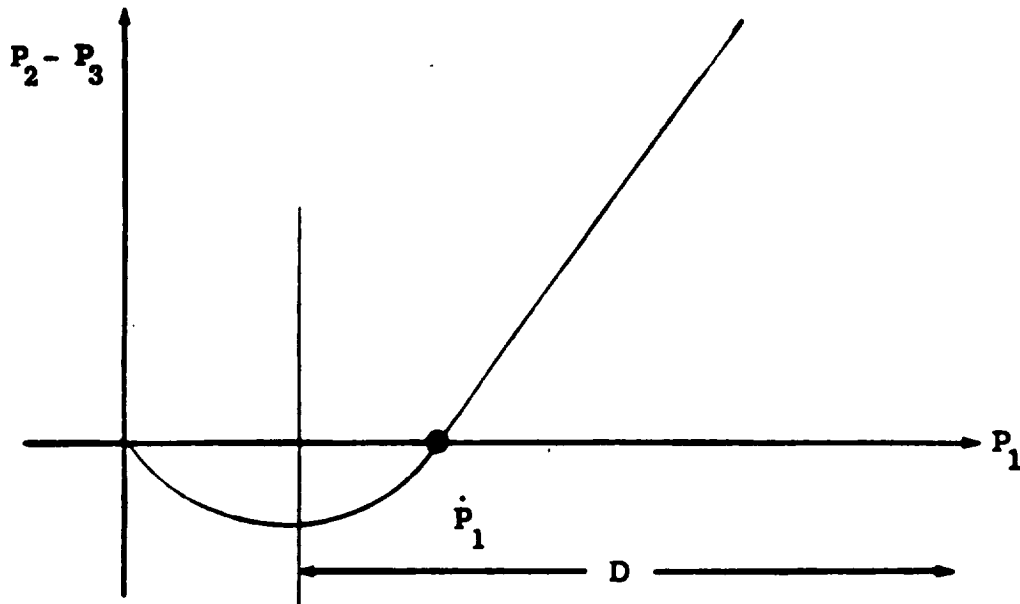


Figure 3-51 Graph of Laminar vs Orifice Restrictor ΔP

It can be seen that in the region D the inverse function of Equation (15) is single valued and $P_2 - P_3$ can be used as a measure of P_1 . If the resistors and orifices A and B are sized so the \dot{P}_1 is the desired reference pressure, then $P_2 - P_3$ can be applied across the control ports of a beam deflection proportional amplifier as an error signal (Figure 3-52).

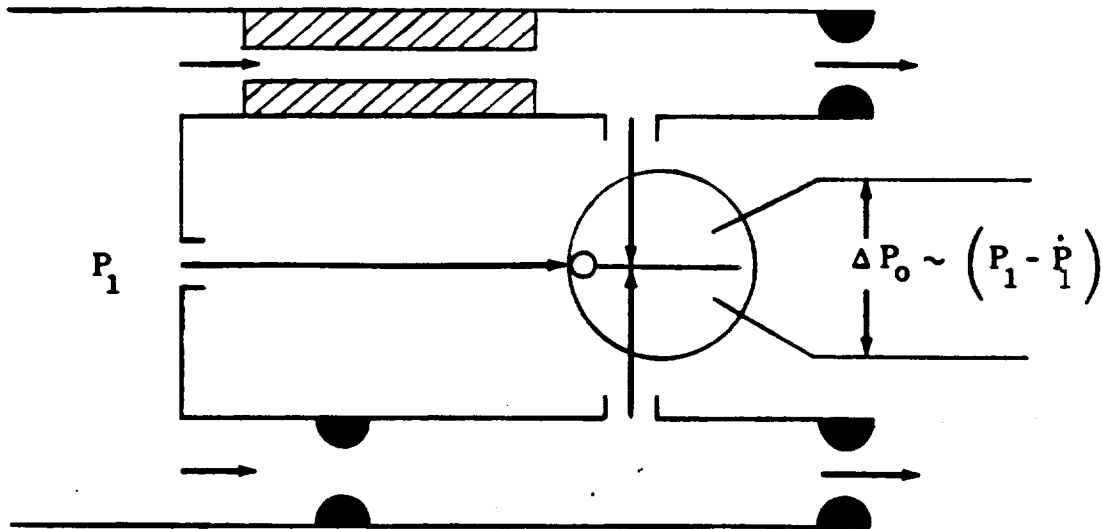


Figure 3-52 Laminar vs Orifice Restrictor Pressure Reference

The more general technique is to use the difference in momentum flux of the flow rates \dot{m}_1 and \dot{m}_2 as the error signal by applying these flows directly to the control ports of a proportional amplifier as shown in Figure 3-53. Then,

$$\dot{m}_1 v_1 - \dot{m}_2 v_2 = C_6 \left(\frac{\dot{m}_1^2 - \dot{m}_2^2}{\rho} \right) = \frac{C_7 T_1}{P_{Iz}} (\dot{m}_1 + \dot{m}_2) (\dot{m}_1 - \dot{m}_2) \quad (16)$$

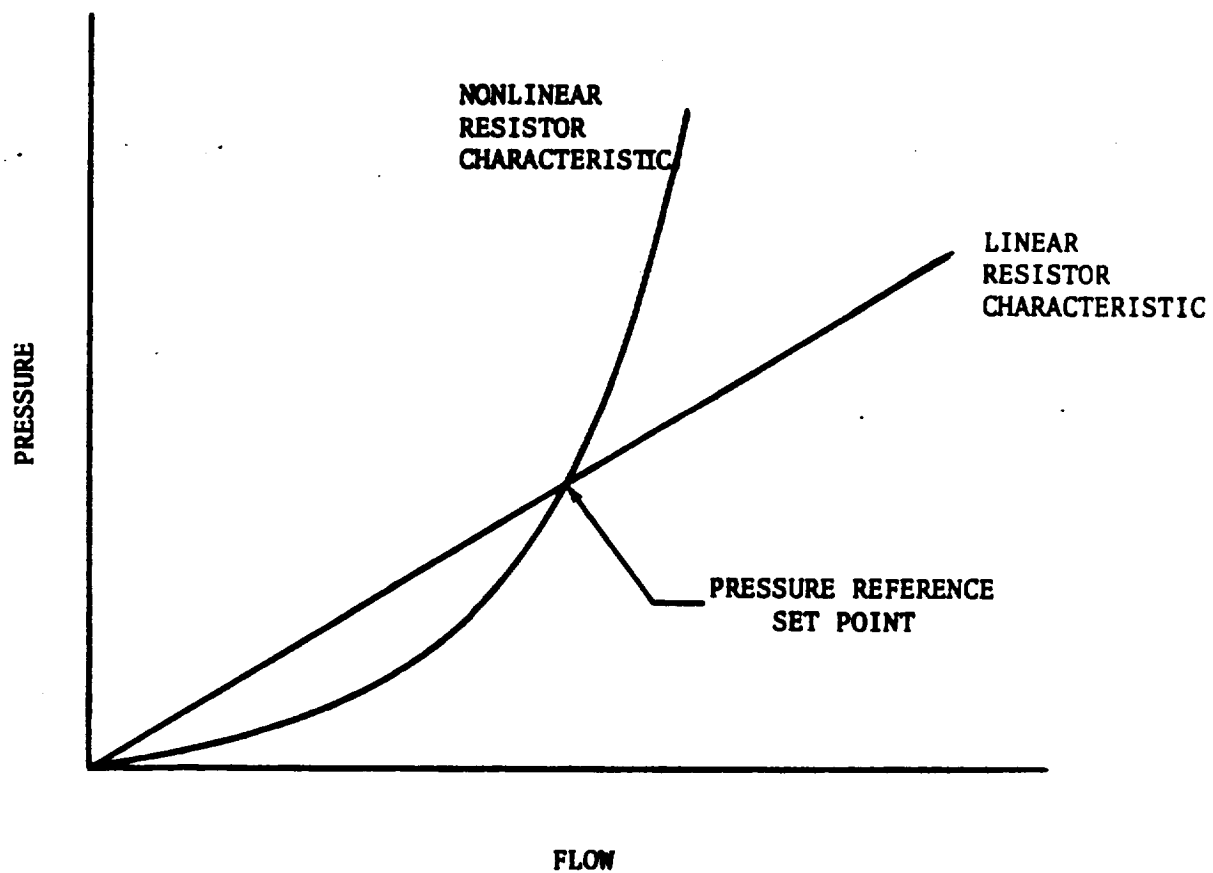
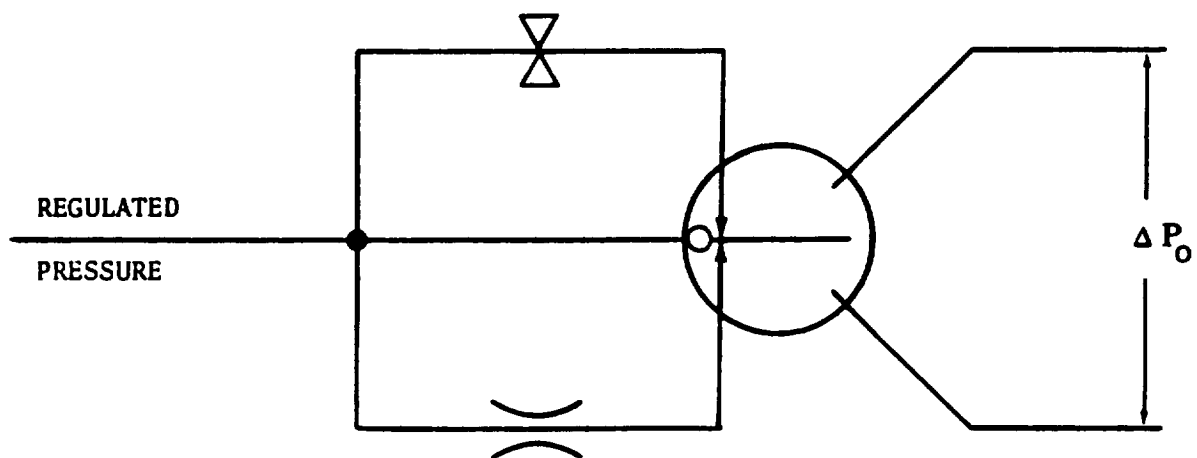


Figure 3-53 Characteristics of Linear-Nonlinear Resistors
As a Pressure Reference

and if the orifices are sized so that $\dot{m}_1 = \dot{m}_2$ at the desired reference pressure \dot{P}_1 ,

$$\dot{m}_1 + \dot{m}_2 \approx 2 \dot{m}_2 = \frac{2C_5 P_1}{\sqrt{T_1}} \quad (17)$$

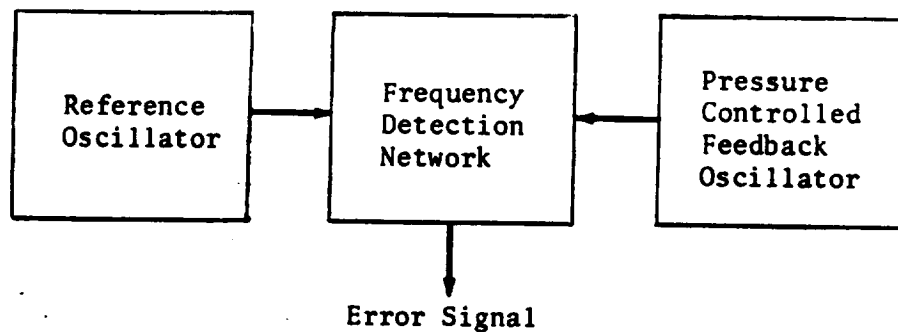
for small perturbations about the set point. Therefore, Equation (16) becomes (where P_{IZ} = pressure in the proportional amplifier interaction zone)

$$\dot{m}_1 v_1 - \dot{m}_2 v_2 = \frac{C_8}{P_{IZ}} \left[\frac{1}{\frac{1}{C_5} + \frac{C_4 T_1}{P_1}} - C_5 \right] P_1^2 \quad (18)$$

which has the same behavior as the function shown in Equation (15) in the neighborhood of \dot{P}_1 and consequently the same conclusions hold.

For a constant upstream pressure, the ΔP across a laminar restrictor is directly proportional to the absolute temperature and the ΔP across an orifice is inversely proportional to the absolute temperature. Consequently, the desired reference pressure will change with variations in fluid temperature, and temperature compensation becomes an important consideration when utilizing a linear restrictor versus a nonlinear orifice as a pressure reference. Several methods have been proposed, which entail compensation of either resistor by adjustment of the resistance as a function of temperature. One scheme utilizes the differential expansion of a contoured needle in an orifice to perform the required compensation. A detailed analysis of all possible methods of compensation is required before this reference scheme would be considered practical.

Fluidic Oscillator Reference - Fluidic oscillators offer a means of achieving precision pressure references. In a fluidic regulator the reference frequency would represent the regulator set point. Its output is then compared with a feedback signal whose frequency represents the analog pressure output of the regulator, i.e., the output could be fed back through a pressure controlled oscillator, so as to generate a frequency signal indicative of the output. This feedback signal and the reference oscillator signal are then compared, and an error signal representing their difference is generated.



The reference oscillator must be made to oscillate at a constant frequency for wide variations in supply fluid temperature and pressure. Theoretical analysis and experimentation have been performed (Reference 3-6), on temperature insensitive oscillators using distributed parameter and lumped RC feedback ducts. Preliminary results have indicated oscillator accuracies of ± 1 percent over a 200°F temperature range.

Although the speed of sound in free space is proportional to the square root of the absolute temperature, the complex speed of propagation of a wave in a duct is a function of the distributed inertance, capacitance, and resistance. The magnitude of the complex speed of propagation, in a duct of constant cross section, for small amplitude waves is given approximately by

$$|C|^4 = \frac{a^4}{1 + \frac{R^2}{\omega^2 L^2}} \quad (19)$$

and for a circular duct on the basis of the ideal gas law

$$|C|^4 = \frac{1}{T^2} + \frac{a_1}{\omega^2 A^2 \rho^2} T^{3/2} \quad (20)$$

where a_1 and a_2 are constants, and

- C = complex speed of wave propagation
- A = free speed of sound
- T = temperature
- R = resistance per unit length of duct
- ω = angular frequency
- L = inertance per unit length
- P = pressure

An examination of Equation (20) shows that for $T = 0$ and for $T \rightarrow \infty$, $|C| = 0$. Therefore, $|C|$ has a maximum value at some discrete temperature and should be less sensitive to temperature in the vicinity of the maximum. An important point is that temperature insensitivity in an oscillator is gained at the expense of pressure sensitivity. This is determined from Equation (20) which shows that for large A, the speed of propagation becomes less sensitive to the pressure.

Considerable effort needs to be expended in the development of fluidic oscillators. The requirements of a reference oscillator are quite stringent, in that it needs to be both pressure and temperature insensitive. However, the right course of action appears to be the optimization of a temperature insensitive oscillator through the use of the inherent characteristics of distributed parameter and lumped RC feedback ducts, then to correct for pressure sensitivity by the use of a pressure controlled oscillator and a frequency discrimination network.

Tuning Fork Fluidic Oscillator - A precision oscillator has been developed recently (Reference 3-7), which consists of a temperature compensated tuning fork, a load insensitive fluidic flip-flop, control transmission lines, and a feedback transmission line. This device has a frequency accuracy of $\pm .002$ percent at room temperature and $\pm .05$ percent over a temperature range of -35°F to 200°F when operated at 400 cps. Although hybrid in nature, this tuning fork oscillator offers the possibility of such an extremely accurate frequency reference that it cannot be overlooked.

Operation of the oscillator is illustrated in Figure 3-54. The supply stream emerges from an aperture in one tine (control) of a tuning fork, and is alternately switched to the two downstream channels as the control tine oscillates. The two downstream channels are used as the control inputs to a load-insensitive flip-flop, which oscillates accordingly. The fluid pulse train emerging from one output channel is fed back and impinged on the other tine of the tuning fork, which maintains oscillation of the fork at its natural frequency. The other flip-flop output channel is used as the output signal. Since the device uses the air pulse only to apply sufficient energy to the tuning fork to sustain oscillation, the oscillator is considerably less sensitive to variations in the speed of sound due to temperature changes which compromise the accuracy of a typical fluidic sonic oscillator.

The tuning fork is a high Q device, i.e, it loses a minimum of energy due to damping and mounting effects, and it can be driven with relatively low power inputs. Temperature compensation of the tuning fork can be accomplished by special alloys, heat treatment, or bimetal construction. The trend should be to small high frequency forks, since higher frequencies result in smaller amplitudes and better accuracy and also minimize the effects of acceleration and vibration.

Fluidic Pressure Regulation

A pressure regulator is defined as a component, or valve, that controls pressure by varying flow as a function of the sensed difference between the actual and the desired value of pressure. In spacecraft systems, the

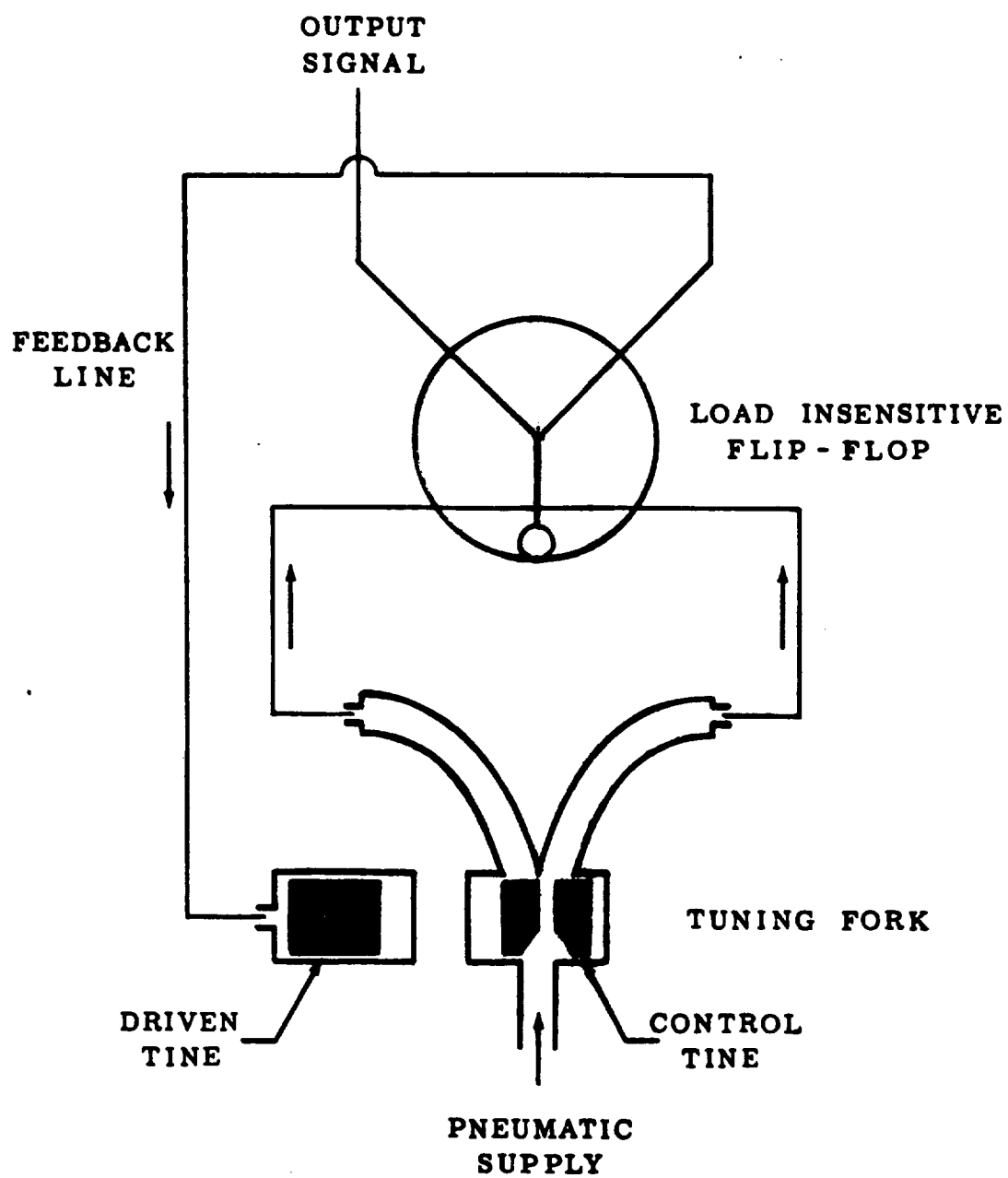


Figure 3-54 Fluidic Tuning Fork Oscillator

term pressure regulator is generally accepted as meaning any device which maintains a predetermined upstream, downstream, or differential pressure by means of a pressure reducing control element. The most common applications are to provide a constant pneumatic pressure in a liquid storage tank for direct expulsion or to maintain pump suction head requirements.

Since gas is more efficiently stored in pressure vessels at high pressure (3000 psig or greater), the pressure reducing regulator is the most common type used in spacecraft systems. Pressure reducing regulators reduce upstream pressure to a predetermined downstream pressure regardless of upstream pressure variations and can be classified as modulating or non-modulating. A modulating pressure regulator can achieve any steady-state flow rate necessary to maintain a constant regulated pressure, and consequently is the most common. A nonmodulating regulator is simply a two-position device which is often referred to as a "bang-bang" regulator. A solenoid valve operated by a pressure switch would be an elementary non-modulating regulator.

The temperature extremes normally encountered in spacecraft applications change regulator set points by thermal contraction or expansion. In spring loaded regulators, simple compensation is accomplished by insulating or caging the reference spring. However, it is a complex problem to accurately predict and/or accurately determine the exposure to changes in temperature, so that complex thermal compensators are the general solution. Vibration poses one of the most difficult design problems since poppets, springs, and bellows are particularly susceptible. Acceleration requirements for spacecraft vehicles also impose severe g-loads along any axis, so that compensation is necessary to accurately maintain the regulator set point.

A fluidic pressure regulator should be simpler and have few, if any, moving parts. Consequently, longer storage life, higher reliability, and greater environmental tolerance should result. Improvements in size, weight, and cost are also possible. These are excellent reasons for

investigating the state-of-the-art of fluidic pressure regulators, and for considering their future application in spacecraft systems.

Throttling Methods - A vortex valve exhibits a variable and controlled impedance. The impedance is produced by a combination of the pressure-flow characteristics of orifices and the radial pressure distribution in vortex flow; the variable impedance is induced by control of the tangential velocity of the vortex field.

An elementary vortex valve configuration is shown in Figure 3-19. With no control flow present, the supply flow enters the vortex chamber and proceeds radially inward toward the outlet orifice. Since the supply port is generally much larger than the outlet orifice, the flow through the vortex valve is determined by the supply pressure, outlet pressure, and the outlet orifice area. Therefore, presuming the outlet orifice is choked, the outlet flow is determined by

$$\dot{m}_o = 0.49 C_d A_o P_s \sqrt{\frac{2g}{RT}}$$

When control flow is injected tangentially into the vortex chamber, a rotational component is imparted to the supply flow. The ensuing vortex field creates a radial pressure gradient which reduces the pressure at the outlet orifice, and thus reduces the outlet flow. The turndown ratio of the vortex valve is defined as

$$\text{Turndown ratio} = \frac{\dot{m}_o (P_c \leq P_s)}{\dot{m}_o (\dot{m}_s = 0)} \bigg|_{P_s = \text{Constant}}$$

Present state-of-the-art vortex valve performance is summarized in Table 3-IV, along with expected performance gains in the next five years.

The static performance characteristics of one of the best available single exit vortex valves is conveniently represented by the family of curves shown in Figure 3-22. This particular valve was considered for use in a fluidic pressure regulator for a fluidic missile control system. The

function of the regulator was to deliver a constant pressure of 15 psig to a fixed orifice load, from a stored nitrogen supply. The minimum supply pressure was specified at 100 psig. From Figure 3-22, it can be seen that the valve will deliver the required output pressure P_o for supply pressures P_s between 650 and 150 psig. The absolute supply pressure ratio $665/165 = 4.0$ is the same as the turndown evaluated at $P_s = 650$ psig, which is $(103 + 15)/30 = 3.94$. It is obvious that for higher supply pressures, the control pressure at turndown would be higher than the required 15 psig regulated pressure. The control to supply pressure ratio, P_c/P_s , at turndown is $750/650 = 1.15$.

An optimized double exit vortex valve will presently give a turndown ratio of 8 for a P_c/P_s ratio of 1.2. This should increase to about 10 in the next five years. It is impractical to use a fixed area orifice to drop the vortex valve supply pressure below the storage tank pressure to obtain the necessary P_c/P_s ratio. This is the case because the pressure dropping orifice becomes sonic during tank blowdown and consequently can not be controlled by the downstream vortex valve even for a slight decrease of the tank pressure.

It has been shown (Reference 3-8) that staging of vortex valves, will give no improvement in turndown, i.e., the overall turndown ratio of two series connected valves (Figure 3-55) will in general be less than the turndown ratios of the individual valves. The primary reason for this is that it would be impossible to operate vortex valve B in a fully turned down condition, since provision must be made for the control flow from valve A when it is in a turned down condition.

Another method of cascading vortex elements is to use a vortex amplifier as a pilot valve which feeds the control and supply ports of a second valve (Figure 3-56). The pilot valve pickoff converts the vortex valve into an amplifier. The differential pressure range between the two pickoff exits then changes much more rapidly than the control pressure, and the central pickoff sees up to 98 percent of the supply pressure with no control flow and almost zero pressure when the pilot valve is turned down.

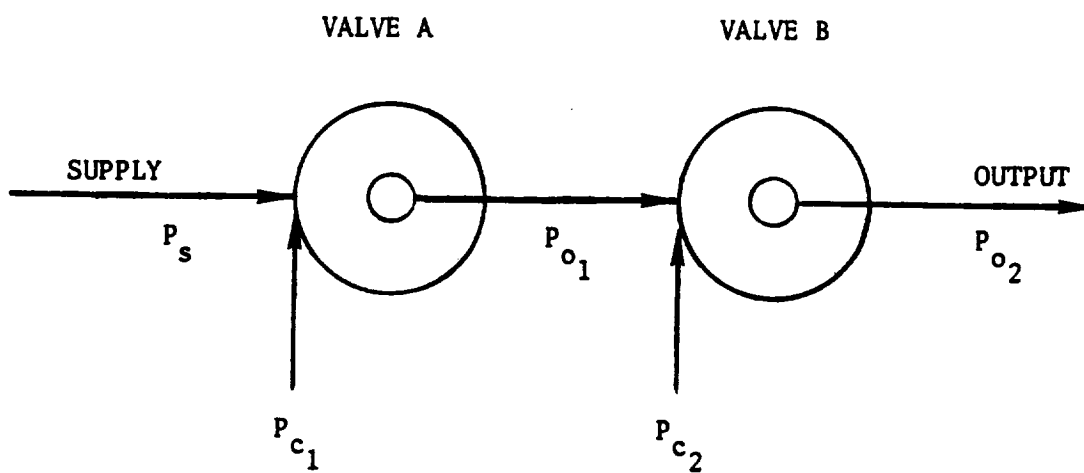


Figure 3-55 Series Connected Vortex Valves

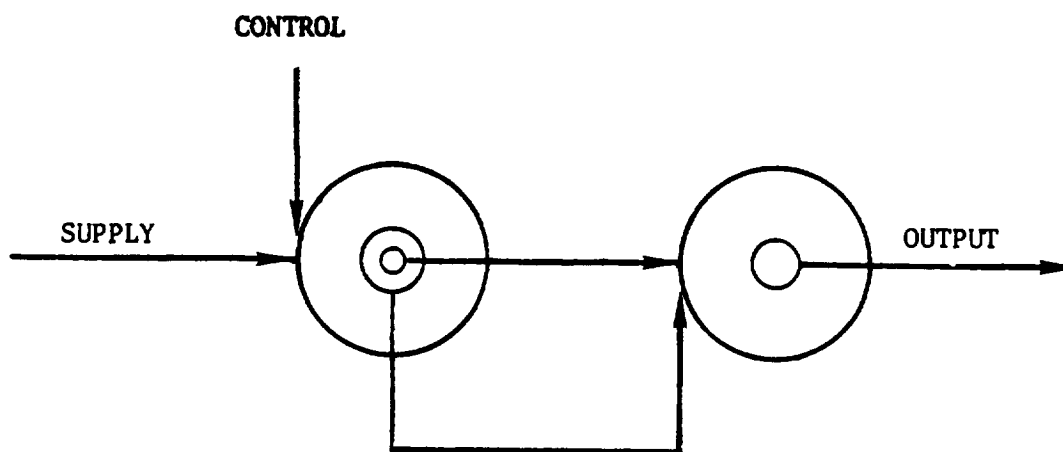


Figure 3-56 Vortex Amplifier - Vortex Valve Cascade

This arrangement should give an overall turndown ratio of from 10 to 20 percent better than for that of a single vortex valve.

The vortex devices discussed previously are characteristic of methods of throttling flow without overboard bleeds. Proportional and bistable amplifiers can also be used as throttling devices, however, these devices must be operated with two output legs, one tied to the regulated load and the other dumped to atmosphere. Consequently, the throttle not only must live with the relatively low power recovery of the amplifiers (about 50 percent), but must also dump flow continuously in the regulation mode. For a blowdown source and a variable load, these power losses may preclude acceptable regulation efficiencies.

Pressure Reference Methods - The deviation of the regulated pressure from the desired value or set point, must be sensed in a high gain circuit so as to provide a feedback signal which can be used to control the throttling element. A pressure reference may require separate devices for its function alone, or the reference can sometimes be an intrinsic part of the feedback circuit.

The most widely used pneumatic pressure reference, which was discussed previously, utilizes the difference in the characteristics of a nonlinear and a linear resistor (Figure 3-53). When the regulated pressure is as desired, the control inputs to the amplifier will be identical and the differential output pressure, ΔP_o , will be zero. If the regulated pressure becomes higher or lower than the set point, there will be a differential output from the amplifier which can be integrated and further amplified in a feedback circuit to adjust the throttling element accordingly.

Another method of detecting shifts in a reference circuit, is to use the pneumatic flow characteristics of a series of equal area orifices. It has been shown (Reference 3-8) that if a series of n orifices is flowed in parallel with a single orifice, the relative quantities of flow in each branch will be a function of the pressure ratio across them. The changes in flow in the two branches can be detected if the branches are in the supply and control lines of a vortex pressure amplifier as shown in

Figure 3-57. One restriction of this reference scheme is that the vent orifice of the vortex pressure amplifier must not be sonic, otherwise its pressure ratio will be effectively independent of changes in the regulated pressure.

Another possible reference scheme is to utilize the output of a pressure controlled fluidic oscillator. A tuned cavity such as a Helmholtz resonator can be used to detect the correct reference pressure, and an optimizing feedback circuit can be used to adjust the throttle. The current state-of-the-art of fluidics is far enough advanced, to permit implementation of a circuit of this type.

The primary problem with all of the pressure reference schemes indicated is temperature sensitivity. Very little effort has been expended to date in the area of temperature compensation, and a concentrated effort should be made to come up with a temperature compensated absolute pressure reference. In particular, fluidic oscillators have been compensated (Reference 3-6) over a wide temperature range by using a distributed parameter feedback duct.

Feedback Methods - These are defined as the circuits that are used to generate signals which are used to control the throttling elements as a function of the deviation of the output pressure from the set pressure. Although the term regulator implies the use of feedback, the requirements of a nonmodulating regulator can be met by programming the effective area of the throttling element as a function of the tank pressure. However, the anticipated future regulator requirements for space systems point to variable load conditions which require closed-loop control.

The vented jet amplifier utilizes the properties of a freely expanding jet impinging on a receiver (Figure 3-28). By confining the jet, and controlling the vent rate of gas from the chamber, useful amplification is achieved. In this device a high pressure source is controlled by a low pressure source. By varying the geometry and spacing of the nozzle and the receiver, several gain characteristics can be obtained. Supply

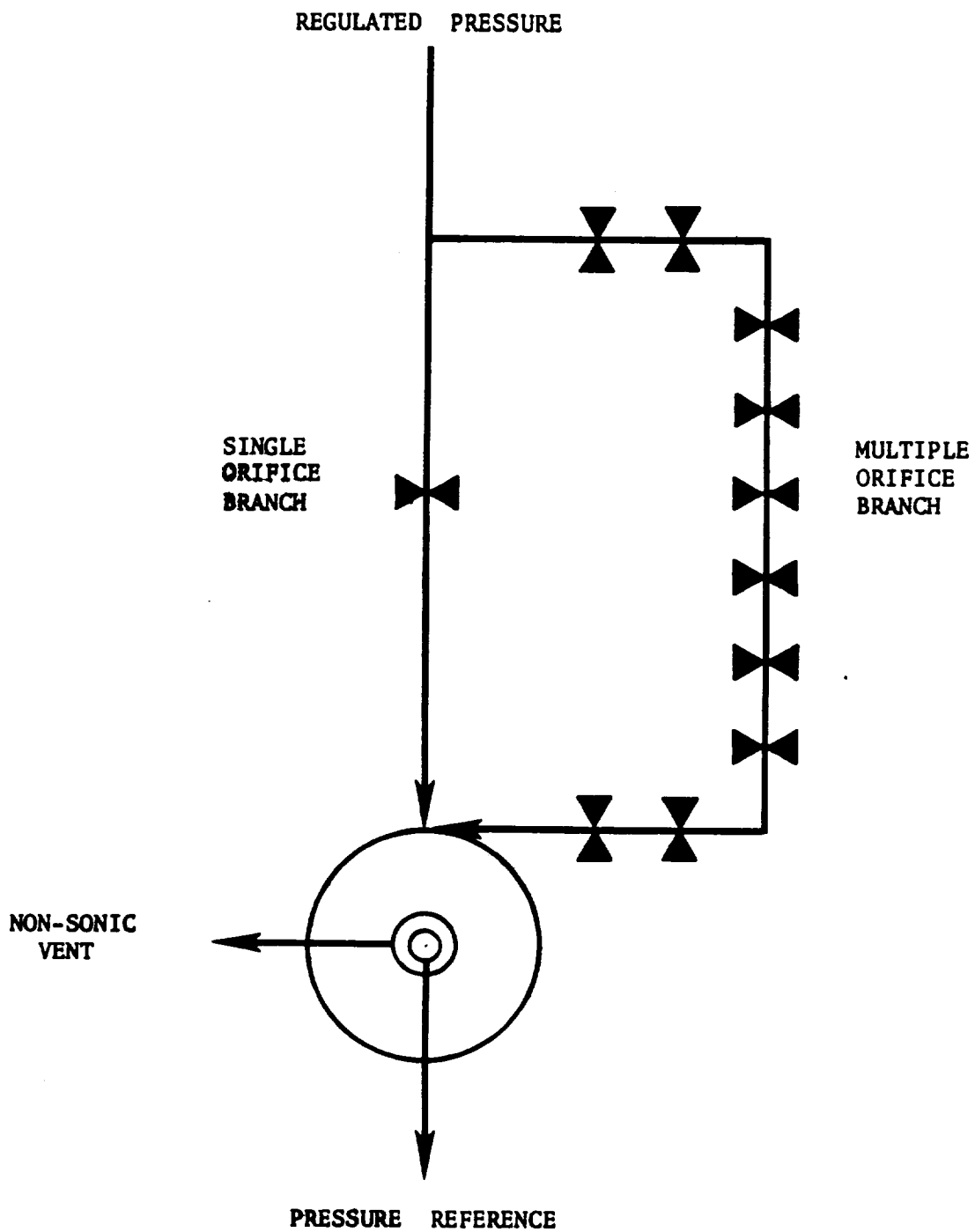


Figure 3-57 Single Versus Multiple Orifice Bridge

pressures are normally controlled by vent to supply pressure ratios, P_v/P_s , of 0.1 to 0.3, with maximum output flow and pressure recoveries on the order of 70 to 90 percent.

Typical performance of a vented jet amplifier with a fixed area load is shown in Figure 3-30. An interesting and useful property of the vented jet is shown in the figure, i.e., if the vent pressure is held at about 50 psig, the output pressure is practically independent of the supply pressure in the range from 250 to 500 psig.

The vented jet amplifier is particularly useful in controlling a vortex throttling element because of its high pressure recovery (>70 percent) when supplying a flowing load. A single-stage feedback amplifier is formed by using a vortex valve to control the vent pressure of the vented jet as shown in Figure 3-58. The use of positive feedback increases the output pressure recovery and reduces the control pressure required to deliver the maximum output pressure.

Stream interaction proportional amplifiers can be interconnected in analog circuits to generate feedback signals. Passive devices are used in these circuits to provide resistive, capacitive, and inductive characteristics. Analog lead-lag, lag-lead, and integration circuits have been successfully fabricated for several applications.

Vortex Regulation Concepts

The vortex valve is the only presently known fluidic device that is capable of throttling flow with acceptable efficiency. However, a major disadvantage is that the vortex valve requires a source of control pressure higher than the supply pressure. Installation of a series orifice in the supply line to obtain the necessary P_c/P_s ratio for control is not practical, since flow turndown will occur only after the orifice becomes subsonic. The following regulator designs are presented as representative of the state-of-the-art efforts in pressure regulation using vortex elements.

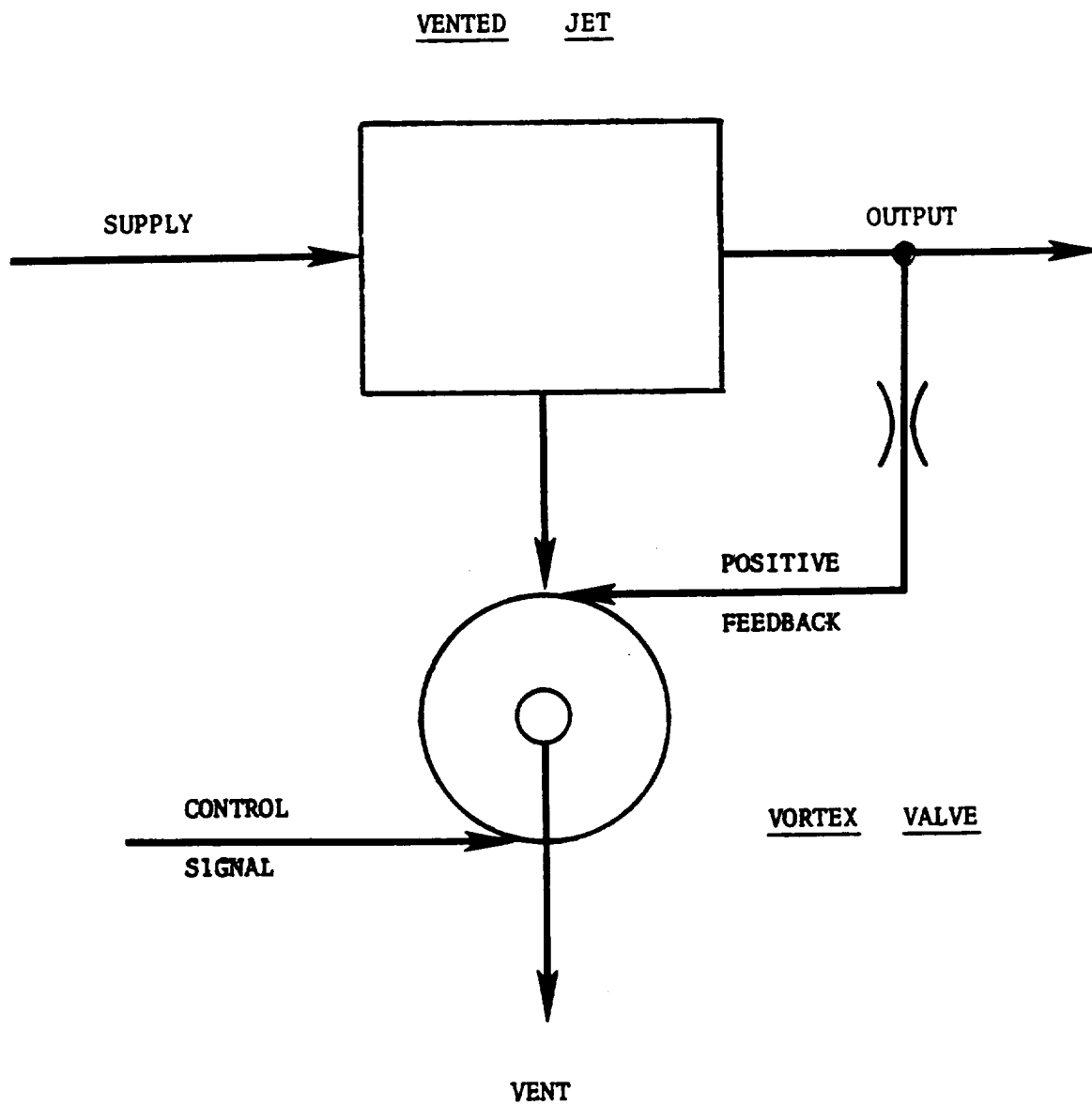


Figure 3-58 Vented Jet - Single Stage Feedback Amplifier

Dual Volume Regulation System - One of the simplest vortex regulation concepts would be to store part of the gas at higher pressure for control purposes (Figure 3-59). If the low pressure supply is at 2000 psig, the control pressure required for supply pressure cutoff would be about 2400 psig. Then if the feedback circuit can deliver a control pressure up to about 80 percent of the high pressure supply, the high pressure supply should be at about 3000 psig. Under these conditions, a dual exit vortex valve with a turndown ratio of 10, would provide a throttling range from 2000 to 200 psig. A further increase in the throttling range should be possible by using the vortex amplifier piloted vortex valve concept discussed earlier.

The necessity of having to store pressurizing gas at two different levels must be considered a disadvantage, since the trend has been for gas storage bottle pressures to increase, particularly in military and aeronautical applications. Theoretically, it can be shown that the weights of single compartment spherical pressure vessels and cylindrical vessels with spherical ends are independent of the storage pressure. However, storage volume decreases inversely as the initial storage pressure, and ullage is also reduced. Another problem, is the possibility of leakage disturbing the required balance between the weights of gas stored in the two volumes. One possible approach to a dual compartment pressure vessel (Reference 3-9), is to use a high pressure vessel installed within a low pressure vessel such that the pressure in the low pressure vessel supports the wall of the high pressure level.

Lag Circuit Regulator - This regulation concept (Figure 3-60) uses a conventional vortex valve and a double delay or lag circuit to control pressure. When the squib valve is opened, fluid flows through the fixed orifices, A_1 and A_2 , and starts to charge the two volumes. Area A_2 is made larger than A_1 so that volume V_2 charges faster than V_1 , which provides control pressure to the confined jet amplifier first, which in turn controls the vortex valve. Initially as the pressure in V_1 is low, the vortex valve is almost completely open. As the pressure in V_1 increases, the vortex valve is completely turned down by the confined jet amplifier, so

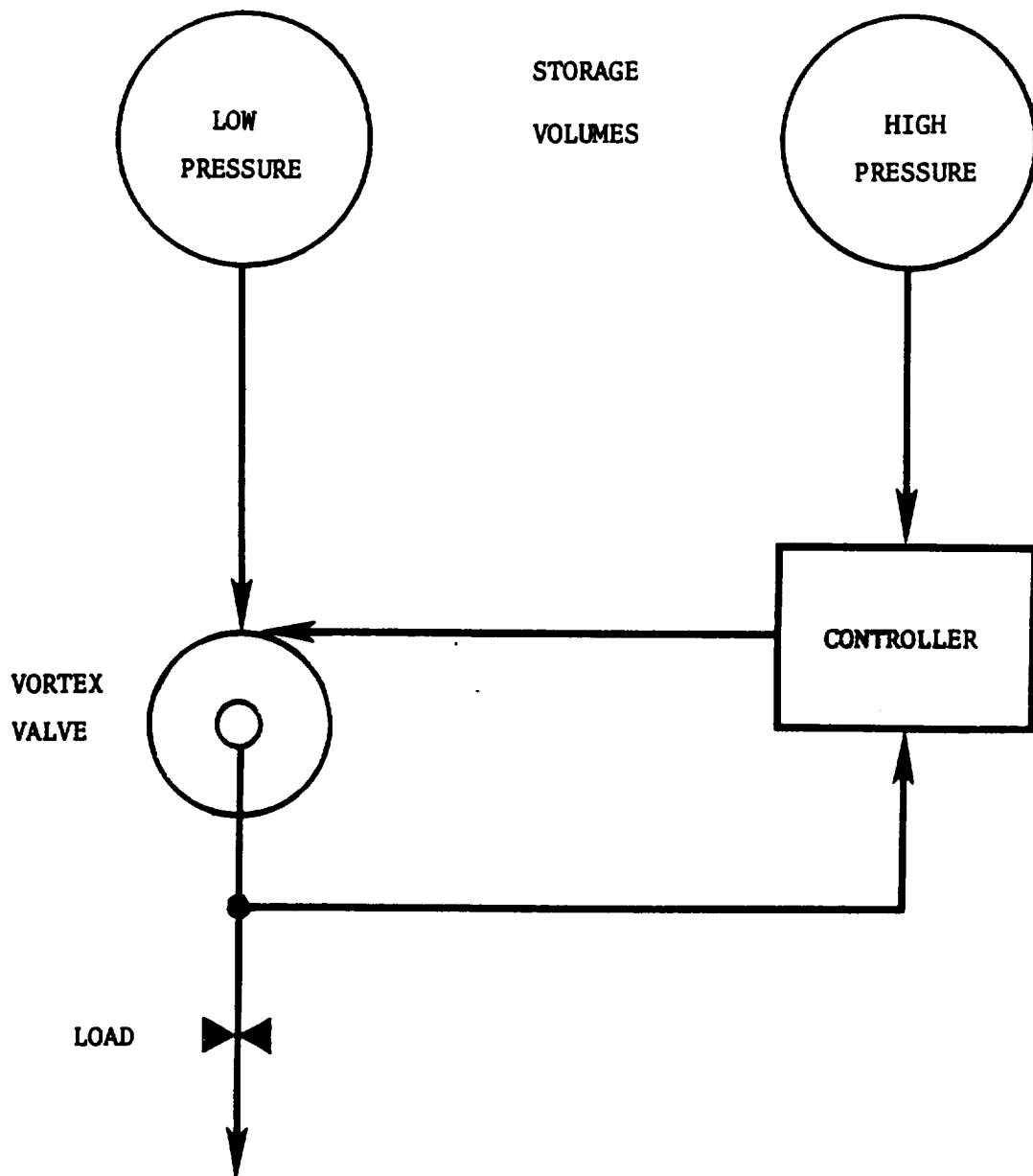


Figure 3-59 Dual Volume Regulation System

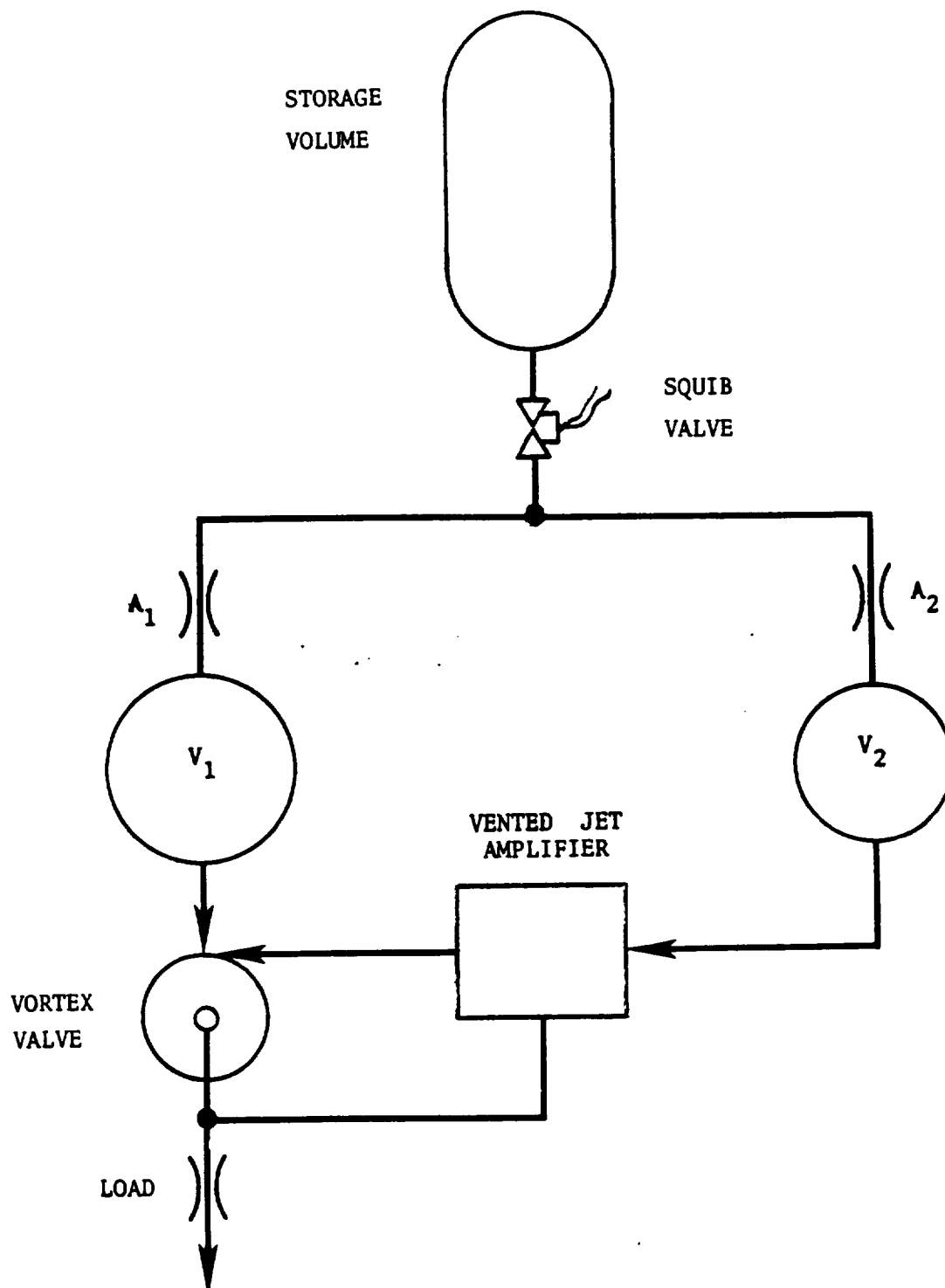


Figure 3-60 Lag Circuit Regulator

that regulated flow is supplied to the load primarily through the vortex valve control port. After V_1 reaches its peak, it will then decay with the storage bottle pressure. Subsequently, when the storage pressure is considerably reduced, the vortex valve will reopen to provide a lower pressure drop path from the supply to the load. The vent of the confined jet amplifier is controlled by the load pressure, which adjusts the output of the confined jet so as to keep the load pressure constant.

This type regulator is capable of operating over a 20 to 1 turndown range, however, it is limited to fixed area loads. Another drawback is that volume V_1 must be considerably larger than the stored volume, and consequently this design is impractical where space is at a premium.

Hybrid Regulator - It becomes obvious, that one approach which avoids the limitations imposed by a single storage tank is to use a variable area as the primary pressure dropping element. The variable area, which must be mechanically positioned, departs from the stated goal of having a pure fluid system with no moving parts. However, the concept appears to represent a practical means of obtaining a high turndown range with a minimum of moving parts and still retaining the other desirable features of a pure fluid system.

A typical hybrid regulator is shown in Figure 3-61. Tank pressure is dropped to a nearly constant supply by the variable mechanical orifice, which essentially increases in area as tank pressure decreases. The vented jet amplifier can then easily adjust the turndown of the vortex valve to accurately regulate the load pressure. This is possible because the effective turndown requirements of the vortex valve are drastically reduced by the variable mechanical orifice.

This type regulator should be capable of operating over an effective turndown range of 20 to 30 to 1. With careful design, the variable area orifice can be made extremely reliable, therefore this hybrid regulator can be effectively used until the state-of-the-art evolves an acceptable pure fluid regulator.

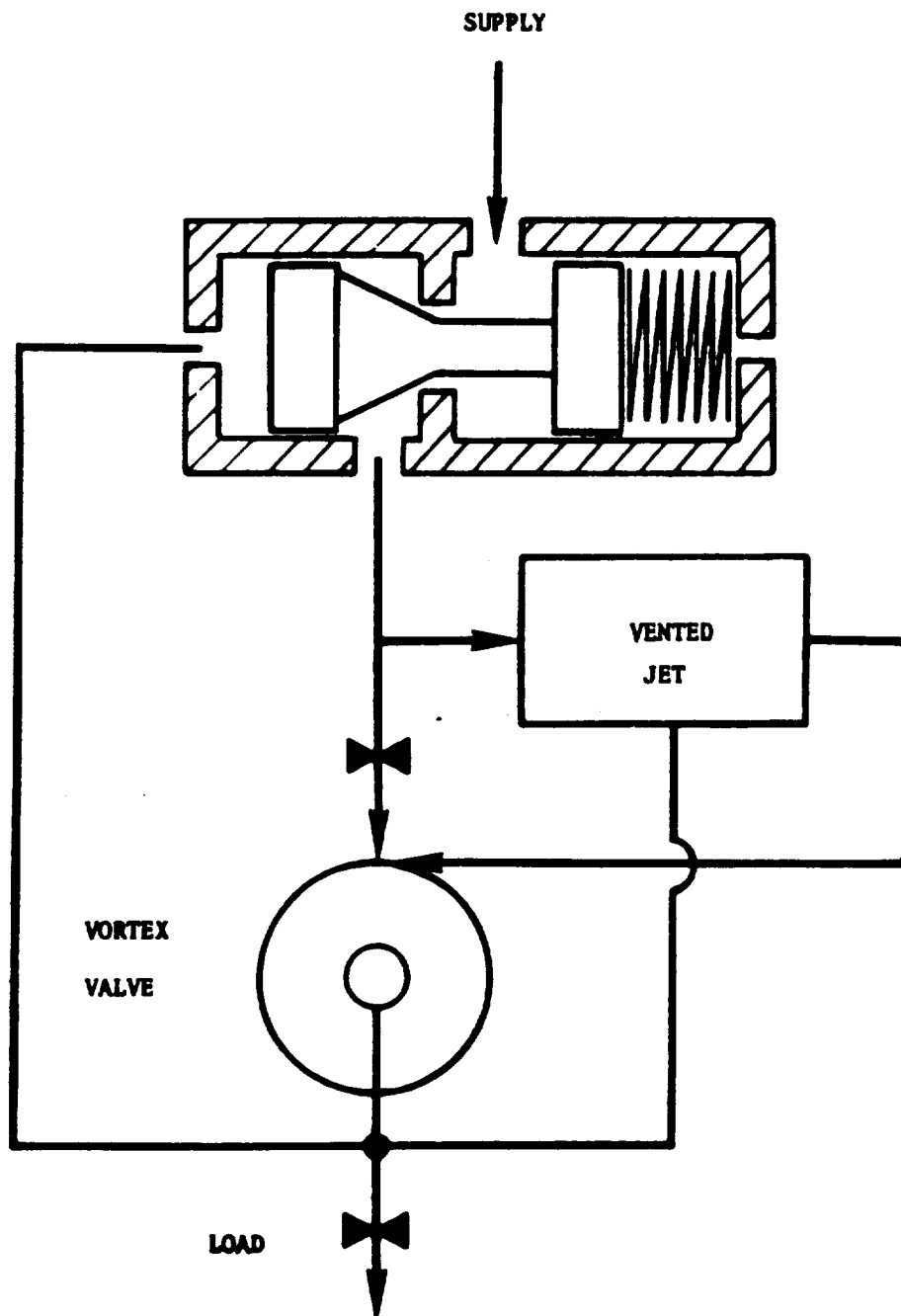


Figure 3-61 Hybrid Regulator Scheme

Proportional Pressure Control System

A schematic of a fluidic feedback system which can be used as a pressure regulator is shown in Figure 3-62. The set point pressure is obtained by connecting the regulated pressure to the supply and the controls of a proportional fluid amplifier. A linear capillary resistor is inserted in one control leg and a nonlinear orifice restrictor in the other. The values of these resistors are adjusted so that the amplifier is zero (at null) at the desired regulated pressure. The differential output of the set point amplifier is fed into a bootstrap integrator, i.e., a proportional amplifier with positive feedback resistors which are adjusted to provide an integrating operation. The output of the integrator is then connected to the control ports of a proportional power amplifier. Regulated fluid is supplied to the load through one output leg of the power amplifier, and proportionally dumps to atmosphere through the other output leg when the load flow demand is decreased. The unregulated pressure source usually is used to supply the power jet of the power amplifier and the other amplifiers are powered from the regulated source.

This type regulator has extremely low power efficiency (25 to 50 percent), because of the venting nature of proportional amplifiers and the fact that it vents to atmosphere to maintain the regulated pressure during low demand periods. However, because of the bootstrap integrator, extremely fine pressure regulation is possible depending on the accuracy and gain of the pressure reference. One possible improvement is the use of the proportional set point and integration circuits to drive a vented jet controlled vortex valve.

New Regulator Concepts

Vented Jet-Vortex Valve Regulator - A possible method of utilizing a vented jet as a regulator is shown in Figure 3-63. This device consists of an in-line vented jet with the vent cavity controlled by a vortex valve. The nozzle to receiver spacing of the vented jet should be close (less than 0.6 times the nozzle diameter) and the diffuser section of the receiver should be carefully designed for good pressure recovery.

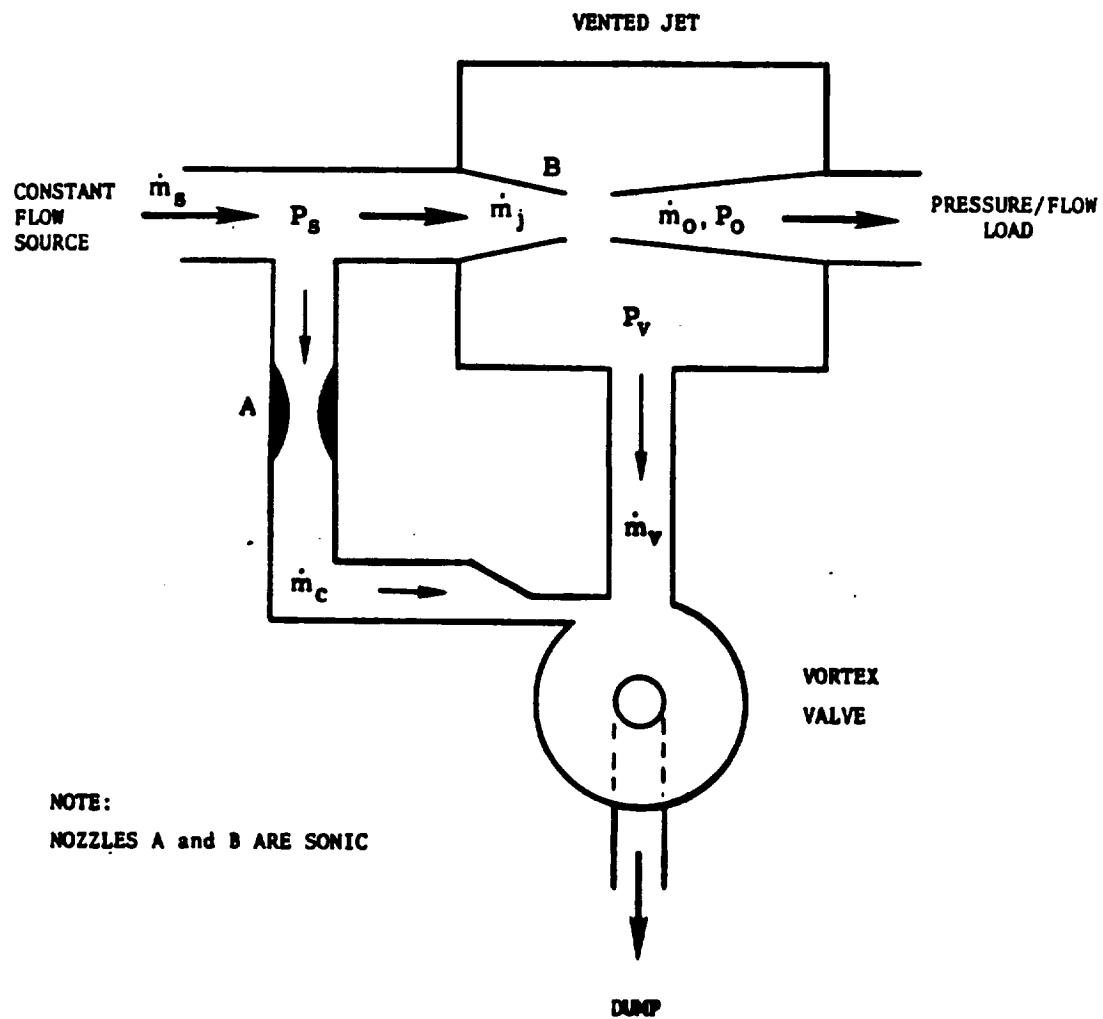


Figure 3-63 Vented Jet-Vortex Valve Regulator Concept

The operation of the device depends on the fact that at any supply pressure P_s there exists a region of operation in which output flow \dot{m}_o and vent pressure P_v can be varied significantly while maintaining almost 100 percent pressure recovery (i.e., $P_o \approx P_s$). A vortex valve is used to control the vent flow and pressure in such a manner as to extend the limits of this high recovery region beyond those obtainable with vent flow flowing through a fixed orifice. For example, as a pressure regulator with fixed supply flow \dot{m}_s operation is as follows:

Because \dot{m}_s is fixed and nozzles A and B are choked (at sonic velocity), the supply pressure P_s and the vortex valve control flow \dot{m}_c are fixed. If it is then assumed that the vented jet is initially operating in the high recovery region ($P_o \approx P_s$), should the load impedance decrease, the output flow \dot{m}_o increases and the vent pressure P_v decreases. However, because of the fixed control flow \dot{m}_c the vortex valve presents a higher impedance to vent flow at low values of P_v than at high values. Actually if P_v drops below a certain critical value, the vortex valve goes into complete turndown and vent flow becomes zero. Therefore, the vortex valve retards the decrease in vent pressure and maintains vented jet operation in the high pressure recovery regime for a broadband of output flows.

As the output impedance increases, the critical point occurs when nozzle B (Figure 3-63) unchokes, after which a further increase in load impedance will affect the flow source. In this case, however, the vortex valve tends to retard the increase in vent pressure, and actually allows lower output flows (even backflow) before nozzle B unchokes.

This device has very low output impedance, constant input impedance, and high pressure recovery. As such, it is a fluidic analog of a cathode follower stage. In general, the device can be used wherever it is desirable to isolate the effects of a variable load on a pressure/flow source. It can be used to convert a load-sensitive device into a load-insensitive device with no significant sacrifice in output pressure. A particular application of the device is as a pressure regulator, since when it is supplied by a constant flow source, it will maintain a near constant

output pressure on a downstream variable load. It should also be useful as a relief valve, in that the downstream load could be a flow source as well as a flow sink.

Preliminary tests were completed with a vented jet regulator operating with a constant supply flow. An output pressure variation of 4 percent (± 2 percent regulation band) was obtained with a load flow variation of 0 to 67 percent of the supply flow (Figure 3-64). Subsequent tests indicated that pressure regulation could be maintained even with significant reverse flow from the output port.

Monopropellant Gas Generator System - The pressure regulation capabilities of the vented jet-vortex valve combination suggest the use of the device as a regulator in a monopropellant gas generator system (Figure 3-65). This pressurization subsystem is conceived as a two-stage monopropellant hydrazine system which provides pressurant for propellant tanks and the working fluid for a fluidic control system. It can accurately regulate the pressurant over a wide flow range, and the estimated duty cycle for the rocket engine firings is about 20 percent.

Vented Jet Performance

The vented jet (Figure 3-28) has considerable potential for application in fluidic pressure regulators. In particular, the device functions with excellent accuracy when regulating a load from a constant flow source such as a monopropellant gas generator system (Figure 3-65). One drawback is an instability in the high gain region (Figure 3-29) that occurs with present receiver configurations. The primary problem appears to be in the receiver configuration, which needs to be modified so as to provide stabilizing negative feedback from the receiver to the vent cavity.

A simple variable geometry vented jet test fixture (Figure 3-66) was fabricated, so as to permit investigation into several possible ways of stabilizing the device in the high gain region.

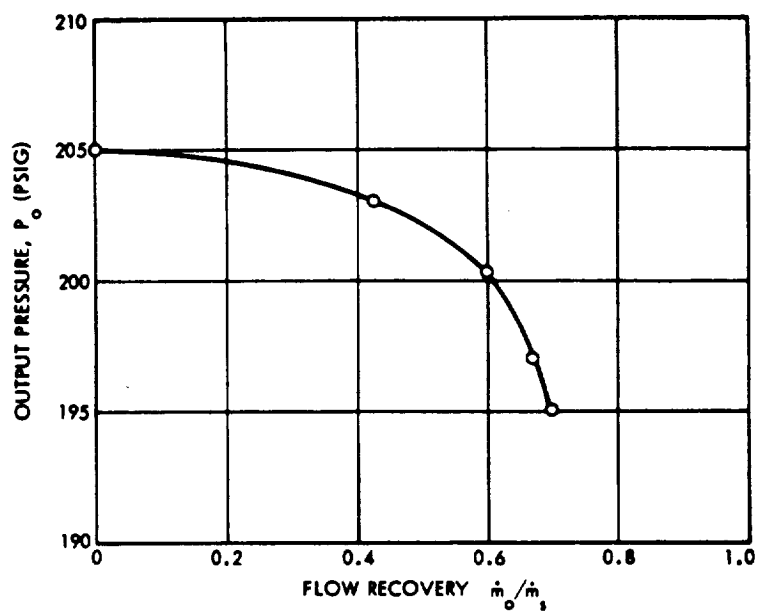
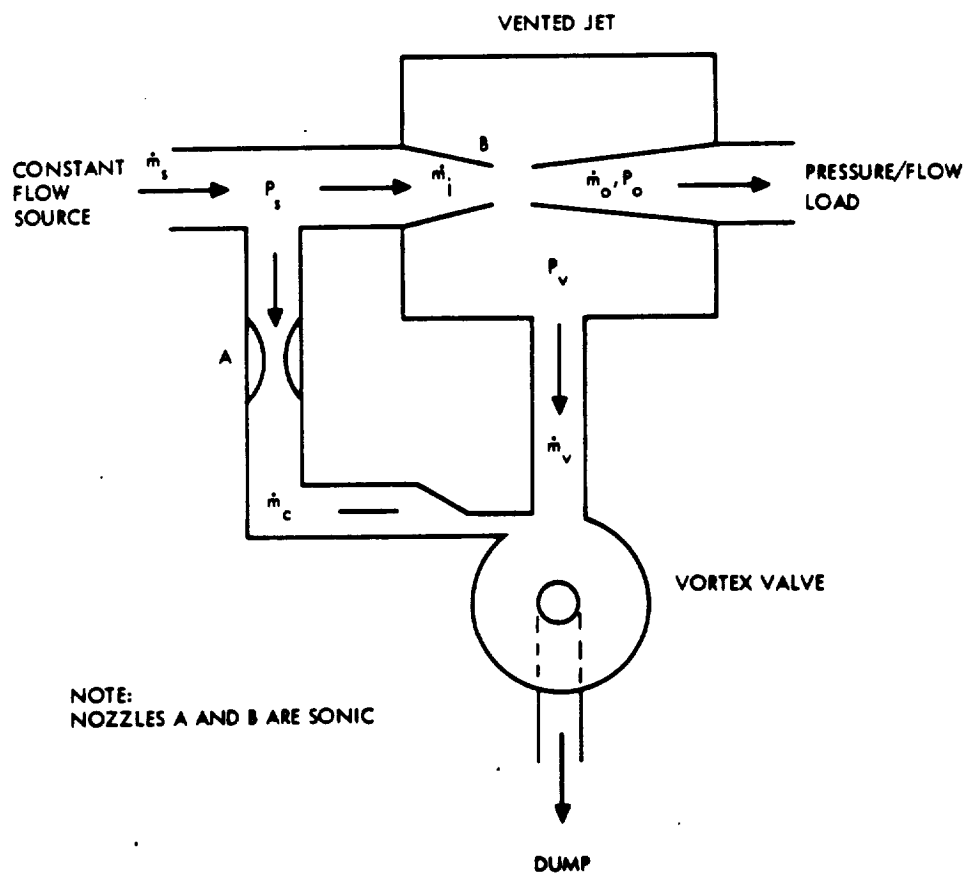


Figure 3-64 Vented Jet-Vortex Valve Regulator Performance

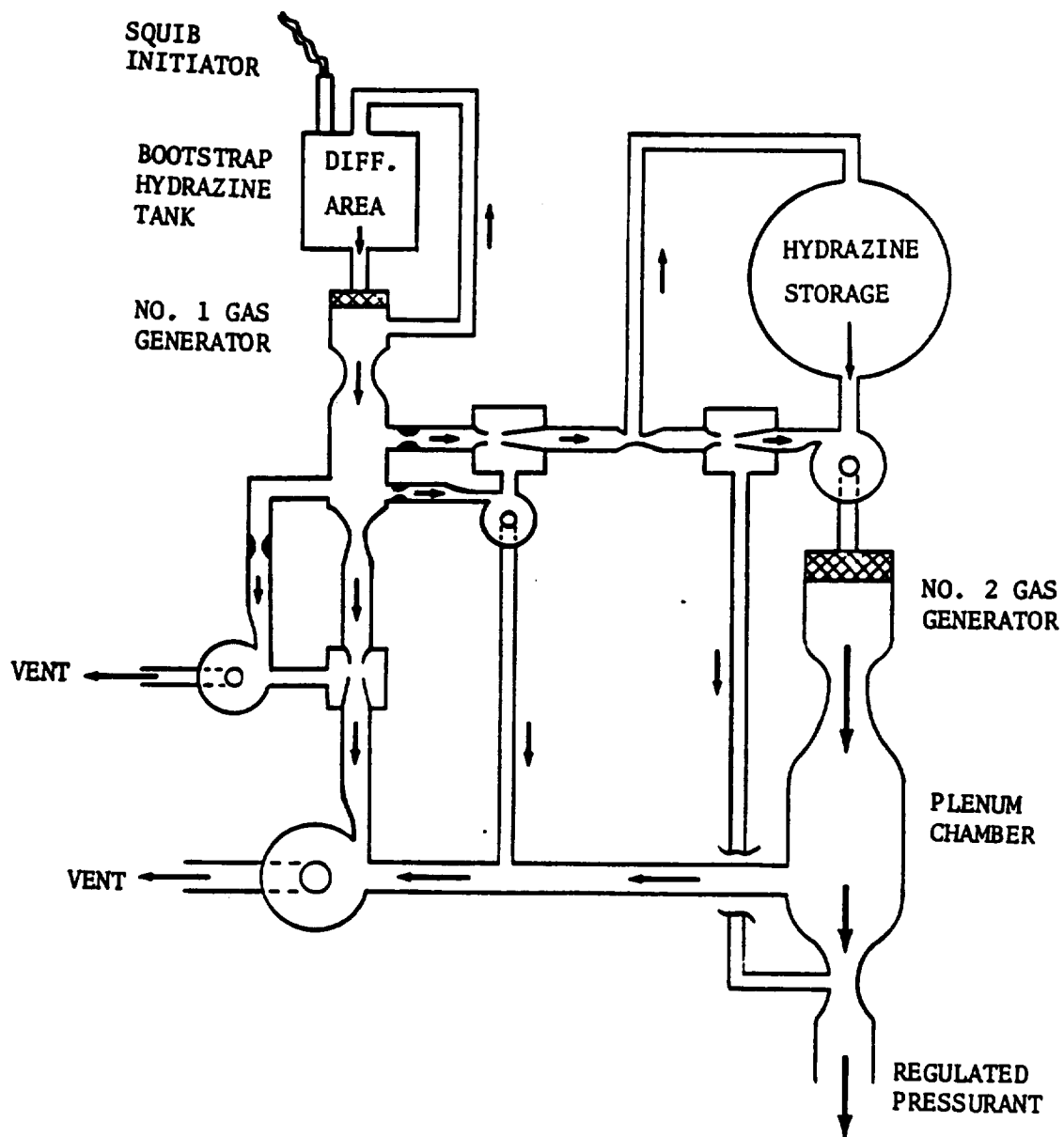


Figure 3-65 Monopropellant Gas Generator System

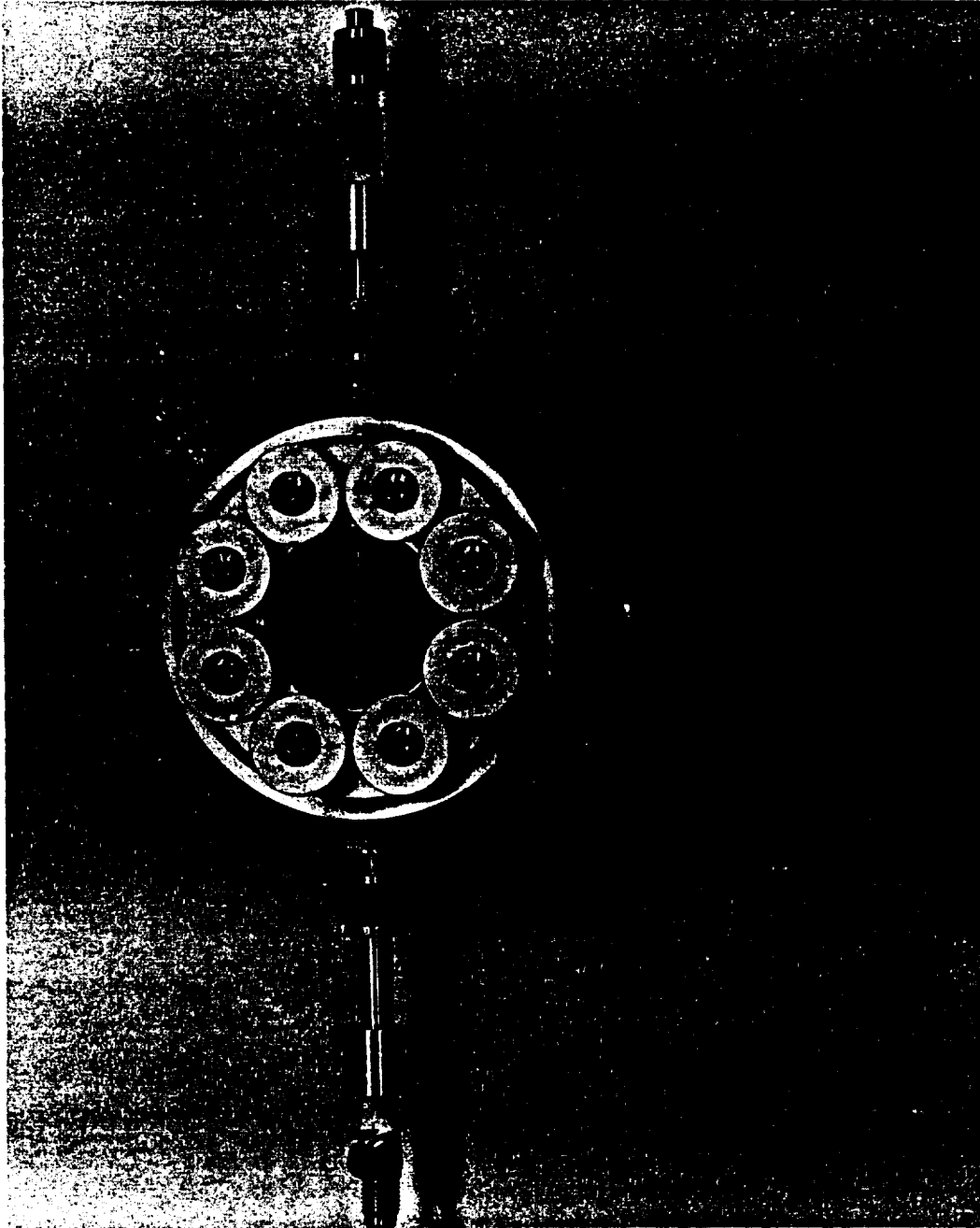


Figure 3-66 Variable Geometry Vented Jet Configuration

ANALYSIS

This section briefly outlines some analytical techniques and tools that could be used to help synthesize and design fluidic systems from a component level and reduce the long time, cost, and uncertainty involved with present repetitive "cut and try" methods. Analysis should be based on component performance data (characteristic curves) which are either made available by the component manufacturer or derived from suitable laboratory testing which is coordinated with the analytical effort. Implementation of analytical techniques will support the system designer in specifying, monitoring, and verifying fluidic component operation in both linear and/or nonlinear system applications. In addition, these techniques should be useful in the specification of the type of testing required for proper component checkout, which will help to ensure successful system design.

Analytical Techniques

In order to perform the analysis of fluidic systems, it will be necessary to model the operation of the components and associated connecting passageways involved from a dynamic as well as a static viewpoint. There are several ways that the dynamic and static analysis of fluidic systems can be approached. Two possible ways are:

1. Fluid dynamic analysis of the detailed complex flow phenomena involved.
2. Fluid circuit analysis analogous to the approach used for electronic circuit design.

The fluid dynamic analysis approach has yielded very little practical information for fluidic system designers to date due to the nonlinearities involved in the controlling partial differential fluid flow equations (Navier-Stokes). This is true both at the component and system levels. Thus, the first approach is not recommended as it does not appear to be applicable to overall fluidic system design at the present time.

A logical area for fluidic system modeling lies in the second approach; i.e., the application of fluid circuit theory as outlined in Reference 3-2 and further discussed in Reference 3-10, in connection with a dynamic analysis design philosophy for fluidic systems. Each of these references points out the logical adaptation of equivalent electrical circuit theory utilizing a mix of lumped and distributed parameters to perform fluidic system modeling. Circuit theory is applicable to the interconnecting lines between circuit elements and is covered in detail in Reference 3-11. It should also be applicable to fluidic components themselves in a manner similar to that used in Reference 3-12 to define the small signal dynamics of various proportional amplifiers by means of derived equivalent circuits, which is an adaption of electronic design techniques.

In areas where application of circuit theory becomes untractable, it will be necessary to use the black box technique, based on extensive fluidic component testing (both static and dynamic), to establish the required analytical transfer functions for the fluidic device in question.

Binary logic design should be based on standard techniques such as Boolean algebra, developed and used in the design of digital computers. These techniques will be helpful in optimizing the selection and combination of bistable fluidic components such as flip-flops, OR-NOR and AND-NAND gates into such digital devices as adders, counters, timers, multivibrators, shift registers, etc., to be used for either sensing, logic or control functions.

Analytical Tools

Circuit Analysis - The analytical tools needed to perform fluidic circuit analysis fall into two categories:

1. Analytical Techniques - Large signal nonlinear problems using graphical techniques and small signal problems using linearizing approximations.

2. Computer Aided Design (CAD) Techniques - Based on programmed solutions generated on analog, digital, or hybrid computers, used to solve either small or large signal linear or nonlinear problems.

In general, the application of purely analytical techniques to the design of fluidic systems will be limited to relatively simple circuits. Techniques for performing analyses for both small signals based on equivalent linear circuits and large signals based on graphical analysis are covered in Reference 3-12. The techniques outlined in detail in Reference 3-12 are similar to the standard procedures that are used for both single and multiple stage electronic circuit design. The only new facet that has been added is the generation of equivalent linear circuits for various proportional fluidic amplifiers. These equivalent circuits include the allowance for the time delays associated with signal propagation.

The application of computer analysis is recommended for the design of relatively large, complex, fluidic systems to achieve a more rapid turn around time than presently available. This approach should also minimize the costs associated with the system design, development, and test cycle.

There are two digital programs, ECAP and SCEPTRE, which are presently being used to aid electronic circuit designers in the design and development of complex electronic circuits. Use of these programs helps minimize the costs associated with the breadboarding and testing of actual hardware, prior to finalizing a design. Since both of these programs are circuit analysis oriented, they also can be gainfully used for computer analysis of complex fluidic systems utilizing fluidic component performance data to characterize and model the equivalent networks.

ECAP (Reference 3-13) is basically oriented to handle small signal or linear circuits. To use the program, an equivalent linear circuit is first established in which any representation of such components as diodes, transistors, etc., can be used provided it can be modeled with conventional linear passive circuit elements, voltage and current sources,

and current sensing switches. The matrix approach is fundamental (solution is not dependent on a transfer function approach) and information on basic network branches (circuit topology) are key entries to the computer. The input to the program is user-oriented, i.e., no translational language is needed. ECAP can perform D-C, A-C, and transient analysis and has options for sensitivity, standard deviation, and worst-case analysis. The latter options are useful in establishing component tolerance criteria which are compatible with overall system performance specifications. Reference 3-12 provides equivalent circuits for fluidic components which can be used in ECAP to perform AC analysis (provide system frequency response) with suitable modifications to include fluidic component and circuit connection time delays.

The SCEPTRE program (see Reference 3-14) was written to allow the designer to perform both D-C and transient analysis of large nonlinear electronic networks. The input format of this program again basically describes the topology of the circuit and the discrete circuit elements. However, unlike in ECAP, these circuit elements may be nonlinear and/or linear. The input format for nonlinearities can be either tables or equations. In addition, active models can be built up from passive elements and stored in a library and recalled for repeated use as needed. Thus, SCEPTRE should especially facilitate fluidic circuit modeling and analysis for large signal cases provided fluidic time delays are accounted for. A typical area of application would be monostable or bistable switching devices used either as relays or to implement logic operations. Modeling involving component cascading would be simplified through the use of the stored model feature. Impedance matching and/or stage isolation in the case of cascaded analog and/or digital components would also be facilitated through the use of SCEPTRE.

Logical Design Analysis - On-line computers can be used to help optimize the design and checkout of both synchronous and nonsynchronous digital logic circuitry which involve fluidic switching hardware. This analytical approach would be especially useful to ensure the acceptable operation of switching networks operating at relatively high speeds.

Timing problems can arise in this case due to inherent fluidic system time delays and the effect of signal noise modification of the signal pulse width, which could cause a loss of signal. An example of the problem involved and solution proposed is given in Reference 3-15.

RESULTS AND CONCLUSIONS

The preliminary objectives of this task have been met. Comprehensive literature and patent searches were completed. Over 600 literature references and about 350 patents were reviewed and a Fluidic Subject Index was organized so as to permit reference to a specific area of interest. The major aerospace and commercial companies and government agencies engaged in fluidics were visited, and the state-of-the-art of fluidics relative to spacecraft liquid propulsion power systems was established.

Propulsion applications of fluidics were also identified and the significant problem areas and future development requirements were summarized. Fluidic fundamentals and definitions have been determined and accepted fluidic terminology, nomenclature, drawing techniques, symbology, and definitions of circuit and performance parameters were documented for reference purposes. The operation, performance, and fabrication of the most common fluidic devices have been discussed relative to various propellants, specific functional parameters and the space environment.

To facilitate component application, the technical problems and major propulsion application areas were identified. Standard application criteria for evaluating engineering systems were also reviewed in relation to the selection of fluidic components for propulsion application. Conceptual studies were also initiated in the areas of fluidic pressure references and regulation. Finally, the analytical techniques and tools that could be used to help synthesize and design fluidic systems from the component level were outlined.

The capabilities of fluidics result from the use of fluid operation and no moving parts. Environmental tolerance has been demonstrated by operation over a temperature range from cryogenics to well over 2000°F. Shock and vibration tolerance has been demonstrated at levels up to 50g's at 5000 cps. The components appear to be unaffected by nuclear and electromagnetic radiation environments. Shelf and operating life should be excellent. Under these environmental extremes, fluidics offers potential

improvements in size, weight, and reliability, particularly where it is advantageous to use a single fluid medium for all control functions and the need to translate information from one medium to another is eliminated.

Future efforts in the application of fluidics to propulsion should be concerned with the elimination of present problem areas and the determination of optimum fluidic component performance criteria. Scaling effects and the effect of temperature and back pressure on the operation of components need to be identified. Electrical to fluid and fluid to electrical transducers and the effect of electrical forces on fluid behavior is another important area. Conceptual studies and prototype evaluation of fluidic concepts which are potentially applicable to propulsion should be continued, i.e., regulation, throttling, and shutoff functions. New areas need to be considered, in particular, analytical design procedures, materials, fabrication, interconnection techniques, and fluidic power supplies.

REFERENCES

- 3-1. Letham, D. L., "Fluidic System Design - Parts 1 through 20", Machine Design, February 17, 1966 through March 16, 1967.
- 3-2. Kirshner, J. M., Fluid Amplifiers, McGraw-Hill Book Co., 1966.
- 3-3. Progress Report on Formulation of Proposed NFPA Recommended Standard for Fluidic Devices, National Fluid Power Association, January 18, 1967.
- 3-4. Fluidic Technology, SAE ARP 993, Society of Automotive Engineers, July 15, 1967.
- 3-5. Aerospace Fluid Component Designers' Handbook, AFRPL, Report No. RPL-TDR-64-25, TRW Systems, March 1967.
- 3-6. Kirshner, J. M. and C. J. Campagnuolo, A Temperature-Insensitive Pneumatic Oscillator and a Pressure-Controlled Pneumatic Oscillator, Volume II, Harry Diamond Laboratories.
- 3-7. Carigan, D. J. and W. K. Clark, Fluidic-Pneumatic Oscillator Uses Tuning Fork for High Accuracy, Hydraulics and Pneumatics, September 1967.
- 3-8. AD 489923: Development of an All-Fluid Pneumatic Pressure Regulator, Bendix Research Laboratories Division, June 1966.
- 3-9. Greenlee, H. R.: Chrysler-Type Oxygen Pressure Vessel Calculations, Designs, and Testing, WADD Technical Report 60-365, May 1960.
- 3-10. Brown, F. T., On the Future of Dynamic Analysis of Fluid Systems, Fluidics, Fluid Amplifier Associates Incorporated, Boston, Mass., 1965.
- 3-11. Krishnayer, R. and T. J. Lechner, An Experimental Investigation of Fluidic Transmission Line Theory, Advances in Fluidics, Proceedings of The 1967 Fluidics Symposium, May 1967, ASME.
- 3-12. Fluidic Systems Design Manual, USAAVLABS Technical Report 67-32, May 1967.
- 3-13. "1620 Electronic Circuit Analysis Program", 1620-EE-02X Users Manual, IBM Technical Publication H20-0170-1.
- 3-14. "Automated Digital Computer Program for Determining Responses of Electronic Circuits to Transient Nuclear Radiation (SCEPTRE)", Volume I - SCEPTRE Users Manual, Air Force Weapons Laboratory, AFWL-TR-66-126, February 1967.
- 3-15. Bauer, P., Fluid Pulse Network Hazards, Advances in Fluidics, Proceedings of the 1967 Fluidics Symposium, May 1967, ASME.

APPENDIX III-A

FLUIDIC LITERATURE BIBLIOGRAPHY

- A-1. Abbey, P. L., Fluid Amplifier State-of-the-Art, Volume I: Research and Development - Fluid Amplifiers and Logic, NASA CR-101, October 1964.
- A-2. Adams, R. B., Application of Fluidic Valves, ASME Paper WA/PID-12, presented at the Winter Annual Meeting, Chicago, Illinois, November 7-11, 1965.
- A-3. Airey, L., M. E. Inglis and D. Reeves, The Fluid Oscillator as a Temperature Sensor, First Conference on Fluid Logic and Amplification, sponsored by the British Hydromechanics Research Association and College of Aeronautics, Cranfield, England, September 9-10, 1965.
- A-4. Aizerman, M. A., Pneumatic and Hydraulic Automation, DDC Report AD-618061, (Foreign Tech. Division, WPAFB, FTD-TT-65-169). Unedited rough draft translation of Mono. Pneumato - 1 Gidroadtomatika, Moscow, 1964. June 1965.
- A-5. Akmenkalns, I. G., E. Pasternak and R. R. Schaffer, Pneumatic to Electric Transducers, IBM Technical Disclosure Bulletin, Volume 5, No. 7, December 1962.
- A-6. Alblas, J. B. and H. G. Cohen, The Deflection of Turbulent Jets Between Bounding Walls, Proc. of Koninkl. Nederl. Akademie Van Wetenschappen, Amsterdam, Series B67, Number 3, 258-288, 1964.
- A-7. Amplifiers That Run On Liquid Diet, Business Week, Pages 130-132, November 7, 1964.
- A-8. Anderson, J. S., Fluid Power, Space/Aeronautics, Volume 44, No. 2, Pages 127-130, 1965.
- A-9. Angrist, S. W., Fluid Control Devices, Scientific American, Volume 211, Pages 81-88, December 1964.
- A-10. Applied Fluidics - Its Impact On Industry - Part 1: Users Guide to Fluidic Information, Hydraulics Pneumatics, Volume 20, No. 2, Pages 65-74, February 1967.
- A-11. A Read-Write Fluidic Memory, Signal, Volume 20, No. 11, Page 106, July 1966.
- A-12. Army Missile Command, Redstone Arsenal, Alabama, Development Of A Pure Fluid Missile Control System, Report No. AMC-RA RG-TR-65-22, DDC Report No. AD-478880, June 1967.
- A-13. Auger, Raymond N., Proximity Detection By Fluidics, Instrument Control Systems, Volume 40, No. 6, Pages 108-111, June 1967.
- A-14. Auger, R. N., Fluid Logic Fills Bottles Fast, Control Engineering, Volume 11, No. 9, Pages 98-99, September 9, 1964.

- A-15. Auger, R. N., Turbulence Amplifiers, Instrumentation in the Chemical and Petroleum Industries, Pages 89-106, 1964. Also, Proceedings of Fifth National Chemical and Petroleum Instrumentation Symposium, Wilmington, Delaware, May 4-5, 1964.
- A-16. Auger, R. N., How To Use Turbulence Amplifiers For Control Logic, Control Engineering, Pages 89-93, June 1964.
- A-17. Auger, R. N., Pneumatic Turbulence Amplifiers, Instruments and Control Systems, Volume 38, Page 130, March 1965. Also, Proceedings of Fifth National Chemical and Petroleum Instrumentation Symposium, Wilmington, Delaware, May 4-5, 1964.
- A-18. Auger, R. N., The Turbulence Amplifier In Control Systems, Proceedings of Second HDL Fluid Amplification Symposium, Volume II, N64-23821, May 26-28, 1964.
- A-19. Avduevskii, V. S., Approximation Method Of Computing The Three-Dimensional Laminar Boundary Layer, DDC Report No. AD-600524, (Foreign Tech. Air Force Systems Command, USSR Report), Wright-Patterson, March 1964.
- A-20. Avery, H. W., R. A. Kantola and R. Ziemba, Fluid Timer For Ordnance Applications, DDC Report No. AD-600661, (General Electric Company Quarterly Report No. 3). (Contract DA19020AMC 0213A), January 15, to April, 1964.
- A-21. Aviv, I., The Design and Construction Of A Pure Fluid Four Bit Comparator, presented at the Second Cranfield Fluidics Conference, Cambridge, England, Paper No. H6 - 1967, NASA N67-21131, January 3-5, 1967.
- A-22. Ayre, V. H. and P. D. Lee, An Analysis Of A Two Axis Fluid Control System For An Artillery Type Missile, paper presented at AIAA/ION Guidance and Control Conference, Minneapolis, Minnesota, August 16-18, 1965.
- A-23. Ayre, V. H. and J. C. Dunaway, Development Of A Hot Gas Bistable Jet Reaction Control Valve, U. S. Army Missile Command, Redstone Arsenal, Alabama, April 13, 1964.
- A-24. Balda, Milan, New System Of Pneumatic Logical Control, DDC Report No. AD-607156 (Foreign Tech. Division Air Force Systems Command, WPAFB), September 1964. Unedited rough draft translation of Automatizace (Czechoslovakia) 1962, Volume 5 No. 3, Pages 58-60.
- A-25. Banta, E. D., Lossless Propagation Of One-Dimensional, Finite Amplitude Sound Waves, Journal of Mathematical Analysis and Applications, Volume 10, Pages 166-173, 1965.

- A-26. Bauer, Peter and Eric E. Metzger, Digital Data Handling Speeds With Pure Fluid (Pneumatic) Circuits, Proceedings of the HDL Fluid Amplification Symposium, Volume II, October 1965.
- A-27. Bauer, Peter, Pneumatic Timer Feasibility Study for Artillery Fuze Application, Bowles Engineering Corporation, DDC Report AD-450413, Contract AF33(657)10705, October 6, 1964.
- A-28. Bantle, K., Counters With Bistable Fluid Elements, Second Cranfield Fluidics Conference, Cambridge, England, Paper No. HS -1967, NASA N67-21122, January 3-5, 1967.
- A-29. Bell, R. W., An Application of Fluid Logic to Telegraphy As A Research Vehicle, First Conference on Fluid Logic and Amplification, sponsored by the British Hydromechanics Research Association and College of Aeronautics, Cranfield, England, September 9-10, 1965.
- A-30. Belsterling, C. A., Development of A Fluid-State Ratio Computer, Part 3: Design Fabrication and Integration of Breadboard System, DDC Report AD-807530, AFFDL-TDR-64-138, October 1966.
- A-31. Belsterling, C. A., Development of Techniques for the Static and Dynamic Analysis of Fluid-State Components and Systems, Final Report No. ARD-FR-037, DDC Report AD-633311, NASA N66-30700, USAAVLABS-TR-66-16, February 1966.
- A-32. Belsterling, C. A., A Fluid State Absolute Pressure Ratio Computer, Proceedings of Third HDL Fluid Amplification Symposium, Volume III, October 1965.
- A-33. Belsterling, C. A. and Ka-Cheung Tsui, Analyzing Proportional Fluid Amplifier Circuits, Control Engineering, Volume 12, No. 8, Pages 87-92, August 1965.
- A-34. Belsterling, C. A. and Ka-Chueng Tsui, Application Techniques for Proportional Pure Fluid Amplifiers, Proceedings of HDL Fluid Amplification Symposium, Volume II, N64-23817, May 26-28, 1964.
- A-35. Bendix Corporation, Southfield, Michigan, Fabrication and Test of A Fluoric Position Servo, Quarterly Report No. BRLD-3133, NASA N66-10701, NASA CR-54776, June 10 - September 10, 1965.
- A-36. Bendix Corporation, Southfield, Michigan, Fabrication and Test of A Fluoric Position Servo, Quarterly Report No. BRLD-3255, NASA N66-27314, NASA CR-54900, September 10 - December 10, 1965.
- A-37. Benedict, E. B., Fluid Amplifier Instrumentation, Paper - Martin Company, Orlando, Florida.
- A-38. Benjamin, T. B., Some Developments in the Theory of Vortex Breakdown, (Aeronautical Research Council, Gt. Brit.) Report No. ARC-27945, DDC Report AD-642179, NASA N67-20608, April 25, 1966.

- A-39. Bermel, T. W. and W. R. Brown, Development of A Pure Fluid NOR Gate and A NOR Logic Binary to Decimal Converter, Proceedings of Third HDL Fluid Amplification Symposium, Volume III, October 1965. Also, ASME Paper 65 WA/AUT-13 presented at the Winter Annual Meeting, Chicago, Illinois, November 7-11, 1965.
- A-40. Bertin, J. and M. Kadosch, Principles and Applications of Axial and Directional Constriction, Bulletin - The Societe Francois Des Meconiciens, 1958.
- A-41. Besant, R. W. and V. Srinivas, Fluid Dynamic Effects of Liquids In Elastic Tubes, Proceedings of HDL Fluid Amplification Symposium, Volume II, October 1965.
- A-42. Betchov, Robert, General Research on the Curvature and Torsion of an Isolated Vortex Filament, DDC Report AD-600459 (Aerospace Corp., Report on Contract ATN6492314), May 1964.
- A-43. Betchov, Robert, Thermal Agitation and Turbulence, IAA - A63-11324, International Symposium on Rarefied Gas Dynamics Second Proceedings, Berkeley, California, August 1960.
- A-44. Bidgood, R. E. and C. J. Charnley, Fluid Units of the Ball Type and Their Application to the Control of a Machine Tool, Cranfield Department of Production and Industrial Administration.
- A-45. Biot, M. A. and T. v Karman, Mathematical Methods in Engineering, McGraw-Hill Book Company, Inc., 1940.
- A-46. Bisshopp, F. E., Internal Angular Momentum and Internal Energy of Fluids, DDC Report AD-612086 (Brown University; Prov. R. I. Report for Contract NONR562 07), January 1965.
- A-47. Bjornsen, Bjorn G., A Fluid-Amplifier Pneumatic Controller, Control Engineering, Page 88, June 1965.
- A-48. Bjornsen, Bjorn G., The Impact Modulator, Proceedings of HDL Fluid Amplification Symposium, Volume II, May 1964.
- A-49. Blackburn, John F., G. Riethof and J. L. Shearer, Fluid Power Control, Technology Press of Massachusetts Institute of Technology and John Wiley and Sons, Inc., New York, 1960.
- A-50. Blanchard, D. L. and C. Sewell, Pure Fluid Technology and Possible Ordnance Applications, DDC Report AD-612503 (Naval Ordnance Lab Report, NOLTR-64-115), December 1964.
- A-51. Blunck, G. C. and C. B. Schuder, The Driving Point Impedance of Fluid Process Lines, ISA Transactions, Volume 2, No. 1, Pages 39-45, 1963.

- A-52. Bolwell, A. J., Sound Switches Fluid Amplifier, Design News, Volume 21, No. 22, Pages 52-53, October 1966.
- A-53. Boksenbom, A. S. and M. E. Laverne, Frequency Response of Linear Systems from Transient Data, NACA Report 977, 1950.
- A-54. Boothe, W. A., A Lumped Parameter Technique for Predicting Analog Fluid Amplifier Dynamics, preprint of paper given at Joint Automatic Control Conference at Stanford University, June 24-26, 1964.
- A-55. Boothe, W. A. and J. N. Shinn, Connecting Elements Into Circuits and Systems, Control Engineering, Volume II, Pages 86-93, September 1964.
- A-56. Boothe, W. A., Feasibility Study - Application of Fluid Amplifiers to Reactor Rod Control, NASA Report CR-59485, prepared for Contract NAS 3-2567.
- A-57. Boothe, W. A., C. G. Ringwall and J. N. Shinn, New Fluid Amplifier Techniques for Speed Controls, Proceedings of SAE 1965 Aerospace Fluid Power Systems and Equipment Conference, Los Angeles, California, Pages 275-281, May 18-20, 1965.
- A-58. Boucher, R. F., Some Considerations in the Development and Operation of Fluidic Devices, presented at Second Cranfield Fluidics Conference, Cambridge, England, Paper No. B7 - 1967, NASA N67-21118, 1967.
- A-59. Boucher, R. F. and E. Markland, Experiments On Symmetrical Wall Re-attachment Amplifiers, presented at First Conference on Fluid Logic and Amplification, sponsored by the British Hydromechanics Research Association and College of Aeronautics, Cranfield, England, September 9-10, 1965.
- A-60. Bouteille, D., New Approach and Recent Developments in Piston Fluid Logic as Applied to General Automation, presented at Second Cranfield Fluidics Conference, Cambridge, England, Paper No. D3 -1967, NASA N67-21128, January 5, 1967.
- A-61. Bowles Engineering Corporation, Silver Springs, Maryland, -CONFIDENTIAL- Design of a Fluidic Missile Control System, Report No. R-5-20-66, DDC Report AD-373973, May 20, 1966.
- A-62. Bowles, Dr. R. E., Analog Pure Fluid Systems, American Helicopter Society Journal, Volume 10, Pages 35-42, January 1965.
- A-63. Bowles, Dr. R. E., A Pure Fluid Hydrofoil Control System, Proceedings of HDL Fluid Amplification Symposium, Volume II, NASA N64-23828, May 26-28, 1964.
- A-64. Bowles, Dr. R. E., Fluid Amplifiers, Design, Theory and Fundamentals for Control Systems, presented at meeting of Society of Automotive Engineers in Kansas City, Missouri, October 3, 1963.

- A-65. Bowles, Dr. R. E., A Second Generation Of Fluid System Applications, Proceedings of HDL Third Fluid Amplification Symposium, Volume III, October 1965.
- A-66. Bowlin, R. C. and R. K. Rose, Dynamic Interaction Analysis and Computer Model Lem Reaction Control Propulsion System, Volume I Technical Discussion, Final Report by General Electric for Grumman Aircraft, March 1965.
- A-67. Bradshaw, R. and M. T. Gee, Turbulent Wall Jets With And Without An External Stream, Reports and Memoranda Number 3252 (previously issued as A.R.C. 22,008) June 1960.
- A-68. Brady, W. G. and G. Ludwig, Theoretical And Experimental Studies Of Impinging Uniform Jets, presented at IAS 31st Annual Meeting, New York, N. Y., IAS Paper No. 63-29, January 21-23, 1963.
- A-69. Brewin, G. M., The Application Of Spring Controlled NOR Units To Machine Switching Operations, Cranfield Fluidics Conference, Cambridge, England, Paper No. J2 - 1967, NASA N67-21133, January 3-5, 1967.
- A-70. Brown, C. C. and J. R. Vince, The Application Of Fluid Jet Devices To A Medical Respirator, paper presented at First Conference on Fluid Logic and Amplification, sponsored by the British Hydro-mechanics Research Association and College of Aeronautics, Cranfield, England, September 9-10, 1965.
- A-71. Brown, C. C., Design And Manufacture Of Pure Fluid Elements, paper presented at Second Cranfield Fluidics Conference, Cambridge, England, Paper No. F4 - 1967, NASA N67-21103, January 3-5, 1967.
- A-72. Brown, D., Fluid Amplification, Metal Working News, January 11, 1965.
- A-73. Brown, F. T. (Ed.), Fluid Jet Control Devices, American Society of Mechanical Engineers, Hydraulic and Automatic Control Division, Winter Annual Meeting and Symposium on Fluid Jet Control Devices, A63-13665, November 28, 1962.
- A-74. Brown, F. T., Fluid Jet Modulators And Systems.
- A-75. Brown, F. T., On The Future Of Dynamic Analysis Of Fluid Systems, Proceedings of HDL Fluid Amplification Symposium, Volume I, October 26-28, 1965.
- A-76. Brown, F. T., On The Stability Of Fluid Systems, Proceedings of HDL Fluid Amplification Symposium, Volume I, May 26-28, 1964.
- A-77. Brown, F. T. and A. K. Simson, Research In Pressure-Controlled Fluid Jet Amplifiers, Massachusetts Institute of Technology for U. S. Army Missile Command, Redstone Arsenal, Alabama, November 1963.

- A-78. Brown, F. T. and S. E. Nelson, Step Response Of Liquid Lines With Frequency-Dependent Effects Of Viscosity, ASME Paper 64-WA/FE-6, December 3, 1964.
- A-79. Brown, W. R. and R. W. Van Tilburg, Fluid Amplifier, Design Engineering, Page 106, May 1965.
- A-80. Bryan, B. G., A Pure Fluid Binary To Decimal Converter, presented at Second Cranfield Fluidics Conference, Cambridge, England, Paper No. H2 - 1967, NASA N67-21280, January 3-5, 1967.
- A-81. Burton, G. T. Jr., J. R. Farron and D. J. Niehaus, Fluid-State Control Systems For Aerospace Nuclear Propulsion Applications, Institute of Aeronautics and Astronautics, Propulsion Joint Specialist Conference, Colorado Springs, Colorado, Paper 65-618, IAA No. A65-26578, June 14-18, 1965.
- A-82. Burton, R. V., Fluid-State Hydraulic Damper, Final Report No. 15-003R, DDC Ad-651104, February 1967.
- A-83. Byrd, J. L., B. J. Clayton and J. G. Williams, Development Of Pure Fluid Missile Control System, (Summary Report FY62), U. S. Army Missile Command Report No. RG-TR-62-7, October 28, 1963.
- A-84. Byrd, J. L. and W. A. Griffith, System And Component Considerations For An All Pneumatic Missile Attitude Control System, AIAA Guidance and Control Conference, Massachusetts Institute of Technology, Cambridge, Massachusetts, August 12-14, 1963.
- A-85. Campagnuolo, C. J. and L. M. Sieracki, A Digital-Proportional Fluid Amplifier For A Missile Control System, Proceedings of the HDL Third Fluid Amplification Symposium, Volume III, October 1965.
- A-86. Campagnuolo, C. J. and A. B. Holmes, Experimental Analysis Of Digital Fluoric Amplifiers For Proportional Thrust Control, paper presented at Second Cranfield Fluidics Conference, Cambridge, England, Paper No. K3 - 1967, NASA N67-21114, January 3-5, 1967.
- A-87. Campagnuolo, C. J., J. E. Foxwell, A. B. Holmes and L. M. Sieracki, Application Of Fluorics To Missile Attitude Control, Proceedings of HDL Third Fluid Amplification Symposium, Volume III, October 1965.
- A-88. Campagnuolo, C. J. and C. Spyropoulos, A Two-State Digital Amplifier Applied To The Army Artificial Heart Pump, DDC Report No. AD-602239, (Harry Diamond Labs, Washington, D. C.), April 1964.
- A-89. Cardon, M. H., Design, Fabrication And Test Of A Fluid Interaction Servovalve, NASA CR-54463 - Bendix Report BRLD 2978, prepared for Contract NAS 3-5212, May 17, 1965.

- A-90. Carafagno, S. P. and J. T. McCabe, Summary Of Investigations Of Entrance Effects In Circular Thrust Bearings, Appendix E - Packed Column Flow Meters, Franklin Institute Interim Report 1-A2049-24, prepared for Contract NONR-2342(00), Task NR-062-316.
- A-91. Carne, C. M., Experiments Using The Momentum Interaction Principle To Produce A Proportional Fluid Amplifier, Paper No. C1 - 1967, NASA N67-21138, January 5, 1967.
- A-92. Carter, V. and J. Fine, Fluid Amplification Technology: A Bibliography Of Direct Contributions, Proceedings of HDL Second Fluid Amplification Symposium, Volume III, May 26-28, 1964.
- A-93. Carwile, C. L., An Analytical And Experimental Study Of The Pressure Of A Small Chamber To Forced Pressure Oscillations, Princeton University Aeronautical Engineering Report No. 595d, October 15, 1962.
- A-94. Chanaud, R. C., A. E. Rodely and D. F. White, A Digital Flowmeter Without Moving Parts, ASME Paper 65-WA/FM-6 presented at the Winter Annual Meeting, Chicago, Illinois, November 7-11, 1965.
- A-95. Champman, W. P., Fluidics: Progress And Growing Pains, Mechanical Engineering, Volume 89, No. 10, October 1967.
- A-96. Chadwick, V. J., A Method Of Using Wall Attachment Devices In An Ultrasensitive Mode, Paper No. B1 - 1967, NASA N67-21123, presented at Second Cranfield Fluidics Conference, Cambridge, England, January 3-5, 1967.
- A-97. Charnley, C. J., R. E. Bidgood and G. E. T. Boardman, The Design Of A Pneumatic Position Encoder, Paper No. 1.5 presented at IFAC/IFIP Symposium on Microminiaturization in Automatic Control Equipment and in Digital Computers - Munich, Germany, October 21-23, 1965.
- A-98. Charnley, C. J. and R. E. Bidgood, The Design Of A Pneumatic Tape Reader, presented at First Conference on Fluid Logic and Amplification, sponsored by the British Hydromechanics Research Association and College of Aeronautics, Cranfield, England, September 9-10, 1965.
- A-99. Charnley, C. J., Fluidics Applied, Control, Volume 11, No. 106, Pages 170-171, April 1967.
- A-100. Chen, Y. N., Experimental Investigation Of Pressure Waves In A Manifold, Sulzer Technical Review, Research Number 1963 (Diesel Engines) Page 41.
- A-101. Clayton, B. J. and T. G. Wetheral, Application Of Pure Fluid Components To Missile Control System, presented to Society of Automotive Engineers Aerospace Fluid Power Systems and Equipment Committee Thrust Vector Control Panel, April 13, 1964.

- A-102. Clayton, B. J. and W. M. Posingies, Development And Flight Test Of A Fluoric Roll Control System, Journal of Spacecraft and Rockets, Volume 4, No. 2, Pages 151-155, February 1967.
- A-103. Clayton, B. J., The Development And Flight Test Of A Pure Fluid Missile Control System, paper presented at AIAA/ION Guidance and Control Conference, Minneapolis, Minnesota, August 16-18, 1965.
- A-104. Cochran, W. L. and R. W. Van Tilburg, The Staging Of Pressure Proportional Amplifiers To Provide Stable Medium Gain, Dual Control, Single Output Pure Fluid Systems, Proceedings of HDL Second Fluid Amplification Symposium, Volume II, May 26-28, 1964.
- A-105. Cohen, H., T. J. Watson and Yih-O Tu, A Theoretical Model For Separation In The Fluid Jet Amplifier, IAA Report A64-10761, (Also IBM Journal of Research and Development, Volume 7, Pages 288-296, October 1963).
- A-106. Coleman, D. D. and K. E. Gray, Theoretical And Experimental Investigation Of The Compressible Free Mixing Of Two Dissimilar Gases, Paper No. 65-822 from the AIAA Aerothermochemistry of Turbulent Flows Conference, December 13-15, 1965.
- A-107. Colston, J. R., A Pneumatic Pure Fluid Speed Control For A 500 KW Steam Turbine Generator, Office of Naval Research Power Branch Report, September 1963.
- A-108. Colston, J. R. and E. M. Dexter, Applications Of Pure Fluid Techniques To A Speed Control, Proceedings of Second Fluid Amplification Symposium, Volume II, May 26-28, 1964.
- A-109. Colston, J. R., A Pure Fluid Speed Governor, presented at meeting of the Society of Automotive Engineers, Phoenix, Arizona, April 14, 1964.
- A-110. Comparin, R. A., On The Limitations And Special Effects In Fluid Jet Amplifiers, Fluid Jet Control Devices, ASME Hydraulic and Automatic Control Division, Winter Annual Meeting and Symposium on Fluid Jet Control Devices, New York, N. Y., Page 65-73, November 28, 1962.
- A-111. Computer-Designed Fluidics Could Open Up New Technology, Product Engineering, Volume 37, No. 23, Pages 40-41, November 1966.
- A-112. Conesco Incorporated, Cambridge, Massachusetts, Development Of Noise Measurement Techniques And Procedures For Use In Fluid Piping Systems, Report No. AD-607588, Conesco Report F-123-1, for Contract NOBS 88557, April 1964.
- A-113. Conrad, P. W., The Effects Of Rotation On The Stability Of Laminar Boundary Layers On Curved Walls, Report No. FLD 9, Mechanical Engineering Department, Princeton University, August 1962.

- A-114. Contractor, D. N. and J. Cain, A Note On The Design Of Flexible-Wall, Volume Resonator Acoustic Filters, DDC Report No. AD-601104, (Hydronautics, Inc., Laurel, Maryland) Contract NOBS 88200, January 1964.
- A-115. Contractor, D. N., Preliminary Studies Of The Sound Generated By Orifices In Pipelines, DDC Report (Hydronautics, Inc., Laurel, Maryland, Contract NOBS 88200, February 1964).
- A-116. Cox, J. E., The Viscous Dissipation Of Energy In Free Turbulent Flows Occurring In Fluid Amplifier Operation, Proceedings of HDL Fluid Amplification Symposium, Volume I, May 26-28, 1964.
- A-117. Craft, D. J., Measuring Techniques For Fluid Devices, presented at First Conference on Fluid Logic and Amplification, sponsored by the British Hydromechanics Research Association and College of Aeronautics, Cranfield, England, September 9-10, 1965.
- A-118. Crocco, Luigi and Cheng, Sin - I, Theory Of Combustion Instability In Liquid Rockets, Butterworth's Publications, Ltd., London, England, 1956.
- A-119. Cronin, R. T., A Hydrodynamic Study Of The Free-Jet Class Of Fluid Jet Amplifiers, Proceedings of HDL Fluid Amplification Symposium, Volume I, May 26-28, 1964.
- A-120. Curtiss, H. A. and C. A. Belsterling, Development Of A Fluid State Ratio Computer - Part 2: System Design And Component Development, DDC Report No. AD-810653, FDL-TDR-64-138, NASA X67-17978, June 30 to November 2, 1964.
- A-121. Curtiss, H. A. and D. J. Liguornik, Research Studies In Proportional Fluid State Control Components - Part 2, DDC Report No. AD-618103 (Astromechanics Research Division, Giannini Controls, Report ARD-TR-013-02, Contract DA36034ORD3722RD, March 1965).
- A-122. Curtiss, H. A., D. G. Feil and D. J. Liguornik, Separated Flow In Curved Channels, Proceedings of HDL Fluid Amplification Symposium, Volume I, May 26-28, 1964.
- A-123. Curtiss, H. A., D. G. Feil and D. J. Liguornik, Separated Flows In Curved Channels With Secondary Injection, Proceedings of HDL Fluid Amplification Symposium, Volume IV, May 26-28, 1964.
- A-124. Daga, A. A., The AF-Relay - Some Applications To Automatic Control Systems, presented at Second Cranfield Fluidics Conference, Cranfield, England, Paper No. J3 - 1967, NASA N67-21108, January 3-5, 1967.
- A-125. Davies, G. E., An Empirical Expression For The Resistance Of Small Bore Tubes To Turbulent Flow, presented at Second Cranfield Fluidics Conference, Paper No. D2- 1967, NASA N67-21140, January 3-5, 1967.

- A-126. Dawson, R. J., Fluid Power, Space Aeronautics, Volume 42, Pages 109-112, September 1964.
- A-127. de Bruyne, N. A., Pneumatic NOR Blocks, paper given at First Conference on Fluid Logic and Amplification, sponsored by the British Hydromechanics Research Association and College of Aeronautics, Cranfield, England, September 9-10, 1965.
- A-128. Defense Documentation Center, Fluid Amplification: A Report Bibliography, DDC Report No. AD-472500, October 1965.
- A-129. Deissler, R. G. and M. Perlmutter, An Analysis Of The Energy Separation In Laminar And Turbulent Compressible Vortex Flows, paper from Lewis Flight Propulsion Laboratory NASA/Cleveland, Ohio. Summary 1931 - 1953.
- A-130. Denker, R. E., Theoretical Analysis Of Fluid Amplifier Design, Proceedings of HDL Fluid Amplification Symposium, Volume II, N64-23820, May 26-28, 1964.
- A-131. Designer Profile: Inventor Of Fluidic Devices Now Applies The Technology, Product Engineering, Volume 38, No. 20, Pages 154-156, September 1967.
- A-132. Dexter, E. M., Application Of Fluidics To Automatic Flight Control, Final Report, USAAVLABS TR-66-71, DDC Report No. AD-645759, NASA N67-22686, September 1966.
- A-133. Dexter, E. M., An Analog Pure Fluid Amplifier, Fluid Jet Control Devices (ASME Hydraulic and Automatic Control Divisions, Winter Annual Meeting, New York, N. Y., 28 November 1962) ASME, Page 41-49 1962.
- A-134. Dexter, E. M. and J. R. Colston, Pure Fluid Controls For Ship's Boiler, Control Engineering, Volume 11, No. 9, Pages 96-97, September 1964.
- A-135. Douglas, J. F. and R. S. Neve, Investigation Into The Behavior Of A Jet Interaction Proportional Amplifier, presented at Second Cranfield Fluidics Conference, Cambridge, England, Paper No. C3 - 1967, NASA N67-21109, January 3-5, 1967.
- A-136. Drazan, P., Optimal Design Of The Control Jet Of A Fluid Amplifier, presented at Second Cranfield Fluidics Conference, Cambridge, England, Paper No. J5 - 1967, NASA N67-21107, January 3-5, 1967.
- A-137. Drohan, (UNIVAC), UNIVAC Shows System Using Fluids For Logic Elements, Electronic News, Page 34, October 19, 1964.
- A-138. D'Sonza, A. F. and R. Oldenburger, Dynamic Response Of Fluid Lines, Transactions of ASME Journal of Basic Engineering, Pages 589-598, September 1964.

- A-139. Ducoffe, A. L. and F. M. White, Jr., The Problem Of Pneumatic Pressure Lag - Part I - Steady-Stage Flow In A Tubing System, Paper No. 63-AHGT-6, Transactions of ASME Journal Of Basic Engineering.
- A-140. Duff, J., K. Foster and D. G. Mitchell, Some Experiments On The Vortex Valve, presented at First Conference on Fluid Logic and Amplification, sponsored by the British Hydromechanics Research Association and College of Aeronautics, Cranfield, England, September 9-10, 1965.
- A-141. Dunaway, J. C. and V. H. Ayre, A Status Report On The Experimental Development Of A Hot Gas Valve, Proceedings of Second Fluid Amplification Symposium, Volume II, May 26-28, 1964.
- A-142. Earles, S. W. E. and J. M. Zarek, Reflection Of Pressure Waves At Sharp-Edged Orifices, The Engineer, Volume 219, Page 383, February 1965.
- A-143. Eige, J. J., Multiple-Ball Pneumatic Amplifiers, Proceedings of HDL Second Fluid Amplification Symposium, Volume II, May 26-28, 1964.
- A-144. Eisenberg, N. A., A Pneumatic Tape-Reader, Proceedings of HDL Third Fluid Amplification Symposium, Volume III, October 1965.
- A-145. Erian, F. and S. Eskinazi, The Wall Jet In A Longitudinal Pressure Gradient, DDC Report No. AD-607474, (Syracuse University Research Institute) Contract NONR669-16, October 1964.
- A-146. Evans, R. A., Applied Fluids Technology, presented at SAE/NASA Conference-Aerospace Vehicle Flight Control, Los Angeles, California, Paper No. 650600, July 13-15, 1965.
- A-147. Fiebig, M., On The Motion Within Fluid Gyroscopes, DDC Report No. AD-608703, (Aeronautical Research Associates of Princeton, Inc., for Contract AF49638-1262), August 1964.
- A-148. Field, R. K., Fluidic Logic Takes To The Air, Electron Design, Volume 15, No. 17, Pages U108-U109, August 16, 1967.
- A-149. Field, R. K., Fluidics: A Simple Pipeline To Rugged Control, Electron Design, Volume 14, No. 20, Pages 17-18, 20-21, August 30, 1966.
- A-150. Fine, J. E., Schlieren Observations Of The Effect Of Sound Injected Into The Power Nozzle Of A Helium-Into-Air Jet, Proceedings of HDL Third Fluid Amplification Symposium, Volume IV, October 1965.
- A-151. Fishlock, D., Fluidics: New Spurt In An Old Technology, New Scientist, Volume 32, No. 527, Pages 722-723, December 29, 1966.
- A-152. Fluid Amplifier, Material Design Engineering, Volume 61, No. 5, Pages 108-110, May 1965.

- A-153. Fluid Amplifiers Face Up To Their Moment Of Truth, Product Engineering, Volume 38, No. 4., Pages 39-46, 49-51, February 13, 1967.
- A-154. Fluid Amps Run Locomotive, Control Engineering, Page 23, July 1965.
- A-155. Fluid Amplifier With Improved Response Time, Control, Volume 9, No. 84, Page 340, June 1965.
- A-156. Fluid Dynamic Solutions To Data Processing And Servotechnical Problems, DISA Information, Pages 7-10, January 1965.
- A-157. Fluid Jet Control Devices At The Moscow Institute Of Automation, Control, Pages 263-265, November 1963.
- A-158. Fluid Logic Systems, Industrial Electron, Volume 3, No. 12, Pages 587-590, December 1965.
- A-159. Fluid Logic, Instrumentation Control Systems, Volume 39, No. 10, Part 1, Pages 93-100, October 1966.
- A-160. Fluid Logic Conference At Cranfield, England, Control, Volume 9, No. 89, Pages 588-589, November 1965.
- A-161. Fluid Logic For Low Cost Automation, Industrial Electronics, Volume 5, No. 4, Pages 167-169, April 1967.
- A-162. Fluid Amplifier State-of-the-Art Report, Volume II-A, Bibliography, General Electric, NASA Report No. CR-734, May 1967.
- A-163. Fluid Technology Held Ready For Growth Into Mighty River, Electronic News, January 11, 1965.
- A-164. Fluidic Control System For Pipelines, Industrial Engineering, Volume 4, No. 10, Page 471, October 1966.
- A-165. Fluidic Summing Junction, Control, Volume 10, No. 95, Page 283, May 1966.
- A-166. Fluidic Gyro Built For Spacecraft Use, Electronic News, Volume 15, No. 5, Page 46, March 1, 1967.
- A-167. Fluidic Controls Win Solid Jobs, Chemical Weekly, Volume 100, No. 21, Pages 57-58, May 27, 1967.
- A-168. Fluidic Devices, Missiles and Rockets, Volume 18, No. 20, Page 54, May 16, 1966.
- A-169. Fluidic Controls A V/Stol, Machine Design, Volume 39, No. 10, Page 26, April 27, 1967.
- A-170. Fluidics Keeps Eagle Eye On Lube System, Machine Design, Volume 38, No. 21, Page 31, September 1966.

- A-171. Fluidics At Frigidaire, Control, Volume 11, No. 105, Page 109, March 1967.
- A-172. Fluidics - New Market For Plastics, Modern Plastics, Volume 44, No. 6, Pages 88-90, 168, February 1967.
- A-173. Fluidics Remove Flash From Die Castings, Hydraulics, Pneumatics, Volume 20, No. 6, Pages 22-23, June 1967.
- A-174. Foss J. F. and J. B. Jones, A Study Of Incompressible Bounded Turbulent Jets, DDC Report No. AD-611189, (Purdue University Research Foundation Report for Contract DA83DAMXDO CSA40A, November 1964).
- A-175. Foster, H. H., and M. F. Heidmann, Effect Of Impingement Angle On Drop-Size Distribution And Spray Pattern Of Two Impinging Water Jets, TN #D872 (NASA), Lewis Research Center, Cleveland, Ohio.
- A-176. Foster, H. H. and M. F. Heidmann, Spatial Characteristics Of Water Spray Formed By Two Impinging Jets At Several Jet Velocities In Quiescent Air, NASA Technical Note D-301, Lewis Research Center, Cleveland, Ohio.
- A-177. Foster, K. and N. S. Jones, An Examination Of The Effect Of Geometry On The Characteristics Of A Turbulent Re-attachment Device, presented at First Conference on Fluid Logic and Amplification, sponsored by the British Hydromechanics Research Association and College of Aeronautics, Cranfield, England, September 9-10, 1965.
- A-178. Foster, K. and D. A. Retallick, Some Experiments On A Free Foil Switching Device, presented at Second Cranfield Fluidics Conference, Cambridge, England, Paper No. D1 - 1967, NASA N67-21104, January 3-5, 1967.
- A-179. Foster, K. and G. A. Parker, Fluid-Logic Control Devices, Industrial Electronics, Volume 4, No. 10, Pages 466-468, October 1966.
- A-180. Foster, K. and A. K. Misra, The Turbulent Re-attachment Amplifier In A Conventional Pneumatic Circuit, paper presented at First Conference on Fluid Logic and Amplification, sponsored by the British Hydromechanics Research Association and College of Aeronautics, Cranfield, England, September 9-10, 1965.
- A-181. Foster, K., Fluidic Circuits Used In A Drilling Sequence Control, presented at Second Cranfield Fluidics Conference, Cambridge, England, Paper No. H4 - 1967, NASA N67-21279, January 3-5, 1967.
- A-182. Four Pneumatic Counters In One, Product Engineering, Volume 36, No. 24, Page 104, November 22, 1965.

- A-183. Fox, H. L. and F. R. Goldschmied, Basic Requirements For An Analytical Approach To Pure Fluid Control Systems, Proceedings of HDL Fluid Amplification Symposium, Volume I, May 26-28, 1964.
- A-184. Fox, H. L., Direct Fluidic Sensors, Instrumentation Technology, Volume 14, No. 9, Pages 67-75, September 1967.
- A-185. Fox, H. L., F. R. Goldschmied and D. L. Letham, Fluid Amplifier Dynamic Characteristics, Volume II, NASA CR-57349, (Sperry Utah Company Final Report on Contract NAS 8-11236), December 30, 1964.
- A-186. Fox, H. L. and O. L. Wood, Fluid Computers, International Science and Technology, Pages 44-50, November 1963.
- A-187. Fox, H. L. and O. L. Wood, The Development Of Basic Devices And The Need For Theory, Control Engineering, Volume II, No. 9, Pages 75-81, September 1964.
- A-188. Franklin Institute, Philadelphia, Pennsylvania, Studies On the Dynamic Performance Of Proportional Fluid Amplifiers, (from Dynamic Performance Analysis of Pure Fluid Amplifiers and Pure Fluid Computational Circuit Studies, NASA N66-35466) NASA N66-35467, Final Report No. F-B2148-1, DDC Report AD-634-527, 1965.
- A-189. Frey, K. P. H. and N. C. Vasuki, Flow Stability For Two-Dimensional Cusp Devices, Proceedings of HDL Fluid Amplification Symposium, Volume I, October 26-28, 1965.
- A-190. Frey, K. P. H., N. C. Vasuki, and P. Trask, New Comprehensive Studies On Sudden Enlargements, Proceedings of HDL Fluid Amplification Symposium, Volume I, October 26-28, 1965.
- A-191. Frock, I. and J. Clements, Fluidic Gage Inspects Auto Parts, Then Accepts Them Or Rejects Them, Hydraulics Pneumatics, Volume 20, No. 6, Pages 97-100, June 1967.
- A-192. Gesell, W. F., Fluidics For Automatic Control, Volume 14, No. 3, Pages 79-83, March 1967.
- A-193. Gant, G. C., A Fluidic Digital Displacement Indicator, presented at Second Cranfield Fluidics Conference, Cambridge, England, Paper No. E1 - 1967, NASA N67-23080, January 3-5, 1967.
- A-194. General Electric Company, Schenectady, New York, Fluid Amplifier Application Studies, NASA Contract Report No. CR-137, NASA N65-12443, December 1964.
- A-195. General Electric Company, Schenectady, New York, Fluid Amplifier State-of-the-Art, Volume II: Bibliography, NASA Contract Report No. CR-102, NASA N64-31700, October 1964.

- A-196. Glaettli, H. H., Basic Properties Of Fluid Mechanic Elements, presented at First Conference on Fluid Logic and Amplification, sponsored by the British Hydromechanics Research Association and College of Aeronautics, Cranfield, England, Paper No. A2 - 1965, NASA N65-36400, September 9-10, 1965.
- A-197. Glaettli, H. H., Mach- And Cavitation Number Effects In Fluid Dynamic Elements And Circuits, presented at Second Cranfield Fluidics Conference, Cambridge, England, Paper No. B8 - 1967, NASA N67-21112, January 3-5, 1967.
- A-198. Glaettli, H. H., Moving Part Versus Non-Moving Part Elements, presented at Second Cranfield Fluidics Conference, Cambridge, England, Paper No. G1 - 1967, NASA N67-21124, January 3-5, 1967.
- A-199. Glaettli, H. H., Remarks On The Limitations Of Pure Fluid Elements, Proceedings of HDL Fluid Amplification Symposium, Volume 1, May 26-28, 1964.
- A-200. Glaettli, H. H., Reunion De Printemps De La Societe Suisse De Physique A Lucerne Le 5 Mai 1962. Journal of Applied Mathematics et de Physique Appliquees), ZAMP, Volume XIII, Pages 500-502.
- A-201. Glaettli, H. H., Similarity Relations And Characterization Of Pure Fluid Elements, Proceedings of HDL Fluid Amplification Symposium, Volume I, October 26-28, 1965.
- A-202. Glasgal, R., Exotic Devices Of The Future?, Electronic Industries, Volume 25, No. 1, Pages 59-61, 101, January 1966.
- A-203. Gluskin, R. S., M. Jacoby and T. D. Reader, A Fluid-Logic Digital Computer, Computer Design, Page 26, June 1965.
- A-204. Gluskin, R. S., FLODAC - A Pure Fluid Digital Computer, AFIPS Proceedings of 1964 Fall Joint Computer Conference, Volume 26, Pages 631-641, 1964.
- A-205. Gluskin, R. S., N. Jacoby and T. D. Reader, The UNIVAC Fluid Computer, Proceedings of 1965 Joint Automotive Control Conference (6th) at Rensselaer Polytechnic Institute, Troy, New York, A65-28816, June 22-25, 1965.
- A-206. Goldschmied, F. R. and D. L. Letham, Analytical Investigation Of Fluid Amplifier Dynamic Characteristics, Sperry Rand Company - Utah - Report - Volume 1, December 30, 1964.
- A-207. Goldschmied, F. R., Dynamic Similarity Analysis Of Compressible Viscous Fluid Pipe Flow, Proceedings of HDL Fluid Amplification Symposium, Volume I, October 26-28, 1965.
- A-208. Goldschmied, F. R. and T. J. Letchner, Feasibility Study Of A Fluidic Control Subsystem, ASME Paper No. 65-WA/AVT-10, presented at Winter Annual Meeting, Chicago, Illinois, November 7-11, 1965.

- A-209. Goldschmied, F. R., Fluid Amplifier Dynamic Characteristics, Volume II, Final Report, NASA CR-57349, NASA N65-19772, December 30, 1964.
- A-210. Goldschmied, F. R., Proposed Test Standards For NOR And NAND Fluid Digital Amplifiers With Some Preliminary Experimental Results, Proceedings of 1965 Joint Automotive Control Conference (6th) held at Rensselaer Polytechnic Institute, Troy, New York, AIAA - A65-28781, June 22-25, 1965.
- A-211. Goldschmied, F. R., Experimental Investigation Of Fluidic And Peristaltic Heart Pumps, presented at AIAA Third Annual Meeting, Boston, Massachusetts, AIAA Paper No. 66-929, November 29 - December 2, 1966.
- A-212. Goodson, R. E. and R. Oldenburger, Simplification Of Hydraulic Line Dynamics By Use Of Infinite Products, ASME Paper No. 62-WA-55, Transactions of ASME Journal of Basic Engineering.
- A-213. Gotoh, K., The Damping Of The Large Wave-Number Disturbances In A Free Boundary Layer Flow, Physical Society of Japan Journal, Volume 20, Pages 164-169, January 1965.
- A-214. Gottron, R. N. and W. Gaylord, A Temperature Control System Using Flueric Components, Proceedings of HDL Third Fluid Amplification Symposium, Volume III, DDC Report No. AD-374344, NASA X67-15579, October 1965.
- A-215. Gottron, R. N., Acoustic Control Of Pneumatic Digital Amplifiers, Proceedings of HDL Fluid Amplification Symposium, Volume I, May 26-28, 1964.
- A-216. Gottron, R. N. and S. D. Weinger, Fluid Amplifiers: Parameters Affecting The Noise In No-Moving-Parts Fluid Devices, DDC Report No. AD-618057, TR-1283 (Contract DA-1P014501A33B), April 15, 1963.
- A-217. Gottron, R. N., Noise Reduction By Jet-Edge Resonator Coupling, Proceedings of HDL Fluid Amplification Symposium, Volume I, May 26-28, 1964.
- A-218. Grant, J., Potential Applications Of Fluidics In Nuclear Plant, presented at Second Cranfield Fluidics Conference, Cambridge, England, Paper No. K2 - 1967, NASA N67-21115, January 3-5, 1967.
- A-219. Gray, W. E. and H. Stern, Fluid Amplifiers: Capabilities And Applications, Reprinted from Control Engineering, Volume 11, No. 2, February 1964.
- A-220. Greber, I., P. E. Koerper and C. K. Taft, Fluid Vortex Amplifier Optimization, Proceedings of HDL Fluid Amplification Symposium, Volume II, October 1965.

- A-221. Greber, I., Bubble Pressures Under Reattaching Laminar Jets And Boundary Layers, Fluid Jet Control Devices, ASME Hydraulic and Automatic Control Divisions, Winter Annual Meeting and Symposium on Fluid Jet Control Devices, New York, N. Y., Pages 33-39, November 28, 1962.
- A-222. Griep, D. J., Fluid Flywheel Attitude Control Systems Study, DDC Report No. AD-606316 (Aerospace Corp., Los Angeles, California) for Contract AF04(695)269, August 1964.
- A-223. Griffin, W. S., Bistable Fluid Jet Amplifier With Low Sensitivity To Receiver Reverse Flow, Technical Reprint from HDL Third Fluid Amplification Symposium, Technical Memo No. TMX - 52120, NASA N65-35797, October 26-28, 1965.
- A-224. Gustofson, R. D., A New Servovalve Concept - The Ball Valve, Proceedings of the Society of Automotive Engineers, Aerospace Fluid Power Systems and Equipment Conference, Los Angeles, California IAA-A65-28067, Paper No. 650318, May 18-20, 1965.
- A-225. Hall, J. F. and L. B. Taplin, Progress Of The U. S. Air Force Research And Technology Division - FDL Program "Synthesis Of Pure Fluid Flight Control System", Paper given at AIAA/ION Guidance and Control Conference, Minneapolis, Minnesota, August 16-18, 1965.
- A-226. Halleen, R. M., A Literature Review On Subsonic Free Turbulent Shear Flow, DDC Report No. AD-606758 (Stanford University for Contract AF49(638)1278), April 1964.
- A-227. Hansen, C. J., A Study Of The Effects Of Environmental Noise On The Performance Of Fluid Amplifiers, Air Force Institute of Technology, Wright-Patterson AFB, Ohio, MS Thesis, Report No. GAM/ME/66A-5, DDC Report No. AD-632396, NASA N66-30142, March 1966.
- A-228. Harry Diamond Laboratories, Fluerics (Fluid Amplification), Report No. TR-1304, DDC Report No. AD-625885, NASA N66-18565, Bibliography August 30, 1965.
- A-229. Harry Diamond Laboratories, Fluid Amplification Symposium - Volume I, "Control Amplification and Fluids", Proceedings of Third Fluid Amplification Symposium, DDC Report No. 611432, NASA N65-22732, October 1965.
- A-230. Harry Diamond Laboratories, Fluerics (Fluid Amplification), No. 23, A Bibliography, Report No. HDL-TR-1338, DDC Report No. AD-649629, January 1967.
- A-231. Harry Diamond Laboratories, Fluid Amplification Symposium, Volume II, Proceedings of Third Fluid Amplification Symposium, October 1965.
- A-232. Harry Diamond Laboratories, Fluid Amplification Symposium, Volume III, Proceedings of Third Fluid Amplification Symposium, October 1965.

- A-233. Harry Diamond Laboratories, Four Fluid Amplifier Controlled Medical Devices - Fluid Amplification Symposium, Volume IV, Proceedings of Third Fluid Amplification Symposium, October 1965.
- A-234. Harry Diamond Laboratories, Fluid Amplification Symposium, Volume I, ASTIA Report No. AD-601499, May 26-28, 1964.
- A-235. Harry Diamond Laboratories, Proceedings Of The Fluid Amplification Symposium, Volume II, ASTIA Report No. AD-601500, May 1964.
- A-236. Harry Diamond Laboratories, Fluid Amplification Symposium, Volume III, ASTIA Report No. AD-601501, May 26-28, 1964.
- A-237. Harry Diamond Laboratories, Proceedings Of The Fluid Amplification Symposium, Volume IV, ASTIA Report No. AD-605289, May 1964.
- A-238. Hart, R. R., Performance Of A Coanda Device As A Pressure Maintainer And As A Switch Or Selector, Paper presented at Second Cranfield Fluidics Conference, Cambridge, England, Paper No. B4, NASA N67-21134, January 1967.
- A-239. Harvey, D. W. and R. P. McRae, Experimental Study Of Fluid Controlled Valves, Proceedings of HDL Third Fluid Amplification Symposium, Volume IV, October 1965.
- A-240. Harvey, D. W. and R. P. McRae, Steady Flow In A Pure Fluid Valve TCV System, Proceedings of HDL Third Fluid Amplification Symposium, Volume IV, October 1965.
- A-241. Harvey, D. W., Transient Theory Of Switching In A Bistable Valve, Proceedings of HDL Third Fluid Amplification Symposium, Volume IV, October 1965.
- A-242. Haugen, J. L., A Fluidic Approach To Control Of VTOL Aircraft, AIAA/JACC Guidance and Control Conference, Seattle, Washington, Pages 749-756, August 15-17, 1966, AIAA New York, 1966.
- A-243. Hawgood, D., Electrical Transducers For Fluidic Systems In Computer Peripherals, presented at Second Cranfield Fluidics Conference, Cambridge, England, Paper No. F3 - 1967, NASA N67-21135, January 3-5, 1967.
- A-244. Hayes, W. F. and C. Kwok, Impedance Matching In Bistable And Proportional Fluid Amplifiers Through The Use Of A Vortex Vent, Proceedings of HDL Fluid Amplification Symposium, Volume I, October 26-28, 1965.
- A-245. Heidmann, M. F. and R. J. Priem, Propellant Vaporization As A Design Criterion For Rocket-Engine Combustion Chambers, NASA TR-67, 1959.
- A-246. Hellbaum, R. F., Flow Studies In A Vortex Rate Sensor, Proceedings of the HDL Fluid Amplification Symposium, Volume II, October 1965.

- A-247. Hemond, Conrad J., Jr., The Transmission Of Sound In A Moving Fluid, DDC Report No. AD-601526 (Hartford University; Connecticut Research Institute for Contract NONR 430100 NR185 802, Report No. 2).
- A-248. Hemond, Conrad J., Jr., The Transmission Of Sound In A Moving Fluid, DDC Report No. AD-604123, (Hartford University; Connecticut Research Institute, Report Number 3).
- A-249. Henke, R., Fluidics And Fluid Power, Machine Design, Volume 37, No. 27, Pages 190, 192, 194, 196-198, November 25, 1965.
- A-250. Heskestad, Gunnar, Two Turbulent Shear Flows, DDC Report No. AD-605595 (John Hopkins University, Baltimore, Maryland for Contract AF49(638)248) June 1963.
- A-251. Hind, E. C. and E. J. Hahn, The Transfer Function Of The Pneumatic Capacitance, ASME Paper 65-WA/AUT-18, presented at the Winter Annual Meeting, Chicago, Illinois, November 7-11, 1965.
- A-252. Hinson, J. L., Study Of A Fluidic Attitude Control System For A Solar Probe Spacecraft, Technical Engineering Report No. ER-14436, NASA CR-80008, NASA N67-18638, November 1966.
- A-253. Ho, S. K., Research On A Non-Destructive Fluidic Storage Control Device, NASA CR-783, June 1967.
- A-254. Hodge, J. and J. G. Hutchinson, Turbulence Amplifiers - Principles And Applications, Paper given at First Conference on Fluid Logic and Amplification, Sponsored by the British Hydromechanics Research Association and College of Aeronautics, Cranfield, England, September 9-10, 1965.
- A-255. Holman, J. P. and E. E. Soehngen, Experimental Studies On The Interaction Of Strong Sound Fields With Free Convection Boundary Layers, Report No. 277, presented at the Boundary Layer Research Meeting of the AGARD Fluid Dynamics Panel, London, England, April 25-29, 1960.
- A-256. Holmes, A. B. and J. E. Foxwell, A Development Report On A Fluid Amplifier Attitude Control Valve System, Proceedings of HDL Fluid Amplification Symposium, Volume III, October 1965.
- A-257. Holmes, A. B., High Pressure Fluoric Control Components, paper presented at ASME Design Engineering Conference and Show, Chicago, Illinois, ASME Paper No. 66-MD-29, May 1966.
- A-258. Holmes, A. B. and J. E. Foxwell, Jr., Supersonic Fluid Amplification With Various Expansion Ratio Nozzles, Proceedings of the HDL Second Fluid Amplification Symposium, Volume IV, May 26-28, 1964.

- A-259. Hope-Gill, C. D., An Experimental Investigation Into The Shape Of Thrust-Augmenting Surfaces In Conjunction With Coanda Deflected Jet Sheets (Part I), DDC Report No. AD-611759 (Institute for Aerospace Studies University of Toronto, Ontario, Canada) Contract DA TC44177G1, December 1964.
- A-260. Horton, B. M., Control, Amplification And Fluids, DDC Report No. AD-612129 (HDL) June 1964.
- A-261. Horton, H. B., Prospects For Fluidics, Instrumentation Control Systems, Volume 39, No. 10, Part 1, Pages 91-92, October 1966.
- A-262. Hot Gas Controls Waiting In The Wings, Control Engineering, Pages 65-66, July 1962.
- A-263. Howie Corporation, Fluid Logic Fundamentals And The Turbulence Amplifier, Howie Corp., Norristown, Pennsylvania, May 1, 1965.
- A-264. Howland, G. R., Fluid State Amplifier And Compensation For The Model NV-B1 Gimbal Actuator, NASA CR-62522 (Bendix Corporation - Final Report BPAD-864-15651R on Contract NAS 8-5407) April 1965.
- A-265. Howland, G. R., Performance Characteristics Of Vortex Amplifiers, Proceedings of the HDL Fluid Amplification Symposium, Volume II, October 1965.
- A-266. Hrubecky, Henry F. and Larry N. Pearce, Flow Field Characteristics In A Model Bistable Fluid Amplifier, Proceedings of HDL Fluid Amplification Symposium, Volume I, May 26-28, 1964.
- A-267. Humphrey, E. G. and D. H. Tarumoto, (Eds.), Fluidics, Fluid Amplifier Associates, Inc., Boston, Massachusetts, 1965.
- A-268. Humphrey, Ronald L. and Francis M. Manion, Low-Pass Filters For Pneumatic Amplifiers, Proceedings of HDL Fluid Amplification Symposium, Volume I, May 26-28, 1964. (Also appeared DISA Information, January 1965, Pages 13-17.)
- A-269. Humphries, J. H. Jr., Fluidic Computers, Datamation, Volume 13, No. 3, Pages 39, 42-44, March 1967.
- A-270. Hurrell, H. G., Analysis Of Injection-Velocity Effects On Rocket Motor Dynamics And Stability, NASA TR-43, 1959.
- A-271. Industry Sponsors Graphic Symbols For Fluidics, Machine Design, Volume 38, No. 9, Pages 29-30, April 14, 1966.
- A-272. Iseman, J. and A. Katz, Angular Speed Control With A Bistable Fluid Amplifier, Product Engineering, Page 133, July 1963.
- A-273. Iseman, J. M., Angular Velocity Regulation With A Fluid Interaction System, Proceedings of HDL Second Fluid Amplification Symposium, Volume III, May 26-28, 1964.

- A-274. Jackomis, William N. and Glen W. Zumwalt, Aerodynamic Throat Nozzle For Thrust Magnitude Control Of Solid Fuel Rockets, ARS Journal, Volume 32, No. 12, Pages 1934-1936, December 1962.
- A-275. Janak, P. H., Experimental And Theoretical Aspects Of A Fluid Amplifier, IAA Report A64-13496, also AIAA Student Journal, Volume I, December 1963.
- A-276. Janow, Carl, Some Aspects Of Fluid Systems For Future Space Missions, paper presented at Society of Automotive Engineers Committee A-6 Meeting, Boston, Massachusetts, September 17, 1964.
- A-277. Jeglum, N. L., Fluid State Devices Used For Proportional Amplification And Flip-Flop Switching, ASME Publication 65MD-27, presented at the American Society of Mechanical Engineers, Design Engineers Conference and Show, May 17-20, 1965.
- A-278. Jeglum, N. L. and C. K. Taft, The New Challenge: Fluid Amplifiers, Mechanical Engineering, Volume 88, No. 1, Pages 36-39, January 1966.
- A-279. Johnson, J. L., A Pure Fluid Absolute Pressure Ratio Sensor, paper presented at AIAA Aerodynamic Testing Conference, Los Angeles, California, AIAA Paper No. 66-748, September 21-23, 1966.
- A-280. Johnson, E. G., Fluidic Jet Engine Controls: Faster, Cheaper, Lighter, Control Engineering, Volume 14, No. 7, Pages 58-62, July 1967.
- A-281. Joklik, O. F., Industrial Scale Manufacture Of Pure Fluidic Devices From Acrylic Material By A Special Casting Process, paper presented at Second Cranfield Fluidics Conference, Cambridge, England, Paper No. F5 - 1967, NASA N67-21102, January 3-5, 1967.
- A-282. Jones, N. S., A Method Of Calculating The Wall Pressure Distribution In A Turbulent Reattachment Bubble, paper presented at Second Cranfield Fluidics Conference, Cambridge, England, Paper No. A3, January 5, 1967.
- A-283. Johnston, Richard Paul, Dynamic Studies Of Turbulent Reattachment Fluid Amplifiers, submitted to the Graduate Faculty of the Schools of Engineering and Mines, University of Pittsburgh, 1963.
- A-284. Jura, S., Some Applications Of Fluid Logic Elements In Devices For Driving Recording Tape, paper presented at Second Cranfield Fluidics Conference, Cambridge, England, Paper No. J1 - 1967, NASA N67-21132, January 3-5, 1967.
- A-285. Kadcsch, M., Attachment Of A Jet To A Curved Wall, Proceedings of HDL Second Fluid Amplification Symposium, Volume IV, May 26-28, 1964.
- A-286. Kadosch, M., Calculation Of The Separation Of A Jet Attached To A Convex Wall, Proceedings of the HDL Fluid Amplification Symposium, Volume I, October 25-28, 1965.

- A-287. Kadosch, M. and C. Pavlin, Mechanical Characteristics Of A Pure Fluid Respirator With Curved Walls, paper given at First Conference on Fluid Logic and Amplification, sponsored by the British Hydro-mechanics Association and College of Aeronautics, Cranfield, England, September 9-10, 1965.
- A-288. Kadosch, M., The Curved Wall Effect, paper presented at Second Cranfield Fluidics Conference, Cambridge, England, Paper No. A4, NASA N67-21120, January 3-5, 1967.
- A-289. Kallavig, John A., Effect Of Receiver Design On Amplifier Performance And Jet Profile Of A Proportional Fluid Amplifier, Proceedings of HDL Fluid Amplification Symposium, Volume II, October 1965.
- A-290. Kantola, R. A. and R. T. Ziemba, Fluid Timer For Ordnance Applications (G. E. Company - Missile and Armament Department, Report 65APB4, for Contract DA 19020AM0213A) DDC Report No. AD-613599, February 1965.
- A-291. Kantola, R. A., Development Aspects Of A Miniature Fluid Counter, 1966 Joint Automatic Control Conference, Seattle, Washington, Pages 150-157, August 17-19, 1966.
- A-292. Kasselmann, J. T. and J. G. Rivard, Development Of An All-Fluid Amplifier For Liquid Rocket Applications, Report No. BC/RLD 3015, NASA CR-54446, November 1965.
- A-293. Katz, Silas, J. M. Goto and R. J. Dockery, Experiments In Analog Computation With Fluids, Proceedings of HDL Second Fluid Amplification Symposium, Volume II, May 26-28, 1964.
- A-294. Katz, S. and G. Roffman, Flueric Feedback Integration and Computation, 1966 Joint Automatic Control Conference, Seattle, Washington, Pages 150-157, August 17-19, 1966.
- A-295. Katz, S. and G. Roffman, Flueric Operation On Pressure Signals, ASME Paper No. 65-WA/PID-2, presented at the Winter Annual Meeting, Chicago, Illinois, November 7-11, 1965.
- A-296. Katz, S. and R. J. Dockery, Staging Of Proportional And Bistable Fluid Amplifiers, HDL Lab Report TR-1165, ASTIA Report No. AD-421613, August 30, 1963.
- A-297. Katz, S., E. T. Winston and P. Hawes, The Response Of A Bistable Fluid Amplifier To A Step Input, Proceedings of HDL Fluid Amplification Symposium, Volume I, May 26-28, 1964.
- A-298. Kaufman, W. F., C. E. Hallum and J. W. Fix, A Pure-Pneumatic Regulator, SAE 1965 Aerospace Fluid Power Systems and Equipment Conference, May 21, 1965.

- A-299. Kelley, L. R., A Fluidic Temperature Control Using Frequency Modulation And Phase Discrimination, 1966 Joint Automatic Control Conference, Seattle, Washington, Pages 123-131, August 17-19, 1966.
- A-300. Kelley, R. E., Parametric Amplification Of Surface And Internal Waves, DDC Report No. AD-605728 (Fluid Dynamic Research Lab, Massachusetts Institute of Technology, for Contract AF AFOSR15663) June 1964.
- A-301. Keto, J. R., Transient Behavior Of Bistable Fluid Elements, Proceedings of HDL Second Fluid Amplification Symposium, Volume III, May 26-28, 1964.
- A-302. Khokhlov, V. A., Hydraulic Power Amplifiers, DDC Report No. AD-413-571 (Translated from Izdatel' stvo ak ademii nauk SSSR, Moskva) 1961.
- A-303. Kirshner, Joseph M., A Definition Of The Mechanical Potential Necessary To A Fluid Circuit Theory, Proceedings of HDL Fluid Amplification Symposium, Volume I, October 26-28, 1965.
- A-304. Kirshner, J. M. (Ed.), Fluid Amplifiers, New York, McGraw-Hill, 1966.
- A-305. Kirshner, J. M. and C. J. Campagnuolo, A Temperature-Insensitive Pneumatic Oscillator And A Pressure-Controlled Pneumatic Oscillator, Proceedings of HDL Fluid Amplification Symposium, Volume II, October 1965.
- A-306. Kirshner, J. M., Progress In Fluid Amplifiers, Machine Design, Volume 36, No. 29, Pages 171-174 and 176-179, December 19, 1964.
- A-307. Kirshner, J. M., Some Topics In Fluid Circuit Theory, paper given at First Conference on Fluid Logic and Amplification, sponsored by the British Hydromechanics Research Association and College of Aeronautics, Cranfield, England, September 9-10, 1965.
- A-308. Klass, Philip J., Fluid/Gas Systems Challenging Electronics, Aviation Week and Space Technology, Volume 81, Pages 36-37 and 39-41, November 30, 1964.
- A-309. Klass, P. J., Fluid Sensors Open Way To Many Systems, Aviation Week and Space Technology, Volume 81, Pages 52, 53, 55 and 59, December 7, 1964.
- A-310. Klein, H. E., Fluid Control: New Challenge To Electronics, Supervisory Management, Page 53, September 1965.
- A-311. Klein, H. E., New Challenger To Electronics, Dun's Review and Modern Industry, Page 48, June 1965.

- A-312. Kline, Stephen J., Some New Mechanisms And Conceptions Of Stall Including The Behavior Of Vaned And Unvaned Diffusers, Progress Report to the National Advisory Committee for Aeronautics under NACA Contract NAW-6500, Stanford University, Stanford, California, March 15, 1957.
- A-313. Koebile, A., Pneumatische Verstaerker, Archiv Fuer Technischis Messen, No-336, Pages 13-16, January 1964.
- A-314. Koenig, G. R., Design Of Inputs And Outputs Of Digital Pneumatic Jet Components For Adaptation To The Standardised Pressure Range, paper presented at Second Cranfield Fluidics Conference, Cambridge, England, Paper No. B5 - 1967, NASA N67-21110, January 3-5, 1967.
- A-315. Kolpin, Marc A., Flow In The Mixing Region Of A Jet, ASRL TR92-3, NASA Grant NsG-31-60, Massachusetts Institute of Technology, Department of Aeronautics and Astronautics, Aeroelastic and Structures Research Laboratory.
- A-316. Kompass, E. J., Fluid Amplifiers As Control Components, Control Engineering, Volume II, Pages 82-85, September 1964.
- A-317. Kompass, E. J., Practical Control System Components, Control Engineering, Volume II, No. 9, Pages 82-85, September 1964.
- A-318. Korst, H. H., Dynamics & Thermodynamics Of Separated Flows, Department of Mechanical and Industrial Engineering, University of Illinois.
- A-319. Krasnoff, E., Theory, Design And Tests Of Flexible Wall Acoustic Filters, DDC Report No. AD-601103, Hydronautics, Inc., Laurel, Maryland, Contract NOBS 88200, September 1963.
- A-320. Krause, F., W. Dahm, A. Hanson and R. Larson, Heat Transfer Below Reattaching Turbulent Flows, Paper No. 65-825, presented at the AIAA Aerothermochemistry of Turbulent Flows Conference, December 13-15, 1965.
- A-321. Krause, E. and V. Zakkay, The Radial Variation Of The Eddy Viscosity In Compressible Turbulent Jet Flows, DDC Report No. AD-617701, New York University Report for Contract AF33(615)1516, May 1965.
- A-322. Kuhlenkamp, A., Hydraulic Computer Amplifiers, Paper No. 1.2 presented at the IFAC/IFIP Symposium on Microminiaturization in Automatic Control Equipment and in Digital Computers, Munich, Germany, October 21-23, 1965.
- A-323. Laakaniemi, R. N., Two Pure Fluid Amplifying Elements, Journal of American Society of Heating, Refrigerating, and Air Conditioning Engineers, Volume 8, No. 1, Pages 102-105, January 1966.
- A-324. Laitinen, P. O., Flow Noise Study Of Water Flowing Through Pipes, DDC Report No. AD-603589, Navy Electronics Lab, San Diego, Calif.

- A-325. Landau, L. D., and E. M. Lifshitz, Fluid Mechanics, Volume 6 of course of theoretical physics, translated from the Russian by J. B. Sykes and W. H. Reid, Published by Pergamon Press, Addison, Wesley Publishing Company, Reading, Massachusetts, 1959.
- A-326. Lane, J. F., The Turbulent Reattachment Fluid Amplifier, Quarterly Bulletin of the Division of Mechanical Engineering and the National Aeronautical Establishment, NASA X67-13434, Report No. DME/NAE-1966, NASA X67-13436, Pages 37-60, September 30, 1966.
- A-327. Lanin, N. D., A Small Scale Continuous Action Pneumatic Computer And Relay Block, DDC Report No. AD-605509 (Foreign Tech. Division Air Force Systems Command, Wright-Patterson AFB), unedited rough draft translation of Mono. voprosy Pnevmo - I Gidroavtomatiki, Mosco, 1960.
- A-328. Lanin, N. D. and V. I. Pashintseva, Methods Of Constructing Pneumatic Computers Of Continuous Action And Ways Of Utilizing Them, DDC Report No. AD-610320 (translation January 9, 1965), Report dated 1959.
- A-329. Lansky, Z. J., Practical Guides To Pneumatic Valve Application, Automation, Page 61, July 1965.
- A-330. Larson, R. H., Basic Devices Used In Fluidic Systems, Automation, Volume 13, No. 12, Pages 72-76, December 1966.
- A-331. Larson, R. W., The Industrial Applications Of Fluidics, Research and Development, Volume 17, No. 12, Pages 26-29, December 1966.
- A-332. Layton, J. P., Summary Technical Report On Transient Pressure Measuring Methods Research For The Period March 1, 1961 Through December 31, 1962.
- A-333. Lechner, T. J., Low Pressure Signal Sensor Amplifier And Analog Computer Using The Impact Modulator As The Basic Active Pure Fluid Device, Part I, Analog Computer, Final Report, DDC Report No. AD-629055, December 1, 1965.
- A-334. Lechner, T. J., Low Pressure Signal Sensor Amplifier And Analog Computer Using The Impact Modulator As The Basic Active Pure Fluid Device, Part II, Low Pressure Signal Sensor Amplifier, Final Report, DDC Report No. AD-629056, December 15, 1965.
- A-335. Lechner, T. J., Fluerics: 19, Low-Pressure Amplifier And Analog Computer, DDC Report No. AD-635227, April 1966.
- A-336. Lechner, T. J. and P. H. Sorenson, Some Properties And Applications Of Direct And Transverse Impact Modulators, Proceedings of HDL Second Fluid Amplification Symposium, Volume II, May 26-28, 1964.
- A-337. Lefer, Henry, All-Pneumatic Missile System On The Horizon, Hydraulics and Pneumatics, Pages 101-111, June 1962.

- A-338. Lefer, H. Lets Look At Fluidics Part I - Where Are We? Where Are We Going? Hydraulics and Pneumatics, Page 113, October 1965.
- A-339. Lemmon, G. V. and E. R. Phillips, Development Of Two Pure Fluid Timers, Proceedings of the HDL Second Fluid Amplification Symposium, Volume II, May 26-28, 1964.
- A-340. Letham, D. L., F. R. Goldschmied and H. L. Fox, Analytical Investigation Of Fluid Amplifier Dynamic Characteristics, Sperry Rand, Utah - Report - Volume II, December 30, 1964.
- A-341. Letham, D. L., Fluidic System Design, Part 2, Analysis, Machine Design, Volume 38, No. 5, Pages 128-135, March 3, 1966.
- A-342. Letham, D. L., Fluidic System Design, Part 3, Fluid Impedance, Machine Design, Volume 38, No. 7, Pages 170-181, March 17, 1966.
- A-343. Letham, D. L., Fluidic System Design, Part 4, Lines, Jets, Machine Design, Volume 38, No. 8, Pages 116-122, March 31, 1966.
- A-344. Letham, D. L., Fluidic System Design, Part 6, Stream-Interaction Amplifiers, Machine Design, Volume 38, No. 15, Pages 171-174, June 23, 1966.
- A-345. Letham, D. L., Fluid System Design, Part 7, Turbulence Amplifiers, Machine Design, Volume 38, No. 16, Pages 157-159, July 7, 1966.
- A-346. Letham, D. L., Fluidic System Design, Part 8, Vortex Amplifiers, Machine Design, Volume 38, No. 17, July 21, 1966.
- A-347. Letham, D. L., Fluidic System Design, Part 5, Practical Fluid Resistors, Machine Design, Volume 38, Pages 134-138, June 9, 1966.
- A-348. Letham, D. L., Fluidic System Design, Part 9, Impact Modulators, Machine Design, Volume 38, No. 18, Pages 146-156, August 4, 1966.
- A-349. Letham, D. L., Fluidic System Design, Part 10, Miscellaneous Devices, Machine Design, Volume 38, No. 19, Pages 169-176, August 18, 1966.
- A-350. Letham, D. L., Fluidic System Design, Part 11, Transducers And Sensors, Machine Design, Volume 38, No. 20, Pages 139-145, September 1, 1966.
- A-351. Letham, D. L., Fluidic System Design, Part 12, Active-Device Characteristics, Machine Design, Volume 38, No. 24, Pages 224-227, October 13, 1966.
- A-352. Letham, D. L., Fluidic System Design, Part 13, Effects Of Circuit Elements, Machine Design, Volume 38, No. 25, Pages 162-165, October 27, 1966.

- A-353. Letham, D. L., Fluidic System Design, Part 14, Circuit Sub-Assemblies, Machine Design, Volume 38, No. 26, Pages 210-218, November 10, 1966.
- A-354. Letham, D. L., Fluidic System Design, Part 15, Circuit Synthesis, Machine Design, Volume 39, No. 1, Pages 124-130, January 5, 1967.
- A-355. Letham, D. L., Fluidic System Design, Part 16, Component Fabrication, Machine Design, Volume 39, No. 2, Pages 217-218, January 19, 1967.
- A-356. Letham, D. L., Fluidic System Design, Part 17, Test Equipment, Machine Design, Volume 39, No. 3, Pages 142-148, February 2, 1967.
- A-357. Letham, D. L., Fluidic System Design, Part 18, Hybrid Devices, Machine Design, Volume 39, No. 4, Pages 231-235, February 16, 1967.
- A-358. Letham, D. L., Fluidic System Design, Part 19, Graphic Symbols, Machine Design, Volume 39, No. 5, Pages 90-92, March 2, 1967.
- A-359. Letham, D. L., Fluidic System Design, Part 20, Application Circuits, Machine Design, Volume 39, No. 7, Pages 201-206, March 16, 1967.
- A-360. Lewis, W. J., Fluid Flow Flight Control Needs No Electronics, Space Aeronautics, Page 126, Volume 41, Report A64-17194, April 1964.
- A-361. Library of Congress, Washington, D. C., Calculation Of Time Characteristics Of Pneumatic Flow Chambers, by V. N. Dmitriev and V. I. Chernyshev, NASA N67-16869, Pages 130-138, from Pure Fluid Devices - Surveys of Foreign Scientific and Technical Literature NASA N67-16861, Report No. ATD-66-107, August 29, 1966.
- A-362. Library of Congress, Washington, D. C., Computation Of The Static Characteristics Of A Pneumatic Relay, by V. N. Dmitriev, NASA N67-16867, Pages 102-116, from Pure Fluid Devices - Surveys Of Foreign Scientific And Technical Literature, NASA N67-16861, Report No. ATD-66-107, August 29, 1966.
- A-363. Library of Congress, Washington, D. C., Electromechanical Systems: Summary Of Data, Report No. ATD-66-74, TT 66-62457, DDC Report No. AD-640430, June 20, 1966.
- A-364. Library of Congress, Washington, D. C., Electropneumatic Transducers Of The IAT And SSSR, by Yu. V. Krementulo, NASA N67-16876, Pages 186-193, NASA N67-16861, Report No. ATD-66-107, from Pure Fluid Devices - Surveys of Foreign Scientific and Technical Literature, August 29, 1966.

- A-365. Library of Congress, Washington, D. C., Improvement Of The Static Characteristic Of A Pneumatic Relay By Means Of Flow Restrictors Of Constant Pressure Drop, by V. N. Dmitriev, NASA N67-16868, Pages 117-129, from Pure Fluid Devices - Surveys of Foreign Scientific and Technical Literature, NASA N67-16861, Report No. ATD-66-107, August 29, 1966.
- A-366. Library of Congress, Washington, D. C., Investigation Of The Characteristics Of Pneumatic Jet Elements, by L. A. Zalmanzon and A. I. Semikova, NASA N67-16883, Pages 227-244, from Pure Fluid Devices - Surveys of Foreign Scientific and Technical Literature, NASA N67-16861, Report No. ATD-66-107, August 29, 1966.
- A-367. Library of Congress, Washington, D. C., On Increasing The Pressure Of The Working Agent In Jet Amplifiers, by B. D. Kosharskii, NASA N67-16875, Pages 181-185, from Pure Fluid Devices - Surveys of Foreign Scientific and Technical Literature, NASA N67-16861, Report No. ATD-66-107, August 29, 1966.
- A-368. Library of Congress, Washington, D. C., Pneumatic Analogue Computer, by N. D. Lanin, NASA N67-16877, Pages 194-196, from Pure Fluid Devices - Surveys of Foreign Scientific and Technical Literature, NASA N67-16861, Report No. ATD-66-107, August 29, 1966.
- A-369. Library of Congress, Washington, D. C., Pneumatic Ratio Controllers Without Mechanical Dividers, by G. T. Berezovets, NASA N67-16865, Pages 85-91, from Pure Fluid Devices - Surveys of Foreign Scientific and Technical Literature, NASA N67-16861, Report No. ATD-66-107, August 29, 1966.
- A-370. Lindahl, J. H., Vortex Senses Aircraft Pitch Rate, Control Engineering, Volume 11, No. 9, Pages 99-100, September 1964.
- A-371. Long, T. A. and E. E. Thompson, Fluid Amplifiers, A DDC Report Bibliography, DDC Report No. AD-344243, November 1963.
-CONFIDENTIAL-
- A-372. Long, M. E., Fluidic, Machine Design, Volume 39, No. 17, Pages 165-166, July 20, 1967.
- A-373. Lowen, J. and J. L. Shearer, The Role Of New Development In Fluid Power Control For Aerospace Systems, IAA Report A63-14947. Paper 593B given at SAE, National Aero and Space Engineering and Manufacturing Meeting, Los Angeles, California, October 8-12, 1962. Contract No. AF-33(616)6120 and AF33(657)7535, October 1962.
- A-374. Lugt, H. J. E. W. Schwiderski, and S. P. Uginciu, Axisymmetric Viscous Fluid Motions Around Conical Surfaces, DDC Report No. AD-600962 (Naval Weapons Lab.) May 1964.

- A-375. Lush, P. A., Investigation Of The Switching Mechanism Of A Large Scale Model Of A Turbulent Reattachment Amplifier, presented at Second Cranfield Fluidics Conference, Cambridge, England, Paper No. A1 - 1967, NASA N67-21129, January 3-5, 1967.
- A-376. Maas, Margaret A., Atmospheric Ports Control In High-Pressure Valve, Design News, September 18, 1963.
- A-377. Maas, Margaret A., Digital Fluid Amplifiers Yield Proportional Control, Design News, Volume 21, No. 8, Pages 20-21, April 13, 1966.
- A-378. Maas, M. A., Fluidics Direct Bottle Packaging, Design News, Volume 21, No. 23, Pages 82-83, November 9, 1966.
- A-379. Maas, M. A., Fluid Amplifier Cycle Respirator, Design News, Page 20, September 25, 1964.
- A-380. Maas, M. A., Fluidic Elements, Start Stop Process Control Pump, Design News, September 1, 1965.
- A-381. Maas, M. A., Fluidics Protect Punch-Press Operator's Fingers, Design News, Page 8, September 15, 1965.
- A-382. Maas, M. A., Turbulence Amplifier Goes Modular, Design News, Volume 21, No. 9, Pages 42-43, April 27, 1966.
- A-383. Makarov, I. and A. Durbov, Electronics, New Rival, DDC Report No. AD-607312 (Foreign Tech. Division Air Force System Command), WPAFB, September 1964, unedited rough draft translation from Izvestuja (USSR), 1964, February 4, Page 5.
- A-384. Malim, T. H., Fluids: The New Look In Controls, Iron Age, Volume 196, No. 1, Page 53-56, July 1965.
- A-385. Mamzic, C. L. and B. L. Johnson, Diverting Valves Cool Burners, Control Engineering, Volume 11, No. 9, Pages 94-95, September 1964.
- A-386. Mamzic, C. L., Fluid Interaction Control Devices, Proceedings of Fifth National Chemical and Petroleum Instrumentation Symposium, Wilmington, Delaware, Pages 79-87, May 4-5, 1964.
- A-387. Manion, Francis M., Development Of A Pressure Controlled Oscillator For Frequency Modulating Systems, Proceedings of HDL Fluid Amplification Symposium, Volume II, October 1965.
- A-388. Mann, J. E., Fluid Amplifier Releases Intermittent Puffs Of Chemical Smoke, Design News, Volume 21, No. 11, Pages 20-21, May 25, 1966.
- A-389. Mann, J. E., Tiny Airfoil Indicates Flow Fluctuations, Design News, Volume 21, No. 7, Pages 44-45, March 30, 1966.

- A-390. Margolis, D. P., Some Aspects Of Curved Turbulent Mixing Important In Fluid Amplifiers And Fluid Logic Devices, Proceedings of HDL Fluid Amplification Symposium, Volume I, May 26-28, 1964.
- A-391. Marris, A. W., On The Generation Of Secondary Velocity Along A Vortex Line, ASME Paper 64-FE-13, presented at Fluids Engineering Conference, Philadelphia, Pennsylvania, May 18-21, 1964.
- A-392. Martin, S. B. and E. R. Phillips, Fluid Timer Development, Proceedings of HDL Third Fluid Amplification Symposium, Volume III, October 1965.
- A-393. Martinez, E., Development Of An Infinite-Input-Impedance Fluidic Amplifier, NASA CR-80023, NASA N67-30159, June 1967.
- A-394. Massachusetts Institute of Technology, Basic Applied Research In Fluid Power Control, Report No. 8998-2, Department of Mechanical Engineering, prepared for Contract AF33(657)7535.
- A-395. Massachusetts Institute of Technology, Basic Applied Research In Fluid Power Control, Report No. 8998-4, Department of Mechanical Engineering, prepared for Contract AF33(657)7535.
- A-396. Massachusetts Institute of Technology, Basic Applied Research In Fluid Power Control, DDC Report AD-603195, Progress Report No. 8998-7 covering period October 1963 - January 31, 1964, prepared for Contract AF-33(657)7535.
- A-397. Massachusetts Institute of Technology, Basic Applied Research In Fluid Power Control, Report No. DSR-5393-1, May 1965, AFFDL-TR-65-79, DDC AD-624885, NASA N66-24792, Progress Report No. 1 for the period of October 15, 1964 to February 1, 1965.
- A-398. Massachusetts Institute of Technology, Basic Applied Research In Fluid Power Control, Report No. DSR-5393-2, September 1965, AFFDL-TR-65-180, DDC AD-625729, NASA N66-18562, Progress Report No. 2, for the period February 1 - May 31, 1965.
- A-399. Massachusetts Institute of Technology, Basic Applied Research In Fluid Power Control, Report No. DSR-593-3, January 1966, AFFDL-TR-65-229, DDC AD-630790, NASA N66-26309, Progress Report No. 3, for the period June 1 - October 15, 1965.
- A-400. Massachusetts Institute of Technology, Basic Applied Research In Fluid Power Control, Report No. DSR-6310-1, August 1966, AFFDL-TR-66-130, SAPR-1, DDC AD-805695, NASA X67-15715, Semi-annual Progress Report No. 1, for the period October 16, 1965 to April 30, 1966.
- A-401. Massachusetts Institute of Technology, Basic Applied Research In Fluid Power Control, Report No. 8998-8, prepared for Contract AF-33(657)7535, FDL-TDR-64-127, September 1964.

- A-402. Massachusetts Institute of Technology, Basic Applied Research In Fluid Power Control, Report No. DSR-8998-9, January 1965, AFFDL-TR-64-193, DDC AD-463892, NASA N65-26245, Final Progress Report.
- A-403. Massachusetts Institute of Technology, Basic Research And Development In Fluid Power Control For The United States Air Force, WADD Tech. Report 60-675, WWRMPT-1, 4th Progress Report for Contract AF33(616)6120, September 1960.
- A-404. Massachusetts Institute of Technology, Basic Research And Development In Fluid Power Control, 8th Progress Report for Contract AF-33(616)6120, Tech. Report ASD-TR-61-349, February 1962.
- A-405. Massachusetts Institute of Technology, Basic Research And Development In Fluid Power Control For The United States Air Force, 9th Progress Report for Contract AF-33(616)6120, Tech. Document Report No. ASD-TDR-62-3, January 1962.
- A-406. Massachusetts Institute of Technology, Engineering Projects Laboratory Report - EPL-1, January 1963.
- A-407. Massachusetts Institute of Technology, Basic Applied Research In Fluid Power Control, Department of Mechanical Engineering Report No. 8998-1, prepared for Contract AF-33(657)7535.
- A-408. Massachusetts Institute of Technology, Research And Development Of Fluid Amplifiers For Turbopropulsion System Control, Report No. DSR-9159-2, Tech. Documentary Report No. APL-TDR-64-82, prepared for Contract AF-33(657)8384, June 30, 1964.
- A-409. Massachusetts Institute of Technology, Research And Development Of A Hot Gas Flight Stabilization System, WADD Tech. Report No. 60-449, Part 1, Volume 1, for Contract AF-33(600)40538, September 1960.
- A-410. Massachusetts Institute of Technology, Research And Development Of Pneumatic Jet Relay System For Propulsion System Control, Report No. DSR-9159-1, March 31, 1963.
- A-411. Mayer, E. A. and P. Maker, Control Characteristics Of Vortex Valves, Proceedings of HDL Second Fluid Amplification Symposium, Volume II, May 1964.
- A-412. Mayer, E. A., Photoviscous Flow Visualization In Fluid State Devices, Proceedings of HDL Fluid Amplification Symposium, Volume II, October 1965.
- A-413. McCabe A. and D. L. Hughes, Characteristics Of Proportional Fluidic Amplifiers, presented at Second Cranfield Fluidics Conference, Cambridge, England, Paper No. C5 - 1967, NASA N67-21127, January 5, 1967.

- A-414. McCloy, D. and R. H. McGuigan, Some Static And Dynamic Characteristics Of Poppet Valves, Paper 23, December 30, 1964.
- A-415. McGlaughlin, D. W., Fluidic Electro-Fluid Converter, 1966 Joint Automatic Control Conference, Seattle, Washington, Pages 132-139, August 17-19, 1966.
- A-416. McGlaughlin, D. W. and C. K. Taft, Fluidic Electro-Fluid Converter, Journal of Basic Engineering, Volume 89, No. 2, Pages 334-340, June 1967.
- A-417. McRee, Donald I., Experimental Study Of A Convergent Nozzle And A Free Jet Flow, Proceedings of HDL Fluid Amplification Symposium, Volume I, October 26-28, 1965.
- A-418. McRee, D. I. and D. A. Small, The R. & D. Challenge of Fluidics, Research and Development, Volume 17, No. 8, Pages 37-40, August 1966.
- A-419. Mehus, T., An Experimental Investigation Into The Shape Of Thrust Augmenting Surfaces In Conjunction With Coanda - Deflected Jet Sheets, Part II, DDC Report No. AD-614617, (Institute of Aerospace Studies, University of Toronto, Ontario, Canada, January 1965).
- A-420. Mellor, G. L. and D. M. Gibson, Equilibrium Turbulent Boundary Layers, DDC Report No. AD-601276 (Princeton University) Contract NONR1858-38, November 1963.
- A-421. Metzger, Eric E. and Charles G. Lomas, Turbulence Amplifier For Integrated Two-Dimensional Fabrication, Proceedings of HDL Fluid Amplification Symposium, Volume II, October 1965.
- A-422. Meyer, C. H., A Fluid Operated Diesel Locomotive Transition Control Unit, Proceedings of HDL Third Fluid Amplification Symposium, Volume III, October 1965.
- A-423. Miles, John W., On Panel Flutter In The Presence Of A Boundary Layer, DDC Report No. AD-605759 (TRW Space Tech. Lab. Los Angeles, California) for Contract AF-18(600)1190, December 1957.
- A-424. Miller, David P., Characteristics Of A Vortex Fluid Throttle, Proceedings of HDL Second Fluid Amplification Symposium, Volume II, May 1964.
- A-425. Mitchell, A. E. and H. R. Müller, Comparison Of A Momentum Device With A Turbulent Reattachment Device, IAA Report No. A64-11716, also Zeitsch Fuer Angewandte Mathematik and Physik, Volume 14, Pages 758-763, November 15, 1963.
- A-426. Mitchell, A. E., Reattachment Of Separated Boundary Layers And Their Effects In Fluid Switching Devices, IBM Research Report No. RZ-81, February 19, 1962.

- A-427. Mitchell, A. E., H. R. Müller and R. H. W. Zingg, Some Recent Developments In The Design Of Fluid Switching Devices And Circuits, 1964 Fluid Power International Conference.
- A-428. Monge, M., Some Industrial Applications Of The Moduflog Systems, paper presented at Second Cranfield Fluidics Conference, Cambridge, England, Paper No. J4 - 1967, NASA N67-21108, January 3-5, 1967.
- A-429. Monge, M., Handling "Fluidics" For Practical Applications, paper presented at First Conference on Fluid Logic and Amplification, sponsored by the British Hydromechanics Research Association and College of Aeronautics, Cranfield, England, Paper No. E5, NASA N66-10658, September 9-10, 1965.
- A-430. Montgomerie, G. A. and T. J. Floyd, Heavy Current Fluidic Devices, paper presented at Second Cranfield Fluidics Conference, Cambridge, England, Paper No. K4 - 1967, January 3-5, 1967.
- A-431. Monolithic Fluid Logic Counts 16 Discrete Numbers, Control Engineering, Volume 12, No. 12, Page 100, December 1965.
- A-432. More On Fluidics Bibliography, Hydraulics and Pneumatics, Volume 20, No. 6, Pages 101-104, June 1967.
- A-433. Morgan, James I., Fluid-Power Components, ASME Publication 65-MD-29, June 1965.
- A-435. Morton, T., The Use Of A Fluid Amplifier In An Intermittent Stream Release Valve For High Altitude Research, Proceedings of HDL Third Fluid Amplification Symposium, Volume III, October 1965.
- A-436. Moynihan, F. A. and R. J. Reilly, Deflection And Relative Flow Of Three Interacting Jets, Proceedings of HDL Fluid Amplification Symposium, Volume I, May 26-28, 1964.
- A-437. Moynihan, F. A., Jet Interaction Noise, Proceedings of HDL Fluid Amplification Symposium, Volume I, May 26-28, 1964.
- A-438. Mueller, Thomas J. and Robert E. Olson, Spreading Rates Of Compressible Two-Dimensional Reattaching Jets, Proceedings of HDL Fluid Amplification Symposium, Volume I, May 26-28, 1964.
- A-439. Müller, H. R., A Study Of The Dynamic Features Of A Wall-Reattachment Fluid Amplifier, The American Society of Mechanical Engineers, Paper 64-FE-10, May 1964. Also Journal of Basic Engineering, Volume 86, Pages 819-826, December 1964.
- A-440. Müller, H. R., Wall-Reattachment Device With Pulsed Control Flow, HDL Fluid Amplification Symposium, Volume I, May 26-28, 1964.

- A-441. Nelson, D. J. and H. Iwata, Application Of Pure Fluid Logic To On-Off Control Systems, Proceedings of HDL Second Fluid Amplification Symposium, Volume IV, May 26-28, 1964.
- A-442. Neve, R. S., A Short Review Of Past Research Into The Properties Of Fluid Jet Amplifiers, Report No. TN-838, NASA N66-10952, February 1965.
- A-443. New Fluidic Devices Control Machines As Well As Missiles, Product Engineering, Volume 37, No. 13, Page 85, June 20, 1966.
- A-444. Norwood, R. E., A Performance Criterion For Fluid Jet Amplifiers, Fluid Jet Control Devices, ASME Hydraulic and Automatic Control Divisions, Winter Annual Meeting and Symposium, New York, N. Y., Pages 59-63, November 28, 1962.
- A-445. Nystrom, K. S., Control Of A Boundary Layer Fluidistor By Means Of Disruptive Discharge, at First Conference on Fluid Logic and Amplification, sponsored by the British Hydromechanics Research Association and College of Aeronautics, Cranfield, England, September 9-10, 1965.
- A-446. O'Connor, T. J., E. H. Comfort and L. A. Cass, Turbulent Mixing Of An Axisymmetric Jet Of Partially Dissociated Nitrogen With Ambient Air, Paper No. 65-823 presented at AIAA Aerothermochemistry of Turbulent Flows Conference, December 13-15, 1965.
- A-447. Oels, R. A., R. F. Boucher and E. Markland, Experiments On Turbulence Amplifiers, paper given at First Conference on Fluid Logic and Amplification, sponsored by the British Hydromechanics Research Association and College of Aeronautics, Cranfield, England, Paper No. D3 - 1965, NASA N65-36348, 1965.
- A-448. Oldenburger, R. and A. F. D'Sonza, Dynamic Response Of Fluid Lines, Journal of Basic Engineering, Transactions of ASME, Pages 589-598, September 1964.
- A-449. Olson, R. E. and R. C. Stoeffler, A Study Of Factors Affecting The Time Response Of Bistable Fluid Amplifiers, American Society of Mechanical Engineers, Fluids Engineering Division, Conference and Symposium on Fully Separated Flows, Philadelphia, Pennsylvania, May 18-20, 1964.
- A-450. Olson, R. E. and Y. T. Chin, Fluid Amplification - 17: Studies Of Reattaching Jet Flows In Fluid-State Wall-Attachment Devices, DDC Report No. AD-623911, NASA N66-15106, September 30, 1965.
- A-451. Olson, R. W., Spreading Rates Of Compressible Two-Dimensional Reattaching Jets Upstream Of Reattachment, Proceedings of HDL Fluid Amplification Symposium, Volume I, October 26-28, 1965.

- A-452. Olson, R. E., Reattachment Of A Two-Dimensional Compressible Jet To An Adjacent Plate, from Fluid Jet Control Devices, ASME Hydraulic and Automatic Control Divisions, Winter Annual Meeting and Symposium, New York, N. Y., Pages 23-31, November 28, 1962.
- A-453. Olson, R. E. and J. F. Camarata, Pressure Recovery Characteristics Of Compressible Two-Dimensional Free Jet Flows, Proceedings of HDL Fluid Amplification Symposium, Volume I, October 26-28, 1965.
- A-454. Olson, R. E. and David P. Miller, The Interaction Of Oblique Shocks And Expansion Waves With A Jet Boundary Mixing Zone, Proceedings of HDL Fluid Amplification Symposium, Volume I, May 26-28, 1964.
- A-455. Orner, P. A., Development Of A Pure Fluid Power Amplifier, 1965 Joint Automatic-Control Conference (6th) Rensselaer Polytechnic Institute, Troy, New York, IAA-A65-28782, June 22-25, 1965.
- A-456. Orner, P. A. and J. N. Wilson, Fluid State Hybrid Control Systems, Proceedings of HDL Third Fluid Amplification Symposium, Volume III, October 1965.
- A-457. Orner, P. A., On The Dynamical Characteristics Of Fluid Amplifiers And Elements, Proceedings of HDL Fluid Amplification Symposium, Volume I, October 26-28, 1965.
- A-458. Osborn, M. J., Fluid Amplifier State-Of-The-Art, Volume II Bibliography (NASA Report CR-102) prepared for George C. Marshall Space Flight Center, under Contract NAS 8-5408, December 3, 1963.
- A-459. Osterle, J. F., W. T. Rouleau, F. J. Young and S. W. Angrist, Unconventional Methods For Influencing Fluid Flow, Technical Document Report No. ASD-TDR-63-776, Volume I, prepared by the Carnegie Institute of Technology, Pittsburgh, Pennsylvania for Contract AF-33(657)9914, November 1963.
- A-460. Ostlund, O. E. and W. G. Beduhn, Fluidic Yaw Damper System, Final Report No. 20230-FR1, AFFDL-TR-67-24, DDC Report No. AD-811542, February 1967.
- A-461. Otsap, B. A., Experimental Study Of A Proportional Vortex Fluid Amplifier, Proceedings of HDL Fluid Amplification Symposium, Volume II, NASA N64-23814, May 26-28, 1964.
- A-462. Parker, G. A. and B. Jones, Experiments With And/And Exclusive-Or Passive Elements, presented at Second Cranfield Fluidics Conference, Cambridge, England, Paper No. C4 - 1967, NASA N67-21119, January 3-5, 1967.
- A-463. Parker, G. A. and B. Jones, A Fluidic Subtractor For Digital Closed-Loop Control Systems, presented at Second Cranfield Fluidics Conference, Cambridge, England, Paper No. H1 - 1967, NASA N67-21105, January 3-5, 1967.

- A-464. Parker, G. A., Digital Fluid Position Encoders, paper given at First Conference on Fluid Logic and Amplification, sponsored by the British Hydromechanics Research Association and College of Aeronautics, Cranfield, England, September 9-10, 1965.
- A-465. Patches Of Fluidic Logic Create Instant Panels, Product Engineering, Volume 38, No. 20, Pages 80-83, September 1967.
- A-466. Pavlin, C., Experimental Study Of A Proportional Fluid Amplifier, Proceedings of HDL Third Fluid Amplification Symposium, Volume III, October 1965.
- A-467. Pavlin, C., Thrust Vector Control Using A Bleed Off-Reinjection Device, Proceedings of HDL Second Fluid Amplification Symposium, Volume IV, May 26-28, 1964.
- A-468. Pay, Rex, Pure-Fluid Guidance Advances Through Research At Giannini, Missiles and Rockets, Pages 28, 31, 32, and 34, December 9, 1963.
- A-469. Payne, Peter R., Curved Jet Flows, Volume I, DDC Report No. AD-616395 for Contract DA-44AM0238T, May 1965.
- A-470. Payne, Peter R., Curved Jet Flows, Volume II, DDC Report No. AD-616357 for Contract DA-44 177AM0238T, May 1965.
- A-471. Pedersen, John R. C., The Flow Of Turbulent Incompressible Two-Dimensional Jets Over Ventilated Cavities, Proceedings of HDL Fluid Amplification Symposium, Volume I, October 26-28, 1965.
- A-472. Peoples, J. A. and W. W. Scott, Photoelastic Effect Shows Fluid Device Performance, Control Engineering, Volume 12, No. 7, Page 98, July 1965.
- A-473. Peracchio, Aldo, The Vortex-Venturi: An Aerodynamic Speed Control For Turbines, Paper No. 63-WA-213, American Society of Mechanical Engineers, New York, N. Y.
- A-474. Phillips, O. M., A Note On The Measurement Of Sound In Liquid Filled Pipes, DDC Report No. AD-601102 (Hydromechanics Inc., Laurel, Maryland) Contract NOBS88200, January 1963.
- A-475. Picatinny Applied Fluidics To Timers, Army Research and Development, Volume 8, No. 4, April 1967.
- A-476. Pneumatic Logic Control: Poised For The Big Plunge, Product Engineering, Volume 37, No. 15, Pages 68-78, July 18, 1966.
- A-477. Pneumatic-Valve Logic Challenges Fluid Amplifiers, Product Engineering, Volume 38, No. 21, Pages 110-112, October 9, 1967.

- A-478. Popov, Y. U., Y. U. Pukhnachev and A. Pushkin, Pneumonics, "Nauka i zhizn" No. 1, Pages 10 to 18, Volume 1, 1965. Also DDC Report No. AD-618319, July 1965.
- A-479. Powell, Alan, An Aerosonics Bibliography, DDC Report No. AD-614594, (California Institute, Department of Engineering) Supplement No. 2 for Contract NONR23362, April 1965.
- A-480. Powell, Alan and T. J. B. Smith, An Aerosonics Bibliography, Supplement No. 1, DDC Report No. AD-600455, (University of California) Contract NONR2336] NRO62229, April 1964.
- A-481. Prete, Sorro, Exploring For Future Hydraulic Requirements, Fluid Power Branch (SEJPF), Vehicle Power Division, September 18, 1964.
- A-482. Proceedings Of The Second Fluidics Seminar On Industrial Applications Of Fluid Amplifiers, Milwaukee, Wisconsin, April 25-26, 1966.
- A-483. Prokopius, P. R., Use Of A Fluidic Oscillator As A Humidity Sensor For A Hydrogen-Steam Mixture, Technical Memo. No. TM X-1269, NASA, August 1966.
- A-484. Prosser, Dennis W. and Michael J. Fisher, Some Influences Of Turbulence On The Noise Of Proportional Fluid Amplifiers, Proceedings of HDL Fluid Amplification Symposium, Volume II, October 1965.
- A-485. Prosser, D. W. and M. J. Fisher, Fluerics: 20 Studies On Two-Dimensional Turbulent Jets, DDC Report No. AD-635195, April 1966.
- A-486. Raber, R. A. and J. N. Shinn, Fluid Amplifier Symbols, Nomenclature and Specification, NASA Report CR-147, prepared for Contract NAS 8-5408, January 1965.
- A-487. Ramanathan, S., The Design Of A Pure Fluid Shaft Encoder, paper presented at Second Cranfield Fluidics Conference, Cambridge, England, Paper No. E4 - 1967, NASA N67-21139, January 3-5, 1967.
- A-488. Reason, J., Boiler Control Proves Analog Fluidics, Control Engineering, Volume 14, No. 3, Pages 59-63, March 1967.
- A-489. Reason, J., Fluidic Press Control Tests New Concepts, Control Engineering, Volume 14, No. 4, Pages 74-77, April 1967.
- A-490. Reid, K. N., Jr., An Experimental Study Of The Static Interaction Of An Axisymmetrical Fluid Jet And A Single Receiver-Diffuser, Proceedings of HDL Third Fluid Amplification Symposium, Volume IV, October 1965.
- A-491. Reid, K. N., Jr., Dynamic Interaction Of A Fluid Jet And A Receiver Load System, Proceedings of HDL Third Fluid Amplification Symposium, Volume IV, October 1965.

- A-492. Reilly, R. J., All-Fluid Devices And Their Application To Gas Turbine Controls, Society of Automotive Engineers, Mid-Year Meeting, Chicago, Illinois, Paper No. 65-504 (SAE Paper 650504) IAA-A65-24801, May 17-21, 1965.
- A-493. Reilly, R. J., Fluid System Works: May Be Best Way To Control Gas Turbine Engines, Society of Automotive Engineers Journal, Volume 74, No. 5, Pages 74-82, May 1966.
- A-494. Reilly, R. J. and F. A. Moynihan, Notes On A Proportional Fluid Amplifier, from Fluid Jet Control Devices, ASME Hydraulic and Automatic Control Divisions, Winter Annual Meeting and Symposium New York, N. Y., Pages 51-57, November 28, 1962.
- A-495. Reisener, W. C., Jr., Pure Fluid Analog - Computational Circuit Studies, from Dynamic Performance Analysis of Pure Fluid Amplifiers and Pure Fluid Computational Circuit Studies, NASA N66-35466, NASA N66-35468, Pages 63-105, DDC Report No. AD-634527, Final Report No. F-B2148-1, 1965.
- A-496. Render, A. B., The Design Of Jet-Interaction Amplifiers Using Supercritical Pressure Ratios, presented at Second Cranfield Fluidics Conference, Cambridge, England, Paper No. B7 - 1967, NASA N67-21118, January 3-5, 1967.
- A-497. Republic Aviation Corporation, Research Investigation Of Hydraulic Pulsation Concepts, DDC Report No. AD-607618, prepared for Contract AF-33(657)10622, also AD-600663, October 1964.
- A-498. Retchen, A. W., Flow Stability In Bistable Fluid Elements, paper presented at Second Cranfield Fluidics Conference, Cambridge, England, Paper No. B6 - 1967, NASA N67-21111, January 3-5, 1967.
- A-499. Richards, E. F. and S. D. Graber, Transition To Turbulence And Wall Attachment Of Miniature Jets, Proceedings of HDL Fluid Amplification Symposium, Volume IV, October 1965.
- A-500. Ringwall, C. G., Investigation Of Water And Steam As The Working Fluid In A Fluid Amplifier Speed Governor For Turbine Generator Sets, ONR Report prepared for Contract NONR4001(00)FBM Amendment No. 2.
- A-501. Rivard, J. G. and J. C. Walberer, A Fluid State Vortex Hydraulic Servovalve, paper presented at 21st National Conference on Fluid Power, Chicago, Illinois, October 22, 1965.
- A-502. Roberts, W. J., Experimental Dynamic Response Of Fluid Lines, MS Thesis, Purdue University, 1963.
- A-503. Roffman, Gary, Absolute Pressure Ratio Measurement For Jet Engine Control, R-RCA-63-17, April 29, 1963.

- A-504. Roffman, Gary and Silas Katz, Predicting Closed-Loop Stability Of Fluid Amplifiers From Frequency Response Measurements, Proceedings of HDL Fluid Amplification Symposium, Volume I, October 26-28, 1965.
- A-505. Roffman, G. L., Staging Of Closed Proportional Fluid Amplifiers, Proceedings of HDL Second Fluid Amplification Symposium, Volume III, May 26-28, 1964.
- A-506. Romanenko, P. N., A. I. Lenot'EV and A. N. Oblivin, A Study Of Resistance And Heat Exchange In The Motion Of Heated Air In Diffusers And Mixers, DDC Report No. AD-601244, (Aerospace Technology Division, Library of Congress), 1961.
- A-507. Rose, R. K., Fluid Amplifier Digital Integrator, NASA Report prepared by the General Electric Company for Contract NAS 8-5408, March 1965.
- A-508. Rose, R. K., Fluid Amplifier Digital Integrator, NASA N66-18313, NASA CR-367, March 1966.
- A-509. Rosenbaum, H. M. and J. S. Cant, A Pneumatic Tape Reader, paper presented at Second Cranfield Fluidics Conference, Cambridge, England, Paper No. E2 - 1967, NASA N67-21101, January 3-5, 1967.
- A-510. Rüdle, M. A., H. J. Wiesner and T. H. Stuttgart, Fluid Devices For Machine Controls, paper given at First Conference on Fluid Logic and Amplification, sponsored by the British Hydromechanics Research Association and College of Aeronautics, Cranfield, England, Paper G2 - 1965, NASA N65-36409, September 9-10, 1965.
- A-511. Rupe, Jack H., On The Dynamic Characteristics Of Free-Liquid Jets And A Partial Correlation With Orifice Geometry, Technical Report No. 32-207, Jet Propulsion Laboratory, California Institute of Technology, Pasadena, California, January 15, 1962.
- A-512. Ritherford, D. E., Fluid Dynamics, Book published by Interscience Publishers, Inc., New York, N. Y., 1959.
- A-513. Rytty, M., Pulsation In The Air Intake Systems Of Turbocharged Diesel Engines, The Brown Boveri Review, Volume 52, 1965.
- A-514. Saghafi, H. T., Static Design Of Pneumatic Logic Circuits, Proceedings of HDL Second Fluid Amplification Symposium, Volume II, NASA N64-23818, May 26-28, 1964.
- A-515. Sarpkaya, T., A Bistable Vortex Oscillator, IAA Report No. A-64-12448; also ASME Transactions, Series E Journal of Applied Mechanics, Volume 30, Pages 629-630, December 1963.
- A-516. Sarpkaya, T., Characteristics Of A Vortex Device And The Vortex-Breakdown Phenomenon, Proceedings of HDL Fluid Amplification Symposium, Volume II, October 1965.

- A-517. Sarpkaya, T., A Theoretical And Experimental Investigation Of The Vortex-Sink Angular Rate Sensor, Proceedings of HDL Fluid Amplification Symposium, Volume II, October 1965.
- A-518. Sarpkaya, T., Characteristics Of Counter-Vortex Oscillators, Proceedings of HDL Second Fluid Amplification Symposium, Volume II, May 1964.
- A-519. Sarpkaya, T., Steady And Transient Behavior Of A Bistable Amplifier With A Latching Vortex, Proceedings of HDL Fluid Amplification Symposium, Volume II, October 1965.
- A-520. Savino, Joseph, M. and Edward G. Keshock, Experimental Profiles Of Velocity Components And Radial Pressure Distributions In A Vortex Contained In A Short Cylindrical Chamber, Proceedings of HDL Fluid Amplification Symposium, Volume II, October 1965.
- A-521. Sawyer, R. A., Analysis Of Time Dependent Jet Attachment Processes And Comparison With Experiment, presented at Second Cranfield Fluidics Conference, Cambridge, England, Paper No. A2 - 1967, NASA N67-21278, January 3-5, 1967.
- A-522. Schrader, E. W., Piezoelectric Crystal Signals Fluid Amplifier Switching, Design News, Volume 21, No. 9, Pages 40-41, April 27, 1966.
- A-523. Schroeder, E. F., Experimental Investigation Of The Performance Characteristics Of A Flow-Instability Sensing Device, Proceedings of HDL Third Fluid Amplification Symposium, Volume IV, October 1965.
- A-524. Schuarz, K. W., B. E. Springett, and R. J. Donnelly, Modes Of Instability In Spiral Flow Between Rotating Cylinders, Journal of Fluid Mechanics, Volume 20, Part 2, Pages 281-289, 1964.
- A-525. Scudder, Kenneth R., Instrumentation, DDC Report No. AD-613711, Harry Diamond Labs Report, 1963.
- A-526. Scudder, K. R., Some Special Circuitry, DDC Report No. AD-613712, Harry Diamond Labs Report, 1964.
- A-527. Seubold, J. G., Turbulent Mixing Of A Two-Dimensional Free Jet, Paper No. 65-821 at the AIAA Aerothermochemistry of Turbulent Flows Conference held December 13-15, 1965.
- A-528. Sevcik, M., Pneumatic Digital Optimizing Device, presented at Second Cranfield Fluidics Conference, Cambridge, England, Paper No. K1 - 1967, NASA N67-21116, January 3-5, 1967.
- A-529. Sewell, C. J., Pure Fluid Technology And Possible Ordnance Applications, Report No. NOLTR-64-115, DDC Report No. AD-612503, NASA N65-25783, March 1965.

- A-530. Shapiro, A. H., Investigation On The Boundary Layer In A Corner, DDC Report No. AD-614689, (MIT Report on Contract DA190200RD4538), March 1963.
- A-531. Sharp, R. and M. Bath, Non-Contact Measurement For Machine Tool Control, paper given at First Conference on Fluid Logic and Amplification, sponsored by the British Hydromechanics Research Association and College of Aeronautics, Cranfield, England, September 9-10, 1965.
- A-532. Sharp, R., A Fluidic Absolute Measuring System, paper presented at Second Cranfield Fluidics Conference, Cambridge, England, Paper No. E3 - 1967, NASA N67-21125, January 3-5, 1967.
- A-533. Shatavsky, S. M., Fluidics And Electronics - Analogies And Symbols, EDN, Volume 12, No. 3, Pages 82-83, February 1967.
- A-534. Shearer, J. L., Candid Look At Fluid Control Systems - 1965, 1965 Joint Automatic Control Conference (6th) Rensselaer Polytechnic Institute, Troy, New York, IAA-A65-28815, June 22-25, 1965.
- A-535. Shearer, J. L., Size And Direction Of Jets Issuing From Two-Dimensional Asymmetric Orifices, from Systems and Controls Laboratory, Page 4, NASA N67-16064, NASA N67-16061, Research Report No. RR-4, NASA CR-80923, October 1966.
- A-536. Sheeran, William J. and Darshan S. Dosawjh, Investigations Of Interacting Underexpanded Jet Flows, Proceedings of HDL Fluid Amplification Symposium, Volume I, May 26-28, 1964.
- A-537. Sher, Neil C., Jet Attachment And Switching In Bistable Fluid Amplifiers, ASME Paper No. 64-FE-19 for presentation at Fluids Engineering Conference - Philadelphia, Pennsylvania, May 18-21, 1964.
- A-538. Shinn, J. N. and W. A. Boothe, Connecting Elements Into Circuits And Systems, Control Engineering, Volume 11, No. 9, Pages 86-93, September 1964.
- A-539. Shinn, J. N. and R. A. Raber, Fluid Amplifier Application Studies Phase II Summary Report, NASA Report CR-137 prepared by General Electric Company for Contract NAS 8-5408, August 1964.
- A-540. Shinn, J. N., Fluid Amplifiers Move Fast, Instrument Society of American Preprint No. 22.2-264, New York, N. Y., October 12-15, 1964.
- A-541. Shinn, J. N., Fluid Amplifier State-Of-The-Art, Volume I, NASA Report CR-101 prepared for George C. Marshall Space Flight Center under Contract NAS 8-5408, September 3, 1963.

- A-542. Shinn, J. N., No Moving Parts Needed! Fluid Amplifiers Perform Electronic-Like Functions, based on report to SAE Subcommittee A-6C, Volume 71, No. 8, August 1963.
- A-543. Shinn, J. N., F. A. Underwood and G. J. Hahn, Procedure For Obtaining Fluid Amplifier Reliability Data, NASA Report prepared by General Electric Company for Contract NAS 8-5408, November 1965.
- A-544. Shook, T. A., T. F. Chen and T. Reader, Fluid Amplification 12 Binary Counter Design, DDC Report AD-617699, (UNIVAC Division of Sperry Rand Corporation for Contract DA49 196AMC34X), November 1964.
- A-545. Shvetsova, V. I., Differential Amplifier For Measuring Small Attenuations, USSR Report Pribery 1 · Tekhnika Eksperimento, Volume 9, Pages 90-92, March-April 1964, in Russian, (IAA Report A64-20036).
- A-546. Sickles, W. E., Viscous Mixing Of Two-Dimensional Jets With Particular Reference To Jets In Ground Proximity, DDC Report No. AD-600499 (Frost Engineering Division Report on Contracts DA44-177AMC71T and IDO21701A04814).
- A-547. Simbulan, Vincent, Increasing Fluid Injection Thrust Vector Control Effectiveness, paper presented at SAE-A6 Meeting, September 14-18, 1964.
- A-548. Simson, A. K., Gain Characteristics Of Subsonic Pressure-Controlled Proportional Fluid Jet Amplifiers, ASME Paper 64-WA/AUT-2 for meeting held November 28, to December 3, 1964.
- A-549. Slezenko, Z. F., The Logical Method For Direct Measurement Of The Boundary-Layer Velocity Profile Of A Nonuniformly Heated Flat Plate, DDC Report No. AD-600809 (Unedited rough draft translation of Inzhenerno-Ezicheskii, Zhurnal (USSR) 1962), April 1964.
- A-550. Smith, E. J., Fluidic Interface Valve Controls Pneumatic Operators, Design News, Volume 22, No. 6, Pages 72, 75, March 15, 1967.
- A-551. Smith, Paul D., An Investigation Of Cylindrical Static Pressure Probes, DDC Report No. AD-604829 (Air Force Institute of Technology Wright-Patterson Air Force Base) (Master's Thesis) June 1964.
- A-552. Society of Automotive Engineers, Proceedings Of The Society Of Automotive Engineers, Aerospace Fluid Power Systems And Equipment Conference, IAA-A65-28019, May 18-20, 1965.
- A-553. Spear, R. C., Second Cranfield Fluidics Conference, Report No. ONRL-C-1-67, March 30, 1967.

- A-554. Sperry Utah Company, Salt Lake City, Utah, Analytical Investigation Of Fluid Amplifier Dynamic Characteristics, Volume I, Report No. NASA CR-244, NASA N65-28691, July 1965.
- A-555. Sperry Utah Company, Salt Lake City, Utah, Analytical Investigation Of Fluid Amplifier Dynamic Characteristics, Volume II, Report No. NASA CR-245, NASA N65-28692, July 1965.
- A-556. Spyropoulos, C. E., A Sonic Oscillator, Proceedings of HDL Second Fluid Amplification Symposium, Volume III, May 26-28, 1964.
- A-557. Stal, H. P. and J. Bulk, The Application Of Fluidics In Numerical Control Of Machine Tools, presented at Second Cranfield Fluidics Conference, Paper No. K2 - 1967, NASA N67-21115, January 3-5, 1967.
- A-558. Stalhuth, W. E., Introduction To Fluidics, Automation, Volume 13, No. 10, Pages 106-109, October 1966.
- A-559. Stanford Research Institute, Menlo Park, California, Bibliography, Fluid Amplifiers For Computation And Control, November 1963.
- A-560. Stanford Research Institute, Menlo Park, California, Fluid Amplifiers, a research report (No. 209) by the Long Range Planning Service, April 1964.
- A-561. Stanford Research Institute, Menlo Park, California, Instrumentation For And Experiments On Tactual Perception, Quarterly Report No. 1 - covering the period September 15, to December 15, 1963.
- A-562. Stefanides, E. J., Fluidic Input Controls Air-Piloted Hydraulics, Design News, Volume 21, No. 10, Pages 24-25, May 11, 1966.
- A-563. Stefanides, E. J., Fluid Logic Unit Controls Locomotive Traction, Design News, Volume 21, No. 6, Pages 30-31, March 16, 1966.
- A-564. Steiner, L. A., Fluid Logic And Control Devices, The Engineer, Volume 220, Pages 330-333, August 27, 1965.
- A-565. Steiner, L. A., Understanding Fluid Amplifiers, Instrument and Control Engineering, July 1965.
- A-566. Steptoe, B. J., Steady-State And Dynamic Characteristic Variations In Digital Wall-Attachment Devices, paper presented at Second Cranfield Fluidics Conference, Paper No. Be, NASA N67-21136, January 3-5, 1967.
- A-567. Stiffler, A. K., Characteristics Of Pressure Controlled Fluid Jet Amplifiers, from Systems and Controls Laboratory, NASA N67-16070, NASA N67-16061, Research Report No. RR-4, NASA CR-80923, October 1966.

- A-568. Strandrud, H. T., Electric-Field Valves Inside Cylinder Control Vibrator, Hydraulics and Pneumatics, Volume 19, No. 9, Pages 139-143, September 1966.
- A-569. Straub, H. H. and J. Meyer, An Evaluation Of A Fluid Amplifier, Face Mask Respirator, Proceedings of HDL Third Fluid Amplification Symposium, Volume III, October 1965.
- A-570. Straub, H. H., Fluid Amplifier Helps Patients Breathe, Control Engineering, Page 120, April 1965.
- A-571. Streeter, V. L., Handbook Of Fluid Dynamics, Section 20: Fluid Transients in Engineering Systems, book published by McGraw-Hill Book Company, Inc., New York, N. Y., 1961.
- A-572. Sulich, J. S., Investigation Of Fluid State Devices For Instrumentation And Computation Of Air Data (FLICA), Final Report No. RLD-3419, AFFDL-TR-66-133, DDC Report No. AD-810265, NASA X67-17992, December 1966.
- A-573. Swartz, E. L., A Fluoric Induction And Gate, Proceedings of HDL Third Fluid Amplification Symposium, Volume IV, October 1965.
- A-574. Taft, C. K., A Fluid Encoding System, Proceedings of HDL Second Fluid Amplification Symposium, Volume II, May 26-28, 1964.
- A-575. Taft, C. K. and R. O. Turnquist, A Fluid State Digital To Analog Converter, Proceedings of HDL Third Fluid Amplification Symposium, Volume III, October 1965.
- A-576. Taft, C. K. and D. W. McGlaughlin, Fluidic Electrofluid Converter, Transactions of ASME, Journal of Basic Engineering, Series D, Volume 89, No. 2, Pages 334-340, June 1967.
- A-577. Taft, C. K., Fluidic Digital Servo Controls Speed-Position With Pulsed Air, Control Engineering, Volume 12, No. 12, Pages 49-53, December 1965.
- A-578. Taft, C. K. and P. E. Koerper, Fluid State Power Amplifier Design, paper presented at 21st National Conference on Fluid Power, Chicago, Illinois, October 22, 1965.
- A-579. Taft, C. K., Impact Of Fluid Amplifiers On Design Of Metal Working Machines, ASME Publication 65-MD-43, June 1965.
- A-580. Tamulis, J. C., Signal Noise In Pure Fluid Amplifiers, NASA CR-62882 (Pennsylvania State University Report NGR-39-009-023, April 1965).
- A-581. Tanney, J. W., Development In Pure Fluid Systems Components And Control Devices (Part I). Reprint of article from DME/NAE Quarterly Bulletin No. A64-20777, April 1964.

- A-582. Tanney, J. W., Development In Pure Fluid Systems Components And Control Devices (Part II). Reprint of article from DME/NAE Quarterly Bulletin No. 1964 (2), A64-26011, June 1964.
- A-583. Taplin, L. B., Synthesis Of Fluidic Flight Control System, Final Report No. RLD-3340, AFFDL-TR-66-184, DDC Report No. AD-804603, NASA X67-14407, November 1966.
- A-584. Timma, E., Analytic Investigation Of Turbulent Flat Jet, Developing In A Co-Stream, DDC Report No. AD-609150 (Foreign Tech. Div. Air Force Systems Command WPAFB). (Unedited rough draft translation of Akademiya, Nauk Estonskoi SSR. Tallinn. Izvestiya, Seriya Fiziko-Matematicheskikh, I Tekhnicheskikh Nauk, Volume 12, No. 1, Pages 57-74).
- A-585. Thomas, J., Fluidics Make Fluidics, Control Engineering, Volume 14, No. 2, Page 96, February 1967.
- A-586. Thomson, A. and M. J. Fisher, The Application Of Fluidics To The Detection Of Burst Fuel Elements In Nuclear Reactors, paper presented at Second Cranfield Fluidics Conference, Cambridge, England, Paper No. K5 - 1967, NASA N67-21130, January 3-5, 1967.
- A-587. Thompson, R. V., The Switching Of Supersonic Gas Jets By Atmospheric Venting, paper presented at Second Cranfield Fluidics Conference, Cambridge, England, Paper No. A5 - 1967, NASA N67-21121, January 3-5-, 1967.
- A-588. Toepfer, H., D. Schrepel and A. Schwarz, Universal Assembly Of Prefabricated Machine Parts For Pneumatic Guidance Control, DDC Report No. AD-608461 (Foreign Tech. Div. Air Force Systems Command WPAFB). (Unedited rough draft translation of Messin - Steuern - Regln, East Germany, 1963).
- A-589. Togino, K. and K. Inoue, Universal Fluid Logic Element, Control Engineering, May 1965.
- A-590. Tomek, R. E., Thermal Switching Of Fluidic Elements, NASA N67-16064, Page 4, from Systems and Controls Laboratory, NASA N67-16061, Research Report No. RR-4, NASA CR-80923, October 1966.
- A-591. Töpfer, H., Pneumatic Logic Elements And Appropriate Peripheral Equipment, Paper No. 1.3 presented at IFAC/IFIP Symposium on Microminiaturization in Automatic Control Equipment and in Digital Computers, held in Munich, Germany, October 21-23, 1965.
- A-592. Trapani, R. D., Fluerics - 22: An Experimental Study Of Bounded And Confined Jets, DDC Report No. AD-644737, NASA N67-20648, November 1966.

- A-593. Tsui, K. C. and J. Stone, Dynamic Performance Analysis of Pure Fluid Amplifiers And Pure Fluid Computational Circuit Studies, Final Report No. F-B2148-1, 1965, DDC Report No. AD-634527, NASA N66-35466, January 1966.
- A-594. Turnquist, R. A., Fluerics (Fluid Amplification), 18, A Fluid-State Digital Control System, DDC Report No. AD-633689, February 2, 1966.
- A-595. Unfried, H. H., An Approach To Broad Band Fluid Amplification At Acoustic Frequencies, Proceedings of HDL Fluid Amplification Symposium, Volume I, October 26-28, 1965.
- A-596. Unfried, H. H., Experiment And Theory Of Acoustically Controlled Fluid Switches, Proceedings of HDL Fluid Amplification Symposium, Volume II, October 1965.
- A-597. USSR, Pure Fluid Control Devices And The Design Of Printed Pneumatic Circuits, Publication OTS: 63-31761, U. S. Department of Commerce, Office of Technical Services, Joint Publications Research Service, Washington, D. C.
- A-598. Van Tilburg, R. W., Area Experience In Moderate Volume Fabrication Of Pure Fluid Devices, Proceedings of HDL Third Fluid Amplification Symposium, Volume III, October 1965.
- A-599. Van Tilburg, R. W., Application Of Optical Fabrication Techniques To The Fabrication And Development Of Fluid Amplifiers And Fluid Circuits, 1 April 1962 - 31 May 1965, DDC Report No. AD-624773, NASA N66-17043, October 29, 1965.
- A-600. Van Tilburg, R. W., Application Of Optical Fabrication Techniques To The Fabrication And Development Of Fluid Amplifiers, DDC Report No. AD-610586, (Corning Glass Progress Report for period ending October 3, 1963).
- A-601. Van Tilburg, R. W., Fluerics: 21, Optical Fabrication Of Fluid Amplifiers And Circuits, DDC Report No. AD-636842, May 1966.
- A-602. Van Tilburg, R. W. and W. L. Cochran, Development Of A Proportional Fluid Amplifier For Multi-Stage Operation, Proceedings of HDL Second Fluid Amplification Symposium, Volume II, May 26-28, 1964.
- A-603. Velkoff, H. R. and J. Bishop, A Study Of A Corona Wind Digital Fluid Amplifier Element, Technical Report No. TR-3, AROD 4942:3-E, DDC Report No. AD-651166, March 1967.
- A-604. Verheist, H. A. M., On The Design, Characteristics And Production Of Turbulence Amplifiers, paper presented at Second Cranfield Fluidics Conference, Paper No. F2 - 1967, NASA N67-21106, January 3-5, 1967.

- A-605. Victory, E. L., Analysis Of Thrust And Flow Augmentation Of A Coanda Nozzle, DDC Report No. AD-617621 (Huyck Research Center, Stanford, Connecticut, Final Report).
- A-606. Vos, C. E., Design, Fabrication And Test Of A Flueric Servovalve, Quarterly Report March 28 - June 28, 1966. Report No. BRLD-3542, NASA CR-72102, NASA N67-13186, June 28, 1966.
- A-607. Vulis, L. A., Turbulent Heat And Mass Transfer In Jet Motion Of A Gas, DDC Report No. AD-605863 (Foreign Tech. Div. Air Force Systems Command WPAFB), edited Machine Trans. of Mono Voprosky Aerodinamiki.
- A-608. Walker, G. K. and B. A. Schumann, A Discussion Of Ness's Analysis For A Turbulent Boundary Layer With Mass Addition, DDC Report No. AD-600627 (General Electric Company MSD Report R61SD49) Contract AF04(647)715, 1961.
- A-609. Walker, G. K. and B. A. Schumann, The Growth Of Turbulent Boundary Layer, DDC Report No. AD-601503 (General Electric Company MSD Report for Contract AF04(645)24, July 1964).
- A-610. Walston, William H., Jr., Transient Response Of A Fluid Line With And Without Bleeds, Proceedings of HDL Fluid Amplification Symposium, Volume II, October 1965.
- A-611. Warren, R. W., Fluid Logic Elements, DDC Report No. AD-613710, Harry Diamond Laboratories, 1964.
- A-612. Warren, R. W., Interconnection Of Fluid Amplification Elements, Proceedings of HDL Second Fluid Amplification Symposium, Volume III, May 26-28, 1964.
- A-613. Warren, R. W., Some Parameters Affecting The Design Of Bistable Fluid Amplifiers, from Fluid Jet Control Devices (ASME Hydraulic and Automatic Control Divisions, Winter Annual Meeting and Symposium, New York, N. Y., Pages 75-82, November 28, 1962.
- A-614. Weinger, S. D., The Effect Of Sound On A Reattaching Jet At Low Reynolds Numbers, Proceedings of HDL Third Fluid Amplification Symposium, Volume IV, October 1965.
- A-615. Weinger, S. D., The Effect Of Sound On The Attachment Of A Jet To An Offset Wall, Harry Diamond Labs - Internal Report R-RCA-6417, August 24, 1964.
- A-616. Weske, J. R. and T. M. Rankin, On The Generation Of Secondary Motions In The Field Of A Vortex, University of Maryland, Technical Note BN-313 dated March 1963.
- A-617. Westerman, W. J., Jr. Mechanically Entrained Fluidic Oscillator, Proceedings of HDL Third Fluid Amplification Symposium, Volume IV, October 1965.

- A-618. Westerman, William J., Jr., The Effect Of Geometric Parameters On The Stability Margin And Switching Characteristics Of Pure Fluid Bistable Elements, Paper - Martin Company, Orlando, Florida.
- A-619. Wetheral, T. G. and J. L. Byrd, Development Of A Pure-Fluid Missile Control System, U. S. Army Missile Command Report No. RG-TR-64-18, December 1964.
- A-620. Wetheral, T. G. and L. C. Atha, Flueric Controls, A Description Of Available Components And Current Applications, ASME Paper No. 65-WA/AUT-21 presented at the Winter Annual Meeting, Chicago, Illinois, November 7-11, 1965.
- A-621. What's In Store For Fluid Amplifiers?, Chemical Engineering, Volume 74, No. 10, Pages 94, 96, 98, May 8, 1967.
- A-622. Wheatley, D. E., Fluidics - A New Technology, Aircraft Engineering, Volume 39, No. 8, Pages 26-30, August 1967.
- A-623. Where's The Profit In Fluid Amplifiers?, Control Engineering, Volume 12, No. 7, Pages 57, 59, December 1965.
- A-624. White, Harry N., Analysis Of The Steady-Flow Pneumatic Resistance Of Parallel Capillaries, Proceedings of HDL Fluid Amplification Symposium, Volume I, October 26-28, 1965.
- A-625. White, H. N., Flueric Pressure Regulation Using A Resistance Set Point, Proceedings of HDL Third Fluid Amplification Symposium, Volume IV, October 1965.
- A-626. Wille, R., Contributions To The Phenomenology Of Free Jets, translated from Zeitscheift für Flugwissenschaften, Volume 11, No. 6, Pages 222-233, June 1963.
- A-627. Williams, J. C., III and F. O. Smetana, Theoretical Study Of A Convergent Nozzle And Free Jet Flow, Proceedings of HDL Fluid Amplification Symposium, Volume I, October 26-28, 1965.
- A-628. Williams, J. E., Reynolds Stress Near A Flexible Surface Responding To Unsteady Air Flow, DDC Report No. AD-601041 (Bolt Beranek and Newman Inc., Cambridge, Massachusetts) Contract NONR394400, June 1964.
- A-629. Wilson, James N., Fluid Amplification: 13, Fluid Analog To Digital Conversion System, DDC Report No. AD-613704 (Case Institute of Technology Report For Contract DA49 186AMC79D), December 1964.
- A-630. Wood, D. E., E. L. Rivest and G. C. Dodson, Signal Processing And Waveform Pattern Recognition For - Analysis Of Signal Origins, Instrumentation And Automation, General Electric TIS Report 65-C-041, September 14, 1965.

- A-631. Wood, O. Lew, Design Guide Pure Fluid Devices, Machine Design, Volume 37, No. 15, Pages 153-180, June 1965.
- A-632. Wood, O. Lew, High-Speed Fluid Amplifier, Machine Design, Volume 37, No. 5, Pages 119-123, March 4, 1965.
- A-633. Wood, O. Lew, Fluidic Devices, Machine Design, Volume 38, No. 22, Pages 108-116, September 22, 1966.
- A-634. Wood, O. Lew, Dithering Jet Overcomes Stiction In A High-Speed Fluid Amplifier, Machine Design, Volume 37, Pages 119-123, March 4, 1965.
- A-635. Woodward, Kenneth, George Mon, James Joyce and Henry Straub, Four Fluid Amplifier Controlled Medical Devices, Proceedings of HDL Second Fluid Amplification Symposium, Volume IV, May 26-28, 1964.
- A-636. Yeaple, F., Analog Fluid Amplifiers Are Waiting In The Wings, Product Engineering, Volume 38, No. 22, Pages 52-54, August 1967.
- A-637. Yeaple, F., Indian-Bead Fluidics Displays And Holds Answers, Product Engineering, Volume 37, No. 23, Pages 38-39, November 7, 1966.
- A-638. Yeaple, F., Pneumatic Amplifiers Boost Low-Pressure Fluidics, Product Engineering, Volume 37, No. 16, Pages 52-54, August 1966.
- A-639. Young, J., Tomorrow's Controls-Fluid Amplifiers Can Oust Electronics, Design Engineering, Volume 10, No. 12, Pages 26-29, December 1964.
- A-640. Young, J.E.R., Fluid Control Device, IBM Technical Disclosure Bulletin, Volume 6, Page 23, August 1963.
- A-641. Zalmanzon, L., Pneumatic Computing And Control Devices, IAA Report A64-16959, (also Academy of Sciences, Institute of Automatics and Telemechanics, MOSCOW, USSR/Engineering Materials and Design, Volume 7, Pages 228-232, - IAA Report No. A64-16957, April 1964.
- A-642. Zappanti, Anthony J., Gas Separation In A Vortex, DDC Report No. AD-604832 (Air Force Institute of Technology, Wright-Patterson AFB) Master's Thesis, May 1964.
- A-643. Zisfein, M. B. and H. A. Curtiss, A High Gain Proportional Fluid State Flow Amplifier, Proceedings of HDL Fluid Amplification Symposium, Volume I, May 26-28, 1964.
- A-644. Zisfein, M. B., The Application Of Fluid State Devices To Process Control Computation, ASME Paper No. 65-WA/PID-11 presented at the Winter Annual Meeting, Chicago, Illinois, November 7-11, 1965.
- A-645. Zumwalt, G. W. and W. F. Walker, The Analysis Of Submerged Jet Flow Fields By A Numerical Field Computation Method, Proceedings of HDL Third Fluid Amplification Symposium, Volume IV, October 1965.

APPENDIX III-B

FLUIDIC PATENT BIBLIOGRAPHY

- B-1. Adams, L. R. and B. J. Greenblott, Fluid Control Apparatus, No. 3168897, dated February 9, 1965, filed December 22, 1961, assigned to International Business Machines Corporation.
- B-2. Adams, R. B., Control Apparatus, No. 3187763, dated June 8, 1965, filed December 17, 1962, assigned to Moore Products Co.
- B-3. Adams, R. B. and C. B. Moore, Flow Control Apparatus, No. 3262466, dated July 26, 1966, filed July 29, 1963, assigned to Moore Products Co.
- B-4. Adams, R. B. and C. B. Moore, Flow Control Apparatus, No. 3267946, dated August 23, 1966, filed April 12, 1963, assigned to Moore Products Co.
- B-5. Adams, R. B. and C. B. Moore, Jet Propelled Boat Steering Apparatus, No. 3247667, dated April 26, 1966, filed September 23, 1963, assigned to Moore Products Co.
- B-6. Adams, R. B., Level Control Apparatus, No. 3267949, dated August 23, 1966, filed March 2, 1964, assigned to Moore Products Co.
- B-7. Adams, R. B., Transducers, No. 3173437, dated March 16, 1965, filed September 22, 1961, assigned to Moore Products Co.
- B-8. Ahern, C. J., Fluidic Flip Flop Devices, No. 3348773, dated October 24, 1967, filed February 10, 1966, assigned to The Bendix Corporation.
- B-9. Allen, C. W. and H. A. Knight, Electro-Pneumatic Translator, No. 3072147, dated January 8, 1963, filed September 29, 1961, assigned to Westinghouse Air Brake Company.
- B-10. Auger, R. N., Fluid Amplifiers, No. 3234955, dated February 15, 1966, filed October 1, 1962.
- B-11. Avery, H. W., Fluid Amplifier Shift Register Circuit, No. 3350008, dated October 31, 1967, filed March 28, 1966, assigned to General Electric Company.
- B-12. Babcock & Wilcox Limited and C. Davy, Method of and Means For Controlling The Flow of a Gaseous Fluid in a Conduit, Duct or the Like, No. 444103, dated January 1936.
- B-13. Bailey, W. R., Fluid Valve Device, No. 3244189, dated April 5, 1966, filed October 4, 1963, assigned to Feedback Systems, Inc.
- B-14. Baldwin, H. A., Fluid Amplifier Systems, No. 3078675, dated February 26, 1963, filed November 2, 1961, assigned to Arizona Research Foundation, Inc.

- B-15. Bauer, P. and E. D. Proctor, Recording Apparatus for Fluid Systems, No. 3267481, dated August 16, 1966, filed March 12, 1964, assigned to Bowles Engineering Corporation.
- B-16. Bauer, P., J. R. Colston and E. U. Sowers III, Presettable Decoder, No. 3339569, dated September 5, 1967, filed May 8, 1964, assigned to Sperry Rand Corporation.
- B-17. Bauer, P., Pressure Band Detector, No. 3340885, dated September 12, 1966, filed May 26, 1964, assigned to Bowles Engineering Corporation.
- B-18. Bauer, P., Pure Fluid Adder, No. 3286082, dated January 17, 1967, filed October 18, 1962, assigned to Sperry Rand Corporation.
- B-19. Bauer, P., Fluid Data Comparator, No. 3299255, dated January 17, 1967, filed October 18, 1962, assigned to Sperry Rand Corporation.
- B-20. Bauer, P. and J. P. Morton, Timing Mechanism, No. 3318523, dated May 9, 1967, filed October 2, 1964, assigned to International Business Machines Corporation.
- B-21. Bauer, P., Fluid Pulse Attenuator, No. 3319659, dated May 16, 1967, filed December 13, 1964, assigned to Sperry Rand Corporation.
- B-22. Bauer, P., Fluid Channel Divider, No. 3282297, dated November 1, 1966, filed July 30, 1964, assigned to Sperry Rand Corporation.
- B-23. Bauer, P., Fluid Multi-Stable Device, No. 3192938, dated July 16, 1965, filed September 5, 1961, assigned to Sperry Rand Corporation.
- B-24. Bauer, P., Fluid Device, No. 3247861, dated April 26, 1966, filed November 20, 1963, assigned to Sperry Rand Corporation.
- B-25. Bauer, P., Fluid Flip-Flop, No. 3246661, dated April 19, 1966, filed October 1, 1963, assigned to Sperry Rand Corporation.
- B-26. Bauer, P., Binary Counter, No. 3182676, dated May 11, 1965, filed April 23, 1962, assigned to Sperry Rand Corporation.
- B-27. Bauer, P., Binary Counter Stages Having Two Fluid Vortex Amplifiers, No. 3193197, dated July 6, 1965, filed April 23, 1962, assigned to Sperry Rand Corporation.
- B-28. Bauer, P., Binary Counter, No. 3219271, dated November 23, 1965, filed November 20, 1963, assigned to Sperry Rand Corporation.
- B-29. Bauer, P., Fluid Pulse Former, No. 3266509, dated August 16, 1966, filed August 26, 1963, assigned to Sperry Rand Corporation.
- B-30. Bauer, P., Fluid Signal Generator, No. 3204652, dated September 7, 1965, filed December 28, 1961, assigned to Sperry Rand Corporation.

- B-31. Bauer, P. and E. U. Sowers III, Fluid Sorter, No. 3169639, dated February 16, 1965, filed August 7, 1963, assigned to Sperry Rand Corporation.
- B-32. Bauer, P., Fluid Vortex Flip-Flop, No. 3258024, dated June 28, 1966, filed February 18, 1964, assigned to Sperry Rand Corporation.
- B-33. Bauer, P., "And" Gate, No. 3191611, dated June 29, 1965, filed January 25, 1963, assigned to Sperry Rand Corporation.
- B-34. Beattie, H. S. and W. F. Voit, Jr., Deserializer and Transducer Therefor, No. 3276690, dated October 4, 1966, filed January 5, 1965, assigned to International Business Machines Corporation.
- B-35. Belsterling, C. A. and R. L. Colcord, Accelerometer Apparatus, No. 3310985, dated March 28, 1967, filed April 7, 1964, assigned to the Franklin Institute.
- B-36. Bjornsen, B. G., T. J. Lechner, Jr. and P. H. Sorenson, Pure Fluid Integrator, No. 3294319, dated December 27, 1966, filed November 30, 1964, assigned to Johnson Service Company.
- B-37. Bjornsen, B. G., Fluid Stream Control Apparatus, No. 3334641, dated August 8, 1967, filed June 25, 1964, assigned to Johnson Service Company.
- B-38. Bjornsen, B. G. and T. J. Lechner, Input Fluid Control Apparatus, No. 3285263, dated November 15, 1966, filed November 1, 1963, assigned to Johnson Service Company.
- B-39. Bjornsen, B. G. and T. J. Lechner, Fluid Control Apparatus, No. 3272215, dated September 13, 1966, filed November 1, 1963, assigned to Johnson Service Company.
- B-40. Blazek, H., Pneumatic Attitude Sensor, No. 3311987, dated April 4, 1967, filed May 19, 1965, assigned to Sperry Rand Corporation.
- B-41. Bliss, D. S. and J. T. Everest, Control of Fluid Curtain Flow in Air Cushion Vehicles, No. 3172495, dated March 9, 1965, filed December 28, 1962, assigned to Hovercraft Development Limited.
- B-42. Blume, W. E., Arrangement for Counting Pieces of Cloth, No. 3327942, dated June 27, 1967, filed October 12, 1965.
- B-43. Bodine, A. G., Oscillatory Fluid Stream Driven Sonic Generator with Elastic Autoresonator, No. 3111931, dated November 26, 1963, filed March 31, 1960.
- B-44. Boothe, W. A. and B. J. Czwakiel, Fluid Amplifier Devices, No. 3285265, dated November 15, 1966, filed April 17, 1964, assigned to General Electric Company.

- B-45. Boothe, W. A., Fluid-Operated Detectors, No. 3285264, dated November 15, 1966, filed March 31, 1964, assigned to General Electric Company.
- B-46. Boothe, W. A., Fluid-Operated Error Sensing Circuit, No. 3260456, dated July 12, 1966, filed September 23, 1964, assigned to General Electric Company.
- B-47. Boothe, W. A., Fluid Control Devices, No. 3181546, dated May 4, 1965, filed November 8, 1962, assigned to General Electric Company.
- B-48. Boothe, W. A., Fluid Amplifier, No. 3233622, dated February 8, 1966, filed September 30, 1963, assigned to General Electric Company.
- B-49. Boothe, W. A., Pure Fluid Logic Circuitry for Integrators and Differentiators, No. 3155825, dated November 3, 1964, filed February 21, 1963, assigned to General Electric Company.
- B-50. Boothe, W. A., Fluid-Operated Logic Circuit, No. 3232533, dated February 1, 1966, filed August 3, 1964, assigned to General Electric Company.
- B-51. Boothe, W. A., Fluid-Operated Error Detecting and Indicating Circuit, No. 3288602, dated January 11, 1966, filed May 28, 1964, assigned to General Electric Company.
- B-52. Boothe, W. A., Fluid Amplifier, No. 3186422, dated June 1, 1965, filed December 31, 1962, assigned to General Electric Company.
- B-53. Bottone, Jr., S., Constant Frequency Fluid-Mechanical Oscillator, No. 3333596, dated August 1, 1967, filed February 12, 1964, assigned to General Electric Company.
- B-54. Bowles, R. E., Pressure Sensing and Measuring Device, No. 3263501, dated August 2, 1966, filed January 9, 1964.
- B-55. Bowles, R. E., Weighted Comparator, No. 3331379, dated July 18, 1967, filed May 31, 1963, assigned to the United States of America.
- B-56. Bowles, R. E., Fluid-Operated Accelerometer, No. 3324730, dated June 13, 1967, filed July 31, 1964, assigned to Bowles Engineering Company.
- B-57. Bowles, R. E., Thruster Apparatus for Craft, No. 3259096, dated July 5, 1966, filed March 10, 1964, assigned to Bowles Engineering Corporation.
- B-58. Bowles, R. E., Visual Readout Device, No. 3249302, dated May 3, 1966, filed January 21, 1963.
- B-59. Bowles, R. E., Pneumatic Eye, No. 3258023, dated June 28, 1966, filed April 12, 1963.

- B-60. Bowles, R. E. and B. M. Horton, Fluid Amplifier, No. 3276259, dated October 4, 1966, filed August 11, 1960.
- B-61. Bowles, R. E., Binary Stage, No. 3223101, dated December 14, 1965, filed May 28, 1963, assigned to the United States of America.
- B-62. Bowles, R. E., Differentiator Comparator, No. 3238959, dated March 8, 1966, filed May 31, 1963, assigned to the United States of America.
- B-63. Bowles, R. E., Passive Pure Fluid Component, No. 3191623, dated June 29, 1965, filed February 21, 1963.
- B-64. Bowles, R. E., Vortex Integrator, No. 3343790, dated September 26, 1967, filed August 16, 1965, assigned to Bowles Engineering Corporation.
- B-65. Bowles, R. E., Pure Fluid Comparator, No. 327212, dated September 13, 1966, filed May 31, 1963, assigned to the United States of America.
- B-66. Bowles, R. E., Fluid Control Systems for Foils, No. 3209714, dated October 5, 1965, filed October 14, 1963.
- B-67. Bowles, R. E. and B. M. Horton, Fluid Oscillator, No. 3185166, dated May 25, 1965, filed April 8, 1960.
- B-68. Bowles, R. E. and R. W. Warren, Perfectionnement Aux Systemes Actionnes Par Un Fluide, No. 127882, dated November 23, 1960.
- B-69. Bowles, R. E. and R. W. Warren, Three Dimensional Jet Vectoring System, No. 320405, dated September 7, 1965, filed February 20, 1964.
- B-70. Bowditch, H. L., Balancing Apparatus for Computers and the Like, No. 3325098, dated June 13, 1967, filed July 2, 1965, assigned to The Foxboro Company.
- B-71. Brooks, J. D., Helical Fluid Signal to Pressure Signal Converter, No. 3336932, dated August 22, 1967, filed October 11, 1965, assigned to the United States of America.
- B-72. Brooks, J. D., Signal Summing Point Device for Hybrid Fluid and Electronic Controls, No. 3266514, dated August 16, 1966, filed April 20, 1964, assigned to the United States of America.
- B-73. Burns, H. L., Cycling Valve, No. 3280832, dated October 25, 1966, filed November 18, 1963, assigned to Retec, Inc.
- B-74. Buratti, G., Analog-Digital Converter Operating with Fluid Dynamics Signals, No. 3279679, dated October 18, 1966, filed December 11, 1964.

- B-75. Caldwell, F. J., R. D. Joyce and C. L. Coleman, Calculating Machines, No. 3311300, dated March 28, 1967, filed July 22, 1964, assigned to The National Cash Register Company.
- B-76. Campagnuolo, C. J., Fluid Jet Momentum Comparator, No. 3323532, dated June 6, 1967, filed February 23, 1965, assigned to the United States of America.
- B-77. Cargill, N. A. and T. D. Reader, Electro-Pneumatic Fluid Amplifier, No. 3071154, dated January 1, 1963, filed October 25, 1960, assigned to Sperry Rand Corporation.
- B-78. Cargill, N. A. and R. D. Reader, Electro-Sonic Fluid Amplifier, No. 3144037, dated August 11, 1964, filed February 16, 1961, assigned to Sperry Rand Corporation.
- B-79. Carlson, Jr., W. L., Cylindrical Fluid Amplifier, No. 3039490, dated June 19, 1962, filed May 11, 1961, assigned to Minneapolis-Honeywell Regulator Company.
- B-80. Chabrier, H. and A. Saint-Joanis, Fluid Actuated Logical Devices, No. 3311301, dated March 28, 1967, filed April 29, 1963, assigned to Societe d'Electrochimie, d'Electro-metallurgie.
- B-81. Chabrier, H. P. and A. Saint-Joanis, Alarm System, No. 3348772, dated October 24, 1967, filed January 2, 1964.
- B-82. Chapin, D. W. and D. H. Fischer, Servo-Actuating Mechanism for Pneumatic Analog Computers, No. 3316815, dated May 2, 1967, filed December 4, 1961, assigned to the Garrett Corporation.
- B-83. Chisel, D. M., Thrust Vector Control, No. 3239150, dated March 8, 1966, filed November 29, 1961, assigned to Continental Aviation and Engineering Corporation.
- B-84. Colston, J. R., Pure Fluid Function Generating System, No. 3250469, dated May 10, 1966, filed August 5, 1963, assigned to Bowles Engineering Corporation.
- B-85. Colston, J. R., Turbine Speed Control, No. 3292648, dated December 20, 1966, filed July 5, 1963, assigned to Bowles Engineering Corporation.
- B-86. Colston, J. R., Temperature Measuring System, No. 3314294, dated April 18, 1967, filed October 4, 1963, assigned to Bowles Engineering Corporation.
- B-87. Colston, J. R., Fluid Pulse Converter, No. 3244370, dated April 5, 1966, filed January 18, 1963, assigned to Bowles Engineering Corporation.

- B-88. Colston, J. R., Pure Fluid Function Generating System, No. 3250469, dated May 10, 1966, filed August 5, 1963, assigned to Bowles Engineering Corporation.
- B-89. Comparin, R. A., Pneumatic Switch, No. 3139895, dated July 7, 1964, filed November 29, 1961, assigned to International Business Machines Company.
- B-90. Connaught, P. M., Pneumatic Thyratrons, No. 3150674, dated September 29, 1964, filed December 28, 1961, assigned to Robertshaw Controls Company.
- B-91. Cooper, F. D., Solids Flow System, No. 3124170, dated March 10, 1964, filed February 27, 1959, assigned to Bituminous Coal Research, Inc.
- B-92. Datwyler, W. F., Fluid Device, No. 3351080, dated November 7, 1967, filed June 24, 1965, assigned to The Bendix Corporation.
- B-93. Davy, C. H., Method of and Means for Superheat Control, No. 2213121, dated August 27, 1940, filed November 11, 1936, assigned to The Babcock and Wilcox Company.
- B-94. Detlefsen, G. C., Diverter Valve, No. 2624364, dated January 6, 1953, filed November 17, 1950, assigned to Crane Co.
- B-95. Dexter, E. M., Fluid Control Device, No. 3338515, dated August 29, 1967, filed April 29, 1964, assigned to General Electric Company.
- B-96. Dexter, E. M. and D. Roland, Rotational-To-Linear Flow Converter, No. 3256899, dated June 21, 1966, filed November 26, 1962, assigned to Bowles Engineering Corporation.
- B-97. Dexter, E. M., Bias Device for Pure Fluid Amplifier, No. 3209775, dated October 5, 1965, filed December 7, 1962, assigned to Bowles Engineering Corporation.
- B-98. Dexter, E. M. and D. R. Jones, Fluid Logic Components, No. 3240219, dated March 15, 1966, filed November 26, 1962, assigned to Bowles Engineering Corporation.
- B-99. Dockery, R. J., Fluid Logic Element, No. 3277915, dated October 11, 1966, filed April 16, 1964, assigned to the United States of America.

- B-100. Duff, B. E., Fluid Flow Control Stage, No. 3180346, dated April 27, filed January 7, 1963, assigned to Midwestern Instruments, Inc.
- B-101. Dunaway, J. C., Actuator For Pure Fluid Amplifier, No. 3289678, dated December 6, 1966, filed February 13, 1964, assigned to the United States of America.
- B-102. Eckert, Jr., A. B. and B. Lyman, Pneumatic Record Sensing Apparatus, No. 3302004, dated January 31, 1967, filed September 5, 1962, assigned to Pitney-Bowes, Inc.
- B-103. Eggers, G., and G. Ernst, Device for Controlling the Jet of a Reaction Propulsion Motor, No. 3020714, dated February 13, 1962, filed June 27, 1957, assigned to Societe National d'Etude et de Construction de Moteurs d'Aviation.
- B-104. Eggers, G. and G. Ernst, Jet Control Apparatus, No. 3036430, dated May 29, 1962, filed June 16, 1959.
- B-105. Eige, J. J., Pneumatic Operational Amplifier System, No. 3266380, dated August 16, 1966, filed November 26, 1963, assigned to Stanford Research Institute.
- B-106. Eige, J. J., Fluid Logic Structures, No. 3319885, dated May 16, 1967, filed May 31, 1963, assigned to Stanford Research Institute.
- B-107. Engholdt, R. K., Injector Pump, No. 3022743, dated February 27, 1962, filed June 19, 1959, assigned to Erie Manufacturing Company.
- B-108. Ernst, A. O. G., J. P. J. Jardinier, and J. Rona, Aerodynamic or Hydrodynamic Servovalve, Especially for Use For the Guidance and Stabilization of Rockets, No. 3285262, dated November 15, 1966, filed August 2, 1963.
- B-109. Etter, T. L., Fluid Pressure Digital Computer, No. 3057511, dated October 9, 1962, filed February 19, 1957, assigned to TRG Incorporated.
- B-110. Evans, R. A., Control Apparatus, No. 3171422, dated March 2, 1965, filed July 10, 1962, assigned to Honeywell Inc.
- B-111. Evans, K. C., Pure Fluid Amplifier and Pure Fluid Amplifier Attitude Control System for Missiles, No. 3278140, dated October 11, 1966, filed February 13, 1964, assigned to the United States of America.
- B-112. Everett, W. S. and J. F. Richards, Fluid Pulsation Dampener, No. 3137316, dated June 16, 1964, filed May 17, 1962.

- B-113. Falconer, D. G., Valves and Fluid Amplifiers, No. 3147668, dated September 8, 1964, filed November 10, 1960.
- B-114. Falconer, D. G., Fluid Sealing Device and Analogue Computer Components, No. 3254837, dated June 7, 1966, filed March 5, 1964.
- B-115. Fedoseev, R. J., Comparators of Pneumatic Analog Signals, No. 3292853, dated December 20, 1966, filed October 16, 1964, assigned to Nauchno-Issledovateijsky Institute Teploenergeticheskogo Priborostroenija.
- B-116. Fox, H. L., G. H. Thorne, Sr., and O. L. Wood, Fluid Logic Vortex Apparatus, No. 3336931, dated August 22, 1967, filed September 16, 1964, assigned to Sperry Rand Corporation.
- B-117. Fox, H. L. and G. H. Thorne, Sr., Fluid Control Apparatus, No. 3208462, dated September 28, 1965, filed September 14, 1962, assigned to Sperry Rand Corporation.
- B-118. Francis, S. A., Fluid Read-Out Device, No. 3200525, dated August 17, 1965, filed May 13, 1963, assigned to Francis Associates.
- B-119. Frantz, W., Liquid Density Computer, No. 3028748, dated April 10, 1962, filed January 18, 1960, assigned to Curtiss-Wright Corporation.
- B-120. Frantz, W., Incremental Digital Fluid Actuator, No. 3164065, dated January 5, 1965, filed December 29, 1961, assigned to Martin-Marietta.
- B-121. Freeman, J. D., Fluid Operated Timer Circuit, No. 3276689, dated October 4, 1966, filed August 14, 1964, assigned to General Time Corporation.
- B-122. Gale, B. M., Fluid Memory Apparatus, No. 3269650, dated August 30, 1966, filed November 27, 1964, assigned to Honeywell Inc.
- B-123. Gehring, A. J., Jr., M. Jacoby and T. D. Reader, Pure Fluid Computer, No. 3190554, dated June 22, 1965, filed June 19, 1963, assigned to Sperry Rand Corporation.
- B-124. Gelin, P., Arrangement for Controlling the Flow of a Fluid, a Means of an Auxiliary Flow, No. 2914916, dated December 1, 1959.
- B-125. Gesell, W. F., Fluid Apparatus, No. 3335737, dated August 15, 1967, filed May 27, 1964, assigned to The Sheffield Corporation.
- B-126. Gesell, W. F., Fluid Apparatus, No. 3258118, dated June 28, 1966, filed June 25, 1964, assigned to The Sheffield Corporation.

- B-127. Glaettli, H. H., Fluid Devices for Computers, No. 3114390, dated December 17, 1963, assigned to International Business Machines Corporation.
- B-128. Glaettli, H. H., Fluid Logical Devices, No. 3122313, dated February 25, 1964, filed May 11, 1961, assigned to International Business Machines Corporation.
- B-129. Gobhai, C. M., Fluid Logic Frequency Treatment, No. 3347251, dated October 17, 1967, filed June 24, 1964, assigned to The Foxboro Company.
- B-130. Gobhai, C. M. and E. Schoppe, Jr., Fluid Logic Pulse Frequency Subtractor, No. 3260457, dated July 12, 1966, filed June 24, 1964, assigned to The Foxboro Company.
- B-131. Gobhai, C. M., Fluid Logic Ring Counter, No. 3250471, dated May 10, 1966, filed June 24, 1964, assigned to The Foxboro Company.
- B-132. Gobhai, C. M., Fluid Logic Half Adder-Subtractor, No. 3239143, dated March 8, 1966, filed June 24, 1964, assigned to The Foxboro Company.
- B-133. Gobhai, C. M., Fluid Logic Half Subtractor, No. 3243115, dated March 29, 1966, filed June 24, 1964, assigned to The Foxboro Company.
- B-134. Gobhai, C. M., Fluid Logic Pulse Frequency Rate System, No. 3241758, dated March 22, 1966, filed June 24, 1964, assigned to The Foxboro Company.
- B-135. Gobhai, C. M. and E. Schoppe, Jr., Fluid Logic Arithmetic Device, No. 3243114, dated March 29, 1966, filed June 24, 1964, assigned to The Foxboro Company.
- B-136. Gongwer, C. A., Fluid Turbulence Detector, No. 3213682, dated October 26, 1965, filed March 6, 1961, assigned to Aerojet-General Corporation.
- B-137. Gottron, R. N., Electro-Fluid Transducer, No. 3311122, dated March 28, 1967, filed January 13, 1964, assigned to the United States of America.
- B-138. Gray, J. L., Fluid Pulse Generator, No. 3202180, dated August 24, 1965, filed February 8, 1963, assigned to Sperry Rand Corporation.
- B-139. Greenblett, B. J., Fluid Controlled Device, No. 3226530, dated December 28, 1965, filed June 5, 1962, assigned to International Business Machines Corporation.

- B-140. Greenblott, B. J., Fluid Controlled Device, No. 3148691, dated September 15, 1964, filed June 7, 1962, assigned to International Business Machines Corporation.
- B-141. Graefe, A. D. and H. D. Hoffman and W. C. Schaffer, Jet Engine Thrust Control System, No. 2934898, dated May 3, 1960, filed September 29, 1953, assigned to Curtiss-Wright Corporation.
- B-142. Grimland, C. J., Analog-to-Digital Converter, No. 3306539, dated February 28, 1967, filed October 6, 1964, assigned to The Geotechnical Corporation.
- B-143. Groeber, E. and G. H. Thorne, Sr., Fluid Logic Device, No. 3266507, dated August 16, 1966, filed September 4, 1963, assigned to Sperry Rand Corporation.
- B-144. Groeber, E., Fluid Logic Apparatus, No. 3232305, dated February 1, 1966, filed November 14, 1963, assigned to Sperry Rand Corporation.
- B-145. Groeber, E., Fluid Oscillator, No. 3342198, dated September 19, 1967, filed January 15, 1965, assigned to Sperry Rand Corporation.
- B-146. Grubb, H. R., Fluid-Operated Shift Register, No. 3250470, dated May 10, 1966, filed December 19, 1963, assigned to International Business Machines Corporation.
- B-147. Grubb, H. R., Fluid Logic Trigger, No. 3253605, dated May 31, 1966, filed December 18, 1963, assigned to International Business Machines Corporation.
- B-148. Gunderson, D. T. and L. A. Weinecke, Edge Position Detector, No. 2539131, dated January 23, 1951, filed November 24, 1948, assigned to Askania Regulator Company.
- B-149. Halista, M. J., Electrical Apparatus, No. 3327223, dated June 20, 1967, filed August 25, 1964, assigned to Honeywell Inc.
- B-150. Hall, R. E., Method of and Means for Translating Sounds, No. 1549196, dated August 11, 1925, filed November 14, 1918, assigned to Hall Radio Corporation.
- B-151. Hatch, Jr., R. W., Fluid Switch, No. 3238961, dated March 8, 1966, filed October 10, 1963, assigned to The Foxboro Company.
- B-152. Hatch, Jr., R. W., Fluid Logic Time Temperature Programmer, No. 3339570, dated September 5, 1967, filed June 24, 1964, assigned to The Foxboro Company.
- B-153. Hatch, Jr., R. W., Fluid Switch System, No. 3327726, dated June 27, 1967, filed June 24, 1964, assigned to The Foxboro Company.

- B-154. Hatch, Jr., R. W., Fluid Logic Dead-Band Control System, No. 3327725, dated June 27, 1967, filed June 24, 1964, assigned to The Foxboro Company.
- B-155. Hatch, Jr., R. W., Fluid Detector by Entrainment, No. 3250116, dated May 10, 1966, filed June 15, 1964, assigned to The Foxboro Company.
- B-156. Hatch, Jr., R. W., Aeriform Fluid Information Transfer Device, No. 3237857, dated March 1, 1966, filed June 24, 1964, assigned to The Foxboro Company.
- B-157. Hatch, Jr., R. W., Fluid Logic Signal Duration Measurement, No. 3237859, dated March 1, 1966, assigned to The Foxboro Company.
- B-158. Hatch, Jr., R. W., Fluid Logic Diffusion Unit Ring Counter, No. 3251547, dated May 17, 1966, filed June 24, 1964, assigned to The Foxboro Company.
- B-159. Hatch, Jr., R. W., Turbulence Fluid Logic Binary Counter Device, No. 3259314, dated July 5, 1966, filed June 24, 1964, assigned to The Foxboro Company.
- B-160. Hausmann, G. F., Directional Control Means for Rockets or the Like, No. 3143856, dated August 11, 1964, filed June 8, 1961, assigned to United Aircraft Company.
- B-161. Hausmann, G. F., Fluid Valve, No. 3016063, dated January 9, 1962, filed July 5, 1960, assigned to United Aircraft Company.
- B-162. Havee, R. M., Fluid Flow Control Device, No. 3194253, dated July 13, 1965, filed June 21, 1962, assigned to Pitney-Bowes, Inc.
- B-163. Hoeton, B. M., Pressure Equalized Fluid Amplifier, No. 3282280, dated November 1, 1966, filed December 17, 1963, assigned to the United States of America.
- B-164. Horton, H. B., Separable Fluid Control System, No. 3283766, dated November 8, 1966, filed April 22, 1963, assigned to Sperry Rand Corporation.
- B-165. Horton, B. M., Fluid Servo System, No. 3111291, dated November 19, 1963, filed September 19, 1960.
- B-166. Horton, H. B., System and Apparatus for Producing, Maintaining and Controlling Laminar Fluid Stream Flow, No. 3182674, dated May 11, 1965, filed July 24, 1961, assigned to Sperry Rand Corporation.
- B-167. Horton, H. B., Delay Line Memory, No. 3075548, dated January 29, 1963, filed September 26, 1960, assigned to Sperry Rand Corporation.

- B-168. Horton, B. M., Negative Feedback Fluid Amplifier, No. 3024805, dated March 13, 1962, filed May 20, 1960.
- B-169. Horton, B. M., Fluid-Operated System, No. 3122165, dated February 25, 1964, filed September 19, 1960.
- B-170. Horton, B. M., Fluid Oscillator, No. 3185166, dated May 25, 1965, filed April 8, 1960.
- B-171. Horton, B. M., Pure Fluid Amplifier, No. 3331382, dated July 18, 1967, filed December 17, 1963, assigned to the United States of America.
- B-172. Horton, B. M., Fluid Scalars, No. 3226023, dated December 28, 1965, filed June 25, 1962.
- B-173. Horton, B. M., Fluid System for Aircraft Control, No. 3137464, dated June 16, 1964, filed September 19, 1960.
- B-174. Horton, H. B., Fluid-Electro Transducer, No. 3258685, dated June 28, 1966, filed April 22, 1963, assigned to Sperry Rand Corporation.
- B-175. Hurvitz, H. Suction Amplifier, No. 3001539, dated September 26, 1961, filed August 15, 1960.
- B-176. Hurvitz, H. Bounded Jet Fluid Amplifiers, No. 3004547, dated October 17, 1961, filed July 22, 1960.
- B-177. Hurvitz, H., Pure Fluid Amplifier, No. 3208463, dated September 28, 1965, filed April 4, 1963.
- B-178. Iverson, I. B., Synchronous Harmonic Computer, No. 3157355, dated November 17, 1964, filed July 3, 1961.
- B-179. Jacoby, M., Binary Counter, No. 3227368, dated January 4, 1966, filed January 22, 1964, assigned to Sperry Rand Corporation.
- B-180. Jacoby, M., Fluid Memory Device, No. 3282503, dated November 1, 1966, filed June 29, 1964, assigned to Sperry Rand Corporation.
- B-181. Joesting, F. D., Pneumatic Transducers, No. 3219049, dated November 23, 1965, filed September 11, 1963, assigned to Honeywell Inc.
- B-182. Joesting, F. D., Fluid Amplifier Control System, No. 3171421, dated March 2, 1965, filed December 7, 1961, assigned to Honeywell Inc.

- B-183. Joesting, F. D., Fluid Flow Control Device, No. 3159208, dated December 1, 1964, filed March 23, 1961, assigned to Honeywell Inc.
- B-184. Joesting, F. D., Two-Stage Fluid Oscillator, No. 3098504, dated July 23, 1963, filed March 26, 1962, assigned to Minneapolis-Honeywell Regulator Company.
- B-185. Johnson, E. G., Fluid Amplifier Apparatus, No. 3171915, dated March 2, 1965, filed May 15, 1962, assigned to Honeywell Inc.
- B-186. Jones, B. A., Fluid Amplification Device for Propulsion System Roll Control, No. 3229461, dated January 18, 1966, filed May 4, 1965, assigned to the United States of America.
- B-187. Jones, B. A., Tertiary Injector for Propulsion System Roll Control, No. 3229460, dated January 18, 1966, filed May 4, 1965, assigned to the United States of America.
- B-188. Jones, D. R., Analog Amplifier Cross Vent, No. 3279488, dated October 18, 1966, filed June 7, 1963, assigned to Bowles Engineering Corporation.
- B-189. Jones, D. R., Fluid Logic Circuit and Shift Register Employing Same, No. 3240220, dated March 15, 1966, filed February 26, 1963, assigned to Bowles Engineering Corporation.
- B-190. Jones, J. E. and J. A. Machmer, Fluid Encoder and Actuator, No. 3314603, dated April 18, 1967, filed November 21, 1965, assigned to International Business Machines Corporation.
- B-191. Jones, D. R. and E. M. Dexter, Bias Device for Pure Fluid Amplifier, No. 3209775, dated October 5, 1965, filed December 7, 1962, assigned to Bowles Engineering Corporation.
- B-192. Katz, S., Fluid Pressure Reference, No. 3313313, dated April 11, 1967, filed April 10, 1964, assigned to the United States of America.
- B-193. Kepler, C. E. and R. E. Olson, Bistable Fluid Valve, No. 3135291, dated June 2, 1964, filed June 14, 1961, assigned to the United Aircraft Corporation.
- B-194. Klein, H. C., Aerodynamic Valves and Apparatus Incorporating Same, No. 3258919, dated July 5, 1966, filed July 23, 1964, assigned to Alfred Teves KG.
- B-195. Krayner, W. L., Force Balance Computing Apparatus, No. 3348771, dated October 24, 1967, filed July 13, 1965, assigned to Calgon Corporation.

- B-196. Laing, N., Fluid Conveying Apparatus, No. 3345961, dated October 10, 1967, filed April 26, 1960.
- B-197. Lee II, L., Fluid Resistor, No. 3323550, dated June 6, 1967, filed May 21, 1964, assigned to The Lee Company.
- B-198. Lewis, G. D., Bistable Valve Control, No. 3330483, dated July 11, 1967, filed October 26, 1964, assigned to United Aircraft Corporation.
- B-199. Lewis, G. D. and B. A. Jones, Bi-Stable Fluid Valve, No. 3276473, dated October 4, 1966, filed July 30, 1963, assigned to the United States of America.
- B-200. Linderoth, E. R., Aerodynamic Check Valve, No. 2727535, dated December 20, 1955, filed January 17, 1950.
- B-201. Lootzook, J. V., Pneumatic or Hydraulic Automatic Control System, No. 3225779, dated December 28, 1965, filed August 18, 1961, assigned to Pneumo-Hydraulic Automatic Control Laboratory of Automatic Control and Telemechanics Institute of the Academy of Sciences of the U.S.S.R.
- B-202. Lorenz, W. T., Fluid Regulator, No. 3198214, dated August 3, 1965, filed October 30, 1963, assigned to R.I.V. Anstalt zur Verwaltung von Realund Immaterialvermogen.
- B-203. Luhrs, J. F., Measuring Apparatus, No. 2217642, dated October 8, 1940, filed March 1, 1938, assigned to Bailey Meter Company.
- B-204. Lupfer, D. E., Method of and Apparatus for Improved Process Control, No. 3197138, dated July 27, 1965, filed June 12, 1961, assigned to Phillips Petroleum Company.
- B-205. Lyman, B., Sheet Handling Apparatus, No. 3236517, dated February 22, 1966, filed April 5, 1963.
- B-206. Mamy, M., Pneumatic Switching Member, No. 3303999, dated February 14, 1967, filed September 16, 1963.
- B-207. Manion, F. M., Automatic Fill Valve, No. 3277914, dated October 11, 1966, filed December 12, 1963, assigned to Bowles Engineering Corporation.
- B-208. Manion, F. M., Differential Fluid Amplifier, No. 3209774, dated October 5, 1965, filed September 28, 1962, assigned to Bowles Engineering Corporation.

- B-209. Manion, F. M., Vortex Transfer Device, No. 3280837, dated October 25, 1966, filed November 20, 1963, assigned to Bowles Engineering Corporation.
- B-210. Manion, F. M., Vented Pure Fluid Analog Amplifier, No. 3282768, dated November 8, 1966, filed November 20, 1963, assigned to Bowles Engineering Corporation.
- B-211. Manion, F. M., Input and Control Systems for Staged Fluid Amplifiers, No. 3282279, dated November 1, 1966, filed December 10, 1963, assigned to Bowles Engineering Corporation.
- B-212. Manion, F. M., Vortex Controlled Fluid Amplifier, No. 3233621, dated February 8, 1966, filed January 31, 1963, assigned to Bowles Engineering Corporation.
- B-213. Manion, F. M., External Vortex Transformer, No. 3216439, dated November 9, 1965, filed December 18, 1962.
- B-214. Marhofer, L. J., Pure Liquid Shift Register, No. 3323722, dated June 6, 1967, filed December 9, 1965, assigned to the United States of America.
- B-215. Markey, F. J., Fluid Jet Edge Position Detector, No. 2919712, dated January 5, 1960, filed May 25, 1956, assigned to GPE Controls, Inc.
- B-216. Mayer, F., Electrohydraulic Actuator, No. 3273594, dated September 20, 1966, filed May 26, 1961, assigned to Inventions Finance Corporation.
- B-217. McCracken, S. T., Fluid Timer, No. 3306538, dated February 28, 1967, filed November 20, 1963, assigned to General Electric Company.
- B-218. McMahan, K. D., Fluid Control Apparatus, No. 2265737, dated December 9, 1941, filed June 21, 1939, assigned to General Electric Company.
- B-219. McNaney, J. T., Binary To Decimal Converter, No. 3263921, dated August 2, 1966, filed July 30, 1965.
- B-220. McNaney, J. T., Temperature Compensating Means for Fluid Displacement Decoder, No. 3237856, dated March 1, 1966, filed May 27, 1964.
- B-221. Meek, J. M., Angular Rate Sensor Utilizing at Least One Fluid Beam, No. 3205715, dated September 14, 1965, filed April 18, 1962.
- B-222. Meier, J. H., Fluid-Controlled Memory with Non-Destructive Readout, No. 3252481, dated May 24, 1966, filed August 29, 1963, assigned to International Business Machines Corporation.

- B-223. Meier, J. H., Tuning Fork Oscillator, No. 3275015, dated September 27, 1966, filed October 29, 1963, assigned to International Business Machines Corporation.
- B-224. Metzger, E. E., Fluid Pulse Width Modulator, No. 3276464, dated October 4, 1966, filed October 21, 1965, assigned to Bowles Engineering Corporation.
- B-225. Mitchell, A. E., Pulse Powered Fluid Device with Flow Asymmetry Control, No. 3326227, dated June 20, 1967, filed December 21, 1964, assigned to International Business Machines Corporation.
- B-226. Mon, J. and J. Joyce, Jr., Fluid Amplifier-Driven Oscillator, No. 3340896, dated September 12, 1967, filed June 7, 1965, assigned to the United States of America.
- B-227. Moore, C. B., Boat Steering Apparatus, No. 3206928, dated September 21, 1965, filed May 16, 1962, assigned to Moore Products Co.
- B-228. Moore, A. D., Calculating Machine, No. 208211, dated June 1, 1937, filed October 11, 1935.
- B-229. Moore, C. B., Control Apparatus, No. 3177888, dated April 13, 1965, filed September 21, 1962, assigned to Moore Products Co.
- B-230. Morey, E. D., Washing Machine, No. 3312234, dated April 4, 1967, filed August 6, 1964, assigned to General Electric Company.
- B-231. Mugele, K., Device for Closing Openings Such as Pressure Openings in Gas Pumps, No. 3348766, dated October 24, 1967, filed March 23, 1965, assigned to Siemens-Schuckertwerke Aktiengesellschaft, Berlin-Siemensstadt.
- B-232. Murphy, F. E., Jr., Stable Fluid Amplifiers, No. 3181545, dated May 4, 1965, filed September 26, 1962, assigned to Corning Glass Works.
- B-233. Neukirch, F., Liquid Catcher for Jet-Pipe Relays, No. 2228015, dated January 7, 1941, filed November 28, 1939, assigned to Askania Regulator Company.
- B-234. Nichols, J. B. and W. E. Wayman, Nozzle Flow Control, No. 2692800, dated October 26, 1949, filed October 8, 1951, assigned to General Electric Company.
- B-235. Norwood, R. E., Electro-Fluid Apparatus, No. 3187762, dated June 8, 1965, filed December 10, 1962, assigned to International Business Machines Corporation.

- B-236. Norwood, R. E., Multi-Stable Fluid Device, No. 3128039, dated April 7, 1964, filed December 20, 1961, assigned to International Business Machines Corporation.
- B-237. Norwood, R. E., Fluid Logic Device, No. 3128040, dated April 7, 1964, filed October 29, 1962, assigned to International Business Machines Corporation.
- B-238. Norwood, R. E., Fluid-Operated Logic Devices, No. 3318329, dated May 9, 1967, filed July 24, 1964, assigned to International Business Machines Corporation.
- B-239. Ogren, H. D., Control Apparatus, No. 3348562, dated October 24, 1967, filed January 30, 1964, assigned to The Foxboro Company.
- B-240. Ogren, H. D., Vortex Rate Sensor, No. 3202237, dated August 31, 1965, filed September 6, 1962, assigned to Honeywell Inc.
- B-241. Palmisano, R. R., Fluid Vortex Oscillator, No. 3311120, dated March 28, 1967, filed July 6, 1964, assigned to the United States of America.
- B-242. Pan, C. H. T., Fluid Amplifiers, No. 3240221, dated March 15, 1966, filed May 8, 1963, assigned to General Electric Company.
- B-243. Phillips, E. R. and M. Jacoby, Visual Fluid Read-Out Device, No. 3305171, dated February 21, 1967, filed July 26, 1965, assigned to Sperry Rand Corporation.
- B-244. Phillips, E. R., Fluid Binary Counter, No. 3342197, dated September 19, 1967, filed May 12, 1964, assigned to Sperry Rand Corporation.
- B-245. Phillips, E. R., Monostable Fluid Amplifier and Shift Register Employing Same, No. 3248053, dated April 26, 1966, filed June 18, 1964, assigned to Sperry Rand Corporation.
- B-246. Phillips, E. R., Fluid Sensor, No. 3270960, dated September 6, 1966, filed September 11, 1964, assigned to Sperry Rand Corporation.
- B-247. Phillips, E. R., Jet Pipe Pneumatic and Gate, No. 3334640, dated August 8, 1967, filed August 1, 1962, assigned to Sperry Rand Corporation.
- B-248. Phillips, E. R., Jet Pipe Pneumatic or Gate, No. 3191612, dated June 29, 1965, filed August 1, 1962, assigned to Sperry Rand Corporation.

- B-249. Phillips, E. R., Pure Fluid Binary Counter, No. 3319886, dated May 16, 1967, filed October 21, 1965, assigned to Sperry Rand Corporation.
- B-250. Plasko, E. R., Fluid Control Means, No. 3275014, dated September 27, 1966, filed September 12, 1963, assigned to American Radiator & Standard Sanitary Corporation.
- B-251. Polter, E. M. and S. N. Zilberfarb, Pure Fluid Velocity Modulated Amplifier, No. 3182675, dated May 11, 1965, filed November 17, 1961, assigned to Sperry Rand Corporation.
- B-252. Posingies, W. M., Control Apparatus, No. 3246863, dated April 19, 1966, filed October 25, 1962, assigned to Honeywell Inc.
- B-253. Przybylko, S. J., Vortex Analog Speed Sensor, No. 3342196, dated September 19, 1967, filed January 4, 1966, assigned to the United States of America.
- B-254. Rawlings, J. L., Fluid Commutating Device, No. 3191625, dated June 29, 1965, filed November 8, 1962, assigned to Sperry Rand Corporation.
- B-255. Reader, T. D., Pulse Generator, No. 3159169, dated December 1, 1964, filed September 4, 1962, assigned to Sperry Rand Corporation.
- B-256. Reader, R. D., Fluid or Gate, No. 3282281, dated November 1, 1966, filed December 23, 1963, assigned to Sperry Rand Corporation.
- B-257. Reader, T. D., Pneumatic Clock, No. 3159168, dated December 1, 1964, filed February 16, 1962, assigned to Sperry Rand Corporation.
- B-258. Reader, T. D., Fluid Shift Register, No. 332643, dated June 20, 1967, filed December 4, 1964, assigned to Sperry Rand Corporation.
- B-259. Reader, T. D., Perforating Mechanism, No. 3176571, dated April 6, 1965, filed June 8, 1962, assigned to Sperry Rand Corporation.
- B-260. Reilly, R. J., Induction Fluid Amplifier, No. 3030979, dated April 24, 1962, filed November 16, 1960, assigned to Minneapolis-Honeywell Regulator Company.
- B-261. Reilly, R. J., Pure Fluid Amplifier, No. 3170476, dated February 23, 1965, filed August 22, 1962, assigned to Honeywell Inc.
- B-262. Rhoades, J. M., Flow Regulator, No. 3324891, dated June 13, 1967, filed April 18, 1961, assigned to General Electric Company.
- B-263. Riordan, H. E., Pneumatic Diode, No. 3068880, dated December 18, 1966, filed December 28, 1961, assigned to General Precision Inc.

- B-264. Riordan, H. E., Pneumatic Computer Element and Circuits, No. 3151623, dated October 6, 1964, filed November 28, 1962, assigned to General Precision Inc.
- B-265. Rose, R. K., Fluid Amplifier Serial Digital Adder Logic Circuit, No. 3350009, dated October 31, 1967, filed March 28, 1966, assigned to General Electric Company.
- B-266. Rose, R. K., Fluid Amplifier Serial Digital Complementer Logic Circuit, No. 3340010, dated October 31, 1967, filed April 26, 1966, assigned to General Electric Co.
- B-267. Russ, D. G., Method and Apparatus for Measuring Thrust in Jet-Type Engines, No. 3233451, dated February 8, 1966, filed February 17, 1961.
- B-268. Saintsbury, J. A., Aerodynamic Flow Reverser and Smoother, No. 3333414, dated August 1, 1967, filed October 13, 1965, assigned to United Aircraft of Canada Limited.
- B-269. Saint-Joanis, A., Fluid Distributor Devices, No. 3326239, dated June 20, 1967, filed December 23, 1963.
- B-270. Samet, F., Binary Flip-Flop Element for Pneumatic Digital Computer, No. 3168898, dated February 9, 1965.
- B-271. Schaefer, J. O., Pneumatic Accumulator, No. 3346184, dated October 10, 1967, filed April 21, 1966, assigned to International Business Machines Corporation.
- B-272. Schonfeld, A. and J. C. Schulte, Fluid Identification and Sorting Device, No. 3241668, dated March 22, 1966, filed October 4, 1963, assigned to Sperry Rand Corporation.
- B-273. Schonfeld, A., M. Jacoby, and T. D. Reader, Keyboard Encoder, No. 3248052, dated April 26, 1966, filed June 25, 1964, assigned to Sperry Rand Corporation.
- B-274. Schonfeld, A. and J. C. Schulte, Fluid Sorter, No. 3241669, dated March 22, 1966, filed August 17, 1964, assigned to Sperry Rand Corporation.
- B-275. Schonfeld, A. and J. C. Schulte, Control and Delay Device for Liquid Fluid Circuits, No. 3331380, dated July 18, 1967, filed November 27, 1964, assigned to Sperry Rand Corporation.
- B-276. Schonfeld, A., Pneumatic Tubing Memory, No. 3270961, dated September 6, 1966, filed November 17, 1964, assigned to Sperry Rand Corporation.

- B-277. Schoppe, E. and C. M. Gobhai, Fluid Logic Bi-Directional Binary Counter Device, No. 3237858, dated March 1, 1966, filed June 24, 1964, assigned to The Foxboro Company.
- B-278. Schuck, O. H., Control Apparatus, No. 3239027, dated March 8, 1966, filed December 26, 1963, assigned to Honeywell Inc.
- B-279. Scudder, K. R., Electro-Pneumatic Transducer, No. 3263695, dated August 2, 1966, filed March 19, 1964, assigned to the United States of America.
- B-280. Seaton, W. J., Bistable Fluid Device, No. 3148692, dated September 15, 1964, filed September 17, 1962, assigned to Sperry Rand Corporation.
- B-281. Severson, A. M., Fluid Amplifier, No. 3080886, dated March 12, 1963, filed September 18, 1961, assigned to Minneapolis-Honeywell Regulator Company.
- B-282. Severson, A. M., Fluid Operated Pump, No. 3176920, dated April 6, 1965, filed May 26, 1961, assigned to Honeywell Inc.
- B-283. Severson, A. M., Controlled Fluid Unit, No. 3144208, dated August 11, 1964, filed October 12, 1962, assigned to Minneapolis-Honeywell.
- B-284. Shinn, J. N., Reversible Fluid Binary Counter, No. 3199782, dated August 10, 1965, filed August 28, 1963, assigned to General Electric Company.
- B-285. Shiiki, A., Digital-Analogue Converter, No. 3288365, dated November 29, 1966, filed June 30, 1965, assigned to Honeywell Inc.
- B-286. Shinskey, F. G., Dead-Time Simulator for Industrial Process Control Apparatus, No. 3292852, dated December 20, 1966, filed January 25, 1962, assigned to Foxboro Company.
- B-287. Smith, Jr., R. T., Fluid Controlled Capstans with Brakes, No. 3270932, dated September 6, 1966, filed January 13, 1964, assigned to Sperry Rand Corporation.
- B-288. Smith, H. V., Pressure Responsive Control System, No. 3344809, dated October 3, 1967, filed January 27, 1965, assigned to Metrol Corporation.
- B-289. Smith, G. L., Fluid Pressure Ratio Sensor, No. 3270561, dated September 6, 1966, filed April 24, 1964, assigned to the United States of America.
- B-290. Sowers, E. U. III, Fluid Amplifier Vacuum Capstan Control, No. 3342392, dated September 1967, filed June 9, 1965, assigned to Sperry Rand Corporation.

- B-291. Sowers, E. U. III, Fluid Power Amplifier Not-Gate, No. 3174497, dated March 23, 1965, filed September 4, 1962, assigned to Sperry Rand Corporation.
- B-292. Sowers, E. U. III, Multi-Frequency Fluid Oscillator, No. 3117593, dated January 14, 1964, filed April 23, 1962, assigned to Sperry Rand Corporation.
- B-293. Sowers, E. U. III, Pure Fluid Pulse Generator, No. 3175569, dated March 30, 1965, filed December 28, 1961, assigned to Sperry Rand Corporation.
- B-294. Sowers, E. U. III, Keypunch Input with Repeat Readout Incorporating Fluid Amplifying Means, No. 3191858, dated June 29, 1965, filed June 5, 1963, assigned to Sperry Rand Corporation.
- B-295. Sowers, E. U. III, Fluid Power Output Device, No. 3282282, dated November 1, 1966, filed February 18, 1964, assigned to Sperry Rand Corporation.
- B-296. Sowers, E. U. III, Fluid Amplifier with Automatic Reset of the Power Stream, No. 3122039, dated February 25, 1964, filed February 16, 1962, assigned to Sperry Rand Corporation.
- B-297. Sorteberg, J., Weighbeam Control System, No. 3289933, dated December 6, 1966, filed April 7, 1965.
- B-298. Sparrow, H. T., Fluid Amplifier Mixing Control System, No. 3091393, dated May 28, 1963, filed July 5, 1961, assigned to Minneapolis-Honeywell Regulator Company.
- B-299. Sparrow, H. T., Pulsed Fluid Amplifier, No. 3176703, dated April 6, 1965, filed March 1, 1962, assigned to Honeywell Inc.
- B-300. Sparrow, H. T., Gas Control System, No. 3171468, dated March 2, 1965, filed May 9, 1961, assigned to Honeywell Inc.
- B-301. Spivak, A. L. and J. A. Russell, Arc Discharge Controlled Fluid Amplifier, No. 3122062, dated February 25, 1964, filed January 23, 1962, assigned to General Electric Company.
- B-302. Spyropoulos, C. E., Pneumatic Relaxation Oscillator, No. 321727, dated November 16, 1965, filed September 10, 1963, assigned to the United States of America.
- B-303. Stern, H., Fluid Control System, No. 3233522, dated February 8, 1966, filed May 28, 1963, assigned to General Electric Company.
- B-304. Sterns, C. F., Hydraulic Computer, No. 3317134, dated May 2, 1967, filed May 25, 1964, assigned to United Aircraft Corporation.

- B-305. Straub, H. W., Light Transducer for Fluid Amplifier, No. 3228411, dated January 11, 1966, filed January 22, 1964.
- B-306. Swartz, E. L., Fluid Oscillator, No. 3320966, dated May 23, 1967, filed December 31, 1964, assigned to the United States of America.
- B-307. Swartz, E. L., Impedance-Matching Fluid Amplifier, No. 3329152, dated July 4, 1967, filed June 12, 1964, assigned to the United States of America.
- B-308. Symnoski, R. V. and C. B. Moore, Pneumatic Measuring Apparatus, No. 3232095, dated February 1, 1966, filed March 23, 1962, assigned to Moore Products Co.
- B-309. Tagaevskaya, A. A. and T. K. Berends, Standardized Modular Systems, No. 3335950, dated August 15, 1967, filed June 10, 1964.
- B-310. Taplin, L. B., W. F. Datwyler, Jr., J. P. Madurski, and T. E. Thompson, Fluid Pulse Control, No. 3302398, dated February 7, 1967, filed June 25, 1963, assigned to the Bendix Corporation.
- B-311. Tesla, N., Valvular Conduit, No. 1329559, dated February 3, 1920, filed February 21, 1916.
- B-312. Testerman, M. K. and P. C. McLeod, Jr., Fluid Oscillator Analyzer and Method, No. 327337, dated September 20, 1966, filed August 12, 1963, assigned to Phillips Petroleum Company.
- B-313. Testerman, M. K. and P. C. McLeod, Method and Apparatus for Determining Fluid Flow Rate, No. 3144767, dated August 18, 1964, filed July 3, 1961, assigned to Phillips Petroleum Company.
- B-314. Thorburn, D. H., Pneumatic Control Unit, No. 3319644, dated May 16, 1967, filed January 19, 1965, assigned to The Power Regulator Company.
- B-315. Topfer, A. and A. Schwarz, Pressurized Fluid Operable Switching Device, No. 3323721, dated June 6, 1967, filed July 20, 1965, assigned to Deutsche Akademie der Wissenschaften zu Berlin.
- B-316. Tooze, M. J., Data Processing Apparatus, No. 3350011, dated October 31, 1967, filed May 16, 1966, assigned to Elliott Brothers (London) Limited.
- B-317. Turick, J. M., Transducer, No. 3266511, dated August 16, 1966, filed October 11, 1963, assigned to Sperry Rand Corporation.
- B-318. Turick, J. M., Fluid Amplifier Control Valve, No. 3266512, dated August 16, 1966, filed October 16, 1963, assigned to Sperry Rand Corporation.

- B-319. Unfried, H. H., Fluid Dynamic Control Device, No. 3282051, dated November 1, 1966, filed February 4, 1965, assigned to Mattel, Inc.
- B-320. Vockroth, Jr., R. W., Comparison Matrix, No. 3288364, dated November 29, 1966, filed November 18, 1964, assigned to Corning Glass Works.
- B-321. Vockroth, Jr., R. W., Fluid Amplifiers, No. 3202179, dated August 24, 1965, filed February 5, 1962, assigned to Corning Glass Works.
- B-322. Vockroth, Jr., R. W., Logic Network for Numerically-Controlled Machine Tools, No. 3250285, dated May 10, 1966, filed February 12, 1963, assigned to Corning Glass Works.
- B-323. Voit, Jr., W. F., Fluid Display and Converter Device, No. 3263922, dated August 2, 1966, filed December 24, 1964, assigned to International Business Machines Corporation.
- B-324. Voit, Jr., W. F., Bistable Fluid Logic Element, No. 3312244, dated April 4, 1967, filed December 24, 1964, assigned to International Business Machines Corporation.
- B-325. Voit, Jr., W. F., Switching Arrangement for Fluid Amplifiers, No. 3266513, dated August 16, 1966, filed March 2, 1964, assigned to International Business Machines Corporation.
- B-326. Voitsekhovsky, B. V., Jet Nozzle for Obtaining High Pulse Dynamic Pressure Heads, No. 3343794, dated September 26, 1967, filed July 12, 1965.
- B-327. Wadey, W. G., Device for Forming Fluid Pulses, No. 3266510, dated August 16, 1966, filed September 16, 1963, assigned to Sperry Rand Corporation.
- B-328. Wadey, W. G., Weighing and Sorting Device, No. 3317039, dated May 2, 1967, filed February 25, 1965.
- B-329. Wadey, W. G., Fluid Logic Control, No. 3191860, dated June 28, 1965, filed January 30, 1963, assigned to Sperry Rand Corporation.
- B-330. Wadey, W. G., Fluid Pulsing Means for Print Hammers, No. 3159099, dated December 1, 1964, filed August 16, 1964, assigned to Sperry Rand Corporation.
- B-331. Wadey, W. G., Tabulating Card Position Sensing Device, No. 3191008, dated June 22, 1965, filed April 11, 1962, assigned to Sperry Rand Corporation.

- B-332. Wadey, W. G., Infrared Record Reader with Fluid Signal Output, No. 3179810, dated April 20, 1965, filed October 4, 1961, assigned to Sperry Rand Corporation.
- B-333. Warren, R. W. and R. E. Bowles, Multi-Channel Fluid Elements, No. 3238958, dated March 8, 1966, filed August 7, 1963, assigned to the United States of America.
- B-334. Warren, R. W., Fluid Vortex Transfer, No. 3207168, dated September 21, 1965, filed January 16, 1963, assigned to the United States of America.
- B-335. Warren, R. W., Respirator, No. 3292623, dated December 20, 1966, filed February 24, 1964, assigned to the United States of America.
- B-336. Warren, R. W., R. G. Barclay and J. G. Moorhead, Pressure Recovery from Bistable Element, No. 3225780, dated December 28, 1965, filed May 20, 1963, assigned to the United States of America.
- B-337. Warren, R. W., Negative Feedback Oscillator, No. 3158166, dated November 24, 1964, filed August 7, 1962, assigned to the United States of America.
- B-338. Warren, R. W., Fluid Time Gate, No. 3180575, dated April 27, 1965, filed January 16, 1963, assigned to the United States of America.
- B-339. Warren, R. W., Fluid-Operated Timer, No. 3093306, dated June 11, 1963, filed June 5, 1961, assigned to the United States of America.
- B-340. Warren, R. W., Fluid Logic Components, No. 3107850, dated October 22, 1963, filed March 17, 1961.
- B-341. Warren, R. W. and E. L. Swartz, Fluid Pulse Width Modulation, No. 3228410, dated January 11, 1966, filed September 30, 1963, assigned to the United States of America.
- B-342. Warren, R. W. and R. E. Bowles, Multi-Channel Fluid Elements, No. 3340884, dated September 12, 1967, filed August 7, 1963, assigned to the United States of America.
- B-343. Warren, R. W. and R. E. Bowles, Three Dimensional Jet Vectoring, No. 3204405, dated September 7, 1965, filed February 20, 1964, assigned to the United States of America.
- B-344. Warren, R. W., Fluid Oscillator, No. 3016066, dated January 9, 1962, filed January 22, 1960.
- B-345. Warren, R. W., Self-Matching Fluid Elements, No. 3272214, dated September 13, 1966, filed October 2, 1963, assigned to the United States of America.

- B-346. Warren, R. W., Pure Fluid Shift Register, No. 3221990, dated December 7, 1965, filed January 30, 1964, assigned to the United States of America.
- B-347. Warren, R. W., High-Speed Counters and Fluid Forward-Backward Counters, No. 3224674, dated December 21, 1965, filed May 11, 1964, assigned to the United States of America.
- B-348. Watrous, R. B., Fluid-Pressure-Operated Computer, No. 2960098, dated November 15, 1960, filed June 29, 1959, assigned to Minneapolis-Honeywell Regulator Company.
- B-349. Welsh, H. F., Fluid Binary Counter, No. 324113, dated March 29, 1966, filed April 20, 1964, assigned to Sperry Rand Corporation.
- B-350. Welsh, H. F., Fluid Shift Register, No. 3201041, dated August 17, 1965, filed March 23, 1964, assigned to Sperry Rand Corporation.
- B-351. Welsh, H. F., Power Jet Clocking, No. 3199781, dated August 10, 1965, filed June 5, 1963, assigned to Sperry Rand Corporation.
- B-352. White, D. R., Fluid Flow Apparatus, No. 2910830, dated November 3, 1959.
- B-353. Widell, G. M., Jet Thrust Vector Control Apparatus, No. 3255971, dated June 14, 1966, filed November 21, 1962, assigned to The Bendix Corporation.
- B-354. Widell, G. M., Vortex Valve, No. 3195303, dated July 20, 1965, filed January 22, 1962.
- B-355. Wilkerson, R. B., Fluid Control Devices, No. 3220428, dated November 30, 1965, filed January 9, 1963, assigned to General Electric Company.
- B-356. Williamson, R. G., Pneumatic Multiplier (Very High Gain Amplifier), No. 3270760, dated September 6, 1966, filed December 19, 1963, assigned to Sperry Rand Corporation.
- B-357. Woodward, K. E., Fluid Amplifier, No. 3053276, dated September 11, 1962, filed April 26, 1961.
- B-358. Woodward, K. E., Fluid Oscillator, No. 3124999, dated March 17, 1964, filed February 1, 1963, assigned to the United States of America.
- B-359. Woodward, K. E., Artificial Heart Pump Circulation System, No. 3208448, dated September 28, 1965, filed February 2, 1962.
- B-360. Wright, C. P., Jet Fluid Amplifier, No. 3283767, dated November 8, 1966, filed May 31, 1963, assigned to International Business Machines Corporation.

- B-361. Zalmanzon, L. A., Method of Automatically Controlling Pneumatic or Hydraulic Elements of Instruments and Other Devices, No. 3295543, dated January 3, 1967, filed February 12, 1960, assigned to Pneumo-Hydraulic Automatic Control Laboratory of Automatic Control and Telemechanics Institute of the Academy of Sciences of the U.S.S.R.
- B-362. Ziberfarb, S. N., Free-Running Oscillator, No. 3266508, dated August 16, 1966, filed April 22, 1963, assigned to Sperry Rand Corporation.
- B-363. Zilberfarb, S. N. and E. M. Polter, Pure Fluid Velocity Modulated Amplifier, No. 3182675, dated May 11, 1965, filed November 17, 1961, assigned to Sperry Rand Corporation.
- B-364. Zilberfarb, S. N., Transducer, No. 3182686, dated May 11, 1965, filed March 28, 1962, assigned to Sperry Rand Corporation.
- B-365. Zilberfarb, S. N., Pure Fluid Operated Counter, No. 3305170, dated February 21, 1967, filed April 1, 1964, assigned to Sperry Rand Corporation.
- B-366. Zilberfarb, S. N., Fluid Device, No. 3247860, dated April 26, 1966, filed April 22, 1963, assigned to Sperry Rand Corporation.
- B-367. Zilberfarb, S. N., Fluid Stream Deflecting Means, No. 3208464, dated September 28, 1965, filed April 22, 1963, assigned to Sperry Rand Corporation.
- B-368. Zilberfarb, S. N., Sequential Fluid Amplifier, No. 3124160, dated March 10, 1964, filed June 29, 1962, assigned to Sperry Rand Corporation.
- B-369. Zisfein, M. B. and G. E. Martin, Fluid Amplifier, No. 3212515, dated October 19, 1965, filed July 13, 1962, assigned to Giannini Corporation.

APPENDIX III-C

FLUIDIC SUBJECT INDEX

The following subject listings are cross referenced to the literature and patent listings in Appendices III-A and III-B.

I. Capabilities

A-1, A-4, A-8, A-9, A-10, A-47, A-50, A-52, A-62, A-72, A-95, A-99, A-110, A-111, A-126, A-131, A-146, A-148, A-149, A-151, A-152, A-153, A-157, A-163, A-168, A-194, A-202, A-219, A-249, A-260, A-261, A-262, A-267, A-278, A-280, A-306, A-308, A-310, A-311, A-316, A-317, A-330, A-338, A-359, A-360, A-367, A-383, A-384, A-394, A-395, A-396, A-397 through A-407, A-418, A-442, A-443, A-465, A-476, A-477, A-481, A-493, A-500, A-510, A-534, A-539, A-540, A-541, A-542, A-558, A-560, A-564, A-565, A-581, A-582, A-585, A-620, A-621, A-622, A-623, A-636, A-639.

II. Commercial Applications

A-2, A-4, A-7, A-10, A-14, A-18, A-29, A-35, A-36, A-44, A-57, A-60, A-65, A-69, A-70, A-80, A-88, A-97, A-98, A-108, A-109, A-137, A-144, A-154, A-158, A-159, A-161, A-164, A-167, A-170, A-171, A-173, A-179, A-181, A-182, A-186, A-191, A-192, A-211, A-218, A-233, A-254, A-267, A-269, A-287, A-331, A-359, A-378, A-379, A-380, A-381, A-422, A-428, A-429, A-443, A-489, A-493, A-510, A-531, A-557, A-562, A-563, A-569, A-570, A-579, A-586, A-635, A-644.

III. Aerospace Applications

A-12, A-20, A-27, A-30, A-32, A-35, A-36, A-50, A-56, A-57, A-61, A-63, A-65, A-81, A-83, A-84, A-85, A-87, A-101, A-102, A-103, A-107, A-120, A-132, A-134, A-146, A-166, A-168, A-169, A-194, A-222, A-225, A-240, A-242, A-252, A-256, A-264, A-267, A-276, A-279, A-280, A-290, A-337, A-360, A-373, A-392, A-408, A-409, A-460, A-468, A-475, A-492, A-493, A-503, A-529, A-572, A-583, A-588, A-619, B-85, B-111, B-141, B-173, B-186, B-187, B-353.

IV. Propulsion Applications

A-12, A-23, A-35, A-36, A-50, A-56, A-61, A-66, A-77, A-81, A-245, A-270, A-410, A-467, A-547, B-69, B-83, B-103, B-108, B-111, B-160, B-186, B-187, B-353.

V. Basic Fluid Flow

A-6, A-19, A-25, A-38, A-40, A-41, A-42, A-43, A-45, A-46, A-49, A-51, A-67, A-68, A-90, A-93, A-100, A-105, A-106, A-110, A-113, A-116, A-118, A-122, A-123, A-129, A-145, A-150, A-174, A-175, A-176, A-189, A-190, A-197, A-213, A-221, A-226, A-250, A-255, A-285, A-286, A-288, A-300, A-304, A-307, A-312, A-315, A-318, A-320, A-321, A-325, A-341, A-374, A-390, A-391, A-417, A-420, A-423, A-426, A-436, A-437, A-438, A-446, A-453, A-454, A-469, A-470, A-471, A-485, A-490, A-491, A-497, A-512, A-513, A-524, A-527, A-530, A-535, A-536, A-546, A-549, A-571, A-584, A-592, A-607, A-608, A-609, A-626, A-627, A-628, A-645.

VI. Digital Elements

A-1, A-7, A-14, A-15, A-17, A-23, A-28, A-29, A-39, A-52, A-59, A-77, A-86, A-96, A-127, A-136, A-177, A-178, A-179, A-180, A-189, A-203, A-210, A-215, A-217, A-221, A-223, A-224, A-238, A-241, A-254, A-257, A-258, A-263, A-266, A-272, A-277, A-282, A-283, A-284, A-285, A-288, A-297, A-301, A-305, A-314, A-322, A-326, A-327, A-345, A-354, A-362, A-365, A-375, A-376, A-377, A-380, A-382, A-385, A-388, A-390, A-419, A-421, A-426, A-427, A-438, A-439, A-440, A-441, A-445, A-447, A-449, A-450, A-451, A-452, A-498, A-499, A-519, A-521, A-528, A-537, A-556, A-566, A-573, A-577, A-587, A-595, A-596, A-603, A-604, A-605, A-611, A-613, A-614, A-615, A-617, A-618, A-632, A-634, B-8, B-23, B-25, B-26, B-28, B-32, B-33, B-98, B-99, B-193, B-198, B-199, B-236, B-245, B-247, B-248, B-256, B-260, B-270, B-280, B-324, B-340.

VII. Analog Elements

A-1, A-7, A-30, A-32, A-33, A-47, A-48, A-91, A-104, A-119, A-121, A-133, A-135, A-136, A-165, A-188, A-277, A-289, A-333, A-334, A-336, A-344, A-348, A-413, A-436, A-437, A-466, A-484, A-490, A-491, A-494, A-496, A-545, A-548, A-602, A-636, A-643, B-36, B-37, B-38, B-39, B-208, B-210.

VIII. Valves and Power Elements

A-2, A-23, A-35, A-36, A-38, A-42, A-66, A-82, A-89, A-121, A-140, A-141, A-220, A-224, A-239, A-240, A-256, A-257, A-258, A-259, A-264, A-265, A-274, A-292, A-298, A-302, A-329, A-346, A-376, A-380, A-385, A-391, A-411, A-412, A-414, A-424, A-430, A-433, A-435, A-455, A-461, A-467, A-473, A-501, A-515, A-516, A-517, A-518, A-520, A-547, A-568, A-578, A-587, A-605, A-606, A-616, A-625, A-638, A-642, A-643, B-13, B-27, B-32, B-73, B-82, B-94, B-108, B-113, B-116, B-161, B-165, B-193, B-194, B-198, B-199, B-202, B-209, B-212, B-213, B-216, B-241, B-262, B-318, B-354.

IX. Passive Elements and Interconnects

A-41, A-55, A-78, A-114, A-115, A-125, A-138, A-139, A-142, A-197, A-207, A-212, A-244, A-247, A-248, A-251, A-268, A-319, A-324, A-342, A-343, A-347, A-352, A-361, A-365, A-417, A-448, A-462, A-474, A-502, A-511, A-610, A-612, A-624, B-197, B-200, B-263, B-268, B-271, B-311.

X. Sensors and Interface Devices

A-3, A-5, A-13, A-52, A-6, A-94, A-147, A-184, A-193, A-214, A-243, A-246, A-299, A-305, A-309, A-333, A-334, A-350, A-364, A-370, A-415, A-416, A-445, A-459, A-483, A-517, A-518, A-522, A-523, A-550, A-568, A-576, A-590, A-603, A-614, A-615, A-638, B-7, B-9, B-35, B-40, B-45, B-54, B-56, B-59, B-77, B-78, B-86, B-136, B-137, B-148, B-149, B-174, B-215, B-221, B-223, B-235, B-240, B-246, B-253, B-279, B-301, B-305, B-317, B-364.

XI. Pneumatic Logic-Moving Parts

A-24, A-44, A-60, A-69, A-114, A-124, A-127, A-143, A-198, A-357, A-476, A-477, A-550, A-589, A-591, A-637.

XII. Digital Systems

A-11, A-16, A-18, A-20, A-21, A-22, A-24, A-26, A-27, A-28, A-29, A-39,
A-44, A-57, A-60, A-64, A-66, A-69, A-80, A-85, A-87, A-88, A-97, A-98,
A-148, A-158, A-159, A-161, A-182, A-186, A-203, A-204, A-205, A-211,
A-254, A-263, A-272, A-273, A-284, A-291, A-296, A-322, A-328, A-339,
A-377, A-378, A-392, A-427, A-431, A-441, A-463, A-464, A-487, A-489,
A-507, A-508, A-509, A-514, A-528, A-544, A-574, A-577, A-594, B-159.

XIII. Analog Systems

A-20, A-22, A-30, A-32, A-34, A-47, A-53, A-54, A-56, A-57, A-62, A-63,
A-64, A-65, A-85, A-107, A-108, A-109, A-120, A-134, A-279, A-293, A-294,
A-295, A-296, A-299, A-333, A-334, A-335, A-354, A-368, A-369, A-488,
A-495, A-505, A-532, B-49.

XIV. Hybrid Systems

A-56, A-57, A-144, A-198, A-357, A-377, A-456, A-562, A-563, A-575, A-629.

XV. Component Performance

A-1, A-26, A-31, A-33, A-34, A-58, A-84, A-86, A-111, A-117, A-135, A-155,
A-185, A-188, A-196, A-199, A-201, A-206, A-209, A-210, A-216, A-217,
A-227, A-251, A-265, A-275, A-297, A-301, A-323, A-340, A-351, A-366,
A-393, A-425, A-439, A-444, A-457, A-472, A-504, A-519, A-543, A-548,
A-554, A-555, A-567, A-580, A-593, A-632, A-633.

XVI. System Analysis and Design

A-31, A-33, A-34, A-45, A-51, A-53, A-54, A-55, A-61, A-64, A-71, A-75,
A-76, A-78, A-84, A-86, A-89, A-97, A-98, A-104, A-130, A-138, A-139,
A-156, A-180, A-183, A-185, A-208, A-209, A-212, A-244, A-251, A-264,
A-271, A-294, A-296, A-303, A-340, A-354, A-358, A-412, A-427, A-486,
A-487, A-505, A-514, A-533, A-538, A-612, A-631.

XVII. Instrumentation Techniques

A-37, A-52, A-58, A-94, A-112, A-117, A-150, A-156, A-332, A-356, A-412, A-472, A-486, A-525, A-526, A-551, A-561, A-572, A-630.

XVIII. Fabrication

A-71, A-89, A-172, A-281, A-355, A-421, A-431, A-588, A-597, A-598, A-599, A-600, A-601.

XIX. Symposia and Abstracts

A-73, A-92, A-128, A-160, A-162, A-195, A-226, A-228, A-229, A-230, A-231, A-232, A-234, A-235, A-236, A-237, A-371, A-432, A-458, A-479, A-480, A-482, A-552, A-553, A-559.

APPENDIX III-D

FLUIDIC STANDARDS

TERMINOLOGY

General

Fluidics - The general field of fluid devices or systems performing sensing, logic, amplification and control functions employing primarily no-moving-part (flueric) devices.

Flueric - An adjective applied in some quarters to fluidic devices and systems performing sensing, logic, amplification, and control functions using no moving mechanical elements.

Elements - The general class of devices in their simplest form used to make up fluidic components and circuits; for example, fluidic restrictors and capacitors, a proportional amplifier or an OR-NOR logic gate.

Analog - The general class of devices or circuits whose output is utilized as a continuous function of its input or control port; for example, a proportional amplifier.

Amplifier - An active fluidic component which provides a variation in output signal greater than the impressed control signal variation. The polarity of the output signal may be either positive or negative relative to the control signal. The level of the control signal may be greater or less than the output level.

Pressure Amplifier - A component designed specifically for amplifying pressure signals.

Flow Amplifier - A component designed specifically for amplifying flow signals.

Power Amplifier - A component designed specifically for increasing signal power.

Vented vs. Closed Amplifier - A vented amplifier utilizes auxiliary ports to establish a reference pressure in a particular region of the amplifier geometry. A closed amplifier has no communication with an independent reference. Terminology usage for the geometry is illustrated in Figures 3-D1 and 3-D2.

Digital - The general class of devices or circuits whose output is utilized as a discontinuous function of its input or control port; for example, a bistable amplifier.

Logic Device - The general category of digital fluidic components which perform logic functions; for example AND, NOT, OR, NOR, and NAND. They can gate or inhibit signal transmission with the application, removal, or other combinations of control signals.

Flip-Flop - A digital component or circuit with two stable states and sufficient hysteresis so that it has "memory". Its state is changed with a control pulse; a continuous control signal is not necessary for it to remain in a given state.

Active - The general class of devices which control power from a separate supply.

Passive - The general class of devices which operate on the signal power alone.

Sensor - A component which senses variables and produces a signal in a medium compatible with fluidic devices; for example, a temperature or angular rate sensor.

Transducer - A component which converts a signal from one medium to an equivalent signal in a second medium, one of which is compatible with fluidic devices.

Actuator - A component which converts a fluid signal into an equivalent mechanical output.

Display - A component which converts a fluid signal into an equivalent visual output.

Specific Elements

Jet Interaction Amplifier - An amplifier which utilizes control jets to deflect a power jet and modulate the output. Usually employed as an analog amplifier. Terminology usage for the geometry is illustrated in Figures 3-D1 and 3-D2.

Wall Attachment Amplifier - An amplifier which utilizes control of the attachment of a free jet to a wall (Coanda effect) to modulate the output. Usually employed as a digital amplifier. Terminology usage for the geometry is illustrated in Figure 3-D3.

Vortex Amplifier - An amplifier which utilizes the pressure drop across a controlled vortex for modulating the output. Terminology usage for the geometry is illustrated in Figure 3-D4.

Boundary Layer Amplifier - An amplifier which utilizes the control of the separation point of a power stream from a curved or plane surface to modulate the output. Terminology usage for the geometry is illustrated in Figure 3-D5.

Turbulence Amplifier - An amplifier which utilizes control of the laminar-to-turbulent transition of a power jet to modulate the output. Terminology usage for the geometry is illustrated in Figure 3-D6.

Axisymmetric Focussed Jet Amplifier - An amplifier which utilizes control of the attachment of an annular jet to an axisymmetric flow separator, (that is, control of the focus of the jet) to modulate the output. Usually employed as a digital amplifier. Terminology usage is illustrated in Figure 3-D7.

Impact Modulator - An amplifier which utilizes the control of the intensity of two directly opposed, impacting power jets thereby controlling the position of the impact plane to modulate the output. Terminology usage is illustrated in Figure 3-D8.

Throat-Injection Amplifier - An amplifier which utilizes auxiliary flow at a nozzle throat for a control signal to modulate the output flow. Pressure level of the control signal may either be above or below local throat pressure to result in a positive or negative (suction) quiescent control flow.

Resistor - Passive fluidic element which because of viscous losses produces a pressure drop as a function of the flow through it and has a transfer function of essentially real components (i.e., negligible phase shift) over the frequency range of interest.

Capacitor - A passive fluidic element which, because of fluid compressibility, produces a pressure across the device which lags net flow into it by essentially 90 degrees.

Inductor - A passive fluidic element which, because of fluid inertance, has a pressure drop across it which leads flow through it by essentially 90 degrees.

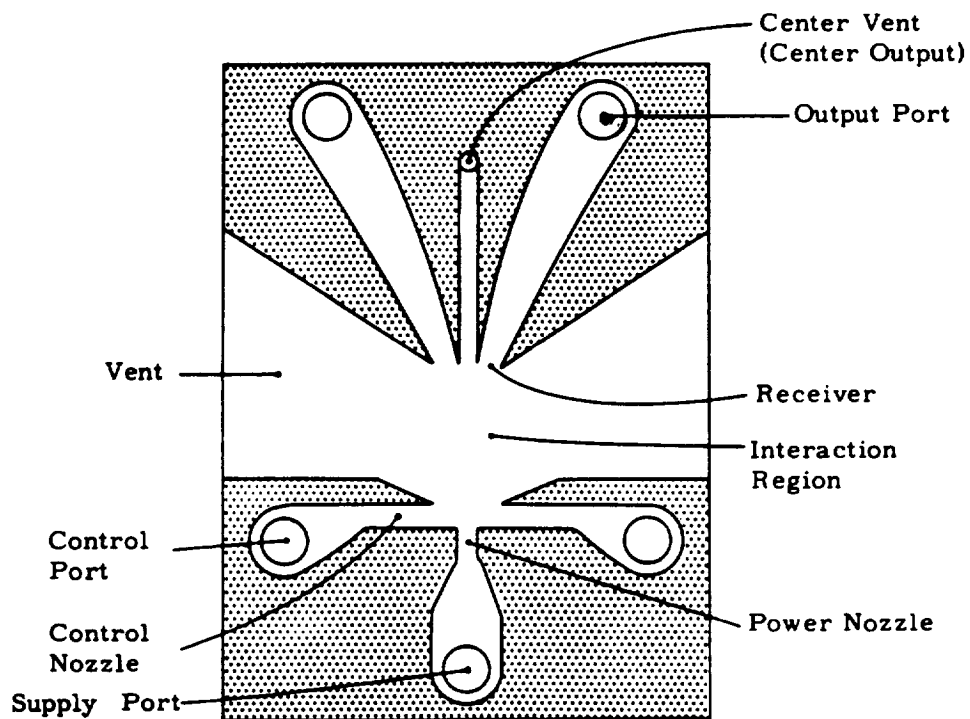


Figure 3-D1 Vented-Jet Interaction Amplifier

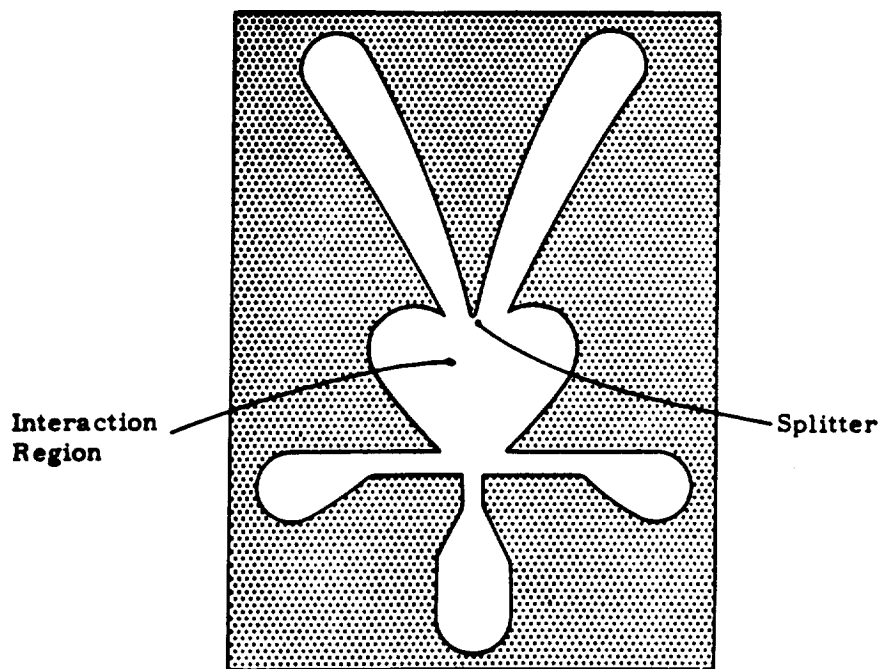


Figure 3-D2 Closed-Jet Interaction Amplifier

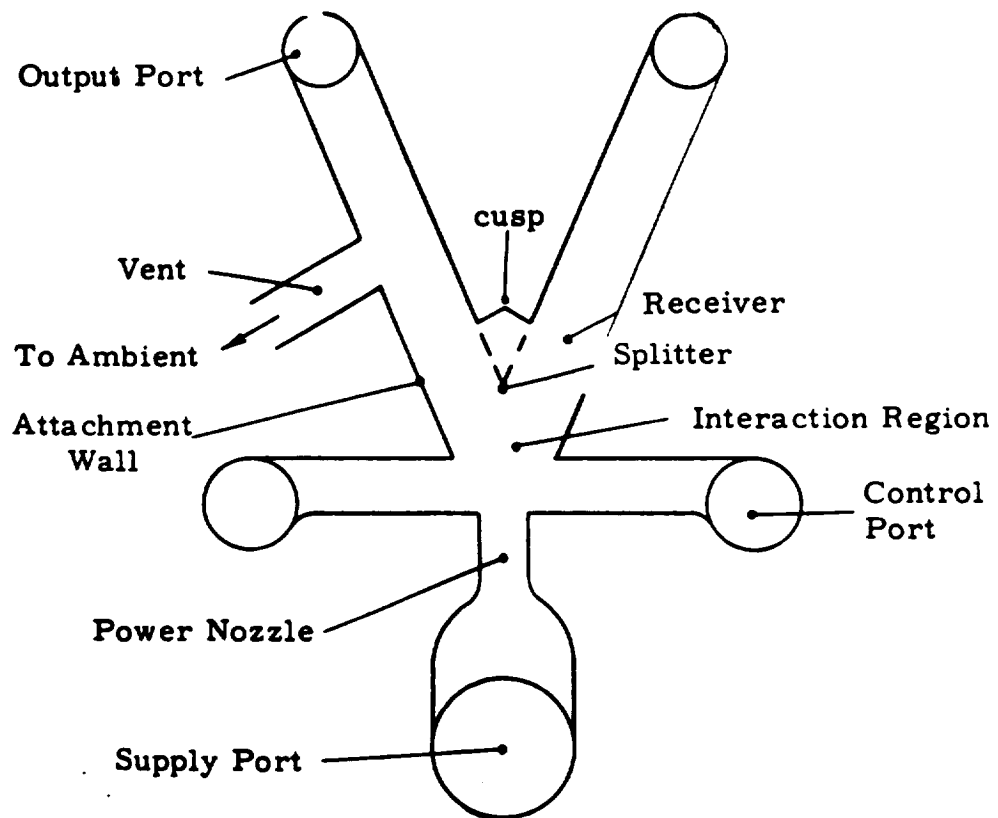


Figure 3-D3 Wall Attachment Amplifier

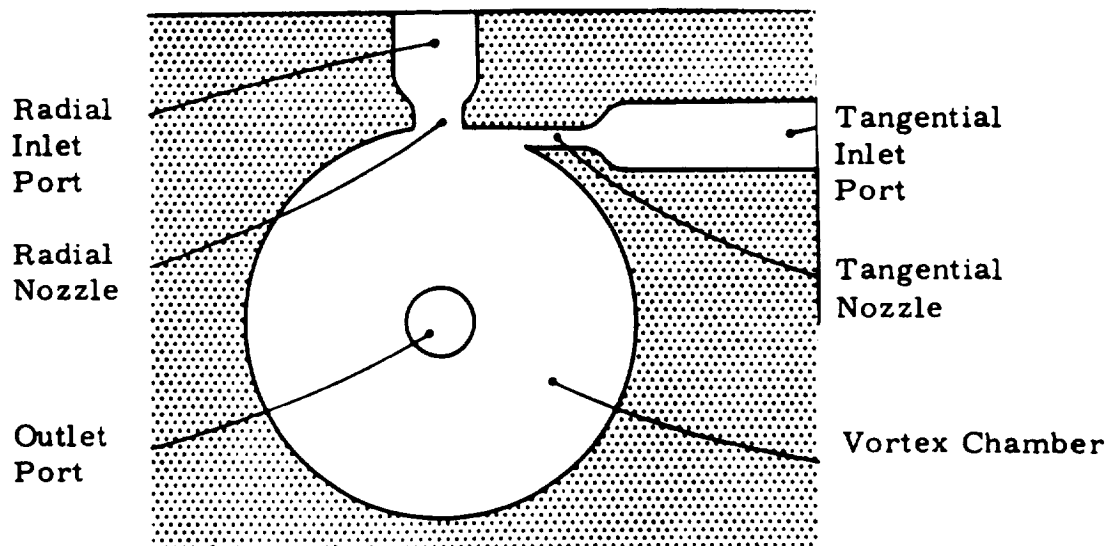


Figure 3-D4 Vortex Amplifier

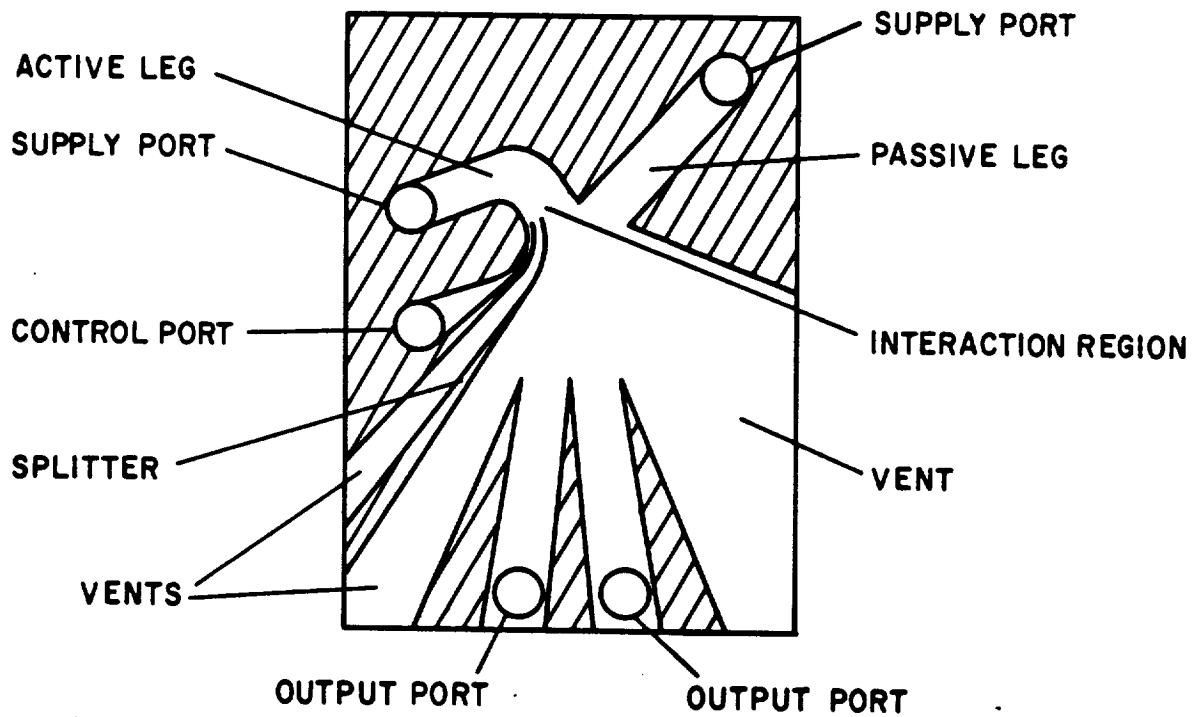


Figure 3-D5 Boundary Layer Control Amplifier (Vents Optional)

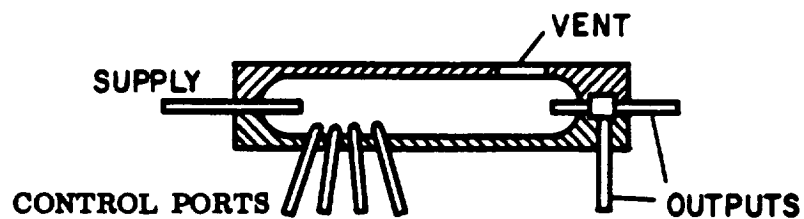
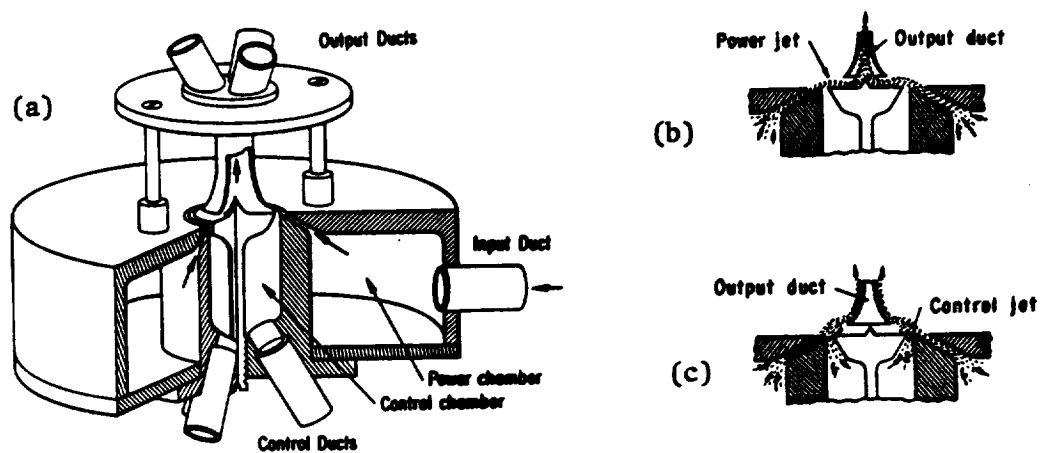
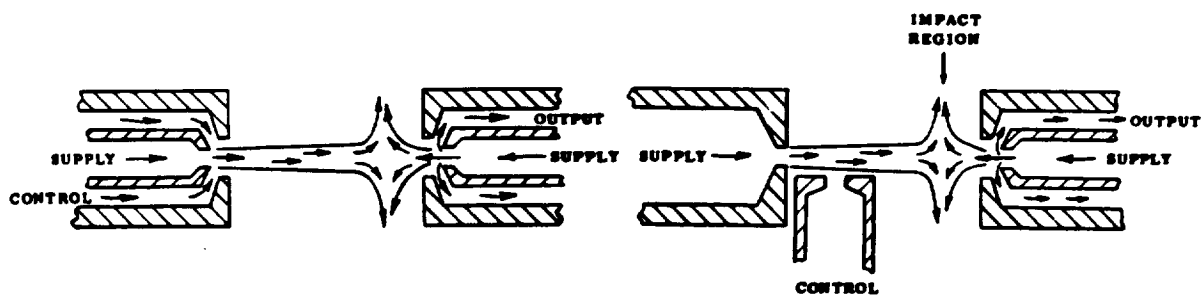


Figure 3-D6 Turbulence Amplifier



Focused-jet amplifier: (a) Typical cross section, (b) Flow pattern with no control flow, (c) Flow pattern with control flow.

Figure 3-D7



Direct Impact Modulator

Transverse Impact Modulator

Figure 3-D8 Impact Modulators

NOMENCLATURE AND UNITS

Basic Quantities

The quantities listed below are general; specific quantities should be identified by subscripts (e.g., P_{02} would be pressure at port 02).

<u>Quantity</u>	<u>Nomenclature</u>	<u>Units</u>
	(std)	(SI)*
Length	-- inch; in	(meter, m)
Force	F pound, lb	(newton; N)
Mass	m lb-sec ² /in	(kilogram; kg)
time	t seconds; sec	(seconds; s)
angle	-- degrees; °	(radians; rad)
frequency	f cycles/sec; cps	(hertz; H _z)
area	A in ²	(m ²)
acceleration	a in/sec ²	(m/s ²)
gravitational constant	g in/sec ²	(m/s ²)
temperature, static	T degrees Rankin °R	(degrees Kelvin; °K)
temperature, total	T ₀ °R	°K
velocity, angular	ω rad/sec	(rad/s)
acceleration, angular	α rad/sec ²	(rad/s ²)
volume	V in ³	(m ³)
weight density	γ lb/in ³	(N/m ³)
mass density	ρ lb-sec ² /in ⁴	(kg/m ³)
weight flow rate	w lb/sec	(N/s)
mass flow rate	ṁ lb-sec/in	(kg/s)
volume flow rate	Q in ³ /sec	(m ³ /s)
velocity, general	u in/sec	(m/s)
velocity, mean	ū in/sec	(m/s)

*The International System of Units

<u>Quantity</u>	<u>Nomenclature</u>		<u>Units</u>
velocity, acoustic	u_c	in/sec	(m/s)
pressure, general	P	lb/in ² or psi	(N/m ²)
pressure, absolute	P_a	psia	(N/m ²)
pressure, gage or drop	P_g	psig	(N/m ²)
power	W	lb-in/sec	(Nm/s)
specific heat ratio	k	dimensionless	
absolute viscosity	μ	lb-sec/in ²	(N-s/m ²)
kinematic viscosity	ν	in ² /sec	(m ² /s)
liquid bulk modulus	β	lb/in ²	(N/m ²)
efficiency	η	dimensionless	
fluid impedance	Z	sec/in ²	(N-s/m ² -kg)
fluid resistance	R	sec/in ²	(N-s/m ² -kg)
fluid capacitance	C	in ²	(kg-m ² /N)
fluid inductance	L	sec ² /in ²	(N-s ² /kg-m ²)
Mach number	M	dimensionless	
Laplace operator	s	1/sec	(1/s)
pressure gain	G_p	dimensionless	
flow gain, average	G_F	dimensionless	
flow gain, incremental	G_{Fi}	dimensionless	
power gain, average	G_p	dimensionless	
power gain, incremental	G_{pi}	dimensionless	
signal - noise ratio	S/N	dimensionless	

General Subscripts

control	c
output	o
supply	s
control, quiescent	co
control differential	cd
output differential	od

SCHEMATICS

The function of the schematics is to enable the circuit designer to employ meaningful and specific symbols in drawings and schematics which will clearly define the function as well as the type of device employed to perform that function.

General

Submerged jet path and flow channels _____

Supply port 0

vent port _____ V

control:

→ arrow-head on control line indicates continual flow required to maintain state, no memory (no hysteresis)

— no arrow-head on control line indicates element has memory (has useful hysteresis).

Logic Notation

$A \bullet B \equiv A \text{ "and" } B$

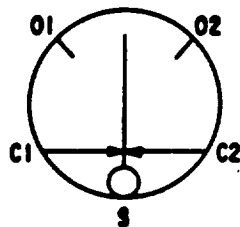
$A + B \equiv A \text{ "or" } B$

$\bar{A} \bullet \bar{B} \equiv \text{"not" } A \text{ and "not" } B$

Port Marking - Port nomenclature shown on schematics need not be used on schematic diagrams; the nomenclature may be useful, however, in correlating test data and specification data with the physical device.

Analog Amplifiers

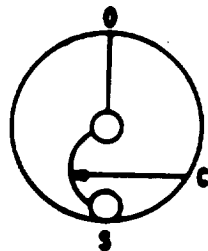
Jet Interaction Amplifier



S - supply
C1 - left control port
C2 - right control port
01 - left output
02 - right output

Operating Principle - Jet interaction (proportional)

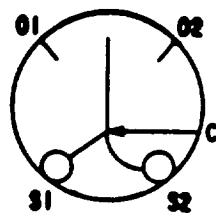
Vortex Amplifier



S - supply
C - control port
0 - output

Operating Principle - vortex

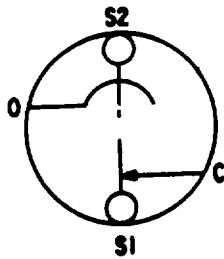
Boundary Layer Control Amplifier



S1 - passive leg supply
S2 - active leg supply
C - control port
01 - left output
02 - right output

Operating Principle - separation point control

Impact Modulator



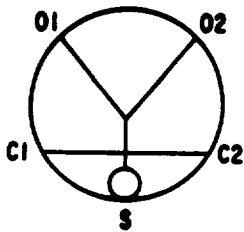
S1 - controlled supply
 S2 - supply
 C - control port
 O - output

Operating Principle - Jet impact

Digital Amplifiers

Wall Attachment Flip-Flop

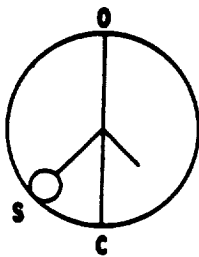
(has memory - relatively wide hysteresis loop)



S - supply
 C1 - left control port
 C2 - right control port
 O1 - left output
 O2 - right output

Operating Principle - wall attachment

Axisymmetric Focussed-Jet Flip-Flop

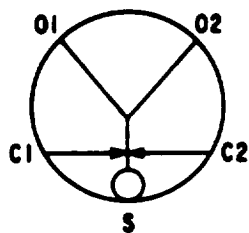


S - supply
 C - control port
 O - output

Operating Principle - annular wall attachment

Digital Amplifier

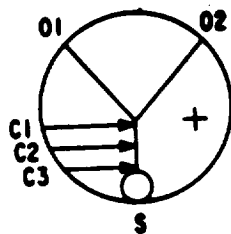
(no memory - essentially zero width hysteresis loop)



S - supply
C1 - left control port
C2 - right control port
01 - left output
02 - right output

Operating Principle - Jet interaction

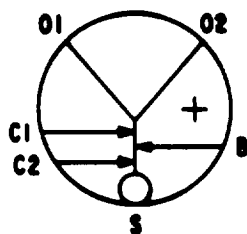
Or-Nor



S - supply
C1, C2, C3 - control ports
01 - $\overline{C1} \bullet \overline{C2} \bullet \overline{C3}$ - output
02 - $C1 + C2 + C3$ - output
+ - indicates Or

Operating Principle - wall attachment, geometrical biasing

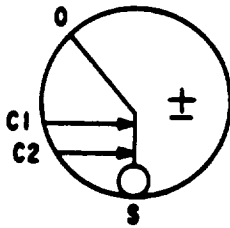
Or-Nor



S - supply
C1, C2 - control ports
01 - left output
02 - right output
B - bias port
+ - Or output

Operating Principle - wall attachment, fluid biased

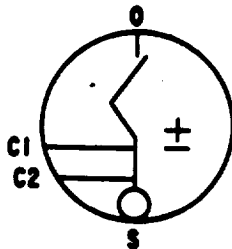
Nor



S - supply port
C1, C2 - control ports
O - output port
± - indicates Nor

Operating Principle - wall attachment

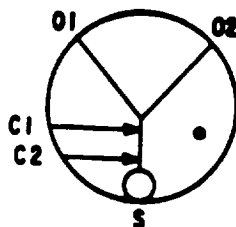
Nor



S - supply
C1, C2 - control ports
O - output
± - indicates Nor

Operating Principle - turbulence

And/Nand

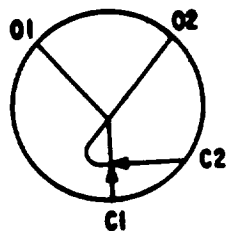


S - supply
C1, C2 - control ports
O1 - $C1 + C2$ output
O2 - $C1 \cdot C2$ output
• - indicates And

Operating Principle - wall attachment

Passive Logic Devices

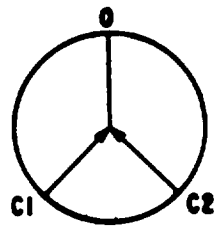
Exclusive Or/And



C1, C2 - control ports
O1 - $C1 \bullet C2$ output
O2 - $C1 + C2$ output

Operating Principle - wall attachment

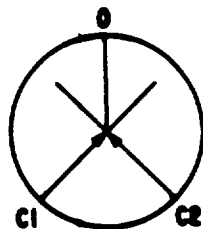
Or



C1, C2 - control ports
O - output

Operating Principle - Jet interaction

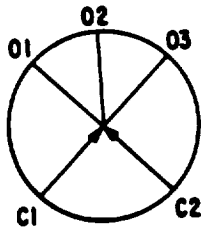
And



C1, C2 - control ports
O - output

Operating Principle - Jet interaction

2/3 And

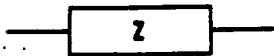


C1, C2 - control ports
01, 02, 03 - outputs

Operating Principle - Jet interaction

General Circuit Elements

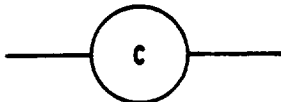
GENERAL IMPEDANCE



CAPILLARY (LAMINAR) RESTRICTION



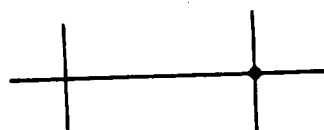
VOLUME CAPACITANCE



RETURN TO RESERVOIR



LINE CROSSING



no connection connection

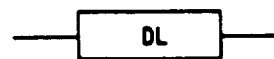
ORIFICE (TURBULENT RESTRICTION)



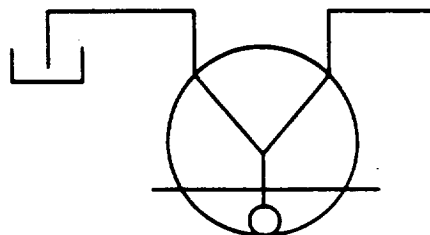
INDUCTANCE



DELAY LINE



EXAMPLE OF RESERVOIR RETURN



DEFINITIONS

General

Fluid Resistance - R; for average value, resistance is the ratio of pressure drop (ΔP) to weight flow rate:

$$R = \frac{\Delta P}{w} \frac{\text{sec}}{\text{in}^2} \left(\frac{\text{Ns}}{\text{m}^2 \text{ kg}} \right)$$

For incremental fluid resistance:

$$R = \frac{dP}{dw} \frac{\text{sec}}{\text{in}^2} \left(\frac{\text{Ns}}{\text{m}^2 \text{ kg}} \right)$$

Fluid Capacitance - C; ratio of integrated weight flow to change in pressure.

$$\text{for gases } C = \frac{V}{k R T} \text{ in}^2 \text{ (m}^2 \text{ -kg/N)}$$

$$\text{for liquids } C = \frac{\gamma V}{\beta} \text{ in}^2 \text{ (m}^2 \text{ -kg/N)}$$

where R is the gas constant.

In general $\Delta P = \frac{1}{Cs} \Delta w$, where ΔP represents a small change in pressure and Δw represents a small change in net weight flow rate. (s = Laplace operator)

Fluid Inductance - L; ratio of pressure change (ΔP) to rate of change of weight flow ($s \Delta w$)

$$L = \frac{y}{gA} \frac{\text{sec}^2}{\text{in}^2} \left(\frac{\text{s}^2 \text{N}}{\text{m}^2 \text{ kg}} \right)$$

where y = channel length and A = channel cross sectional area.

In general $\Delta P = Ls \Delta w$, where ΔP represents a small change in pressure drop along a channel and Δw represents a small change in weight flow rate.

Digital Elements

Pressure Gain - The ratio of the output pressure change to control pressure change required for switching to occur. Data shall be taken in the vicinity of the operating point and load shall be specified.

Flow Gain - The ratio of the output flow change to control flow change required for switching to occur. Data shall be taken in the vicinity of the operating point and load shall be specified.

Power Gain - The ratio of the change in output power to the change in control power required for switching to occur. Data shall be taken in the vicinity of the operating point and load shall be specified.

Pressure Amplification - The ratio of the absolute value of the maximum output pressure divided by the absolute value of the maximum control pressure shall be used to determine the pressure amplification. Data is understood to be at the switch points and load shall be specified.

Flow Amplification - The ratio of the maximum output flow level divided by the maximum control flow shall be used to determine flow amplification. Data is understood to be at the switch points and load shall be specified.

Power Amplification - The ratio of the output power to the control power in the switching region shall be used to determine the power amplification. Load shall be specified.

Fanout - The number of digital elements which can be controlled from the output of a single identical element operating at a common power nozzle pressure. It should be noted that fanout may be affected by operating speed.

Response - An indication of response characteristics is the propagation delay which occurs in response to an approximate step control of recommended amplitude. Propagation delay is the time between the instant the control reaches 50% of final value and the instant the output reaches 50% of the final value as indicated in Figure 3-D9. Load shall be specified if the response is load sensitive.

Noise - The peak-to-peak amplitude of the pressure noise of the device in psi will be listed. Load shall be specified.

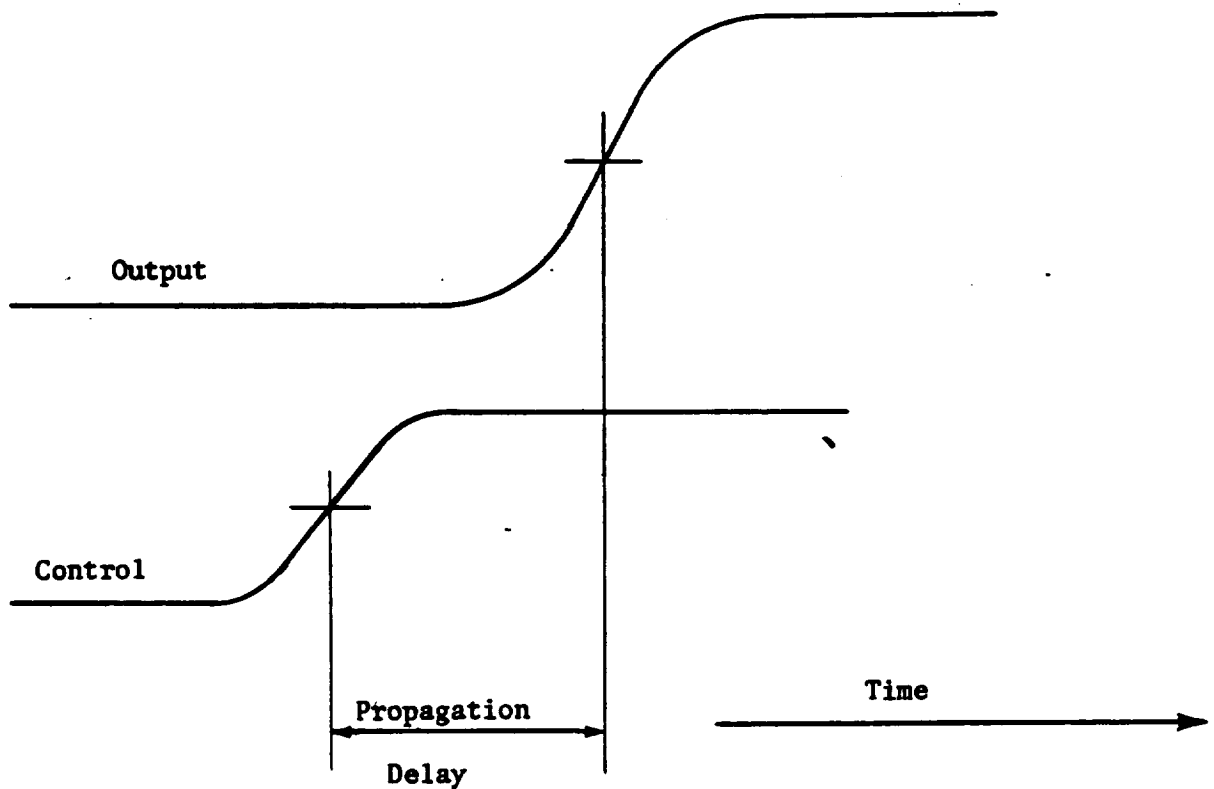


Figure 3-D9 Propagation Delay Definition

Hysteresis - Width of the hysteresis loop as measured on a control output curve and expressed as a percentage of the supply conditions, e.g., flow hysteresis is the hysteresis loop width (measured on a control output flow curve) divided by the supply flow. (See Figure 3-D10). Flow Hysteresis (%) = $\Delta w / w_s \times 100$.

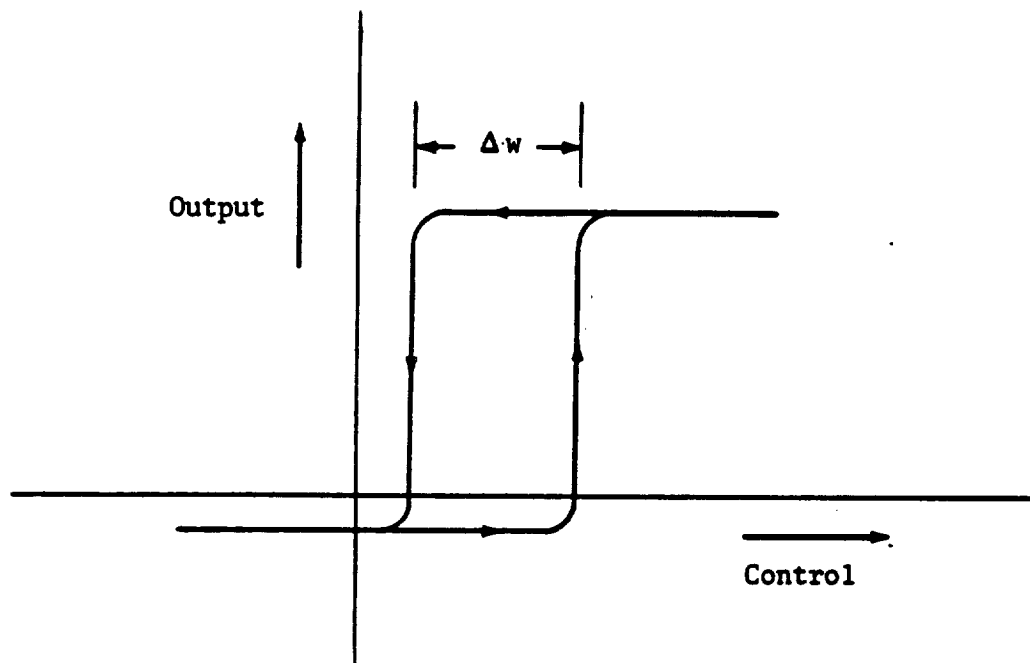


Figure 3-D10 Hysteresis Definition

Control Impedance - Z_C , the ratio of control pressure change to flow change measured at a control port; value may depend on operating point since output pressure-flow curve may not be linear.

Output Impedance - Z_O , the ratio of output pressure change to flow change measured at an output port; value may depend on operating point since output pressure-flow curve may not be linear.

Proportional Elements

Pressure Gain - The slope of the curve of output pressure versus control pressure (See Figure 3-D11) in the vicinity of the operating point shall be used to establish pressure gain.

Flow Gain - The slope of the curve of output flow versus control flow (See Figure 3-D12) in the vicinity of the operating point shall be used to establish gain.

Power Gain - The change in output power divided by the change in control power. Power gain shall be calculated around the operating point for small changes (less than 10% of saturation) of control power.

Pressure Amplification - The ratio of the absolute value of output pressure divided by the absolute value of the control pressure shall be used to determine the pressure amplification. End point values of the useful range or saturation values may be used (See example Figure 3-D11).

Flow Amplification - The ratio of the outlet flow divided by the control flow shall be used to determine the flow amplification. End point values of the useful range or saturation values may be used (See example Figure 3-D12).

Power Amplification - The ratio of the outlet power to the control power shall be used to determine the power amplification. As in pressure and flow amplification, the end point values of the useful range or saturation values may be used.

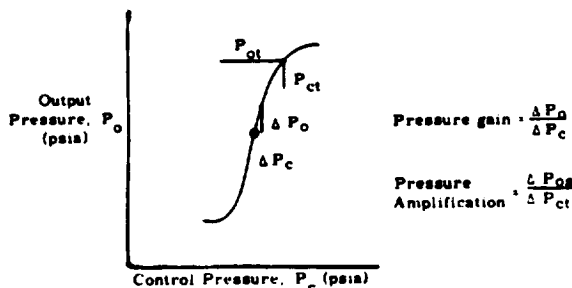


Figure 3-D11. Pressure Gain Definition

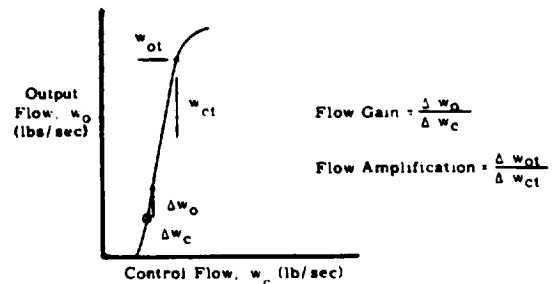


Figure 3-D12. Flow Gain Definition

Frequency Response - Frequency response is fully described by a gain/phase plot. An indication of frequency response is the frequency at which the output signal lags the control signal by 45 degrees for a specified load and control amplitude.

Noise - The peak-to-peak amplitude of the pressure noise of the device in psi will be listed. Element load used during test shall be specified.

Saturation - The maximum output value regardless of control magnitude. (See Figure 3-D13).

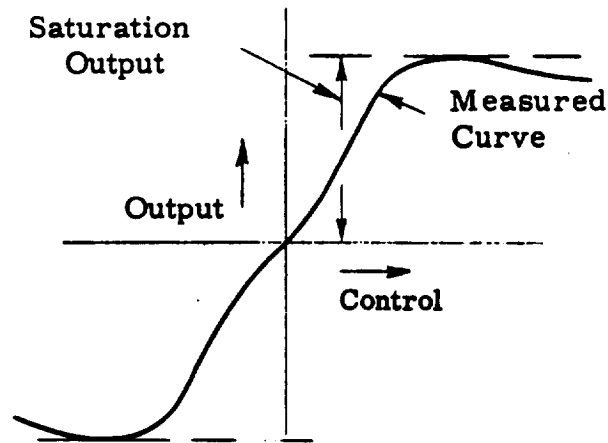


Figure 3-D13 Saturation Definition

Linearity - Deviation of the measured curve from the straight-line average gain approximation; defined as the ratio of the peak-to-peak output deviation to peak-to-peak output range (range should be stated if other than maximum output level) expressed as a percentage. (See Figure 3-D14).

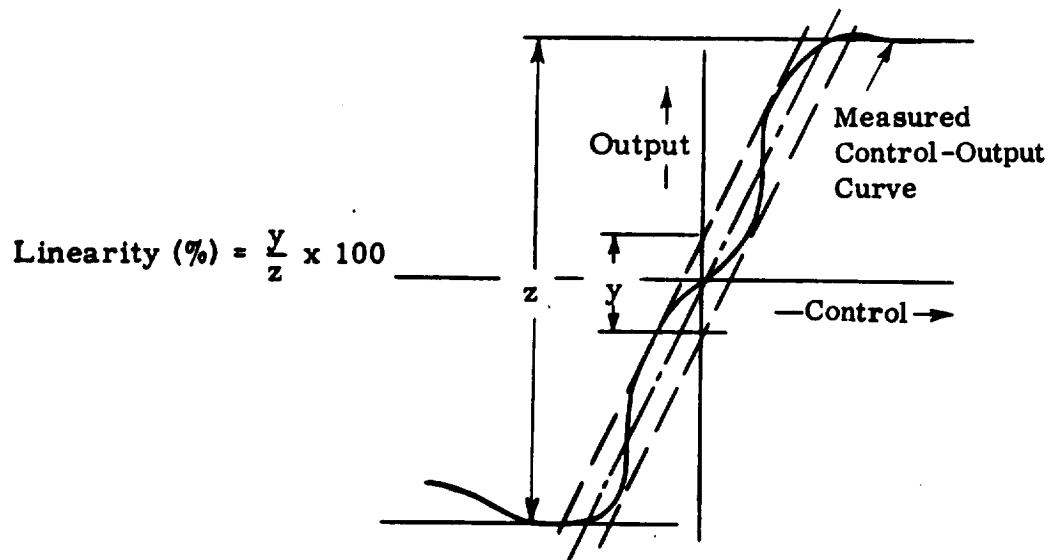


Figure 3-D14 Linearity Definition

Hysteresis - Total width of hysteresis loop expressed as a percent of peak-to-peak saturation control signal. Measurement to be at frequencies below those where dynamic effects become significant. (See Figure 3-D15).

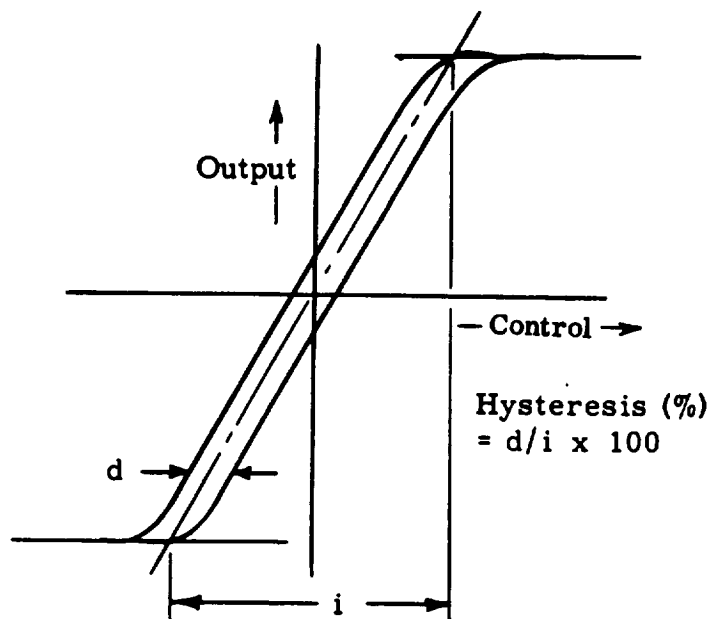


Figure 3-D15 Hysteresis Definition

Control Impedance - Z_C , the ratio of pressure change to flow change measured at a control port. Numerical value may depend on operating point since control pressure-flow curve may not be linear. (See Figure 3-D16). For active elements the power source should be connected for measurements.

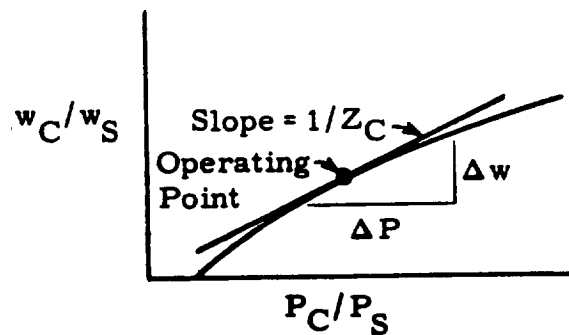


Figure 3-D16 Control Impedance Definition

Output Impedance - Z_O , the ratio of pressure change to flow change measured at an output port. Numerical value may depend on operating point since output pressure-flow curve may not be linear. (See Figure 3-D17).

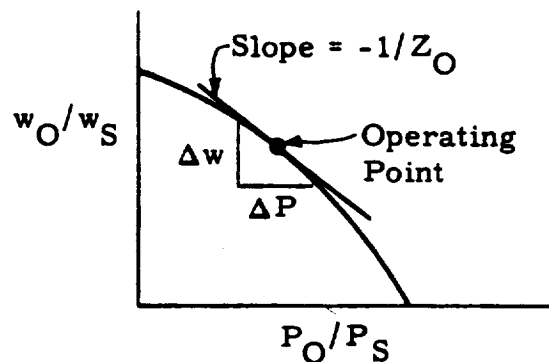


Figure 3-D17 Output Impedance Definition

IV. VALVE ACTUATOR STUDY

This study reports the results of work performed to investigate the performance, applications, and limitations of actuation devices used to operate valves for controlling the flow of liquid chemical rocket propellants. Several problem areas are defined. New approaches to valve actuation were investigated and several concepts presented.

	<u>Page</u>
VALVE ACTUATOR RATING ANALYSIS CHART	4-3
ACTUATOR STUDY	4-4
Electromechanical Actuators	4-4
Pneumatic Actuators	4-10
Hydraulic Actuators	4-12
Chemical Actuators	4-13
Thermal Actuators	4-15
Manual Overrides	4-15
HIGH SPEED SOLENOID VALVE ACTUATION STUDY	4-16
CONCEPTUAL STUDIES	4-36
Monopropellant Actuator Concept	4-36
Bipropellant Actuator Concept	4-39
Other Chemical Actuators	4-40
Thermal Actuator Concept	4-40
Lightweight Electromagnetic Actuator	4-44
Beryllium Thin Films	4-49

VALVE ACTUATOR RATING ANALYSIS CHART

A rating analysis was used to document the results of the surveys and to define the areas where an advancement in the state of the art of valve actuation is required. The rating analysis is presented in a chart on the following page. A rating is assigned to each type of actuator in defining its performance with propellants and in the space environment.

The ratings assigned to the various combinations of actuators and parameters are defined as follows:

RATING

1	A problem exists for which there is no satisfactory solution under the present state of the art.
2	A problem exists but a solution may be available within the present state of the art.
3	Satisfactory - i.e., within the state of the art.
U	Necessary information upon which to base a judgment was unobtainable.
NA	Parameter not applicable.

In some cases as indicated on the chart, a differentiation in values was made for manned missions.

All the ratings were based on the actuator operating in space for up to 10 years. The time, temperature and environmental parameters, i.e., radiation and vacuum, were considered in rating the propellants, functional parameters and application-to-valve types. Ratings pertaining to actuator performance with propellants were based on compatibility of material of construction. The functional parameters were rated based on expected actuator performance requirements in the next 5 to 10 years.

4-3-12

[illegible]

U - UNAVAILABLE INFORMATION
NA - NOT APPLICABLE UNANNOUNCED (DIGIT ONLY)

WANTED

NOTE:

- a. STORED ENERGY CONCEPTS DESCRIBED ON PAGE 4-B
- b. LIQUEFIED PETROLEUM GAS
- c. METHANE, PROPANE, BUTANE
- d. NORMALLY ONE CYCLE ONLY
- e. 300°F, 60 HOURS, 6 CYCLES

[illegible]

ACTUATOR STUDY

The objectives of this study are to briefly describe the various types of actuators which are used or may be used for actuating valves on chemical spacecraft rocket engines. Actuator applications are briefly discussed; however, emphasis was placed on the limitations of the various actuator types. The category of actuators investigated under this study are: electromechanical, pneumatic, hydraulic, chemical and thermal.

The above actuator types were considered in applications to the following valve types: flow metering, shutoff, relief, cold gas regulator, hot gas regulator, liquid regulator, gas disconnect and liquid disconnect. Actuator performance was considered and included the effects of propellants on the actuator materials of construction. Also considered were the functional requirements such as temperature, power, operating life, contamination, response, weight, effects of vibration and leakage; and the effects of the space environments for a period of up to 10 years.

The effort undertaken to achieve these objectives included a literature survey, interviews with several agencies, analysis of applications, limitations of actuation techniques and, where applicable, a review of problem areas presently recognized by valve users throughout the aerospace industry.

Electromechanical Actuators

The electromechanical valve actuators in common use for application to liquid propulsion controls operating in space include the solenoid, motor drive and torque motor. The solenoid and torque motor valve actuators in present use are principally applicable to small shutoff valves and on pilot valves for use on pneumatic and hydraulic actuators. Motor drives are presently used where higher actuation forces are required and for positioning the metering pintle in the larger flow metering valves. Piezoelectric actuators are being investigated and used experimentally. They hold promise for future spacecraft use.

Solenoid Valve Actuators

The solenoid actuator is applicable to short stroke valves and valves requiring low force output and high response. Size, weight, power and response increases with an increase in stroke and solenoid force requirements. A limitation of the solenoid is the continuous applied current necessary to hold the plunger at the end of its stroke. If the duration of lock-up is long, the coil temperature may increase and cause insulation failure. Latching solenoids which mechanically lock the plunger in position are commonly used to avoid the necessity for long term holding currents. Magnetic latching utilizing a permanent magnet which holds the plunger in position is common for small solenoid valves.

Solenoid valve actuators operating in propellants represent a severe limitation since high performance magnetic core materials, being high iron alloys, are attacked by a number of the fuels and oxidizers. In addition, these materials are rather difficult to plate since they exhibit surface imperfections which are difficult to bridge. If a tight plating is not accomplished, corrosion will cause rapid unit failure. Plating materials such as nickel and chromium have been used in plating the magnetic core materials; however, a flaking of these platings has been observed in propellants such as hydrazine and this has resulted in functional valve failures. The plating materials used were compatible with the propellants; however, it is possible that some small imperfections in the plating, as installed, due to wear, or due to dimensional changes resulting from residual stresses or magnetostriction of the core, allowed some propellant to contact the core material. This would allow corrosion to commence under the plating, causing it to flake off.

Techniques are being sought to overcome these problems. One such technique was developed by the Parker Aircraft Company for use on the Apollo Project and consists of a vapor deposited gold barrier plating which is then diffused into the core surface. This coating was successful in providing the required protection against N_2O_4 , hydrazine and the nitric acid formed due to water flush of the system. Chrome diffusion coatings effectively prevent core material corrosion but the temperatures involved in the

diffusion process must be carefully controlled or a transition from alpha to gamma phase iron will occur with an accompanying reduction in magnetic properties. The quantity of chrome must be carefully controlled as it also degrades the magnetic properties of the materials. If wet coils are used, the core potting material must withstand the propellant, and insulation flaking must be controlled or contained to prevent valve contamination.

A technique involving complete encapsulation of the magnetic core material with an austenitic stainless steel sheath has been employed, as have ferritic stainless steel cores. Both of these approaches markedly decrease core performance, resulting in larger coils, higher power levels, or slower valve response.

Techniques involving the use of a diaphragm to separate the core material from the propellant have been used successfully. The diaphragm also provides flexure type bearing for the valve poppet and thus eliminates any sliding, moving parts. A typical valve is shown schematically in Figure 4-1. If high pressures are used in a valve of this design the pressure across the diaphragm must be balanced. One typical approach to this is to pierce the diaphragm with a small hole and use it as a bearing only. If this is done, the core material must once again be protected from propellant attack.

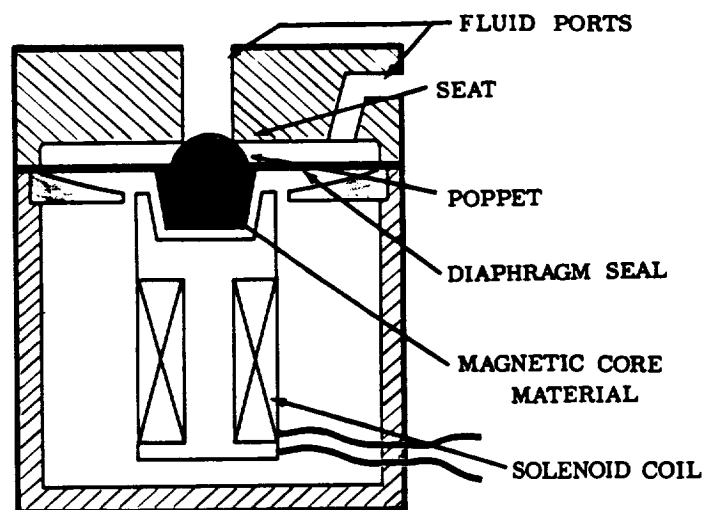


Figure 4-1. Schematic: Diaphragm Sealed Solenoid Valve

Solenoid actuators are within the state of the art for temperatures to 20°K or less, but are limited at higher temperatures due to material softening, winding insulation breakdown, and loss of magnetic properties in the core material.

Solenoids for use at temperatures in excess of 1000°F have been fabricated on a special order basis. The use of beryllium as a winding material for high and low temperature solenoid applications is attractive due to its high softening temperature, tenacious insulating anodic oxide film and low electrical resistivity. The use of beryllium for both high and low temperature applications has been investigated. The results of these investigations appear in the Advanced Valve Technology Interim Report, dated 1 November 1966, (Report No. 06641-6004-R000, Contract NAS 7-436).

Motor Drive Actuators

Electric motor driven valve actuators are used principally in large valves with modest response requirements. They are particularly useful in the fine positioning of pintles in precision metering valves and in heavily loaded shutoff valves.

Material compatibility limitations with motor driven actuators are similar to those in solenoid valves when they are immersed in propellants. These have been overcome in some cases by canning the motor rotor and field in a nonmagnetic stainless steel. This, however, does decrease motor performance. Problems are caused in dc motors due to commutation requirements. Since many propellants are electrical conductors, immersed brushes cannot be used. Lubricants required for use on bearings and gears may not be propellant compatible. These problems may be partially overcome by sealing the motor from the propellant; however, zero leakage (10^{-7} sccs) dynamic shaft seals are not within the present state of the art. Bellows or diaphragm hermetic shaft feed throughs may be used but these are bulky and are limited in pressure capabilities and cyclic life.

When shaft seals are used, the motor housing is often pressurized with a gas such as nitrogen to approximately the propellant pressure. This reduces

the pressure difference across the seal and minimizes the possibility of leakage into the motor. Exposure to the propellant vapor must be assumed in this type system.

Motor drives exposed to space vacuum may experience brush arcing, lubricant loss and cold welding of sliding parts. This may be partially alleviated through the use of brushless motors, special brushes, lubricants and materials, or by hermetically sealing the motor.

Minimizing the power input to servo motors used in positioning metering valves is an important consideration. A recent concept being developed by the Jet Propulsion Laboratory minimizes the power input required to a servoactuator through the use of a spring energy storage element analogous to a hydraulic accumulator. A low-powered electric motor of .02 hp running continuously is employed to produce momentary power output of .602 hp. The system operates as follows:

The electric motor drives the spring mechanism through a gear reducer. The spring output is attached to a reversing planetary drive, which also incorporates governors for speed control. Reversal of direction is accomplished by a brake system which can hold one of the ring gears stationary while the other is left free. The output is taken by a ball-nut and converted into linear motion for use in positioning (as for a valve pintle).

The following is a brief resume of the system's design goals:

Initial breakaway force	1000 lb
Available start force (springs)	400 lb
Available operating force	200 lb
Available stroke	1 in.
Time for 1 in. stroke	.05 sec
Peak output power	.602 hp
Average input power	.02 hp

The average output power cannot exceed the steady-state input power so the duty cycle for continuous operation is 1-1/2 seconds between full stroke cycles. The springs store enough energy for 4 complete cycles without depending on the input motor.

Torque Motor Actuators

Torque motor actuators are used primarily in small-to-medium metering and shutoff valves. They are often used in positioning spool type servo-valves. Torque motor actuators which are directly immersed in propellants share the magnetic material and insulation compatibility problems experienced with both the solenoid and motor driven actuators.

Several valve manufacturers have used flexible elements to isolate the torque motor from the propellant. These elements include the diaphragm pivots and flexing, thin-walled tubes. The diaphragm seal must be kept thin, to minimize torque and therefore, is normally limited to relatively low pressures. Diaphragm deflection with pressure may change critical air gaps, causing changes in actuator performance. This may be minimized by filling the motor cavity with an incompressible fluid such as an oil, to eliminate diaphragm flexing with line pressure changes. An oil fill has also been used to act as a vibration damper, particularly in the thin-walled tube designs. The thin-walled tubes used in some design have been found to fatigue, causing premature failures, particularly under vibration. A definite need has been expressed for a reliable low torque hermetic seal for use with torque motor actuators.

Piezoelectric Valve Actuators

Piezoelectric valve actuators are not presently in use in spacecraft; however, they hold promise for use in both shutoff and metering type valves. Piezoelectric actuators operate due to the change in dimension in certain materials when they are placed in an electric field. Changes of dimension of approximately 0.1 percent are readily obtainable with high force levels. These deflections require relatively high voltages which may range from approximately 300 to 3,000 volts depending on the material properties and

actuator configuration. Materials exhibiting good piezoelectric properties are normally quite brittle in nature. They have high compressive strength but relatively low (on the order of 10 times less) tensile strength. Any actuator design must take these material limitations into account. One typical approach to limiting this problem is preloading the piezoelectric material in compression.

The advantages of the piezoelectric actuator include low power consumption, precise positioning capabilities and high output force levels. When used on spacecraft which carry electric propulsion systems, the voltages required are easily obtained; otherwise, some type of power conditioning is required. If a large number of valves aboard are using piezoelectric actuation, the weight penalty for the power conditioning should be small.

Pneumatic Valve Actuators

Pneumatic actuators are used on large valves where the weight, power and size of an electromechanical actuator might be too great; and in metering valves such as pressure regulators, flow regulators and relief valves. They are the obvious choice in gas systems. Pneumatically actuated valves are piloted with small solenoid or torque motor actuated valves when an electrical actuation signal is required.

Where liquid propellant valves are used, pneumatic pressure for actuation is supplied from a separate source. This source may be a pressurized gas cylinder or a gas generator drawing fuel from the propellant line itself. The advantages of pneumatic actuation include:

- 1) High actuation forces in a small lightweight package
- 2) Overboarding of gases rather than liquid propellants

Most pressurant gases such as nitrogen, hydrogen, helium, argon or oxygen exhausting directly to space vacuum will not cause a freezing or snow problem when the gas is initially at room temperature, unless there is considerable water vapor present in the gas supply. Exhausting of moist gases could possibly result in a freezing (snow) problem.

Gas system relief valves and regulators are examples of pneumatic actuated valve types applicable over a broad range of sizes. Pneumatic actuators have an extremely wide range of operating temperatures from well below 20°K (36°R) to as high as a material may be made to contain the working fluid.

The advantages of pneumatically driven piston actuators are light weight, small size and design simplicity. Limitations are possible piston dynamic seal leakages, particularly at temperature extremes, and rubbing bearing problems. Piston actuators have been operated at temperatures ranging from 36°R to over 2000°F.

Bellows sealed pneumatic actuators provide a hermetic sealing capability over an extended range of temperatures and pressures. They do, however, complicate the design. Bellows actuators are more sensitive to vibration than piston or diaphragm types and tend to be heavier, particularly at high pressures. Life is limited by the fatigue life of the bellows material. Bellows sealed actuator designs tend to be heavier and larger than piston actuators for the same pressure and stroke capability.

Diaphragm sealed pneumatic actuators also provide a hermetic seal over a broad temperature and pressure range. They are relatively insensitive to vibration and light in weight for short stroke requirements. These actuators are limited in stroke for reasonable diaphragm diameters. Diaphragm actuators will withstand high overpressures without damage if the diaphragm is supported by a backing plate reproducing the free diaphragm contour at that deflection.

Pneumatic rotary positive displacement actuators include vane, Roots, gear and nutating disc motors. These have weight and size advantages in large valve sizes. Their complexity, leakage and the rubbing contacts involved in the bearings, gears, seals, etc., limit their use to large-sized valves.

Pneumatic turbine actuators are small in size and weight for their power output but require relatively large quantities of gas for operation. This limits their use to relatively specialized applications.

Hydraulic Actuators

Hydraulic actuators have been used for valves in spacecraft where actuation forces exceed the level normally attainable with solenoid actuators for the same size and weight. They are generally used to actuate large shutoff valves and metering type valves such as pressure regulators, flow regulators and relief valves. Like the pneumatic valve actuator, hydraulic units are often piloted with a small solenoid, or torque motor actuated valve.

Electromechanically actuated pilot valves are not normally isolated from the propellant, and therefore the compatibility problems discussed in the electromechanical actuator section must be considered.

The comments presented in the pneumatic actuator section with regard to the various actuator types generally apply also to hydraulically powered actuators. The actuator working fluid is normally the propellant itself. Long term exposure of actuator construction materials to propellants may constitute a compatibility problem. This is particularly true if moisture enters the system since corrosive acids are formed when water mixes with most storable propellants.

Seal materials may also present a compatibility problem, particularly in long term use. Most elastomers are attacked to some degree by strong oxidizing agents. Such long term attack could result in seal leakages or swelling which could cause actuator malfunction.

Another problem encountered with hydraulic actuators utilizing propellants involves overboarding of the propellant upon actuation. The freezing of propellants upon venting to space has been demonstrated on several occasions. Testing has shown that with a N_2O_4 system this has resulted in valve seizing due to a buildup of solid propellant on the valve. This was solved by exhausting the propellant through an opening in a shield plate which prevented frozen propellant from striking the valve. The freezing

of liquid propellants when vented to space vacuum has also been demonstrated for cryogenic propellants such as liquid oxygen, and hydrogen as well as pressurants such as liquid nitrogen and liquid neon. Freezing is a problem which must be considered in the design of liquid propellant valves and actuators venting to space. The use of heaters has been employed in some valves and lines to control this problem as has exhaust duct design.

Hydraulic actuators must operate within a narrower range of environmental temperatures than pneumatic actuators due to the freezing and vaporization characteristics of the propellants used. Actuators utilizing a liquid at low temperatures and the vapor at elevated temperatures can be produced. The vapor characteristics as well as the liquid properties must be considered in these designs.

Chemical Actuators

The only type of chemical valve actuator in general use on rocket engines is the solid propellant squib. Concepts for chemical actuation utilizing monopropellant and bipropellant combustion products are described in a later section.

Solid Propellant Squib

The most common chemical valve actuators in use are the squib or solid propellant explosive type. These are separated into two basic types, the deflagrating squibs and the detonating squibs. The deflagrating types are high rate gas generators and perform work by expansion of high temperature, high pressure gas. The detonators depend on a high intensity shock wave to drive the actuator.

Evaluation of squib cartridges after exposure to a variety of environmental conditions was performed as a part of previous Advanced Valve Technology studies. The results of these investigations are presented in the Advanced Valve Technology final reports dated July 1964 and August 1965 (Reports Number 8651-6032-SU000 and 8651-6042-SU000, Contract Number NAS 7-107).

The above referenced investigations indicated several problem areas. These included:

- 1) Severe degradation in performance after exposure to 300°F sterilization temperatures with some propellants
- 2) Leakage at ceramic insulator connector pins after firing
- 3) Fixed volume bomb tests gave insufficient data for repeatable squib performance evaluation

A concept originally reported as part of the Advanced Valve Technology Program for a work output tester (Pyromite was reduced to practice by a commercial vendor, and this device was found to give repeatable results in evaluating squib work outputs.

Reliability testing of squib actuators may have a significant program cost impact. This is due to the large number of charges which must be fired to assure proper performance in service. In addition the actual unit to be flown cannot be tested. Typically, ten times the required end use units must be fired from the same batch without a single failure to establish that the actuator will perform properly.

Initiation of explosive actuators in spacecraft is normally electrical. Both directly coupled and spark gap coupled bridgewires have been used. The directly coupled bridgewire type of initiator can be set off by currents induced in lead wires due to radio and radar transmission and other fluctuating electrical fields in the area. Spark gap coupled bridgewires are used to help overcome this problem. The firing of squibs by transmitting coherent radiation to them from a laser via a fiber optics bundle has been demonstrated by Space Ordnance Systems, Incorporated, El Segundo, California. This holds promise for future squib initiation.

Thermal Actuators

Thermal actuators are not presently used in spacecraft valve actuation. They are generally applicable to valves which do not require a fast response time. Examples of thermal valve actuators in commercial use are lawn sprinkler valves and fire sprinkler valves.

When thermal actuators are used, incorporating the control and actuating heat source with the spacecraft thermal management system should be considered since the spacecraft may contain several heat sources which utilize a coolant loop to carry the excess heat to a space radiator. If this is the case, actuation energy may be provided by ducting the hot or cold side coolant to the valve actuator. Control of the coolant loop flow could be provided by fluidic diverters and logic (see Section III), if this is compatible with the mission objectives. An added advantage is the utilization of heat energy that is otherwise wasted. This could result in a net saving in spacecraft power requirements. Several types of thermal actuators may be devised for valve actuation. The type chosen will depend on force level, response, heat source and control principle employed.

Manual Overrides

Manual actuator overrides have not been normally required on spacecraft valving in the past, though they have been used in aircraft and missile ground support applications. The manual override capability must be considered in systems evaluations of manned spacecraft systems where it may affect overall system reliability. Manually controlled valves have been used as primary and secondary controls in the life support systems on the Mercury and Gemini capsules. The use of manual controls or functions in these applications simplified overall system design and improved reliability. The use of man as an adaptive control element in a system has been demonstrated in aircraft ground and initial space systems. Further study is required on specific missions and systems to maximize the advantages of man's adaptive and analytic nature with respect to mission success probability.

HIGH SPEED SOLENOID VALVE ACTUATOR STUDY

Introduction

Solenoid actuated valves for use on spacecraft rocket propulsion systems are designed for minimum weight, minimum size, low electrical power consumption and high speed. These requirements can be enhanced when solenoid valve actuators are driven by circuits which provide a large electrical energy impulse during actuation and automatically switch to a modest holding power required during steady-state operation. The electrical impulse supplied from the electrical drive circuit should provide maximum energy force without reduced steady holding force. The electrical impulse energy required during actuation is stored in single or multiple capacitors which are electrically charged slowly. This technique avoids an impulse demand on the spacecraft electrical power source.

This study considers the general requirements and characteristics of impulse solenoid drive circuits and some of the practical limits on operating speed of solenoid actuators. Methods of improving other factors that limit speed are also discussed.

The characteristics of solenoid actuator circuits are studied by use of the general nonlinear variable coefficient differential equation describing the current-voltage characteristic of an active solenoid actuator. This equation is linearized for limited time intervals by appropriate adjustment of coefficients during selected portions of the operating transient. Appropriate operating intervals are selected by consideration of typical current-voltage characteristics. Armature motion effects are included by using variable coefficients for armature position and velocity during the motion interval.

Principles of Operation

A dc solenoid valve actuator usually obtains the electrical actuation power from a constant voltage, low impedance dc power supply. A semiconductor circuit is usually used to obtain nearly ideal switching. The

solenoid actuator includes an iron or iron alloy magnetic circuit which has a nonlinear relationship between magnetizing current and magnetic flux density; hence, accurate analysis is not possible using a single linear differential equation with constant coefficients. It is possible to understand the current-voltage, pull-in time behavior of solenoid actuators by using a linear differential equation with variable coefficients to account for armature motion. The nonlinear current flux density relationship is conveniently accounted for by readjusting the initial parameter conditions at selected intervals during the operation transient.

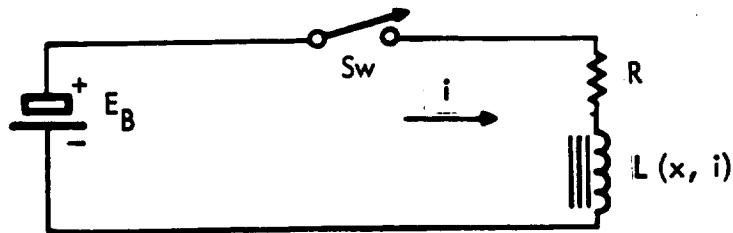


Figure 4-2. Solenoid Actuator Circuit

Figure 4-2 represents a simplified solenoid actuator circuit suitable for analyses of the current-voltage relationship of a solenoid actuator. The general nonlinear differential equation describing the current-voltage relationship of an active solenoid actuator is:

$$E(t) = \frac{d}{dt} [L(x,i) i(t)] + R i(t) \quad (1)$$

where

$E(t)$ = voltage applied to solenoid actuator as a function of time

$L(x,i)$ = apparent inductance of solenoid actuator as a function of armature position, x , and current $i(t)$

$i(t)$ = electric current flowing in the solenoid actuator as a function of time

The time intervals (Figure 4-3) are defined as follows:

- 1) The time o-a, immediately following application of electrical power but prior to armature motion
- 2) The time a-b, from initiation of armature motion until the armature reaches nearly full travel but has not decelerated
- 3) The time b-c, when deceleration and rebound of the armature appears near full travel
- 4) The time interval c-d, after armature motion following acutation has ceased

During this initial pre-motion interval, o-a, after application of power, the magnetizing current is low due to current rate limiting by the solenoid inductance. The solenoid inductance is much lower than the inductance at higher currents when the armature is partially closed. The inductance is low at low magnetizing currents because the nonlinear characteristic of iron and iron alloys results in a low initial magnetic permeability at low magnetizing forces and the air gap. The air gap accounts for most of the magnetizing force. Equation (2) may be used for the current-voltage characteristic during the initial interval o-a.

$$E_{oa}(t) = L_{oa} \frac{di}{dt} + Ri, \quad 0 \leq t \leq a, \quad i(0) = 0 \quad (2)$$

where

L_{oa} = the initial inductance (assumed constant)

$E_{oa}(t)$ = actuator applied voltage during interval o-a

During the initial motion interval a-b, the inductance increases with time due to armature motion and the increasing magnetizing force applied to the magnetic circuit. The inductance is a function of current and armature position during this interval; however, a suitable inductance, $L_{ab}(x)$, which is a function of armature position but independent of current, may be selected to fit this portion of the characteristic. For $L_{ab}(x)$, which is position dependent only, Equation (1) becomes Equation (3).

The circuit inductance in Equation (1) is a function of current, $i(t)$, and armature position, x , and hence requires an apriori knowledge of L for all expected operating combinations of i and x ; this is not usually available. Approximate values of L which are independent of i may be selected for appropriate time intervals of a typical current-voltage transient.

This approximation simplifies Equation (1) and enables an understanding of the current-voltage/time characteristic including the effects of armature position and velocity. The typical current-voltage transient of an active solenoid actuator, Figure 4-3, illustrates the choice of time intervals and provides the basis for the appropriate simplified differential equations which are applicable during each selected time interval.

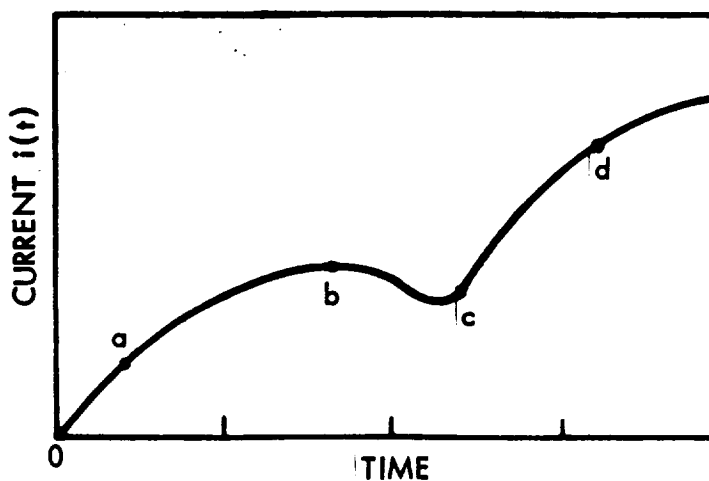


Figure 4-3. Typical Current Transient Characteristic Curve for Solenoid Valve Actuator

$$E(t) = \frac{d}{dt} \left[L_{ab}(x) i(t) \right] + R i(t)$$

$$E_{ab}(t) = i(t) \frac{d}{dt} L_{ab}(x) + L_{ab}(x) \frac{d i(t)}{dt} + R i(t)$$

$$E_{ab}(t) = i(t) \frac{dL_{ab}(x)}{dx} \frac{dx}{dt} + L_{ab}(x) \frac{d i(t)}{dt} + R i(t) \quad (3)$$

for $a \leq t \leq b$, $i(a) \leq i(t) \leq i(b)$

where $L(x)_{ab}$ = inductance for $x(a) \leq x \leq x(b)$

$E_{ab}(t)$ = applied voltage for interval a-b

Equation (3) differs from the non-motion Equation (2) by the addition of a velocity dependent voltage and a position dependent coefficient for the rate of change of current.

During the final motion interval when deceleration and rebound exist, the inductance, $L(x)$, is nearly constant at a final position value L_c , hence for the final motion interval, b-c-d, depicted in Figure 4-3.

$$E_{bd}(t) = i(t) \frac{dL_c}{dx} \frac{dx}{dt} + L_c(x) \frac{d i(t)}{dt} + R i(t) \quad (3a)$$

$i(b) \leq i(t) \leq i(d)$, $b \leq t \leq d$

$E_{bd}(t)$ = applied voltage for interval b-d

During the interval when armature motion ceases after application of power $L(x) = L_d$ and $\frac{dL(x)}{dx} = 0$, hence:

$$E_{de}(t) = L_d \frac{d i(t)}{dt} + R i(t), \quad d \leq t \leq e \quad (4)$$

$E_{de}(t)$ = applied voltage for interval d-e

Breakaway Time

During the initial linear operating interval (o-a, Figure 4-3), prior to breakaway, the armature force and breakaway speed will be proportional to the applied voltage from equation (1) $E_b = L_{oa} \frac{dI_o}{dt}$, $I(o) = 0$, at $t = 0$

$$\text{hence, } \frac{dI(o)}{dt} = \frac{E_b}{L_{oa}}, \quad \frac{\Delta I_{oa}}{\Delta t_{oa}} \approx \frac{E_b}{L_{oa}} \quad (5)$$

$$\text{and } \Delta t_{oa} \approx L_{oa} \frac{\Delta I_{oa}}{E_b},$$

where: Δt_{oa} = breakaway time

ΔI_{oa} = breakaway current

L_{oa} = initial inductance of the solenoid actuator

E_b = voltage applied to the solenoid actuator

Operating Time

Subsequent to breakaway, the armature velocity, $\frac{dx}{dt}$, will be proportional to the applied voltage; hence, the armature pull-in speed is proportional to applied voltage for linear circuit operation. If the magnetic force is a monotonically increasing function of current but is less than a proportional rate of increase, a diminishing improvement in pull-in velocity will result with increasing current.

The cusps in the $I(t)$ curve of Figure 4-3 between b and d are due to armature bounce. This characteristic will depend on construction of the actuator. For example, a stiff spring and hard stop for the armature at the full limit of travel may have conspicuous bounce cusps unless the armature motion is damped by fluid damping and armature friction. The bounce characteristic cannot be used as final criteria of solenoid quality since

poppet clearances, stop hardness, fluid viscosity, pressure, etc., will differ between valves. It is obvious that a fast solenoid actuated valve with conspicuous bounce characteristics is unsuitable for controlling pulses of fluid flow whose pulse width is comparable to the bounce interval.

Electrical Impulse Drivers

High actuator speed may usually be obtained from electrical impulse solenoid drivers. Spacecraft power supplies are usually low voltage and may provide a limited peak demand and steady power to a solenoid actuator. The actuator power consumption is also limited by size, weight, and temperature rise. An impulse electrical supply may supply high peak powers to a solenoid actuator during actuation without excessive actuator heating. The transient and steady power demand of the impulse supply may be small compared to the solenoid holding power. The weight and power consumption of an impulse driver should be less than required for a larger solenoid actuator to achieve a corresponding result from a constant voltage supply. In addition, a fail-safe circuit is desired which will provide power at reduced impulse if a component malfunction develops. A capacitor storage impulse driver can meet these basic weight and power requirements.

The capacitor storage impulse driver charges N capacitors in parallel while the solenoid actuator is off or in a steady holding condition. The capacitors automatically connect with their voltage in series aiding with the power supply when the valve is actuated. When the capacitor stored energy is depleted, the capacitor automatically connects for recharge and standby until a valve actuation requires the impulse energy. This capacitor switching logic corresponds to the practice used for many years for high voltage impulse generators exemplified by the Marx trigger circuit. Figure 4-4 illustrates the logic of a capacitor storage solenoid actuator driver.

The breakaway time may be reduced by a factor $\frac{1}{(N+1)}$ times by N series connected capacitors charged to the power supply voltage. For N capacitors

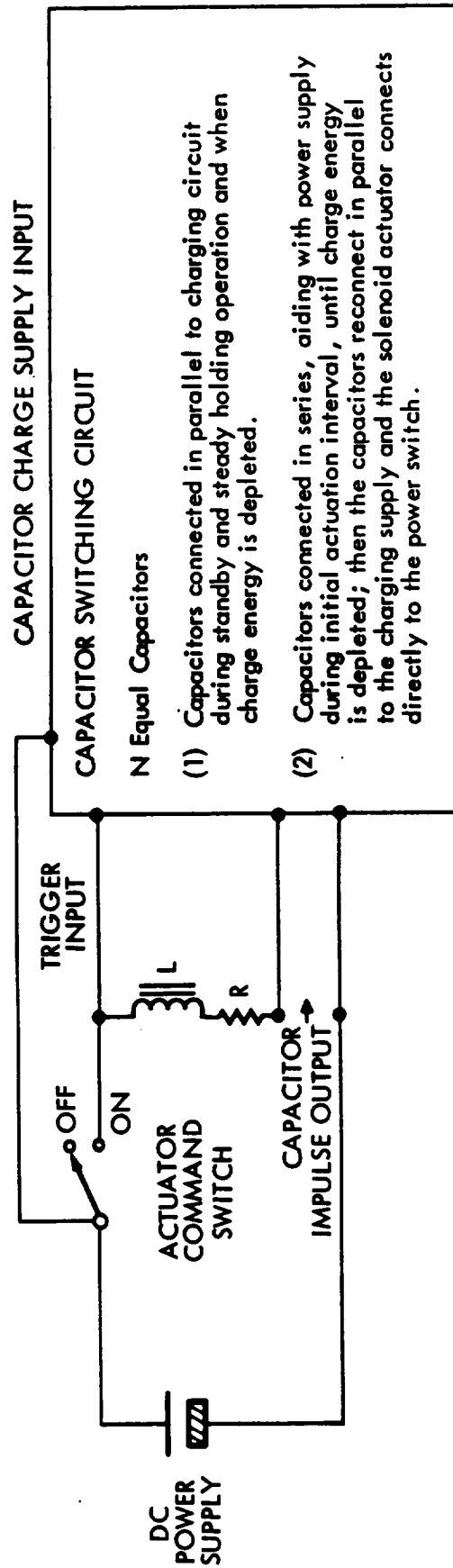


Figure 4-4. Capacitor Impulse Actuator Driver

the breakaway time, Δt_{oaN} , is:

$$t_{oaN} = \frac{L_{oa} \Delta I_{oa}}{(N+1)E_b} = \frac{\Delta t_{oa}}{(N+1)} \quad (6)$$

If we select an approximate initial inductance value for $L(x)_{ab}$ which is independent of magnetizing current, the pull-in time, Δt_{ac} is also improved by the factor, $\frac{1}{N+1}$, when N charged capacitors are series connected.

For N capacitors, the pull-in time, Δt_{acN} , is:

$$\Delta t_{acN} = \frac{\Delta i_{ac}}{(N+1)} \quad (7)$$

The actual improvement in Δt_{acN} will be less than given by Equation (7), depending on the degree of magnetic circuit saturation.

Equations (5) and (6) assume the charge stored in each of the N capacitors is sufficient to supply the solenoid current for the time intervals Δt_{oaN} and Δt_{acN} with a negligible decrease in capacitor voltage; however, a decrease in capacitor voltage is required to supply the current to the solenoid actuator. If we assume the rate of change of current is constant at the initial value at $t = 0$, $\frac{di(0)}{dt}$, we can make a conservative estimate of the capacity and number of capacitors required for a desired improvement in pull-in time, Δt_{ac} . The pull-in speed improvement factor, A , assuming a linear differential equation is:

$$A = N + 1 = \frac{\Delta t_{ac}}{\Delta t_{acN}} \quad (8)$$

where: N = number of series capacitors in the current impulse supply

Δt_{acN} = pull-in time with N capacitors

Δt_{ac} = pull-in time with only the constant voltage supply

A = pull-in speed improvement factor for N capacitors

The capacitors supply the solenoid current ($i(t)$) for a time Δt_{ocN} with a corresponding decrease in charge, ΔQ_c , and voltage, ΔE_c ,

$$\Delta Q_c = C \Delta E_c = \int_0^{\Delta t_{oc}} i(t) dt \quad (9)$$

where: ΔQ = decrease in charge of each capacitor
 ΔE_c = decrease in voltage of each capacitor

Using the conservative assumption that

$$\frac{di}{dt} \sim \frac{d i(o)}{dt}$$

$$\Delta Q_c = \int_0^{\Delta t_{oc}} i(t) dt \sim \int_0^{\Delta t_{oc}} t \frac{d i_o}{dt} dt$$

$$\Delta Q_c \sim \frac{\Delta t_{oc}^2}{2} \frac{d i_o}{dt} \quad (10)$$

$$\frac{d i_o}{dt} = \frac{(N+1)E_b}{L_o}$$

For N capacitors, ΔQ_N and C_N are:

$$\Delta Q_N \sim \frac{\Delta t_{oc}^2}{2} \left(\frac{(N+1)E_b}{L_o} \right) \cong C \Delta E_c \quad (11)$$

$$C_N \sim \frac{(N+1)E_b \Delta t_{oc}^2}{2L_o \Delta E} \quad (12)$$

Equation (12) will give the required capacity for each capacitor, C , corresponding to a given decrease in capacitor voltage, ΔE , during the time, Δt_{oc} . A conservative value of ΔE is 10 percent of E_b . For $\Delta E = .1E_b$ Equation (12) becomes:

$$C_N \approx \frac{(N+1) \Delta t_{oc}^2}{.2L} \quad (13)$$

from Equation (8) the number of capacitors, N , is:

$$N \approx \frac{\Delta t_{oc}}{\Delta t_{ocN}} - 1 = A - 1 \quad (14)$$

Equations (11) and (12) give a conservative value for the capacity of each capacitor, C_N , and the number of capacitors, N . It is possible to obtain the same speed improvement with a larger N than given by Equation (13) with a corresponding decrease in C ; however, the capacitor total weight and energy storage density does not improve and additional switching components are required. A lower value of C than given by Equation (12) may produce the desired speed improvement factor A since the Equation (12) is a conservative approximation. Experimental successive approximations based on an initial trial value given by Equation (11) is an appropriate method to determine a precise value of C_N required for the desired Δt_{acN} .

Electrical Requirements of Impulse Circuits

The current, power, and energy requirements for the capacitor discharge solenoid driver may be determined when the capacity, C_N , the number of capacitors, N , and the power supply voltage, E_b , are selected. The capacity C_N and N are determined by speed requirements using Equations (13) and (14).

The total stored energy, T_{CN} , in the N capacitors, is:

$$T_{CN} = \frac{N C E_b^2}{2} \quad (15)$$

Where: T_{CN} is the total capacitor stored energy in Joules or Watt seconds
 C_N is in Farads
 E_b is in Practical Volts

The energy loss in the capacitors is small; hence, most of the energy stored in the capacitors is delivered to the solenoid during the driving impulse.

The energy supplied by the power supply circuit to charge the capacitors exceeds the energy stored in the capacitor by the charging circuit losses, T_r , which are largely dissipated in the charging resistance. The charging circuit loss is always equal to the energy stored in the capacitor.

For N capacitors:
$$T_{rN} = T_{CN} = \frac{N C E_B^2}{2} \quad (16)$$

The total energy delivered by the power supply, T_b , to charge the capacitors is for N capacitors:

$$T_b = N C E_B^2 \quad (17)$$

The peak charging current for N capacitors, \hat{I}_c , is:

$$\hat{I}_{cN} = \frac{N E_b}{R_c} \quad (18)$$

where R_c is the charging circuit resistance in ohms, the charging current, $I_{cN}(t)$, is for N capacitors:

$$I_{cN}(t) = \frac{N E_B}{R_c} e^{-t/R_c C_N} \quad (19)$$

where: t is the time in seconds after application of the charging voltage, E_b , in volts, and e is the natural base = 2.718.

The voltage on the charging capacitor, $E_c(t)$, is:

$$E_c(t) = E_b \left[1 - e^{-\frac{t}{RC_N}} \right] \quad (20)$$

Typical values of $\frac{E_c(t)}{E_b}$ for selected values of t/RC_N are given in the following table:

Table 4-1.

t/RC_N	4.6	3	2.3	1.61
$\frac{E_c(t)}{E_b}$.99	.95	.90	.80

The power demand from the battery $P_b(t)$, during charging is for N capacitors

$$P_b(t) = \frac{N E_b^2}{R} e^{-t/RC_N} \quad (21)$$

The capacitor charging time, t_1 , to a specified fraction of the supply voltage, $\frac{E_c(t)_1}{E_b}$, will also determine \hat{I}_c for a given C , t_1 is:

$$t_1 = -RC \ln \left(1 - \frac{E_c(t_1)}{E_b} \right) \quad (22)$$

The \hat{I}_{cN} corresponding to t_1 is for N capacitors:

$$\hat{I}_{cN} = \frac{N E_b}{R_c} = \frac{N C E_b \ln \left(1 - E_c(t_1)/E_b \right)}{-t_1} \quad (23)$$

An independent choice of charging time t_1 and \hat{I}_{CN} is not possible unless C is permitted to vary from the value defined by Equation (13). Since the C determined by Equation (13) is a conservative estimate for C , some reduction in C is possible. If \hat{I}_{CN} is limited by the power supply capability then the value of charging time, t_1 , corresponding to the permitted peak charging current, I_{CN} , must be used. Hence:

$$t_1 = \frac{N C E_b \ln \left(1 - E_c(t_1)/E_b \right)}{I_{CN}} \quad (24)$$

Limiting Speed of Operation

Equation (12) suggests the speed improvement factor A will continue to increase in proportion to N ; however, there are practical limits to A beyond which a diminishing improvement in A is obtained with increasing N . Some of the factors causing severe deviations from the linear relationship of Equation (8) are:

- 1) The bulk of the magnetic material becomes saturated at $\Delta t < \Delta t_{ocN}$.
- 2) The rate of increase of current and magnetic induction is too rapid to permit full penetration of the magnetic field into the magnetic structure, thus limiting the possible rate of increase of the total magnetic force.
- 3) The breakaway force required for a solenoid armature has been assumed constant; however, it may have additional force requirements which are dependent on the rate of application of breakaway force.
- 4) The mechanical friction forces are assumed to be proportional to velocity. Additional nonlinear forces proportional to the square of the velocity may be important when valve fluid loads with velocity squared forces are important.
- 5) Good magnetic materials are subject to inelastic deformation and plastic or fluid flow when the rate of application of magnetic stress exceeds the stress propagation velocity in the magnetic material.

The above five limiting factors show improved operating speed can be obtained with an electrical impulse driver for low values of the improvement factor A. The speed limits which may be realized in properly constructed solenoid actuators can approach the speeds obtained by magnaforming or explosive actuated actuators; however, repeated cycle operation will obviously be sacrificed. The upper speed limit of the electrical impulse solenoid driver corresponds to the speed of magnaforming techniques.

Improvement of Limiting Speed

When the practical operating speed limit of existing solenoid actuators have been realized with an electrical impulse driver, the above five factors limiting further speed improvement may be considered to select methods which will yield the greatest improvement in speed.

Some of the methods for improvement of each limiting factor are:

1) Improvement of Bulk Saturation Flux Density - If the active magnetic structure is saturated for $\Delta t < \Delta t_p$, the depth of penetration due to a rapid buildup of magnetizing induction is not limiting the actuation speed. A higher acceleration force and speed may be obtained by using a magnetic material with a higher saturation flux density obtainable by improved heat treatment and/or alloy composition. If this is not possible, it is necessary to increase the active cross-sectional area of the magnetic circuit transverse to the direction of magnetic field. In the case of the moving armature, this change should be accomplished without increasing the mass of the armature; i.e., the increased armature cross-sectional area must be accompanied by an equal squared thickness or length reduction.

In cases where higher saturation magnetic materials are available, the pull in speed is improved in direct proportion to the square of the saturation flux density, assuming the magnetic field penetration remains complete.

$$\frac{\Delta t_{p1}}{\Delta t_{p2}} = \frac{B_{2 \text{ sat}}^2}{B_{1 \text{ sat}}^2} \quad (25)$$

where: Δt_{p1} = pull-in time with magnetic material No. 1
 Δt_{p2} = pull-in time with magnetic material No. 2
 B_{1sat} = saturation flux density of magnetic material No. 1
 B_{2sat} = saturation flux density of magnetic material No. 2

A common example of improvement in magnetic material is the substitution of optimum annealed permendur^R for low carbon steel or pure ingot iron. The saturation flux density by this substitution may be improved from 12 to 15 kilogauss for low alloy iron to 20 to 22 kilogauss when permendur is used. The corresponding pull in speed ratio would be:

$$\frac{\Delta t_{p1}}{\Delta t_{p2}} = \left(\frac{B_{2sat}}{B_{1sat}} \right)^2 = \left(\frac{22}{12} \right)^2 = 3.68 \text{ times}$$

2) Improvement of Magnetic Field Penetration Velocity - When the rate of increase of magnetic force on the armature is limited by the rate of increase of magnetic field penetration to the full dimension of the armature and magnetic circuit, improvement in performance requires a material or construction change which allows a faster buildup of the magnetic field. A decrease in electrical conductivity or magnetic material thickness will permit a faster increase in magnetic field. The propagation constant for a magnetic wave in a conducting, homogeneous, isotropic, linear magnetic material is:

$$\gamma = \sqrt{j \omega \mu g} = \alpha + jB ; \alpha = B = \sqrt{\frac{\omega \mu g}{2}} \quad (26)$$

where: γ = the complex magnetic wave propagation constant
 α = the magnetic wave attenuation constant in nepers per meter
 B = the magnetic wave phase constant in radius per meter
 j = $\sqrt{-1}$ the imaginary factor
 ω = $2\pi f$ where f is the real wave frequency
 μ = permeability of the magnetic material in Henry's per meter
 g = conductivity of the magnetic material in ohm meters

The attenuation of the magnetic wave in the magnetic material may be reduced by reducing μ or g or both. The reduction of μ is somewhat unattractive because a higher magnetizing current is required to obtain a desired flux density and mechanical force. The conductivity may be reduced by appropriate alloying elements and heat treatment. The conductivity reduction should not be accomplished by a corresponding reduction of permeability, μ , or saturation flux density, B_{sat} . The bulk conductivity of a given material may be reduced by compressing small insulated particles together to obtain the bulk configuration. Insulated laminations assembled to fit the desired physical shape may also be used. The method of subdivision and assembly must cause a minimum degradation of the apparent bulk magnetic properties. Examples of magnetic wave attenuation improvement by alloying are the substitution of silicon steel for high purity ingot iron and the substitution of 2 percent vanadium permendur for 50/50 permendur. The use of high purity compressed insulated iron powder or flake for bulk iron magnetic structures is not attractive for high force solenoid actuators because of the poorer bulk magnetic properties of the compressed materials. Magnetic materials with low conductivity and low magnetic wave attenuation such as ferrites are available; however, their saturation flux density of 4 kilogauss precludes their use in high force density actuators.

A survey of the methods to improve the speed of magnetic field penetration and the consequent limiting speed of armature force buildup indicates bonded laminates of high saturation magnetic alloys will produce the highest actuator speed and force density. Laminates of .001-inch-thick sheets are available resulting in apparent bulk permeabilities and saturation flux densities which are 90 to 95 percent of the static characteristics for the solid material. It is possible by use of insulated magnetic laminates to obtain full magnetic force speeds less than 0.1 millisecond. The laminate bonding must have sufficient strength to endure the acceleration and shock loads which are possible with high speed buildup or decay of magnetic force.

3) Improvement of Breakaway Speed - A solenoid actuator usually works against a spring force which is installed to insure return of the actuator armature to a required unenergized position. An initial preload force is

included in the spring to assure armature return for all operating conditions and maintain stability under environmental accelerations. Reduction of spring preload will reduce the breakaway time and the minimum shock and acceleration tolerance. It is assumed that materials and surface finishes are selected to minimize static friction.

4) Improvement of Dynamic Friction - Dynamic friction will limit the speed of operation for a given applied magnetic force. Valve actuators are required to move a valve closure against a fluid stream velocity and pressure. It is possible to design valve closure mechanisms which balance the fluid forces on the closure element with identical forces on a balancing element. This technique may complicate the design and reduce reliability; hence, the application must be carefully considered.

5) Improving Speed Limit By Inelastic Deformation of Actuator

Materials - The maximum saturated magnetic pressure obtainable from the best available magnetic materials is approximately 600 psi which is much lower than the permissible stress in most structural and magnetic materials; hence, this inelastic deformation of actuator materials is not limiting for efficient solenoid actuators operating at near saturation flux densities. Electromagnetic forming or deformation requires much higher magnetic field intensities for the transformation of the electrical energy into mechanical kinetic energy prior to the material deformation. This electromagnetic forming transformation of electrical energy to mechanical forming forces does not appear to be an efficient method of operating solenoid actuators.

Ideal Impulse Voltage Characteristic

The electromechanical factors limiting speed of electromechanical actuators and the basic requirements to improve the speed with a multiple capacitor impulse driven circuit have been considered. Voltage time characteristics obtained with the multiple capacitor impulse driver is not an ideal characteristic, but it does represent a good compromise consistent with requirements of reliability and simplicity. An ideal impulse drive voltage

characteristic may be established which will give maximum speed for minimum electrical energy consistent with electrical and mechanical stress limits. Figure 4-5 represents an idealized impulse voltage time characteristic considering the material stress limits.

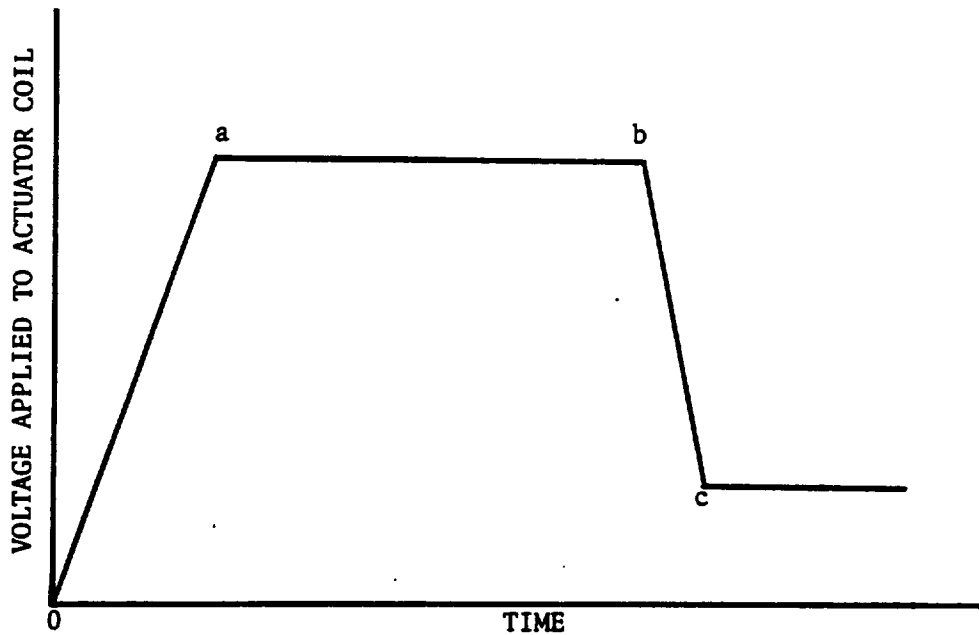


Figure 4-5. Ideal Solenoid Drive Impulse

The maximum impulse voltage E_{ab} (Figure 4-5) of the ideal impulse driver is determined by the coil electrical insulation requirements. This voltage represents the greatest rate of change of current and magnetic force obtainable with acceptable electrical insulation life. The impulse voltage must be applied and removed at a limited rate during intervals 0-a and b-c (Figure 4-5) because the impulse voltage propagates the coil at a low velocity, causing large voltage differences between adjacent turns and layers of the actuator coil. The large voltage differences can cause voltage overstress of the interturn and interlayer insulation. For maximum speed, the full impulse voltage, E_{ab} (Figure 4-5), must be sustained during armature motion. After the armature position is static following actuation,

the actuator voltage may be gradually reduced to a voltage, E_{ce} , which is sufficient to hold the armature position against the return spring, fluid and external acceleration forces.

It is possible to construct a circuit which will generate a nearly ideal turn-on pulse similar to Figure 4-5 for driving solenoid actuators; however, the component, weight and reliability will not compare favorably with the multiple capacitor impulse driver. The switching logic for the low voltage trapezoid impulse driver circuit can be identical to the capacitor circuit, except the capacitor energy storage components are replaced by lumped or uniformly distributed L-C transmission line elements with a round trip propagation time equal to the desired impulse time.

Conclusion

The speed and performance of solenoid actuators can be improved by use of electrical impulse driver circuits with a reduction in weight and electrical power demand and consumption. Low voltage series-parallel capacitor switching circuits are an effective way to obtain impulse voltages for this purpose. The approximate capacitor requirements can be easily determined by the speed improvement ratio required for a given actuator design recognizing other practical factors limiting speed.

A nearly ideal impulse driver circuit can be constructed; however, the weight, simplicity and reliability are less favorable than the simple capacitor switching impulse driver.

CONCEPTUAL STUDIES

Monopropellant Actuator Concept

Liquid hydrazine monopropellant gas generators have been developed for use in spacecraft rocket engines and for spacecraft propellant pressurization systems. A concept incorporating an integral actuator and monopropellant gas generator was conceived and tested during this reporting period. This actuation technique is capable of producing high pressures from small quantities of fuel, resulting in high actuation forces. The measured work output of the unit compared very favorably to that of squib type actuators (see Advanced Valve Technology Final Report Number 8651-6042-SU000, August 1965).

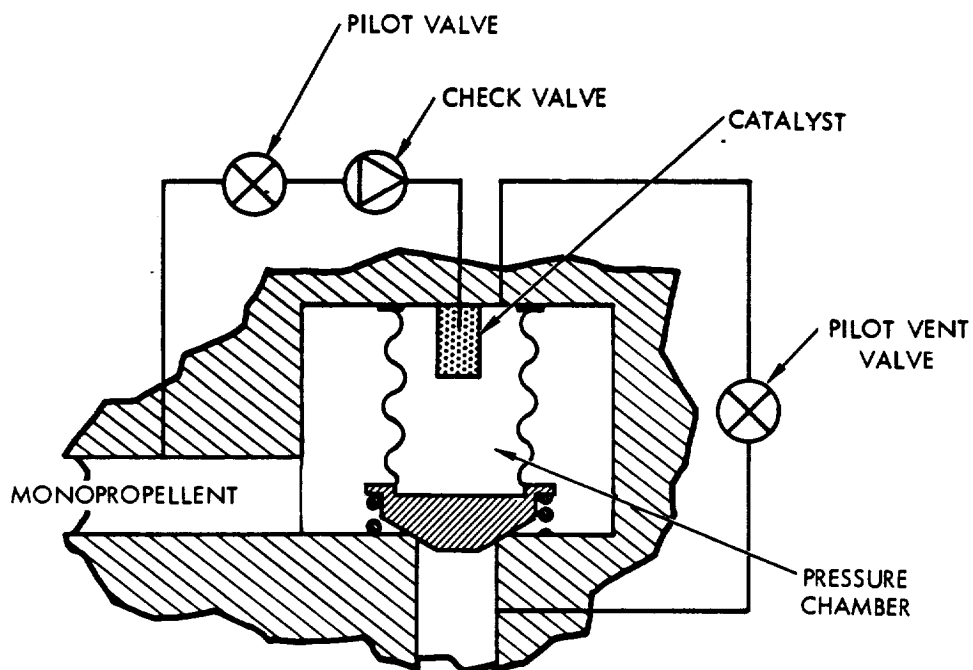


Figure 4-6. Schematic: Monopropellant Chemical Actuator
(For Normally Open Valve)

The operation of the monopropellant unit shown in Figure 4-6 is as follows. Since the valve is shown normally open, initially there is flow through the

valve. When turn-off is desired, a pilot valve is pulsed, allowing a predetermined amount of monopropellant to flow through it, the check valve, and catalyst, into the actuator's pressure chamber. The pressure thus formed, acts against the piston or bellows head of the actuator to close the valve. The effects of high pressure on the pilot valve are minimized by the check valve, which prevents back flow in the actuated condition. When the valve is to be opened, the pilot vent valve is opened, venting the pressure from the actuator. The vented gas may be directed back into the line or overboard. If more positive opening is desired, a second actuator similar to the first but arranged to act in the opposite direction may be used. Three-way pilot valves may be used to replace the separate pilot and pilot vent valves. The advantage of using two separate valves for piloting is that they need to be opened only momentarily for valve actuation, reducing power requirements without the use of latching solenoid type valves.

Feasibility Tests

A monopropellant actuator was constructed and tested to determine the feasibility of the design. Hydrazine was used as the working fluid. Successful actuations with restraining loads to 265 lb were demonstrated. Piston transfer times as low as 60 ms for a 2.75 in. stroke were observed.

The system used in performing these tests is shown schematically in Figure 4-7. Recordings were taken of valve current, fuel volume injected, actuator stroke, actuation pressure and restraining pressure versus time.

Test firings were performed for fuel supply pressures ranging from 150 to 350 psi and restraining pressures from 100 to 600 psi. A typical plot of pressure and displacement versus time is shown in Figure 4-8.

After a total of 25 test firings the actuator was disassembled for examination. A strong odor of ammonia typical of hydrazine reactions was noted. The presence of catalyst "fines" was observed in the actuation chamber. The actuator elastomer seals seemed unaffected by the test firings. No erosion

of the actuator internal surfaces was evident. A photograph of the disassembled actuator after test is shown in Figure 4-9.

The monopropellant actuator concept has been demonstrated to be feasible. Actuation with high force level has been demonstrated with fuel consumption over an order of magnitude less than if direct line piloting was used. It is felt this approach has promise for applications in spacecraft valves and should be pursued further for specific applications. The concept may also find application in other spacecraft actuation functions such as boom extension, spacecraft positioning on planet surfaces and in powering tools for space maintenance functions.

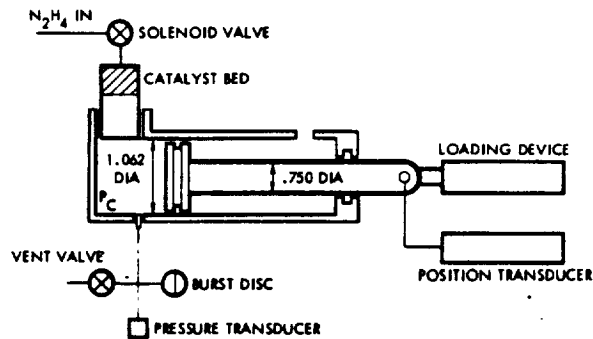


Figure 4-7. Schematic: Monopropellant Chemical Actuator Concept Tests

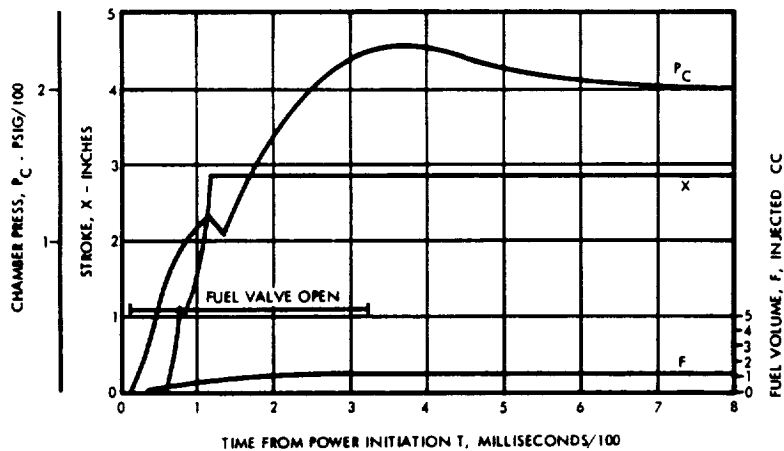


Figure 4-8. Performance Curve - Monopropellant Chemical Actuator

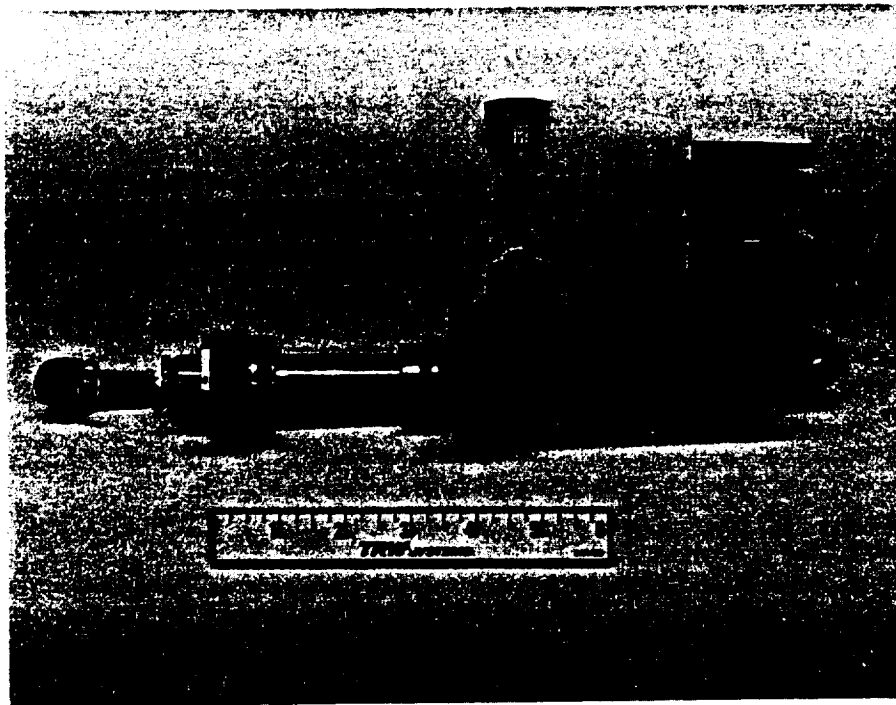


Figure 4-9. Monopropellant Chemical Actuator Test Unit

Bipropellant Actuator Concept

The bipropellant actuator is very similar to the monopropellant unit described above. It is apparent that a hybrid (liquid-solid) actuator containing a quantity of fuel or oxidizer internally could also be utilized. Figure 4-10 illustrates a bipropellant chemical actuator applied to a normally closed valve. Operation is very similar to the monopropellant unit except that both fuel and oxidizer injection is necessary. Positive actuation in both directions may also be obtained, eliminating the spring used for closure. The bipropellant actuation concept may also be applied to other spacecraft actuation functions requiring high force levels. The advantages of using propellant combustion for actuation are similar to those for squibs used for actuating explosive valves, except that many actuation cycles are possible.

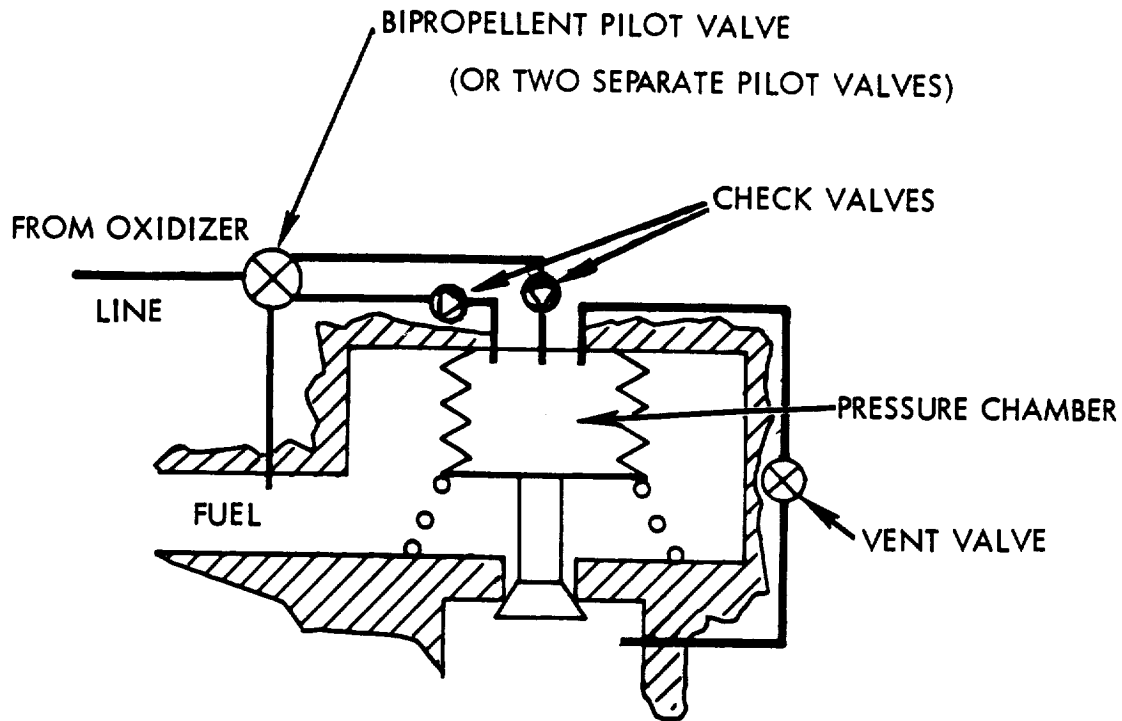


Figure 4-10. Schematic: Bipropellant Chemical Actuator
(For Normally Closed Valve)

Other Chemical Actuators

Electrochemical, photochemical and biochemical actuators have been proposed. These act due to a volume change associated with a chemical reaction driven by one of the above techniques. These types of actuators are not used at the present time and more data as to their possible characteristics is required.

Thermal Actuator Concepts

The types of thermal actuators include the following: solid differential expansion actuators, liquid or vapor expansion actuators, state change and phase change actuators (Polyphase). Schematic diagrams shown in Figures 4-11 and 4-12 illustrate possible mechanizations of these techniques.

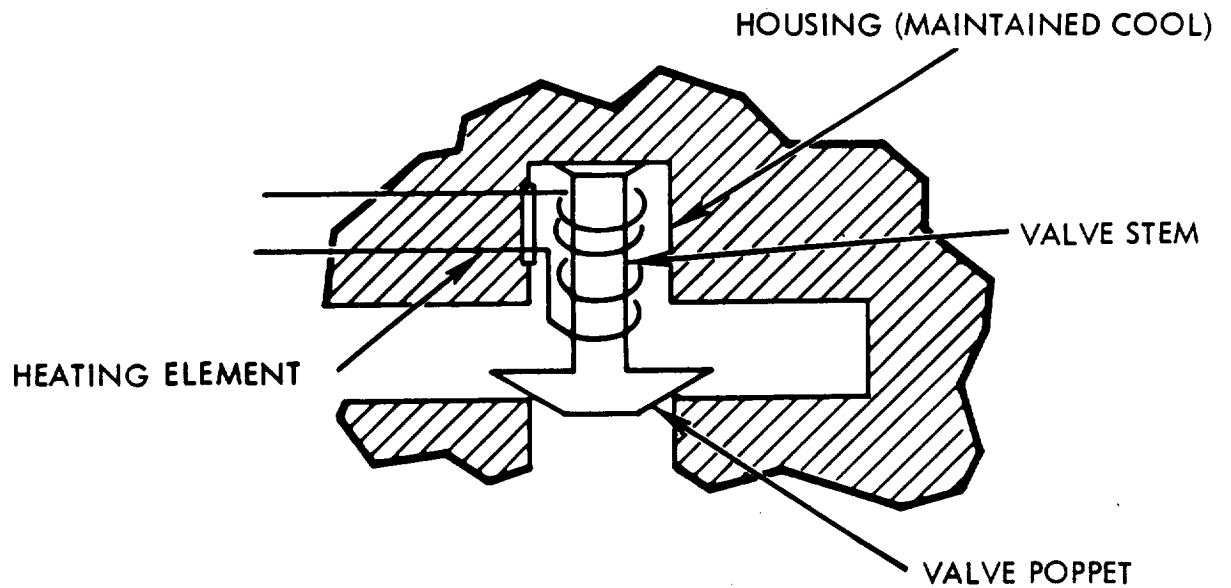


Figure 4-11. Schematic: Differential Expansion Actuated Valve

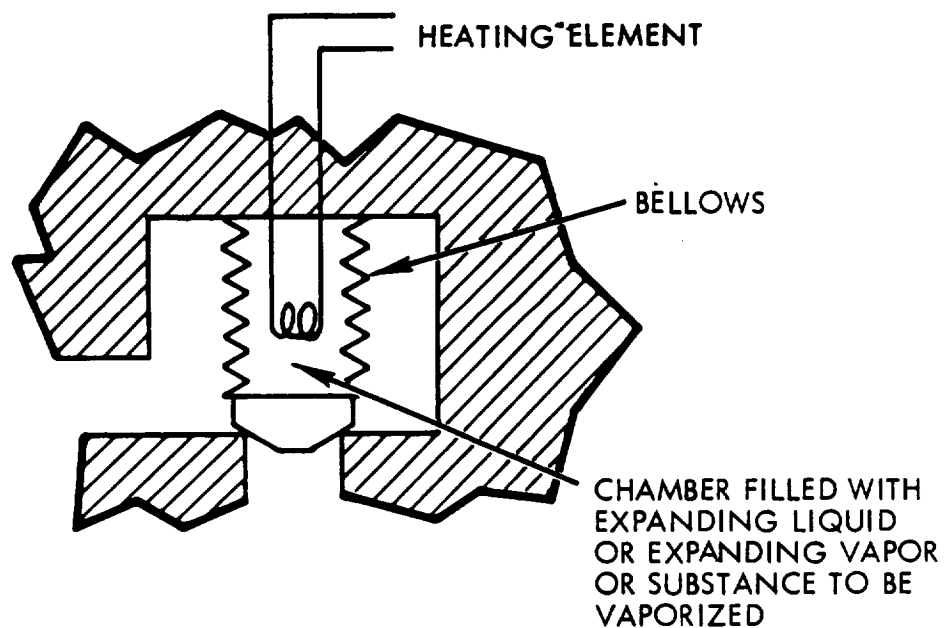


Figure 4-12. Schematic: Thermally Expansive Fluid or Polyphase Actuator Actuated Valve

Thermal actuators have slower response than solenoid actuated valves due to the thermal lags associated with transferring heat into or out of a system. These lags are controlled by the relative temperature difference between the heater and the object to be heated, the heat transfer coefficient between the two, and the thermal inertia of both. For constant heater output and constant specific heat, the time rate of change of temperature may be described as

$$\frac{dT}{dt} = \frac{Q}{(W_1Cp_1 + W_2Cp_2 + \dots)} \quad (1)$$

where

- T = Temperature
- t = Time
- Q = Heat input into area to be heated
- W = Weight of heated part
- Cp = Specific heat of heated part

The actual temperature of the part at any time t may then be described as:

$$T = T_o + \frac{Qt}{(W_1Cp_1 + W_2Cp_2 + \dots)} \quad (2)$$

where

T_o is the initial temperature of the part

From Equation (2) it is evident that the valve response may be improved (minimizing the actuation time) by increasing heat input and, decreasing the mass and specific heat of the actuating part. Figure 4-13 schematically illustrates a concept where this has been considered. In this valve a thin bimetallic diaphragm is used to provide high actuation forces in a snap acting manner while minimizing the mass of the actuating element.

In the valve shown in Figure 4-13, heat may be introduced directly to the actuation diaphragm, electrically or from a separate source, opening the

valve. The propellant then impinges on the diaphragm and provides an effective means for removing heat from it. This allows rapid closure when the heater is turned off.

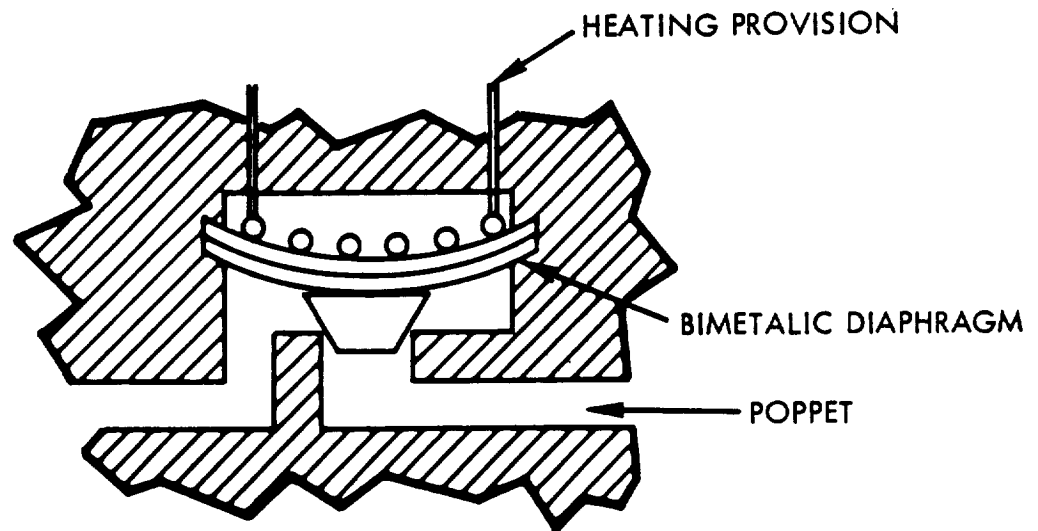


Figure 4-13. Schematic: Snap Action Differential Expansion Actuated Valve

Lightweight Electromagnetic Actuator

The objective of this study is to investigate beryllium as an electrical conductor of electromagnetic actuators. This study is a continuation of previous work reported under Contract NAS 7-107 (References 1 and 2) and NAS 7-436 (Reference 3).

Work reported in this section describes electrical resistivity data on very pure beryllium metal from cryogenic temperatures typical of all cryogenic propellants up to 1800°F.

Beryllium Wire Technology

Introduction

Beryllium metal has many electrical and physical characteristics which make it inherently superior to all other electrical conductors for high temperature electrical machinery operating at temperatures up to 1800°F and cryogenic temperatures near -330°F. Some of the salient characteristics which make beryllium most attractive when compared to conventional electrical conductors are:

- 1) Low density
- 2) High tensile strength
- 3) High Young's modulus
- 4) Thin adherent self-electrical insulating anodize film
- 5) Good thermal and electrical conductivity
- 6) Best combinations of above properties at 1000°C and -190°C

At high temperatures near 1800°F or above:

Beryllium is the only good electrical conductor, offering a near optimum combination of high thermal conductivity, high space factor insulation and good mechanical properties.

At low temperatures near -330°F :

Beryllium has the highest electrical conductivity in combination with the best overall mechanical properties.

The desirable properties of beryllium for high-and-low temperature electrical machinery applications are attendant with a very undesirable brittle characteristic of commercially available beryllium forms. Presently available beryllium wire requires specialized manufacturing methods for electrical machinery applications.

The potential application of beryllium is most attractive for high-and-low temperature spacecraft electrical machines; for example, a high temperature beryllium turboelectric generator could result in great weight saving due to: low density, high tensile strength, high Young's modulus combination, and thus would permit much higher operating speeds at 1000°C than other good electrical conductors. Beryllium motors and actuators could also operate successfully in high temperature environments of rocket engines, eliminating the weight of temperature protection structures. Low temperature applications are most attractive when cryogenics are on board for other purposes. A cryogenic beryllium ac machine offers the greatest possible power, efficiency and weight reduction of any electrical conductor. Cryogenic ac turboelectric generators could be coupled to nuclear reactor power supplies with a negligible weight requirement for electrical machines.

Results

This report includes results obtained with extreme purity beryllium. The work on ultra refined beryllium at cryogenic temperatures was done by Nuclear Metals Corporation. The material refined by Nuclear Metals was high purity Pechinny commercial beryllium as noted on Figures 4-14 and 4-15. Figure 4-14 compares the resistivity of super refined beryllium and very pure copper from cryogenic temperatures to 1800°F . Figure 4-15 compares the resistivity density product of beryllium and copper. The resistivity density product is a more significant figure of merit for comparison of electrical conductors in spacecraft actuator and electrical applications since minimum system weight is a dominant requirement.

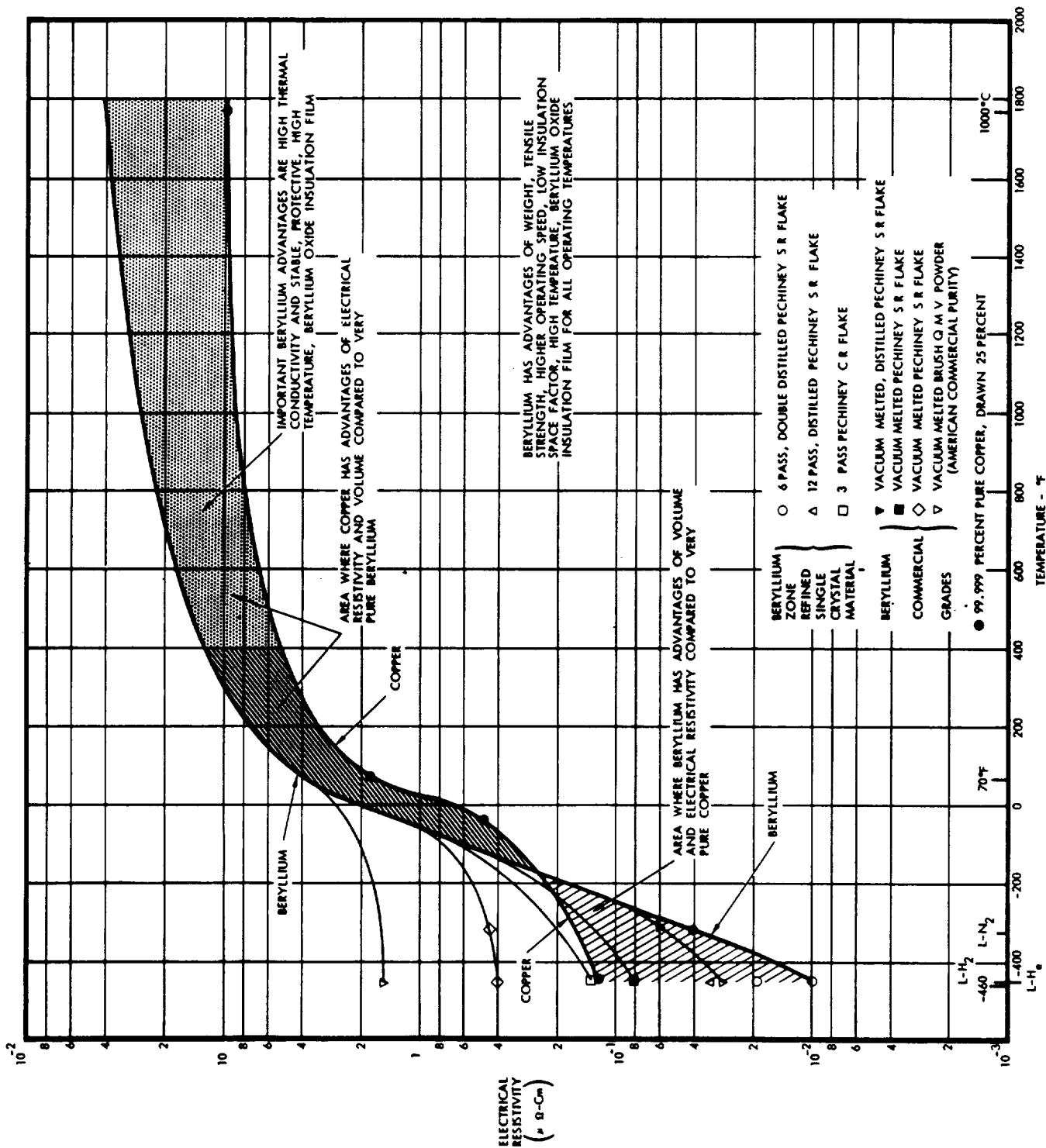


Figure 4-14. Resistivity of Ultra Pure Beryllium and Copper

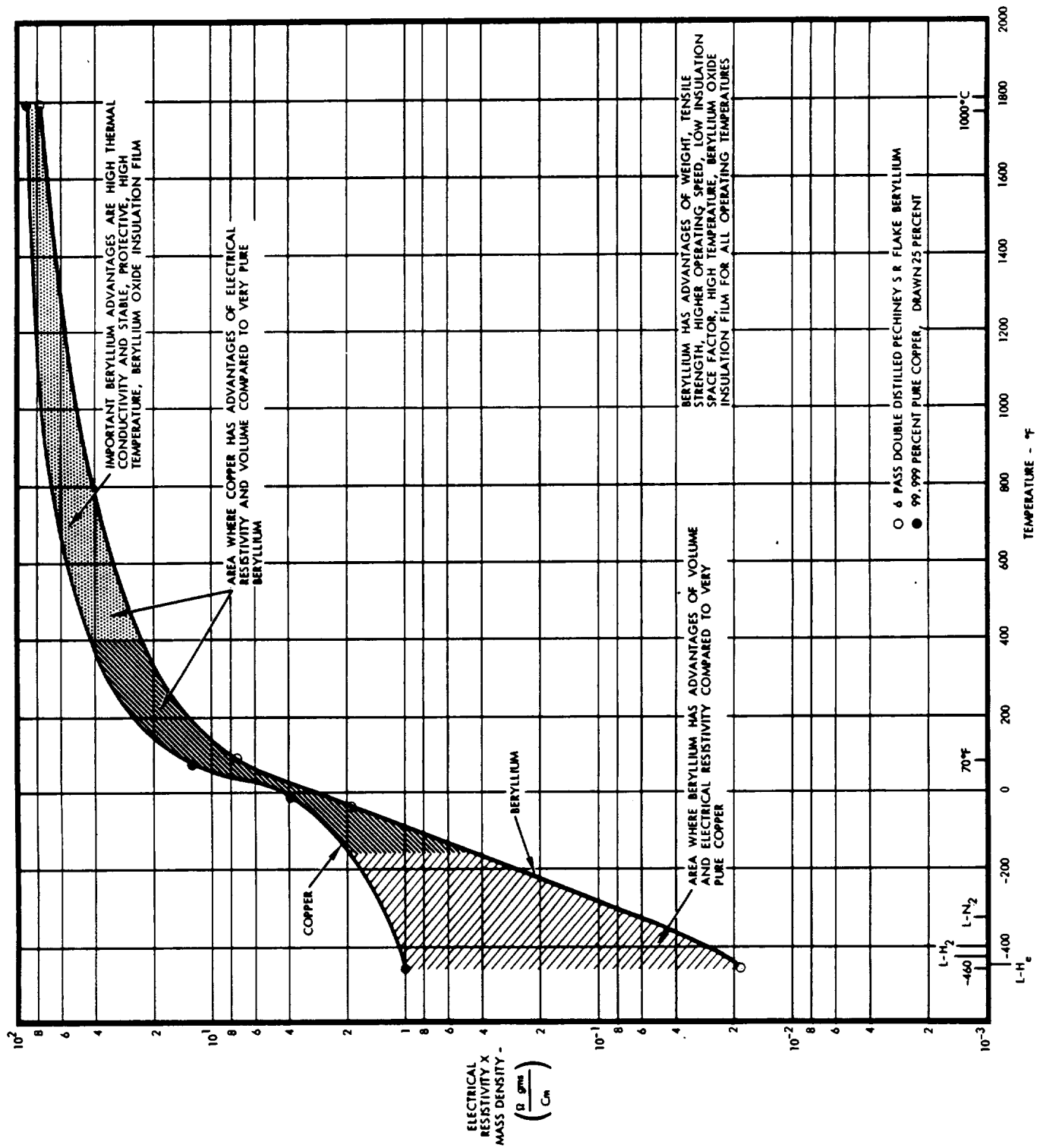


Figure 4-15. Resistivity and Density Product of Pure Beryllium and Copper

Recommendations

The development and application of beryllium in high performance spacecraft electrical machines require a continued effort until a practical basis for production of such machines is established. The initial emphasis in development must be on two problems:

- 1) Beryllium wire technology for electrical machines
 - a. Improve wire ductility
 - b. Eliminate mechanical flaws and occlusions in wire
 - c. Improve surface finish and mechanical tolerances
 - d. Improve mechanical and electrical properties of the anodize insulating film
- 2) Application of beryllium wire to cryogenic and high temperature actuators and other electrical machines
 - a. Specific design studies to establish the comparative characteristics and specific improvements possible in a typical cryogenic and high temperature electrical machine
 - b. Construct and evaluate performance of a high temperature and a cryogenic electrical machine

The above program would provide the continued stimulus and progress essential to realize the inherent qualities of beryllium conductors in applications to electrical machinery.

Beryllium Thin Films

It may be possible to fabricate beryllium electrical conductors having the desired low resistivity and high ductility by deposition of beryllium film on a substrate in continuous process. This experimental investigation illustrates the properties of vapor deposited films on fused silica, and beryllium oxide substrates. The film may be used on the substrate or removed for the electrical application. Beryllium was deposited on selected substrates by electron beam evaporation for this experiment.

Experimental Investigation

A series of beryllium thin films were prepared using electron beam heating evaporation techniques. The material used was 99.99 percent pure beryllium obtained from Electronic Space Products, Inc., No. K-446B, Grade 4N. Typical impurities listed by the supplier are - 1 ppm Cr, 3 ppm Fe, 5 ppm Mn, 2 ppm Ni, and 30 ppm Si.

Film deposits were made by supporting target substrates above the beryllium evaporation source on a chimney. With this configuration, a circular target plane of approximately 6.5 cm was formed. Films were deposited Si O₂ (quartz), Al₂O₃ (aluminum oxide), and Be O (beryllium oxide) substrate. A mask for the standard Hall specimen configuration was used for test samples, (References 4 and 5).

Films not exceeding 1000^oA thickness could be formed on quartz; thicker films showed a matte surface and separated completely from the substrate. Stresses in the separated film caused the film to curl.

Films formed on Be O and Al₂O₃ had a matte surface corresponding to substrate surface as shown in Figures 4-16 and 4-17.

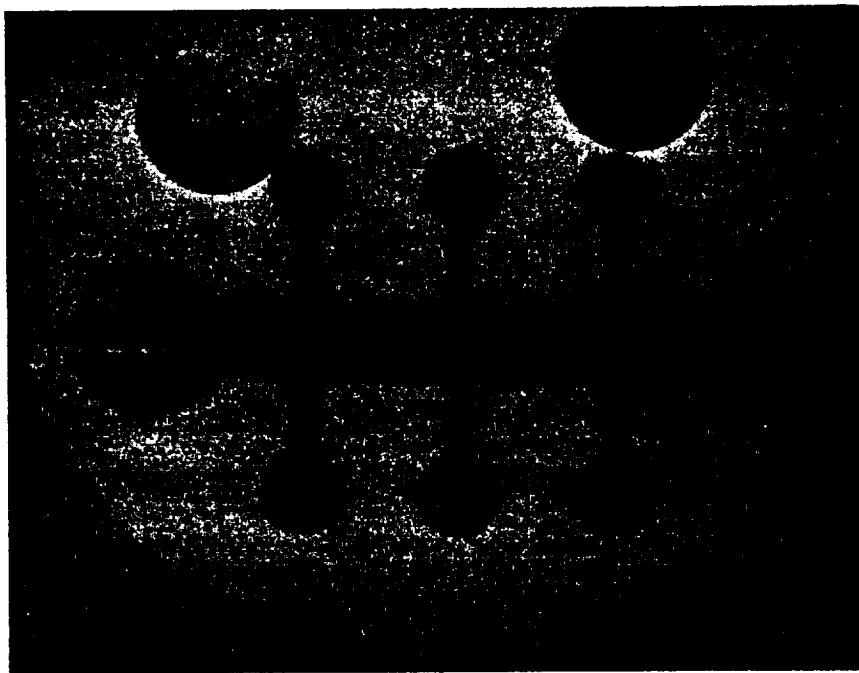


Figure 4-16. Beryllium Film Deposited on Beryllium Oxide Substrate

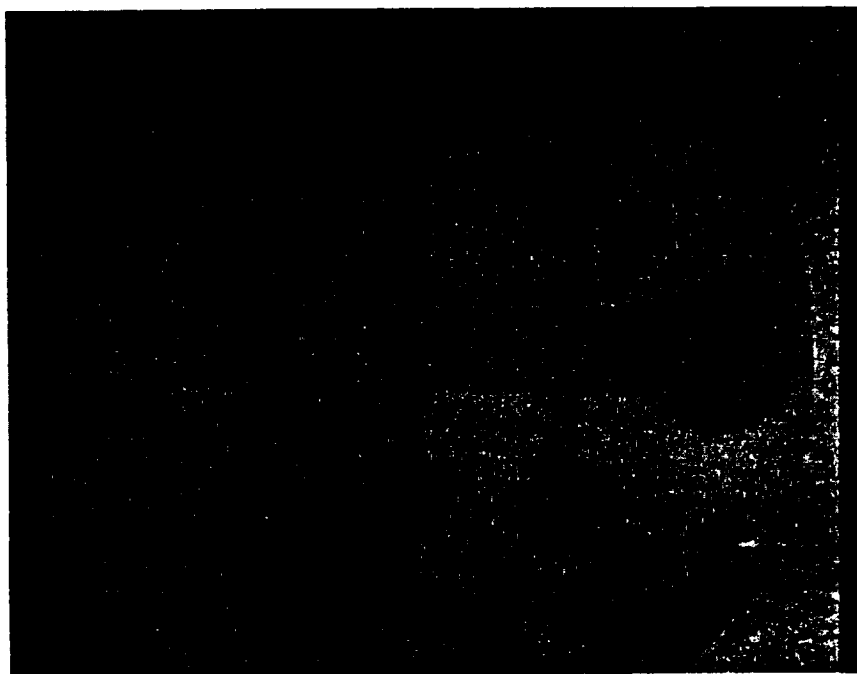


Figure 4-17. Beryllium Film Deposited on Aluminum Oxide Substrate

The tabulated film thickness values are approximate values calculated from an assumed bulk resistivity of 2.78×10^{-6} ohm cm. Experimental interferometer measurements were unsuccessful, because beryllium is a "dark" metal with significant spectral absorption in the near UV and visible wavelengths.

Overcoating with a "bright" metal such as aluminum may be used for accurate interferometer thickness measurement, but this was not done. Since the thickness values are calculated from a measured surface resistance (4 point method), and an assumed bulk resistance value, there is some uncertainty in the absolute value. This method does not impair the accuracy of the relative resistance-temperature characteristic.

Three beryllium films with different thicknesses were measured for total solar absorptance and normal emittance. The results are given in Table 4-2.

TABLE 4-2.

	α	ϵ
1. Thick Film (500-1000Å)	.45	.06
2. Moderate Thickness Film (300-500Å)	.61	.10
3. Very Thin (50-100Å) Slightly Transmitting	.66*	.20*

*Some quartz effect.

Typical electrical measurements and the calculations are illustrated below:

Surface Resistance (4 point probe)

$$R_s = \frac{V}{I} \times 4.45 \text{ (ohms per square)}$$

$$R_s = \frac{.022}{0.1} \times 4.45 = 0.98 \text{ (ohms per square)}$$

Film Thickness (4 point probe, assuming $\rho_{Be} = 2.78 \times 10^{-6} \text{ } \Omega \text{ cm}$, @25°C)

$$\rho = R_s \times t$$

$$t = \frac{\rho}{R_s} = \frac{2.78 \times 10^{-6} \text{ ohm-cm}}{0.98 \text{ ohm}} = 2.84 \times 10^{-6} \text{ cm} = 284 \text{ } \text{\AA}$$

Resistivity (Bridge Method)

$$\rho = \frac{V}{I} \times \frac{W \times t}{L}, \quad L = 2W \text{ for configuration}$$

$$\rho = \frac{1.25 \times 10^{-1}}{10^{-1}} \times \frac{2.84 \times 10^{-6}}{2} = 1.8 \times 10^{-6} \text{ ohm-cm}$$

Hall Coefficient

$$R_H = \frac{V_H \times t}{I \times H} \times 10^8$$

$$R_H = \frac{1.3 \times 10^4 \times (2.84 \times 10^{-6} \text{ cm})}{10^{-1} \times (4 \times 10^3 \text{ gauss})} \times 10^8 = 9.2 \times 10^{-5} \text{ cm}^3/\text{coulomb}$$

(Positive sign indicates hole rather than electron carrier)

Hall Mobility

$$\mu_H = \frac{R_H}{\rho} = \frac{9.2 \times 10^{-5}}{1.8 \times 10^{-6}} = 51.2 \text{ cm}^2/\text{volt-sec}$$

Three Be thin films on quartz were evaluated at room temperature using the above relationships. Subsequent measurements of relative resistivity (bridge method) down to LN_2 temperatures were performed. The results are shown in Figure 4-18. Where the data points are not given at LN_2 temperature, electrical contact separation occurred on the sample. For comparison, bulk resistance curves of iron and copper are also shown in Figure 4-18. Film B is not believed to represent a room temperature resistivity lower than copper because of the uncertainty in the thin film thickness.

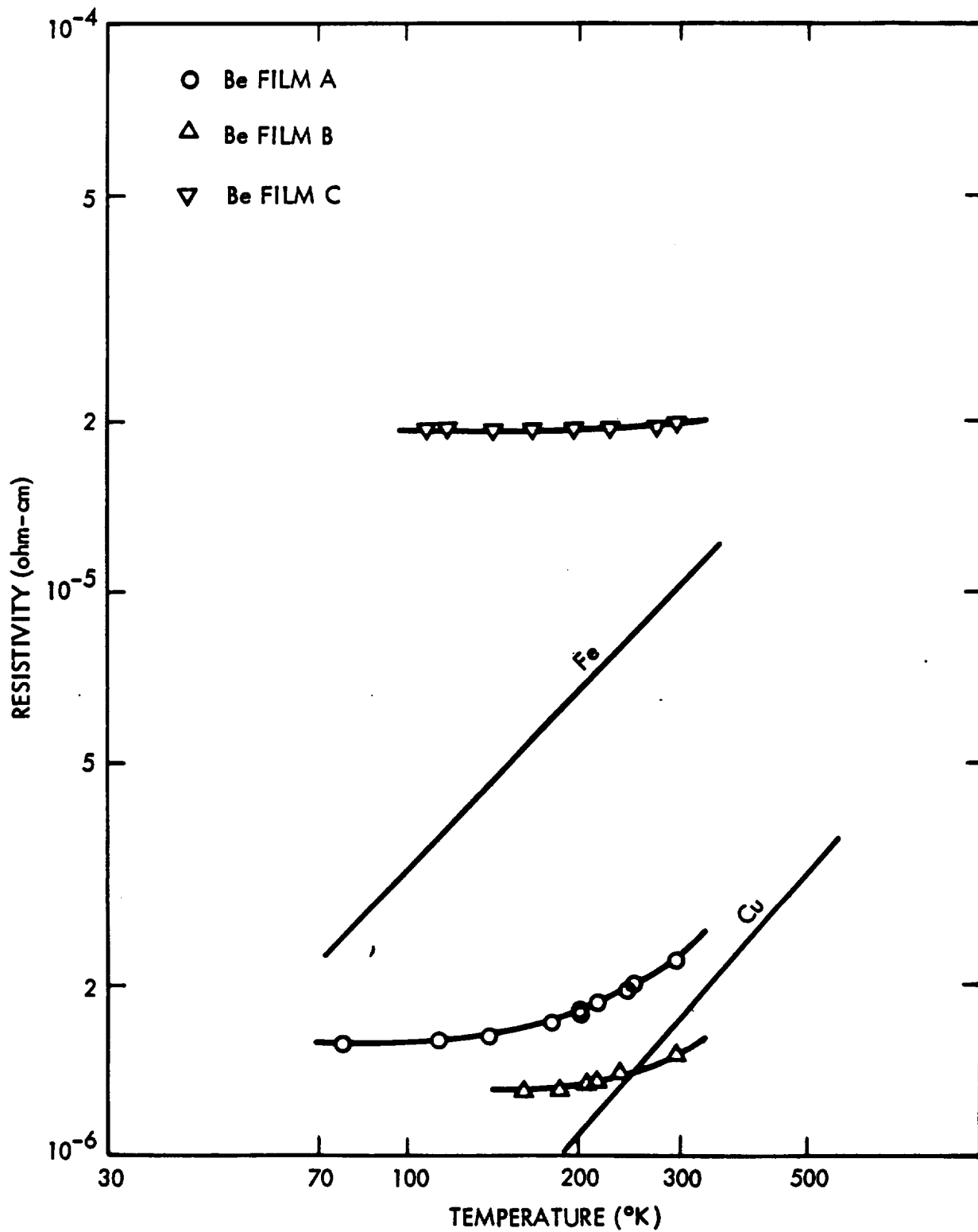


Figure 4-18. Resistivity Data for Evaporated Beryllium Thin Films

Conclusions and Recommendations

Pure beryllium films prepared by the experimental method described here are not suitable for high efficiency solenoid actuator windings where the low bulk resistivity of high purity beryllium is required. This limitation of resistivity of deposited films is due to the limited thickness of films which were produced by vapor deposition methods used. Thin films have higher resistivity than the observed bulk resistivity because surface boundary controlled scattering of charge carriers dominates the conduction process.

The thin beryllium films prepared exhibit a very low temperature coefficient of resistance which is approximately 3 times better than other commercially used thin film materials used for resistance components. Beryllium thin films are especially interesting for precision and power resistor applications because of the protective oxidation resistant property of beryllium at high temperatures and the high recrystallization temperature.

Characteristics of three beryllium films deposited on a quartz substrate are given in Table 4-4.

TABLE 4-4.

Characteristics of Three Beryllium Films Deposited on Silica Substrates

Parameter	Film A	Film B	Film C	Published Bulk Values
Surface Resistance, R_s (ohm/square)	0.245	1.335	76-174	
Thickness, t , (Å)	1130	208	37-16	
Resistivity, ρ @ 25°C (ohm cm)	2.2×10^{-6}	1.53×10^{-6}	19.5×10^{-6}	2.78×10^{-6}
Hall Coefficient, R_H @25°C (cm ³ /coulomb)	1.32×10^{-4}	9.4×10^{-5}	9.8×10^{-5}	2.4×10^{-4}
Hall Mobility, μ_H μ_H @25°C (cm ² /volt-sec)	60.0	61.5	5.0	86.5

The application of beryllium thin films to high precision, high stability resistors and high temperatures, and high power resistors for electronic and electrical power applications deserves continued investigation because the results obtained here are superior to the corresponding characteristics of commercially available thin film resistors.

REFERENCES

1. "Advanced Valve Technology for Spacecraft Engines," Contract NAS 7-107, 19 June 1964, TRW Systems Group, Report No. 8651-6033-SC000.
2. "Advanced Valve Technology for Spacecraft Engines," Contract NAS 7-107, August 1965, TRW Systems Group, Report No. 8651-6042-SU000.
3. "Advanced Valve Technology for Spacecraft Engines," Contract NAS 7-436, November 1966, TRW Systems Group, Report No. 6641-6004-R000.
4. Charles Kittel, Introduction to Solid State Physics, Third Edition, John Wiley and Sons, New York, 1966.
5. K. Lark-Horvitz and Vivian A. Johnson, Methods of Experimental Physics, Volume 6, Part B, Academic Press, New York and London, 1959.

IN-FLIGHT LEAKAGE MEASUREMENTS

The objectives of this study are to determine the requirements for in-flight valve leakage measurements, review the present state of the art in leakage measurement, determine the limitations of present techniques, and where possible, evolve concepts to overcome these limitations.

In-flight leakage measurement requirements include a sensitivity of 10^{-7} std cc/sec, operation in zero-g and high vacuum environments, and proper function after launch accelerations and vibrations. Accuracy of the instrument should be better than five percent, and calibration should be traceable to NBS standards.

The following organizations are engaged in in-flight leakage instrument development, or were contacted as part of this study. This list is not inclusive and there may be other companies engaged in in-flight leakage measurements.

- Air Force - Edwards Air Force Base, California
- Army - Army Missile Command, Redstone Arsenal, Alabama
- Douglas Aircraft Co., Huntington Beach, California
- General Electric Co., Valley Forge, Pennsylvania
- NASA - MSFC, Huntsville, Alabama
- NASA - MSC, Houston, Texas
- Nassau Instrument, Princeton, New Jersey
- North American Aviation, Canoga Park, California
- Parametrics Corp., Boston, Massachusetts
- Ratheon, Boston, Massachusetts
- Rosemont Engineering, Minneapolis, Minnesota
- Space Labs, Inc., Van Nuys, California
- TRW Systems Group, Redondo Beach, California
- Tylan, Inc., Torrance, California

V INSTRUMENTATION AND MEASUREMENTS

This section includes the results of a study performed for the purpose of determining the requirements for instrumentation and measurements related to valve qualification testing and in-space flight valve measurements. A discussion of the presently used technology is given. Requirements are defined and several concepts presented.

	<u>Page</u>
In-flight Leakage Measurements	5-2
Valve Positioning Indicators	5-7
Conceptual Studies	5-18

the partial pressure of the oxygen or hydrogen present in the atmosphere exposed to the detector. An advantage of this type of sensor is that it generates its own power, sometimes sufficient for operating a sensitive relay. Disadvantages include a lifetime limited by the quantity of oxidizer (or reducing agent) packaged in the unit and by its exposure to the reducing agent (or oxidizer) being sensed. Errors have occurred in H_2 sensors due to O_2 entering the cell, resulting in a reaction similar to that occurring in catalytic sensors. Sensitivities on the order of 1 percent of the lower explosion limit of hydrogen in air mixtures have been attained.

Catalytic sensors measure the heat dissipated in a reaction between the fluid being sensed and an oxidizer (or reducing agent) in a catalytic burner. This type of sensor has been used in laboratory and commercial installations for measuring O_2 and H_2 concentrations. The oxidizer (or reducing agent) must be stored within the unit or supplied from an externally stored supply.

Radiation sensors sense the radiation level in a line or area into which a fluid component could leak. This radiation is supplied by a radioactive tracer material added to the leaking fluid. The tracer material may be mixed with the propellant initially or it may be added as part of the leak sensing operation. An example of the latter case is a system in which the leakage is passed through a platinum dioxide sponge impregnated with Kr_{85} . As the leaking fluid passes through the sponge it entrains some of the radioactive Kr_{85} which is sensed by a radiation detector in a shielded area downstream. The sensitivity of these systems depends on the quantity of the tracer added to the leaking fluid. When a radioactive material is added to the bulk propellant, sensitivity is limited by the undesirable effects of radiation on the propellant, structure, and personnel in the area. When the entrainment approach is used the sensitivity and life of the system must be traded off; the higher the sensitivity, the shorter the life for a given size limit.

Mass spectrometers measure the anode to cathode current in an electrically and magnetically deflected beam of ions. The electric and magnetic fields

The principle methods being considered for in-flight leakage measurement include the following:

- Electrothermal Flow Meters
- Fuel Cells
- Catalytic Sensors
- Radiation Sensors
- Mass Spectrometers
- Acoustic Sensors
- Burst Diaphragms
- Thermal Sensors

Table 5-1 presents a rating comparison of the various leakage measurement techniques considered. These ratings are based on ground performance and do not reflect size or weight considerations.

Electrothermal flow meters operate on the principle that the heat transfer from a warm body in a flow stream varies with the Reynolds number of the flow. The electrothermal flow meter is extremely simple and requires no moving parts. The parts exposed to propellants may be easily encapsulated in a compatible material. The limitations of the instrument include a lack of sense information, errors due to convective currents when used in a gravity field and cryopumping errors when used in some cryogenic propellant applications. Leakage sensitivities of 25 cc per hour of liquid propellant have been obtained in a .625 inch diameter line. This is probably close to the lower limit of Reynolds numbers detectable by this method. A marked improvement in sensitivity (cc/hr or cc/sec) may be attained by reducing the diameter of the flow channel in the sensing area, thus increasing the flow velocity.

Fuel cells operate on a reverse electrolysis principle wherein a voltage is generated between two plates during the reaction of an oxidizer and a reducing agent. This principle has been applied to commercial oxygen and hydrogen concentration monitors. These generate a voltage proportional to

TABLE 5-1.
COMPARISON OF IN-FLIGHT LEAKAGE MEASUREMENT METHODS

INSTRUMENT	External Leakage	Internal Leakage	Sensitivity	Accuracy	Gases	Liquids	Propellant Limitations
Electrothermal Flow Meters	3 ^a	3	2 7 x 10 ⁻³ cc/sec (liquid)	2	3	3	None.
Fuel Cell	2 ^a	2	U	2	2	2	Oxidizers & Reducing Agents Only.
Catalytic Sensor	2 ^a	2	U	2	2	2	Oxidizers & Reducing Agents Only.
Radiation Sensor	3 ^a	3	3	3	3	3	None.
Mass Spectrometer	3 ^a	3	3 10 ⁻¹¹ sccs	2	3	Vapors Only	Vapors Only.
Acoustic Sensor	2 ^a	2	U	2	3	3	None.
Burst Diaphragm	2 ^a	2	1-3	1	3	3	None.
Thermal Leak Sensor	3 ^a	3	3 4.5 x 10 ⁻⁷ cc/sec (liquid)	2	1-2	2-3	None.

a - Leakage must be collected and delivered to sensor.

1 - Poor
2 - Fair
3 - Good
U - Unknown

are adjusted so that only the ions with the proper charge to mass ratio strike the cathode. Ionization is normally accomplished by passing the sample over a hot wire.

Mass spectrometers are in general use in ground leakage measurements of hydrogen and helium and other gases and their use has been proposed for flight systems. They may also be used as an analytic tool to determine leakage sample composition. Successful operation of a mass spectrometer tube at cryogenic temperatures has been demonstrated. Further work in this area is required to produce a spaceborne system. The mass spectrometer has higher sensitivities than any of the methods listed with the possible exception of the radiation type sensor.

Acoustic leakage sensors normally measure the velocity of an acoustic wave transmitted in the direction of flow and compare it with the velocity of one transmitted against the direction of flow. This approach has been used in commercial flow meters and is capable of relatively high sensitivity.

Burst diaphragms have been used as go no go and long term inspection leakage surveillance devices on rocket engines. The diaphragm closes off a cavity into which leakage will potentially flow. When a certain quantity of fluid leakage has occurred the diaphragm ruptures. A problem is encountered when this approach is used with cryogenic propellants. Cryogenics may cause cryopumping in the measurement cavity with resulting diaphragm implosion. This may be partially overcome by venting the measurement cavity through a small orifice but this markedly reduces sensitivity. Remote readout may be provided to indicate diaphragm failure. Data is principally qualitative and once failure occurs, no further leakage monitoring is possible.

Thermal leakage sensors sense the temperature change due to the isenthalpic expansion of the leaking fluid across the valve seal and compare it to the bulk fluid temperature. These sensors are extremely simple and they may be easily encapsulated in propellant compatible materials. Sensitivities of 3.66×10^{-6} cubic inches per hour with water and 4×10^{-4} cubic inches per hour with hydrazine have been obtained.

be used to obtain consistent results. For example, consistent repeated on-off transients can usually be obtained for solenoid actuators by using a gated, precision regulated power supply in a temperature and humidity controlled laboratory. The on-time of the gate is adjusted slightly in excess of the on transient time of the solenoid actuator. This procedure greatly reduces the heating usually caused by steady actuator coil excitation. This heating changes the coil resistance which affects the final coil current and the time constant of the transient characteristic. A one shot multivibrator or triggered single cycle square wave generator or pulse width timing switch may be used for gating the power supply. Figure 5-1 illustrates a system which is useful for obtaining consistent, repetitive, on-off current and voltage transients for a solenoid actuator coil. Figure 5-2 is an illustration of a current and voltage on transient trace for a solenoid valve obtained with the system shown in Figure 5-1. Frequent repeated transient tests were made with all results being exact replicas of Figure 5-2.

The current transient obtained with the poppet position blocked closed is a useful comparison reference. The current transient obtained with a moving poppet may be compared to determine the starting time for armature motion. A blocked armature current transient with a distinctly faster than normal rise time is indicative of shorted actuator coil turns. It is also possible to detect shorted turns with the poppet blocked closed, by measuring the incremental inductance on a low level audio frequency bridge. Low bridge excitation at high audio frequencies will minimize or eliminate the effects of poppet motion or buzz, 1 to 10 KHZ should be sufficient. Low inductance relative to a statistically normal production inductance is indicative of shorted turns. Shorted turns should be cause for rejection because it is indicative of faulty coil winding and will usually cause a large change in pull-in-time.

Comparison of blocked and moving poppet current transients of a solenoid valve will give information on the time of motion initiation. A double exposure photograph with both transients on one photograph will give a precise overlay comparison of both transients or a memory oscilloscope may

VALVE POSITION INDICATOR STUDY

Introduction

Position indication for solenoid valves is normally obtained from the transient current and voltage characteristic of the actuator coil. In some cases the current and voltage time traces are not properly interpreted resulting in rejection of the valve during qualification tests. Other position indicator techniques utilize a mechanical linkage coupling the position transducers such as an LVDT, resistance potentiometer, or photometric device to the linkage. On or off status may also be confirmed by precisely located switching devices coupled to the linkage. Many actuators do not couple to the valve mechanism through a mechanical linkage and conventional position indicating and measuring devices cannot be used. Solenoid valves without external position measuring devices may use various in-situ methods for position determination which are constructed as part of the actuator assembly. Position measuring methods suitable for solenoid valves which do not permit mechanically coupled external measuring devices are also considered.

Current and Voltage Transient Data

There is a relationship between armature velocity-position characteristic and the transient current-voltage characteristic. This relationship is complicated and a simple, unique, direct and linear relationship does not exist between actuator armature position and the transient current-voltage characteristic. This relationship is considered in detail in Section IV of this report under the High Speed Solenoid Actuator Study. Limited information on armature motion can be obtained from the time derivative of the actuator coil on-off current/voltage characteristic. The derivative may be augmented, biased or clamped and stored to obtain a useful display of the result if the actuator coil on-off current voltage is stable and consistent, independent of environmental effects, supply voltage, load and source impedance, fluid pressure, etc. These qualifying restraints do not usually exist and therefore this method is not used extensively.

Information obtained from the actuator current/voltage on-off transient is very useful for laboratory study where carefully controlled conditions can

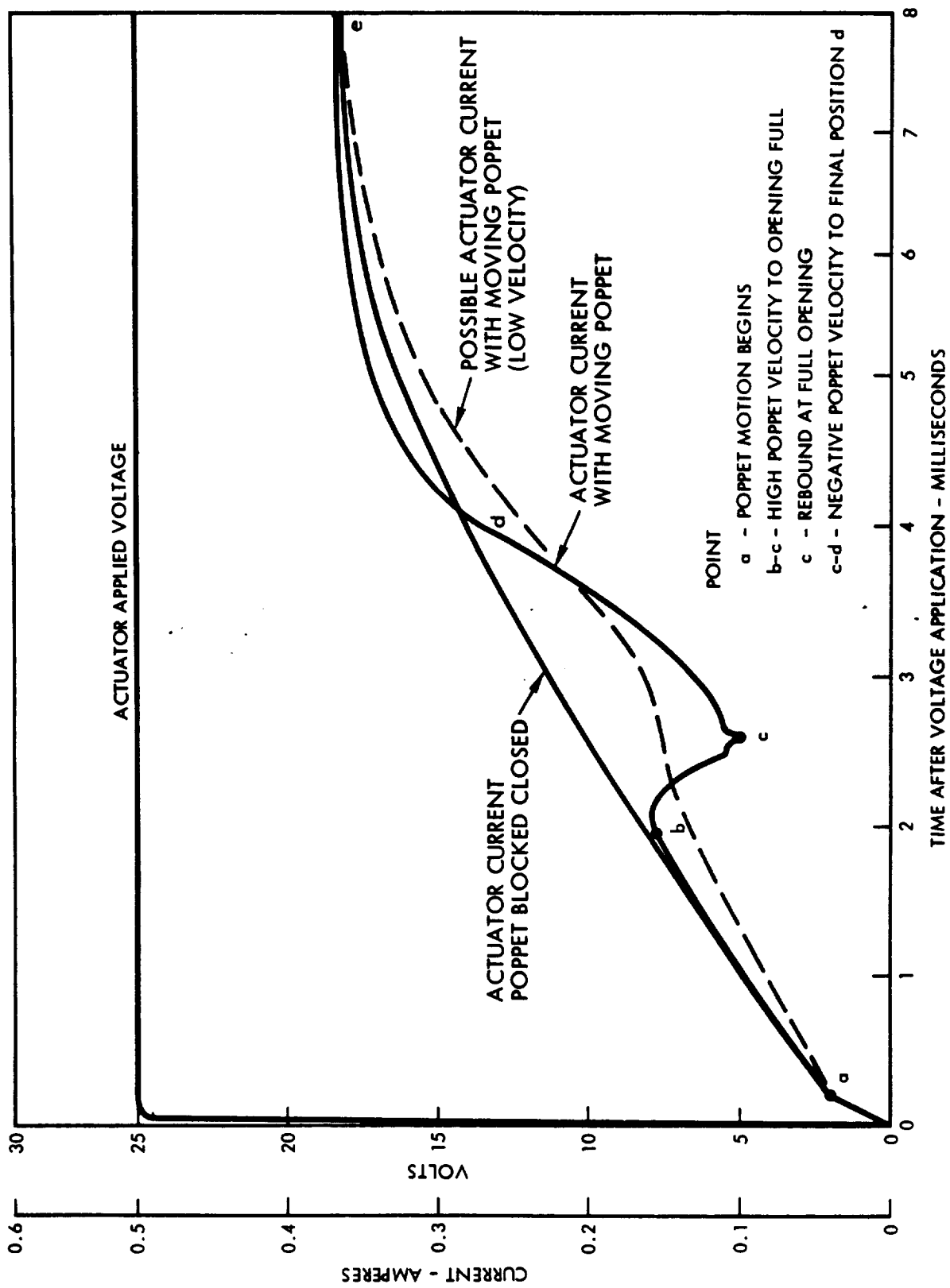


Figure 5-2. Typical Current Voltage Transient Characteristics of a Solenoid Valve with Blocked and Moving Poppet

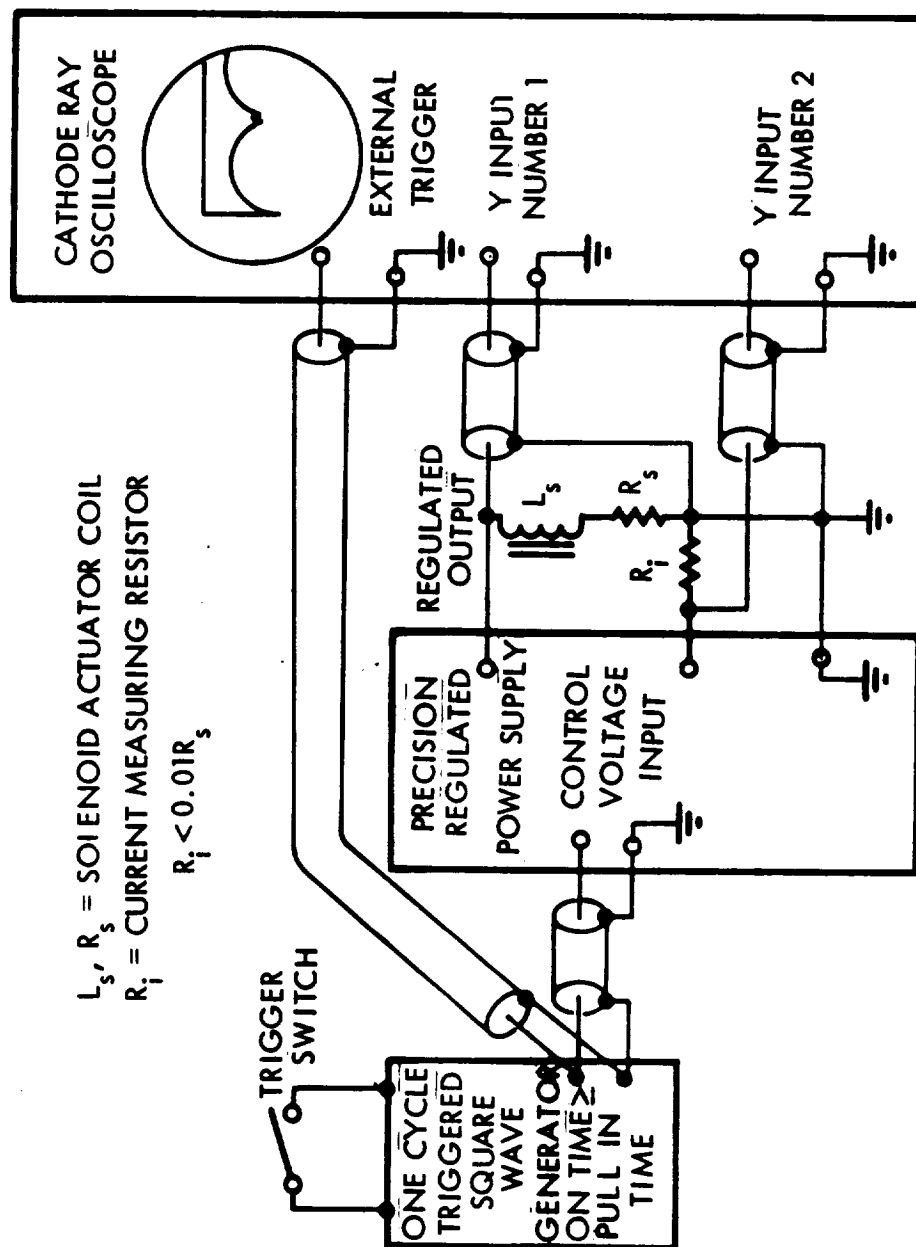


Figure 5-1. Repetitive Solenoid Actuator On-Off Transient Test Setup

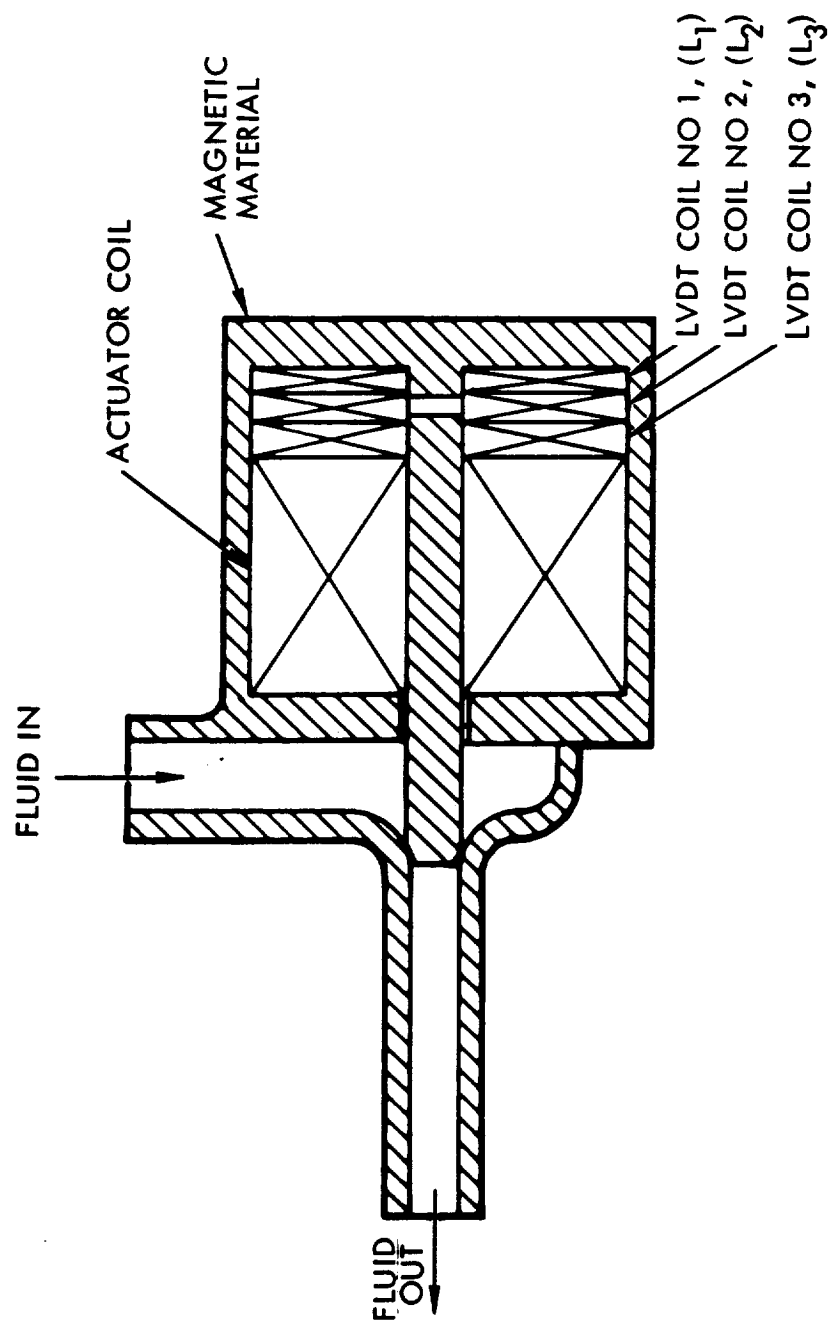


Figure 5-3. Solenoid Valve with In-Situ LVDT Position Sensor

be used for direct visual comparisons. The results of such a visual or photographic comparison may be similar to Figure 5-2. It is apparent that point a in Figure 5-2 is the point where the unblocked poppet motion begins because this is where the two current traces begin to depart from each other due to poppet motion. The deviation from the blocked armature transient on path a-b is small due to low armature velocity during this interval; hence, existing practice has assumed armature motion begins at b and is complete at c. It is possible for a solenoid actuator to have a current transient similar to the dashed curve on Figure 5-2 with normal armature travel with conditions of high viscous or fluid damping, in this case the completion of armature travel is not well defined, yet the fluid flow characteristics of the valve opening may be acceptable.

In-situ Valve Position Indicators

The following in-situ position sensing methods are considered.

1. LVDT Coil
2. Magnetoresistance Resistors
3. Hall Effect Magnetic Sensors
4. Photometric Transducers

LVDT Coils

A carefully matched pair of differentially opposed coils may be installed on the inside radius of the driving coil as shown in Figure 5-3. The coils may be located to produce a null output for either the fully closed or fully open position enabling very small deviations from the fully open or closed position to be measured precisely. Three coils may be installed to enable measurement of deviations from fully open and fully closed position. One pair of the three provides null output at the fully open position and the second pair is null output at the fully closed position. The real time position information obtainable during switching transients is limited because the changing actuator field caused by the solenoid coil current transient contributes somewhat to the LVDT output indication. The static null position measurements can be very accurate and quantitative nominal



deviations from null are affected only slightly by environmental factors and coil excitation.

Figure 5-4 is a diagram illustrating the use of in-situ LVDT coils for measurement of the static on and off position of the solenoid actuator. Carefully placed in-situ LVDT coils promise to be a very sensitive and precise method of measurement for static on and off position errors for in-flight and laboratory measurements.

Magneto Resistance Sensors

An electrical resistance which changes when exposed to a magnetic field can be used in a position sensor technique. The resistance is temperature sensitive, consequently matched pairs of magneto resistors exposed to identical temperature must be used in a differential opposing circuit to cancel temperature effects. Three magneto resistors may be in-situ in the solenoid actuator to obtain null outputs for the desired on and off actuator positions. The null outputs are insensitive to actuation coil transient excitation, operating, and environmental conditions. The magneto resistance error sensing system can give real time actuator position information during actuator on-off transients if the inductive coupling of switching transients to the magneto resistance sensor circuits is precisely compensated by an identical opposing inductive coupling. The magneto resistance sensor system can operate directly from the spacecraft ac or dc power supply without complicated power conditioning systems.

Magneto resistance sensors offer advantages of accurate real time transient and static position information, simple power supply requirements and high position error sensitivity.

Figure 5-5 illustrates the installation of three matched magneto resistors to assure immunity from temperature changes and to obtain position error information for the actuator on and off conditions. Figure 5-6 illustrates a system using in-situ magneto resistors to obtain information.

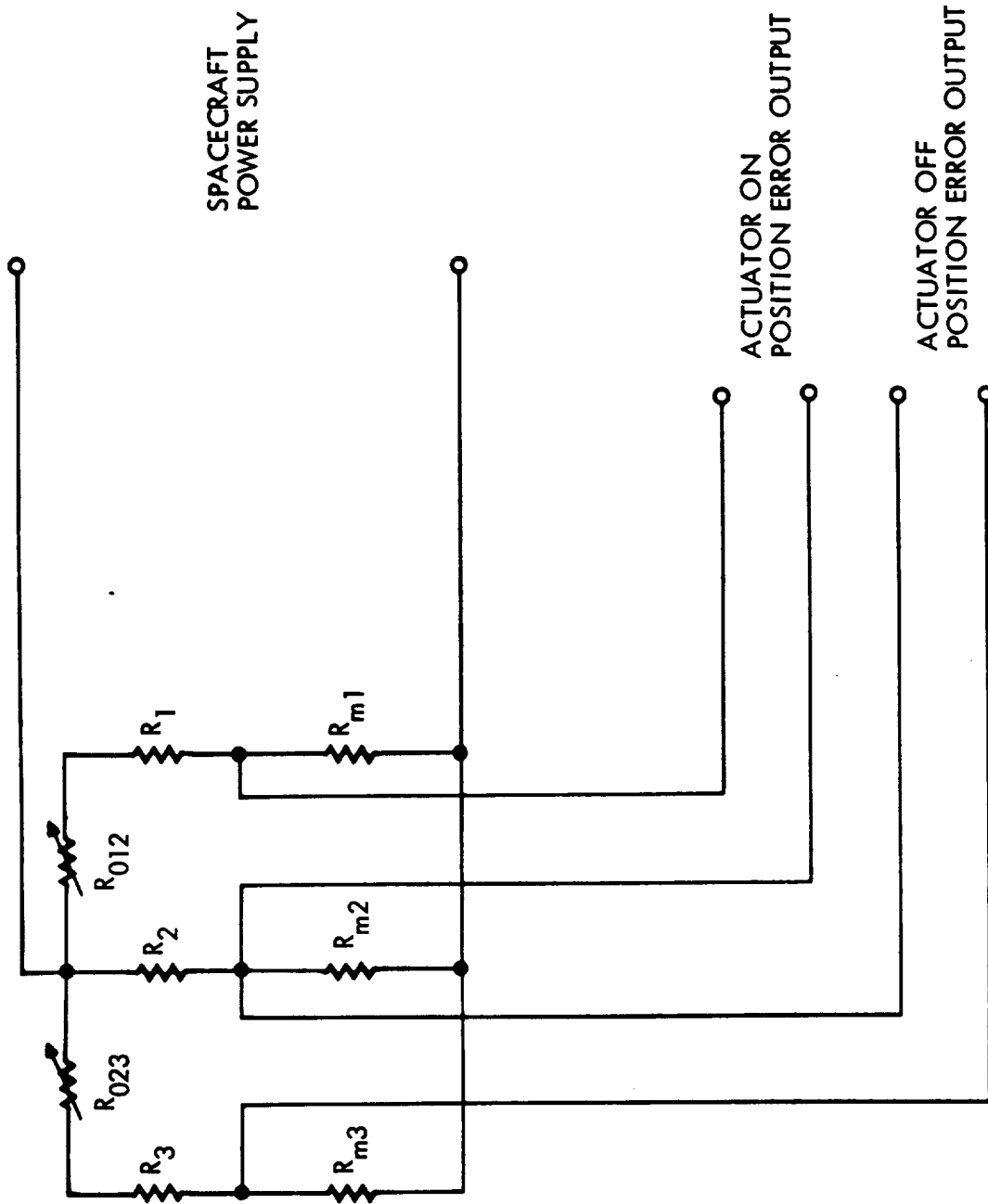


Figure 5-6. Solenoid Actuator In-Situ Magneto Resistance Position Error Measuring System

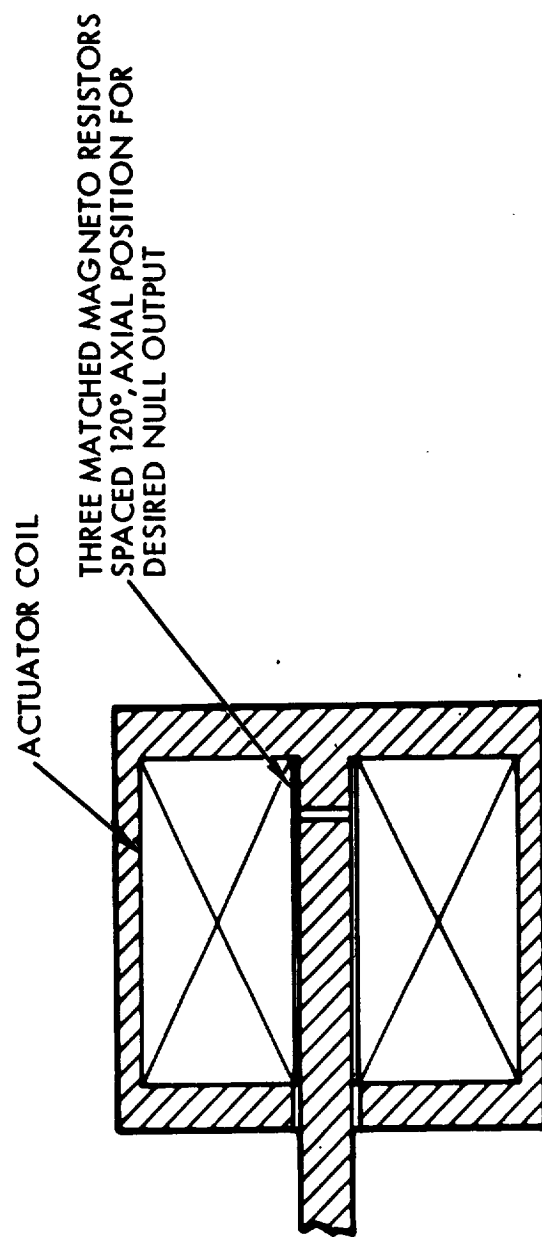
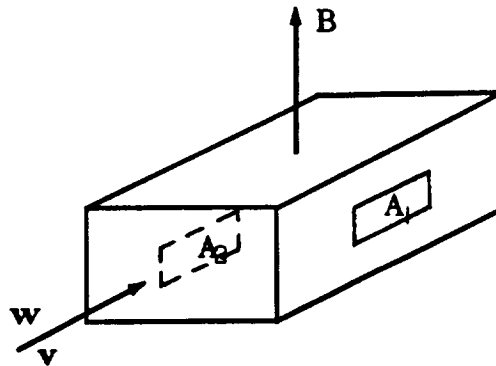


Figure 5-5. Solenoid Valve with In-Situ Magneto Resistance Position Sensors

CONCEPTUAL STUDIES

Electromagnetic Meter

The electromagnetic meter concept traces back to Faraday, however, it still has basic advantages for high reliability systems in that it has no moving parts. The principle involved is that motion of a substance in a magnetic field results in an induced voltage.



As shown in the sketch when a flow w (or velocity v) occurs perpendicular to the magnetic field vector B a voltage V will result between plates A_1 and A_2 . This voltage is proportional to fluid velocity and is independent of symmetric velocity distributions across the duct.

$$V = \oint (\mathbf{v} \times \mathbf{B}) \cdot d\mathbf{l} - \iint \frac{\partial \mathbf{B}}{\partial t} \cdot d\mathbf{s} \quad (1)$$

where l is the width of the channel, t is time, and ds is incremental area.

Figure 5-7 shows a flow meter concept utilizing an ac magnetic field to allow flow measurement of insulating and poorly conducting fluids. The use of a periodically varying magnetic field also eliminates problems due to electrolysis, polarization, stray electromagnetic fields, and flow induced electrostatic fields.

The meter's output is again described by equation (1) however, two magnetic

Hall Effect Position Sensors

A Hall effect transducer produces an output voltage proportional to the magnetic flux density perpendicular to the sensor surface. The installation and characteristics are similar to the magneto resistance sensors described. Hall effect transducers are less sensitive than the corresponding magneto resistance transducer and in addition, require a resistance null error balance adjustment.

Photometric Position Error Sensing

Very compact, solid state, infrared or visible light sources and sensors are available which may be used in-situ in solenoid actuators. The light source sensor system is installed with the light beam transverse to the actuator motion and properly located with respect to the actuator armature end boundary to obtain a null output from the photometric system at the desired on or off position. The circuit concepts and performance characteristics are believed to be comparable to the magneto resistance sensor system, however, a transparent, nearly constant light transmission path must be available transverse to the armature motion. If the armature is operated in the propellant, the fluid must offer little attenuation to the transverse light beam.

Conclusions and Recommendations

Actuator motion data inferred by processing the on-off current and voltage transient of solenoid actuator coils does not provide a simple dependable means of measuring on and off actuator position errors. This type of data is valuable in laboratory studies of actuator performance where controlled conditions enable consistent results. Techniques for using the on-off current and voltage transients for laboratory investigation can extend beyond accepted practices. Efforts should continue to demonstrate and describe suitable laboratory techniques.

The in-situ methods described here for armature on-off position error measurement deserve further experimental investigation as methods for in-flight actuator position measurement. These methods can provide static and dynamic position information.

fields in opposite directions are used to cancel the effects of the second term. The induced voltage for each coil is then described by:

$$V = \oint (\mathbf{v} \times \mathbf{B}) \cdot d\mathbf{l} \quad (2)$$

where, if the magnetic field is varying sinusoidally

$$\mathbf{B} = B_0 \cos \omega t \quad (3)$$

ω is the radian frequency or, $\omega = 2\pi f$, where f is the frequency. Substituting and solving we obtain

$$V = v l B_0 \cos \omega t \quad (4)$$

Two coils were used with magnetic fields, and therefore induced voltages, in opposite directions. This cancels the effects of spurious fields. Connecting these in series, as shown in the sketch, Figure 5-7, doubles the output signal.

Thus:
$$V = 2 v l B_0 \cos \omega t \quad (5)$$

It is seen that the voltage must be of the form:

$$V = V_0 \cos \omega t \quad (6)$$

therefore:
$$V = 2 v l B_0 \quad (7)$$

The following numeric example illustrates the potential sensitivity of the meter in a large duct.

Take: $B_0 = 1.8 \text{ webers/meter}^2$
 $v = .1 \text{ meter/sec}$
 $V_{0 \text{ min}} = 10^{-6} \text{ volts.}$ Minimum voltages easily measured with routinely available equipment.
 Flow channel = 4 cm x .4 cm, $a = 1.6 \text{ cm}^2$ (area equivalent to .5625 in. dia. tube)
 $l = 4 \text{ cm}$

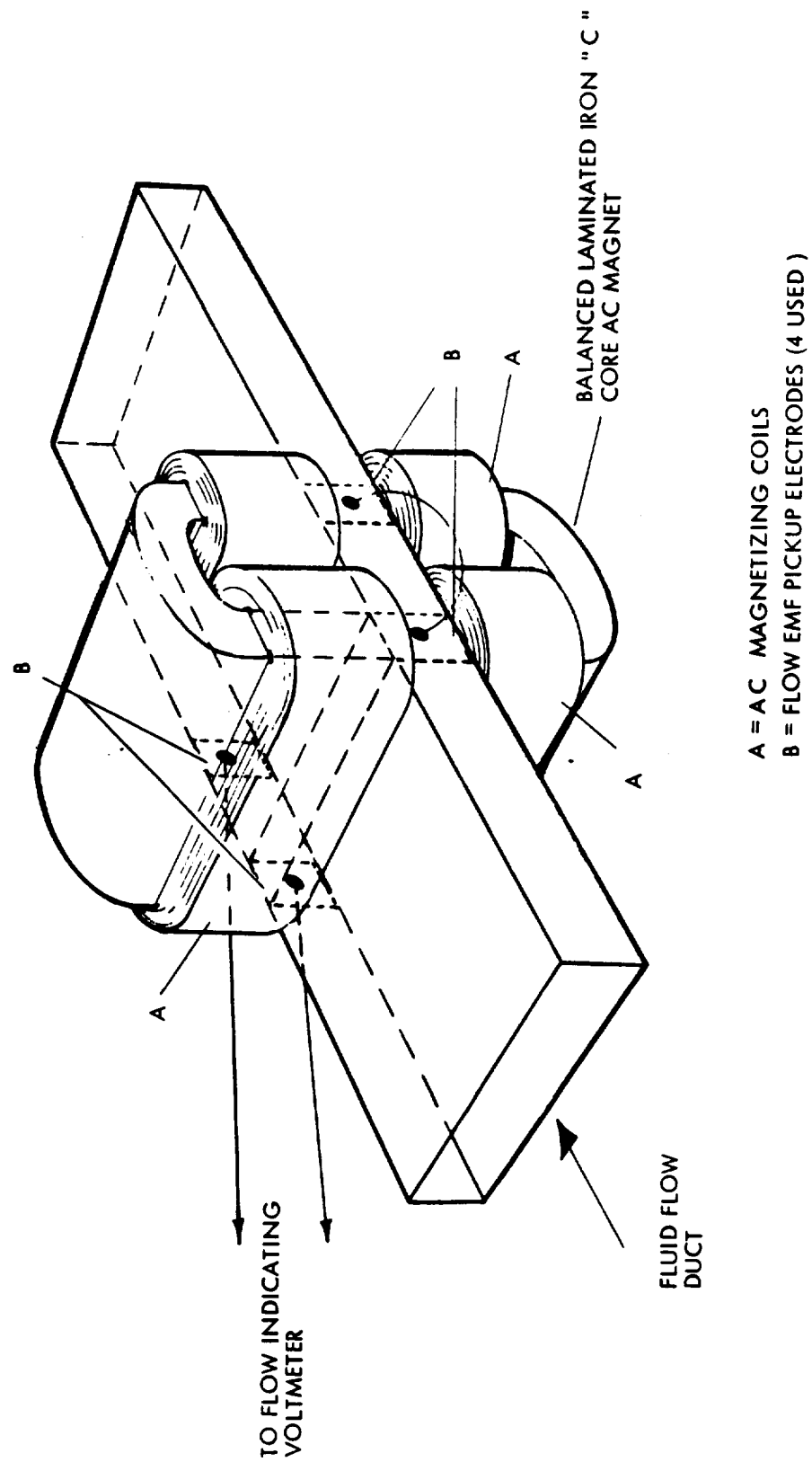
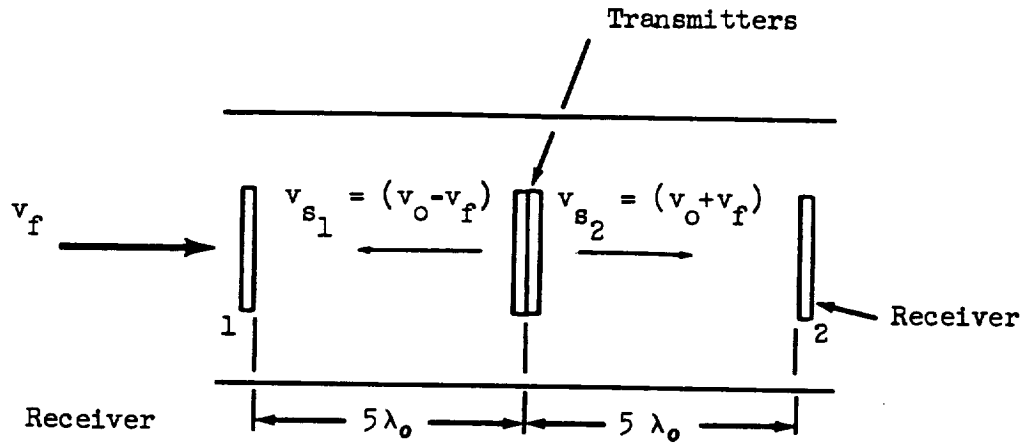


Figure 5-7. AC Electrohydrodynamic Fluid Flow Meter



The time for the sound wave to travel between the transmitter and the upstream receiver is:

$$t_1 = \frac{5\lambda_o}{v_{s1}} \quad (1)$$

and between the transmitter and downstream receiver

$$t_2 = \frac{5\lambda_o}{v_{s2}} \quad (2)$$

With no flow the time becomes:

$$t_o = \frac{5\lambda_o}{v_o} \text{ in both cases.} \quad (3)$$

Now, if we compare the phase of the wave arriving at the upstream receiver to that arriving at the downstream receiver, the time difference is:

$$t_{\phi} = (t_1 - t_o) + (t_o - t_2)$$

Then:
$$V_o = 2 \times .1 \frac{\text{meter}}{\text{sec}} \times .04 \text{ meter} \times 1.8 \frac{\text{webers}}{\text{meter}^2}$$

$$V_o = 1.44 \times 10^{-2} \text{ volts}$$

Flow rate, $q = va$ (8)

$$\begin{aligned} q &= 10 \frac{\text{cm}}{\text{sec}} \times 1.6 \text{ cm}^2 \\ &= 16 \frac{\text{cm}^3}{\text{sec}} \end{aligned}$$

and the specific signal is:

$$V_{o_{sp}} = 9 \times 10^{-4} \frac{\text{volts}}{\text{cm}^3/\text{sec}}$$

If $V_{o_{min}} = 10^{-6}$ volts as noted, the minimum flow which may be sensed is:

$$q_{min} = 1.11 \times 10^{-3} \text{ cm}^3/\text{sec}$$

or approximately .244 in.³/hr. The sensitivity will be considerably higher for smaller ducts. More sophisticated voltage measurements could improve the sensitivity by as much as a factor of a thousand. Approximately 25 in.³/hr sensitivities are presently attained with electrothermal type flow meters.

Acoustic Meters

Acoustic meters have been made which measure the deflection of an acoustic beam transmitted perpendicular to a fluid flow. The frequency measurement of the repetition rate of a self triggered acoustic wave transmitted over a known distance with and against a fluid flow has also been used. A more sensitive acoustic flow meter may be made which measures the Doppler phase shift of a sound wave when traveling with, and against the fluid velocity in a duct. This phase shift is directly translatable into a fluid velocity measurement and therefore gives a flow measurement. A possible arrangement is shown schematically below.

this gives:

$$t_{\phi} = \frac{1.8 \times 10^{-4}}{360 \times 10^5}$$

$$t_{\phi_{\min}} = 5 \times 10^{-13} \text{ sec}$$

Substituting for v_{s_1} and v_{s_2} in equation (5)

$$t_{\phi} = 5 \lambda_o \left(\frac{1}{(v_o - v_f)} - \frac{1}{(v_o + v_f)} \right)$$

$$t_{\phi} = \frac{10 \lambda_o v_f}{v_o^2} \left[\frac{1}{\left(1 - \frac{v_f}{v_o}\right) \left(1 + \frac{v_f}{v_o}\right)} \right]$$

Since v_f is small compared to v_o , in our case this reduces to:

$$t_{\phi} = \frac{10 \lambda_o v_f}{v_o^2} \tag{9}$$

then for the example

$$t_{\phi} = \frac{10 \times 5 \times 10^{-2} \times .33 \text{ ft/sec}}{(5 \times 10^3)^2 \frac{\text{ft}^2}{\text{sec}^2}}$$

$$t_{\phi} = 6.6 \times 10^{-9} \text{ sec}$$

If we choose a tube area of 1.6 cm^2 , as before, the flow rate, q , is

$$q = 16 \frac{\text{cm}^3}{\text{sec}}$$

or

$$t_{\phi} = t_1 - t_2 \quad (4)$$

then

$$t_{\phi} = \frac{5 \lambda_o}{v_{s_1}} - \frac{5 \lambda_o}{v_{s_2}}$$

$$t_{\phi} = 5 \lambda_o \left(\frac{1}{v_{s_1}} - \frac{1}{v_{s_2}} \right) \quad (5)$$

the time required for one wave to occur is

$$T = \frac{1}{f} \quad (6)$$

then the phase shift is

$$\phi = ft_{\phi} \text{ } 2\pi \text{ radians} \quad (7)$$

$$\phi = ft_{\phi} (360) \text{ degrees} \quad (8)$$

Now let us examine a numeric example to illustrate sensitivity.

Let:

$$f = 10^5 \text{ cps}$$
$$v_o = 5 \times 10^3 \text{ ft/sec}$$
$$\lambda_o = 5 \times 10^{-2} \text{ ft}$$
$$180^\circ \text{ phase change} = 10 \text{ volts}$$
$$V_{\min} = 10^{-6} \text{ volts as before}$$

Then we may sense a phase shift of:

$$\phi_{\min} = 180 \times \frac{10^{-6}}{10} = 1.8 \times 10^{-5} \text{ deg.}$$

Acoustic Pressure - Leakage Measurement Technique

The acoustical method of pressure and leakage measurement described below has the advantage of being insensitive to the pressure or absence of gravity fields. It may be made quite rugged to withstand a spacecraft launch environment or allow field use on the ground

The concept is based on measuring the acoustic impedance or transmission characteristics of a chamber or line. A sound wave is produced by exciting the input transducer at a known level. The intensity of the wave at the receiver or output transducer is then examined. A schematic of the system (Figure 5-8) illustrates the concept.

The pressure is calculated from the wave intensity and physical dimensions of the transducers, chamber and the species present. Preliminary calculations indicate a receiver intensity of 1.63×10^{-16} watts/cm² (0 db) for mean chamber pressures of 10^{-8} torr and an input transducer motion of 10^{-4} times the chamber volume is possible. This signal strength should be easily detectable.

Leakage measurements may be made by monitoring pressure over a known time with a known chamber volume. Since chamber volume may be precisely determined, an extremely sensitive leakage measurement is obtainable.

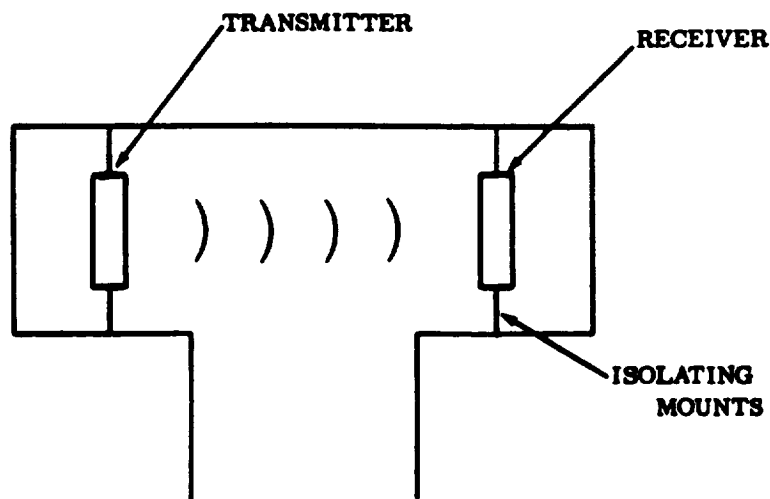


Figure 5-8. Acoustic Pressure Measuring Device

then

$$\begin{aligned}q_{\min} &= \frac{t_{\phi \min} q}{t_{\phi}} \\&= \frac{5 \times 10^{-13}}{6.6 \times 10^{-9}} \times 16 \\&= 1.21 \times 10^{-3} \frac{\text{cm}^3}{\text{sec}}\end{aligned}$$

or .266 in³/hr

This is two orders of magnitude better than electrothermal flow meters and might be improved further with more sophisticated sensing techniques and optimized tube geometry.

REFERENCES

1. Kraus, J. D., Electromagnetics, McGraw-Hill, New York, N. Y., 1953.
2. Shercliff, J. A., Electromagnetic Flow Measurement, Cambridge University Press, Great Britain, 1962.

THE FORMATION OF SURFACE FILMS BY ELECTRON BOMBARDMENT

Final Report of Work Carried Out
at the School of Chemistry
University of Bradford

by

Professor M. W. Roberts
and
Dr. J. R. H. Ross *

9 October 1967

SUMMARY

A study has been made of the adsorption of the tetramethylsilane molecule on evaporated films of tungsten and iron at 20°C and above. The method adopted involved ultra-high-vacuum techniques and a combination of volumetric and mass-spectrometric measurements, the nature of the adsorbed layer being further characterized by exchange with gaseous deuterium. Tungsten was found to dissociate tetramethylsilane to a much greater extent than did iron; the breakdown was particularly marked with respect to the cleavage of carbon-silicon bonds, as evidenced by the appearance of methane in the gas phase. The effect of electron bombardment of the adsorbed layer, both in the absence and presence of excess silane, has been studied briefly on tungsten films; in the presence of excess silane, electrons were found to cause further reaction of the silane. The rate of reaction appeared to be governed by either the electron current or by the pressure of the silane, depending on the conditions. This would indicate that at any pressure a certain proportion of the surface is covered by adsorbed molecules which are capable of reacting, and these will react if struck by an electron. Reaction was also found to occur if several layers of silane were adsorbed physically by cooling the surface to -195°C, and the surface was bombarded with electrons; the rate was found to depend on the electron current.

*The experimental work was done by R. H. Colburn, with the assistance of R. E. Jones and T. P. Solheim.

VI THIN FILM STUDY

Thin organic film coatings applied to metal substrates using electron beam bombardment techniques are being investigated. Applications of these films may include anti-cold welding coatings, lubrication, propellant compatibility and seal technology. Film formation studies include varying the electron to monomer (siloxane) ratio followed by laboratory tests for chemical compatibility, vacuum thermal stability and mechanical stress. Two universities are under subcontract to perform fundamental investigations of the chemical kinetics of electron polymerized siloxane DC 704 film and to examine the possible use of other monomer materials as films.

The final report representing the period from 9 October 1966 to 9 October 1967 submitted by the University of Bradford, England, and the final report representing the period of performance from 1 July 1966 to 1 July 1967 submitted by Dartmouth College, Hanover, New Hampshire are reproduced in the following pages.

	<u>Page</u>
The Formation of Surface Films By Electron Bombardment	6-2
Physical and Chemical Properties of Thin Polymer Films	6-24

The initial adsorption step will be intimately tied up with adhesion properties of any polymer formed. The metals chosen for the study were tungsten and iron because by analogy with the adsorption of hydrocarbons, widely different extents of dissociation might be expected.

PREVIOUS STUDIES

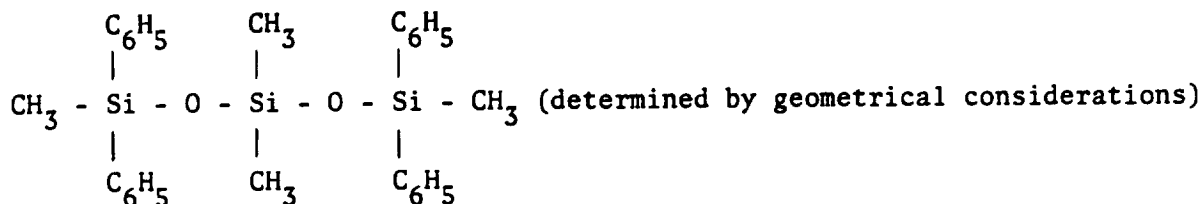
Continuous or polymer films have been formed by any one of a number of methods:

- (1) Electron bombardment,¹⁻⁹
- (2) U. V. radiation,¹⁰⁻¹¹
- (3) In a discharge tube,¹²⁻¹⁵

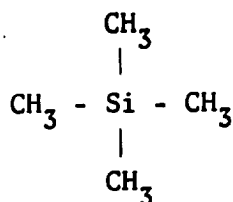
In general, the method of formation has been dictated by the vapor pressure of the monomer. If the vapor pressure is greater than about 1 mm Hg., then the discharge tube method is most convenient, but the method has several disadvantages, the main one being that the energy of the particles in a discharge is not uniform and therefore the properties of the resultant polymer cannot be controlled accurately. A very large number of monomers have been used in these studies, ranging in complexity from methane¹³, to styrene^{13,15}, ferrocene¹³, and various siloxanes¹⁴. Polymerization by the ultra-violet method is limited to molecules containing double bonds which may be excited by the radiation e.g., such molecules as butadiene¹⁰ and methylmethacrylate¹¹. Polymers formed by this method tend to be soft and flexible with properties more like those of the bulk polymer; and there are also difficulties due to gas-phase polymerization and deposition on the quartz windows. Electron beam polymerization is the most easily controlled method. Monoenergetic electrons may be used and clearly defined patterns may be obtained by focusing the electron beam. The disadvantage of the method is that the polymerization rate is lower, as the monomer pressure is restricted to about 10^{-3} mm. Polymers have been formed from vacuum greases^{1,2}, diffusion pump oils², butadiene⁶, epoxy resins⁹, and various methyl siloxanes⁵.

OBJECT OF STUDY

The object of the study is to gain an understanding of the physical structure and the chemical kinetics of continuous film formation and the importance of the electron/monomer ratio. Of particular interest in this context is the monomer DC704, a tetramethyltetraphenylsiloxane of molecular weight 484, probably with the structure:



Owing to the extremely low vapor pressure of this material at 20°C and the consequent difficulty of handling it quantitatively, as well as the very large number of product gases which might be expected, (e.g. CH₄, H₂, C₆H₆, silanes, lower siloxanes, etc.) it was decided to commence by studying the simpler molecule, tetramethylsilane,



This molecule has a much higher vapor pressure and can therefore be admitted to an evaporated metal film quantitatively through -80°C traps, which exclude mercury from the film. The silicon atom of tetramethylsilane has a similar type of bonding to that of the central silicon atom of DC704 and also the products of any reaction would be much simpler than from DC704. Previously there have been no studies of the adsorption of silicon compounds by clean metal surfaces, and it was therefore believed necessary to study this reaction before using the electron bombardment method of application.

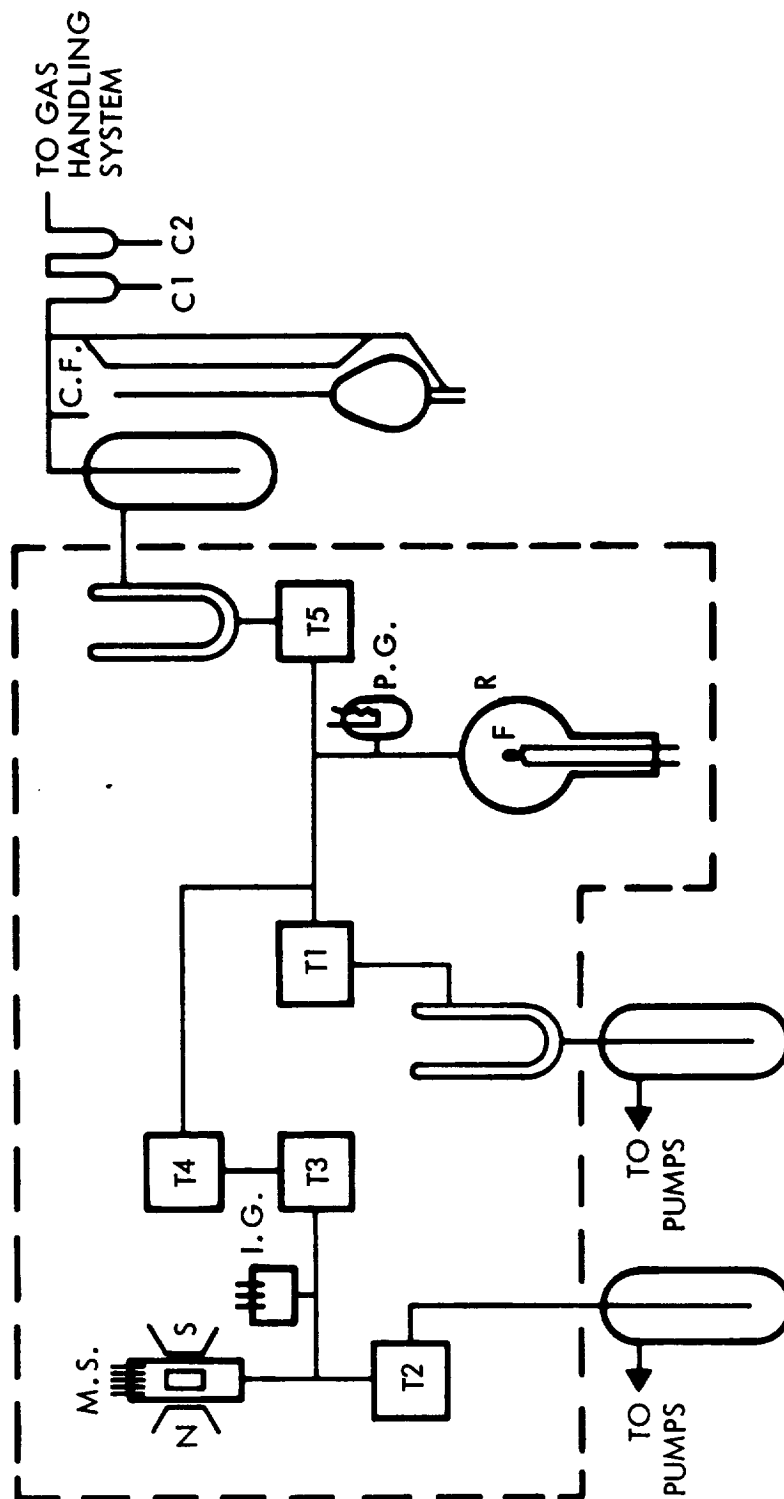


Figure 6-1. Experimental System

APPARATUS AND EXPERIMENTAL METHOD

Three features are required of the apparatus to be used:

1. It should be possible to prepare atomically clean metal surfaces of reasonably high area: this can be achieved by thermal evaporation of the metal onto a glass substrate under ultra-high vacuum conditions (i.e., $\leq 10^{-8}$ mm Hg.).
2. It should be possible to dose gases onto the metal films thus prepared in a quantitative fashion; the gases may be dosed from storage bulbs, through a series of mercury cut-offs, into a known volume which includes a McLeod gauge with which the pressure may be measured, and hence to the metal film.
3. It should be possible to analyze the product(s) of any reaction with the metal film; considering the small quantities of gas involved, the only technique which allows accurate analysis is that of mass-spectrometry.

Figure 6-1 shows the apparatus which has been constructed to meet these requirements. T_1 to T_5 inclusive are bakeable metal valves; the remainder of the system is constructed of Pyrex glass. The area within the dotted lines may be enclosed in an oven which is capable of operation at temperatures up to 350°C , but which is generally used at about 250°C . The traps outside the oven may be surrounded by tube furnaces and baked at the same temperature, and the McLeod gauge and cut-offs C_1 and C_2 may be flamed with an air-gas flame.

A typical procedure for an experiment is as follows:

(a) The entire system is baked for a period of upwards of six hours; after the first hour, the bakeout is interrupted in order to carry out the initial outgassing (and in the case of the iron, reduction) of the metal filament (see later).

(b) Traps 1 and 3 are surrounded by Dewar flasks containing liquid nitrogen, and trap 5 by a flask containing a solid CO_2 /acetone mixture (-80°C).

After the film has been formed, valves T_1 , T_3 , T_4 , and T_5 are closed, and a dose of tetramethylsilane is admitted to the section T_5C_1 and the pressure is measured. A pressure of 1×10^{-3} mm of tetramethylsilane in this volume corresponds to 2.50×10^{-3} cc or 6.77×10^{16} molecules. Similar, but not necessarily equal factors apply to the other gases encountered in the study. Calibration factors have also been obtained relating pressures in the volume T_5C_1 to the resultant pressure on expansion into the volume $T_4T_1C_1$, i.e., the reaction volume. The purity of the tetramethylsilane can be checked by condensing it in the cold-finger (CF) at -195°C , when its vapor pressure is about 2×10^{-5} mm Hg., which shows that it is clear of non-condensable gases such as O_2 and N_2 . After the dose has been measured, it is admitted to the film by opening T_5 . After several minutes, a liquid nitrogen trap is put around the cold-finger and the tetramethylsilane is condensed back to T_5C_1 ; the completion of the removal of the silane can be checked with the Pirani gauge, P.G. The composition of any non-condensable product gas can be found by opening T_4 wide and T_3 slightly until a pressure of about 10^{-7} mm Hg. is obtained in the mass-spectrometer tube, if necessary using slight adjustment of T_2 . The peak heights of the various ions in the ion chamber are then measured and the pressure of non-condensable gas is measured concurrently with the McLeod gauge. T_4 is closed after each mass-spectrometer scan but T_2 and T_3 are not touched during the course of an experiment. The extent of reaction of tetramethylsilane may be obtained at any stage by closing the valve T_5 , measuring the non-condensable pressure (P_{nc}) (i.e., H_2 and/or CH_4), removing the -195°C trap and measuring the total pressure (P_T). The condensable fraction throughout assumed to be tetramethylsilane; it cannot be measured using the Omegatron mass-spectrometer as the voltage of the ionising electrons in the Omegatron is 208 volts, which causes excessive fragmentation of the silane molecule. If it were possible to operate the spectrometer with a lower ionising potential (about 20V) it would be possible to measure the components in the gas phase at any time without condensing out the tetramethylsilane. The relative sensitivity of the mass-spectrometer for hydrogen and methane (Y/x) may be obtained by

(c) The oven is turned off and the glassware and valves are allowed to cool slowly towards room temperature.

(d) When the glassware is still hot, outgassing of the metal filament (F) in the reaction vessel (R) is commenced and the ion gauge is outgassed. When the pressure has fallen well below 10^{-6} mm Hg., the filament of the Omegatron mass-spectrometer (MS) is turned on and outgassed.

The outgassing and film-throwing procedures for the two metals are as follows:

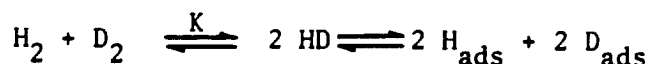
Tungsten

The filament is wound from about 15 cms of 0.2 mm diameter tungsten wire. This is attached to the 0.5 mm tungsten rods of the glass-metal seals by means of nickel clips, which enables the filament to be removed after throwing the film, allowing the weight of the film to be determined. The filament is outgassed at a current of 4.6 amps, with occasional bursts at 6.0 amps, and when a pressure less than 10^{-8} mm Hg. is attained, the film is formed with the walls of the reaction vessel at room temperature at a current of 6.2 amps.

Iron

The filament is wound from about 12 cms of 0.5 mm diameter "Spec pure" iron wire. After the initial short bake, the filament is reduced in 1 cm of H_2 at $1000^\circ C$, and is then outgassed at a current of 2.7 amps ($\sim 880^\circ C$), followed by the prolonged bake. The final outgassing is carried out at 2.7 amps, with bursts to 3.4 amps ($\sim 1100^\circ C$), until the pressure is less than 10^{-8} mm at 3.4 amps. The film is formed at a current of 3.6 amps with the reaction vessel at $-80^\circ C$. The film is sintered at $150^\circ C$ for about 10 minutes; the pressure during this step does not rise above 5×10^{-9} mm. Before throwing the film of either metal, traps 1, 2 and 5 are topped up, and trap 3 is filled with liquid nitrogen and trap 4 is filled with powdered solid CO_2 .

with hydrogen atoms bound to the carbon skeleton. The equilibrium is:



$$K = 2.87 \text{ at } -80^\circ\text{C}, \quad 3.24 \text{ at } 20^\circ\text{C}^{16}$$

If it is assumed that the proportions of hydrogen and deuterium in the gas phase are the same as on that part of the surface which is in equilibrium, then knowing the volumes of deuterium and tetramethylsilane added to the system, the number, n , of exchangeable hydrogen atoms per silane molecule can be calculated at any time. Experiments of this type were carried out in a reaction vessel (R) of the type shown in Figure 6-1.

2. The effect of electrons on the adsorbed layer.

3. The effect of electrons in the presence of an excess of tetramethylsilane. Only preliminary studies have been carried out in this category.

Figure 6-2 shows the reaction vessels used in categories (2) and (3).

2(a) incorporates a gun of tetrode construction. A cadmium sulphide coated disk which can be moved in and out of the electron beam from a side-arm facilitates focussing of the gun. It also serves the dual purpose of protecting the gun during the deposition of the evaporated film. Electrical contact to the film is made by a platinum foil sealed into the glass and attached to a tungsten rod sealed through the pyrex (C). This reaction vessel has the disadvantage that only a small proportion of the film is hit by primary electrons, while the rest of the film is hit by secondaries. Therefore, it is not possible to talk of the extent of reaction in terms of the number of layers formed, as it is not obvious on what proportion of the total surface reaction occurs. 2(b) is of diode construction, and with it the total film area is bombarded with electrons. The cathode is a small

solving two simultaneous equations:

$$P_{T_1} = x \cdot (h_{H_2^+})_1 + y \cdot (h_{CH_3^+})_1$$

and
$$P_{T_2} = x \cdot (h_{H_2^+})_2 + y \cdot (h_{CH_3^+})_2$$

where subscripts 1 and 2 correspond to two different sets of readings, $h_{H_2^+}$ and $h_{CH_3^+}$ are the peak heights for hydrogen and CH_3^+ ions respectively, and x and y are the partial pressures of hydrogen and methane, respectively, in the reaction vessel giving rise to unit H_2^+ and CH_3^+ peak heights. The method works if the relative pressures of hydrogen and methane are different from one measurement to the other. In some of the preliminary experiments, the leak rate was varied during the experiment and so the experiments had to be abandoned. From the calculated partial pressures of H_2 and CH_4 the number of molecules of H_2 and CH_4 (in H_2 and in CH_4) desorbed per adsorbed tetramethylsilane molecule can be calculated.

Three types of experiment have been carried out:

1. Adsorption at 20°C, followed by desorption of products at various temperatures. In some of these experiments, the reaction vessel was then cooled to -80°C and deuterium was added, and the exchange reaction was followed mass-spectrometrically. The relative sensitivities for H_2 , HD, and D_2 may be obtained by a similar method as for H_2 and CH_4 , or may be obtained before the experiment by equilibration of known mixtures of H_2 , HD and D_2 by the hot metal filament with the leak conditions to be used for the experiment. The relative sensitivities for H_2 , HD and D_2 do not vary as much with leak conditions etc., as does the relative sensitivity for H_2 and CH_4 . The exchange experiments depend on the assumption that gaseous deuterium will equilibrate with adsorbed hydrogen atoms and gaseous hydrogen molecules and that this equilibrium will occur more rapidly than

loop of 0.2 mm tungsten wire which may be outgassed in the same way as the filament (F). Currents up to several milliamps at 50-500 V can be achieved with this arrangement.

RESULTS AND DISCUSSION

(a) Adsorption Experiments

Some typical experiments are reported in Table 6-1 for adsorption at 20°C on tungsten and in Table 6-2 for iron, at the same temperature. For iron, the coverage of the surface with silane is shown relative to the krypton monolayer determined after the experiment.

$$\Theta = \frac{V_{\text{Si(CH}_3)_4\text{ads}}}{V_{\text{Kr}}}$$

For comparison with these figures, a value of Θ has been estimated for tungsten from the weights of the film using some data relating film weight and volume of the krypton, V_{Kr} determined previously. V_{Kr} was in some cases determined after the adsorption of tetramethylsilane, and was found to be lower than that estimated, i.e., there is a decrease in the surface area apparent of the gaseous krypton atoms after the adsorption of the silane. This decrease in area must be attributed to "blocking of pores" by the large silane radicals involved, permitting krypton adsorption on the geometric surface only, i.e., the uptake of krypton corresponded to an area of about 120cm², or approximately the geometric area of the inside wall of the reaction vessel. This is of importance when considering the build-up of polymer above the layer of chemisorbed silane, as each "completed layer" will correspond to less than the initial amount of silane chemisorbed. Tables 6-1 and 6-2 also show results of experiments where deuterium was added to the system after cooling to -80°C where such equilibrium experiments were carried out. Values of n are accurate to about ± 1.0 , but two significant figures are shown to indicate trends in

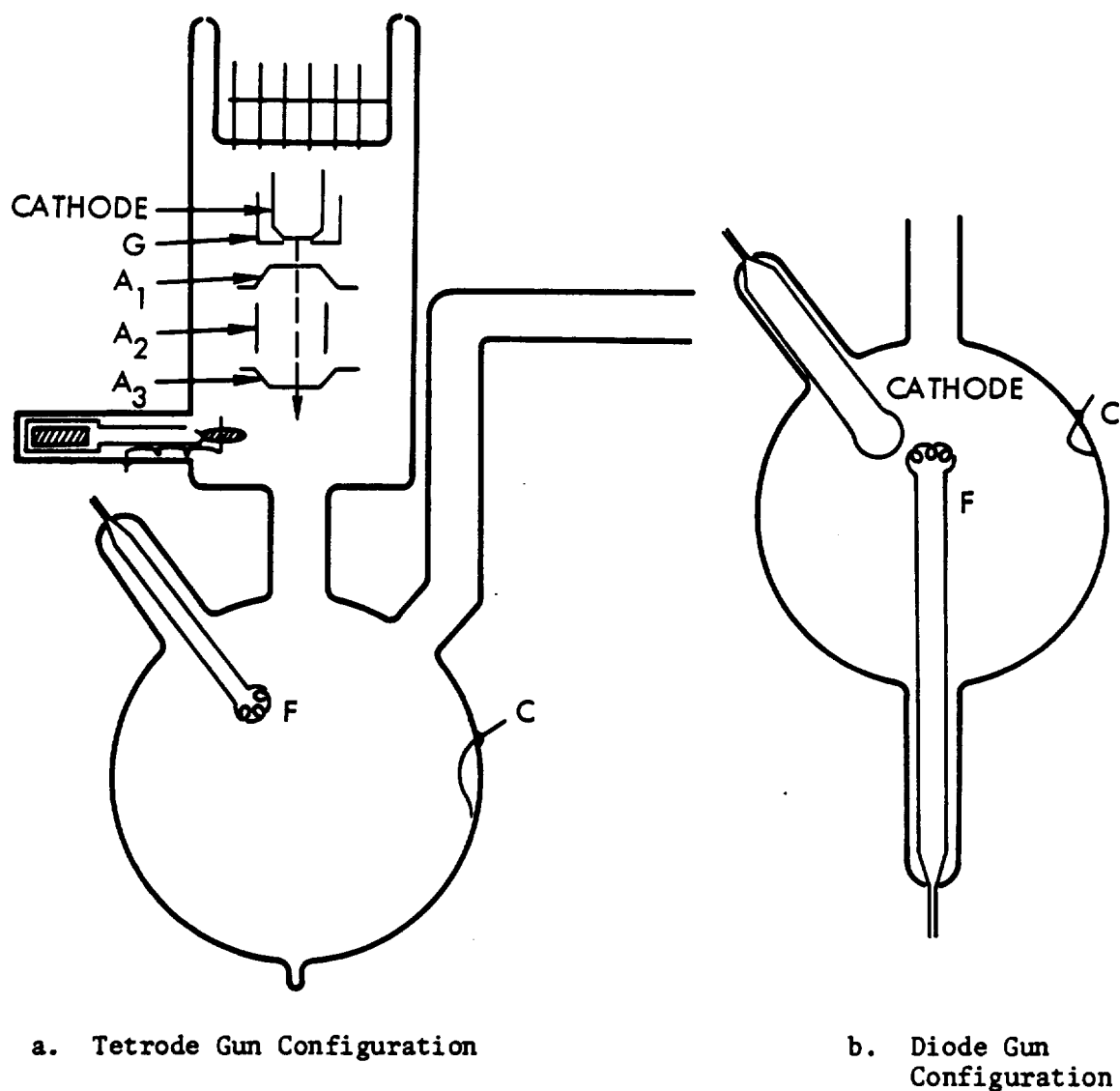


Figure 6-2. Reaction Vessels

TABLE 6-2.

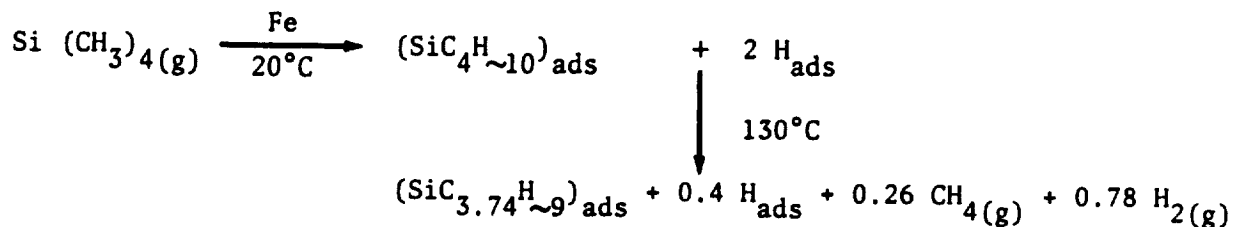
THE ABSORPTION OF TETRAMETHYLSILANE ON IRON FILMS

Run	V_{Kr} (cc x 10 ³ , s. t. p.)	$V_{Si(CH_3)_4}$ Adsorbed	θ	T°C	Temperature = T°C		Exchange			
					Surface Composition	n_{CH_4}	n_{H_2}	n at -80°C	n at 20°C	
1	-	5.80	-	130°	SiC _{3.74} H _{9.40}	0.26	0.78	2.0	9.8	
2	8.95	4.64	0.52	114°	SiC _{3.68} H _{9.37}	0.32	0.68	1.2	7.6	
3	9.18	4.25	0.47	152°	SiC _{3.73} H _{7.26}	0.27	1.83	-	-	
4	-	5.69	-	132°	SiC _{3.92} H _{10.44}	0.08	0.67	-	-	
5	8.62	4.15	0.48	162°	SiC _{3.90} H _{8.87}	0.10	1.36	2.4	9.3	
8	10.15	3.43	0.34	20°	SiC ₄ H ₁₂	(i.e., no products)			2.3	8.0

TABLE 6-1.
THE ADSORPTION OF TETRAMETHYLSILANE ON TUNGSTEN FILMS

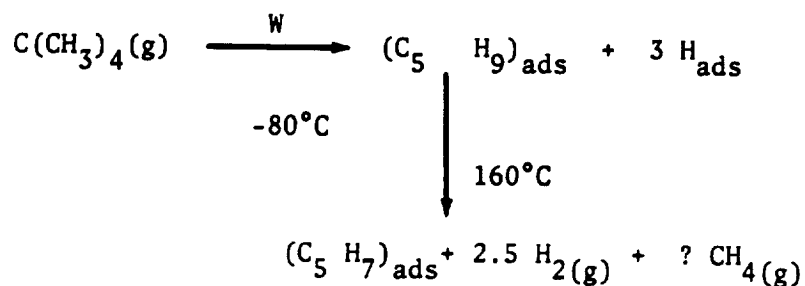
Run	Film Weight (mg)	V_{kr} Estimated (cc x 10 ³ , s.t.p.)	$V_{Si(CH_3)_4}$ Adsorbed	θ	Temperature = 20°C			Temperature = T°C			Exchange		
					Surface Composition	Gas Phase n_{CH_4}	Gas Phase n_{H_2}	T°C	Surface Composition	n_{CH_4}	n_{H_2}	n at -80°C	n at 20°C
7	11.7	43.4	17.2	0.39	SiC _{3.70} H _{10.20}	0.3	0.31	120°	SiC _{3.20} H _{5.40}	0.82	1.67	-	-
8	6.7	19.30	8.6	0.45	-	-	-	50°	SiC _{3.55} H _{8.56}	0.45	0.82	3.9	8.1
9	10.9	38.6	10.4	0.27	SiC _{3.21} H _{8.84}	0.79	0.0	130°	SiC _{2.11} H _{4.08}	1.89	0.162	1.0 3.0	3.4
11	7.4	22.3	11.8	0.53	SiC _{3.68} H _{10.72}	0.32	0.0	124°	SiC _{3.09} H _{5.79}	0.91	1.30	3.6	3.9
12	8.7	28.4	14.9	0.53	SiC _{3.53} H _{10.12}	0.47	0.0	128°	SiC _{2.18} H _{3.14}	1.82	0.74	2.4	3.2
13	9.7	32.5	16.4	0.51	SiC _{3.96} H _{11.12}	0.04	0.36	Not heated above 20°C				2.0	-

As for tungsten, the adsorption of the silane at 20°C followed by heating to 130°C may be depicted by a scheme of the type:

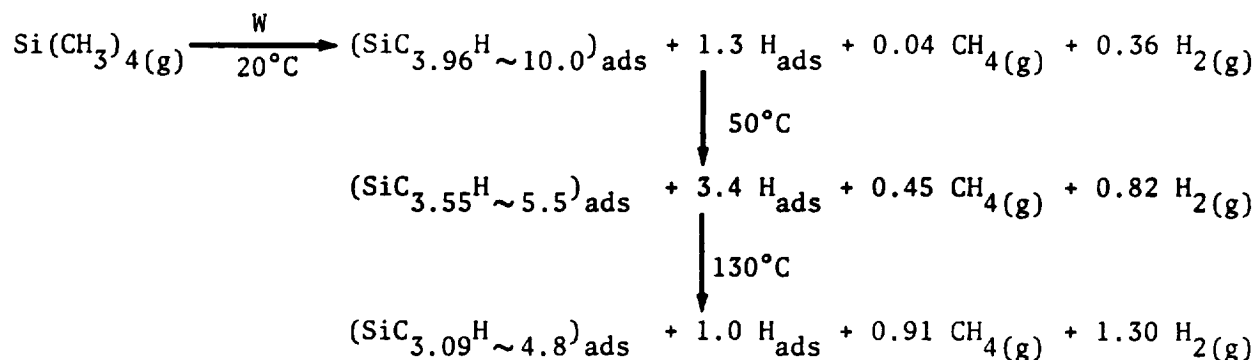


The actual values of n_{H_2} and n_{-80° vary slightly from run to run, but they indicate that little or no further hydrogen is liberated from the silane on heating apart from that which appears as gas phase methane. Again, there is no evidence whether or not Si-C bond cleavage has occurred on the surface, but iron causes considerably less breakdown than tungsten as evidenced by the gas phase products.

It is interesting at this stage to compare these results with the adsorption of hydrocarbon on metal films. Figure 6-3 shows the number of exchangeable hydrogens found at various temperatures after the adsorption of neopentane, $\text{C(CH}_3)_4$, by films of tungsten at -80°C (a), and after heating the adsorbed species to 160°C (b). The exchange at -80°C allows the surface radical to be characterized and is of most interest; the results at higher temperatures however serve to illustrate the point made above concerning the exchange at higher temperatures, showing a gradual change of some sort in the adsorbed radical. The scheme evolved for the adsorption of neopentane on tungsten is:



n. The silane would appear to be adsorbed according to the equation:



This scheme is deduced from the data shown in Table 6-1. The composition of the surface phase is only approximate. The actual proportion of $\text{CH}_4(\text{g})$ and $\text{H}_2(\text{g})$ appears to vary from run to run, and although part of this variation may be due to the uncertainty in the relative sensitivity for the two masses in the mass spectrometer, it is probable that such a variation does occur; for example in some runs only methane was observed at 20°C but in all the runs hydrogen was observed at higher temperatures, and so the lack of hydrogen at 20°C was not an instrumental error. The breakdown of carbon-hydrogen bonds and of carbon-silicon bonds occurs at room temperature. Further C - H bond cleavage occurs at between 20°C and 50°C , but the majority of the freed hydrogen atoms is not liberated to the gas phase until higher temperatures and then some of them appear in methane. No evidence can be obtained concerning Si-C bond cleavage and $\text{CH}_4(\text{g})$ may be formed either via adsorbed monocarbon species or by direct desorption from the skeleton.

The adsorption of tetramethylsilane on iron at 20°C occurs to approximately the same extent as on tungsten (see Table 6-2), and it may be noted that the estimated V_{Kr} values for tungsten must be of the correct order. The difference in absolute uptakes of the silane is due to the high surface area of tungsten films compared with that of iron films.

The presence of very small quantities of methane was inferred, but this was not conclusive due to the presence of rather large background methane peaks in the mass-spectrometer set-up used. The uptakes of neopentane were very similar to those obtained in the present work for tetramethylsilane. It would appear that the central silicon atom causes very different behavior; the weaker C-Si bond (about 10 kcal/mole less than the C-C bond) appears to break much more easily, resulting in desorption of methane. Θ values for the adsorption of tetramethylsilane on tungsten and iron were approximately 0.4 to 0.5. It can be shown that one krypton atom is adsorbed for every 2 to 3 metal sites, and so one silane molecule is adsorbed per 4 to 7 sites. Thus, for example, the surface radical on tungsten at 20°C, $\text{SiC}_{\sim 3.5}\text{H}_{\sim 10}$ occupies somewhere between 3 and 6 metal sites, which is quite possible according to its size: its cross sectional area is about 30 \AA^2 while that of tungsten is 7 \AA^2 .

Table 6-3 shows the results of an experiment at 20°C in which dose (1) represents incomplete adsorption, dose (2) represents complete adsorption, and dose (3) the slightly enhanced adsorption after pumping the system for several minutes. $V_{\text{Si(CH}_3)_4\text{ads}}$ corresponds to the total amount of the silane adsorbed, whereas $V_{\text{H}_2(\text{g})}$ and $V_{\text{CH}_4(\text{g})}$ corresponds to the amount of hydrogen and methane in the gas phase at any time. It will be seen that from dose (1) to dose (2) the proportion of desorption of products; relative to the amount of the silane adsorbed increases, indicating displacement of both methane and hydrogen during the enhanced adsorption. Pumping the reaction vessel allows further reaction to proceed and this reaction must occur on sites vacated by desorbed material of some sort. That hydrogen only was involved was shown in another experiment by pumping only section T_5C_1 (Figure 6-1) and then expanding into this volume from $T_iT_4T_5$, when an increase in the amount of hydrogen, but not of methane, was found.

Table 6-4 shows that the adsorption of the silane at 20°C increased gradually with time. The relative proportion of carbon in the radical hardly

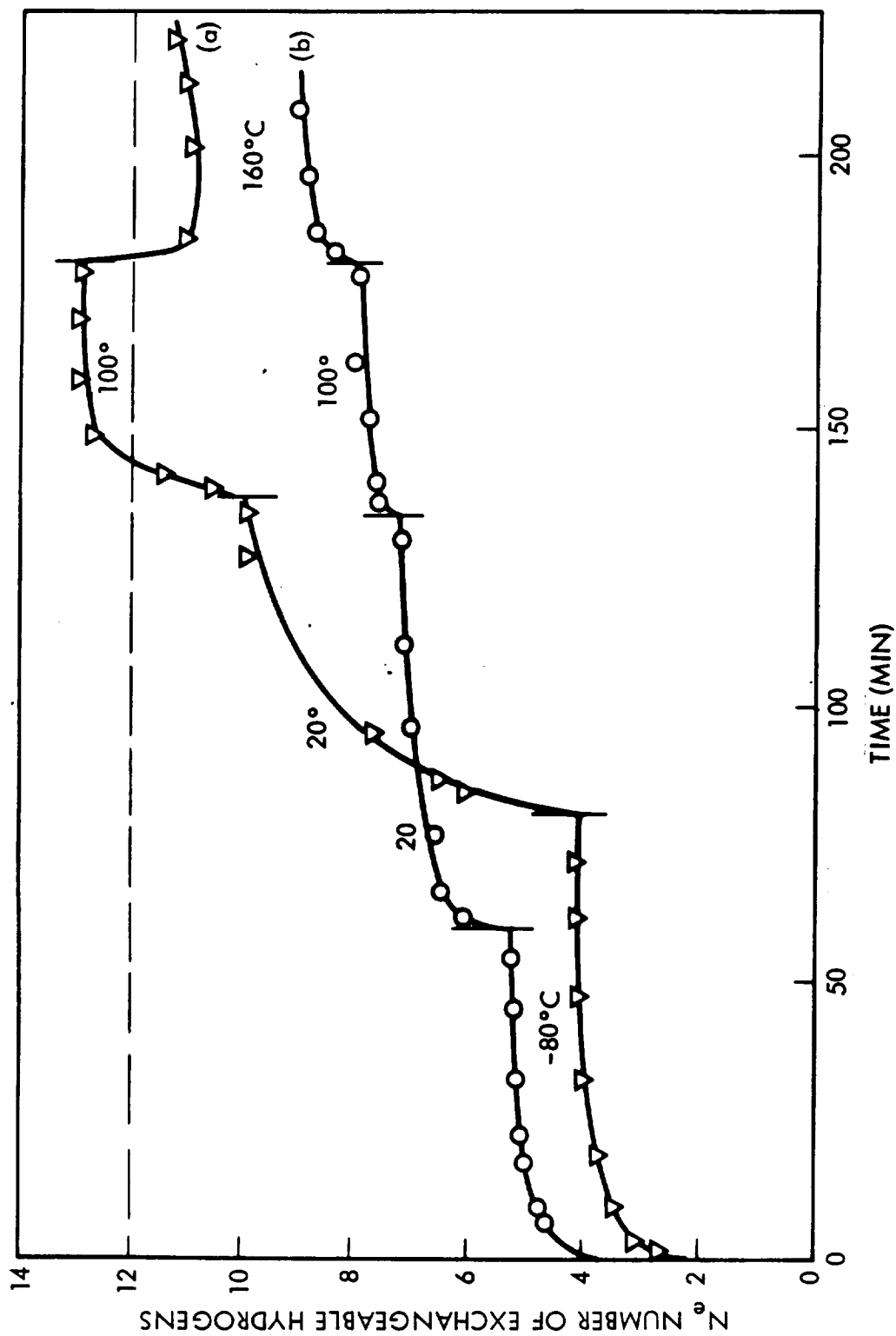


Figure 6-3. No. of Exchangeable Hydrogens at Various Temperatures After
 a) Adsorption of Neopentane $C(CH_3)_4$ by Films of Tungsten At
 -80°C and b) After Heating the Adsorbed Specifics to 160°C

changed, but that of hydrogen decreased, indicating that the gradual process is due to the displacement of adsorbed hydrogen by the excess silane. This type of rate process was observed with neopentane on tungsten¹⁷, when the neopentane was found to displace a pre-adsorbed layer of hydrogen by a rate process. These results will explain to some extent the variation of V_{CH_4}/V_{H_2} shown in Tables 6-1 and 6-2, this ratio determined by both whether an excess of silane was added and by how long the silane was left in contact with the surface.

The adsorption results show that tungsten causes much more breakdown of the silane on adsorption at 20°C and that the higher the temperature to which the surface is raised, the more nearly the surface composition approaches that of silicon carbide (SiC). The composition of the surface layer will have considerable effect on the properties of the polymer formed, e.g., on its adherent properties.

(b) The Effect of Electron Bombardment

Four preliminary types of experiment have been carried out at 20°C, in all cases after adsorption of tetramethylsilane at 20°C.

- (i) Bombardment of the surface in the presence of a vapor pressure of 10^{-5} mm of silane.
- (ii) Addition of silane to the surface after (i) or after bombardment in the absence of a source of silane.
- (iii) Bombardment in a vapor pressure of 10^{-3} mm of silane.
- (iv) Bombardment of a physically adsorbed layer at -195°C.

Table 6-5 shows the results of an experiment which was designed to cover each of the above points in turn. The number of electrons striking the surface (e), the total number of silane molecules reacting (m'), and (where appropriate) the number of molecules striking the surface (m), all in the total time of the experiment, are shown, together with the number

TABLE 6-3.
(see text)

Dose	$V_{\text{Si}(\text{CH}_3)_4 \text{ ads}}$ (cc x 10^3 , s.t.p.)	$V_{\text{H}_2(\text{g})}$ (cc x 10^3 , s.t.p.)	$V_{\text{CH}_4(\text{g})}$ (cc x 10^3 , s.t.p.)	Surface Composition
1	12.8	1.12	2.98	$\text{SiC}_{3.77}^{\text{H}}10.90$
2	15.2	3.08	6.22	$\text{SiC}_{3.59}^{\text{H}}9.95$
3	16.38	0.54	0.82	-

TABLE 6-4

THE INCREASE IN ABSORPTION OF TETRAMETHYLSILANE ON A TUNGSTEN FILM WITH TIME

Time; (min.)	$V_{\text{Si}(\text{CH}_3)_4 \text{ ads}}$ (cc x 10^3 , s.t.p.)	$V_{\text{H}_2(\text{g})}$ (cc x 10^3 , s.t.p.)	$V_{\text{CH}_4(\text{g})}$ (cc x 10^3 , s.t.p.)	Surface Composition
2	4.98	1.15	0.72	$\text{SiC}_{3.86}^{\text{H}}10.96$
8	5.00	1.69	0.79	$\text{SiC}_{3.85}^{\text{H}}10.71$
22	5.85	2.33	0.91	$\text{SiC}_{3.84}^{\text{H}}10.58$
42	6.05	2.80	0.97	$\text{SiC}_{3.84}^{\text{H}}10.43$

of electrons necessary to cause one molecule of silane to react (e/m'). The electron voltage throughout was 100V.

It would appear that process (i) is inefficient in producing reaction, in that only one in 270 electrons causes any reaction. Although more molecules than electrons strike the surface, it would appear that insufficient molecules reach the surface in the correct form to react. However, the fact that when excess silane is admitted to the surface (case ii) further reaction occurs, would indicate that some sort of active surface has been generated by the electron. The uptake shown in case (ii) corresponds to about one geometric monolayer. Both cases (iii) and (iv) appear to be efficient processes. In (iii), the pressure has been raised sufficiently so that each electron which reaches the surface is capable of causing reaction i.e., the supply of molecules in suitable conformation to react has been increased. The rate of reaction therefore depends on either the pressure or the electron current; in the former case, (e.g., case i), $e/m' > 1$, whereas in the latter, $e/m' \approx 1$ (case iii). Bombardment of a quantity of physically adsorbed silane also gave considerable reaction (case iv), with the extent of reaction again being determined by the number of electrons striking the surface.

Future work involving tetramethylsilane will be directed towards ascertaining (a) which of processes (iii) or (iv) produces more effective polymers, (b) the actual all-over chemical structure of the polymers as obtained by continuous mass-spectrometric analysis of the gas phase, and (c) the effect of parameters such as substrate temperature, pressure, and electron current, both on the rate of polymer formation and on its properties. Several confirmatory experiments on the formation of the adsorbed layer are still outstanding. Work should be accomplished using an Omega-tron capable of analysis of the gas phase, at low ionising voltages; there by enabling analysis to be made during reaction, and of very fast scan rates, such that very fast reactions may be studied.

TABLE 6-5.
THE EFFECT OF BOMBARDING THE SURFACE WITH ELECTRONS UNDER VARIOUS CONDITIONS

Conditions	Current μA	Time Minutes	Number of Electrons Striking Surface e	Extent of Reaction (molecules) m^{-2}	e/m^2	Molecule Impingement Rate m^{-2}
(i) Bombardment in v.p. of 10^{-5} mm of $\text{Si}(\text{CH}_3)_4$ at 20°C	400	19	2.7×10^{18}	1×10^{16}	270	2.9×10^{20}
(ii) Addition of excess $\text{Si}(\text{CH}_3)_4$ to the surface after (i) and after repeating (i) again (20°C)	400	19	2.7×10^{18}	7×10^{16}	40	-
	200	11	7.9×10^{17}	3.5×10^{16}	23	-
(iii) Bombardment in v.p. of 10^{-3} mm of $\text{Si}(\text{CH}_3)_4$ at 20°C	100	8	2.9×10^{17}	3.9×10^{17}	1	1.4×10^{22}
(iv) Bombardment with several physically adsorbed layers at -195°C	100	3	1.08×10^{17}	8.1×10^{16}	1	-

PHYSICAL AND CHEMICAL PROPERTIES OF THIN POLYMER FILMS

Final Report to TRW Systems
under Purchase Order K 4231-SC
Dartmouth College
Hanover, New Hampshire

by

Robert W. Christy

1 July 1966 - 1 June 1967

PHOTOCURRENTS THROUGH THIN POLYMER FILMS

INTRODUCTION

Thin insulating films can be formed on a substrate in vacuum when the substrate is simultaneously bombarded by an electron beam and by molecules of an organic or silicone monomer. The dielectric films thus formed have exceptional insulating properties, good adhesion, excellent temperature stability, and are unaffected by most solvents. The mechanism of the film formation is the free-radical polymerization of the molecules adsorbed on the surface, under the action of the bombarding electrons. The molecules are cross-linked by the electron beam to form a solid polymer film. The rate of deposition of the solid film depends on the substrate temperature, electron beam current density, and flux of molecules per unit area. The influence of these factors which is observed experimentally is satisfactorily explained by a phenomenological kinetic theory, which also involves the electron cross-section for the cross-linking reaction and the mean time of stay of the molecules on the surface.^{1,2}

The electrical properties of the thin polymer films have been previously studied in detail.^{3,4} Sandwiches consisting of a polymer film between two metal films show nonlinear current-voltage characteristics which have not yet been satisfactorily explained. In addition they exhibit aging when

Future plans are to run a program involving a study of polymers formed from a varied range of monomers. The emphasis of this work will initially be on comparing the physical and chemical properties of various polymers prepared under identical conditions. Properties to be studied will include adhesion strength, chemical inertness, electrical properties, infra-red adsorption, etc. Various metal substances will also be used which will be in the form of metal ribbons.

due to free carriers produced in the polymer film itself. This volume photoconductivity, which gives further information on energy levels, should predominate in thicker films.

EXPERIMENTAL PROCEDURE

The sandwiches were constructed by evaporating a metal strip, called the electrode, onto a glass microscope slide. This strip was covered with a thin layer of DC 704 silicone oil polymerized by electron bombardment. Over this layer at right angles to the electrode was evaporated a second, semitransparent, metal strip, called the counterelectrode. The finished sandwich was removed from the evaporating system to an evacuable sample holder with electrical leads and optical window for the dark current and photocurrent measurements. Dark current was measured by connecting a voltmeter in parallel with the sample, and connecting an ammeter and variable DC emf across this combination. The photocurrent is the additional current observed in a similar arrangement when a monochromatic light was shone on the counterelectrode. The photocurrents were generally comparable with the dark currents. Since the counterelectrode was partially transparent, photoemission from both electrodes could occur simultaneously.

Sandwich Construction

The glass slide substrates were cleaned in an ultrasonic cleaner, first in detergent solution, rinsed in distilled water, and then in alcohol.

The substrate was mounted in the vacuum system on a rotatable substrate carrier, which can position the substrate over either of two evaporating filaments or an electron gun (see Figure 6-4). The substrate is protected by a solenoid-actuated shutter. The aluminum metal was evaporated from tungsten wire baskets at a rate of approximately $30 \text{ \AA}/\text{sec}$ at pressures around 5×10^{-6} Torr. The electrodes were about 1500 \AA thick and 1.8 mm wide, giving an active area of about 3.2 mm^2 . Electrical connection to the electrode was made by indium-soldering nickel-wire leads to the glass substrate.

exposed to air; this aging may be related to the number of free radicals remaining in the film after the electron bombardment. These properties presumably depend on the distribution of conduction electron energy levels in the polymer.

Regarding the polymer valence-electron structure from the standpoint of band theory, the energy levels of the conduction band states can be further elucidated by photoemission of electrons into the thin film insulator from metal electrodes. Measurement of the photocurrent as a function of photon energy and bias voltage applied to metal-insulator-metal sandwiches should give the variation of the conduction band height through the thickness of the insulating film. This technique has been successfully applied to a similar investigation of aluminum oxide insulating films.⁵

In the following we report the results of photocurrent measurements on aluminum-polymer-aluminum sandwiches. The polymer was formed by electron bombardment of DC 704, a tetramethyltetraphenyltrisiloxane made by the Dow-Corning Company. In all these sandwiches the electron/molecule ratio during formation of the polymer was maintained at the same relatively large value, and the substrate was at room temperature. All current-voltage and photocurrent measurements were made at room temperature, with only a few minutes' exposure of the sample to air. In each case the thickness of the polymer film was of the order of 200 Å. The aluminum film toward the incident light was semitransparent, so that photoemission from both aluminum films can be expected.

The photocurrent measurements were made in the wavelength range from 350 to 620 mμ (2.0 to 3.5 eV). At wavelengths longer than about 550 mμ (below 2.2 eV) the polymer film is relatively transparent,³ so that any photocurrent may be due to emission from the metal electrodes. At about 410 mμ (3.0 eV), the absorption by the polymer film becomes of the order of 10%. Thus at shorter wavelengths (high energy) the current due to photoemission from the electrodes may be complicated by absorption or by a photocurrent

The electron gun was a diode flood gun, using an oxide-coated cathode. The anode aperture had a diameter of 6.3 mm, and was about 2 mm from the cathode, and about 12.5 cm directly below the substrate. The normal operating conditions were as follows:

anode voltage	0 V
cathode voltage	-400 V
filament current	3.3 A

During formation of the polymer film on the substrate, a bias of +90 V was applied to the electrode, so that all secondary electrons were presumably collected. (Lampblack was coated onto the mask in front of the substrate, in order to minimize secondary electron production by primary electrons which hit the mask.) The net current to the substrate was normally about 300 μ A, and the rate of film formation was about 25 Å/min. The mask had a diameter of 13 mm, giving a uniform polymer spot of approximately this diameter. Over the polymer spot there was room to evaporate four separate counterelectrodes, of different thicknesses if desired. Since the counterelectrode thickness is only of the order of 100 Å, aluminum is probably a better material than silver for this film: Silver films of this thickness tend to be discontinuous⁶, whereas aluminum is more likely to be continuous.

The source of DC 704 which provides the flux of molecules is a small cylinder which is mounted 3.5 cm from the substrate at an angle of 50° from the normal. It is a copper cylinder 1/2" ID and 1" long with wire wrapped around it for a heating element. A thermocouple is mounted in the base to measure the temperature of the oil. The films reported here were made with the oil at room temperature, but the temperature variability is provided so that the molecule flux can be varied in future experiments. During the formation of the polymer films the vacuum system is trapped with liquid nitrogen; the rate of formation due to back-streaming pump oil is negligible, but nevertheless the pump contains DC 704 so that any contamination is a higher order effect.

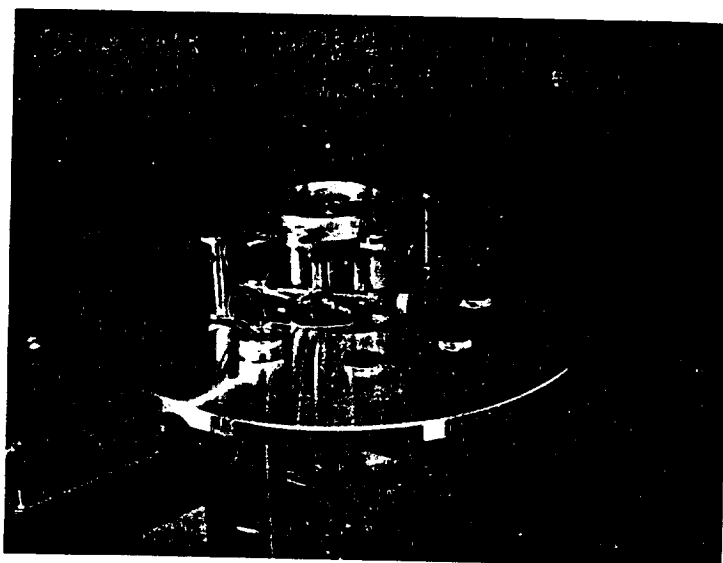


Figure 6-4. Substrate Holder and Source Assembly
in Vacuum System

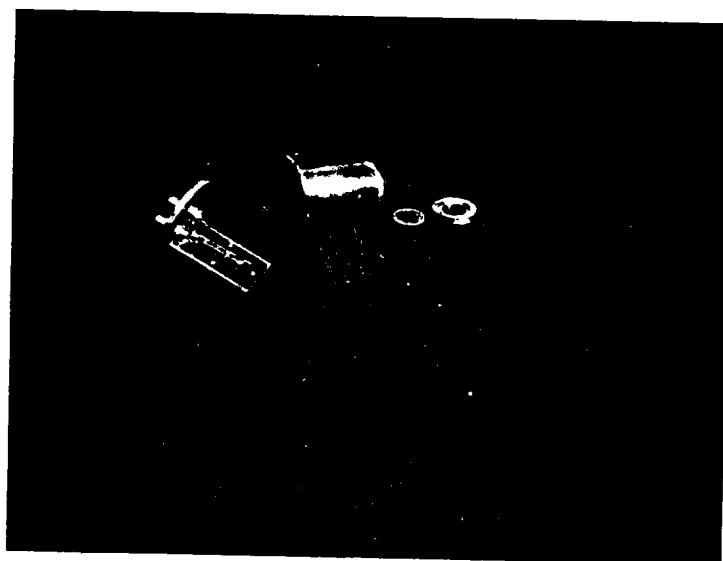


Figure 6-5. Specimen Holder for Electrical and
Photoelectric Measurements

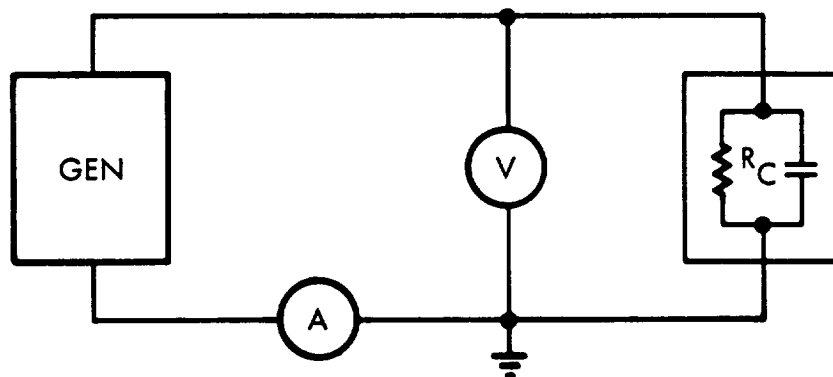


Figure 6-6. Circuit for Measurement of Dark Current

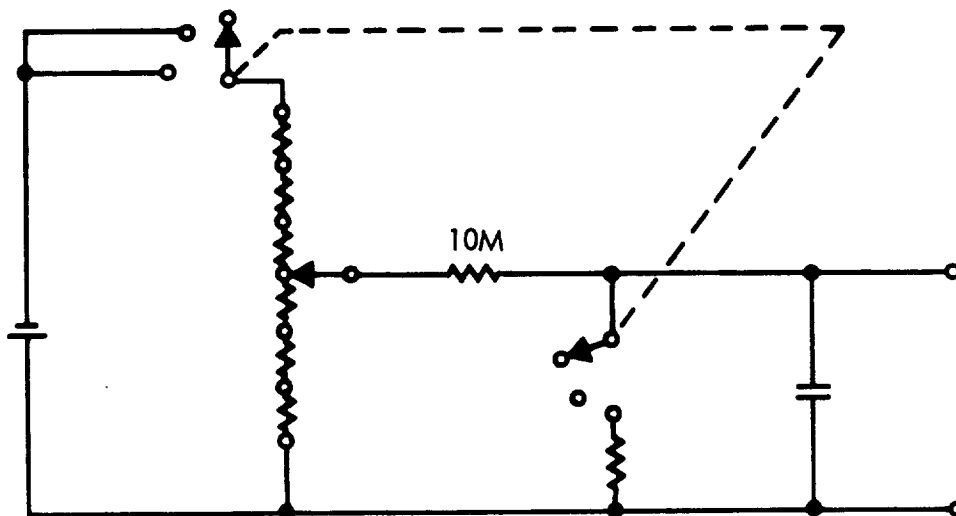


Figure 6-7. Voltage Generator for Circuit of Figure 6-6
All resistors are $1\text{ k}\Omega$ except as noted.

Electrical Measurements

A sample holder was constructed for the electrical and photoelectric measurements on the finished metal-polymer-metal sandwiches (see Figure 6-5). The specimen is enclosed in a copper can for purposes of electrostatic shielding; four electrical leads enter through BNC connectors. This can may be evacuated, so that the measurements can be made under vacuum conditions. (Rapid aging of the insulating films occurs during exposure to air.) A quartz window with O-ring seal admits visible and uv light for the photoelectric measurements. Electrical leads are attached to the specimen electrodes (aluminum films) by soldering them to the glass substrate with indium.

The circuit (Figure 6-6) for measuring the V-I characteristics (dark current) of the completed sandwiches consists of a generator which supplies a voltage that increases at an approximately constant time-rate; a high-impedance voltmeter (General Radio Electrometer-Amplifier Type 1230A), a micromicroammeter (Hewlett-Packard Model 425A), and an X-Y recorder (Moseley Model 135) to record the voltmeter and ammeter outputs. The voltage generator output is the voltage across a large capacitor which is charged through a high resistance by a battery (Figure 6-7). For example, with a 9 V battery, 10 M Ω resistor, and 68 μ F capacitor, the output voltage rises from 0 to 1 V in about 50 sec. Slower rates are obtainable by dropping the battery voltage. In the circuit connections used, the ammeter measures the current through the voltmeter as well as the current through the sample. Because the voltmeter input impedance is about $10^{14} \Omega$ its effect is negligible. All leads are shielded.

Photocurrents could be measured using the same circuit as for the dark current, but with a constant (though variable) voltage source, simply by shining a light on the specimen and noting the increase of current. In this method, however, the current is observed to change with time after the light is turned on, and again after it is turned off. In order to eliminate the dependence of the observations on such trapping and space-charge effects, a pulsed-light technique was used. This was accomplished

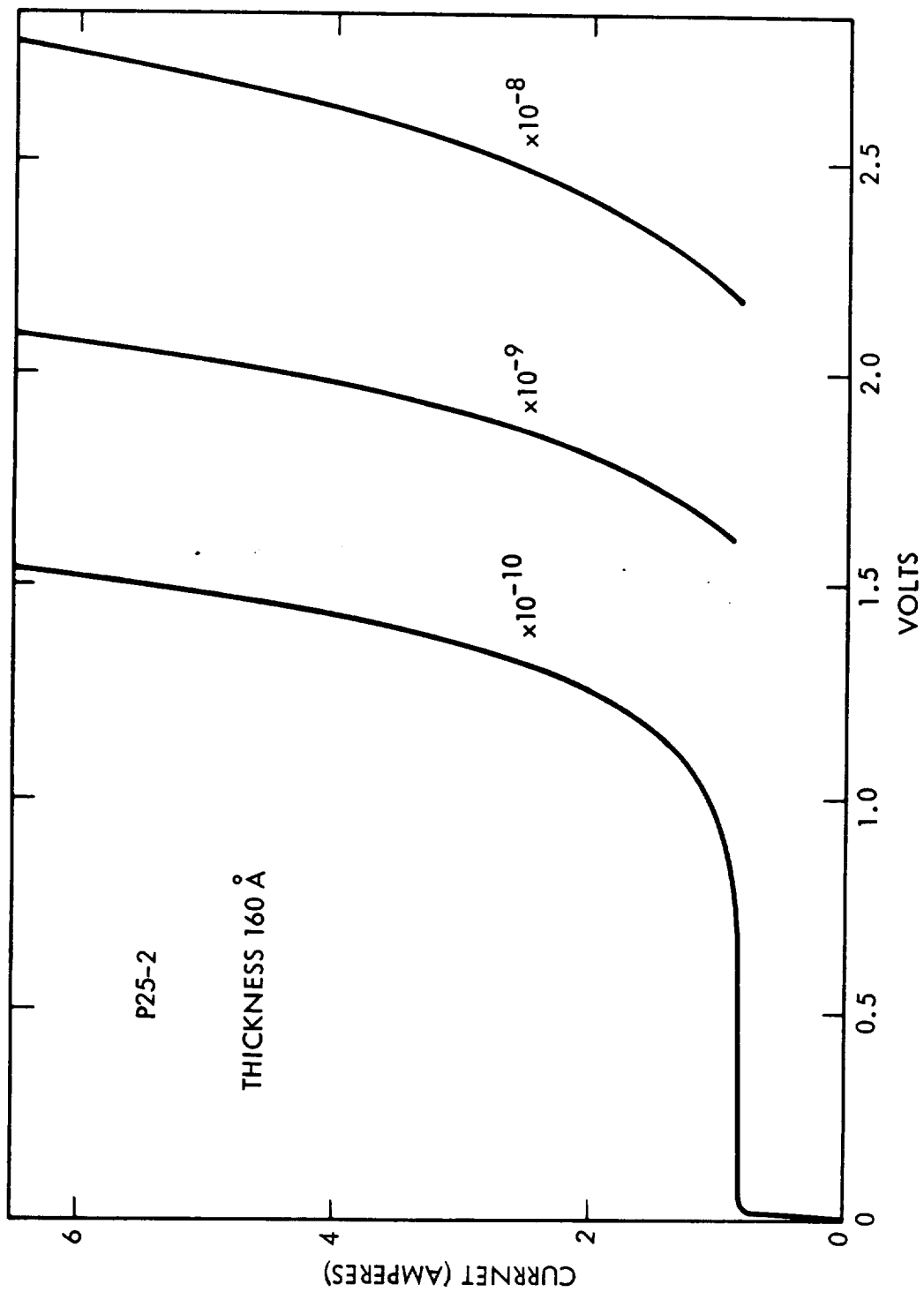


Figure 6-8. Dark Current of Aluminum-Polymer-Aluminum Sandwich

by limiting the exposure to light to three light pulses of 0.1 sec duration. Shorter pulses could not be used because capacitance of the sandwich introduced rise times of the order of several milliseconds. The photocurrent pulse appeared as a voltage across a 10 M Ω resistor which replaces the ammeter in Figure 6-6. The voltage pulse was amplified 1000x by a Tektronix Type 122 low-level preamplifier, and displayed on a Tektronix Type 545 oscilloscope which had a 60-cycle filter before its input. The current was calculated by measuring photographs of the oscilloscope trace, using the voltage scale calibration of the oscilloscope. For the low-level signals, a TMC Mod. CAT-1024 Computer-of-Average-Transients permits to eliminate the random noise from the signal by averaging over a number of sets of three pulses. Its output could be either photographed or recorded on the recorder.

Light Source

The monochromatic light was obtained at the exit slit of a Bausch and Lomb 250-mm grating monochromator. The sources were Bausch and Lomb tungsten lamp and high pressure mercury arc accessory to the monochromator. The slits were set at 4 mm, giving a pass band of 50 Å. Intensities at all wavelengths used were of the order of 1000 $\mu\text{W}/\text{cm}^2$. A rotating shutter at the exit slit was used to pulse the light incident on the sample, which is about 8 cm from the exit slit in the evacuated, shielded sample chamber.

The monochromator output intensity at the position of the sample was calibrated with an E G & G Spectroradiometer, Model 580, or with a Leybold 557-36 Thermopile and EMR Mod. 33-B Ten-cycle amplifier.

EXPERIMENTAL RESULTS

The V-I curve for the dark current of a typical aluminum-polymer-aluminum sandwich is shown in Figure 6-8. The curve is approximately linear at low voltage (not apparent on the scale in the figure), and exponential at higher voltage as observed previously⁴. Both the rate of film formation and the magnitude of the current are in reasonable agreement with previous

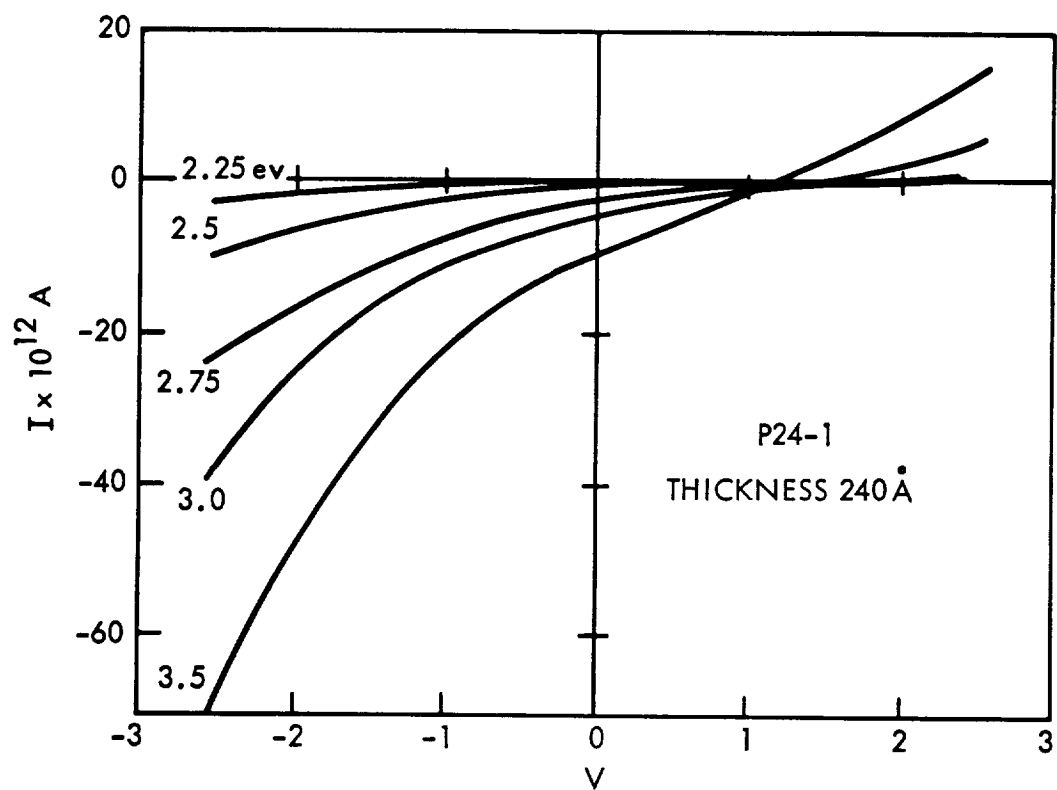


Figure 6-9. Photocurrent as a Function of Applied Bias Voltage, for Several Different Photon Energies

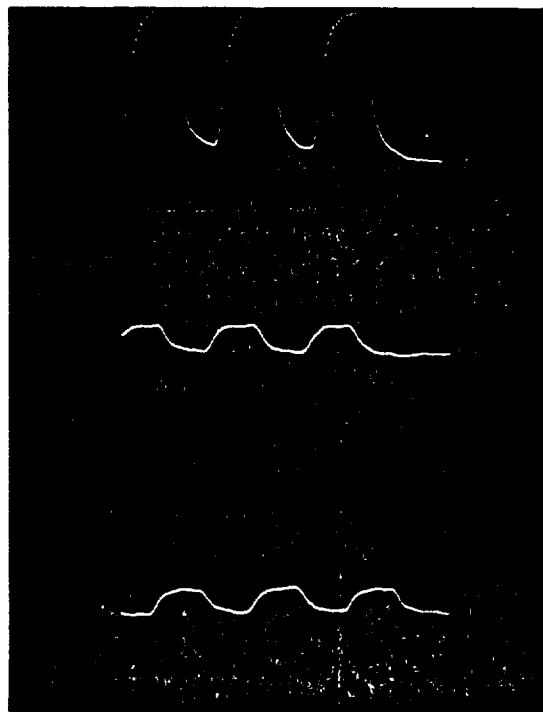


Figure 6-10. Photocurrent Pulses at Different Wavelengths

results^{1,4} applicable to a relatively large electron/molecule ratio.

The non-zero current at zero voltage is due to the capacity of the sandwich. The sample is effectively a parallel combination of resistance R and capacitance C . The linearly increasing applied voltage V gives a constant charging current into this capacitance,

$$I_0 = C \, dV/dt,$$

which constant current is added to the current through the sample resistance, V/R . The zero-voltage current can be used to give a measure of the capacity of the sandwich, and therefore of the thickness of the polymer film, from the formula (in MKS units)

$$C = \epsilon A/s,$$

where $A = 3.2 \times 10^{-6} \, \text{m}^2$ was the area and s the thickness of the polymer. The relative dielectric constant has been determined³ to be 2.8 for somewhat thicker polymer films.

The capacity can also be measured using an AC bridge. The bridge measurements give results somewhat smaller than the estimate of C obtained from the V - I curves. The quoted thicknesses are calculated from the bridge measurement of C , so as to be comparable with previously reported work⁴. (The capacity of the present films was measured at room temperature; the value at liquid nitrogen temperature or below may be about 10% smaller.⁴)

Figure 6-9 shows the dependence of the photocurrent upon the voltage applied to the sandwich for several fixed photon energies. The curves have been normalized for the dependence of light intensity on wavelength. Positive voltage means that the counterelectrode is positive with respect to the electrode, and positive current corresponds to electrons going from the electrode to the counterelectrode. These curves are obtained from oscilloscope traces of the type shown in Figure 6-10. The three traces

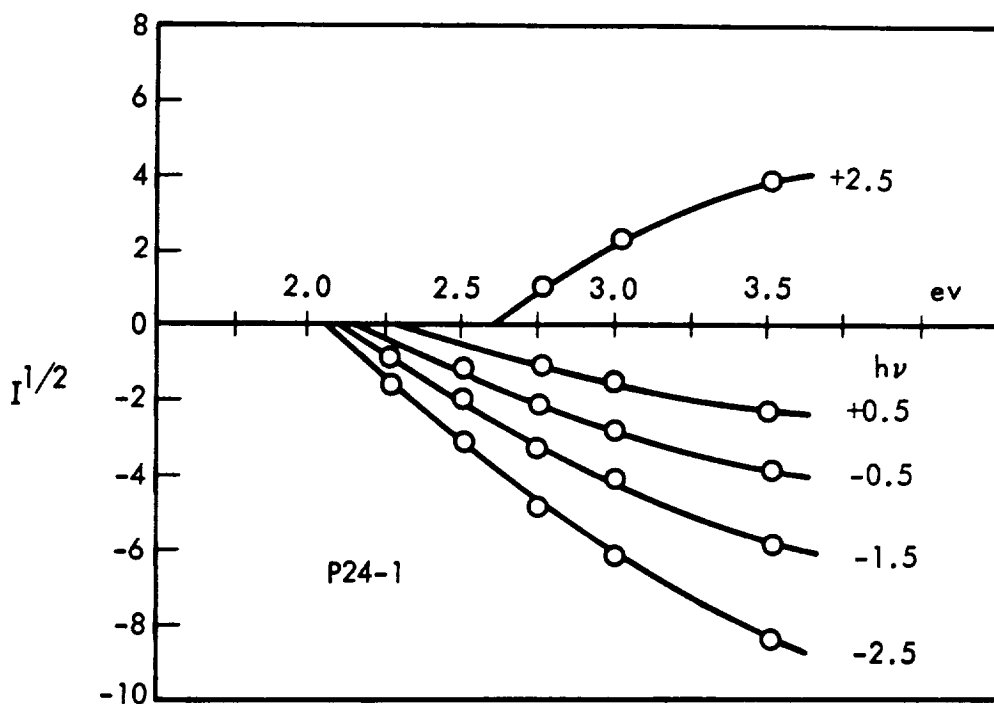


Figure 6-11. Fowler Plot of Photocurrent Vs. Photon Energy, for Different Bias Voltages

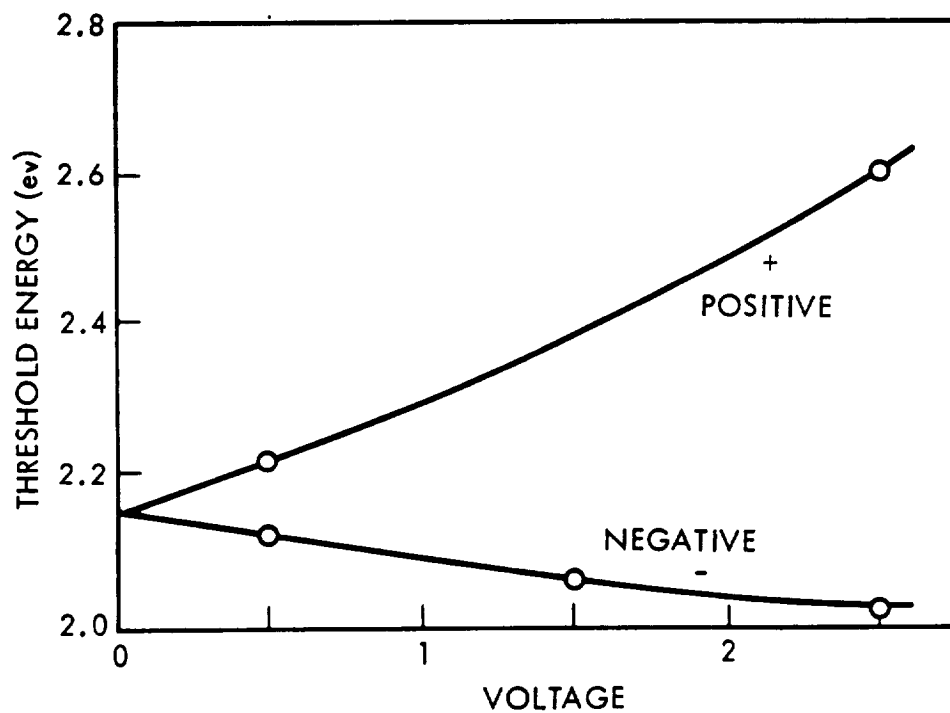


Figure 6-12. Threshold Energy from Figure 6-11 Vs. Bias Voltage

are for wavelengths of 354, 413, and 440 $m\mu$ and + 2V bias, with sweep speed 0.1 sec/cm, sensitivity 20 $\mu V/cm$ (sample P26-1). The photocurrent increases both with increasing bias voltage and increasing photon energy. The asymmetry seen in Figure 6-9 appears to be typical of the sandwiches studied under the stated conditions. For zero bias, the electrons move predominantly toward the electrode rather than the counterelectrode.

DISCUSSION

Two different sources of photon-produced charge carriers can be considered in order to explain the experimental photocurrent curves: 1) carriers excited from the conduction band states of the metal electrode into conducting states of the insulator and transported from the boundaries through the insulator, and 2) carriers excited from non-conducting to conducting states in the volume of the insulator itself. In either case the conductivity would depend on the number of carriers produced and the "Schubweg," i.e. the mean distance traveled before retrapping of the carrier. The Schubweg depends on the applied electric field and on the density of trapping centers for the carriers.

The analysis of photoemission from the electrodes shows⁷ that in first approximation the current should be proportional to $(\nu - \nu_0)^2$, where ν is the photon frequency and ν_0 is the threshold frequency. Thus a plot of $I^{1/2}$ versus photon energy should be linear near the cutoff for photoemission (Fowler plot). A Fowler plot of the data in Figure 6-9 is shown in Figure 6-11. These curves show an approximately linear dependence, with a threshold frequency which depends on bias voltage. The threshold photon energy is shown as a function of bias voltage in Figure 6-12. Using this model, Geppert has shown^{8,5} how the shape of the bottom of the conduction band can be obtained from Figure 6-12. This analysis would give a barrier height of about 2.0 eV at the counterelectrode, rising to about 2.15 eV in a distance equal to one-tenth of the thickness. Beyond this point the bottom of the conduction band would have to bend down again, in order to account for the negative current at zero bias. These results are not unreasonable, but the other branch of the curve in Figure 6-12,

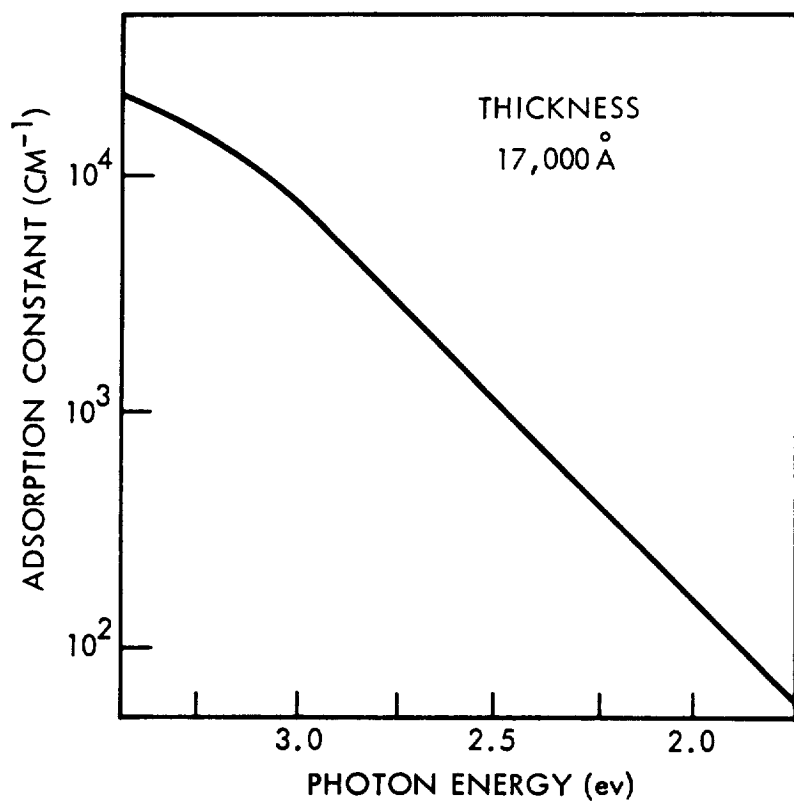


Figure 6-13. Optical Absorption Constant of a Polymer Film as a Function of Wavelength

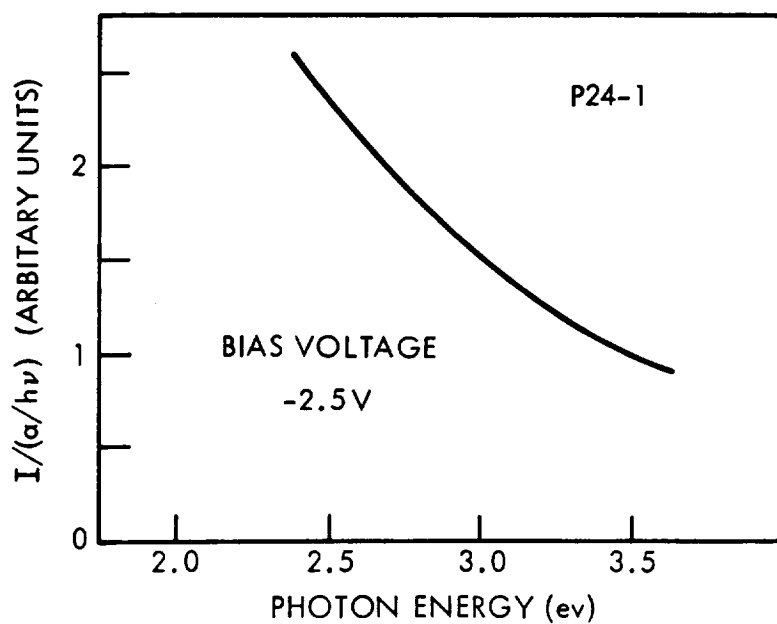


Figure 6-14. Quantum Yield Assuming Photocurrent is Due to Volume Photoconductivity in the Polymer

corresponding to positive (counterelectrode) bias is difficult to understand. For large positive bias the current is positive, corresponding to electron emission from the electrode. It seems impossible that the barrier height should be greater than 2 eV in this circumstance. Similar arguments would appear to apply if hole conduction is assumed instead of electron conduction.

Another possibility is that the charge carriers are produced in the volume of the polymer film rather than at the metal electrodes. There is probably some photon absorption in the polymer throughout the wavelength range investigated. The absorption by the present films is too small to measure, but it has been measured in a thick (17,000 Å) polymer film produced under similar conditions by H. T. Mann. The absorption constant α is shown in Figure 6-13 as a function of photon energy. A photocurrent I depends on α as follows.⁹

$$I = (\eta N_a e / t) (w / s),$$

where η is the quantum yield (i.e. the number of charge carriers produced per photon absorbed), N_a is the number of photons absorbed in time t , e is the electron charge, w is the Schubweg, and s is the sample thickness. If N_i is the number of photons incident, then

$$N_a = N_i (1 - e^{-\alpha s}) \approx \alpha s N_i \quad \text{for } \alpha s \ll 1.$$

Putting

$$N_i = At J / h\nu$$

where A is the sample area, J is the incident light intensity, and $h\nu$ is the photon energy, we get

$$I = \alpha \eta (w / s) (J A s e / h\nu).$$

Inserting the appropriate values for the known quantities, we find

REFERENCES

1. R. W. Christy, J. Appl. Phys. 31, 1680 (1960).
2. H. T. Mann, Electrochem. Techn. 1, 287 (1963).
3. H. T. Mann, J. Appl. Phys. 35, 2173 (1964).
4. R. W. Christy, J. Appl. Phys. 35, 2179 (1964).
5. K. W. Shepard, J. Appl. Phys. 36, 796 (1965).
6. R. S. Sennett and G. D. Scott, J.O.S.A. 40, 203 (1950).
7. R. H. Fowler, Phys. Rev. 38, 45 (1931).
8. D. V. Geppert, J. Appl. Phys. 34, 490 (1963).
9. F. C. Brown, The Physics of Solids (W. A. Benjamin, Inc., New York, 1967).

$$I \approx \alpha \eta (w/s) 10^{-12} \text{ A.}$$

If $\eta(w/s) = 1$ (its maximum possible value), then

$$I \approx \alpha 10^{-12} \text{ A.}$$

Thus for α greater than 10^2 cm^{-1} we get the observed order of magnitude of photocurrent in the correct wavelength range. The electric field (bias voltage) dependence comes in through the Schubweg, so that (w/s) must be less than 1. The nonlinearity with voltage is not normally expected, but it is not impossible. The only wavelength dependent quantities in the equation for I are I , η , α , and $h\nu$ (since the wavelength dependence of J has been normalized out). Plotting the experimental values of $I/(\alpha/h\nu)$ would give the wavelength dependence of the quantum yield. This is shown in Figure 6-14. While α changes by a factor of 20, η varies only by a factor of about 2.

Whatever the correct explanation of the source of the photoelectrons, the existence of a photocurrent for zero applied field very likely means that there is an internal field in the insulator. Since about + 1.5 V is required to reduce the current to zero for the sample in Figure 6-9, the bottom of the conduction band is presumably lower by this amount on the side toward the substrate. This difference might occur if conditions changed during the course of the electron bombardment, for example if collection of secondary electrons were greater in the initial stages. It should be noted that some other samples showed considerably smaller asymmetry.

Measurement of photocurrents through polymer films has been shown to be a useful tool for the study of the electronic structure of the polymer. It remains to use this tool to investigate the effects of polymer thickness, electron/molecule ratio during formation, and aging in air. One could expect that volume photoconductivity would predominate for thicker films and emission from the electrodes for thinner films.

	<u>Copies*</u>
Mr. Henry Pohl PESD Energy - RCS Branch Chief NASA Manned Spacecraft Center Houston, Texas 77058	1
Mr. Richard Carter Langley Research Center Langley Station Hampton, Virginia 23365	1
Mr. Clarence A. Syvertson Mission Analysis Division NASA Ames Research Center Moffett Field, California 24035	1
<u>NASA CENTERS</u>	
Ames Research Center Moffett Field, California 94035	1
Goddard Space Flight Center Greenbelt, Maryland 20771	1
Jet Propulsion Laboratory California Institute of Technology 4800 Oak Grove Drive Pasadena, California 91103	1
Langley Research Center Langley Station Hampton, Virginia 23365	1
Lewis Research Center 21000 Brookpark Road Cleveland, Ohio 44135	2
Marshall Space Flight Center Huntsville, Alabama 35812	2
Manned Spacecraft Center Houston, Texas 77058	2
John F. Kennedy Space Center Cocoa Beach, Florida 32931	1

*(Technical Library unless indicated otherwise)

INTERIM REPORT DISTRIBUTION LIST

CONTRACT NAS 7-436

	<u>Copies*</u>
NASA Headquarters Contracting Officer, BCA Patent Office, AGP Washington, D.C. 20546	1
Dr. Robert Levine Chief, Liquid Propulsion Technology NASA Headquarters, Code RPL Washington, D.C. 20546	1
Mr. Frank Compitello Office of Advanced Research and Technology NASA Headquarters Washington, D.C. 20546	1
Mr. Louis Toth Jet Propulsion Laboratory 4800 Oak Grove Drive Pasadena, California 91103	2
NASA Scientific and Technical Information Facility P. O. Box 33 College Park, Maryland 20740	25
Mr. Vincent L. Johnson Director, Launch Vehicles and Propulsion, SV Office of Space Science and Applications NASA Headquarters, Washington, D.C. 20546	1
Mr. Edward Z. Gray Director, Advanced Manned Missions, MT Office of Manned Space Flight NASA Headquarters, Washington, D.C. 20546	1
Mr. Joseph G. Thibodaux, Jr. Code EP, Propulsion and Power Division NASA Manned Spacecraft Center Houston, Texas 77058	1
Mr. Keith D. Chandler, R-P&VE-PA NASA Marshall Space Flight Center Huntsville, Alabama 35812	1

*(Technical Library unless indicated otherwise)

INDUSTRY CONTRACTORSCopies*

Aerojet-General Corporation
P. O. Box 296
Azusa, California 91703

1

Aerojet-General Corporation
P. O. Box 1947
Technical Library
Bldg. 2015, Dept. 2410
Sacramento, California 95809

1

Aeroneutronic - Philco Corporation
Ford Road
Newport Beach, California 92663

1

Aerospace Corporation
2400 East El Segundo Blvd.
P. O. Box 95085
Los Angeles, California 90045

1

Arthur D. Little, Inc.
20 Acorn Park
Cambridge, Massachusetts 02140

1

Astrosystems International, Inc.
1275 Bloomfield Avenue
Fairfield, New Jersey 07007

1

Atlantic Research Corporation
Edsall Road and Shirley Highway
Alexandria, Virginia 22314

1

Bell Aerosystems Company
P. O. Box 1
Buffalo, New York 14240

1

Bendix Systems Division
Bendix Corporation
3300 Plymouth Road
Ann Arbor, Michigan

1

Boeing Company
P. O. Box 3707
Seattle, Washington 98124

1

Boeing Company
P. O. Box 3707
Seattle, Washington 98124
Attn: William W. Kann

1

*(Technical Library unless indicated otherwise)

GOVERNMENT INSTALLATIONS

Copies*

Aeronautical Systems Division
Air Force Systems Command
Wright-Patterson Air Force Base
Dayton, Ohio 45433

1

Arnold Engineering Development Center
Arnold Air Force Station
Tullahoma, Tennessee

1

Space and Missile Systems Organization (SAMSO)
2400 E. El Segundo
El Segundo, California 90045

1

Bureau of Naval Weapons
Department of the Navy
Washington, D. C.

1

Defense Documentation Center Headquarters
Cameron Station, Building 5
Attention: ITSIA
5010 Duke Street
Alexandria, Virginia 22314

1

Air Force Rocket Propulsion Laboratory
Research and Technology Division
Air Force Systems Command
Edwards, California 93523

1

U. S. Army Missile Command
Redstone Arsenal, Alabama 35809

1

U. S. Naval Ordnance Test Station
China Lake, California 93557

1

CPIA

Chemical Propulsion Information Agency
Applied Physics Laboratory
8621 Georgia Avenue
Silver Springs, Maryland 20910

1

*(Technical Library unless indicated otherwise)

	<u>Copies*</u>
Rocketdyne (Library 586-306) North American Aviation, Inc. 6633 Canoga Avenue Canoga Park, California 91304	1
Space General Corporation 9200 East Flair Avenue El Monte, California 91734	1
Astro-Electronics Division Radio Corporation of America Princeton, New Jersey 08540	1
Reaction Motors Division Thiokol Chemical Corporation Denville, New Jersey 07832	1
Stanford Research Institute 333 Ravenswood Avenue Menlo Park, California 94025	1
TRW INC TRW Systems Group One Space Park Redondo Beach, California 90278	1
Research Laboratories United Aircraft Corporation 400 Main Street East Hartford, Connecticut 06108	1
Aerospace Operations Walter Kidde and Company, Inc. 567 Main Street Belleville, New Jersey 07109	1
Florida Research and Development Pratt and Whitney Aircraft United Aircraft Corporation P. O. Box 2691 West Palm Beach, Florida 33402	1
Rocket Research Corporation 520 South Portland Street Seattle, Washington 98108	1
Solar Division of International Harvester Company 2200 Pacific Highway San Diego, California	1

*(Technical Library unless indicated otherwise)

	<u>Copies*</u>
Missile and Space Systems Division McDonnell Douglas Corporation 3000 Ocean Park Boulevard Santa Monica, California 90406	1
General Dynamics/Astronautics Library and Information Services (128-00) P. O. Box 1128 San Diego, California 92112	1
Re-Entry Systems Department General Electric Company 3198 Chestnut Street Philadelphia, Pennsylvania 19101	1
Grumman Aircraft Engineering Corporation Bethpage, Long Island, New York	1
Ling-Temco-Vought Corporation Astronautics P. O. Box 5907 Dallas, Texas 75222	1
Lockheed Missiles and Space Company P. O. Box 504 Sunnyvale, California 94088 Attn: Technical Information Center	1
The Marquardt Corporation 16555 Saticoy Street Van Nuys, California 91409	1
Denver Division Martin Marietta Corporation P. O. Box 179 Denver, Colorado 80201	1
McDonnell Douglas Corporation P. O. Box 516 Municipal Airport St. Louis, Missouri 63166	1
Space and Information Systems Division North American Aviation, Inc. 12214 Lakewood Boulevard Downey, California 90241	1

*(Technical Library unless indicated otherwise)

	<u>Copies*</u>
Stratos Western Division of Fairchild-Hiller Corporation 1800 Rosecrans Boulevard Manhattan Beach, California	1
Vacco Valve Co. 10350 Vacco Street South El Monte, California	1
Valcor Engineering Corp. 365 Carnegie Avenue Kenilworth, New Jersey 07033	1
Whittaker Corporation 9601 Canoga Avenue Chatsworth, California 91311	1
Wintec Corp. 343 Glasgow Inglewood, California	1

*(Technical Library unless indicated otherwise)

	<u>Copies*</u>
Accessory Products Division of Textron, Inc. 12484 E. Whittier Blvd. Whittier, California 90602	1
Calmec Manufacturing Corporation 5825 District Blvd. Los Angeles, California 90022	1
Carleton Controls Corporation East Aurora, New York 14052	1
J. C. Carter Company 671 W. Seventeenth Street Costa Mesa, California 92626	1
Holex Incorporated 2751 San Juan Road Hollister, California 95023	1
M. C. Manufacturing Company P. O. Box 126 Lake Orion, Michigan 90501	1
Moog Servocontrols, Inc. Proner Airport East Aurora, New York 14052	1
National Waterlift Co. 2220 Palmer Avenue Kalamazoo, Michigan 49001	1
Ordnance Engineering Associates, Inc. 1030 East North Avenue Des Plaines, Illinois	1
Parker Aircraft 5827 W. Century Boulevard Los Angeles, California 90009	1
Pelmec Division Quantic Industries, Inc. 1011 Commercial Street San Carlos, California	1
Pyronetics, Inc. 10025 Shoemaker Avenue Santa Fe Springs, California 90670	1

*(Technical Library unless indicated otherwise)

